

An Analysis of the Subfloor Cavity Climate in a Residential Building

Sabrina Sequeira
BS (summa cum laude)

Submitted in fulfilment of the requirements
for the degree of
Doctor of Philosophy

University of Tasmania
School of Architecture and Design
School of Engineering

October, 2014

STATEMENTS

Declaration of Originality

This thesis contains no material which has been accepted for a degree or diploma by the University or any other institution, except by way of background information and duly acknowledged in the thesis, and to the best of my knowledge and belief no material previously published or written by another person except where due acknowledgement is made in the text of the thesis, nor does the thesis contain any material that infringes copyright.

Authority of Access

This thesis may be made available for loan and limited copying and communication in accordance with the Copyright Act 1968.

ABSTRACT

As roof and wall insulation have become standard practice in residential building design and construction, the conditions in the subfloor cavity have gained relative importance to a building's thermal performance. However, the modelling of the subfloor cavity is considered a weak point in many building thermal performance software programs. Recent research suggests that improvements to the subfloor model are crucial to improving the accuracy of Australia's benchmark building thermal performance program, AccuRate. Another recent study finds fault with the criteria that established the current standard for subfloor ventilation design, questioning the subfloor's ability to maintain the subfloor humidity below the design limit. These findings suggest the need for a review of the subfloor thermal model.

As very little measured data on Australian subfloor conditions exist, this research seeks to explore the subfloor conditions experimentally. This research investigates the subfloor cavity climate of a small residential scale test cell for a period of over one year. Energy and mass transfer relationships linking subfloor ventilation, ground evaporation and the subfloor and outdoor climate conditions are explored theoretically and using observed data. The observed data are compared to design limits, previous research findings and AccuRate's predictions.

The relative humidity in the subfloor is found to exceed the ventilation design limit. The conditions that lead to mould or decay are complex and when compared to these limits the data are on the threshold of conditions thought to be conducive to deterioration.

The subfloor climate conditions are found to vary based on time elapsed since construction. Between one year and five years after construction, the subfloor air temperature, specific humidity and ground moisture evaporation rate are observed to drop considerably. Though the relative humidity remains constant over this time, both the energy and moisture in the subfloor are reduced, changing the role of the subfloor vents. Whilst initially the net effect of the vents is to nearly always decrease both the moisture and energy of the subfloor air, six years after construction the vents are shown to increase moisture 24% of the time, and energy 35% of the time.

This shift in subfloor climate over time is found to affect the apparent accuracy of the AccuRate subfloor model. Previous research, based on data collected one year after construction, had shown that the observed subfloor temperature was several degrees above AccuRate's predicted subfloor temperature. However, when considering data six years after construction, this study finds that the observed and AccuRate temperatures are more closely aligned.

These results emphasize the importance of building thermal performance research to consider the time elapsed since building construction, as ground temperature and moisture stabilization have a noticeable effect on the subfloor climate.

ACKNOWLEDGEMENTS

This research would not have been possible without the financial support from CSIRO and the Tasmanian Government Department of Workplace Standards.

I am very thankful for the support that my colleagues, friends and family provided during my candidature.

My supervisors Roger Fay and Jane Sargison kept me on the straight and narrow path to completion. I appreciate their guidance, smiles and patience. My earlier supervisor Florence Soriano provided much technical and personal guidance.

Dong Chen from CSIRO was always willing and enthusiastic to engage in technical discussion. I appreciate his prompt and knowledgeable responses to my varied questions.

I benefited greatly from the presence of my compatriots in the research process Phil McLeod, Detlev Geard, and Mark Dewsbury, and am thankful for their eagerness to discuss ideas and research methods. Additional thanks to Detlev for assistance with AccuRate and to Mark for his diverse and innumerable contributions.

Many thanks to past and present members of the School of Architecture & Design and the Centre for Sustainable Architecture with Wood including Gregory Nolan, Michael Lee, Victoria (Kong) Pearce, Stephen Wright, and Janice Bowman, for helping organize the data acquisition and providing general support. Many thanks as well to those in the School of Engineering including Andrew Bylett, Pete Seward, David Morley, Cal Gerard, Bernie Chenery, James Lamont and Hayden Honeywood, for providing support as needed.

I also appreciate the large effort devoted to the CFD model by Jean Cailleau from the University of Nantes; the soil sampling performed by Ray Mayne; the guidance regarding the BRL radiation model from John Boland from the University of South Australia; the early conversations and assistance from Angelo Delsante, retired from CSIRO; and the feedback from Des Fitzgerald from the School of Mathematics & Physics.

I have much gratitude for Kate Stark, Jonny Stark, Jennifer Lorrimar-Shanks and Jon Shanks, who let neither infants nor impending childbirth stand in the way of proofreading this document.

Thanks to Bruce Fleet and my community for supporting my household in a variety of ways over the course of the last six years. Finally, I have much adoration and appreciation for my Sofia and Eliza, who do not realize how much they have sacrificed.

TABLE OF CONTENTS

Statements	ii
Abstract	iii
Acknowledgements	v
Table of Contents	vi
List of Tables.....	x
List of Figures	xi
Abbreviations and Definitions	xv
1 · Introduction.....	1
1.1 Background, aim and scope.....	1
1.2 Structure of the thesis.....	3
2 · Background	5
2.1 Introduction.....	5
2.2 Australian residential building.....	5
2.2.1 House Energy Rating software.....	6
2.2.2 Concerns about HER software	8
2.2.3 Recent research on empirical validation of AccuRate	9
2.3 Subfloor construction.....	11
2.3.1 Construction requirements.....	11
2.3.2 Origin of the construction requirements	13
2.4 Modeling of subfloor thermal performance	15
2.4.1 Subfloor climate model.....	17
2.4.2 Subfloor ventilation model.....	20
2.5 Experimental support of subfloor modeling theory	22
2.5.1 Subfloor ventilation experimentation.....	22
2.5.2 Subfloor climate experimentation	25
2.6 Conclusion.....	27
3 · Research Design.....	29
3.1 Introduction.....	29
3.2 Research questions and method overview	29
3.3 Research design for Investigation 1, Subfloor Ventilation.....	31
3.3.1 Investigation 1 Inputs	32

3.3.2	Investigation 1 Analyses	33
3.3.3	Investigation 1 Outputs	34
3.4	Research design for Investigation 2, Subfloor Climate.....	34
3.4.1	Investigation 2 Inputs	35
3.4.2	Investigation 2 Analyses	36
3.4.3	Investigation 2 Outputs	37
3.5	Test facility	37
3.6	Conclusion.....	42
4	Investigation 1 Design and Results: Subfloor Ventilation	43
4.1	Introduction	43
4.2	Assessment of test site using computational fluid dynamics	43
4.2.1	TC2 in isolation.....	44
4.2.2	TC2 in presence of TC1 and TC3.....	47
4.2.3	CFD summary.....	51
4.3	Tracer gas test method and instrumentation	52
4.4	Observed data reduction.....	54
4.5	Generation of theoretical data	56
4.6	Results of ventilation test.....	57
4.7	Conclusion.....	61
5	Investigation 2 Design: Subfloor Climate	62
5.1	Introduction	62
5.2	Measurements	62
5.2.1	Summary of sensors and other measurements.....	62
5.2.2	Weather sensors	67
5.2.3	Temperature.....	69
5.2.4	Humidity.....	70
5.2.5	Heat flux.....	70
5.2.6	Radiation	71
5.2.7	Air speed	71
5.3	Data acquisition.....	71
5.4	Data reduction.....	74
5.4.1	Data handling and error checking.....	74
5.4.2	Summary of data and anomalies present.....	84
5.5	Additional measured data and calculations.....	86
5.5.1	Wood moisture.....	87
5.5.2	Soil moisture	87
5.5.3	Additional weather data and calculations.....	88

5.5.4	Environmental temperature	90
5.5.5	Air, moisture and energy flows	91
5.5.6	Daily maximum and minimum calculation	93
5.6	Generation of AccuRate data	94
5.6.1	Overview of method for running AccuRate	94
5.6.2	Standard AccuRate inputs	95
5.6.3	Non-standard AccuRate inputs	97
5.6.4	Summary of differences between AccuRate runs	105
5.6.5	AccuRate data reduction	106
5.7	Conclusion	106
6	Investigation 2 Results: Subfloor Climate	107
6.1	Introduction	107
6.2	Presentation of observed data	107
6.2.1	Outdoor climate	108
6.2.2	Room and subfloor climate	117
6.2.3	Air, moisture and energy flows in the subfloor	136
6.2.4	Different time periods and historical data	140
6.3	Presentation of AccuRate data	149
6.3.1	AccuRate Run 1 results	150
6.3.2	AccuRate Run 2 results	155
6.4	Correlation of residuals	161
6.5	Measurement system analysis	175
6.6	Conclusion	176
7	Discussion: Subfloor Ventilation and Climate	177
7.1	Introduction	177
7.2	Trends in observed subfloor data	177
7.2.1	Subfloor ventilation	177
7.2.2	Temporal variations	179
7.2.3	Spatial variations	180
7.2.4	Seasonal variations	182
7.2.5	Effect of ground cover and ceiling hatch	183
7.2.6	Subfloor moisture and deterioration criteria	184
7.3	Trends in AccuRate data	186
7.4	Sources of error and limitations	191
8	Conclusions and Recommendations	193
8.1	Findings	193
8.2	Recommendations for further research	195

References	198
Appendix	203

LIST OF TABLES

Table 2.1: Subfloor ventilation and clearance (BCA 2011).....	12
Table 3.1: Test cell fabric matrix.....	40
Table 4.1: Site influence on TC2 roof air speed.....	52
Table 4.2: Site influence on TC2 subfloor inlet vent air speed.....	52
Table 4.3: Terrain classification parameters (Deru and Burns 2003).....	56
Table 5.1: AccuRate climate inputs (Geard 2011).....	63
Table 5.2: Sensor set - minimum	64
Table 5.3: Sensor set - total.....	65
Table 5.4: Wood moisture measurements locations.....	66
Table 5.5: Soil sample locations	66
Table 5.6: Time periods for reduced data set.....	86
Table 5.7: Atypical AccuRate inputs for this research.....	95
Table 5.8: Framing factor material thickness adjustments.....	96
Table 5.9: Ventilation models.....	101
Table 5.10: Climate file format (Geard 2011).....	103
Table 5.11: Observed weather parameters integrated into AccuRate climate file	104
Table 6.1: Subfloor SE corner relative humidity, time spent above 80% and 85%	124
Table 6.2: Soil moisture content	134
Table 6.3: Correlation of AR1 subfloor temperature to observed temperatures.....	152
Table 6.4: Daily minimum and maximum residuals (ODB – AR1), averaged by month.....	154
Table 6.5: Average daily minimum and maximum residuals (ODB – AccuRate) from 2007 (Dewsbury 2011).....	155
Table 6.6: Correlation of AR2 subfloor temperature to observed temperatures.....	158
Table 6.7: Daily minimum and maximum residuals (OE – AR2), averaged by month	161

LIST OF FIGURES

Figure 2.1: Climate zones based on relative humidity (BCA 2011).....	13
Figure 2.2: Subfloor cavity heat (Q) and moisture (g) flows (Kurnitski and Matilainen 2000)	17
Figure 3.1: Research process map for Investigation 1, Subfloor Ventilation	32
Figure 3.2: Research process map for Investigation 2, Subfloor Climate	35
Figure 3.3: Test site from the northwest	38
Figure 3.4: Aerial photo of test site	38
Figure 3.5: Site plan, not to scale (Dewsbury 2011)	39
Figure 3.6: Diagram of wall cavity and subfloor obstruction (Dewsbury 2011)	41
Figure 3.7: Photo of wall cavity and subfloor obstruction (Dewsbury 2011)	41
Figure 3.8 Subfloor cavity	41
Figure 3.9: Subfloor vent.....	41
Figure 3.10: North wall of test cell	42
Figure 3.11: South wall of test cell.....	42
Figure 3.12: East wall of test cell	42
Figure 3.13: West wall of test cell	42
Figure 4.1: CFD results, TC2 in isolation, wind from W.....	45
Figure 4.2: CFD results, TC2 in isolation, wind from NW	47
Figure 4.3: CFD results, wind from W	48
Figure 4.4: CFD results, wind from N.....	49
Figure 4.5: CFD results, wind from NW.....	51
Figure 4.6: Tubes for injecting and sampling SF6 (Dewsbury 2011).....	54
Figure 4.7: Dispersement of SF6 via fan (photograph by Mark Dewsbury)	54
Figure 4.8: Observed and theoretical subfloor ventilation data.....	57
Figure 4.9: Subfloor ventilation by wind octant.....	59
Figure 4.10: Ventilation from NW octant by wind component	60
Figure 5.1: Location plan of sensors and wood moisture probes (not to scale)	67
Figure 5.2: Wind speed and direction sensors	68
Figure 5.3: Mounted Vaisala temperature and humidity sensors.....	68
Figure 5.4: AD592 temperature sensors	69
Figure 5.5: PT100 sensors.....	70
Figure 5.6: Heat flux sensor.....	71
Figure 5.7: Overhead view of data loggers	72
Figure 5.8: Master spreadsheet of data in 10-minute increments	76
Figure 5.9: Process map for error-checking 10-minute interval data.....	77
Figure 5.10: Range check summary	78

Figure 5.11: Portion of AS30 range check sensor violations output file.....	79
Figure 5.12: Portion of step check summary table.....	80
Figure 5.13: Portion of HF20 range check sensor violations output file.....	80
Figure 5.14: Graphical instrumentation checks	81
Figure 5.15: Thermocouple spiking.....	83
Figure 5.16: Ground cover in subfloor.....	85
Figure 5.17: Missing ceiling hatch.....	86
Figure 5.18: Wood moisture sensing.....	87
Figure 5.19: Soil moisture test.....	88
Figure 5.20: Flow of water through subfloor.....	92
Figure 5.21: Missing plasterboard panels on south wall.....	96
Figure 5.22: Incorporating missing plasterboard panels into AccuRate.....	97
Figure 5.23: Bypassing thermostat settings in scratch file	98
Figure 5.24: Energy usage for space conditioning	98
Figure 5.25: Bypassing heat addition in scratch file	100
Figure 5.26: Default subfloor ventilation model	100
Figure 5.27: Modified subfloor ventilation model	101
Figure 5.28: Default climate file	102
Figure 5.29: Replacement of NA values in on-site climate file.....	105
Figure 6.1: Outdoor air temperature, TP1-3.....	109
Figure 6.2: Outdoor relative humidity, TP1-3	110
Figure 6.3: Outdoor specific humidity, TP1-3.....	111
Figure 6.4: Wind speed at test cell roof, TP1-3.....	112
Figure 6.5: Wind rose.....	113
Figure 6.6: Precipitation	113
Figure 6.7: Global irradiation	114
Figure 6.8: Outdoor ground heat flux.....	115
Figure 6.9: Outdoor ground heat flux versus global radiation.....	116
Figure 6.10: Outside ground temperature	116
Figure 6.11: Outdoor heat flux versus difference between air and ground temperature.....	117
Figure 6.12: Room dry bulb and globe temperatures, by month.....	118
Figure 6.13: Subfloor and outdoor air temperatures, by month.....	118
Figure 6.14: Subfloor temperature, by hour.....	119
Figure 6.15: Subfloor centre temperatures, by month.....	119
Figure 6.16: Subfloor centre and corner air temperatures, by month.....	120
Figure 6.17: Subfloor centre and NW air temperatures, by month.....	120
Figure 6.18: Subfloor centre and east side air temperatures, by month	121

Figure 6.19: Temperature difference, subfloor globe - dry bulb air temperature	122
Figure 6.20: Subfloor and outdoor relative humidity, by month.....	123
Figure 6.21: Subfloor relative humidity, by hour.....	123
Figure 6.22: Relative humidity throughout subfloor, by month.....	124
Figure 6.23: Subfloor SE corner relative humidity during cool months	126
Figure 6.24: Subfloor temperature during cool months.....	127
Figure 6.25: Subfloor specific humidity, TP1-3.....	129
Figure 6.26: Specific humidity throughout subfloor, by month	130
Figure 6.27: Subfloor centre and east side heat flux	131
Figure 6.28: Subfloor centre ground temperatures, by month.....	132
Figure 6.29: Comparison of subfloor and outdoor ground temperatures	133
Figure 6.30: Subfloor heat flux versus air and ground temperature difference.....	134
Figure 6.31: Wood moisture content	135
Figure 6.32: Subfloor centre relative humidity vs ventilation.....	136
Figure 6.33: Net moisture exiting subfloor vents.....	137
Figure 6.34: Net moisture exiting vents versus outside relative humidity.....	137
Figure 6.35: Subfloor cavity moisture sources versus ventilation.....	138
Figure 6.36: Ground moisture evaporation as a function of ventilation.....	138
Figure 6.37: Ground moisture evaporation vs. evaporation potential.....	139
Figure 6.38: Net energy exiting subfloor vents.....	140
Figure 6.39: Net energy exiting subfloor vents versus outdoor specific humidity	140
Figure 6.40: 2007 Subfloor and outdoor air temperatures (Sequeira et al. 2010b)	141
Figure 6.41: Subfloor temperature vs. outdoor temperature, by time period.....	142
Figure 6.42: Subfloor temperature, by time period and season	143
Figure 6.43: Subfloor specific humidity vs. outdoor specific humidity, by time period	144
Figure 6.44: Subfloor specific humidity, by time period and season	145
Figure 6.45: Subfloor relative humidity vs. outdoor relative humidity, by time period.....	146
Figure 6.46: 2007 Ground moisture evaporation vs. subfloor ventilation (Sequeira et al. 2010b).....	147
Figure 6.47: Evaporation vs. evaporation potential, by time period.....	148
Figure 6.48: Subfloor evaporation vs. evaporation potential, TP1 and TP3 winter data	149
Figure 6.49: Observed and AR1 room temperatures for selected weeks	150
Figure 6.50: Observed and AR1 subfloor temperatures for selected weeks.....	151
Figure 6.51: AR1 temperature vs. observed subfloor temperatures.....	152
Figure 6.52: 2007 Simulated subfloor temperature versus observed subfloor dry bulb temperature (Dewsbury 2011)	153
Figure 6.53: Observed and AR1 daily min. and max. subfloor temperatures, July 2012.....	154
Figure 6.54: Observed and AR2 room temperatures for selected weeks	156

Figure 6.55: Observed and AR2 subfloor temperatures for selected weeks.....	156
Figure 6.56: AR2 temperature vs. observed subfloor temperatures.....	158
Figure 6.57: Observed and AR2 daily min. and max. subfloor temperatures, July 2012.....	159
Figure 6.58: Monthly average of AR1 and AR2 daily residuals	159
Figure 6.59: Correlation of room residuals with subfloor residuals (OE-AR2), TP3	162
Figure 6.60: Correlation of subfloor residuals (OE-AR2) with various parameters, TP3, batch 1.....	163
Figure 6.61: Correlation of subfloor residuals (OE-AR2) with various parameters, TP3, batch 2.....	164
Figure 6.62: Residuals by hour, TP3.....	166
Figure 6.63: Environmental temperatures by hour, TP3.....	166
Figure 6.64: Subfloor temperatures by hour on July 01 2012	167
Figure 6.65: Correlation of room residuals to subfloor residuals by hour, TP3	168
Figure 6.66: Correlation of daily room residuals to subfloor residuals, TP3.....	168
Figure 6.67: AccuRate vs. observed temperature, 9am, TP3	169
Figure 6.68: Correlation of subfloor residuals (OE-AR2) w/various parameters, 9am,TP3,batch 1	170
Figure 6.69: Correlation of subfloor residuals (OE-AR2) w/various parameters, 9am,TP3,batch 2.....	171
Figure 6.70: AccuRate vs. observed temperature, 4pm, TP3.....	172
Figure 6.71: Correlation of subfloor residuals (OE-AR2) w/various parameters, 4pm,TP3,batch 1	173
Figure 6.72: Correlation of subfloor residuals (OE-AR2) w/various parameters, 4pm,TP3,batch 2	174
Figure 7.1: Example characteristics of residuals, using contrived data.....	187

ABBREVIATIONS AND DEFINITIONS

ABARES – Australian Bureau of Agricultural and Resource Economics and Sciences

ABCB – Australian Building Codes Board

ABS – Australian Bureau of Statistics

ACH – air changes per hour

AccuRate – Australia’s benchmark building thermal performance simulation program

Air – atmospheric air, which consists of dry air and water vapour.

AR1, AR2 – AccuRate run 1 or 2

BCA – The Building Code of Australia

BOM – Bureau of Meteorology

BRANZ – Building Research Association of New Zealand

CEM – dataTaker brand channel expansion module connected to DT0

CFD – computational fluid dynamics

CSIRO – Commonwealth Scientific and Industrial Research Organisation

CSV – comma-separated variable, a file format and extension

DCCEE – Department of Climate Change and Energy Efficiency

DEWHA – Department of Energy, Water, Heritage and the Arts

DOE – Department of Energy

DT0, DT2 – dataTaker brand DT500 data loggers

DT80 – dataTaker brand data logger connected to DT2

DXD – file extension for DeTransfer data file

GUI – graphical user interface

HER – House Energy Rating

IC – integrated circuit, a type of temperature sensing device

LBL, or LBNL – Lawrence Berkeley National Laboratory

NatHERS – National House Energy Rating Software Scheme

ODB – observed dry bulb (temperature)

OE – observed environmental (temperature)

R^2 or R-squared – coefficient of determination, indicating how well data fits a linear model

Residuals – temperature difference, calculated as observed temperature minus AccuRate temperature

RMY – reference meteorological year

RTD – resistance temperature detector, a type of temperature sensing device

SF₆ – sulphur hexafluoride

TC – thermocouple

TP1, TP2, TP3 – time period 1, 2 or 3

UniSA – University of South Australia

UTAS – University of Tasmania

1 • INTRODUCTION

1.1 Background, aim and scope

This research considers the residential building industry in Australia.

Forty-one percent of the energy used in a typical Australian household is consumed for space heating and cooling (Department of Energy, Water, Heritage and the Arts, or DEWHA 2008). The Australian government aims to reduce this energy demand through improvements in the thermal design of housing. The government legislates this through the Australian Building Codes Board's (ABCB) Building Code of Australia (BCA). The BCA stipulates that new residential buildings meet or exceed a pre-defined energy efficiency standard, termed a star rating. A star rating represents the amount of space heating and cooling energy a building would be expected to use to maintain adequate temperatures during specified times in its occupied rooms.

Quantifying the predicted energy usage and determining the star rating for an individual building requires the use of a software program compliant with Australia's National House Energy Rating Software Scheme (NatHERS). AccuRate is the benchmark building thermal performance simulation program established by the Australian government (Department of Climate Change and Energy Efficiency, or DCCEE 2014). AccuRate was developed at Australia's national science agency, the Commonwealth Scientific and Industrial Research Organisation (CSIRO). The user inputs a building's design and location, and AccuRate makes assumptions about the climate and occupants' behaviour, and then performs a series of calculations. One of the outputs of AccuRate is the building's star rating. Thus, as the star rating is the basis for the government's regulation, the government has an interest in ensuring the accuracy of the AccuRate program.

In addition to its regulatory use, AccuRate can also be used as a design tool. It is used early in the design phase of a building to assist a designer make informed decisions based on the building fabric and layout's effect on thermal performance. As AccuRate assists a designer to decide between one construction material or system and another, commercial industry groups also have an interest in the accuracy of the program.

As the usage of AccuRate has increased, so have calls for its accuracy to be confirmed. The *Australian* newspaper twice brought national attention to possible errors in the software (Thomas 2010a; Thomas 2010b). Soon after, research from the University of Tasmania (Dewsbury 2011) demonstrated a positive correlation between the accuracy of AccuRate's room model and the accuracy of the subfloor model in a building with an enclosed-perimeter platform-floor, making it possible that the accuracy of the subfloor affected the accuracy of the room. Hence, attention is directed toward the subfloor.

The subfloor cavity, also known as the crawl space, of a building is quite different to other zones in a building because generally it is unoccupied, it contains no provisions for space heating or cooling, it interacts directly with the open ground below and the walls have permanent openings through which ventilation naturally occurs. Research concerning other zones of a building is not always directly applicable to the subfloor because of these unique traits.

The subfloor design requirements are aimed at maintaining a low relative humidity in the subfloor. The purpose of this is to maintain the subfloor climate at a state that would hinder the deterioration of the wood. Thus, this study considers not only the accuracy of AccuRate's thermal modelling of the subfloor cavity but also the subfloor's effectiveness at maintaining conditions that would hinder deterioration.

A review of research on subfloors returns mostly theoretical results. A model quantifying the amount of air flow passing through the subfloor cavity was recently incorporated into the AccuRate program (Delsante 2007). The model was developed theoretically and there were no experimental studies to support it. Other research traces the history of the subfloor ventilation design criteria and indicates that the calculations leading to the current BCA guidelines appear flawed (Williamson and Delsante 2006b). This work was also theoretical without the support of sufficient experimental data.

Moreover, the review of research returns very little experimental data gathered from Australian subfloor cavities. One study does present experimentally measured subfloor temperature and humidity data but there are very few ventilation or weather data with which to compare them (Olweny et al. 1998). Other studies from the USA, UK, Finland and New Zealand do present more data, but they are of limited value due to differences in the building design and construction methods used in Australia.

The literature lacks a broad analysis of the subfloor cavity as a whole, comprising observations taken over at least one year and a comparison of those data to theoretical predictions. **Therefore, the aim of this research is to investigate experimentally the subfloor cavity conditions of a residential building.**

The research contained in this thesis pertains only to buildings designed to comply with the Building Code of Australia. It considers a building with a suspended floor where the cavity beneath the floor is exposed to the bare ground below, and the sides are enclosed by a perimeter wall whose surface is broken only by subfloor vents. This is a commonly used form of construction for single family residential dwellings in Australia. This work is relevant to buildings in a cool temperate climate.

This research compares observed subfloor parameters to observed weather conditions and associated heat and mass transfer processes. Observed data are compared to theoretical data as predicted by AccuRate, as well as historical data. It is outside the scope of this research to investigate the effect of the subfloor conditions on the thermal performance of the interior of the building.

1.2 Structure of the thesis

The research is documented as follows.

Chapter 2 introduces the House Energy Rating software and its role in the building industry. Recent research on the empirical validation of the AccuRate program directs the focus towards subfloors. The origin of the design of the subfloor is discussed as well as theory regarding the pertinent heat and mass transfer processes. A review of relevant experimental data is performed and it is found that much of the theory is unsubstantiated by experimental data.

Chapter 3 describes the research plan designed to address the shortcomings in our understanding of the subfloor. Four research questions are presented as well as an overview of the resulting experimental method. The experimental method consists of two separate investigations. Investigation 1 concerns the subfloor ventilation model. Investigation 2 is more complex as it involves the relationships between measured parameters and their associated heat and mass transfer processes. A brief summary of each investigation is provided. The test facility used for both investigations is described.

Chapter 4 describes the design and presents the results of Investigation 1 in relation to subfloor ventilation. First the test site is assessed using computational fluid dynamics. Then the test procedure, instrumentation and data handling procedure are described. The observed ventilation data are then compared to theoretical prediction.

Chapter 5 describes the design of Investigation 2 in relation to subfloor climate. The measurement system is described, including the sensors, their installed location, and the data acquisition system. The data reduction method is then detailed. All calculations performed on the observed data are

provided in this chapter, as well as the procedure for adjusting the AccuRate program to best represent the test site and weather conditions.

Chapter 6 presents the results of Investigation 2, following on from the description of the design presented in Chapter 5. Data from observed parameters outside and within the test building are provided and their variation by location is explored. Relationships between the observed parameters and air, moisture and energy flows are also examined. The observed data is compared to the predicted data from AccuRate and the differences between the two series of data are explored to find their influences. Both the observed and AccuRate data are compared to historical data.

The implications of the results presented in Chapters 4 and 6, the uncertainty in several presented parameters and an assessment of the limitations of the research are discussed in Chapter 7. Conclusions and recommendations for further research are provided in Chapter 8.

Additional information is provided in the Appendix and referred to throughout the thesis as appropriate.

2 • BACKGROUND

2.1 Introduction

This chapter introduces Australia's building industry with a focus on the energy that the residential sector uses for heating and cooling of its buildings. Thermal performance building simulation models are then discussed, as they are a tool used in assessing this energy usage. Research into the simulation models' accuracy is examined, which directs attention onto the subfloor cavity of buildings. The design and construction of subfloor cavities are presented. The status of the modelling theory relevant to subfloors is examined, as well as the experimental data that exists to support the current theoretical understandings.

2.2 Australian residential building

In 2008-2009 the residential sector accounted for 7.5% of Australia's domestic energy use (Australian Bureau of Agricultural and Resource Economics and Sciences, or ABARES 2011). The residential sector's consumption of energy contributes significantly to Australia's stationary energy greenhouse gas emissions (Department of Energy, or DOE 2008).

The current and projected trend in Australian residential building is that the number of households consistently increases while the number of occupants per household consistently decreases. It is estimated that the number of occupied residential households will have increased 61%, from six to almost 10 million, between 1986 and 2020. During those years total residential floor area is expected to have increased 145%, from 685 million square metres to nearly 1,682 million square metres (DOE 2008). The demand for heating and cooling, also known as space conditioning, is also projected to increase. Thus the amount of energy used to maintain an Australian home is an area of great concern.

Space conditioning accounts for 41% of the energy used in Australian households (Australian Bureau of Statistics, or ABS 2008). In 2008, more than three-quarters of Australian households had a heater and two-thirds had a cooler (air conditioner or evaporative cooler). One way to reduce the

heating and cooling energy usage in homes is through the design of the building itself. This method of energy reduction targets energy usage on the demand side. If a building is designed of such dimensions, materials and construction detail that the internal environment remains consistently comfortable for the occupants, then the need for the occupants to actively control their environment using energy-consuming heaters and coolers would be reduced. Furthermore, in the event that a heater or cooler is indeed used, the building should be designed such that the energy is used efficiently.

The Australian Building Codes Board (ABCB) is following this demand-side methodology for reducing the energy usage in buildings. The ABCB regulates the design of all commercial and residential buildings in Australia. The regulations are compiled in the three-volume Building Code of Australia (BCA).

Volume 2 of the BCA pertains specifically to small residential buildings. By means of these regulations the ABCB is targeting a reduction in residential buildings' anticipated space conditioning energy loads. This aim is made clear in the performance requirement of Volume 2 P2.6.1 (BCA 2011) which states that "a building must have, to the degree necessary, a level of thermal performance to facilitate the efficient use of energy for artificial heating and cooling." The ABCB further highlights "the need to consider the installation of energy efficiency measures in a building where there is a likelihood that an artificial heating or cooling system will be installed in the building irrespective of the initial design."

The ABCB then enforces this objective in the mandated construction practices targeted at energy efficiency in residential buildings in Volume 2 Part 3.12.0 of the BCA (BCA 2011). There are two routes for a building to comply with these energy efficiency regulations. One option under the deemed-to-satisfy provisions is that the building satisfies each of the listed energy efficiency provisions. The other option is that the building meets or exceeds minimum energy rating criteria when assessed using a compliant NatHERS program. Thus, House Energy Rating (HER) software programs play a significant part in the energy efficiency regulations of the building industry.

2.2.1 House Energy Rating software

As of 2014 three compliant NatHERs software programs exist for rating the thermal performance of Australian homes. The current benchmark NatHERs program set by the Australian government is AccuRate (DCCEE 2014). By this it is meant that other programs may be used but their output must be proven to be similar to AccuRate's. AccuRate is set as the benchmark because its output was validated against a set of international reference thermal performance programs (Delsante 2004). The other two compliant software packages are FirstRate 5 and BERS Professional. They

each offer alternative user interfaces but both are based on the Chenath Engine, the same calculation engine of AccuRate (DCCEE 2014).

AccuRate was developed at CSIRO, and is the result of a major overhaul of other previously existing programs. This overhaul project was funded by Australia's Energy Efficiency & Greenhouse Group and was administered by the Australian Greenhouse Office (Delsante 2005). AccuRate's calculation engine consists of a set of equations based primarily on theoretical physics with some adjustments having been incorporated into the program to represent findings from experimentation. The program treats each room of a building as an individual zone, with the roof cavity identified as a zone and the subfloor cavity, if one exists, being identified as a distinct zone as well. The calculation engine consists of equations representing physical relationships describing the heat and mass flow through the building. Ventilation models exist in the program to represent the flow of air through the openings of each zone.

When using AccuRate to assess a building's thermal performance, the user provides the program with the post code for the building's location. Based on this the program then assigns the building to a climate zone and assumes a typical annual climate pattern. This characteristic climate is called the Reference Meteorological Year, RMY. The RMY data is compiled by Australia's Bureau of Meteorology, BOM, for each climate zone based on at least 25 years of recorded temperature, humidity, solar radiation, and wind speed and direction data (DCCEE 2014). The user also inputs information about the site exposure to wind. Then the user inputs a comprehensive set of information about the building itself including the dimensions, orientation, materials, construction details, window coverings and any fixed shading the building is affected by.

AccuRate assumes behaviour patterns for the occupation of each room, taking into account the function of the room and the times of day it is expected to be used. AccuRate also assumes requirements for what defines the occupants' thermal comfort. This takes into account considerations such as the occupants' acclimatisation to the local climate, the impact of the RMY climate on the room, and the time of day. For example, it is assumed that a sleeping space needs to be maintained at a thermally comfortable condition only between the hours of 4pm and 9am. Between 4pm and midnight, and between 7am and 9am, the thermal comfort range is defined as a minimum air temperature of 18 °C. Between midnight and 7am, however, the thermal comfort minimum drops to 15 °C (DCCEE 2014).

AccuRate then calculates the temperatures in each zone and compares them to the thermal comfort range. In the event that the temperature is outside the range the program attempts to remedy this. Firstly, the program checks if the disparity can be resolved by natural methods, such as opening a window. Windows are assumed to be operational at all hours, though they may only be adjusted once every three hours. Secondly, the program considers low energy mechanical means of cooling,

such as ceiling fans. Lastly, if the discrepancy still cannot be resolved, the program assumes that mechanical heaters or coolers must be used (DCCEE 2014).

The program then calculates the amount of energy required to bring the zone temperature within the thermal comfort band. This procedure is repeated for every hour throughout the year and the amount of required heating and cooling energy usage is summed. This annual space conditioning energy demand is then divided by the total conditioned floor area and an adjustment is applied based on conditioned floor area and location. The intent of the adjustment is to compensate for the tendency of larger buildings to more easily achieve a better energy rating due to their smaller ratio of surface area to floor area (Delsante 2005). The result is an adjusted annual space conditioning energy usage per unit floor area for the entire building.

This value is compared against a predefined table of values called a starband. Each climate zone has a unique starband which takes into account the local climate. From this comparison the star rating results. The star rating can range from zero to ten. A 0-star house does very little to mitigate the occupants' discomfort due to extremes in weather, and thus requires a large amount of heating or cooling energy to make the home comfortable. In contrast a 10-star house provides the occupants with a thermally comfortable environment without any need for artificial heating or cooling (DCCEE 2012).

It is this star rating that is regulated in the BCA. It is therefore essential that a building's star rating output from the AccuRate program bears a strong relationship to the amount of energy that would actually be required to maintain that home in that location at an acceptable level of thermal comfort. As of 2014 most states have a 6-star minimum requirement, with Tasmania's requirement for detached residential buildings still at 5-star (BCA 2011).

In addition to this regulatory aspect, AccuRate is used as a design tool. Building industry professionals use the star rating as a metric in assessing trade-offs when deciding upon building design, orientation or choice of materials. For example, a building designer may be deciding between two different flooring materials which might only directly affect one room of the building. The building designer may be paying particular attention to the temperatures in that one room. Thus, it is not only important that AccuRate as a whole is accurate, but that the individual components of the program are accurate as well.

2.2.2 Concerns about HER software

Because of the substantial influence the building simulation programs can have on the building industry, the accuracy of these programs has come into question several times in recent years. On July 27th, 2010 The Australian, Australia's largest selling national daily newspaper, printed a short article highlighting an undescribed issue in the software (Thomas 2010a). The article states that

“the true energy efficiency of new Australian homes built to reduce greenhouse gas emissions is in question due to fundamental errors in the key software tool that performs the calculations ... The software tool designed by the CSIRO produces consistently false results and distorts the energy ratings of homes.”

The article then states that the errors caused by the software were confirmed by CSIRO scientist Dr. Zhengdong Chen. Chen stated that the CSIRO along with the DCCEE, which manages the software, were investigating the issue and at present they did not know what the extent of it was. The article then finishes with some comments from researchers. One researcher, University of Adelaide Associate Professor Terry Williamson, called for an “independent inquiry and a full examination of the software,” though Dr. Holger Willrath, principal of the Solar Logic firm which produces the BERS Professional program, doubted the errors were quite so significant.

Within a week of publishing the first article, The Australian published a much longer article mentioning the drastic differences in star ratings uncovered when a team of energy assessors used three different software programs to assess the same residential buildings (Thomas 2010b). This article provides comments from various industry representatives about the detrimental effect that inaccurate or inconsistent software packages can have on the building industry. This article also concludes with researchers’ comments. Williamson denounced blind faith in the software, and Willrath called for more funding to continue the software’s improvement.

These newspaper articles highlight a contested political issue and are rumoured to contain misquotes. Though they do not identify technical details, the articles make known that some errors do indeed exist in the software and that the effects are significant enough to be noticed by both researchers and standard users. While scientists and researchers may differ in their opinion regarding the extent that the error causes, they do agree that an investigation into the software is necessary.

2.2.3 Recent research on empirical validation of AccuRate

At the time that The Australian articles were being published, research was already underway at the University of Tasmania (UTAS) to investigate the accuracy of the AccuRate program. This research has since been published in two PhD theses (Dewsbury 2011; Geard 2011).

The purpose of both research programs was to empirically validate the AccuRate program and identify aspects of the software requiring improvement. The research focused on assessing the ability of the software to predict a room’s temperature over a period of time when the room had no mechanical heating or cooling applied. Both research programs concentrated only on lightweight residential buildings in a cool temperate climate (Dewsbury 2011; Geard 2011).

Dewsbury's research program involved the construction of three purpose-built test buildings in Launceston. Each consisted of only one internal room of the same size. Geard's research was undertaken on complete residential houses outside Hobart. Dewsbury's research program, due to the simpler building design, was more straightforward than Geard's and Dewsbury's is discussed in more detail.

The three test buildings were situated in close proximity to each other but positioned such that one would never cast a shadow on the other. They differed slightly in construction material. One was plywood clad with a platform-floor over an unenclosed subfloor. The second was clad in brick with a platform-floor over an enclosed subfloor. The third was also clad in brick but instead of a platform floor the building's floor was a concrete slab-on-ground (Dewsbury 2011). Brick veneer and timber are two of the most commonly used outside wall materials for Australian buildings, together accounting for over half of all dwellings (ABS 2008). Thus the test buildings were representative of contemporary Australian building practice.

The test ran over a period of several months in 2007. There was no heating or cooling energy supplied during this time and so the internal temperatures of each building were free to vary as needed. This is referred to as being in a free-running mode. Measurements of the inside of the test building and the surrounding weather were recorded during this time. A thermal simulation was then run using the AccuRate program. In addition to the standard AccuRate inputs, the simulation used many non-standard inputs to best match the exact design and construction of the test building and weather conditions it was subjected to. AccuRate was altered to essentially ignore the thermal comfort level bands and thus mimic the free-running state. AccuRate was also supplied the actual on-site measured weather data and so it bypassed using the RMY data, to eliminate the effect of differences between actual and reference climate data. Other modifications were made as well (Dewsbury 2011). Thus, the cause of any differences between measured and simulated data could best be attributed to calculations in the simulation engine.

As AccuRate was altered to run in free-running mode, no star rating was output. The research instead focused on temperature, as temperature drives the space conditioning load and therefore is strongly linked to space conditioning energy usage. For each building the AccuRate program output the room's temperature by the hour over the entire duration of the test. This simulated temperature was then compared to the measured temperature and an analysis between the two data sets was performed. For each building, the simulated temperature for each room was consistently different from the measured temperature in that room (Dewsbury 2011). For the building with an enclosed subfloor, the room temperature residuals (the difference between the measured and simulated value at any given time step) displayed a positive linear relationship and strong correlation with the subfloor temperature residuals, indicating that the simulation error in these two

zones was likely linked (Dewsbury 2011). In both the room and subfloor, the software was consistently under-predicting the temperatures.

In the building with the exposed subfloor, statistical analysis of the data indicated that the relationship between the room and subfloor values be further reviewed. In the slab-on-ground building, the room residuals were similar to that of the enclosed-subfloor building. This and additional analysis considering all three buildings again indicated that the error in the room residuals were due to errors in the subfloor or ground model. The research eliminated numerous sources of error by accounting for thermal bridging due to non-standard framing factors and measured air ventilation rates (Dewsbury 2011).

The research recommends that before any development be made to the AccuRate room model, improvements are first required for the roof space, subfloor and ground models (Dewsbury 2011). The research concludes that an urgent assessment of the measured ground temperature under buildings and the further development of the subfloor model in AccuRate are needed, and that these two investigations are top priorities when rated on their certainty of effect on simulation and perceived importance based on current construction requirements.

The Launceston research program similarly recommends that AccuRate's subfloor model be reviewed as a priority (Geard 2011). Thus, a review of the subfloor space encompassing both the theoretical modelling and experimental data is needed.

2.3 Subfloor construction

The term subfloor, or crawl space, refers to the air space underneath the floor in a platform-floor, also known as a suspended floor, building. The subfloor volume is usually bound by the ground below and the floor above. It is not common building practice in Australia to cover the ground with a membrane. Floor insulation was only mandated within the last several years (BCA 2011). Therefore, when considering existing buildings, the subfloor space is often in contact directly with the bare ground below and flooring above.

The space may be unenclosed on the sides, in which case outside air is generally free to pass through. This is often the case when the building is clad with a lightweight material. Alternatively the space may be enclosed, in which case a subfloor wall is present which greatly limits the amount of air which can flow through the subfloor.

2.3.1 Construction requirements

Acceptable construction practices for subfloor framing of residential buildings are regulated in Volume 2 Part 3.4.1 of the BCA (BCA 2011). Here it is stipulated that the subfloor must be cleared of all building debris and vegetation. It is also mandated that enclosed subfloors must provide for

ventilation by means of openings in the subfloor perimeter wall. These openings allow natural ventilation, air movement driven by wind and temperature differences, to occur. The term ‘enclosed subfloor’ indicates that the perimeter of the subfloor wall is broken only by these required openings.

These perimeter wall openings must be evenly spaced and placed not more than 600 mm in from the corners to ensure that no stagnant air spaces occur within the subfloor (BCA 2011). It is common practice to install a screen or vent in the opening to limit vermin from accessing the subfloor. The openings are therefore referred to as the subfloor vents, and the area of these openings is referred to as the ventilation area or vent area. If the vents are blocked by other constructions such as patios or paving, then additional vents must be provided to yield an equivalent amount of ventilation area. Internal subfloor walls are also regulated to allow for adequate ventilation and to reduce the occurrence of stagnant air spaces. They must have an unobstructed ventilation area equal to that required of the adjacent external walls, and these vents must also be evenly distributed throughout the wall.

A barrier must be installed between the subfloor cavity and wall cavity to limit any air movement between the two zones (BCA 2011). When such a barrier is present the junction is referred to as being obstructed. One of the effects of this barrier is that air is restricted to entering and exiting the subfloor only through the vents in the subfloor perimeter wall.

The height of the subfloor space is also regulated, depending on whether or not the building occurs in a termite inspection area. The requirements for minimum subfloor ventilation area per length of wall and minimum height of floor above ground surface are summarized in Table 2.1, taken from Table 3.4.1.2 in the BCA (BCA 2011).

Table 2.1: Subfloor ventilation and clearance (BCA 2011)

CLIMATE ZONE (see Figure 3.4.1.2)	Minimum sub-floor ventilation (mm ² /m of wall)		Minimum height from ground surface (mm)	
	No membrane	Ground sealed with impervious membrane	Termite inspection not required	Termite inspection required (see note)
1	2000	1000	150	400
2	4000	2000	150	400
3	6000	3000	150	400
Note: On sloping sites, 400 mm clearance may be reduced to 150 mm within 2 m of external wall/s in accordance with Figure 3.4.1 Diagram b .				

The climate zones referred to in Table 2.1 are defined in Figure 2.1 , taken from Figure 3.4.1.2 from the BCA (BCA 2011), where Climate Zones A, B and C are equivalent to 1, 2 and 3, respectively.

The climate zones indicated in Figure 2.1 are defined by their typical outdoor relative humidity as measured at 9am and 3pm in January and July. Nearly all of coastal Australia and the entire state of Tasmania lie in the highest humidity area of Climate Zone 3.

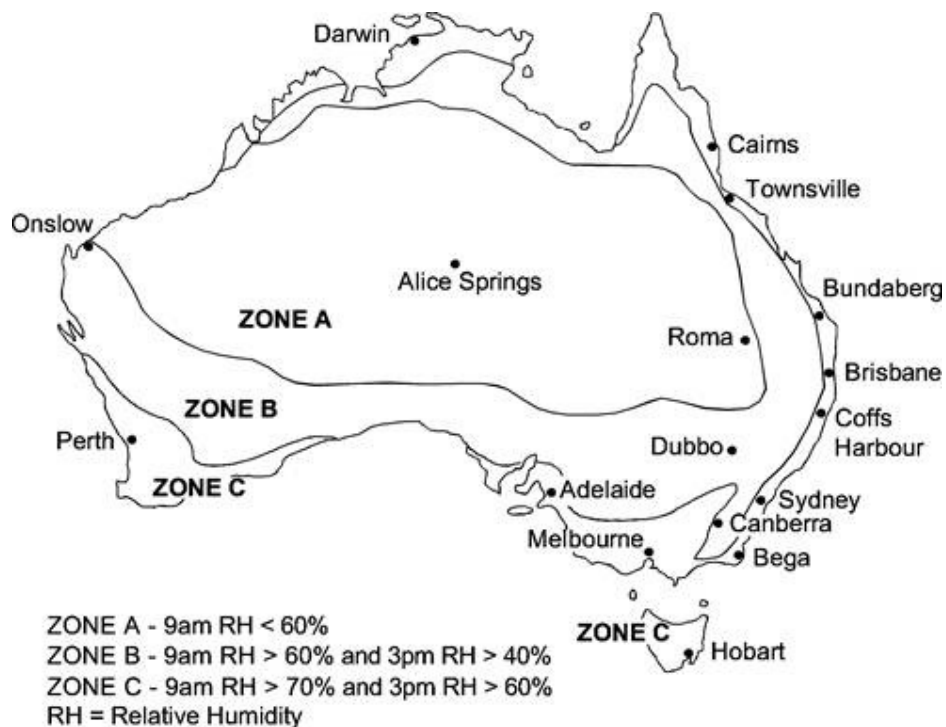


Figure 2.1: Climate zones based on relative humidity (BCA 2011)

As shown in Table 2.1, as the outdoor relative humidity of a building's location increases so too does the amount of subfloor ventilation required. In the event that the ground or subfloor area is damp or subjected to frequent flooding, the required subfloor ventilation area as defined in Table 2.1 increases by 50% and a sealed ground cover impervious to moisture must be installed.

2.3.2 Origin of the construction requirements

Much of the design of the subfloor is driven by the desire to allow for adequate ventilation throughout the space. The BCA in Volume 2 Part 3.1.3.5 states that "in suspended floor areas it is important that termite activity is not encouraged by inadequate subfloor ventilation ... Air flow is critical. Air flow will not only restrict the growth of fungus which attacks subfloor members (which makes them more susceptible to termite attack), but also creates a climatic atmosphere less conducive to termite activity (BCA 2011)." The BCA mandates the ventilation in an effort to prolong the life of the subfloor materials. This claim is confirmed in research (Williamson and Delsante 2006b) which explores the origins of the subfloor ventilation requirements.

The BCA's ventilation requirements are traced back to research performed at CSIRO and published by I. S. Cole in 1997, which defined how much ventilation area was needed to control a subfloor's humidity. The requirement was that subfloor relative humidity should be kept below 80%. Field measured data formed the basis of that work (Williamson and Delsante 2006b).

The prediction for subfloor humidity was based on subfloor ventilation, ground moisture evaporation and outdoor humidity (Williamson and Delsante 2006b). It is not known what assumptions were made about the conditioning of the room space above, and if these conditions affected the subfloor model. The subfloor ventilation model predicted the rate of subfloor ventilation as a function of vent area and outdoor wind speed. That model originated with P. J. Walsh at CSIRO in 1975 (Williamson and Delsante 2006b). The ground moisture evaporation model stemmed from ground moisture research (Abbott 1983) from the Building Research Association of New Zealand (BRANZ). By fusing the ventilation and ground evaporation models together, ventilation areas were proposed that would ensure that the subfloor humidity would stay within an acceptable limit. Subfloor ventilation area requirements were defined as a function of outdoor humidity, as the zone demarcations in Table 2.1 indicate.

Various components of the subfloor ventilation requirements have been assessed in the literature. The environmental conditions needed for mould growth to occur have been investigated. In addition to high humidity other conditions are required for mould growth to occur, such as a minimum air temperature limit or a criterion for minimum time spent at high humidity (Williamson and Delsante 2006b). One study from a Nordic climate states that the relative humidity must remain above 80% over a period of several months for mould growth to occur (Samuelson 1994). An assessment of 17 houses in New Jersey, USA, showed that humidity alone did not correctly predict the moisture content of the joists and it was suggested that wet or dry bulb temperatures be considered as predictors as well (Stiles and Custer 1994). A study of 121 homes in the northwest USA, including a mix of both older homes and newer homes, found that regardless of the subfloor humidity the only instances where wood decay was observed in the subfloor occurred only where plumbing leaks existed or where the wood was in direct contact with the ground (Tsongas 1994). It would therefore appear conservative to base the ventilation design criteria on subfloor humidity alone.

The model for ground moisture evaporation has also been investigated (Williamson and Delsante 2006b). The model originates from a New Zealand field study where it was determined through experimental field work that the rate of moisture evaporation from the ground beneath a suspended floor was a linear function of the difference between the saturation pressure of air at the ground temperature and the vapour pressure of the subfloor cavity air (Abbott 1983). It is important to note that when dealing with psychrometry, the study of gas-vapour mixtures, a strict definition of 'air' must be observed. In this context and throughout this work, air refers to atmospheric air, which is a mixture consisting of both dry air and water vapour, also known as moisture. Moisture may also refer to water in the liquid state.

That linear function, after allowing for a change in nomenclature from original form and conversion to SI units, becomes (Williamson and Delsante 2006b):

$$\dot{m}_{evap} = 1.111 \times 10^{-5} \times (p_{sat_g} - p_{v_sf}) \quad 2.1$$

where \dot{m}_{evap} is the rate of ground moisture evaporation [kg/(m²*sec)]; p_{sat_g} is the saturation pressure of air at ground temperature [kPa]; and p_{v_sf} is the vapour pressure of the subfloor cavity air [kPa]. Thus, the rate of ground moisture evaporation is a function of the ground surface temperature in the subfloor and the subfloor air temperature and humidity.

Further manipulation of the ground moisture evaporation model of Equation 2.1 and a comparison to the 1997 work done at CSIRO indicate that the two models are off by a factor of approximately 100, in the directed of the 1997 CSIRO work under-predicting the evaporation. A detailed mathematical account of the equations in question is provided elsewhere (Williamson and Delsante 2006b), which indicates that the error is likely in the CSIRO work.

Thus, is it noted that the foundation on which the BCA bases its subfloor ventilation requirements quite possibly under-predicts the amount of ground evaporation. This raises the issue of whether or not subfloors designed to these ventilation requirements actually conform to the original intent of maintaining acceptable humidity levels. Though it is not known how this inconsistency affects the subfloor thermal performance model, it is known that the predicted humidity does not drive the building regulations to the extent that predicted temperature does. Thus, attention is redirected to the thermal performance of the subfloor rather than its moisture performance.

2.4 Modeling of subfloor thermal performance

As was discovered in the UTAS research (Dewsbury 2011), errors in the thermal performance modelling of a building's subfloor very likely drive the errors in the thermal performance of the building as a whole. This therefore calls for an investigation into AccuRate's subfloor modelling. However, the detailed calculations from AccuRate's simulation engine are not publicly available. As a result, an assumption is made that AccuRate's subfloor model follows the general principles used in other subfloor models. This can be substantiated on occasion, as AccuRate's authors or current owners have released pertinent information regarding the subfloor modelling via published works and personal communication.

What first must be investigated is how the subfloor interacts with the room above. AccuRate treats the subfloor space as a zone and models the heat flow between the internal zones of the building and the subfloor zone (Delsante 2005). Heat flow is driven by a difference in temperature and is impeded by thermal resistance. Hence the temperatures in each zone, the heat transfer between adjacent zones and the thermal resistance between adjacent zones are all crucially linked and must

be modelled in unison. An examination of the interaction between subfloor zone temperatures and subfloor heat transfer processes in subfloor models is presented in Section 2.4.1. Further exploration into the thermal resistance of suspended floors is presented here.

A recent study (Williamson and Delsante 2006a) provides a summary of the modelling of the thermal resistance, commonly referred to as the R-value, of suspended floor systems from the International Standards Organization's (ISO) 13370 "Thermal performance of buildings – Heat transfer via the ground – Calculation methods" and the Chartered Institution of Building Services Engineers (CIBSE) Environmental Design Guide A - 1998. The ISO 13370 model is based on the CIBSE methodology.

The ISO 13370 method to calculate the thermal resistance of a suspended floor system is represented by Equation 6 in ISO 13370 (Williamson and Delsante 2006a). The equation is stated in terms of thermal transmittance, the inverse of thermal resistance, in the following equation:

$$\frac{1}{U} = \frac{1}{U_f} + \frac{1}{U_g + U_x} \quad 2.2$$

where U is the overall thermal transmittance of the suspended floor system [$\text{m}^2\text{K}/\text{W}$]; U_f is the thermal transmittance of the suspended part of the floor, including the effect of any thermal bridging [$\text{m}^2\text{K}/\text{W}$]; U_g is the thermal transmittance for heat flow through the ground [$\text{m}^2\text{K}/\text{W}$]; and U_x is an equivalent thermal transmittance between the subfloor space and the outside accounting for heat flow through the walls of the subfloor space and by ventilation of the subfloor space [$\text{m}^2\text{K}/\text{W}$].

The thermal transmittance term U is the crucial link between the subfloor thermal performance and the interior thermal performance. Therefore it is important to understand its constituents. U_f is a function of material properties, dimensions and construction details. U_g considers heat flow into the ground to and from the subfloor cavity. This model is complex. The ground is modelled as a semi-infinite solid providing resistance between indoor and outdoor temperatures, having a distributed capacitance. It consists of a separate steady state and transient component, as the cyclic nature of the ground temperature fluctuation is significant (Delsante 1997).

U_x represents the generally horizontal component of heat flow to and from the subfloor cavity directly through the walls and through the ventilation openings within the walls. U_x is defined by Equation 9 of ISO 13370 (Williamson and Delsante 2006a) as the sum of two terms, one representing the heat flow through the walls and the other representing the ventilation component of the heat transfer.

Thus, as can be inferred from Equation 2.2, understanding the thermal resistance of a suspended floor system requires not only knowledge of the floor itself, but also knowledge of the heat flow into the ground, through the subfloor walls and through the subfloor vents. Of these three, subfloor ventilation modelling is further explored in Section 2.4.2.

2.4.1 Subfloor climate model

The AccuRate subfloor zone is comprised of three other zones (Delsante 2005). One represents the subfloor air; one represents the underside surface of the floor system at the top of the subfloor cavity; and the last represents the surface at the top of the subfloor floor.

A similar model has been described in research from Finland (Kurnitski and Matilainen 2000). The model represents a subfloor with the junction between the subfloor and wall cavity obstructed. The model is summarized in Figure 2.2 which represents the heat and moisture flows throughout the subfloor cavity.

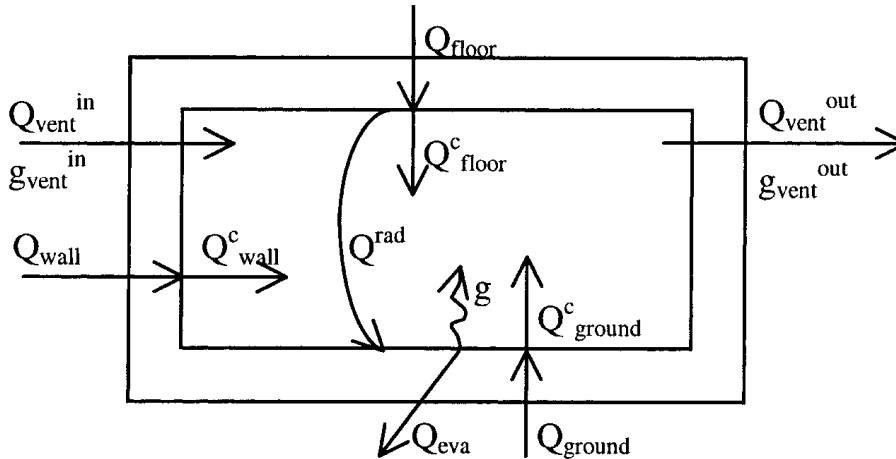


Figure 2.2: Subfloor cavity heat (Q) and moisture (g) flows (Kurnitski and Matilainen 2000)

The inner rectangle in Figure 2.2 represents the inside surface bounding the subfloor cavity. The straight and long-curved arrows represent energy flows and the jagged arrow represents moisture flow. The superscript 'c' marks convection.

The study then considers the subfloor air zone and then provides the following energy balance (Kurnitski and Matilainen 2000) over this zone:

$$C \frac{\partial T_{air}}{\partial t} = Q_{floor}^c + Q_{ground}^c + Q_{wall}^c + Q_{vent}^{in} - Q_{vent}^{out} \quad 2.3$$

where C is the heat capacity of the air [J/K]; T_{air} is the air temperature in the subfloor [K];

Q_{floor}^c , Q_{ground}^c and Q_{wall}^c are rates of convective heat transfer between the subfloor air and the floor, ground and wall [W]; and Q_{vent}^{in} and Q_{vent}^{out} are the rates of heat flux in and out of the subfloor cavity due to subfloor ventilation [W].

The left hand side of Equation 2.3 represents the energy being stored in the air as an increase in temperature and equates this to the sum of heat flows convected between the air and the surrounding surfaces, plus the net incoming energy transfer via the vents. The convection terms are each a function of the surface temperature, air temperature, the area of the surface and a convective heat transfer coefficient (Kurnitski and Matilainen 2000). In the AccuRate software it is known that each convective heat transfer coefficient is itself a function of surface temperature, air temperature, direction of heat flow and the air speed over the surface. The air speed over the surface is a function of the ventilation rate in the subfloor space and the surface area. This calculation is known to be an area of great uncertainty (Delsante 2005). Explicit definitions for Q_{vent}^{in} and Q_{vent}^{out} are not provided (Kurnitski and Matilainen 2000) but it is straightforward to calculate that they, too, are a function of subfloor ventilation rate.

Equation 2.3 mostly matches the graphic provided in Figure 2.2, with the exception of the heat of evaporation term, Q_{eva} , which is present in the figure but omitted from the equation. The term Q_{eva} is defined as the product of g , the rate of moisture evaporation from the ground [kg/s], and latent heat of vaporization, which is assumed to be a constant value of 2.5×10^6 J/kg (Kurnitski and Matilainen 2000). Thus Q_{eva} has units of Watts. It is stated in a separate publication (Kurnitski 2000, page 20) that this evaporation term should be included in the subfloor air energy balance “if evaporation is remarkable.” Therefore it appears that Q_{eva} is omitted from Equation 2.3 due to an assumption of its insignificant value in comparison to the other terms. It is known that the Q_{eva} term is omitted from the subfloor air energy balance in the Accurate model as well (Chen 2010).

One known difference in the subfloor air zone modelling between AccuRate and the model summarized in Equation 2.3 is that AccuRate does not consider convection between the subfloor walls and the subfloor air (Delsante 2005). In the AccuRate model the internal surface of the walls are coupled directly to the subfloor air. The subfloor air therefore exchanges heat via convection with only two surfaces, the ground and the floor, in the AccuRate model.

It is noted that the model of Equation 2.3 (Kurnitski and Matilainen 2000) does not consider the energy stored in the air as a change in moisture. The left hand side of Equation 2.3 only considers the enthalpy stored in the dry air as a change in temperature, as enthalpy for dry air is the product of the heat capacity of the air and its temperature. Nowhere in the equation is there representation for the enthalpy stored in the air as a change in moisture. It is not known whether this omission is accidental or whether the enthalpy due to change in moisture was assumed insignificant.

The study from Finland then considers the ground surface zone (Kurnitski and Matilainen 2000) and provides the following energy balance:

$$Q_{ground} = Q_{ground}^c - Q^{rad} + Q_{eva} \quad 2.4$$

where Q_{ground} is the heat flux conducted to the ground surface from the subground [W] and Q^{rad} is the heat flux radiated between the ground surface and the underside of the floor [W]. Q^{rad} is defined to be a function of the emissivities and temperatures of the ground surface and under-floor surfaces only. Thus, the model assumes that the only surfaces in the subfloor that radiate heat are the ground and floor.

The AccuRate program is known to model the ground surface zone radiation similarly. The surfaces bounding the top and bottom of the subfloor are modelled as parallel plates with a view factor of one (Delsante 2005). As far as radiation is concerned they essentially only see each other, and the walls do not participate in the radiative heat exchange.

The research from Finland also provides a mass balance over the subfloor air cavity (Kurnitski and Matilainen 2000). As there are two components of air, there are two possible mass balances which could be provided. The following mass balance for water is provided:

$$V \frac{\partial v_{air}}{\partial t} = g_{vent}^{in} + g - g_{vent}^{out} \quad 2.5$$

where V is the volume of the subfloor [m³]; ∂v_{air} is the absolute humidity of the subfloor air [kg moisture/m³]; and g_{vent}^{in} and g_{vent}^{out} are the moisture flows entering and exiting the subfloor via the vents [kg/s].

The left hand side of Equation 2.5 represents the amount of moisture being stored in the subfloor air. This is equated to the sum of the net moisture brought into the subfloor via the subfloor vents plus the amount of moisture entering the subfloor air space via evaporation from the ground. It is not known what moisture modelling, if any, is performed by the AccuRate program.

The subfloor vents may actually have the net effect of introducing moisture into the subfloor, represented by a positive value of $g_{vent}^{in} - g_{vent}^{out}$. This is especially possible in the summer months when the outdoor air is relatively warm and has a high capacity for holding moisture.

The term g represents the rate of ground moisture evaporation. Water evaporates when saturated air at the water's temperature has a vapour pressure exceeding the vapour pressure of the surrounding air. This association is demonstrated by the two pressure terms in the evaporation prediction in Equation 2.1. In the case of subfloors, moisture is not evaporating from a free pool of water but from soil. The implications of this difference must be considered.

Experiments have shown that when a soil's moisture content exceeds a critical value, which varies by soil type, the equilibrium relative humidity of the soil is near 100 percent (Abbott 1983). In these conditions the apparent vapour pressure is independent of soil type and the evaporation behaviour for the soil is essentially identical to that of free water. In this case, evaporation is considered to occur at the ground surface.

However for soils with moisture content below that critical value the equivalent relative humidity of the soil has been shown to strongly depend on soil type (Abbott 1983). In these conditions the vapour pressure and hence evaporation properties cannot be predicted without detailed knowledge of the soil type. In this case, a significant amount of evaporation takes place beneath the soil surface, from perhaps as far as half a metre down, and diffuses to the surface (Trethowen 1988).

The evaporation term g links the moisture mass balance from Equation 2.5 to the evaporation energy term Q_{eva} used in the energy balances of Equations 2.3 and 2.4. These energy balances represent several methods of heat transfer, all of which are driven by temperature differences. This indicates that the thermal performance and moisture characteristics of the subfloor space are fundamentally related and must be examined in unison.

2.4.2 Subfloor ventilation model

Subfloor ventilation affects the subfloor climate model and the thermal resistance of the subfloor, and thus it also warrants investigation.

The ventilation model used in AccuRate (Delsante 2007) is the sum of two components: the stack component, which represents the buoyancy effect caused by the air temperature difference between the subfloor and outdoors, and the wind component, which is caused by the wind pressure on the outside face of the building at the location of the subfloor vents. Each component is a function of both weather and building geometry.

The presence of a barrier between the subfloor and wall cavity restricts the entry and exit of the subfloor air to the subfloor vents. When there is no barrier present the flow path of air is known to be complex. It is well documented that air from the subfloor travels up the wall and mixes with the roof cavity air (Bassett 1988, Rose 1994). A subfloor with an unobstructed junction would therefore have a relatively more influential stack component of ventilation than a subfloor with an obstructed junction would have.

The subfloor ventilation equation that AccuRate uses for a detached building with an obstructed wall cavity junction (Delsante 2007) is as follows, after being adjusted for nomenclature and unit consistency:

$$\bar{V} = \frac{aP}{A_f L_{sf}} (A_1 + B_1 \times f_1 \times v_{met}) \quad 2.6$$

where \bar{V} is the subfloor ventilation rate in air changes per hour [ACH]; a is the area of subfloor ventilation openings per length of subfloor wall perimeter [m²/m]; P is the subfloor wall perimeter [m]; A_f is the subfloor ground surface area [m²]; L_{sf} is the height of the subfloor space [m]; A_1 is a constant value of 96.12 m/hr; B_1 is a constant value of 304.6 s/hr; f_1 is a wind shielding factor [unity]; and v_{met} is the meteorological wind speed [m/s] at a height above ground level of 10 m. Note that a is often considered in units of mm²/m and thus the equation may

require a conversion factor of $\frac{1m^2}{10^6 mm^2}$ to be applied.

AccuRate's subfloor ventilation model is a linear function of wind speed. The terms a , P , A_f , and L_{sf} of Equation 2.6 are all building geometry parameters and thus constant in time. The wind shielding factor, f_1 , is a function of the building site's exposure and thus also constant. Its value depends on whether the site exposure is classified as exposed, open, suburban or protected. The meteorological wind speed, v_{met} , is the wind speed as measured at a height of 10m and is sometimes referred to as the airport wind speed (Williamson and Delsante 2006b). It is measured in an area of flat terrain and no local flow obstruction.

The first component of Equation 2.6, the term that includes the constant A_1 , is the stack component. The basis for AccuRate's stack component originates from a model which references British Standard 5925, "Code of practice for ventilation principles and designing for natural ventilation", and is a function of several building geometry constants and the outdoor and subfloor air temperatures (Delsante 2007). Thus it is a function of time and can also vary from building to building. However, since the ventilation rate of a subfloor with an obstructed wall cavity junction

should have very little temperature dependence, a constant value for stack component is used in AccuRate.

The wind component of Equation 2.6 is a linear function of meteorological wind speed. The constant term, B_1 , takes into account an assumed pressure coefficient near the subfloor vent location, dependence of that pressure coefficient with angle, a discharge coefficient and an assumed vent blocked factor (Delsante 2007). Wind direction is not taken into account. Note, however, that elsewhere it is suggested that a vent effectiveness factor depending on wind direction be included in the wind component of ventilation. The recommended value is a scalar of 0.5 to 0.6 for winds perpendicular to the inlet vent and 0.25 to 0.35 for diagonal winds (American Society of Heating, Refrigerating and Air-Conditioning Engineers, or ASHRAE 2005). AccuRate uses a constant value for discharge coefficient of 0.6.

The wind component used in AccuRate is similar to the ISO 13370 wind component of ventilation for naturally ventilated subfloor spaces. The ISO13370 wind ventilation model was recently revisited (Williamson and Delsante 2006a) and its wind shielding factor was traced back to an infiltration model developed in the 1970s and 1980s by Max Sherman at Lawrence Berkeley Labs (LBL, or LBNL) in the USA. However when starting fresh and applying the LBL model to subfloor space three shortcomings were found and as a result new wind shielding factors are recommended (Williamson and Delsante 2006a). These new factors have not been incorporated in AccuRate.

2.5 Experimental support of subfloor modeling theory

Though several research works have been published in the last several years regarding subfloor modelling, most of the focus has been theoretical. There are few experimental studies to support the theory relevant to current Australian subfloor building practices.

2.5.1 Subfloor ventilation experimentation

One informative study from the University of South Australia (UniSA) presents measured subfloor ventilation data and compares it to the theoretical ventilation predicted by the EnCom2 building thermal performance program (Olweny et al. 1998). The study considered two private and occupied houses in the Melbourne, Victoria area throughout 1997. One house was weatherboard clad and the other house was brick veneer. The weatherboard house had much a larger subfloor ventilation area ($97,600 \text{ mm}^2/\text{m}$) than the brick house had ($3,300 \text{ mm}^2/\text{m}$). The weatherboard house was assumed to have minimal airflow between the subfloor and wall cavity, whereas the brick house was known to have no obstruction between the two spaces.

Passive tracer gas ventilation testing was performed on both houses. Although the test ran over a period of several months, only five subfloor ventilation data points per house were obtained due to the nature of passive tracer gas testing. Measured data show that the weatherboard house had an average subfloor ventilation rate 2 to 3 times that of the brick house (Olweny et al. 1998). The weatherboard house had a peak ventilation rate of 86 ACH while the brick house subfloor ventilation rate always averaged below 25 ACH. When fitted to a linear function of wind speed, the data for each house had high variation, although each showed a good match to prediction. For the brick house the ventilation area used in the theoretical ventilation equation was expanded to include the wall cavity cross-sectional area, as this was a probable flow path for the subfloor air. The weatherboard house data had an R^2 (coefficient of determination, or square of the correlation coefficient) of 0.45. The low value does not indicate great confidence in the linear model, though a low R^2 often is the result of a low number of data points.

The difference in construction between these houses and houses built to current Australian practice is not trivial. The weatherboard house had an obstructed junction between the subfloor and wall cavity but the area of subfloor ventilation was about 20 times the BCA requirement. The brick house had subfloor wall ventilation openings similar to current Australian standard but due to the unobstructed junction the stack effect was likely more significant than in current practice. However, since the blocking of the junction between the subfloor and wall cavity is a relatively new requirement in subfloor construction, most experimental subfloor ventilation studies use buildings with an unobstructed junction. Still, it is worth considering these studies for any other insight into ventilation that they may provide.

One British study (Edwards, Hartless, and Gaze 1990) analysed 56 subfloor ventilation data points and compared them to theory. There was no mention of a blocked junction between the subfloor and wall cavity, but due to the publication year it can be assumed that it was unobstructed. The house used in this research was semi-detached with subfloor ventilation provided by vents on only two sides of the house. The ventilation area of 985 mm²/m is similar to current Australian practice. The 14 data points were measured at a time when the wind was blowing onto the vents, ranging in wind speeds up to 4 m/s and resulting in ventilation up to 2 ACH. The study found that the ventilation rate is linearly related to wind speed.

Another British study considered a test house in Garston, Watford (Hartless and White 1994) and analysed measured subfloor ventilation data. In this study the test house had a floor area of 42 m², a subfloor height of 0.22 m and subfloor ventilation area of 1,230 mm²/m. The floor was not soil but a concrete oversite which was suspended over the bare ground. The subfloor had one wall running through it and the wall cavity junction was unobstructed. Windspeed was measured from 15 m high mast. Ventilation was measured via tracer gas test using sulphur hexafluoride (SF₆) and

ranged from 3 to 13 ACH (Hartless and White 1994). The data from this study were later re-examined. It was found that the subfloor ventilation was stack dominated when the difference between subfloor and outdoor temperature was over 6 °C and that wind only became a significant influence when it was above 3.5 m/s (Hartless 1996).

The subfloor and wall cavity junction of this test house was later blocked (Hartless 1996) and subfloor ventilation was again measured using the tracer gas method with SF₆. Two months of data were recorded. The researchers compared the measured ventilation to a temperature-corrected wind speed, defined as the ratio of wind speed to the difference between subfloor and outdoor temperature. The ventilation was stack dominated only when the temperature-corrected wind speed ratio was less than or equal to 0.7. The ventilation was wind dominated when the temperature-corrected wind speed ratio was equal or greater to 11.

It is interesting that in this test house the stack effect was significant even with a blocked wall cavity junction, as this would have reduced the vertical path available for any warm buoyant air to rise through. This suggests that leaks in the floor may have provided an alternate flow path, or that the wind speed effect may have been reduced due to sheltering in the vent vicinity (Hartless 1996). It is, however, notable that the stack component of ventilation did play a major role in a building with an obstructed wall cavity junction.

Another study provides a qualitative assessment of subfloor ventilation, investigating the pattern of airflow throughout a subfloor cavity in a laboratory setting (Harris and Dudek 1994). The test chamber had a 3 m by 3 m suspended floor with a subfloor height of 0.5 m. Air was mechanically forced by fan into the subfloor perpendicular to the wall through ventilation openings yielding an equivalent area of 1500 mm²/m. Glass panels formed the floor of the test chamber and smoke was injected into the air stream so that the air movement pattern could be identified in plan view.

Different vent configurations were tested. The inlet vents were varied from one near the corner, to one inlet vent near the centre of the wall, to two vents each near a corner on the same wall. For each inlet vent configuration, different outlet vent configurations were also tested: one vent on the side wall or one vent on the opposite wall near the closer corner, middle of the wall, or near the farther corner. All combinations of inlet and outlet vent configurations yielded thorough mixing of the subfloor air. But the airflow pattern changed depending on the configuration of only the inlet vents (Harris and Dudek 1994). The pattern was not affected by the positioning of the outlet vents. This finding supports the idea that only the windward vents need be considered when quantifying ventilation or assessing the impact of wind direction angle.

2.5.2 Subfloor climate experimentation

There are also experimental research publications that investigate the relationship between subfloor ventilation, ground moisture evaporation and subfloor humidity, and the effects that these processes have on various temperatures.

The UniSA study, in addition to assessing subfloor ventilation in two Melbourne houses as described in Section 2.5.1, also provided monthly averages of key climate parameters (Olweny et al. 1998). The two houses had nearly identical subfloor air temperatures except for during the summer months of January and February when the weatherboard house temperature (the house with the greater subfloor ventilation) were 1-2 °C higher. Both subfloors had similar ground surface temperatures except for during February, at the end of summer, when the weatherboard house values were higher. In both subfloors the ground surface temperatures had the same annual trend as the subfloor air temperatures, though the ground surface temperatures were consistently several degrees lower.

Both houses had a subfloor relative humidity that varied less than the outdoor relative humidity. Like the outdoors, both houses had a relative humidity that peaked in the cooler months of May through September. Throughout the entire year the weatherboard house had a noticeably lower subfloor relative humidity and lower soil moisture content than the brick house had. The soil moisture content of the weatherboard house varied throughout the year and was highest in summer, lowest in the late autumn and early winter, while that of the brick house remained relatively constant. Both houses had a similar soil type. An assessment of ground moisture evaporation was not reported (Olweny et al. 1998). Although there may be other unidentified differences between the two houses and sites, the data suggest that the higher ventilation rate has driven a higher rate of ground moisture evaporation but that this has still resulted in lower subfloor humidity.

This finding was duplicated in the investigation into the subfloor conditions under an apartment building in Finland (Kurnitski 2000). In this study the natural subfloor ventilation rate had a positive correlation with ground moisture evaporation rate and a negative correlation with relative humidity. The subfloor ventilation ranged from 0.25 to 2.5 ACH. Each of these linear correlations had an R^2 of 0.4 based on a sample size of approximately two hundred data points. A separate study, which possibly used the same data set and building, reports the findings when mechanical subfloor ventilation was intentionally varied (Kurnitski and Matilainen 2000). This data also showed that eliminating subfloor ventilation brought about a nearly saturated air state.

The similarity between subfloor air temperature and ground surface temperature found in the UniSA study (Olweny et al. 1998) has also been observed in other studies. It was found that the

ground surface temperature under the Finland building was nearly identical to the subfloor air temperature with a difference never exceeding 2 °C (Kurnitski 2000). In the study of the Watford, UK, building with the obstructed wall cavity junction, it is also reported that the subfloor air temperature correlated quite well with the concrete oversite temperature (Hartless 1996).

It is interesting to note that these trends exist amongst buildings in different locations and with differing construction. The Finland study was performed using a multi-storey apartment building and the subfloor ground was not level with the outside, but rather it was dug into the ground. The subfloor floor sat approximately 1 m under ground level and the subfloor height was 0.9 m (Kurnitski 2000). However, none of these studies have shown the resulting quantification and comparison of energy flows throughout the subfloor.

What has been reported are measurements of the mass flows in subfloors, particularly the mass flow rate of water evaporation from the ground. This corresponds to the g term from Figure 2.2 and Equation 2.5. Research from New Zealand reports on a comprehensive survey involving 60 subfloors from houses in the cool temperate climates of Auckland, Wellington and Christchurch (Trethowen 1998). Lysimeters were used to measure the ground moisture evaporation directly. Subfloor ventilation was not measured but half of the houses had more than 3500 mm²/m of vent area. One house in Wellington averaged as high as 111 g/m² per hour in the summer, averaging 85 g/m² per hour throughout the year. The corresponding subfloor ventilation area for this house is not known.

When combining the data from the 1998 study (Trethowen 1998) and the 1983 study of Auckland subfloors (Abbott 1983), the average evaporation rate amongst all of the houses was 17 g/m² per hour (Trethowen 1994). This average is much lower than the evaporation rate that the Wellington house encountered, and large variation amongst the data was noted. A separate assessment of the 1983 data (Abbott 1983) finds that even apparently dry soil was evaporating approximately 10 g/m² per hour (Bassett 1988).

These values are higher than what was calculated for the Finland apartment building. In the Finland study, the evaporation rate was not directly measured but instead calculated as a function of the measured moisture content of the air and the subfloor ventilation rate, a relationship which can be deduced from Equation 2.5. The evaporation rate was found to be less than 8 g/m² per hour in cases where the subfloor ventilation rate ranged from 0.25 to 2.5 ACH (Kurnitski 2000). This is at the low end of the range of values found in the New Zealand buildings (Trethowen 1998). As stated earlier in this section, the Finland study did find a correlation between subfloor ventilation rate and ground moisture evaporation rate (Kurnitski 2000). The lower evaporation rate could then be justified by assuming that the Finland building had a ventilation rate at the lower end of the

range that the New Zealand houses had, or that the ground and climate conditions were significantly different.

However, it was found that when considering data from all 60 New Zealand houses that the ground moisture evaporation rate showed no clear correlation with either the subfloor vent area or the soil moisture content (Trethowen 1994). This supports the prevalent idea that the relationship between subfloor ventilation, subfloor humidity and ground moisture evaporation is very site dependent.

It is also worthwhile to quantify and compare the sources of moisture entering the subfloor. Moisture enters subfloor air either by evaporation from the ground or by direct transport via the subfloor vents (Equation 2.5). Research on a test house in Devon, UK, addressed this in a semi-detached house with the three exposed subfloor walls providing subfloor ventilation rates up to 18 ACH. The subfloor was open to bare ground with a ground surface area of 5 m by 8 m and a subfloor height of 0.35 m. The subfloor had internal walls which split the space into four zones. It was found that the vent contribution to subfloor moisture was an order of magnitude greater than the evaporation contribution (Hartless and Llewellyn 1999). There are no other known measured data for comparison with this ratio.

2.6 Conclusion

The drive towards energy efficient housing in Australia has brought attention to the building thermal performance simulation program, AccuRate. Recent experimental work indicates that the subfloor modelling in AccuRate could be improved and that the ground temperatures underneath a building need more investigation. This has in turn prompted a review of the subfloor climate.

Fundamental theory shows that the air movement, moisture movement and heat transfer processes in the subfloor are highly linked and very likely these relationships are site specific. Some thorough and enlightening experimental research work has been performed in a variety of different climates to substantiate different elements of the theory. Subfloor ventilation has been quantified in several separate studies but very few data points exist from a subfloor design representative of current Australian building practice. Ground moisture evaporation from subfloors has been quantified but most of the data has wide variations which cannot easily be correlated to other subfloor processes. The remaining data span a very limited range of ventilation rates. Several studies present experimentally obtained temperatures and humidities and compare these to each other. However, no study has been found that links such data to their associated energy transfer processes.

Thus, results from prior experimental studies are not immediately applicable for comparison with the modelling theory relevant to current Australian subfloor design. The predicted models for

subfloor air movement, moisture movement and heat transfer processes lack experimental confirmation. Only once this is done can their complex correlation be investigated.

3 • RESEARCH DESIGN

3.1 Introduction

The subfloor model in AccuRate represents complex air, moisture and heat transfer processes. Existing analyses of measured data do not adequately investigate the complex nature of these processes. Hence more experimental data is needed to support the model.

This chapter describes an experimental procedure for obtaining this needed subfloor data. First, research questions are posed, the scope of the research is stated, and an overview of the research design is provided. The research is divided into two investigations and each is linked to the research questions it addresses. The design of each investigation is described in greater detail with the inputs, analyses, and outputs of each being summarized. Finally the test site and test building used to collect the experimental data are discussed.

3.2 Research questions and method overview

Chapter 2 presents a summary of the current state of knowledge regarding subfloors. Subfloor ventilation and climate models are discussed and their connection to the moisture performance of the subfloor is made clear. The AccuRate building thermal performance simulation program is introduced as the benchmark building thermal performance simulation program in Australia, and although the full details of its calculation engine are not known, it is known to have its basis in the other published models and its output needs experimental validation. Areas of uncertainty in the understanding of the models have been identified, and it is demonstrated that the theoretical models need experimental data to support them. To explore these areas of uncertainty, this research addresses the following four questions.

Research Questions:

1. How accurate is the subfloor ventilation model in AccuRate?
2. Are the subfloor ventilation requirements effective at maintaining a relatively dry subfloor?

3. How accurate is AccuRate's predicted subfloor temperature?
4. How can the AccuRate subfloor model be improved?

This research focuses mainly on the subfloor cavity and not the other zones of a building. Thus it is not within the scope to quantify the thermal resistance of the suspended floor system or to investigate its dependence on subfloor ventilation or specific subfloor climate conditions. It is also outside the scope to investigate the relationship between the room and subfloor thermal performance. This research only considers a naturally ventilated subfloor where the junction between the subfloor cavity and the wall cavity is obstructed such that air is essentially unable to flow between the two spaces. The presence of such an obstruction is mandated in the BCA (BCA 2011). It is outside the scope of this research to perform an in-depth investigation into the links between subfloor humidity, wood moisture content, mould growth or wood decay.

An experimental method was selected to address the research questions. The options for experimentation are laboratory testing and field testing.

Laboratory testing would involve the construction of a test building in a maintained environment, whereas a field test building would be situated outdoors where the environmental conditions fluctuate naturally. The main benefit of a laboratory test is that the climate could be controlled. For example, in a field test it may be very rare to encounter climate data with an inverse relationship between outdoor air temperature and radiation, but in a laboratory test this condition could be intentionally investigated. However, the drawbacks of a laboratory test are the large space required and the ongoing cost of maintaining the facility. Additionally, and importantly, a laboratory test would not allow for proper assessment of the ground evaporation. Thus a field test was deemed more suitable for this research.

Two buildings were available for field testing. One was a small unoccupied test cell just north of Launceston (Dewsbury et al. 2007) and the other was an occupied house just south of Hobart (Geard, Nolan, and Fay 2008). Both buildings have a suspended floor with an obstructed junction between the subfloor and wall cavity. Both buildings would have been available for subfloor research and already had some instrumentation and data logging equipment on-site. With relatively minor adjustments to existing equipment and the purchase of additional dedicated instrumentation, a subfloor test program could have been devised using either building.

The Launceston test cell was selected for this research because its design and environment are more tightly controlled. The Launceston test building has a square floor plan with no windows. It exists for research purposes only and thus has no occupants. It is situated on mostly flat land with relatively little exposure to wind obstruction (Dewsbury 2011). The Hobart house's floor plan is more complex and it is occupied. It also has more neighbouring buildings and a fence situated very

close by (Geard 2011). Thus, the Launceston test cell allows for more straightforward analysis. They alone are used in this research and the Hobart houses are not.

A research method was devised using the instrumented test cell to address the four research questions. This method involves two separate investigations, each requiring a separate test to be run using the same test cell. These tests need not be performed simultaneously. The first test is a subfloor ventilation test. This can be performed in just a few days as long as a suitable range of wind speeds is encountered. The second test, the subfloor climate test, involves measuring the local weather and other parameters of interest throughout the subfloor. Data for the climate test is to be observed over as long a time period as possible to ensure that weather conditions vary as much as possible.

The following two investigations are run as follows to address the four research questions:

1. Investigation 1, Subfloor Ventilation. The observed subfloor ventilation rate is compared to that predicted by AccuRate. The suitability of the test site is assessed using computational fluid dynamics to predict where departures from theory may arise. This investigation uses data from the subfloor ventilation test and addresses Research Question 1.
2. Investigation 2, Subfloor Climate. There are no forced conditions imposed on the test cell; it reacts naturally to the weather conditions without mechanical assistance from either ventilation or space conditioning. Monitoring a test building in this free-running state is a task similar to that performed in other research studies (Delsante 2006; Dewsbury, Nolan, and Fay 2008; Geard, Nolan, and Fay 2008; Sugo, Page, and Moghtaderi 2004, 2005). The observed weather and subfloor climate data are presented and the subfloor relative humidity is assessed. Parameters of interest including moisture and energy flows are calculated and presented. The observed subfloor temperature is compared that predicted by AccuRate. The differences between these two parameters, called the residuals, are assessed statistically. Correlations between the subfloor residuals and various parameters are explored. This investigation uses data from both tests as calculations employ the observed ventilation rate rather assuming the theoretical ventilation rate. This investigation addresses Research Questions 2, 3 and 4.

Investigation 1 is further explored in Section 3.3 and Investigation 2 is further explored in Section 3.4. The test facility is described in Section 3.5.

3.3 Research design for Investigation 1, Subfloor Ventilation

The first investigation aim is to address Research Question 1 by providing a comparison between the observed and predicted subfloor ventilation rate, as defined in Section 3.2. The research

method for Investigation 1 is summarized visually in a process map in Figure 3.1. Each column of the process map is now described in more detail.

3.3.1 Investigation 1 Inputs

The first column in Figure 3.1 represents the input data.

The first group of inputs comprises the building geometry and site terrain terms, including the building's floor area, the subfloor height above ground level, and assessment of the local terrain. These are constant values that can be measured or assessed at any time during the investigation.

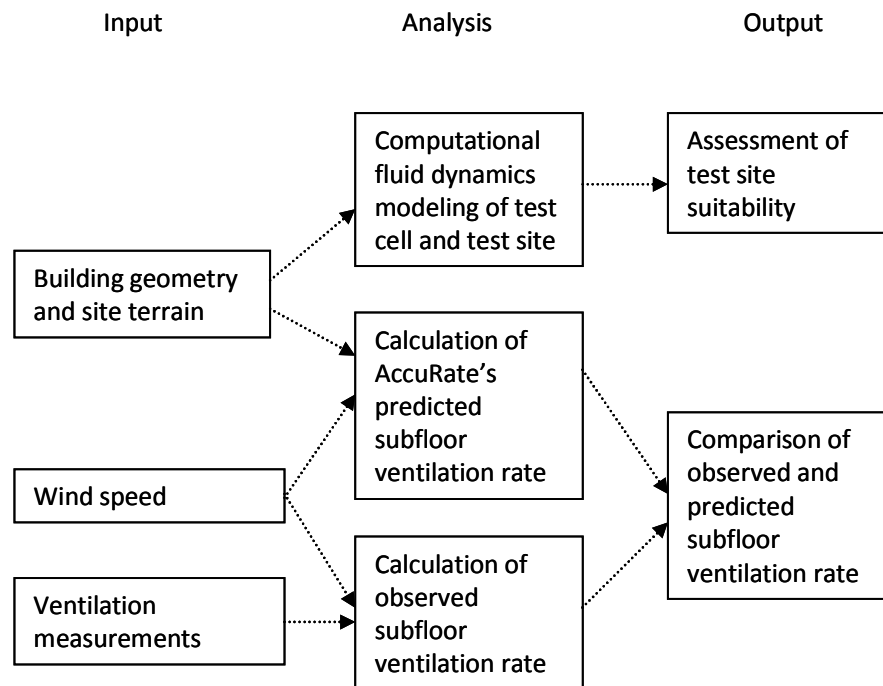


Figure 3.1: Research process map for Investigation 1, Subfloor Ventilation

The next input is wind speed. This is a time-dependent series of data. As shown in Equation 2.6 in Section 2.4.2, the only weather parameter expected to drive subfloor ventilation is the meteorological wind speed. Meteorological wind speed at a variety of sites is available from the Bureau of Meteorology (BOM). However, as the closest BOM site is approximately 18 kilometres away, it is instead preferred to measure wind speed on-site. The on-site weather station records wind speed at the building height (Dewsbury 2011), not 10m above ground level, so this height difference must be accounted for in the analysis.

The last group of inputs includes anything used for the experimental measurement of subfloor ventilation. For a tracer gas decay test this includes the tracer gas concentration as a function of time.

3.3.2 Investigation 1 Analyses

The second column in Figure 3.1 represents various manipulations of the inputs.

The first analytical task is a computational fluid dynamics (CFD) assessment of the test cell. The purpose of this task is to gauge to what extent the ventilation in the subfloor can be influenced by the test cell surrounds. This involves modelling the test cell in isolation to assess the surrounding wind pattern, and then noting how this wind pattern changes when nearby buildings are included in the model.

The next group of analyses calculates AccuRate's predicted theoretical rate of subfloor ventilation. The entire AccuRate program does not necessarily need to be run because the subfloor ventilation model for a detached building with an obstructed wall cavity junction is completely identified in Equation 2.6. Equation 2.6 inputs meteorological wind speed but the test cell records building height wind speed. Therefore a conversion method between these two values must be used. This conversion formula is a function of both the wind speed measurement height and an assessment of terrain. This formula and all calculations used to tailor the theoretical subfloor ventilation rate to suit test conditions are provided in Section 4.5.

The final group of analyses addresses the experimentally obtained ventilation data. There are several available methods for measuring ventilation in buildings and many of those methods are feasible if the ventilation is expected to be constant in time. However if the ventilation is expected to depend on wind, and therefore time, a tracer gas test is an ideal choice. There are several types of tracer gas tests, including pulse injection, decay, constant injection rate and constant concentration. Pulse injection and constant injection tests are very similar. If the ventilation rate varies with time, then the decay method and constant concentration method give more accurate results. Of the decay and constant concentration tests, the decay test requires less set-up time and lower cost, and it yield more data points in the same amount of time. (McWilliams 2002; Roulet and Vandaele 1991). Thus, the decay test is the preferred method of tracer gas test and is used in this research.

At the time this research commenced, a tracer gas decay ventilation test had already been performed on the test cell room, roof and subfloor by Deakin University's Mobile Architectural Built Environment Laboratory, MABEL (Dewsbury 2011; Sequeira et al. 2010a). Testing occurred over a period of only two days but it encompassed a broad range of wind speeds and provided a sufficient number of data points. Wind speed, wind direction and tracer gas concentration were recorded as a function of time as described in Section 4.3. MABEL provided the raw data but all processing was performed by the author as described in and 4.4. Thus, as all needed inputs were available the data was found suitable for use in this research.

3.3.3 Investigation 1 Outputs

The third column of Figure 3.1 represents the outputs of the investigation. The first output is the CFD assessment of test site suitability. This is a qualitative assessment indicating what other key areas should be explored with the observed data. For example, the CFD analysis may suggest that winds direction may have great impact on the test cell, or that the relationship between the building height wind speed and meteorological wind speed may become non-linear.

The next output is a comparison between the observed and theoretical subfloor ventilation rate. As the ventilation rate is expected to be a linear function of windspeed, both the observed and theoretical subfloor ventilation rates are summarized by their adder and scalar on windspeed. Other relationships in the data, as prompted by the CFD analysis or trends observed in the literature, are then explored.

All results of this investigation are provided in Chapter 4.

3.4 Research design for Investigation 2, Subfloor Climate

The second investigation is more complex than the first as it involves the entire subfloor climate. The aim of this investigation is to address Research Questions 2, 3 and 4 as defined in Section 3.2. The experimental component of this investigation is conducted over several seasons to ensure that as much variation as possible occurs amongst the weather inputs.

The research method for Investigation 2 is summarized visually in a process map in Figure 3.2. As the process map shows, the four groups of input data lead into several components of analysis before the data can be output into a meaningful format. This process map demonstrates the link between Investigation 1 and Investigation 2, as the fourth input into Investigation 2 is the observed ventilation data as output from Investigation 1. Each column of the process map is now described in more detail.

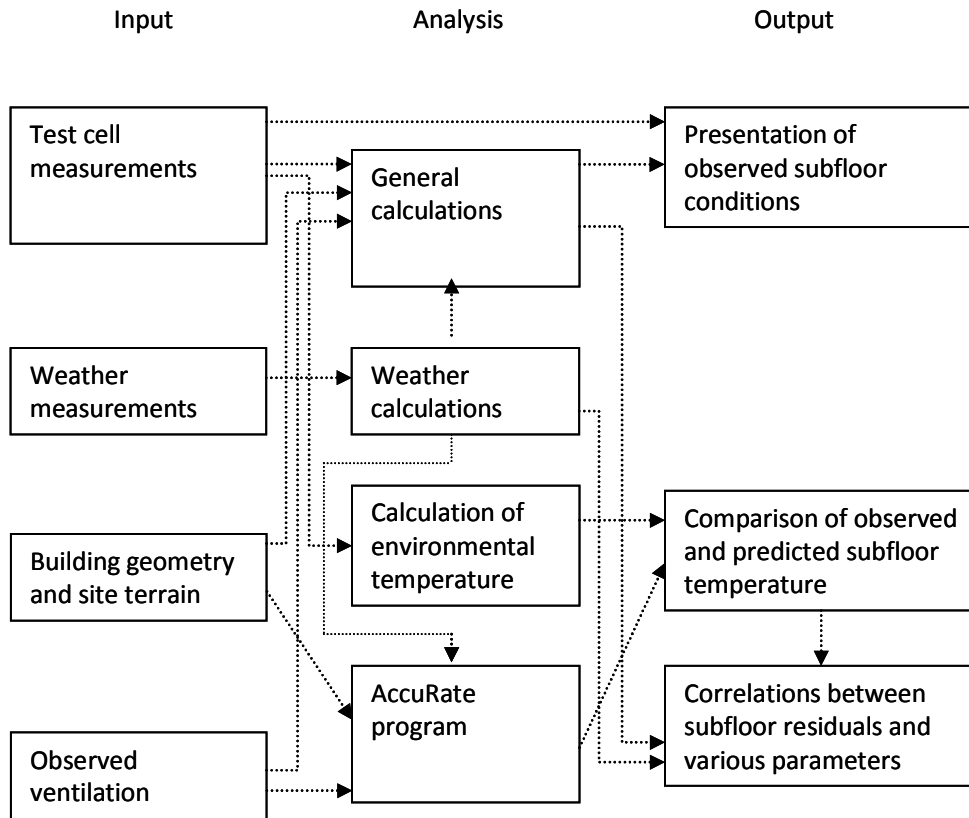


Figure 3.2: Research process map for Investigation 2, Subfloor Climate

3.4.1 Investigation 2 Inputs

The first column of boxes in Figure 3.2 represents the input data for the subfloor climate investigation. The first group of inputs comprises the test cell measurements. These are measurements recorded at numerous locations inside the test cell room, the subfloor or in the immediate surrounds of the test cell. Temperatures, humidity, air speed, radiation and heat flux are measured via affixed instruments and recorded in 10-minute intervals to one of two data loggers. Moisture content measurements for wooden subfloor elements and the soil are recorded manually.

The second group of inputs comprises the weather measurements. Like the majority of the test cell measurements, the on-site air temperature, humidity, radiation, wind speed and wind direction are also measured via affixed instruments and recorded in 10-minute intervals to one of two data loggers. Additional parameters to supplement this data are purchased from BOM. This includes atmospheric pressure and precipitation.

Instrumentation, equipment and procedures for measuring, organizing and reducing the test cell and site-recorded weather data are described in detail in Sections 5.2 to 5.4.

The third group of inputs comprises the building geometry and site terrain. These are all constant values that can be measured or assessed at any time during the investigation. The fourth input group is the observed ventilation. This input represents the output of the ventilation test of Investigation 1. The data consist of a set of constant values representing adders and scalars on wind speed.

3.4.2 Investigation 2 Analyses

The second column of Figure 3.2 represents the calculations and manipulations performed on the data. These have been sorted into four groups.

In order of simplicity, the first set of analyses involves ‘Calculation of environmental temperature’, shown as the third group in the Analysis column. This calculation is needed to perform a direct comparison between the observed test cell temperatures and the corresponding AccuRate output temperature. AccuRate does not output an air temperature but an ‘environmental temperature’. The process of calculating environmental temperature from measured test cell temperatures is explained in Section 5.5.3.

Another set of analyses is the ‘Weather calculations’, shown as the second group in the Analysis column. Some of the on-site and BOM weather data must undergo a dedicated set of calculations before they are input into further calculations or the AccuRate program. For example, the measured atmospheric pressure is modified to reflect the altitude of the test cell; the specific humidity of the outdoor air is a function of local atmospheric pressure; diffuse radiation is a function of the measured global solar radiation; and direct solar radiation is a function of both the calculated diffuse radiation and directly measured global solar radiation. These weather calculations are detailed in Section 5.5.3.

The third set of analyses is for ‘General calculations’ as shown in the top group in the process map. This represents all remaining calculations for determining various parameters. All four groups of input data are used in this analysis. For example, subfloor ventilation is calculated as a function of measured wind speed and the observed ventilation constants; ground moisture evaporation and other moisture flows are calculated as a function of the subfloor ventilation, test cell and weather measurements; and various energy flows are calculated as a function of the moisture flows and all other groups of inputs. The formulas are based upon the conservation of mass, conservation of energy and various thermodynamics relationships. These are developed in Section 5.5.5.

The final set of analyses, shown as the bottom group in the Analysis column of Figure 3.2, is undertaken by running the AccuRate program. Building geometry and site information are inputs to the program. AccuRate uses those inputs and applies assumptions as necessary to perform a multitude of calculations. However, as the accuracy of AccuRate’s output is under investigation, it

is important that any avoidable assumptions in the program are kept to a minimum. For example, AccuRate typically assumes a weather pattern using the building's postal code and the associated RMY data. In this research the RMY data is replaced with the observed weather conditions. This reduces the likelihood that inaccuracy in the program's output is due to the difference between observed and reference weather conditions. Several other atypical modifications to AccuRate are needed. This non-standard use of the program requires the following of a procedure mapped out in recent research (Dewsbury 2011; Geard 2011) and necessitates guidance from CSIRO. The detailed procedure for running AccuRate and modifying the program inputs to match the observed on-site conditions is described in Section 5.6.

3.4.3 Investigation 2 Outputs

Finally, the third column of the process map in Figure 3.2 represents the output of the subfloor climate investigation.

The first output group comprises the presentation of the observed subfloor conditions. Temperature and humidity at several locations throughout the subfloor are presented and compared to outside conditions. The subfloor humidity is assessed in detail. Ground temperature and heat flux values also are presented. Moisture flows are presented and the relationship between ground moisture evaporation, subfloor ventilation and subfloor humidity is explored. Various energy flows are presented and their values compared. Comparisons are presented between these observed data, observed data from published literature, and theoretical predictions.

The second output group comprises the comparison of observed and predicted subfloor temperatures. Here, the observed subfloor temperature is compared to the subfloor temperature as predicted by AccuRate. The differences between these values, called the residuals, are summarized and compared to those found in previous research. Then, as represented by the third output group in the process map, correlations are made between these residuals and various parameters of interest. The AccuRate residuals are compared to residuals from published literature. As the entirety of the AccuRate calculation engine is not known, the AccuRate program is essentially treated as a black box in this investigation. However, from these comparisons and correlations, inferences about the accuracy of the AccuRate program are made and potential avenues for its improvement are identified.

All results from this investigation are shown in Chapter 6.

3.5 Test facility

The test facility used in this research was constructed on the University of Tasmania's campus in Newnham, Launceston in 2006. It is the centre test cell in a row of three instrumented test cells, all

constructed for the purpose of conducting thermal performance research. The design and construction of the test cells have been documented extensively (Dewsbury 2011; Dewsbury et al. 2007; Dewsbury and Nolan 2006; Dewsbury, Nolan, and Fay 2008) as the test cells had previously been used for an empirical validation of AccuRate (Dewsbury 2011). Figure 3.3 shows the test cell site as seen from the northwest at ground level.



Figure 3.3: Test site from the northwest

The site is semi-rural and an aerial photo from 12th January 2008 is shown in Figure 3.4 (GoogleEarth 2013). This image was recorded at approximately 320 m above ground level.

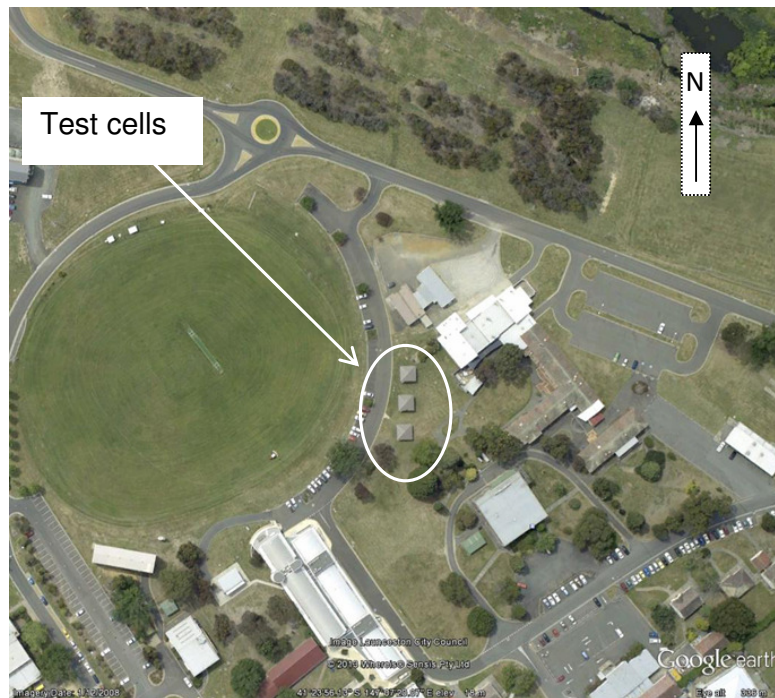


Figure 3.4: Aerial photo of test site

The three test cells are at the centre of the image. To the east of the site there are some buildings at a distance and to the west the site is relatively clear except for one narrow street light pole, a street with occasional parking and one small tree in the parking area. Further to the west and northwest is a large clearing for the university's oval. To the north there are buildings and to the south are more trees. The ground at the test site slopes gently downhill to the north (Dewsbury 2011). The test cells were purposefully spaced such that one would never overshadow another (Dewsbury et al. 2007). This ensures that the amount of direct solar radiation received by any one of the test cells would not be affected by the presence of the other two test cells. Distances between the test cells and surrounding objects are shown in the site plan in Figure 3.5.

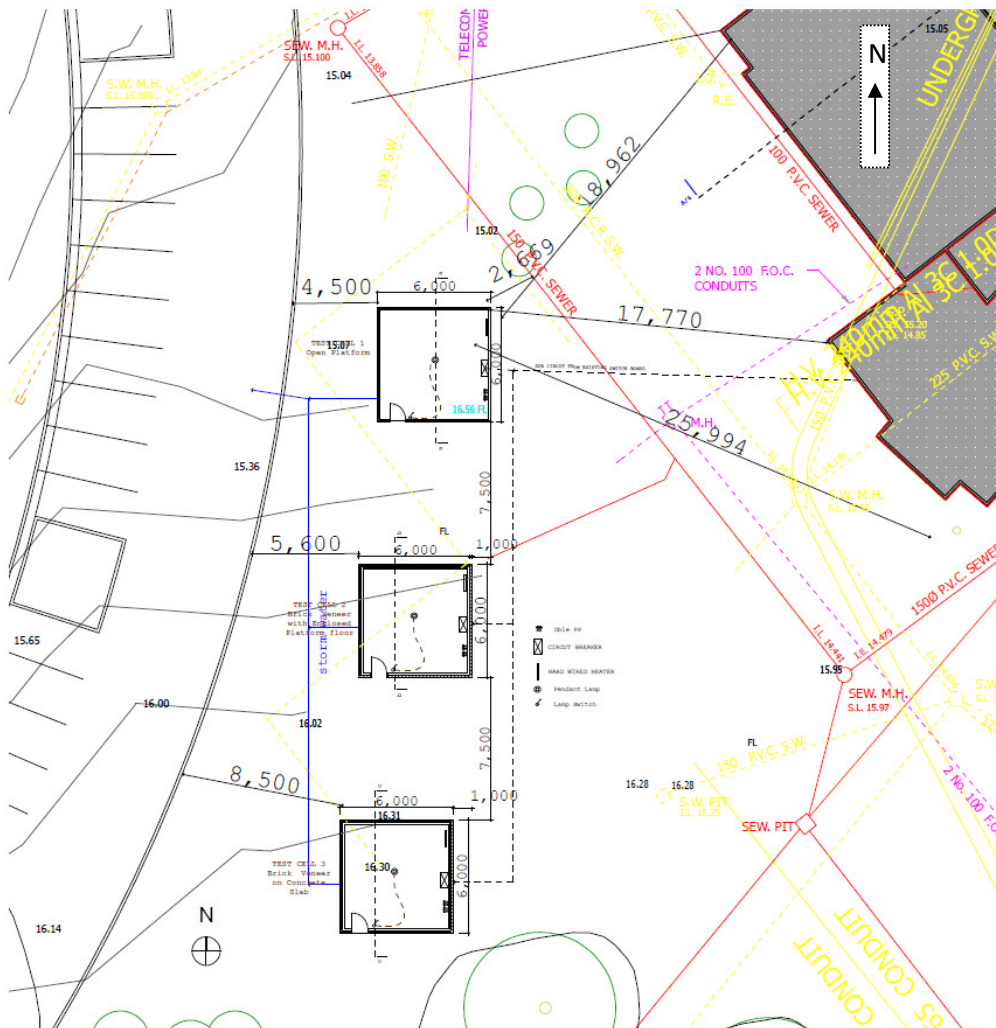


Figure 3.5: Site plan, not to scale (Dewsbury 2011)

West of the test site there is a curb and the ground height drops slightly to allow for a road with parking. Cars are often parked on the road during daytime hours when university classes are in

session. The parking area is approximately 10 metres from the test cells and parking spaces are denoted by flat white dots as seen in Figure 3.3

The three test cells each are square with an outside wall perimeter of 6 m. Each have an identical indoor floor area of 30 m² (5.480 m x 5.480 m) but have differing construction materials (Dewsbury et al. 2007). The test cell used in this research, Test Cell 2, is in the centre. Test Cell 1 has a suspended floor and an unenclosed subfloor and lies to the north by 7.5 m and to the east by 1.0 m. Test Cell 3 lies to the south by 7.5 m and to the west by 1.0m and has a slab on ground floor construction.

Drawings for Test Cell 2 are provided in Appendix A.1. These include the footing plan, floor plan, roofing plan, elevations and section drawings.

The test cell was designed to comply with current Australian building practice. The fabric matrix for the test cell (Dewsbury 2011) is provided in Table 3.1. Floor carpet was not included in the original construction and was installed in 2007.

Table 3.1: Test cell fabric matrix

Item	Specification
Footings	Treated poles set in a concrete pier
	Concrete strip footings for brick veneer wall
Sub-floor	110 Extruded clay brick veneer
Floor	Carpet, 19mm Particle board deck on timber bearer and joists
Walls	10mm Plasterboard, 90mm softwood stud framing, R2.5 rockwool wall batt insulation, reflective foil wrap, 50mm cavity, 110 clay brick
Ceiling	10mm Plasterboard, R4.0 Glass wool ceiling batt
Roof	Softwood truss, battens, reflective foil sarking, Colorbond sheet metal roofing

The test program began at a time when floor insulation was not required per the BCA. Floor insulation became a requirement in 2010 (BCA 2011), and the possibility existed to install it to make the research more representative of current practice. However it was desired to limit any fabric changes to the test cell to allow for more direct comparison with prior research. Also, it was already determined that investigating the thermal resistance of the floor system was outside the scope of this research. Thus, floor insulation was intentionally not installed.

Care was taken beyond that of typical construction to minimize the amount of undesired air movement between zones of the building. Wall wrap and roof sarking joints were taped instead of just being overlapped (Dewsbury 2011). The test cell was also carefully constructed to have the wall cavity and subfloor junction blocked, thus limiting air movement between the cavities. The cavity seal design is shown in Figure 3.6 with Figure 3.7 showing a photograph of the obstruction taken during construction.

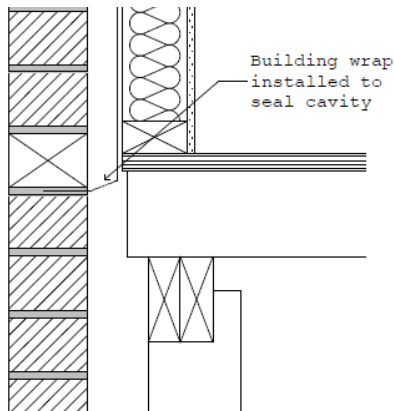


Figure 3.6: Diagram of wall cavity and subfloor obstruction (Dewsbury 2011)



Figure 3.7: Photo of wall cavity and subfloor obstruction (Dewsbury 2011)

The subfloor is open to the bare ground below. This is visible in the photograph of Figure 3.8 which is taken from the access door and looks across to the southwest corner. Subfloor ventilation is provided by two 230 mm x 165 mm vents on each side of the building. The eight subfloor vents each have the equivalent wall area of two bricks. Each vent contains 9 rows and 13 columns of 11 mm square openings, as shown in Figure 3.9.



Figure 3.8 Subfloor cavity

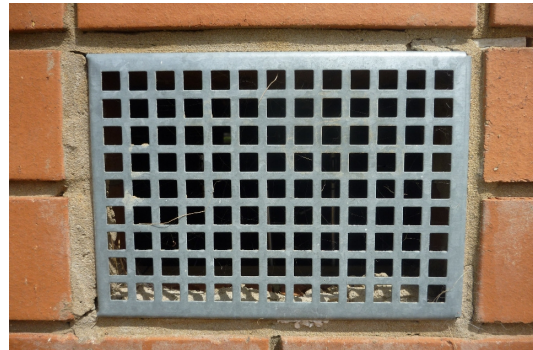


Figure 3.9: Subfloor vent

The location of the subfloor vents varies slightly between the four faces of the building, as shown in Figure 3.10 through Figure 3.13. On the north and south faces of the building the vents are shifted toward one side to accommodate the subfloor access door and test cell door steps. The east and west wall vents are spaced more symmetrically. All eight vents are at the same height but due to the sloping ground the south wall vents are flush or within 4 cm to the ground while the north wall vents are 20 cm above ground level. The southern vent on the west wall is 3 cm above ground level though it appears closer due to the long grass.



Figure 3.10: North wall of test cell



Figure 3.11: South wall of test cell



Figure 3.12: East wall of test cell



Figure 3.13: West wall of test cell

The test cell has the capability of housing and powering instrumentation and data logging equipment. The instrumentation used for each investigation is discussed in Sections 4.3 and 5.2.

3.6 Conclusion

An experimental procedure has been defined which addresses gaps in the knowledge about subfloor climates. Theoretical understanding of the physical interactions expected to occur in the subfloor has shaped the procedure of the research. Desired outputs of the research have been defined and linked through various analyses to their needed inputs and ensure that all physical properties needing measurement have been identified. The available test building is typical of standard Australian building practice, ensuring that results are relevant.

4 • INVESTIGATION 1 DESIGN AND RESULTS: SUBFLOOR VENTILATION

4.1 Introduction

In Chapter 3 research questions are proposed and the scope of the research is bound. The research is divided into two investigations. The design and results from Investigation 1 are presented in this chapter.

This chapter assesses the wind pattern around the test site and presents the results relevant to Research Question 1 regarding the accuracy of the subfloor ventilation model in AccuRate. First a qualitative analysis of the test site is performed using computational fluid dynamics to determine the site's influence on the wind pattern around the test cell. Then the subfloor ventilation test procedure and data reduction process are described. Finally the observed subfloor ventilation is compared to the theory.

4.2 Assessment of test site using computational fluid dynamics

The three test cells described in Section 3.5 were designed and constructed before the commencement of this research. They were built to satisfy the needs of the previous research team making broad investigations into building thermal performance. Previous research was not as focussed on the subfloor ventilation, however. As discussed in Section 2.4.2 and shown in Equation 2.6, the environmental factor expected to primarily drive the ventilation is wind speed. Nearby buildings and other structures can influence the local wind pattern around the test cell. Thus it is necessary to assess any effect that the presence of Test Cells 1 and 3 (TC1 and TC3) may have on the air flow pattern around Test Cell 2 (TC2).

Computational fluid dynamics, CFD, was used to assess the test site on a qualitative basis with the purpose of identifying any unexpected wind flow patterns around TC2 due to its placement between TC1 and TC3. As the assessment is predominantly qualitative, an uncertainty analysis was not performed on the results. The CFD analysis was performed by researchers at the UTAS School

of Engineering (Sequeira et al. 2010a), with general guidance provided by the author. ANSYS software was used with post-process performed using CFX Post. The three test cells were modelled in CFD though other buildings in the area were not included in the model. The model included a clearance of 6 m around the houses and 15 m above. The flow was incompressible, laminar flow. The mesh size for the test cells was such that the rooves were divided into 20 elements, the walls into 30 and the base into 40. The fluid domain was divided into 70 elements along the N-S direction, 35 in the E-W direction and 35 in the vertical direction. The model totalled 1,545,000 elements. The results were considered after 110 iterations, which yielded convergence.

The TC2 entrance steps on the south side were not included. Due to symmetry, winds from only one quadrant were analysed. Since the predominant wind in the area is from the northwest, this quadrant was selected. Other obstructions in this quadrant were then assessed. The drop in ground level of the footpath just metres to the west of the test cells was found to have a negligible effect on air flow. However, the presence of cars in the car park was found to disrupt the air flow near Test Cell 2. For simplification, both the footpath and cars were then removed from the model (Sequeira et al. 2010a), and the effect of the cars on air flow is left for future study.

Three wind directions were studied: north, northwest and west. For each wind direction the air flow and pressure around TC2 was assessed with TC2 in isolation, and then again in the presence of the other test cells. The differences could then be attributed to the presence of TC1 and TC3. When TC2 is in isolation, the north wind was not assessed because it can be considered to have the same effect as a wind from the west due to symmetry. Thus, only five different scenarios were considered. The base scenario to which all others are referenced is the scenario with a westerly wind and TC2 in isolation. For each scenario the free stream air speed at 20 m elevation was set to 1.5 m/s. Generally wind speed is studied at the height of 10 m; however, 20 m was used as it improved the stability of the model.

4.2.1 TC2 in isolation

TC2 is considered in isolation with a westerly wind and a northwesterly wind.

The CFD results from the westerly wind are shown in Figure 4.1. Figure 4.1(a) shows the air movement around TC2 when viewed from the south. The air speed is lowest about halfway up the height of the building. At the roof of the test cell the air speed is above the free stream air speed. The air speed is lower on the east side of the test cell due to the presence of the boundary layer. Figure 4.1(b) shows the top view of the air flow around TC2 at 1 m above the ground, close to the height of the subfloor vents. The air flow is mostly symmetrical about the E-W axis. On the west side, the air approaching the bluff test cell has a reduced speed and on the north and south sides

the speed increases. The boundary layer on the north and south side detaches from the building. This view also shows that the air on the east side is mostly stagnant.

The pressure throughout the subfloor is shown in Figure 4.1(c). The highest pressure occurs outside the west side, the windward side. The pressure outside the east side, the side blocked from the wind, is lower because it is in the wake of the boundary layer. This is similar to the pressure inside the subfloor. The lowest pressure occurs on the north and south due to the high speed of the air moving past. Differences in symmetry along the E-W axis are minor and presumably caused by differences in subfloor vent location. Air speed throughout the subfloor is shown in Figure 4.1(d). Air enters the subfloor through the two vents on the west, the windward side, which had the highest pressure. Air exits the subfloor through the four vents on the north and south sides via aspiration. Very little air exits through the east side vents.

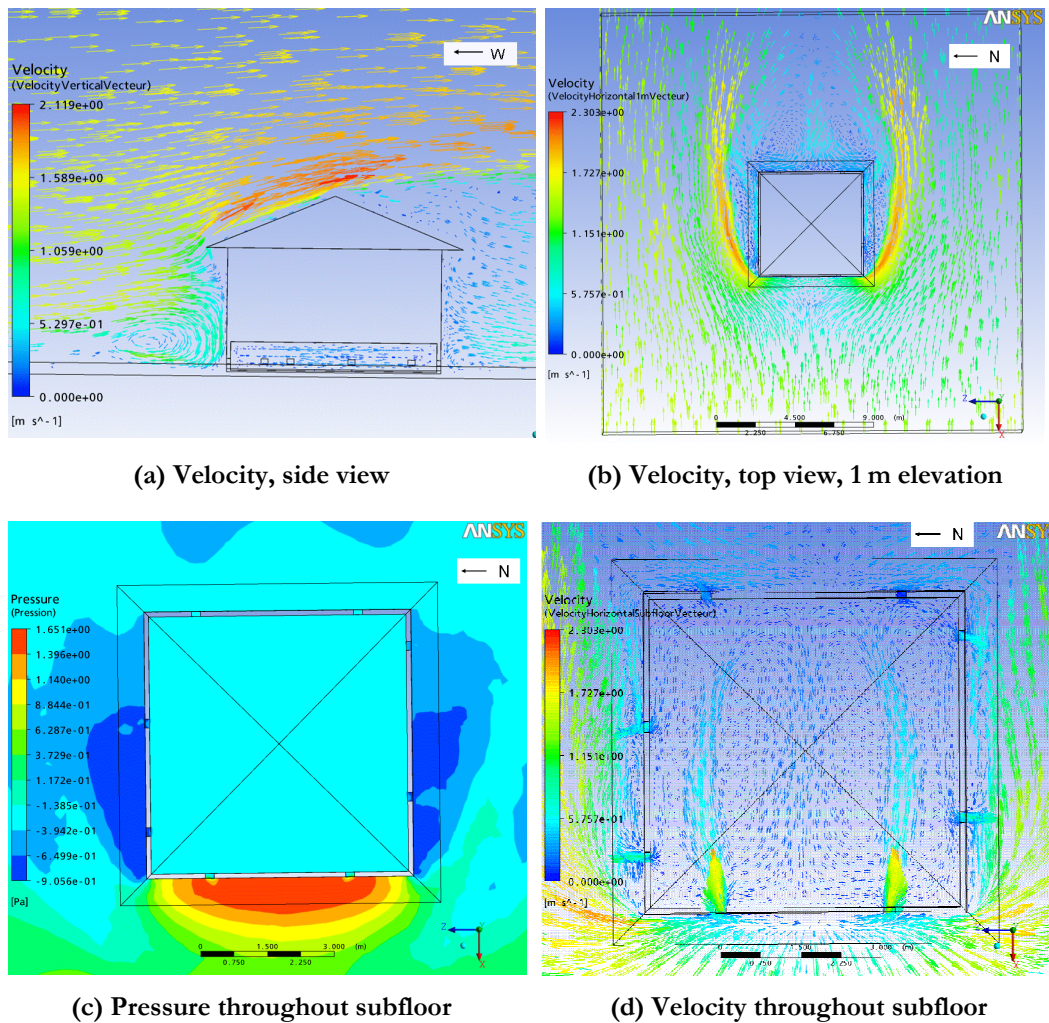
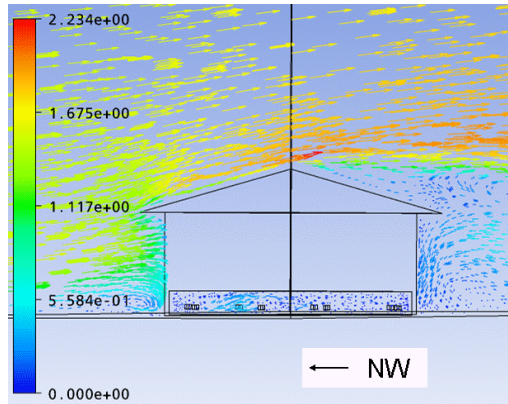


Figure 4.1: CFD results, TC2 in isolation, wind from W

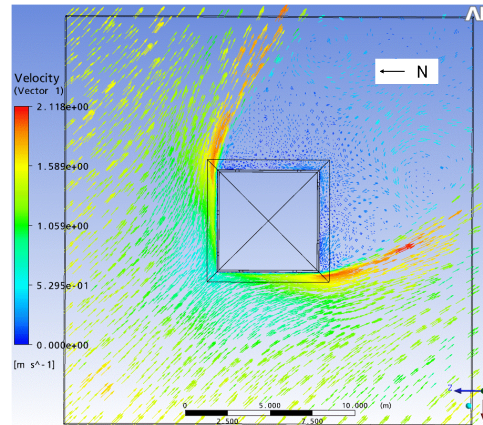
Due to symmetry, wind from the north was not modelled when TC2 is in isolation. Though there are slight differences the subfloor vent spacing between these two sides, the effect of this difference is assumed to be minor.

The CFD results from a northwesterly wind are shown in Figure 4.2. Figure 4.2(a) shows the air flow around TC2 when looking from the southwest toward the northeast, perpendicular to free stream wind movement. Similar to the base scenario, the air speed at the roof height is higher than the free stream air speed. The air speed is lower on the southeast side of the building. Figure 4.2(b) shows the top view at 1 m elevation. Air speed is reduced at the northwest corner and it increases along the length of the north and west faces of the building. The east and south faces of the building are in the wake of the boundary layer separation region. The air flow appears mostly symmetrical about the NW-SE axis.

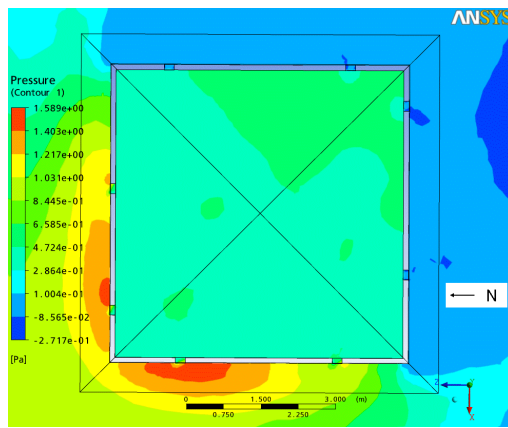
The pressure throughout the subfloor is shown in Figure 4.2(c). The highest pressure region is outside the corner on the windward side. The pressure outside the south and east sides is lower, and lower than that of the subfloor cavity as well. The asymmetry along the NW-SE axis is minor, and presumably due to the differences in vent location. Air speed throughout the subfloor is shown in Figure 4.2(d). Air enters the subfloor through the four vents on the north and west sides and exits through all four vents on the south and east sides. This is in contrast to the base scenario where some vents are stagnant.



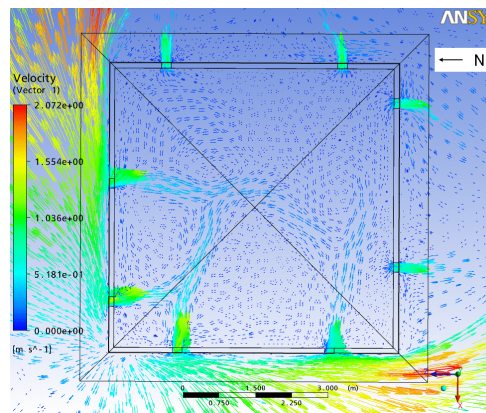
(a) Velocity, side view



(b) Velocity, top view, 1 m elevation



(c) Pressure throughout subfloor



(d) Velocity throughout subfloor

Figure 4.2: CFD results, TC2 in isolation, wind from NW

4.2.2 TC2 in presence of TC1 and TC3

The effects of TC1 and TC3 on TC2 are considered with a westerly wind, a northerly wind, and a northwesterly wind. The CFD results from a westerly wind are shown in Figure 4.3.

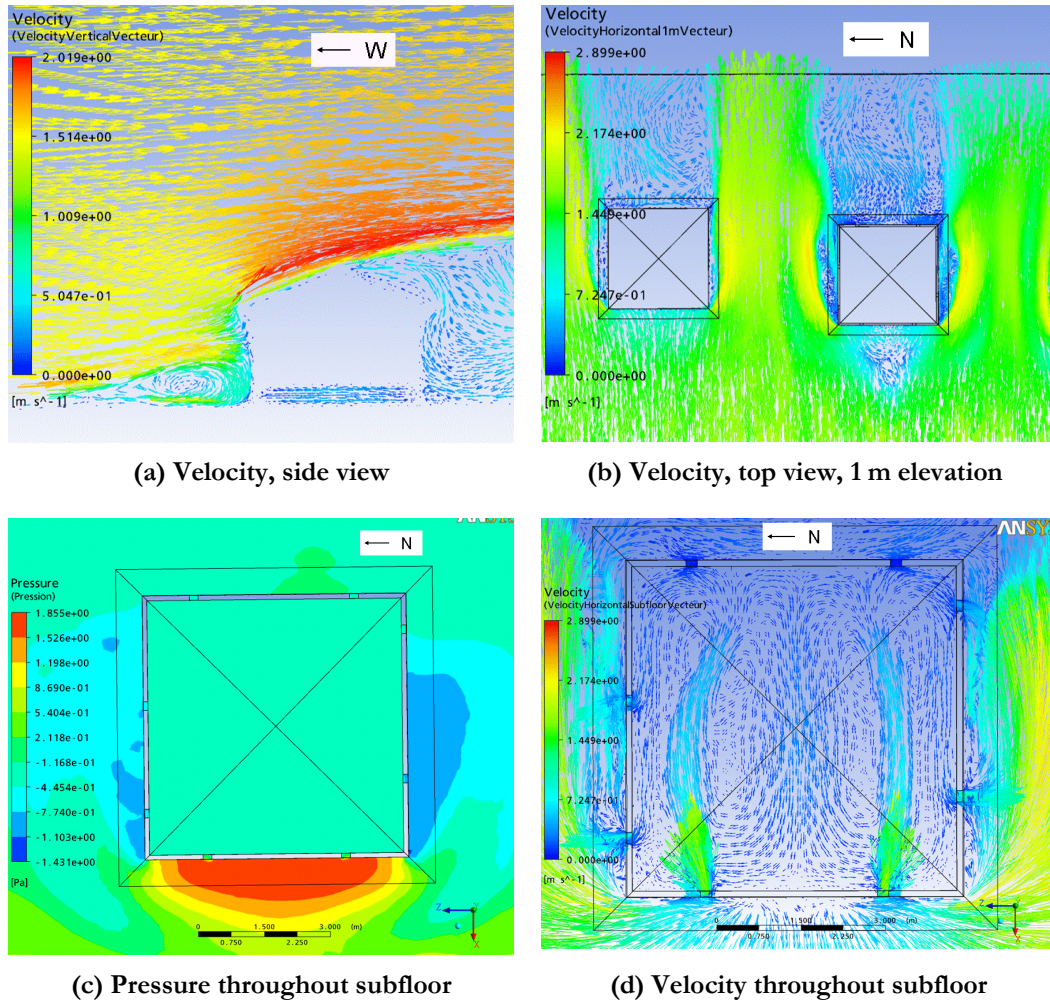
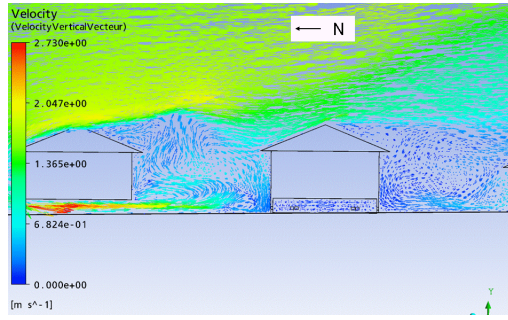


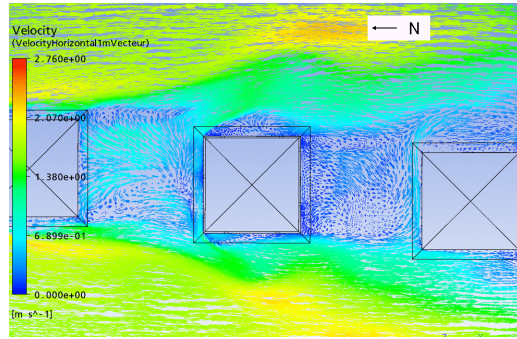
Figure 4.3: CFD results, wind from W

The air flow in this scenario is similar to that of the base scenario. Figure 4.3(a) shows the air flow around TC2 when viewed from the south. The air speed at the roof height is higher than the free stream air speed, and on the east side the speed is much lower. Figure 4.3(b) shows the top view of the air flow around TC2 at 1 m above the ground. The air speed is decreased at the west side of the building, then increased at the north and south sides, with the boundary layer detaching from the building on each side. The subfloor pressure in Figure 4.3(c) and air speed in Figure 4.3(d) are also similar to the base scenario. Air enters the subfloor from the windward side, the side with the highest pressure. Air then aspirates out the four vents on the north and south sides, where the outside pressure drops below that of the subfloor. There is minimal air movement though the east side vents, which is in the wake of the boundary layer separation region and where the outside pressure is similar to that inside the subfloor cavity.

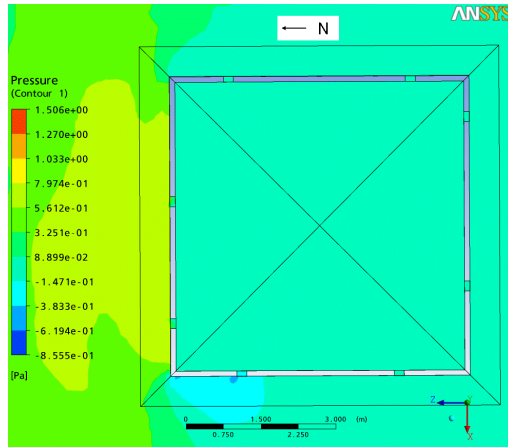
The CFD results from a northerly wind are shown in Figure 4.4.



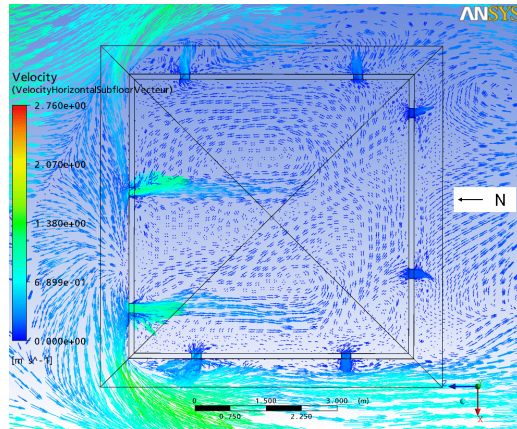
(a) Velocity, side view



(b) Velocity, top view, 1 m elevation



(c) Pressure throughout subfloor



(d) Velocity throughout subfloor

Figure 4.4: CFD results, wind from N

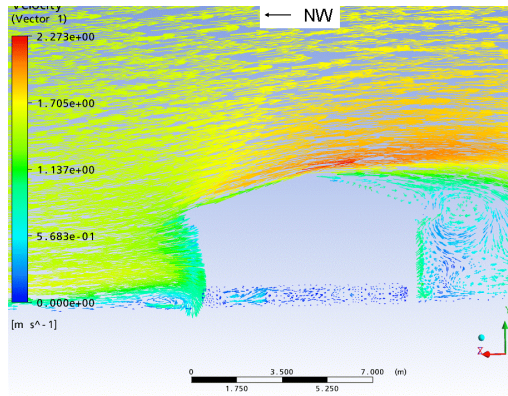
The air flow in this scenario is quite different to that in the base scenario. Figure 4.4(a) shows the air flow around TC2 when viewed from the west. TC2 lies in the wake of the boundary layer formed when the free stream air impacts upon TC1. Some of this air passes over the roof of TC1 and its speed increases above 1.5 m/s. This air then diffuses resulting in air speed at the TC2 roof lower than that of the free stream. Other air impacting TC1 is diverted underneath TC1 and flows through its open subfloor cavity. This air then enters the wake at approximately the height of TC2's subfloor vents. The 1 m elevation top view of Figure 4.4(b) also shows this wake effect. The air exiting from TC1's subfloor cavity enters the wake and then joins the bulk flow on the east and west sides of TC2.

Compared to the base scenario shown in Figure 4.1(c), Figure 4.4(c) shows less pressure on the windward side of TC2. Figure 4.4(d) shows the air flow through the subfloor vents. Flow enters the subfloor from the two north vents and exits primarily from the four east and west vents, with less exiting from the two south vents.

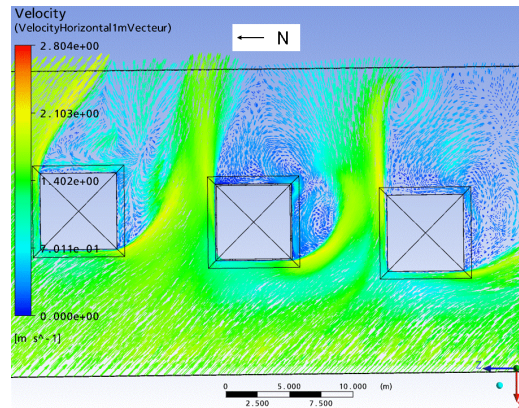
Though not modelled it is expected that a southerly wind would have a similar impact as a northerly wind on TC2, but with less subfloor ventilation as TC3 is slab-on-ground construction and cannot funnel air underneath. Even though TC3 has a lower height than TC1, TC2 would still be expected to lie in the wake as the wind is directed overhead.

The fifth and final scenario is a northwest wind. The CFD results for this scenario are presented in Figure 4.5 and are similar to the isolation scenario of Figure 4.2. Figure 4.5(a) shows the air flow pattern around TC2 when viewed from the southwest toward the northeast. The air increases in speed as it passes over the roof of the building. The air speed is lower on the southeast side of the building. Figure 4.5(b) shows the air flow at 1 m elevation. As with the case when TC2 is in isolation, air speed is lower at the northwest corner and increases along the length of the north and west faces of the building. The east and south face of the building are in the wake of the boundary layer separation region. However, there is no longer symmetry along the NW-SE axis. The wake of the boundary layer on the south side of TC2 is limited by the presence of TC3. This constricts the air movement between TC2 and TC3, resulting in reduced air speed along the west side of TC2. However, there is no such constriction on the wake at the east side of TC2. Therefore the air on the north side of TC2 has a higher speed (Sequeira et al. 2010a).

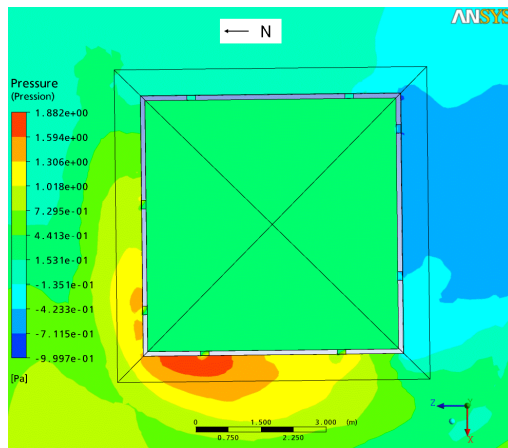
The asymmetry in air speed is also evident in the pressure at the subfloor vents, shown in Figure 4.5(c), with a higher pressure on the west side than on the north side. Air movement through the vents and throughout the subfloor is shown in Figure 4.5(d). Air enters the vents from the four vents on the north and west sides of the test cell and it exits from the four vents on the south and east sides. Similar to the scenario when TC2 is in isolation, there are no stagnant vents.



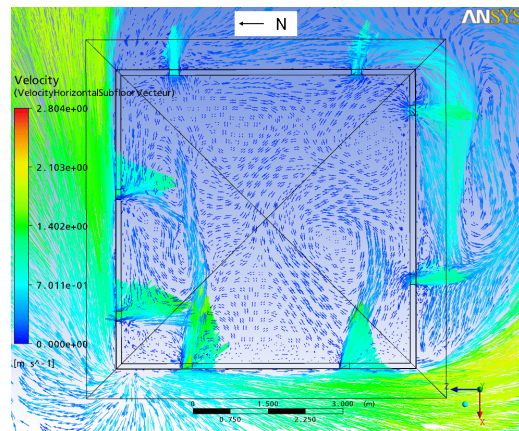
(a) Velocity, side view



(b) Velocity, top view, 1 m elevation



(c) Pressure throughout subfloor



(d) Velocity throughout subfloor

Figure 4.5: CFD results, wind from NW

4.2.3 CFD summary

A summary of the TC2 roof air speeds is provided in Table 4.1. When TC2 is in isolation the wind direction does not affect the air speed at the roof of the building, and the roof air speed is greater than the free stream wind speed. When the surrounding test cells are considered, a wind from the west or northwest still has essentially the same impact on TC2. However, the impact of a northerly wind on the TC2 roof air speed is substantially affected by the presence of TC1. This is the only scenario considered where the roof air speed drops below that of the free stream wind speed.

CFD was also run with TC2 in isolation with varying free stream wind speeds. It was found that the relationship between roof air speed and free stream air speed was always linear. Therefore, the results from this study are expected to apply to a range of wind speeds.

Table 4.1: Site influence on TC2 roof air speed

Wind direction	TC2 in isolation Wind speed [m/s]	TC1, TC3 present Wind speed [m/s]
North	1.9 *	1.3
West	1.9	1.9
Northwest	1.9	2.0

Wind speed at 20 m elevation is 1.5 m/s

* assumed via symmetry

The different scenarios are also observed to have different effects on the air speed at the subfloor vent locations. For each scenario the air speed flowing through the centre of each vent was summed for each vent with inward flow. This represents the total air speed into the vents and could be correlated to the subfloor ventilation. The calculation is rudimentary in that it does not consider the variation of the speed across the surface of each vent, and how this variation changes with wind direction. The results are shown in Table 4.2. The wind direction does indeed impact the subfloor vent air speed. In isolation the subfloor vent wind speed resulting from a northwesterly wind is 22% higher than from a westerly wind. When the surrounding test cells are considered for both the west and northwest directions there is a slight increase in vent wind speed. However, the presence of the surrounding cells considerably reduces the inlet vent air speed when the wind is from the north.

Table 4.2: Site influence on TC2 subfloor inlet vent air speed

Wind direction	TC2 in isolation %	TC1, TC3 present %
North	0 *	-39
West	base	+5
Northwest	+22	+29

* assumed via symmetry

CFD results indicate that wind direction may indeed influence the subfloor ventilation and should be further explored with the observed data.

4.3 Tracer gas test method and instrumentation

The goal of the subfloor ventilation test was to determine the observed subfloor ventilation rate as a function of wind speed. The tracer gas decay test was performed before the commencement of this research project. Testing of all zones of all three test cells was conducted though only the analysis of the data from the subfloor ventilation test of Test Cell 2 is presented in this thesis. The test procedure and associated instrumentation have been documented extensively elsewhere (Dewsbury 2011; Luther 2008) and is only summarized here.

Deakin University's Mobile Architectural Built Environment Laboratory, MABEL, conducted tracer gas testing on the subfloor of TC2 between the 6th and 8th of March 2007 before the test cell was carpeted (Luther 2008). Testing was also conducted on the carpeted test cell in September of 2007 but the data appeared incorrect. This research therefore utilizes the March 2007 data.

Two separate 24-hour ventilation tests were performed. On day 1 Test Cells 2 and 3 were simultaneously tested and on day 2 Test Cells 1 and 2 were simultaneously tested. A two-hour pause at the end of day 1 allowed for transfer of instrumentation from Test Cell 3 to Test Cell 1. The equipment pertinent to the subfloor ventilation test on Test Cell 2 was not modified during the entire 50-hour period (Sequeira et al. 2010a).

The subfloor tracer gas test was conducted using the decay method with the gas sulphur hexafluoride, SF₆. Tracer gas decay testing consists of a dosing period followed by a decay period. The amount of tracer gas injected is at all times kept low enough so as not to significantly alter the density of the air (Roulet & Vandaele 1991). SF₆ was injected into the subfloor and sampled from the subfloor using tubes inserted through the west vent on the south wall of the subfloor, as shown in Figure 4.6. During both the dose and decay periods a gas analyser was used to measure the concentration of SF₆ in parts per million (PPM). Each dose-decay cycle lasted approximately 45 minutes and yielded a unique ventilation rate. Therefore, the test yielded many data points in a short amount of time. During the dosing period the gas was injected into the subfloor space directly into the path of a fan operating at low speed, as shown in Figure 4.7. The fan was used to encourage uniform mixing of the SF₆. It is not expected that the fan would have greatly changed the ventilation rate being measured, due to the insignificance of the fan pressure. After the dosing was stopped the SF₆ concentration was allowed to decay. This process was repeated continuously for the duration of each test (Sequeira et al. 2010a).

Wind speed and direction during the test period were measured from an on-site weather station mounted on the north side roof of the centre test cell, at approximately 0.5m above the roof peak. The measurements were recorded in 10-minute intervals. Details of the instrumentation and data logging equipment for recording the wind speed have been documented elsewhere (Dewsbury 2011).



Figure 4.6: Tubes for injecting and sampling SF6 (Dewsbury 2011)

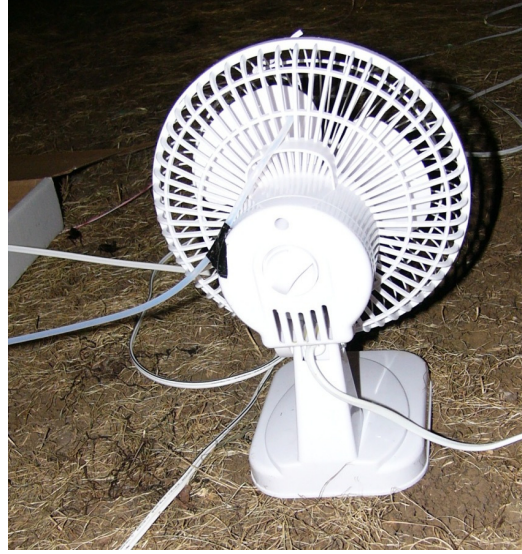


Figure 4.7: Dispersement of SF6 via fan (photograph by Mark Dewsbury)

4.4 Observed data reduction

Though the test was conducted by an outside consultant (Luther 2008) the data was reduced and analysed as part of this research project. Data provided included SF6 gas concentration from the gas analyser, and wind speed and direction from a separate instrumentation system recorded on a data logger. The ventilation rates were calculated as a function of gas concentration and elapsed time. However, the resulting data points occur at a time that was not synchronized with the measurement interval of the data logger. The wind speed and direction were then found at the desired time points via interpolation.

Firstly the ventilation rates were found. The slope of gas concentration was used to differentiate between each dose-decay cycle where a positive slope indicated dosing and a negative slope indicated decay. Once the decay processes were isolated, the ventilation rates for each decay period were found using the two-point average decay method (Sherman 1990) as follows:

$$\bar{V} = \frac{\ln\left(\frac{C_i}{C_f}\right)}{T} \quad 4.1$$

where \bar{V} is the subfloor ventilation rate in air changes per hour [ACH]; C_i is the initial gas concentration of the time period of interest (PPM); C_f is the final gas concentration of the time period of interest (PPM); and T is the duration of the time period.

Ideally the slope of the decay (C_i / C_f) remains constant during the decay period, but for these tests it did not, indicating that the ventilation rate was varying with time. It is known that in this situation the variability of tracer gas decay test results can be significant (Roulet & Vandaele 1991). The calculation of ventilation rate was therefore very sensitive to the time in each decay period at which the decay slope was sampled. To accommodate this sensitivity, the decay slope was sampled at a consistent time after the start of each decay period for each dose-decay cycle. In addition, calculations were based upon a moving average of the slope, to reduce the effect of any fluctuations (Sequeira et al. 2010a). The analysis yielded 28 data points from the first day of testing and 21 points from the second day.

To pair these 49 data points with their corresponding wind speeds, some manipulation of the wind speed data was then required. Wind speed and direction were measured in ten-minute intervals, while each decay process took approximately 30 to 45 minutes. Therefore a 30-minute moving average of wind speed was calculated to best represent the average windspeed during the decay times. This was performed as a vector average instead of a simple scalar average. The measured wind speed was separated into north-south and east-west components. A moving average of each component was performed separately and they were then vectorially summed to produce the average wind speed and direction (Sequeira et al. 2010a).

Next this observed wind speed at the building roof height was projected to the meteorological reference height of 10 m. This standard method of relating wind speed at different heights has been used in similar research (Deru and Burns 2003; Swami and Chandra 1988; Williamson and Delsante 2006a). The formula to relate wind speed at any height to the wind speed at 10 m is:

$$\frac{v}{v_{met}} = \alpha \times \left(\frac{H}{H_{met}} \right)^\gamma \quad 4.2$$

where v is the wind speed at the location of interest [m/s]; v_{met} is the wind speed [m/s] at a height above ground level of 10 m; H is the height above ground level of the location of interest [m]; H_{met} is the meteorological reference height of 10 m; and both α and γ are defined in Table 4.3 as a function of the terrain class.

Table 4.3: Terrain classification parameters (Deru and Burns 2003)

Class	γ	α	Description
I	0.10	1.30	ocean or other body of water with at least 5km of unrestricted expanse
II	0.15	1.00	flat terrain with some isolated obstacles(buildings or trees well separated)
III	0.20	0.85	rural areas with low buildings, trees, etc.
IV	0.25	0.67	urban, industrial, or forest areas
V	0.35	0.47	center of large city

Using Class III values from Table 4.3, sometimes called “Open” terrain, a scalar of 1.36 is applied to the measured wind speed at measurement height of 4.9 m to project the value to the reference height of 10 m. Thus the observed data are reduced to a set of 49 data points, with each observed ventilation value paired to a corresponding meteorological wind speed.

The prediction of Equation 4.2 and Table 4.3 show that wind speed in an area of open terrain is generally expected to decrease from its free stream speed at 10 m upon approach to the ground. However, per the CFD results the test cell roof peak lies in an area expected to have a local flow obstruction which would causes a contradiction in this general trend. As shown in Table 4.1 the CFD predicts a west or northwest wind results in a roof air speed higher than the free stream wind speed. The roof air speed measurement location may or may not fall within this area of locally-adjusted air speed. There is no separate, independent local wind speed measurement to determine the relationship between roof wind speed and free stream air speed. Thus there is uncertainty in the outcome when projecting wind speed to different heights, especially as Equation 4.2 and Table 4.3 give only general guidance and do not account for local obstructions.

4.5 Generation of theoretical data

The formula to predict subfloor ventilation as a function of windspeed is presented in Equation 2.6 with all variables defined in Section 2.4.2. The first term, which is not dependent on wind speed, is called the stack component and the second term, which contains the wind speed v_{met} , is the wind component. That formula can be adjusted to the following form:

$$\bar{V} = A + B \times terrain_{eaves} \times v_{met} \quad 4.3$$

where A is the ventilation adder or stack term [ACH]; B is the ventilation scalar on eaves-height wind speed [ACH*s/m]; and $terrain_{eaves}$ is a scalar to project the wind speed from 10 m to the height of the eaves. Various pressure coefficients in the AccuRate program refer to the height of the eaves. Hence the formula is written as above, with the subfloor ventilation model inputting the meteorological wind speed and then multiplying it by a terrain scalar to determine the wind speed at the eaves height.

When AccuRate is run the program outputs the values for the A , B , and $terrain_{eaves}$ parameters for each zone used in the internal calculations. AccuRate was run to model the test cells as described in Section 5.6. and for the subfloor zone the AccuRate ventilation values were found to be A of 0.67, B of 1.56, and $terrain_{eaves}$ of 0.67. Thus the theoretical formula for subfloor ventilation as a function of meteorological height becomes:

$$\bar{V} = 0.67 + 1.05 \times v_{met} \quad 4.4$$

where the constant term **0.67** represents the stack effect [ACH] and the constant term **1.05** represents the wind effect [ACH s/m]. This equation pertains only to this building and site.

Some of the AccuRate values can be confirmed using known formulas. The terrain scalar $terrain_{eaves}$ of 0.67 can be found using Equation 4.2 to project the wind speed at 10 m to the eaves height of 3.0 m using Class III values from Table 4.3. The stack term A of 0.67 can be found to within 3% via Equation 2.6 with a ventilation area a of 6000 m²/m, a subfloor wall perimeter P of 24 m, a subfloor ground surface area A_f of 33.4 m², and a height of the subfloor space L_{sf} of 0.6 m. The wind term B of 1.56 could not be replicated by following published formulas.

4.6 Results of ventilation test

The data from both days of tracer gas testing is compared to the theoretical prediction of Equation 4.4 and shown in Figure 4.8.

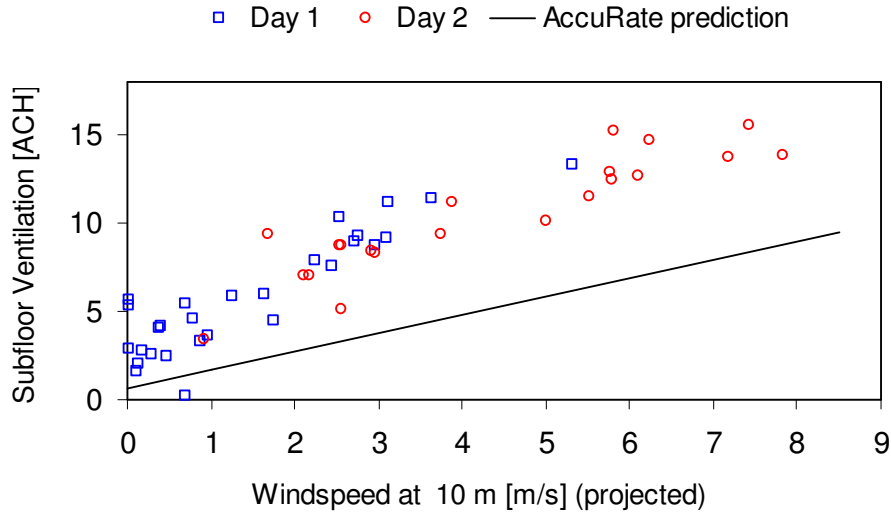


Figure 4.8: Observed and theoretical subfloor ventilation data

The two days of data provide consistent results. The data show a clear correlation to wind speed, though the ventilation values are higher than expected by AccuRate. The data indicate a larger stack

effect and higher wind sensitivity than the theory predicts. A linear regression of all 49 data points yields a best-fit line of:

$$\bar{V} = 3.3 + 1.7 \times v_{met} \quad 4.5$$

which shows both the larger stack and wind terms than the theoretical prediction provided in Equation 4.4. The linearity of the data is good, with an R^2 (coefficient of determination, or square of the correlation coefficient) value of 0.85.

The variation of the observed subfloor ventilation is within the range reported in the literature discussed in Section 2.5.1. This is a much tighter fit than the data measured in two private homes in Melbourne, Australia (Olweny et al. 1998). A linear regression of that data yields an R^2 of 0.45 for the weatherboard house and 0.54 for the brick veneer house, though it is noted that each house had only five observed data points. The subfloor ventilation from the Watford, UK, test house yielded R^2 values of 0.76 and 0.94. However, that data was fit to a temperature-corrected wind speed. This was necessary as the stack effect played a larger role in their ventilation characteristic, due to the ability of the subfloor air to travel up the wall cavity (Hartless and White, 1994).

A 10% uncertainty in tracer gas decay tests is not uncommon. Contributors to this include non-uniform gas mixing, contamination of sample containers, and errors due to the gas analyser itself include calibration drift, detector bias and reading near the sensitivity threshold (American Society for Testing and Materials, 2006). Specific to this test, additional uncertainty would stem from the synchronizing of data sets and interpolation of wind speed.

AccuRate theory takes only wind speed and not wind direction into account, though due to the site layout winds from differing directions can be expected to produce differing amounts of subfloor ventilation. The experimental studies in the literature do indeed show the effect of wind direction has on subfloor ventilation. One test building with vents on only two sides was found to have subfloor ventilation differ by 30% depending on wind direction (Edwards et al. 1990). Similarly, the Watford, UK, test house showed a 25% difference in the subfloor ventilation rate depending on wind direction (Hartless 1996).

To investigate this phenomenon, both days of data were sorted into wind speed octants, representing the direction the wind was coming from. Additionally, to reduce any effect of wind obstructions, all data that were collected during daytime hours and those that contained a westerly wind component were then removed, as it is possible that these points could have been affected by the air flow disruption from cars being parked in the nearby car parking area. This reduced the Day 1 data set to 25 points and the Day 2 data set to 15 points (Sequeira et al. 2010a).

The Day 1 data are from four octants, with the northwest and east being the most prevalent, with the other two octants being west and southwest. The Day 2 data are mostly from the northwest

octant, with only one point each from the north octant and south octant. This reduced data is graphed versus wind speed and the results are provided in Figure 4.9.

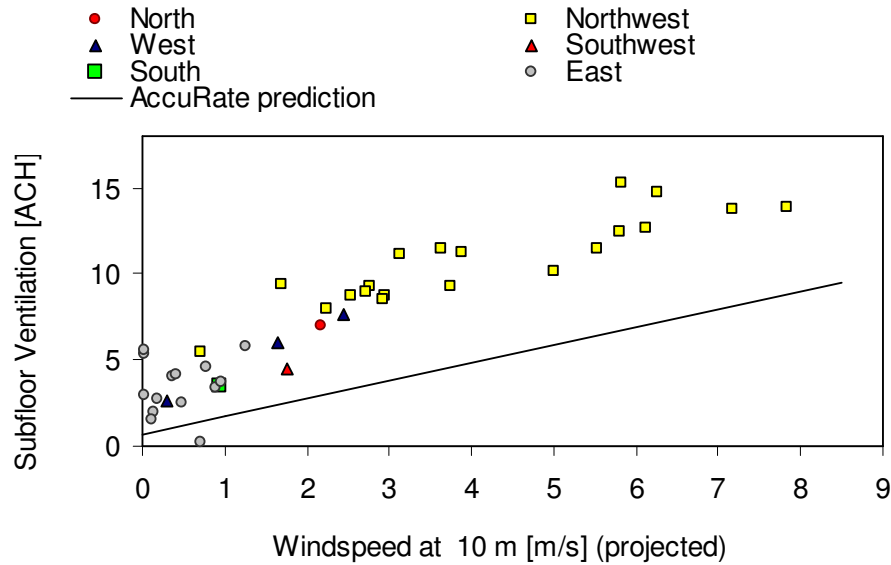


Figure 4.9: Subfloor ventilation by wind octant

The low speed data points are mostly from the east and they are observed to have a large amount of scatter. Because there are so few data points at higher wind speeds from any octant other than the northwest octant, a quantitative comparison between octants cannot be made. However, the few data points from the north, west, southwest, and south octants do lie within the family of northwest data points, though they only occur at low wind speeds.

The CFD results in Table 4.2 indicate that the wind direction should affect the air speed at the vents such that the northwest winds produce the highest vent speeds and the north or south winds produce the lowest vent speeds. However, as discussed in Section 2.4.2, the literature also states that the vent effectiveness is a function of wind angle, and that for the same wind speed a diagonal wind results in approximately half the ventilation as a perpendicular wind (ASHRAE 2005). It is possible that both these predictions are correct but essentially counteract each other, and that a northwest wind does result in a higher speed at the vent, but then due to the ineffectiveness of the incidence angle the resulting subfloor ventilation is the same as if the wind was originating from a perpendicular angle.

The total wind speed represents a fusion of the two components of the wind, the north-south component and the east-west component. As shown in Figure 4.5(b) the presence of TC3 reduces the air speed on the south and west sides of TC2 and directs air into the west sides vents, while on the north side the wind is funnelled under TC1 and the air speed is relatively high along the face of TC2. It is possible that one component alone is driving the ventilation.

Figure 4.10 shows the Day 1 and Day 2 ventilation data from the northwest octant graphed against the north-south wind speed component and east-west wind speed component. There are 20 data points in total. Similar experimental data exists in the literature for the Watford, UK, test house (Hartless and White 1994) though the only graphs provided are subfloor ventilation rate versus time and component wind speed versus time, so a direct comparison between ventilation and wind component is not easily achieved.

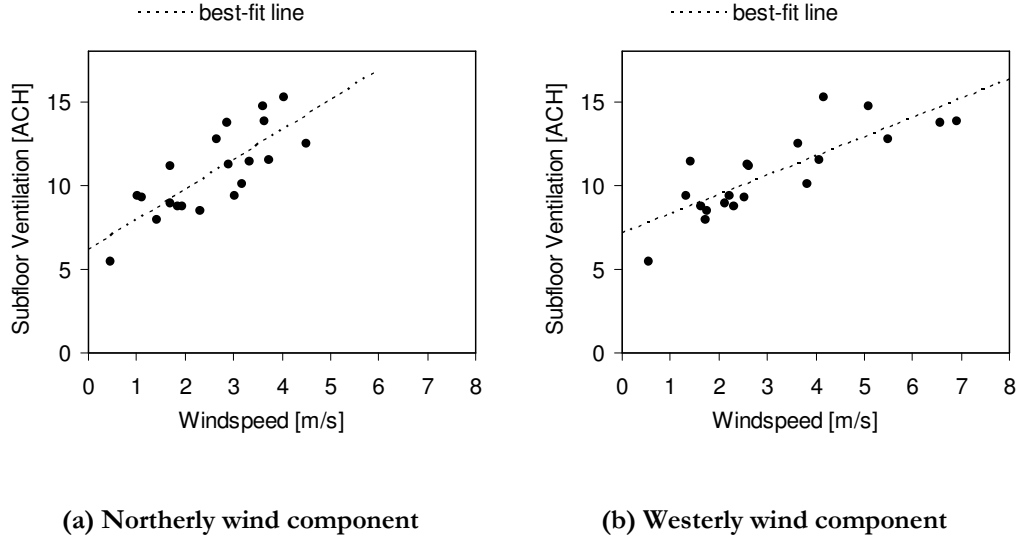


Figure 4.10: Ventilation from NW octant by wind component

These graphs show that the ventilation has a slightly stronger sensitivity to the northerly component of the wind than to the westerly component. This is visible from the trendline in Figure 4.10(a) being steeper than in Figure 4.10(b). This is also supported by the following best-fit multiple linear regression:

$$\bar{V} = 5.7 + 1.0 \times v_{met,N} + 0.7 \times v_{met,W} \quad 4.6$$

where $v_{met,N}$ is the northerly component of the wind speed at meteorological height; $v_{met,W}$ is the westerly component of the wind speed at meteorological height; and the coefficient of the northerly wind speed component is slightly larger than the coefficient of the westerly wind speed component. The adjusted R^2 of 0.78 indicates that this line has a good fit to the data (Sequeira et al. 2010a).

However, it is observed that the westerly wind speed component has higher peak values than the northerly wind speed component, and it is the data points with these higher speeds that appear to dampen the ventilation's sensitivity to westerly wind component. Indeed, if the two data points with westerly wind components of over 6 m/s are removed, the remaining 18 data points reveal that the ventilation has nearly identical sensitivity to both the northerly and westerly wind speed

components. This result is what would be expected if there were no other test cells surrounding Test Cell 2. Thus, the effect of the surrounding buildings on the TC2 subfloor ventilation does not appear significant (Sequeira et al. 2010a).

4.7 Conclusion

CFD analysis of the test site shows the expected wind pattern around Test Cell 2. Neither the presence of the surrounding tests cells nor the wind direction is expected to influence the wind speed at the measurement location, except if the wind is from the direct north or south. As the predominant wind direction of the area is from the northwest, this should have a minimal effect in a long-term test, and thus the site is deemed suitable for conducting Investigation 2.

Subfloor ventilation data observed from the tracer gas decay test are presented and shown to be dependent on wind speed, thus supporting the theoretical model. However, the observed values are higher than predicted and indicate a stronger dependence on temperature than expected. In addition, the observed sensitivity of ventilation to wind speed is over 60% higher than that predicted in AccuRate. The observed ventilation shows no dependence on wind direction, and thus the layout of the test site itself does not appear to greatly affect the measured subfloor ventilation rate.

The observed subfloor ventilation is used again in this research in Investigation 2 in Chapters 5 and 6. Observed ventilation is input into AccuRate to bypass the default values and thus isolate differences between observation and prediction due to factors other than the ventilation models. Discussion of the CFD and subfloor ventilation test results, and the effect of errors on the AccuRate results are provided in Section 7.2.1.

5 • INVESTIGATION 2 DESIGN: SUBFLOOR CLIMATE

5.1 Introduction

In Chapter 3 the four research questions are proposed and the scope of the research is bound. The research is divided into two investigations, and Chapter 3 summarizes each. Investigation 1 considers subfloor ventilation and the design and results of the subfloor ventilation test are presented in Chapter 4. The design of the second investigation is addressed in this chapter.

The aim of this chapter is to describe the procedure needed to obtain the Investigation 2 observed and theoretical data sets, ensure their integrity and convert them into usable formats. Sections 5.2 through 5.5 describe the equipment and procedure used for measuring, recording, and processing all the observed data. Section 5.6 then describes the procedure for generating the theoretical AccuRate data set.

5.2 Measurements

Investigation 2 requires the handling and organization of a host of instrumentation, much of which was acquired during previous test cell research and then refurbished and calibrated prior to the commencement of the current research. A variety of sensors were used with the minimum goal of providing AccuRate with a complete set of inputs.

5.2.1 Summary of sensors and other measurements

The first task in selecting a set of sensors was to ensure that all needed measurements were recorded. The summary of inputs needed for Investigation 2 is listed in the first column Figure 3.2. Building site and terrain are easily assessed, and the observed subfloor ventilation was already found as discussed in Chapter 4. Hence the minimum sensor set measures the weather parameters needed for AccuRate or other calculations, and the parameters needed to calculate the

environmental temperature of the subfloor. The AccuRate weather input parameters were known from previous research (Dewsbury 2011; Geard 2011) and are shown in Table 5.1.

Table 5.1: AccuRate climate inputs (Geard 2011)

Subject	Measured Parameter	Units
Site Measurements	Dry bulb (air) Temperature (tenth of a degree)	°C
	Moisture content (tenth of gram per kilogram)	g/kg
	Atmospheric air pressure (tenths of kilopascals)	kPa
	Wind speed (tenth of metres per second)	m/s
	Wind direction	0-16, 0=calm, 1=NNW
	Cloud cover	0-8, 0=no cloud, 8=full cloud
	Global solar radiation	W/m ²
	Diffuse solar radiation	W/m ²
	Normal direct solar radiation	W/m ²
	Solar altitude	0-90
	Solar azimuth	0°-359°. 0°=N, 90°=E

Dry bulb temperature can be directly measured. Moisture content, or specific humidity, can be calculated from dry bulb temperature, relative humidity and atmospheric air pressure, all of which can be directly measured. Wind speed and wind direction can be directly measured. Cloud cover can be provided by the Bureau of Meteorology. Global solar radiation can be directly measured. The diffuse and normal direct solar radiation can either be measured or calculated as a function of global radiation, building location and solar altitude. Solar altitude and azimuth are functions of the building location.

It was desired to have as many weather inputs recorded on-site as feasible. With this in mind, the following weather parameters were recorded on-site with the specific purpose of inputting into AccuRate: dry bulb air temperature, relative humidity, wind speed, wind direction and global solar radiation. All other inputs needed for the AccuRate climate file were calculated, purchased or assumed, as described in Sections 5.5.3 and 5.6.3.

The subfloor environmental temperature is a function of subfloor dry bulb air temperature and subfloor globe temperature, as described in Section 5.5.4. These two parameters complete the minimum sensor set shown in Table 5.2.

Table 5.2: Sensor set - minimum

Purpose	Parameter	Unit
AccuRate	Dry bulb air temperature	° C
AccuRate	Relative humidity	%
AccuRate	Wind speed	m/s
AccuRate	Wind direction	°
AccuRate	Global horizontal irradiance	W/m ²
Subfloor	Dry bulb air temperature	° C
Subfloor	Globe temperature	° C

In addition to the seven sensors needed as minimum, 43 other sensors were used to provide supporting data. Each of these 50 sensors was assigned a unique ID and is listed in Table 5.3, where RTD is resistance temperature detector, IC is integrated circuit, and TC is type K thermocouple. The majority of these sensors were used and described in previous research on the test cells (Dewsbury 2011) with only the heat flux sensors, the RTDs and the thermocouples being newly purchased for the current research. All the sensors included in Table 5.3 were installed and connected to the data acquisition system as described in Section 5.3.

Table 5.3: Sensor set - total

Sensor ID	Description	Type *
Weather -----		
AD10	Wind direction	
AS10	Wind speed	
RA14	Global horizontal irradiance	
RH10	Relative humidity	
TA10	Air temp	
External -----		
RA10	Global radiation on wall, east side	
RA11	Global radiation on wall, south side	
RA12	Global radiation on wall, west side	
RA13	Global radiation on wall, north side	
RA15	Vertical radiation	
RA16	Diffuse radiation	
HF20	Heat flux near ground surface, outside east wall	
TG20	Underground temp 150mm, outside east wall	RTD
TG21	Underground temp 600mm, outside east wall	RTD
Room -----		
TA37	Air temp at room centre, 600 mm height	IC
TA38	Air temp at room centre, 1200 mm height	IC
TA39	Air temp at room centre, 1800 mm height	IC
TB32	Globe temp at room centre, 1200 mm height	IC
TS38	Top-of-floor surface temp at room centre	TC
Subfloor -----		
AS30	Air speed, NW vent, middle height, east alignment	
AS31	Air speed, NW vent, middle height, centre alignment	
AS32	Air speed, NW vent, middle height, west alignment	
AS33	Air speed at subfloor center (N-S airflow)	
HF30	Heat flux near east wall	
HF31	Heat flux at subfloor centre	
RH30	Relative humidity near SE corner	
RH31	Relative humidity near NW corner	
RH32	Relative Humidity at subfloor centre	
TA30	Air temp near NE corner	IC
TA31	Air temp near SE corner	IC
TA32	Air temp near SW corner	IC
TA33	Air temp near NW corner	IC
TA34	Air temp near east wall	RTD
TA35	Air temp at subfloor centre	IC
TA36	Air temp at subfloor centre	RTD
TA40	Air temp just behind NW vent	IC
TB30	Globe temp near east wall	RTD
TB31	Globe temp at subfloor centre	RTD
TG30	Underground temp 150mm at subfloor centre	RTD
TG31	Underground temp 600mm at subfloor centre	RTD
TS30	Surface temp of brick, inside east wall	TC
TS31	Surface temp of brick, inside south wall	TC
TS32	Surface temp of brick, inside west wall	TC
TS33	Surface temp of brick, inside north wall	TC
TS34	Underfloor surface temp near E wall	TC
TS35	Ground surface temp near E wall	TC
TS36	Underfloor surface temp at subfloor centre	TC
TS37	Ground surface temp at subfloor centre	TC
TS39	Pier surface temp at subfloor centre	TC
TS40	Temperature embedded in brick, inside east wall	TC
* for temperature sensors only		

In addition to the data recorded by the data acquisition system, wood moisture at six locations was recorded manually. One location was in the room and the other five were in the subfloor. Three

measurements were taken at the subfloor centre in both a joist and the floor board, and the other two subfloor locations were in joists near the northwest and southeast corners. These locations are listed by ID in Table 5.4. The instruments and procedure for obtaining wood moisture is described in Section 5.5.1.

Table 5.4: Wood moisture measurements locations

ID	Description
WM33	Wood moisture. Room, centre, top of floor board
WM30	Wood moisture. Subfloor, centre, north side of joist
WM31	Wood moisture. Subfloor, centre, south side of joist
WM32	Wood moisture. Subfloor, centre, bottom of floor board
WM34	Wood moisture. Subfloor, NW corner, bottom of floor board
WM35	Wood moisture. Subfloor, SE corner, bottom of floor board

The subfloor soil was manually sampled at five locations, all in the northern side of the subfloor. These locations are listed in Table 5.5. The method for calculating soil moisture is provided in Section 5.5.2.

Table 5.5: Soil sample locations

ID	Location from subfloor door
SM1	1.5 m in
SM2	2 m in, 4 m to right
SM3	2 m in, 1 m to right
SM4	1 m in, 2 m to right
SM5	0.5 in from each side at NW corner

The locations of the 50 sensors are shown in Figure 5.1, along with the locations of the six wood moisture probes and the five soil moisture locations.

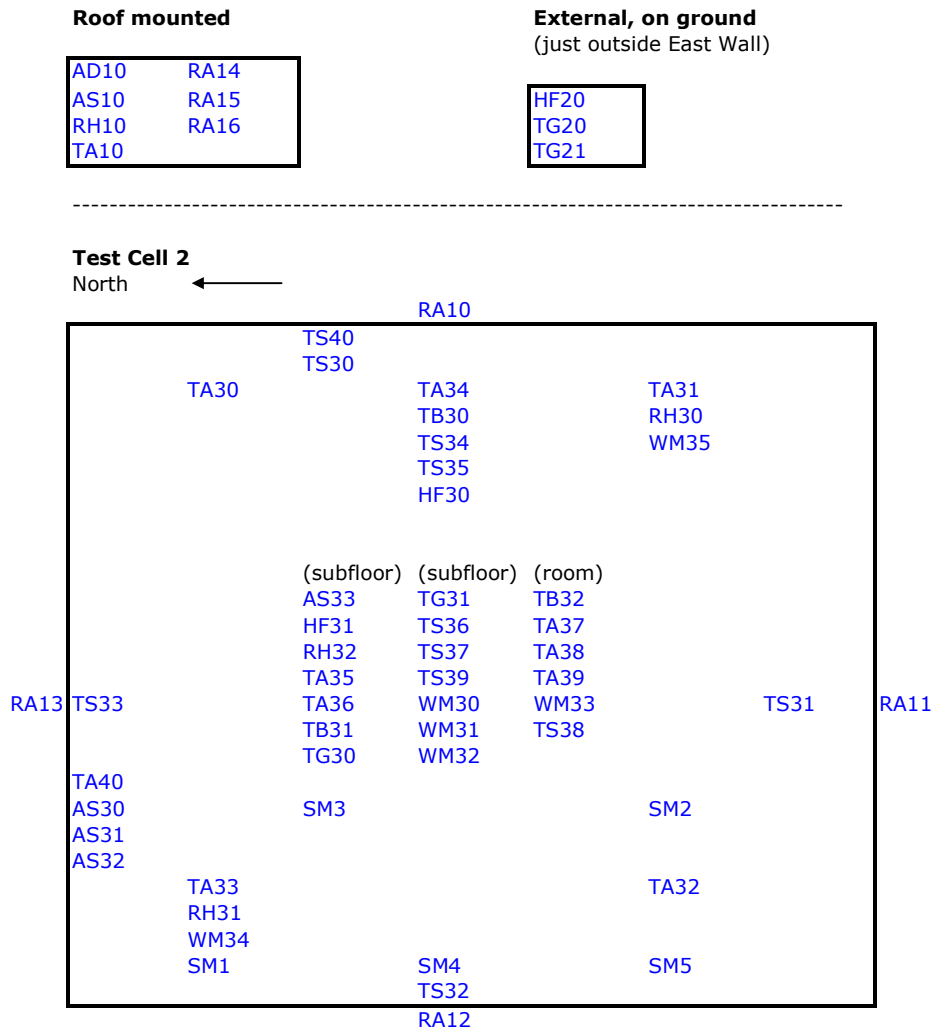


Figure 5.1: Location plan of sensors and wood moisture probes (not to scale)

The majority of the sensors were calibrated, installed, and connected to the data acquisition system by the Launceston instrumentation company Industrial Technik, under guidance of the author. Calibration and sensor accuracy information is provided in Appendix A.2.1. The data acquisition system is described further in Section 5.3.

5.2.2 Weather sensors

The five sensors used for minimum weather measurement were all used in the previous research program on the test cells.

Wind speed (AS10) and direction (AD10) were measured via a Pacific Data Systems PDS-WD/WS-10, with a speed threshold of 0.5 m/s, accuracy of 0.5 m/s and a directional accuracy of 2°. The wind speed is a three-cup array, each cup of 60 mm diameter, and the direction is a 400

mm vane arm. Wind angle was calibrated on-site in April 2011. The sensors were mounted above the roof peak, just to the north. Figure 5.2 shows the sensors and installation.

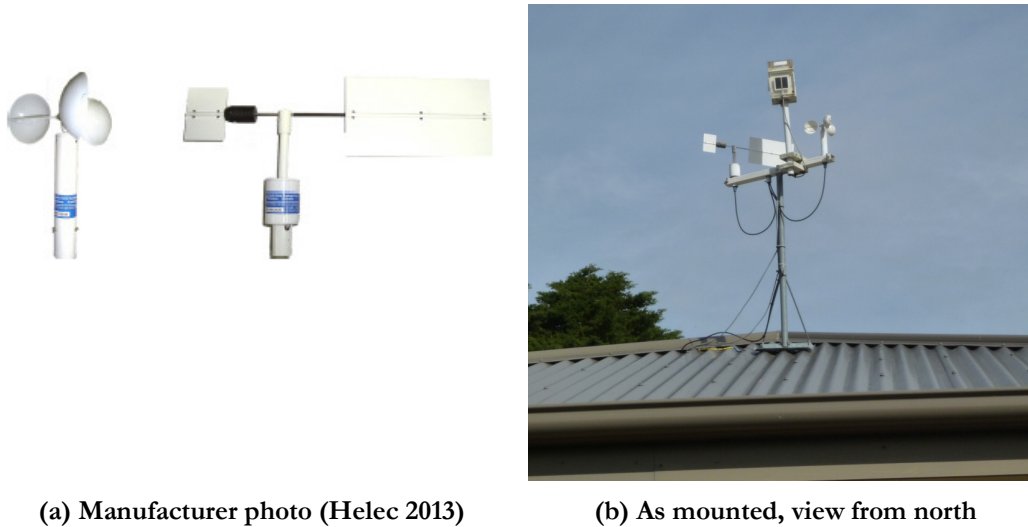


Figure 5.2: Wind speed and direction sensors

The outdoor temperature and humidity (TA10 and RH10) were measured using a Vaisala HUMICAP HMP45A sensor mounted on a pole stand fixed to the fascia board below the gutter on the north side roof near the west side, about 1 m above the roof peak. This is shown in Figure 5.3. The pole was moved in June 2010 from its location at the roof peak where it was mounted during previous research. The sensing elements are underneath a curved shield which protects them from radiation and rain. Both the temperature and humidity sensors were calibrated by Industrial Technik in October 2010.



Figure 5.3: Mounted Vaisala temperature and humidity sensors

Global horizontal irradiance (RA14) which comprises both the diffuse and direct radiation is measured via a SolData 80SPC pyranometer mounted on the wind speed pole facing directly upward. The sensor consists of a photovoltaic cell in a sealed epoxy resin, mounted on a sheet of acrylic. The side of the pyranometer mounting block is visible at the very top of the mounted sensors shown in Figure 5.2(b).

5.2.3 Temperature

All the integrated circuit temperatures were recorded using Analog Devices AD592CN sensors. These had been used in previous test cell research and were all calibrated on-site by researchers from UTAS School of Architecture and Design and Industrial Technik during June 2010, using equipment provided by Industrial Technik. Photographs of a sensor and the thermal calibration block are provided in Figure 5.4. Most of the AD592CN sensors were used to measure dry bulb air temperature. In the subfloor the wiring was attached to the joists such that the sensing element was suspended freely. One AD592CN sensor was used to measure the globe temperature inside the room. Globe temperature is an approximation for mean radiant temperature (Awbi 2003). The globes consisted of 150 mm copper spheres painted with matte black paint, with internal structure to suspend a sensing element at their centre. The globes were fabricated for previous research and their construction is documented elsewhere (Dewsbury 2011). A photo of one is shown in Figure 5.5(a).

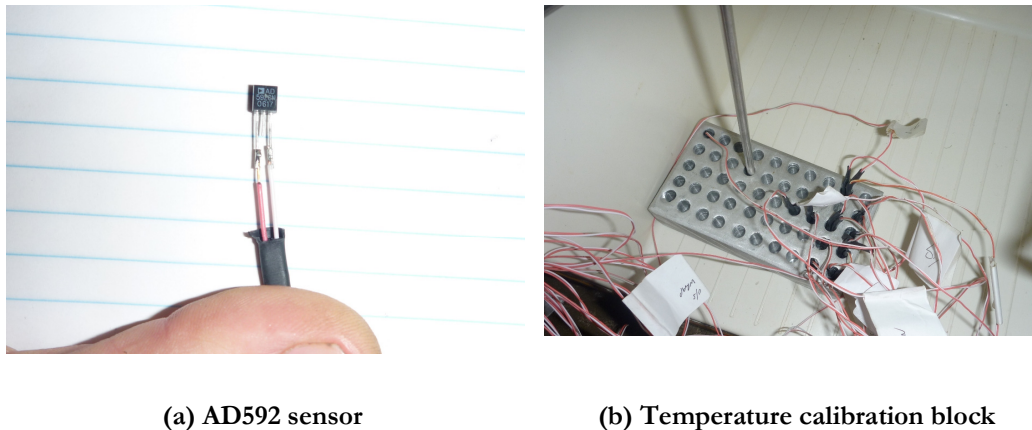


Figure 5.4: AD592 temperature sensors

The RTD temperature measurements were recorded on Pico Technology PT100 sensors. These eight sensors were purchased new via Industrial Technik in October 2010 and were calibrated for the present research in September 2012. All eight PT100 sensors were installed in the subfloor or just outside the east wall of the test cell. Two were used to measure dry bulb air temperature. Two were used to measure globe temperature. The remaining four were used to measure ground temperature. The ground temperature sensors were 150 mm and 600 mm long with the

temperature sensing element at the tip. The ground sensors at the subfloor centre were buried straight down, but those outside the test cell were buried at an angle so that the leads and the body of the sensor would remain underneath the test cell footing and thus be more secure. The sensing elements were still at 150 mm and 600 mm depth below ground surface to be consistent with those ground temperatures at the subfloor centre. A PT100 sensor installed outside for ground temperature measurement is shown during installation in Figure 5.5(b).

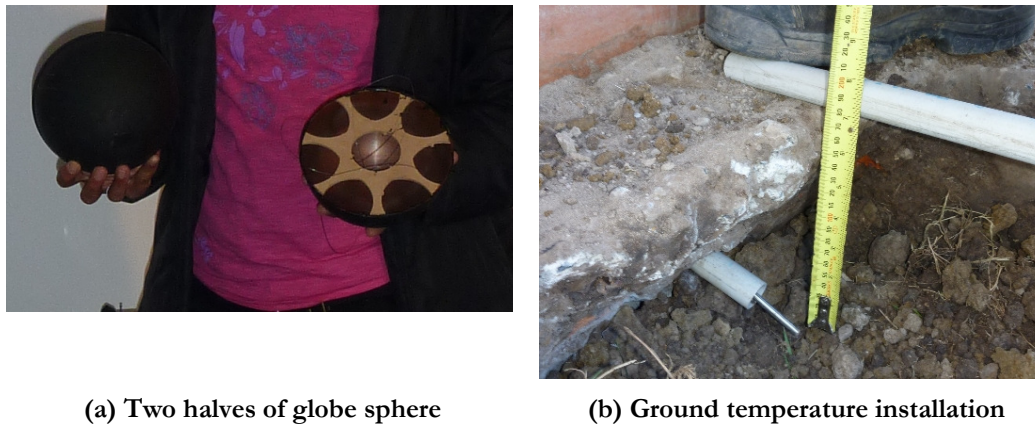


Figure 5.5: PT100 sensors

11 thermocouples were used to measure surface temperatures throughout the subfloor. These were calibrated in September 2012 and frequently had erratic readings. Though the thermocouple data went through the data reduction process of Section 5.4, the results from the thermocouples are not presented in this research.

5.2.4 Humidity

The three humidity sensors installed in the subfloor were Vaisala Humidity Transmitters, HMW40U. They were mounted on the joists at three location to assess the variation in humidity. These were all used in previous test cell research and were calibrated by Industrial Technik in September 2010.

5.2.5 Heat flux

Three new Hukseflux Thermal Sensors HFP01SC were bought for this research. They have the ability to be self-calibrating sensors but that feature was not activated during the duration of this investigation due to programming complications in the data acquisition system. They were calibrated by the vendor in February and March of 2010. The sensor is a ceramic wafer with a conduction similar to that of soil that works by measuring the temperature difference from top to bottom and uses that to calculate the heat flux. A heat flux sensor is shown in Figure 5.6.

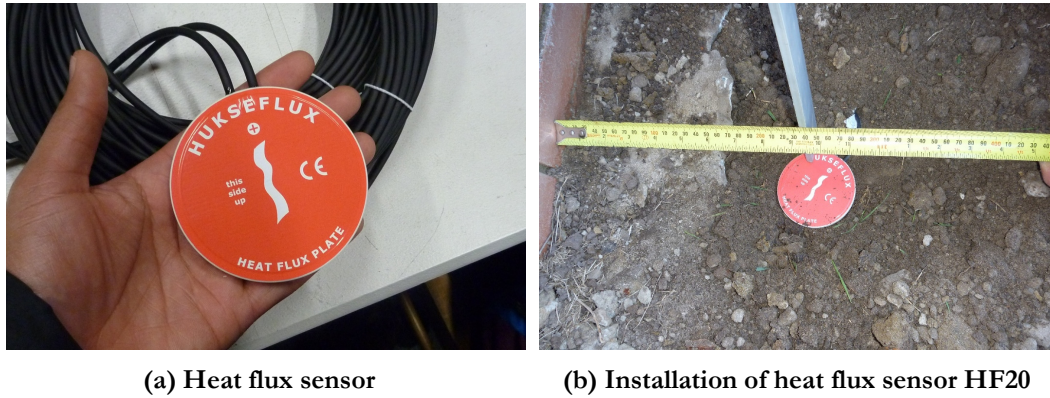


Figure 5.6: Heat flux sensor

5.2.6 Radiation

Radiation was measured on each face of the building using SolData 80SPC Pyranometers, using the same model as used for the global irradiation. Radiation from the roof of the test cell, the normal direct radiation and diffuse radiation, were also recorded.

5.2.7 Air speed

Four anemometers were installed, all TSI Air Velocity Transducer, Model 8455. These are hot-wire anemometers. Three were calibrated in March 2010 and one was calibrated in November 2009. They were stored in closed containers until their installation in December 2010.

5.3 Data acquisition

The data logging units used for this research were dataTaker brand. All were used for previous research on the test cells and were subsequently refurbished before the commencement of the present research. All data loggers were mounted on a table along the south side of the test cell, near the eastern wall. Two DT500 data loggers were used, referred to as DT0 and DT2. A Channel Expansion Module Series 3, referred to as the CEM, was connected to DT0. The fourth data logging unit was a DT80, connected to DT2. The arrangement of data loggers is shown in Figure 5.7 where DT0 is toward the top (west), DT2 is in the middle and the CEM is at the bottom (east). The DT80 is also at the east side and oriented perpendicular to the others. A data acquisition schematic showing the connections from all sensors to the data logging units is provided in Appendix A.2.2.

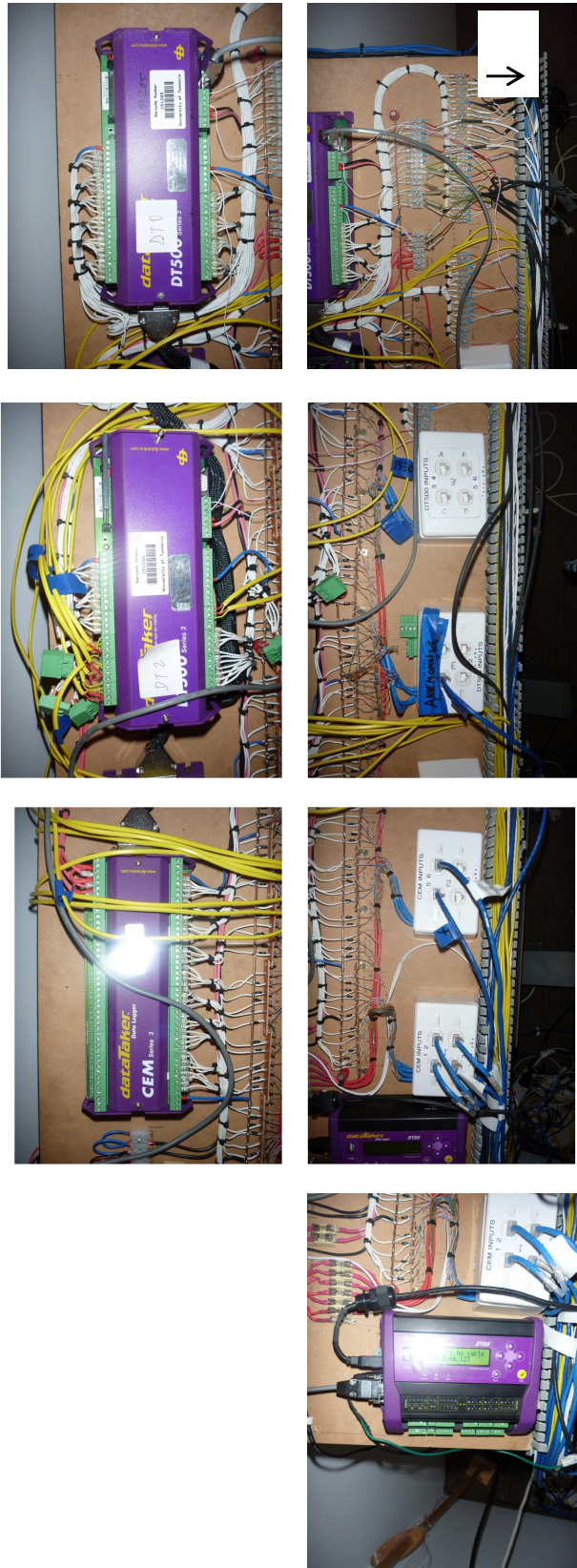


Figure 5.7: Overhead view of data loggers

The dataTaker software (DeTransfer V3.27) enabled communication from a laptop in the test cell to the data loggers. The same laptop was left in the test cell throughout the duration of the test period. Though remote access was possible on these units it was not activated due to programming complications. Communication to the CEM and DT0 was via manual connection from the laptop to the DT0, and similarly communication to the DT80 and DT2 was via connection from the laptop to DT2. Communication with the data loggers consisted of setting the time stamps, uploading programming scripts, and retrieving data. The time stamps on the DT0 and DT2 were manually entered and synchronized to within seconds. Standard time was used throughout this research to avoid any data processing complications due to daylight savings time.

The data acquisition programming scripts uploaded to both DT0 and DT2 are provided in Appendix A.2.2. These two scripts call for the recording of the data from the 50 sensors of Table 5.3 to occur every 10 minutes. Close to the top of each script are lines that begin with “S1=...” or “S15=...”, and so on. These lines contain definitions to convert the raw data to engineering units, or definitions of any linear shifts that need to be applied to the data, such as the application of calibration factors. The IC temperature and heat flux sensors each had individual calibration factors applied via the data acquisition scripts. These lines of script also define engineering units, which are simply text fields added to the end of the data values. There is no inherent meaning to the engineering units. Most of the lines between the “BEGIN” and “END” statements identify which values are to be stored to the data logger memory. These lines of code indicate any specifications about how the data from each channel of the logger is to be recorded, applies any needed conversions as long as they are already defined earlier in the program, and assigns each bit of data its unique 4-character ID. The script uploaded to DT0 identifies sensor values from both the CEM and DT0, where the “1:” at the beginning of a statement refers to the CEM. Thus the line “8+V(S6,“TA10”,X,N)” refers to the “+” port of channel 8 of DT0, whereas the line “1:3-V(S4,“RH30”,X,N)” refers to the “-” port of channel 3 of the CEM. Similar terminology is used in the script uploaded to DT2 to differentiate between sensors wired to DT2 and the DT80.

DT0 and DT2 each had memory cards installed. Data was never manually cleared from the memory cards on the data loggers. When the memory cards reached capacity, the newest data would automatically overwrite the oldest data. The DT2 memory card could hold a much longer date range of data because there were fewer sensors connected to the DT80 and DT2 than to the CEM and DT0.

Data was manually downloaded from the DT0 and DT2 memory cards approximately every 2 ½ weeks during the 1 ½ year research period, a total of 33 times. The data file was output in a DeTransfer proprietary format with a .dxd extension (DXD). Each downloaded data set contained the entire sensor set stored on the memory card of that logger, spanning from a time far back

enough to duplicate what had previously been downloaded, to the present time. On a few occasions the time between downloads was inadvertently left too long and the earliest data from DT0 and the CEM were overwritten on the memory card and thus irretrievable.

5.4 Data reduction

5.4.1 Data handling and error checking

The data from all 50 sensors have undergone the data reduction process described in this section, though the results from some sensors, such as the thermocouples and some pyranometers, are not presented.

Soon after download each data file was converted from the DXD format to a comma-separated variable (CSV) format, and then read into Excel. Excel 2003 was mostly used. The files were organized with each row representing the date and time, and each column representing a different sensor's value. If a datum was missing the cell was left blank. An Excel script was then run to identify any missing time steps or duplicated time steps. Errors caught during this process were then corrected manually. On a few occasions the downloaded data were corrupt with the presence of too many or missing commas. Sometimes the data was salvageable. A visual inspection of the data in Excel was also performed to ensure that the values did not mistakenly shift into neighbouring columns. This was a manageable task as each downloaded data file contained approximately 4,500 rows of data.

The next step was to add another column to both the DT0 and DT2 downloaded data spreadsheets for "Notes" representing nuances in the data. A Note was added to each row of data as required. For example, Note 002 indicated that people may have been inside the test cell and Note 006 indicated that the heat flux sensor values were still in mV and not engineering units. A total of 16 Notes were used during the duration of the investigation. Some time ranges had multiple Notes in effect while many had none.

Once the downloaded data from each logger passed inspection and had the appropriate Notes indicated, it was then fused into a master data spreadsheet. The column locations for each sensor in the DXD and CSV files remained constant throughout the test period as they were driven by the data acquisition scripts. This minimized the chances for data fusion errors to occur. Nevertheless, every time new data was fused into the master spreadsheet, numerous spot checks of the data were performed to ensure no errors had been made.

From the master spreadsheet, batch alterations were then made to the data. These alterations occurred for two reasons. The first was to correct for "Noted" issues. For example data marked with Note 006 had the heat flux values converted from mV to the engineering units of kW/m², and

then had the value of 006 removed from the note field. The second reason was to apply calibration factors to a sensor if it was not already loaded into the data logging scripts. The wind direction (AD10) sensor is one that was calibrated in the master data spreadsheet. A log of all alterations was kept, including the date the alteration was made and the affected rows of data. A portion of the master spreadsheet of data is shown in Figure 5.8. Some columns were no longer used but were still retained. The best date and time is in Column A, Notes are in Column F, and sensor data starts in column with Column G, though column H was ignored. In the small time period sampled as an example in Figure 5.8, the HF20 sensor data in Column G was not available.

At this stage the master spreadsheet contained approximately 4 million bits of data. This was proving unwieldy for a visual program like Excel, so the data was saved as a CSV file which could then be read easily into other programs. Several programs were then considered for bulk data processing, including Matlab, R, SAS and SPSS. All four have statistical capability, but Matlab and R have superior graphical capability. Both Matlab and R have large, varied user bases. R was selected for the processing of the data, because it was free of cost, and the known willingness of other R users to provide assistance with troubleshooting coding errors. R version 2.13.0 was used with the 'chron' and 'openair' packages installed. All scripts used in this research were written by the author specifically for this research.

A data reduction process then commenced with the first goal of scouring the 10-minute interval data for errors. Five R scripts were written to support this task: `instr_range.R`, `instr_step.R`, `instr_maxmin.R`, `instr_graphs.R` and `instr_ave.R`. Those five scripts along with other files that they reference are included in Appendix A.2.2. An overview of the error-checking process is shown in Figure 5.9. The data file is input through several data checking processes, with versions backed up at every step.

	A		B		C		D		E		F		G	H	I	J	K	L	M
1	DTstandard		DTmeas		Day		Date		Time		Note		HF20	HF20HEATER	TG20	TG21	RA14	RA15	RA16
2	2011/02/24	12:10	2011/02/24	13:10	1	2011.02.24	2011.02.24	13:10	13:10	003-014-015	NA	NA	NA	-0.046	17.8	18.1	0.696	0.404	-0.321
3	2011/02/24	12:20	2011/02/24	13:20	1	2011.02.24	2011/02/24	13:20	13:20	003-014-015	NA	NA	NA	-0.046	17.8	18.1	0.475	0.278	-0.271
4	2011/02/24	12:30	2011/02/24	13:30	1	2011.02.24	2011/02/24	13:30	13:30	003-014-015	NA	NA	NA	-0.047	18.0	18.3	0.483	0.278	-0.287
5	2011/02/24	12:40	2011/02/24	13:40	1	2011.02.24	2011/02/24	13:40	13:40	003-014-015	NA	NA	NA	-0.043	17.9	18.1	0.963	0.658	-0.231
6	2011/02/24	12:50	2011/02/24	13:50	1	2011.02.24	2011/02/24	13:50	13:50	003-014-015	NA	NA	NA	-0.043	18.0	18.2	0.748	0.568	-0.2
7	2011/02/24	13:00	2011/02/24	14:00	1	2011.02.24	2011/02/24	14:00	14:00	003-014-015	NA	NA	NA	-0.044	17.9	18.1	0.989	0.705	-0.163
8	2011/02/24	13:10	2011/02/24	14:10	1	2011.02.24	2011/02/24	14:10	14:10	003-014-015	NA	NA	NA	-0.045	18.0	18.1	1.043	0.727	-0.181
9	2011/02/24	13:20	2011/02/24	14:20	1	2011.02.24	2011/02/24	14:20	14:20	003-014-015	NA	NA	NA	-0.044	18.1	18.2	0.929	0.577	-0.282
10	2011/02/24	13:30	2011/02/24	14:30	1	2011.02.24	2011/02/24	14:30	14:30	003-014-015	NA	NA	NA	-0.048	18.0	18.2	0.651	0.426	-0.241
11	2011/02/24	13:40	2011/02/24	14:40	1	2011.02.24	2011/02/24	14:40	14:40	003-014-015	NA	NA	NA	-0.048	18.1	18.1	0.367	0.226	-0.249
12	2011/02/24	13:50	2011/02/24	14:50	1	2011.02.24	2011/02/24	14:50	14:50	003-014-015	NA	NA	NA	-0.047	18.1	18.3	0.554	0.342	-0.287
13	2011/02/24	14:00	2011/02/24	15:00	1	2011.02.24	2011/02/24	15:00	15:00	003-014-015	NA	NA	NA	-0.046	18.2	18.2	0.455	0.274	-0.274
14	2011/02/24	14:10	2011/02/24	15:10	1	2011.02.24	2011/02/24	15:10	15:10	003-014-015	NA	NA	NA	-0.047	18.2	18.2	0.339	0.198	-0.217
15	2011/02/24	14:20	2011/02/24	15:20	1	2011.02.24	2011/02/24	15:20	15:20	003-014-015	NA	NA	NA	-0.048	18.2	18.2	0.319	0.169	-0.208
16	2011/02/24	14:30	2011/02/24	15:30	1	2011.02.24	2011/02/24	15:30	15:30	003-014-015	NA	NA	NA	-0.049	18.3	18.2	0.345	0.174	-0.218
17	2011/02/24	14:40	2011/02/24	15:40	1	2011.02.24	2011/02/24	15:40	15:40	003-014-015	NA	NA	NA	-0.045	18.2	18.1	0.336	0.182	-0.217
18	2011/02/24	14:50	2011/02/24	15:50	1	2011.02.24	2011/02/24	15:50	15:50	003-014-015	NA	NA	NA	-0.045	18.3	18.2	0.322	0.167	-0.213
19	2011/02/24	15:00	2011/02/24	16:00	1	2011.02.24	2011/02/24	16:00	16:00	003-014-015	NA	NA	NA	-0.043	18.3	18.1	0.352	0.188	-0.223

Figure 5.8: Master spreadsheet of data in 10-minute increments

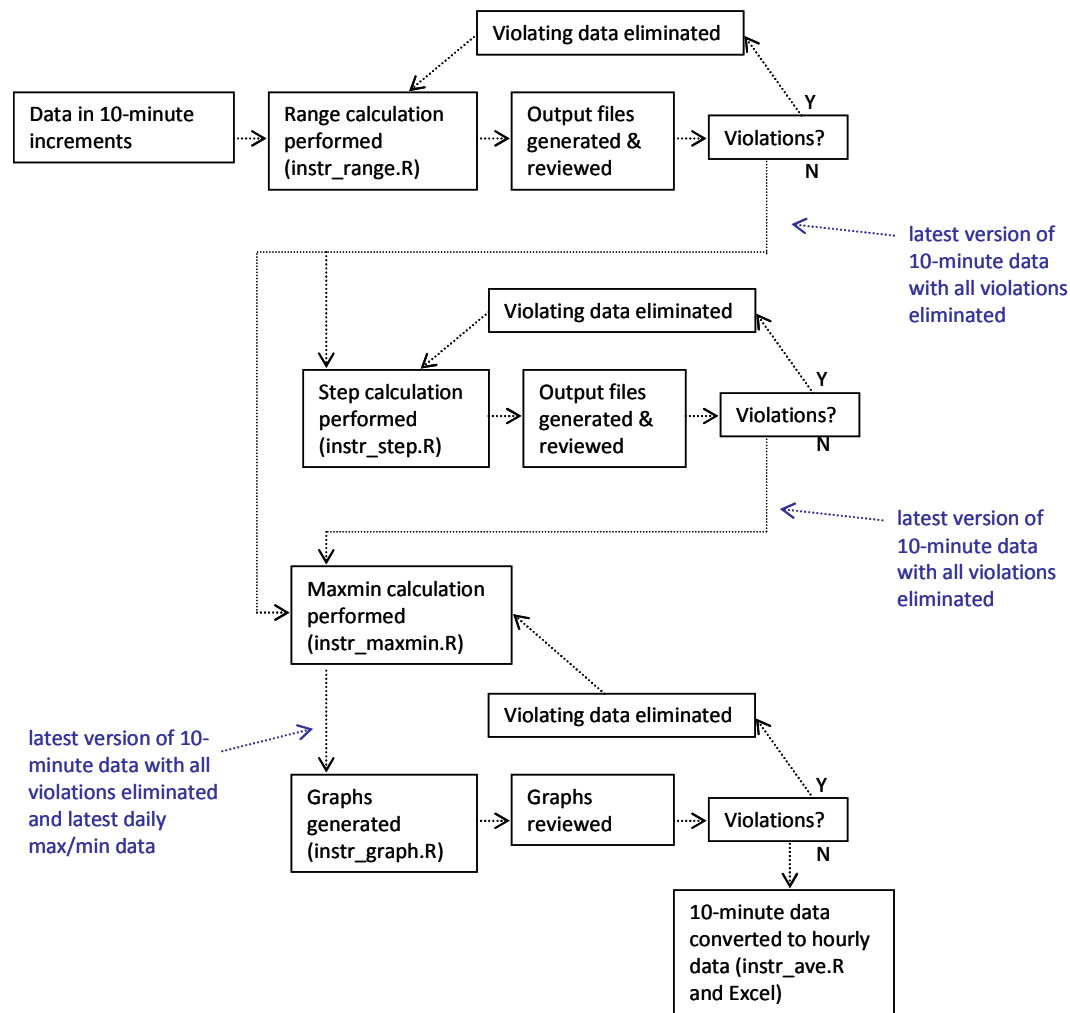


Figure 5.9: Process map for error-checking 10-minute interval data

The first stage of error checking was the range check. This was performed by the `instr_range.R` script, which read in the 10-minute interval data in CSV format. The purpose of the range check was to compare each sensor's value to a pre-defined minimum and maximum limit of acceptable values. The limits were defined based on known sensor values from previous experimentation. The script took approximately 90 minutes to run and when completed it produced a summary table as shown in Figure 5.10. The summary table lists the sensors in the order they appear in the master spreadsheet and in all subsequent CSV data files. It then states the minimum and maximum sensor limits and the number of input rows of data. Figure 5.10 shows only 62,135 input rows of data for each sensor because of row number limitation in Excel 2003. A subsequent running of the `instr_range.R` script then contained the additional 19,513 rows of data. The summary table then lists the sum of missing values found, and finally the number of range violations.

Summary of Range Violations Check. Run at Fri Oct 19 14:55:30 2012

Parameter	Min	Max	# Inputs	# NA	# Violations
HF20	-50	50	62135	6935	3259
TG20	5	25	62135	6935	0
TG21	5	25	62135	6935	0
RA14	-1.3	1.3	62135	6935	10
RA15	-1.3	1.3	62135	6935	0
RA16	-1.3	1.3	62135	6935	0
RH10	35	100	62135	6935	3202
TA10	-5	38	62135	6935	0
RA10	-1.3	1.3	62135	6935	0
RA11	-1.3	1.3	62135	6935	0
RA12	-1.3	1.3	62135	6935	0
RA13	-1.3	1.3	62135	6935	0
AS33	0	5	62135	6935	39097
HF30	-10	10	62135	6935	0
HF31	-10	10	62135	6935	69
RH30	35	100	62135	6935	0
RH31	35	100	62135	6935	0
RH32	35	100	62135	6935	0
TA30	-5	38	62135	6935	0
TA31	-5	38	62135	6935	0
TA32	-5	38	62135	6935	0
TA33	-5	38	62135	6935	0
TA35	-5	38	62135	6935	0
TA36	-5	38	62135	6935	0
TG30	7	23	62135	6935	0
TG31	7	23	62135	6935	0
AS30	0	5	62135	6935	12355
AS31	0	5	62135	6935	11578
AS32	0	5	62135	6935	13448
TB32	-5	38	62135	6948	0
TA37	-5	38	62135	6948	0
TA38	-5	38	62135	6948	0
TA39	-5	38	62135	6948	0
TA40	-5	38	62135	6948	0
AD10	0	360	62135	3817	134
AS10	0	16	62135	3816	3632
TA34	-5	38	62135	3799	0
TB30	-5	38	62135	3799	0
TB31	-5	38	62135	3799	0
TS30	0	38	62135	3799	0
TS31	0	38	62135	3799	0
TS32	0	38	62135	3799	0
TS33	0	38	62135	3799	0
TS34	5	25	62135	3799	1611
TS35	5	25	62135	3799	859
TS36	5	25	62135	3799	1359
TS37	5	25	62135	3799	27
TS38	5	25	62135	3799	1827
TS39	5	25	62135	3799	816
TS40	0	38	62135	3799	171

Figure 5.10: Range check summary

The easiest method to investigate each sensor's violations was to look through the violations output file that `instr_range.R` produced for each sensor. A portion of one file is shown in Figure 5.11. The file lists the date and time, with the date always in year-month-day format, original sensor value, then outputs a range error indication by a 1 in the error column if an error is present, and a 0 if not. The next column, titled correction, is the column where violating data is corrected. The default values are the original sensor values. In the example of Figure 5.11 some negative air speed values in error were corrected back to 0, under advisement from instrumentation technicians. Other times, when the data were unsalvageable an "NA" was place in the correction column, to make clear that the data was intentionally omitted. This method was used because the R program identifies missing data with either a blank space or an NA. In many cases, the error violation did not indicate an instrumentation error, but indicated that the expectations of what the sensors' value should have been were incorrectly set. Thus if the values appeared reasonable, for example high internal temperatures on a hot summer afternoon, then limits were re-adjusted and the `instr_range.R` script was re-run.

DTstandard	orig	error	correction
2011.03.04 06:00	0.1	0	0.10
2011.03.04 06:10	0.16	0	0.16
2011.03.04 06:20	0	1	0.00
2011.03.04 06:30	-0.03	1	0.00
2011.03.04 06:40	0.15	0	0.15
2011.03.04 06:50	-0.03	1	0.00
2011.03.04 07:00	-0.03	1	0.00
2011.03.04 07:10	0.03	0	0.03

Figure 5.11: Portion of AS30 range check sensor violations output file

Once all the violations for each sensor were investigated, the corrected values for each amended sensor were fused back into the master data file. The entire column of data was transferred every time in order to reduce the likelihood of mistakes. Then the range checking process was repeated on the amended data. The output from the second pass was first checked to ensure that data amendments were correctly entered. Only two passes were needed for the range check, though additional passes were performed out of curiosity. Logs were retained of all sensor amendments.

The next stage of error checking was the step check. The purpose of this was to determine if a sensor's value changed too quickly for a 10-minute interval. This iterative process was conducted similarly to the range check. An output summary table was created, a portion of which is shown in Figure 5.12.

```

Summary of Step Violations Check. Run at Tue Jan 15 16:46:08 2013
Parameter MaxStep # Inputs # NA # Violations
TA30      1.2      62135      6940      60
TA31      1.2      62135      6940      65
TA32      1.2      62135      6940      36
TA33      1.2      62135      6940      62

```

Figure 5.12: Portion of step check summary table

Each sensor's violations were listed in a spreadsheet, an example of which is shown in Figure 5.13. In this example, the errors indicated that the step limits were too strictly set. Four iterations of step checks were run on the 10-minute interval data, with all amendments to the data logged.

```

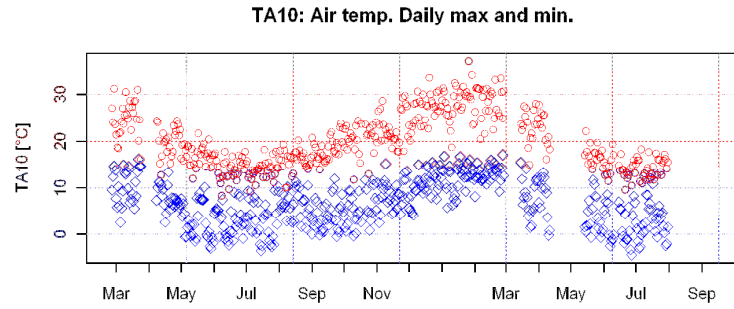
DTact      orig      step      error      upload
2011.03.17 09:00     -9.7      0.7        0      -9.7
2011.03.17 09:10     -8.6      1.1        0      -8.6
2011.03.17 09:20     -6.6      2.0        0      -6.6
2011.03.17 09:30     -4.0      2.6        1      -4.0
2011.03.17 09:40     -0.7      3.3        1      -0.7
2011.03.17 09:50      2.9      3.6        1       2.9
2011.03.17 10:00      6.7      3.8        1       6.7
2011.03.17 10:10     10.4      3.7        1     10.4

```

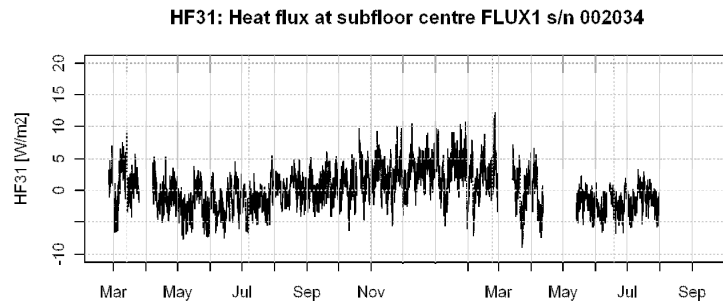
Figure 5.13: Portion of HF20 range check sensor violations output file

Due to the nature of some of the step errors, it was useful to conduct the step checks and graphical checks concurrently. Before the graphical checks could be performed, the data underwent another set of calculations. These calculations found each sensor's daily minimum and daily maximum values, called the daily maxmin data. If a sensor had any missing data on a single day, then neither the maximum nor minimum value were calculated for that sensor for that day. The R script to perform this is `instr_maxmin.R`.

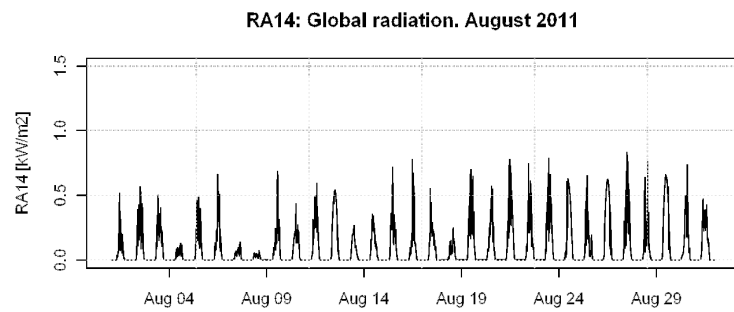
The maxmin data and the latest 10-minute interval data were input into the R script, `instr_graph.R`, used to create graphs. The graphing script employed a series of nested loops to create four types of graphs, termed the maxmin graphs, the alldata graphs, the monthly graphs and the weekly graphs. These graphs were created for all 50 sensors though they contained data for only one sensor at a time. The maxmin graphs contained the maxmin data and spanned the entire test period. The alldata graphs contained the 10-minute interval data and also spanned the entire test period. The monthly and weekly graphs both contained the 10-minute interval data separated into monthly or weekly batches. A total of approximately 4,850 of these single-sensor graphs were generated each of the four times the graphical checks were performed. These instrumentation-checking graphs are not included in the Appendix but an example of each type of graph is provided in Figure 5.14.



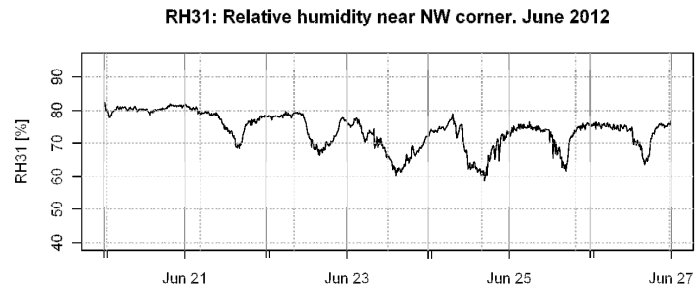
(a) Maxmin



(b) Alldata



(c) Monthly



(d) Weekly

Figure 5.14: Graphical instrumentation checks

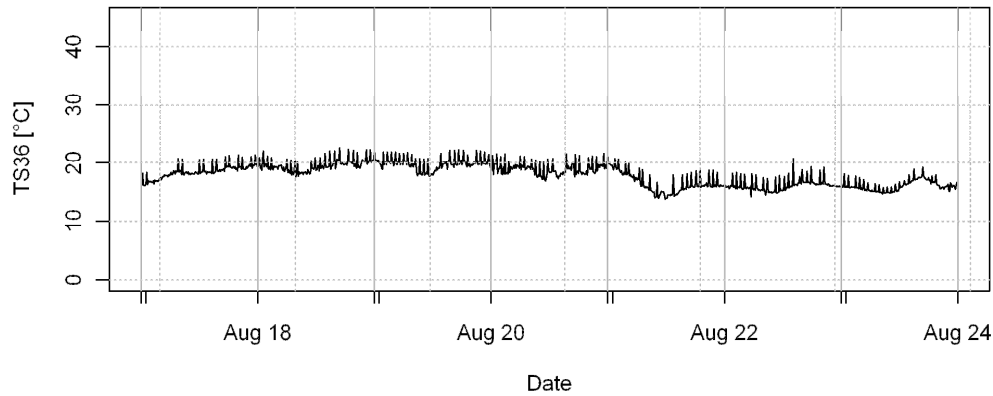
The thermocouples had an excessive amount of scatter and they required additional assessment. Weekly graphs showing several batches of thermocouples together were generated and assessed. The generation of these graphs was also performed via the `instr_graph.R` script provided in Appendix A.2.2. All the generated graphs were visually assessed by the researcher, though sometimes only for seconds since there were nearly 20,000 in total. Nevertheless, the process was effective at identifying abnormalities in the data that either the range checking or steps checking missed. In the event that the graphical checks identified data that were questionable and needed to be deleted, the sensor's step check output files were altered. Thus, there were an equal number of passes through the step checks and graphical checks.

The thermocouple data displayed intermittent spikes and so formulae were written in Excel to identify data spikes. These formulae were included into the step check output file for each thermocouple in question. An example of thermocouple spiking and the correction is shown in Figure 5.15. For many thermocouples several passes of spike correction were needed.

Once all the error checks on the 10-minute interval data were complete, the data were then averaged into hourly intervals. This task completed the process shown in Figure 5.9. Instead of averaging it would have been an easier task to sample the data at hourly intervals, and there are advantages and disadvantages associated with each method. Averaging the data lessens the effect of poor quality or missing data points, however it dampens values that may change quickly with time, such as global radiation between 8 and 9am. In previous research (Dewsbury 2011; Geard 2011) an average was used and therefore that method was selected for the present research.

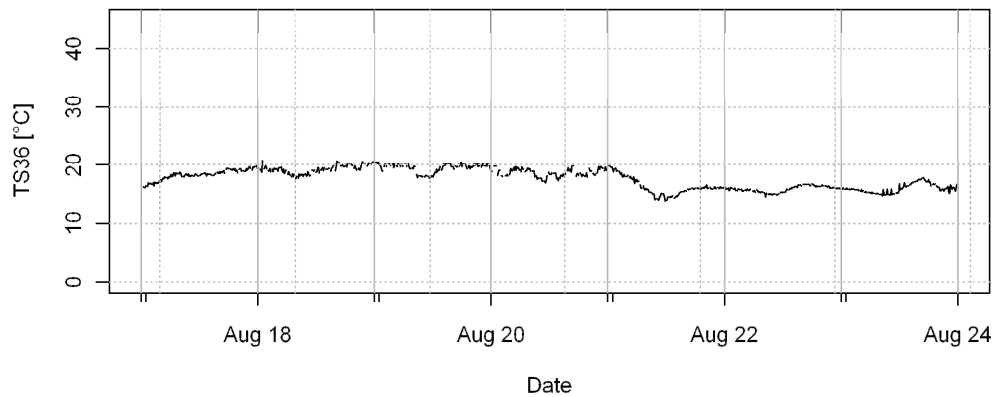
The averaging for most sensors was performed by the R script `instr_ave.R`. The average for each hour comprised values from 20 minutes before the hour to 30 minutes after the hour. For example the 11:00am data was an average of the data at 10:40, 10:50, 11:00, 11:10, 11:20 and 11:30. In the event that any of those six values were missing, the average was calculated based on the remaining values. Wind velocity, measured by wind speed and wind direction, required special treatment as the scalar function of averaging does not apply readily to vector quantities. There are several methods for performing this function, and it was decided to repeat what previous test cell researchers (Geard 2011) had done. Thus average hourly wind speed was a simple scalar average as for the vast majority of the other sensors. However average hourly wind direction was calculated manually in Excel. It was taken as the angle of the resultant vector formed by the summation of the six input wind vectors. Thus, average hourly wind direction was a function of both the 10-minute wind speed and wind direction.

TS36: Underfloor surface temp at subfloor centre. August 2011



(a) Before correction

TS36: Underfloor surface temp at subfloor centre. August 2011



(b) After correction

Figure 5.15: Thermocouple spiking

Once the hourly averaging was complete, the error checking process of Figure 5.9 was repeated on the hourly data. This required a slight modification to the range checking script, the step checking script and the maxmin script to account for the change in number of data points. No change was needed for the graphing script. The summary output files from the range check and step check were viewed, as well as the more than 4700 resulting graphs. As expected, there were no new errors discovered in the hourly data, and the error checking process was deemed complete.

5.4.2 Summary of data and anomalies present

The reduced data set contained values for 50 sensors spanning 13,609 hours, though there were many patches of missing data for various sensors. There were five notes remaining in the data. One note indicated that people were present in the test cell and/or the lights were on. Another note indicated that the door had been opened as people entered or exited the test cell. There are few instances of either of these notes occurring and as the effect of these situations on the subfloor was expected to be minimal, they are mostly disregarded. The third note indicated if the local time was on daylight savings. This note assisted in data processing and did not affect the quality of the data.

The two remaining notes indicated issues that would possibly have a larger affect on the data and they had to be dealt with more rigorously. One issue is that for a long portion of the test period a ground cover was left in the subfloor, as shown in the photograph of Figure 5.16 which was taken from just inside the subfloor door. The ground cover was a thin plastic sheet about 1 metre wide, running the length of the east side of the ground, from the subfloor door on the north nearly reaching the south wall. Approximately 1/5 of the ground surface was covered. The sheet was not pulled flat nor was it sealed at the edges, and there were several air pockets between the sheet and the ground. This was not expected to have a large effect on the bulk air properties of the subfloor, but it was expected to have a localized effect on the moisture and heat transfer under the sheet. When the sheet was removed on 22nd February 2012 a musty smell was noted and there was visible moisture on the ground where the sheet had been. The discovery of the plastic sheet did not extend the test period, though it did add a level complexity to the processing and analysis of the results, as provided in Section 6.2.4.



Figure 5.16: Ground cover in subfloor

The second issue is that the ceiling hatch cover was left off, thus allowing the possibility of free air movement between the test cell room and the roof cavity. The photo of Figure 5.17 shows the missing 600 mm square ceiling hatch, though this photo was taken before the test period commenced and as such there are other items strewn about the test cell room. The ceiling hatch was put back on about one month after the ground cover was removed. This was expected to influence the room temperature but not have a considerable affect on the subfloor air temperature.



Figure 5.17: Missing ceiling hatch

The final reduced data set was organized into three time periods, denoting what issues were present. A summary is provided in Table 5.6. Time Period 1, TP1, spans the first year of the test period and comprises the time when the ceiling hatch was off and the ground cover was on. Time Period 2, TP2, includes the few weeks when the ground cover was removed but the ceiling hatch was still off. Time Period 3, TP3, contains the last several months when both the ground cover was off and the ceiling hatch was on.

Table 5.6: Time periods for reduced data set

Time Period	Dates	Weeks	Ceiling Hatch	Ground Cover
TP1	2011/Feb/24 00:00 - 2012/Feb/22 15:00	1 - 52	Off	On
TP2	2012/Feb/22 16:00 - 2012/Mar/22 11:00	52 - 57	Off	Off
TP3	2012/Mar/22 12:00 - 2012-Sep-13 00:00	57 - 81	On	Off

The data spanned a total of 81 weeks, 568 days, though not all weeks contained valid data.

5.5 Additional measured data and calculations

This section describes data obtained in addition to the 50 sensors recorded by the data acquisition system, such as the wood moisture, soil moisture and purchased weather measurements. This section also describes various calculations summarized by the top three boxes in the Analysis column of Figure 3.2. Most of the calculations described in Sections 5.5.3 through 5.5.5 were performed in R via the script `ana_calcs.R`, which is in Appendix A.2.2.

5.5.1 Wood moisture

Wood moisture was measured using a Deltron DCR22 Timber moisture meter as shown in Figure 5.18(a). Wood moisture sensors are essentially multimeters that work by measuring the electrical conductivity of the wood or measured medium, then correlating that resistance to a moisture content. The probe consists of two metal prongs which are placed on or into the medium to be tested. To simplify the measurement method for the current research, pairs of silica bronze nails were permanently inserted into six different locations in the test cell. Wires attached to the nails were led back to a readout box inside the test cell, shown in Figure 5.18(b). Readings were taken manually throughout the test period by touching the sensor probes to the corresponding pins in the readout box. Data samples were taken sporadically throughout the test period.

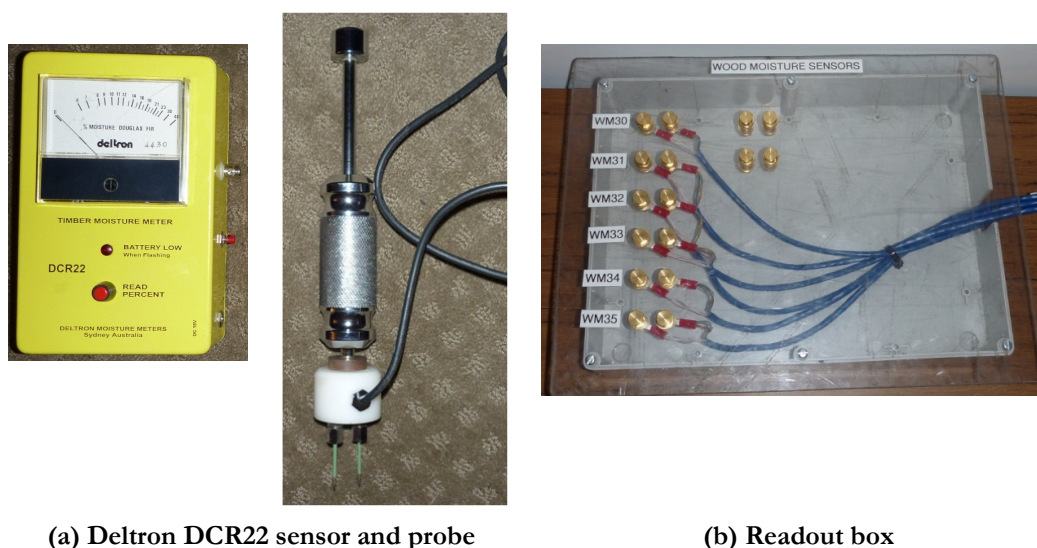


Figure 5.18: Wood moisture sensing

5.5.2 Soil moisture

Soil samples were taken on 22nd February 2012, immediately after the ground sheet was removed. About 200 grams were taken at each of the five locations listed in Table 5.5. Sample SM1 was taken from an area that the ground sheet had covered, and SM3 was taken at the edge of the area where the ground sheet had covered. The samples were enclosed in sealed plastic bags until the test start date of 20th March 2012.

Soil moisture content was measured according to the procedure described in Australian Standard 1289 (2000), which involved heating the soil to a temperature of 110 °C for 24 hours and measuring the reduction in mass, which equates to evaporated moisture. The oven used was the Qualtex 5076 at the University of Tasmania School of Engineering Geomechanics Laboratory. Three samples from each of the five locations were tested. The samples were each placed in small

metal dishes then placed on the same tray and heated together. Photos of the oven and samples are shown in Figure 5.19.

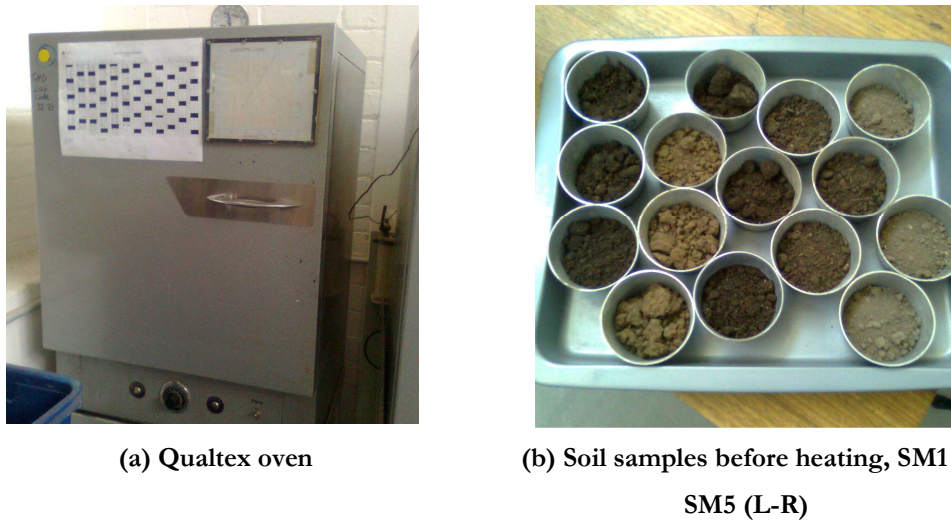


Figure 5.19: Soil moisture test

5.5.3 Additional weather data and calculations

The purchase of additional weather data was required to supplement the on-site observed data. Calculations based on the purchased and on-site weather data were needed for calculating other weather parameters of interest, some of which were to be inputted into AccuRate.

A data set was purchased from the Bureau of Meteorology, BOM. The data were recorded from the Launceston Airport Weather Station, Station Number 091311, a distance of approximately 14 kms from the test cell. The parameters purchased were mean sea level air pressure and precipitation since 9am. Cloud cover was desired but it was not available.

The data set required slight manipulation. Firstly it had to be converted from half hourly to hourly. The data was averaged in Excel. Averaging was used instead of simply sampling the hourly values to match the processing of the site-measured data. The weighting of each hourly value was 50% from the current hour, 25% from the previous half hour and 25% from the following half hour, with missing values omitted from the calculation.

Once the data was in hourly format it was truncated to match the exact hours of the total test period and was then merged with the site-measured data using R. Then the air pressure was manipulated. BOM measures total air pressure at altitude then increases it to correct for that altitude, providing the pressure at sea level. To conform with the site-measured data this pressure

needed to be corrected back to the altitude of the test cell, 15 m. To do this the pressure was reduced by 1.19 kPa for every 100 m (Cengel and Boles 2006), a minor adjustment.

Once the air pressure was known, specific humidity of both the outdoor air and subfloor air could be calculated. Specific humidity for the outdoor air was calculated as follows (Cengel and Boles 2006):

$$\omega_{os} = \frac{0.622 \times P_{v,os}}{P_T - P_{v,os}} \quad 5.1$$

where ω_{os} is the specific humidity of the outdoor air [kg moisture/ kg dry air]; 0.622 is the ratio of the gas constants of air and water; $P_{v,os}$ is the vapour pressure of the outdoor air [kPa]; and P_T is the total air pressure [kPa]. $P_{v,os}$ is a function of the outdoor air dry bulb temperature and relative humidity.

Diffuse and direction radiation also needed to be calculated. First was the diffuse radiation. To do this the BRL model was used (Boland 2013; Lauret, Boland, and Ridley 2010). The format of the model was an Excel program with an embedded Visual Basic macro. The model inputted the global radiation at every hour as measured on-site, as well as the latitude and longitude of the test cell. The model provided the diffuse solar fraction for every hour, which was then multiplied by the global radiation to arrive at the diffuse radiation. The model automatically corrected the data at low sun angles, though this correction required manual manipulation in work by previous researchers (Dewsbury 2011).

Once diffuse radiation was found, direct radiation could be found as they are related through the equation (Batlles et al. 2000):

$$DirectRadiation = GlobalRadiation - \frac{DiffuseRadiation}{\sin(SolarAltitude)} \quad 5.2$$

where all radiation terms are in the units of W/m². Solar altitude for a reference meteorological year, RMY, was used and it was sourced from the default climate file used in AccuRate. The diffuse and direct radiation data were then merged with the other observed data using R.

Additional calculations were then performed on the weather data. Wind speed measured at the building height was projected to the meteorological height of 10 m. This involved multiplying the measured speed by a factor of 1.36, as derived in Section 4.4. Wind direction was sorted into groups, or bins, for easier handling and ease of inputting into AccuRate. There were 16 bins total, each representing a circular segment of 22.5°. If the wind speed was zero then the wind bin was 0.

Otherwise, bins 1 through 16 were assigned such that bin 16 indicated a wind from the north, bin 4 indicated wind from the east, bin 8 indicated a wind from the south and bin 12 indicated a wind from the west. At this point, all the weather parameters needed for AccuRate were calculated, though formatting of the weather data as described in Section 5.6.3 was still required.

5.5.4 Environmental temperature

From the observed data, temperatures for the room and subfloor had to be identified to compare to AccuRate's output temperatures. However, the temperature AccuRate outputs does not relate directly to dry bulb temperature but rather it is similar to what is known as environmental temperature, also referred to as equivalent temperature. Environmental temperature is a combination of dry bulb air temperature and mean radiant temperature. Environmental temperature better represents a person's thermal comfort than dry bulb temperature alone, as it accounts for heat transfer not only due to convection but to radiation as well (Williamson 1984).

Mean radiant temperature can be approximated by globe temperature, the temperature inside a black matte sphere, in contrast to dry bulb temperature which is generally measured in the free stream air and shielded from radiation. Globe and dry bulb temperatures are affected differently by weather conditions. If both measurements are taken concurrently in a room, direct sunlight would have the effect of increasing the globe temperature greatly but would only have a secondary effect on the dry bulb temperature. Research on test houses (Geard 2011) where the interior was exposed to solar radiation shows that the globe temperature is higher than the dry bulb air temperature, and that this difference is due to solar gain. Any air movement in the room would have a greater effect on the dry bulb temperature than the globe temperature. Previous research considering the test cell room (Dewsbury 2011) references literature to show that the test cell room dry bulb and globe temperatures were expected to be equal

For this research where neither the room nor subfloor is subjected to direct sunlight, and even in the subfloor which is subject to slight air movement, it is not expected that the values for dry bulb temperature and globe temperature would differ greatly.

Environmental temperature is calculated as a weighted sum of the mean radiant temperature and dry bulb temperature, where the weighting depends on the heat transfer coefficients of radiation and convection, respectively. Although previous research on the test cells considered only dry bulb temperature (Dewsbury 2011), it was confirmed with CSIRO that environmental temperature was the best temperature to use for comparison with AccuRate (Chen 2013a). The formula for environmental temperature used in this research is (Williamson 1984):

$$T_E = \frac{6}{5}T_{MR} - \frac{1}{5}T_{DB} \quad 5.3$$

where T_E is the environmental temperature, T_{MR} is the mean radiant temperature, and T_{DB} is the dry bulb temperature, all in °C. Globe temperature and dry bulb temperature were measured in both the room and subfloor, with the globe temperature approximating the mean radiant temperature. The dry bulb temperature of the subfloor was taken from the subfloor centre RTD sensor, TA36, and the dry bulb temperature of the room was the average of the three IC dry bulb temperature sensors at different heights: TA37, TA38 and TA39. The averaging of the three dry bulb temperatures was done to account for temperature stratification as recommended by CSIRO in previous test cell research (Dewsbury 2011).

5.5.5 Air, moisture and energy flows

The rate of ventilation through the subfloor was calculated as a linear function of the windspeed. The windspeed at meteorological height in m/s was multiplied by 1.7 then an adder of 3.3 was applied to arrive at the ventilation in ACH. These values were derived from the tracer gas test and were provided in 4.5 of Section 4.6.

The mass of moisture in the subfloor cavity air was calculated as a function of the dry bulb temperature and relative humidity of the subfloor air. First the saturation pressure was found from thermodynamic tables as a function of the dry bulb temperature (Cengel and Boles 2006). This was multiplied by relative humidity to yield the vapour pressure. With the vapour pressure calculated, the total air pressure known, the dry bulb temperature measured and the subfloor volume a known constant of 20.04 m³, the mass of moisture in the subfloor cavity air was then calculated using the ideal gas law. The mass of moisture in a subfloor-sized volume of outdoor air was calculated using the same procedure as a function of the measured outdoor temperature and relative humidity.

The mass of moisture exiting the subfloor cavity through the vents in kg/hour was then calculated as the product of the mass of moisture in the subfloor in kg and the rate of subfloor ventilation in ACH. Key to this calculation was the assumption that the subfloor air had adequate mixing. Similarly, the mass of moisture entering the vents was calculated using the same method but instead substituted the mass of moisture in a subfloor-sized volume of outdoor air. For that calculation, it was assumed that the outdoor air at the weather station represented the properties of the air outside the subfloor vents. The net moisture exiting the vents was then found as the difference between the mass of moisture exiting and entering.

To calculate the amount of ground moisture evaporation, the law of conservation of mass was applied to the subfloor cavity. The flows of moisture through the subfloor cavity are shown

schematically in Figure 5.20, where the net evaporation represents the amount of evaporation minus the amount of condensation, and the moisture storage rate represents the change in moisture in the subfloor air over time.

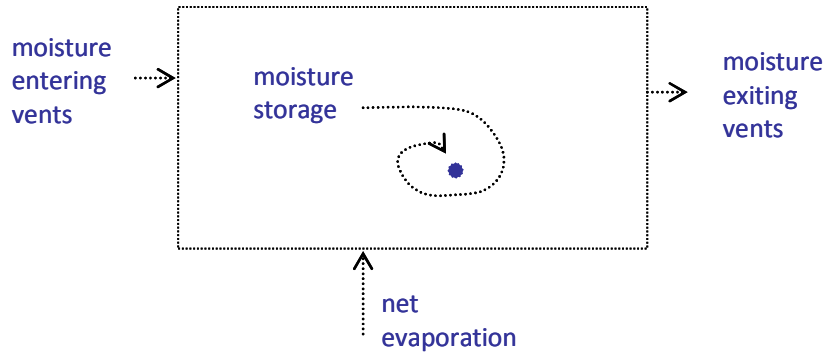


Figure 5.20: Flow of water through subfloor

According to the law of conservation of mass, the mass entering a control volume equals the sum of what exits the control volume plus the net amount of mass that gets stored inside (Cengel and Boles 2006). Pertaining to the subfloor cavity the conservation of mass for water thus becomes (Sequeira et al. 2010b):

$$\dot{m}_{w,in} + \dot{m}_{evap} = \frac{\partial[m_{w,sf}]}{\partial t} + \dot{m}_{w,out} \quad 5.4$$

where $\dot{m}_{w,in}$ is the mass flowrate of water entering the subfloor cavity via the vents [kg/hour];

\dot{m}_{evap} is the mass flowrate of water via evaporation from the ground or other surfaces in the

subfloor [kg/hour]; $m_{w,sf}$ is the total mass of water present in the subfloor cavity [kg]; $\frac{\partial[m_{w,sf}]}{\partial t}$

is the rate of change of mass of water present in the subfloor cavity [kg/hour], or the net rate of

water storage into the subfloor; and $\dot{m}_{w,out}$ is the mass flowrate of water exiting the subfloor cavity

via the vents [kg/hour]. This equation is equivalent to that provided in Equation 2.5 (Kurnitski and

Matilainen 2000). \dot{m}_{evap} was then calculated from Equation 5.4 as the three other terms had already been calculated.

As Figure 5.20 shows, moisture is introduced into the subfloor by two means: the subfloor vents and evaporation from the ground or other subfloor material. Most of the evaporation is assumed to come from the ground as exposed wood is expected to change its moisture content very slowly in relation to the other moisture flows.

Subfloor ground moisture evaporation has been predicted to be a function of the vapour pressure deficit, which is the difference between the saturation pressure of air at the ground temperature and the vapour pressure of the air in the subfloor cavity. This relationship is described in Section 2.3.2. These pressures take into account the air and ground temperatures and air and ground moistures. However, considering only these influences for evaporation is a simplification of a complex system, as ground evaporation rate is also influenced by other environmental factors including radiation, air speed at the surface and amount of moisture present (Strangeways 2003). More complex evaporation models exist which tie in these additional environmental factors and predict evaporation to be a function of the pressure deficit multiplied by an air speed term, then added to a radiation term (Shuttleworth 2007).

The subfloor cavity is not exposed to solar radiation, and the amount of moisture present in the subfloor ground is not known. But what has been measured is the wind speed. It is therefore expected that evaporation would not only correlate with the pressure deficit, but also with the product of pressure deficit and wind speed. This product is termed the evaporation potential.

The amount of energy in the subfloor air is the sum of the energy in the dry air and the energy contained in the water vapour. In equation form this is:

$$H_{sf} = m_{a,sf} h_{a,sf} + w_{sf} m_{a,sf} h_g \quad 5.5$$

where H_{sf} is the total enthalpy of the subfloor cavity air [kJ]; $m_{a,sf}$ is the mass of dry air in the subfloor cavity [kg]; $h_{a,sf}$ is the enthalpy of the dry air in the subfloor cavity [kJ/kg]; w_{sf} is the specific humidity of the subfloor air [kg moisture/ kg dry air]; and h_g is the enthalpy of saturated vapour [kJ/kg]. All the terms on the right hand side are found using general psychrometric methods (Cengel and Boles 2006) and are functions of atmospheric pressure, subfloor temperature and relative humidity, and the volume of the subfloor. Thus, the total enthalpy of subfloor air can be calculated. Similarly, the total enthalpy in a subfloor-sized volume of outdoor air was found using the air properties measured on the roof-mounted weather station.

The rate of energy exiting the subfloor cavity through the vents was then calculated as the product of the enthalpy of the subfloor air and the rate of subfloor ventilation. Similarly, the rate of energy entering the subfloor cavity through the vents was calculated as the product of the enthalpy of the subfloor-sized volume of outdoor air and the subfloor ventilation. The net energy exiting the vents was then found as the difference between the energy exiting and entering.

5.5.6 Daily maximum and minimum calculation

Once all the calculations were performed on the observed data, the daily maxima and minima of certain parameters were calculated and combined with daily extrema of the directly measured

values to create the observed daily “maxmin” data set. If a parameter is missing at any hour then neither the maximum nor the minimum was calculated for that day. This task was performed by the script `ana_maxmin.R` and is provided in Appendix A.2.2. This script has higher algorithmic efficiency than does the similar script used in the data reduction of instrumentation.

5.6 Generation of AccuRate data

AccuRate data are now generated to represent the actual construction of the test cell and the weather conditions it encountered. This fulfils the last Analysis task shown in Figure 3.2. The method for generating AccuRate data to match experimental data has been well documented in recent publications (Dewsbury 2011; Geard 2011). The procedure used in this research follows suit with deviations noted.

5.6.1 Overview of method for running AccuRate

In typical use the inputs to AccuRate are a building’s design and location. The following information is input into the program: the building’s dimensions, materials and orientation; the location via postcode; site information including exposure, ground reflectance, which depends on area ground cover, and shading; and actual building construction details such as gaps around doors and windows.

AccuRate assumes typical standard material properties unless these have overridden by the user. The RMY climate conditions for 69 climate zones each compiled from at least 25 years of BOM data are pre-loaded into the program and AccuRate selects the pertinent one based on the input post code. The program then makes assumptions about the building residents’ preferences and behaviour. Heat loads representing appliance use, people and lighting are added to various zones at various hours depending on the zone type. Occupancy settings for thermal comfort are also maintained. For living spaces, a minimum temperature of 20 °C is maintained from 7am until midnight. Sleeping spaces are maintained from 4pm to 9am and the minimum temperature varies by hour from 15 °C to 18 °C. The programs assumes the residents would open windows when possible for cooling and would other times use mechanical heating and cooling to maintain the temperature within the comfort bands (DCCEE 2012).

The program then outputs the annual sum of energy usage required to maintain the thermally comfortable interior. It also outputs the hourly temperatures in each zone of the building.

The AccuRate program had to be modified from that of standard usage to represent the unique circumstances of this test situation. Atypical AccuRate modifications pertaining to this research program are summarized in Table 5.7. The unique circumstances of this research are listed in the first column. The AccuRate inputs required to incorporate these circumstances are listed in the

second column and they are sorted as to whether or not they are standard inputs that can be modified by the typical user via AccuRate's graphical user interface, GUI. There was no way to represent either the missing ceiling hatch or the subfloor ground cover in AccuRate. The method of integrating these AccuRate inputs are discussed in Sections 5.6.2 and 5.6.3.

Table 5.7: Atypical AccuRate inputs for this research

Test circumstance	AccuRate input	Type of input *	
		Standard	Non - standard
Framing factor known, missing panels	Adjust building fabric	x	
Free-running (no space conditioning)	Bypass thermostat settings		x
No occupants, no appliances	Bypass heat addition		x
Actual ventilation known	Override default ventilation		x
Actual on-site weather data known	Override RMY climate data		x
Ceiling hatch missing for part of test	None		
Ground cover in place for part of test	None		

* A standard input can be modified by the typical user

AccuRate was run twice to achieve two different outcomes. The first run was AccuRate Run 1, AR1, with the purpose of closely matching the previous research performed on the test cell. The second run was Accurate Run 2, AR2, which incorporated some corrections to better represent the test cell. The differences between AR1 and AR2 are provided in Section 5.6.4. The AccuRate inputs for both runs are in Appendix A.3.

For both runs AccuRate Version 1.1.4.1 was used, which uses Engine 2.13. This was the same version used in previous research on the test cell (Dewsbury 2011) and was the current version accredited by the Australian government (DCCEE 2012). The data reduction procedure for both runs of AccuRate is provided in Section 5.6.5.

5.6.2 Standard AccuRate inputs

Information is input into AccuRate via the following tabs on the GUI panel: Project, Constructions, Zones, Shading, Elements and Ventilation. The program's help menu provides assistance on what information is required for each tab. The AccuRate inputs for this research were based on those used for previous test cell research (Dewsbury 2011) then modified as needed. The GUI panel inputs for both AR1 and AR2 are provided in Appendix A.3.

Atypical inputs entered via the GUI panel include adjustments to building fabric to match observed precise framing factors and missing wall panels.

The framing factor represents the ratio of wall area with framing to the entire wall area and adjustments to framing factor can make a substantial difference to the total thermal resistance of a building element (Dewsbury et al. 2009). The framing factor for this test cell was calculated during previous test cell research using photographs taken during construction. This was then converted

to adjusted wall thermal resistance values using the isotherm planes method in preference to the parallel paths method. This adjusted thermal resistance value was then translated to a revised wall thickness and was input into AccuRate as such. A similar method was used to obtain revised floor and ceiling thicknesses (Dewsbury 2011). The framing factor adjustments are provided in Table 5.8.

Table 5.8: Framing factor material thickness adjustments

Construction	Material	Thickness (mm)	
		Original	Revised
Floor	Particle board	21	19
North Wall	Rockwool insulation	83	61
South Wall	Rockwool insulation	83	59
Ceiling	Glass fibre insulation	176	158

Adjustments to the area of the north and south test cell walls were needed to account for missing plasterboard panels. Each the north and south wall are missing two panels summing to 0.2 m². The missing north wall panels are visible in Figure 5.17 and the missing south panels are shown in Figure 5.21. This photo was taken while the data logging system was under configuration and during the test period the data logger table was directly in front of the panels.

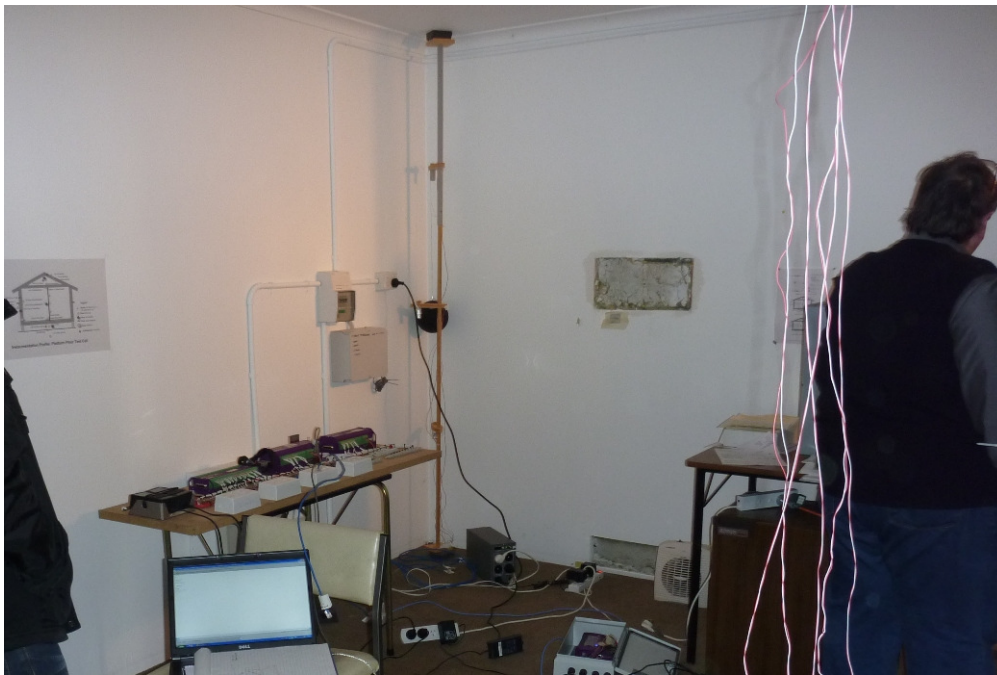


Figure 5.21: Missing plasterboard panels on south wall

The missing panels were incorporated into AccuRate by defining a new wall construction that was missing the plasterboard, as shown in Figure 5.22. Each the north and south external walls had the lengths of existing wall shortened by 0.08 m (Walls 1 and 3) and had 0.08 m of the new wall

inserted (Walls 5 and 6) to include a new wall area of 0.20 m² while keeping the gross wall area for each side constant.

Test cell: External walls main data						
Wall	Construction	Azi (deg.)	L (m)	H (m)	Area (gross) (m ²)	Area (net) (m ²)
1	brick veneer framing factor East west no	0	5.40	2.44	13.18	13.18
2	brick veneer framing factor East west no	90	5.48	2.44	13.37	13.37
3	Brick veneer Wall Bridged South	180	5.40	2.44	13.18	11.45
4	brick veneer framing factor East west no	270	5.48	2.44	13.37	13.37
5	north wall without plasterboard (base wa	0	0.08	2.44	0.20	0.20
6	south wall without plasterboard (base wa	180	0.08	2.44	0.20	0.20

Figure 5.22: Incorporating missing plasterboard panels into AccuRate

5.6.3 Non-standard AccuRate inputs

Not all required edits could be implemented through the AccuRate GUI. When AccuRate runs it accesses several other files. One is the scratch file and one is the climate file. Edits to both of these files were needed for this research. The typical user would not normally edit these files.

The first non-standard edit was to bypass the thermostat settings to represent the free-running condition. The thermostat settings are defined in the scratch file. They represent the occupancy settings as described in Section 2.2.1 and Section 5.6.1. The default thermostat settings of Figure 5.23(a) show that the thermostat settings are not active during the early hour of the morning, denoted by 0.0, but then the comfort range of 20.0 °C to 22.5 °C is set. These settings are modified in the appropriate section of the scratch file as shown in Figure 5.23(b) to set all temperatures to zero, disabling the temperature control. The effect of this edit is to bypass the addition of energy to control the temperature, allowing the resulting temperature to fluctuate unhindered.

```

C      Heating thermostat settings [hours 1-12]
3 1501 0.0 0.0 0.0 0.0 0.0 0.0 0.0 20.0 20.0 20.0 20.0 20.0
C      Heating thermostat settings [hours 13-24]
3 1502 20.0 20.0 20.0 20.0 20.0 20.0 20.0 20.0 20.0 20.0 20.0
C      Cooling thermostat settings [hours 1-12]
3 1503 0.0 0.0 0.0 0.0 0.0 0.0 0.0 22.5 22.5 22.5 22.5 22.5
C      Cooling thermostat settings [hours 13-24]
3 1504 22.5 22.5 22.5 22.5 22.5 22.5 22.5 22.5 22.5 22.5 22.5
C

```

(a) Default

```

C      Heating thermostat settings [hours 1-12]
3 1501 0.0 0.0 0.0 0.0 0.0 0.0 0.0 0.0 0.0 0.0 0.0
C      Heating thermostat settings [hours 13-24]
3 1502 0.0 0.0 0.0 0.0 0.0 0.0 0.0 0.0 0.0 0.0 0.0
C      Cooling thermostat settings [hours 1-12]
3 1503 0.0 0.0 0.0 0.0 0.0 0.0 0.0 0.0 0.0 0.0 0.0
C      Cooling thermostat settings [hours 13-24]
3 1504 0.0 0.0 0.0 0.0 0.0 0.0 0.0 0.0 0.0 0.0 0.0
C

```

(b) Modified

Figure 5.23: Bypassing thermostat settings in scratch file

The effect of this thermostat setting can be seen in one of the AccuRate output files, energy.txt, as shown in Figure 5.24. This shows a portion of the file summarizing the amount of energy required to maintain the test cell within the comfort band zone. This file shows that for the entire test period no energy is added.

```

Total number of conditioned zones = 1

Month Day Hour      ----      Test cell---
                        Heat      Cools      CoolL
2 24 0      0.0      0.0      0.0
2 24 1      0.0      0.0      0.0
2 24 2      0.0      0.0      0.0
2 24 3      0.0      0.0      0.0
2 24 4      0.0      0.0      0.0
2 24 5      0.0      0.0      0.0
2 24 6      0.0      0.0      0.0
2 24 7      0.0      0.0      0.0
2 24 8      0.0      0.0      0.0
2 24 9      0.0      0.0      0.0
2 24 10     0.0      0.0      0.0
2 24 11     0.0      0.0      0.0
2 24 12     0.0      0.0      0.0
2 24 13     0.0      0.0      0.0
2 24 14     0.0      0.0      0.0
2 24 15     0.0      0.0      0.0

```

Figure 5.24: Energy usage for space conditioning

The next non-standard edit was to bypass heat addition. AccuRate models a heat gain as both sensible and latent heat to represent the heat given off by the building's occupants and appliances. This value was changed to be a constant 30 W sensible heat gain, to represent the heat released by the data logging equipment. The change was integrated into AccuRate via an edit to the scratch file, with the appropriate relevant sections of both the default scratch file and edited scratch file provided in Figure 5.25. The changes to the scratch file in order to bypass the thermostat settings and heat gain were performed in previous research on the test cell (Dewsbury 2011).

```

C      Sensible internal heat gain (watts), [hours 1-12]
3  1401  100  100  100  100  100  100  100  460  160  113  113  113
C      Sensible internal heat gain (watts), [hours 13-24]
3  1402  113  113  113  113  113  175  1175  325  325  100  100
C      Latent internal heat gain (watts), [hours 1-12]
3  1403  0  0  0  0  0  0  0  273  73  37  37  37
C      Latent internal heat gain (watts), [hours 13-24]
3  1404  37  37  37  37  37  55  655  55  55  55  0  0
C

```

(a) Default

```

C      Sensible internal heat gain (watts), [hours 1-12]
3  1401  30  30  30  30  30  30  30  30  30  30  30  30
C      Sensible internal heat gain (watts), [hours 13-24]
3  1402  30  30  30  30  30  30  30  30  30  30  30  30
C      Latent internal heat gain (watts), [hours 1-12]
3  1403  0  0  0  0  0  0  0  0  0  0  0  0
C      Latent internal heat gain (watts), [hours 13-24]
3  1404  0  0  0  0  0  0  0  0  0  0  0  0
C

```

(b) Modified

Figure 5.25: Bypassing heat addition in scratch file

The third non-standard AccuRate input was the overriding of default ventilation values to match the observed ventilation. The ventilation models for the roof, room and subfloor of the test cell are provided in the scratch file. Each model provides the zone ventilation as a linear function of meteorological wind speed. The model takes the wind speed, applies a reduction factor, $WsRed$, to arrive at wind speed at the building eaves height. It then applies a scalar, B , and an adder, A , to arrive at zone ventilation in air changes per hour. The model in equation form is identical to Equation 4.3 with the *terrain_{eaves}* term renamed to $WsRed$. The values for A , B and $WsRed$ are defined in the scratch file and the appropriate section of the scratch file containing default values of 0.67, 1.56 and 0.67 respectively for the subfloor zone is provided in Figure 5.26. As discussed in Section 4.5 the value of 0.67 of $WsRed$ can be verified by projecting the windspeed at eaves height of 3 m from the meteorological height of 10 m.

```

C Name, volume, infiltration data, wind speed reduction factor, typ
C      Name  Vol  A  B  WsRed  Type  EstSG  FlorZ  G
3  3      Sub Floor  20.0  0.67  1.56  0.67SubFlA  1  6

```

Figure 5.26: Default subfloor ventilation model

The scratch file is then modified to integrate the observed subfloor ventilation with values as shown in Figure 5.27. Other research projects requiring the modification of AccuRate's default ventilation models (Dewsbury 2011; Geard 2011) used this approach. The product of B , 2.53, and

WsRed, 0.67, yields 1.7 which matches the scalar in Equation 4.5. Similarly the A value of 3.29 matches the adder in Equation 4.5.

```
C Name, volume, infiltration data, wind speed reduction factor, typ
C      Name      Vol      A      B WsRed  Type EstSG FlorZ G
3   3      Sub Floor  20.0  3.29  2.53  0.67SubFlA      1      6
```

Figure 5.27: Modified subfloor ventilation model

The tracer gas ventilation test described in Chapter 4 yielded results for the roof and room of the test cell as well as for the subfloor. The data for the roof and room were reduced and input into AccuRate for this research as well as the test cell research of others (Dewsbury 2011). A summary of the ventilation model values for all zones is provided in Table 5.9. The AR1 and AR2 ventilation values are compared to default AccuRate values and values used in previous research on the test cell (Dewsbury 2011). In previous research the observed ventilation scalar for all zones was mistakenly input as a function of meteorological wind speed instead of eaves-height wind speed. This error was subsequently repeated in other building research programs (Geard 2011). It was confirmed by CSIRO (Chen 2013b) that indeed the ventilation scalar must be input as a function of eaves-height wind speed not the meteorological wind speed, and that correction is evident in the scalars of AR2 being higher. The ventilation values of AR1 match those of previous research, though they are modified slightly to keep only two digits after the decimal point as in the default model.

Table 5.9: Ventilation models

Zone	Default		Previous research (Dewsbury 2011)		AR1		AR2	
	A*	B*	A	B	A	B	A	B
Room	0.12	0.04	0.00	0.021	0.00	0.02	0.00	0.03
Roof	2.00	1.00	0.40	0.258	0.40	0.26	0.40	0.34
Subfloor	0.67	1.56	3.292	1.91	3.29	1.91	3.29	2.53

* A is an adder, and B is the scalar on eaves-height wind speed

The integration of observed weather data into AccuRate is the last of the non-standard AccuRate inputs and the only one that does not require modification to the scratch file. Based on the input postcode AccuRate selects the appropriate climate file out of 69 climate files consisting of RMY data. For this research the contents of the entire default Launceston climate file have been overwritten with the observed climate data. This process of overriding the default RMY data with observed data has been documented elsewhere (Dewsbury 2011; Geard 2011) though this research streamlines the process with the use of R scripts.

The default climate file contains the RMY data for every hour of the year, starting the 1st of January. The file is a text file where each row is 54 characters long and each row represents one hour. The beginning of the Launceston climate file is shown in Figure 5.28.

```

LT930101 0 141 90 994 36136111111 0 0 0 0 011119
LT930101 1 144 92 994 32166111111 0 0 0 0 011119
LT930101 2 146 91 994 28166100000 0 0 0 0 011119
LT930101 3 147 96 993 23166111111 0 0 0 0 011119
LT930101 4 147 98 993 17156111111 0 0 0 0 011119
LT930101 5 147101 993 15158100000 8 7 2 411711119
LT930101 6 147102 994 9158111111 97 81 861410811119
LT930101 7 152105 994 7158111111 264153 31225 9911119
LT930101 8 168108 995 10158000000 459167 55836 9011119
LT930101 9 178109 994 14154111111 635177 67647 7911119
LT93010110 197110 994 22143111111 763211 68658 6411119

```

Figure 5.28: Default climate file

The formatting of the climate file is described extensively in other publications (Dewsbury 2011; Geard 2011) and is summarized in Table 5.10.

First the length of the climate file was adjusted to exactly match the test period. This process was done by hand as it simply required doubling the length of the file, then truncating the beginning and end to achieve the required 13,609 rows. The start date and time of midnight on 24th February 2011 exactly matched the observed data but the end date and time of the lengthened climate file was midnight 14th September 2012, one day later than that of the observed data due to the observed data encompassing a leap year. The lengthened climate file was named climate23_long.txt.

Table 5.10: Climate file format (Geard 2011)

Columns 1 and 2 contain a two letter code for the site (eg HO for Hobart)
Columns 3 and 4 contain the last two digits of the year number eg 07 for 2007
Columns 5 and 6 contain the month number (zero-filled) eg 01 for January
Columns 7 and 8 contain the day number (zero-filled) eg 01 for first of the month
Columns 9 and 10 contain the hour number 0-23 (0=midnight, 1=1am etc)
Columns 11 to 14 contain the Dry Bulb (Air) temperature in tenths of degrees C
Columns 15 to 17 contain the Moisture Content in tenths of g per kg
Columns 18 to 21 contain the Atmospheric (Air) Pressure in tenths of kPa
Columns 22 to 24 contain the Wind Speed in tenths of metres per second
Columns 25 to 26 contain the Wind Direction 0-16 (0=CALM, 1=NNE, ..., 16=N)
Column 27 contains the Cloud Cover 0-8 (0= no cloud; 8= full cloud)
Column 28 contains the Flag for Dry Bulb Temp. (0=Actual, 1=Estimated)
Column 29 contains the Flag for Moisture Content (0=Actual, 1=Estimated)
Column 30 contains the Flag for Atmospheric Pressure (0=Actual, 1=Estimated)
Column 31 contains the Flag for Wind Speed (0=Actual, 1=Estimated)
Column 32 contains the Flag for Cloud Cover (0=Actual, 1=Estimated)
Column 33 contains the Flag for Wind Direction (0=Actual, 1=Estimated)
Columns 34 to 37 contain Global Solar Radiation on a horizontal plane (Wh/m ²)
Columns 38 to 40 contain Diffuse Solar Radiation on a horizontal plane (Wh/m ²)
Columns 41 to 44 contain the Normal Direct Solar Radiation (Wh/m ²)
Columns 45 to 46 contain Solar Altitude in degrees (0 to 90)
Columns 47 to 49 contain the Solar Azimuth in degrees (0 to 359, 0=N, 90=E, ...)
Column 50 contains the Flag for Global Solar Radiation. (0=Actual, 1=Estimated)
Column 51 contains the Flag for Diffuse Solar Radiation (0=Actual, 1=Estimated)
Column 52 contains the Flag for Normal Direct Solar Radiation (0=Actual, 1=Estimated.)
Columns 53 and 54 contain the first two digits of the year number, e.g. 20 for 2010
Columns 55 to 60 are blank

Next the default climate data were overwritten. Of all the contents of the climate file, only the data actually used in AccuRate calculations were considered. Manipulation of the climate file was performed by the `ana_climate.R` script, provided in Appendix A.3. This script replaced each row of the lengthened climate file with the observed weather data. This script formats each parameter as required, which includes converting to appropriate units, truncating data and applying fixed-width fields. The source data for this script were the observed data which were either measured on-site or purchased from BOM, some of which then went through the calculations listed in Section 5.5.3.

The observed parameters input to the script as well as their required units and source are provided in Table 5.11.

Table 5.11: Observed weather parameters integrated into AccuRate climate file

Parameters	Unit	Source
Date and time	--	Directly measured
Outside temperature	1/10 °C	Directly measured
Specific humidity	1/10 g moisture / kg dry air	Calculation described in Section 5.5.3
Pressure	hPa or mbar	Calculation described in Section 5.5.3
Windspeed at 10 m	1/10 m/s	Calculation described in Section 5.5.3
Wind direction	constant, 0-16	Calculation described in Section 5.5.3
Cloud cover	constant, 1-8	Constant assumed
Global solar radiation	W/m ²	Calculation described in Section 5.5.3
Diffuse solar radiation	W/m ²	Calculation described in Section 5.5.3
Direct solar radiation	W/m ²	Calculation described in Section 5.5.3

All the observed weather parameters have been discussed except for cloud cover which is used in AccuRate to calculate the night time sky losses. This primarily affects the roof of a building. Cloud cover was not available with the BOM data set. It had been previously shown that cloud cover had a minimal impact on test cell temperatures, and therefore it was expected that the effect on subfloor climate would be reduced further. Therefore, a constant value of 4 was used for cloud cover, representing 50% cloud cover, as had been done in previous test cell research (Dewsbury 2011).

Once the observed data were fused into the climate file, there was no longer the one-day mismatch between the climate and observed dates and times due to the leap year. However, there were now NA values present in the climate file, representing missing weather data. The date and time of each row of data missing any weather parameter was recorded. Then, each row with missing weather data was replaced by the corresponding default data from the lengthened climate file. This way, there were no missing data in the climate file. This replacement of data is also performed in the `ana_climate.R` script provided in Appendix A.3. The replacement of NA values is shown in Figure 5.29.

LT11022421	170	721013	29	54111111	0	0	0	0	011120	
LT11022422	153	731013	7	44111111	0	0	0	0	011120	
LT11022423	128	711013	2	44111111	0	0	0	0	011120	
LT110225	0	120	721013	0	44111111	0	0	0	0	011120
LT110225	1	112	711013	0NA411111	0	0	0	0	0	011120
LT110225	2	108	711013	0NA411111	0	0	0	0	0	011120
LT110225	3	114	751013	8	44111111	0	0	0	0	011120

(a) NA values present

LT11022421	170	721013	29	54111111	0	0	0	0	011120	
LT11022422	153	731013	7	44111111	0	0	0	0	011120	
LT11022423	128	711013	2	44111111	0	0	0	0	011120	
LT110225	0	120	721013	0	44111111	0	0	0	0	011120
LT110225	1	140	451005	0	05111111	0	0	0	0	011119
LT110225	2	136	471005	0	05100000	0	0	0	0	011119
LT110225	3	114	751013	8	44111111	0	0	0	0	011120

(b) NA values replaced with default climate data

Figure 5.29: Replacement of NA values in on-site climate file

5.6.4 Summary of differences between AccuRate runs

The purpose of AR1 is to correspond with the ‘As-Built/Climate’ AccuRate output data provided by a previous research team (Dewsbury 2011). The same version of AccuRate was used, 1.1.4.1, which uses AccuRate Engine 2.13.

The AccuRate input files were kept as similar as possible to those used in previous research and only differed where needed to represent changes in the fabric of the test cell or the climate. An entirely new climate file was prepared for AR1 representing the 2011-2012 observed weather, as described in 5.6.3. The AR1 input file incorporated 10 mm medium-colour carpet and 8 mm underlay as well as the missing wall panels on both the north and south walls. The test cell was not carpeted until mid-2007, which was after the previous research team’s data had already been gathered. In addition, the ventilation scalar and adder were kept nearly the same with the only change being that the values were truncated as shown in Table 5.9.

The purpose of AR2 is to better represent the test cell and climate. The AccuRate input files for this run were based on those for AR1 with modification made as needed. AR2 moves the subfloor access door to the north side from the south side, as it was incorrectly modelled before. The ‘Ventilation’ tab of AccuRate was modified to show the lengths of all sides to be 5.9 m instead of 5.5 m. Also the ventilation scalar on windspeed is increased by 31% as shown in Table 5.9.

5.6.5 AccuRate data reduction

The same data reduction procedure was performed on both AR1 and AR2 output data files. For each run, an output data file containing hourly temperatures in the roof, test cell and subfloor zones for 81 weeks was generated. The data were then compared to the log of missing weather data generated during the creation of the climate file. At any time step containing missing data and for the ensuing 12 hours, the corresponding AccuRate data was deleted and never revisited. The purpose of the 12-hour delay was to mitigate the effect of step changes in the on-site climate file on the AccuRate output data. The script that performed this task is `acc_check.R`, provided in Appendix A.4.

The final AccuRate data set for each AR1 and AR2 spanned 81 weeks though only 57 of those weeks contained data. 48 of those weeks occurred in TP1, 1 occurred in TP2 and 8 occurred in TP3. The 8 weeks in TP3 occur only in winter. AccuRate was unable to properly model the plastic subfloor ground cover or the missing ceiling hatch. Thus the time period best represented by AccuRate is TP3.

The daily maxima and minima for each zone temperature were calculated for each AccuRate run. This task was performed by the script `acc_maxmin.R` and is provided in Appendix A.4.

5.7 Conclusion

The minimum set of sensors and an array of supplementary sensors were installed and gathered data for 1 ½ years. Data purchased from BOM and hand-measurements completed the set of observed data. The data acquisition and reduction procedures were carried out using as many automated processes as possible to minimize manual errors and yield reproducible results. Two runs of AccuRate were performed to satisfy two purposes. Adjustments to the program, outside the capability of the typical user, were introduced to best represent the actual environmental conditions encountered by the test cell. The set of observed data and both sets of theoretical data are prepared for analysis and comparison.

6 • INVESTIGATION 2 RESULTS: SUBFLOOR CLIMATE

6.1 Introduction

Chapter 5 described the procedure for obtaining the Investigation 2 observed data and preparing the corresponding theoretical AccuRate data. The aim of this chapter is to present those results relevant to Research Questions 2, 3 and 4, which pertain to assessing the moisture in the subfloor, the accuracy of AccuRate's predicted subfloor temperature and the methods for improvement to AccuRate's subfloor model.

The outdoor and subfloor climate data are presented and relationships between parameters are investigated. Air, moisture and energy flows between the subfloor and outdoors are next presented. The observed data are then compared to historical data.

Next, the AccuRate data are presented and compared to the observed data and historical data. Differences between the AccuRate and observed data are presented and explored for correlations with outdoor climate conditions.

Finally, a measurement system analysis is presented. Discussion of the results is provided in Chapter 7.

6.2 Presentation of observed data

This section presents the observed test cell data. Data are presented from the entire test period, Time Periods 1, 2 and 3 as defined in Section 5.3, unless otherwise specified. Air temperature refers to dry bulb temperature unless otherwise specified.

Boxplots are often used. The outline of each box denotes the first and third quartiles with the centreline denoting the second quartile, or median. Outliers are shown by the open dots. For a normal distribution, as the number of data points increases the median becomes roughly equivalent

to the mean. For many parameters there are very few data points in August or September 2012 and thus the data from those months have been removed from the boxplots.

6.2.1 Outdoor climate

The outdoor dry bulb air temperature (TA10) by month is shown in Figure 6.1(a). The uncertainty in outdoor temperature based on calibration data is 0.6 °C. The temperature averages a minimum during the winter month of July and a maximum during the summer month of January. August has the least variation in temperature while January has the greatest. When considering the year from March 2011 through February 2012 the average was 13.2 °C. The temperature reached above 30 °C on 11 days: two days in December, four days in January and 5 days in February. It reached a maximum of 35.0 °C at the end of January. The temperature fell below 0 °C on 30 days: 12 days in May, 7 days in June, 8 days in July, 2 days in September and 1 day in October. It reaches a low of -3.4 °C in mid July.

The outdoor temperature hourly profile is provided in Figure 6.1(b). The lowest average hourly temperature occurs at 5am and the highest occurs at 1 to 2pm.

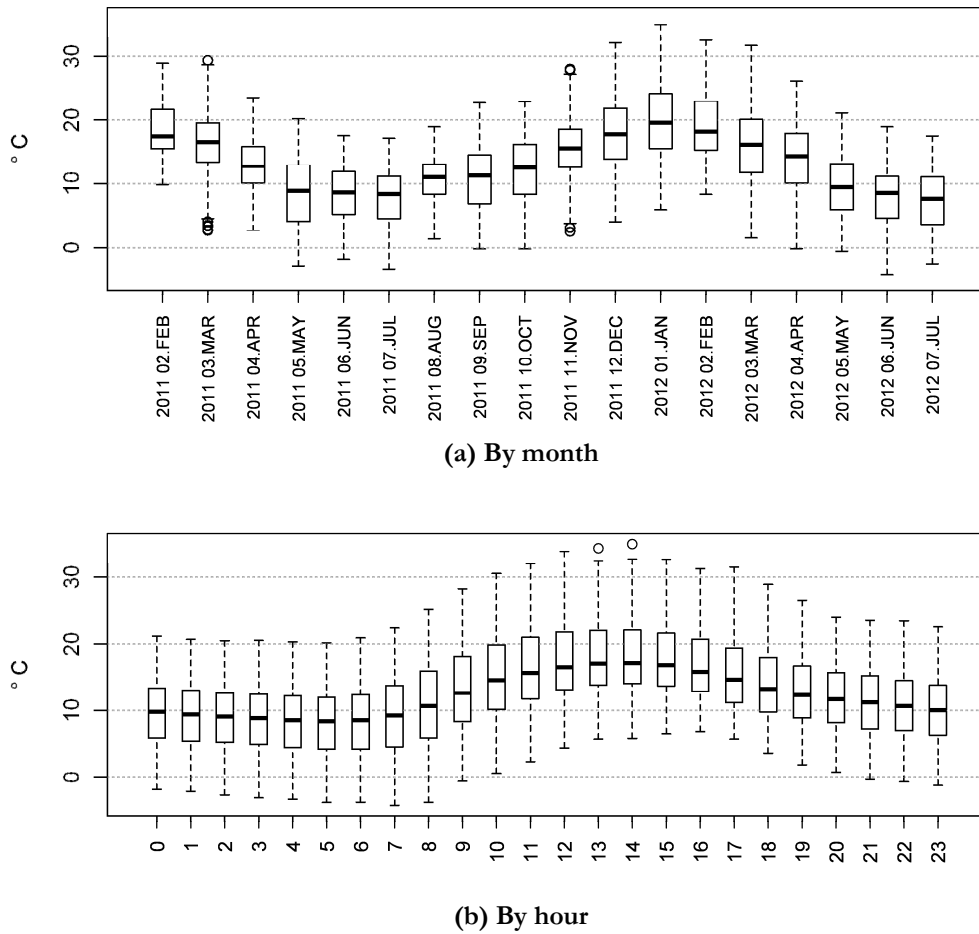


Figure 6.1: Outdoor air temperature, TP1-3

The outdoor relative humidity (RH10) by month is shown in Figure 6.2(a). The uncertainty in outdoor relative humidity based on calibration data is 0.8%. As expected, the outdoor relative humidity is lowest in the warm months when the temperature is highest, and highest in the cool months when the temperature is lowest. The hourly profile is shown in Figure 6.2(b). The relative humidity is highest in the morning hours and then starts to drop at about 7am, just as the air temperature starts to rise. The humidity is lowest just after noon and then slowly increases throughout the evening.

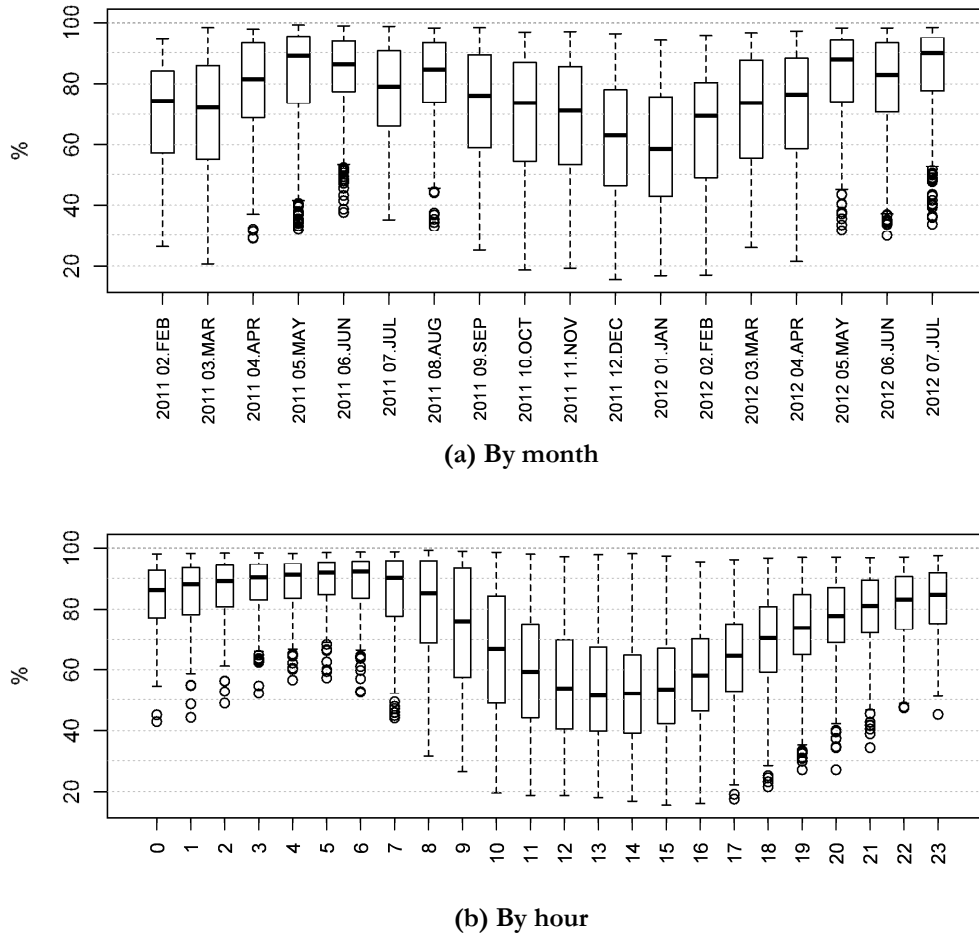


Figure 6.2: Outdoor relative humidity, TP1-3

The outdoor specific humidity by month is shown in Figure 6.3(a). The uncertainty is calculated to be 0.2 g/kg, based on the uncertainty of temperature of 0.6 °C and the uncertainty in relative humidity of 0.8%. In general, the specific humidity is higher in the warmer months and lower in the cooler months, though August 2011 went against this trend. The hourly profile is shown in Figure 6.3(b). The hourly variation in specific humidity is quite small compared to the range of the data, indicating that the amount of moisture in the outdoor air changes very slowly over time.

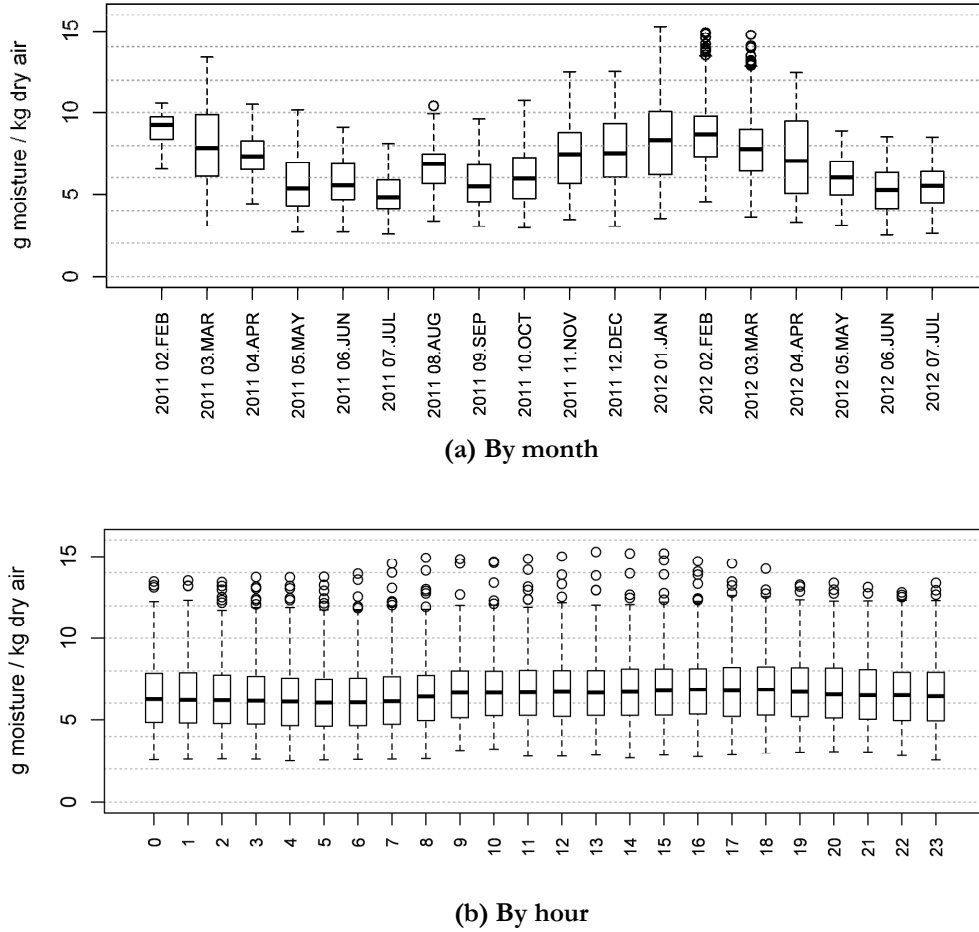


Figure 6.3: Outdoor specific humidity, TP1-3

The monthly wind speed (AS10) profile is shown in Figure 6.4(a). The uncertainty in wind speed is estimated at 1 m/s, which is twice the manufacturer's stated accuracy. There is no apparent correlation between wind speed and month. The hourly wind speed (AS10) profile is provided in Figure 6.4(b). The wind is generally calmer in the early hours of the morning and then it peaks at approximately 3pm.

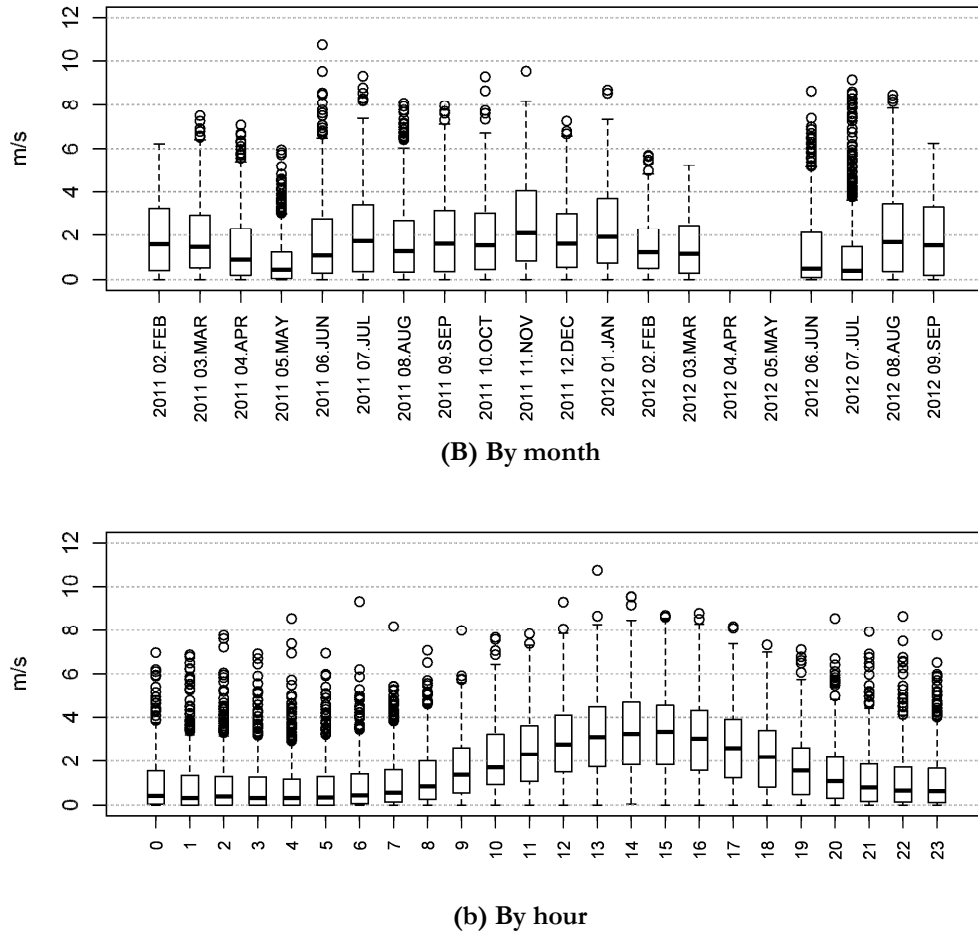
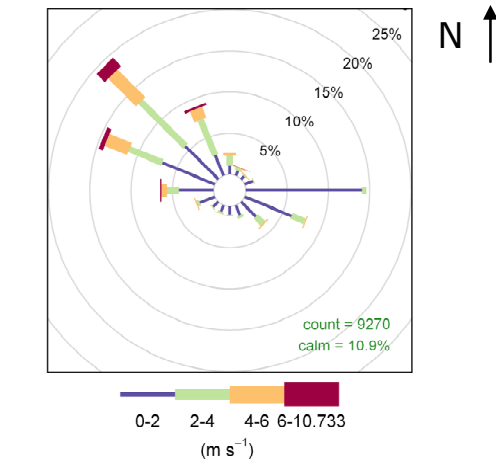


Figure 6.4: Wind speed at test cell roof, TP1-3

The predominant wind directions as measured from the test cell roof are from the northwest and east, with nearly all winds above 4 m/s coming from the northwest. This is shown in the wind rose of Figure 6.5. The uncertainty in wind direction, based on on-site calibration, is 4°. This profile is consistent across all seasons.



Frequency of counts by wind direction (%)

Figure 6.5: Wind rose

The precipitation by month is shown in Figure 6.6. These data were purchased from BOM and represent the amount of rainfall since 9am local time. The value is reset just after 9am each day. March 2011 and May 2012 received more precipitation than other months.

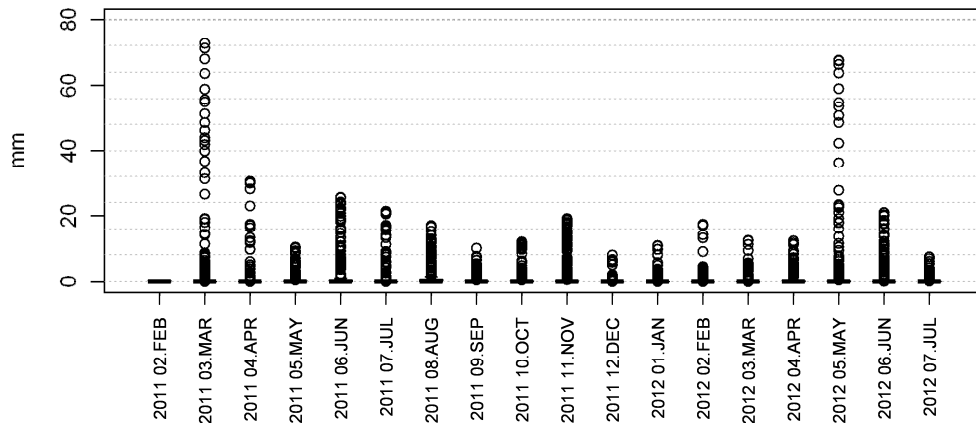


Figure 6.6: Precipitation

The monthly profile of global irradiation is shown in Figure 6.7(a). The uncertainty is approximately 0.05 kW/m^2 , based on twice the manufacturer's stated accuracy. As expected, the maximum daily global radiation is highest during the summer months and lowest during the winter months, and the minimum daily global radiation is always 0. The average maximum daily radiation during the summer of December 2011 through February 2012 was 883 W/m^2 . The hourly profile of global irradiation is shown in Figure 6.7(b). The radiation peaks at noon.

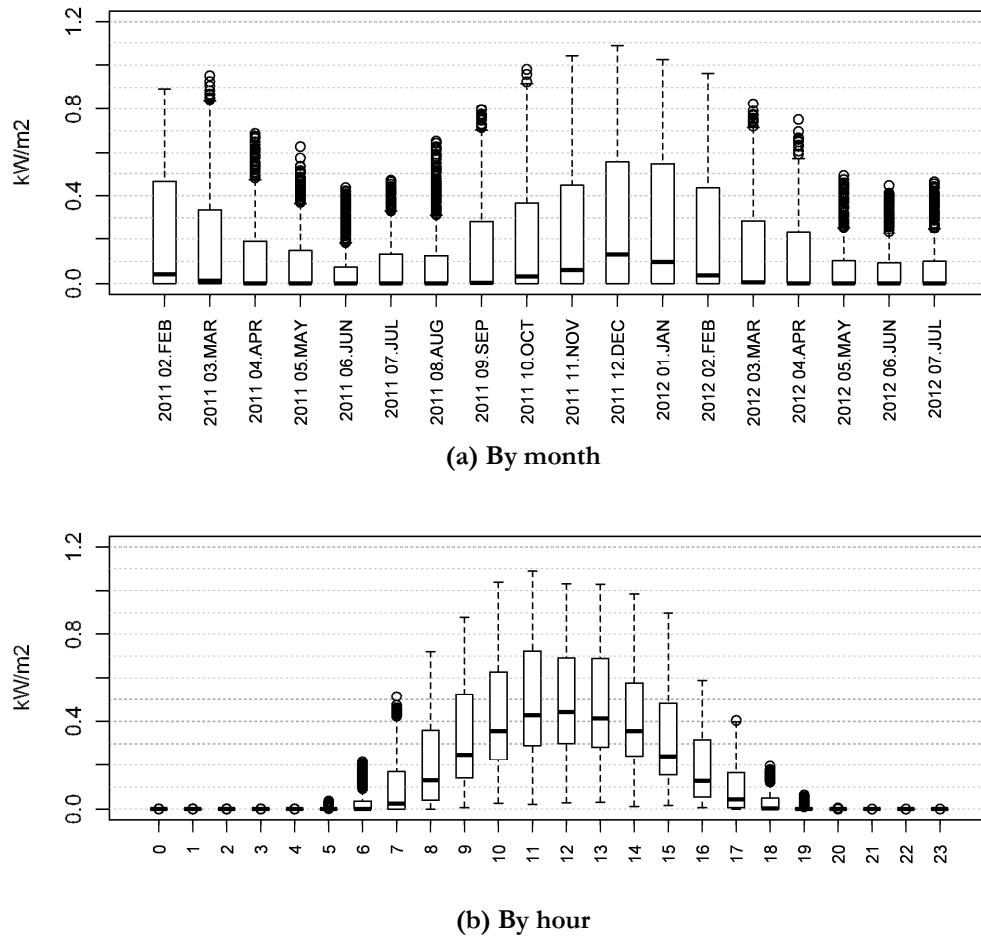


Figure 6.7: Global irradiation

The ground heat flux just outside the east wall of the test cell is shown in Figure 6.8. A positive value indicates a downward flow of heat. The monthly profile is provided in Figure 6.8(a). The maximum daily heat flux into the ground varies with season as expected, with the highest value in the summer months when the global radiation is also highest. On seven days throughout the March 2011 – February 2012 year, the maximum daily heat flux value was negative, indicating that the heat did not flow downward on those days. This occurred on two days in March, two days in April, one day in June, one day in August and one day in October. The minimum daily heat flux has very little seasonal variation. A negative value of heat flux occurred every day, indicating that at some point on every day heat was flowing upward from the ground. The outside heat flux shows a clear hourly trend, as shown in Figure 6.8(b), with the peak values occurring just after the peak global irradiation, at 1pm. Generally heat flows downward into the ground between the hours of 10 am and 6 pm, and upward at other times.

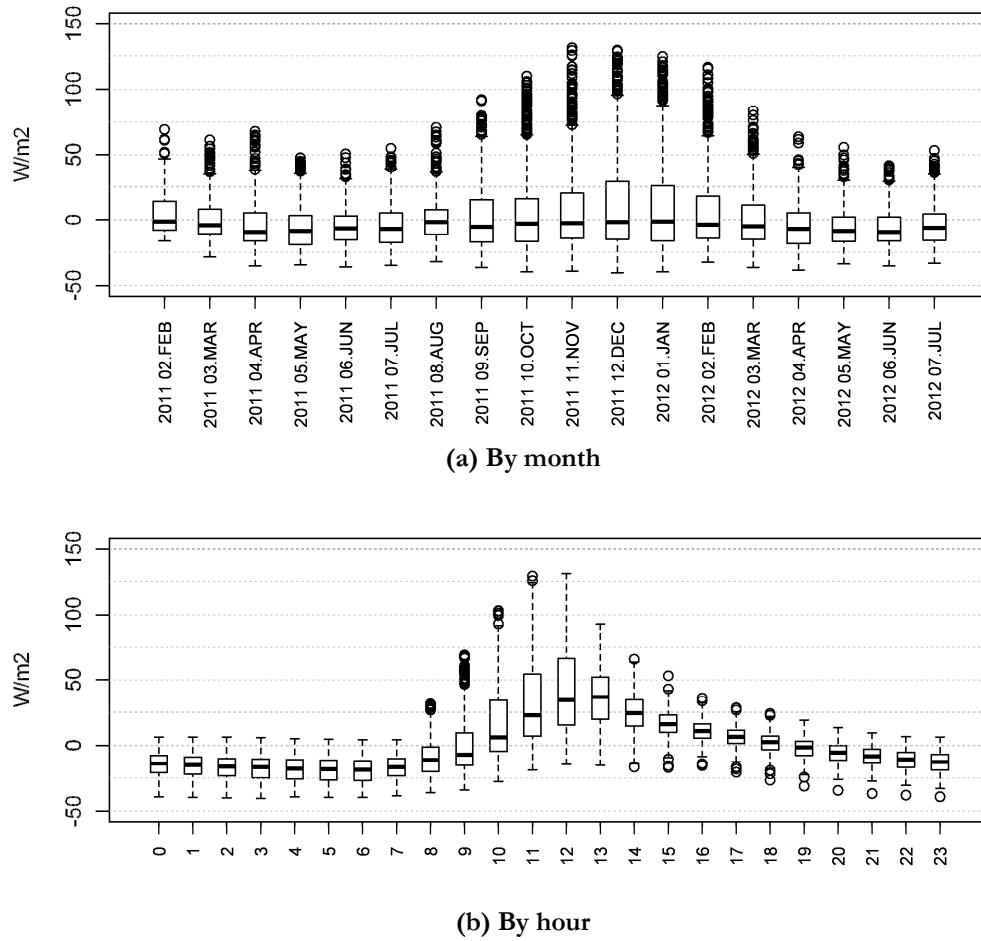


Figure 6.8: Outdoor ground heat flux

The linear relationship between outdoor ground heat flux (HF20) and global irradiation (RA14) is shown in Figure 6.9. 64% of the variation in heat flux (R^2) can be attributed to the radiation. The slope is positive, indicating that as radiation increases, heat flux into the ground does also. The value of the slope indicates that of all the incident radiation on the ground surface, only 8.3% of that energy enters the ground.

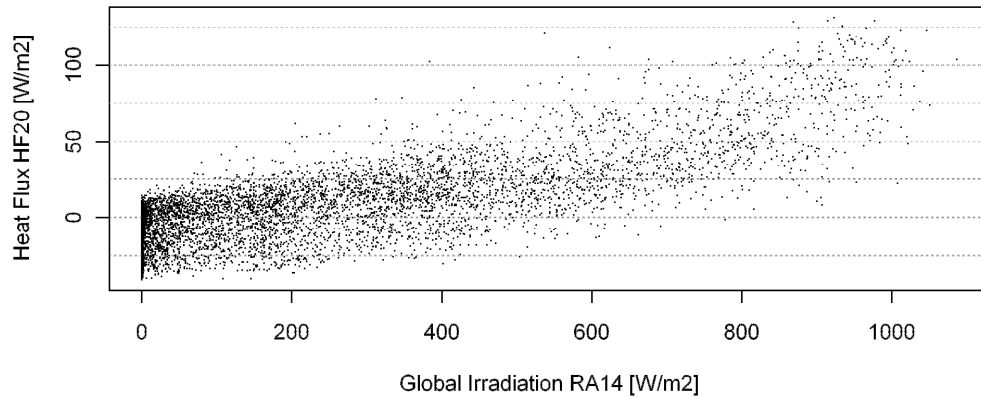


Figure 6.9: Outdoor ground heat flux versus global radiation

The ground temperature outside the east wall of the test cell is shown in Figure 6.10. The ground temperature uncertainty was within 0.3 °C, as described in Appendix A.2.1. The average outside air temperature from March 2011 through Feb 2012 of 13.2 °C is indicated on the graph. This is less than the annual average ground temperatures of 14.4 °C at 150 mm deep and 14.2 °C at 600 mm deep. It is common that the average annual ground surface temperature and air temperature are similar (McInnes 2005). There is greater range in the temperature at 150 mm than at 600 mm deep, as expected. The seasonal trend of ground temperature is also as expected with the lowest temperature occurring in winter in July and the highest temperature occurring in summer in January. The average monthly 150 mm temperature drops below the average monthly 600 mm temperature at the beginning of autumn and it rises above in mid-winter.

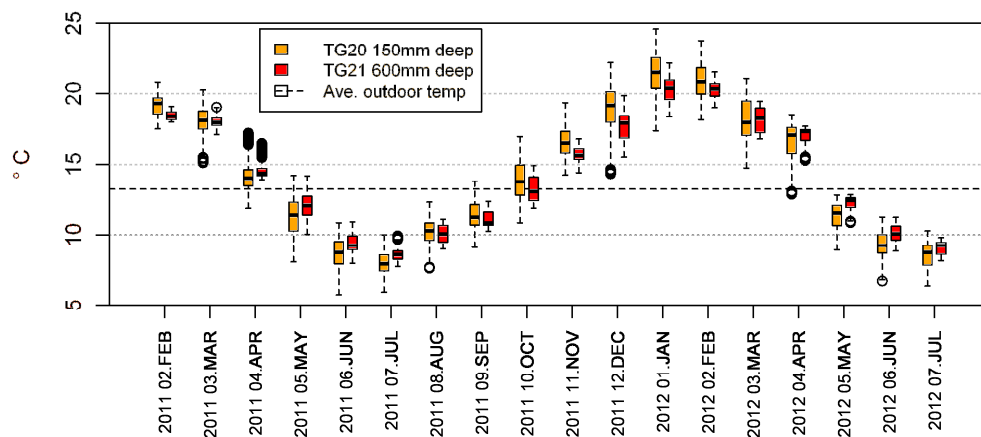


Figure 6.10: Outside ground temperature

Fourier's law of steady-state heat conduction relates the rate of heat transfer through a medium, the temperature change with depth and the medium's thermal conductivity (Cengel and Boles 2006). This law can be applied to estimate the thermal conductivity of the soil near the ground surface. Ground surface temperature is needed to calculate the temperature change with depth, but ground

surface temperature is not available. The average daily air temperature is similar to the average daily ground surface temperature (McInnes 2005), and ground temperature prediction models based on ground surface temperature have shown to be successful when substituting air temperature for ground surface temperature (Wu and Nofziger 1999). Thus, if the air temperature is substituted for ground surface temperature to calculate the temperature change with depth into the soil, then the heat flux is related to the temperature change as shown in Figure 6.11, where the temperature change is between the air temperature and ground temperature at 150 mm deep. The correlation has an R^2 of 0.64.

Considering the slope evident in Figure 6.11 and knowing that the vertical distance between the two soil temperature measurement locations is 150 mm, the soil thermal conductivity is estimated to be 0.63 ± 0.09 W/mK. The uncertainty stems from an assumed uncertainty in heat flux of 10%, and the uncertainty in the temperature difference of 0.6°C . This is within the typical range of 0.06 to 2.18 W/mK for soils (Hillel 2004).

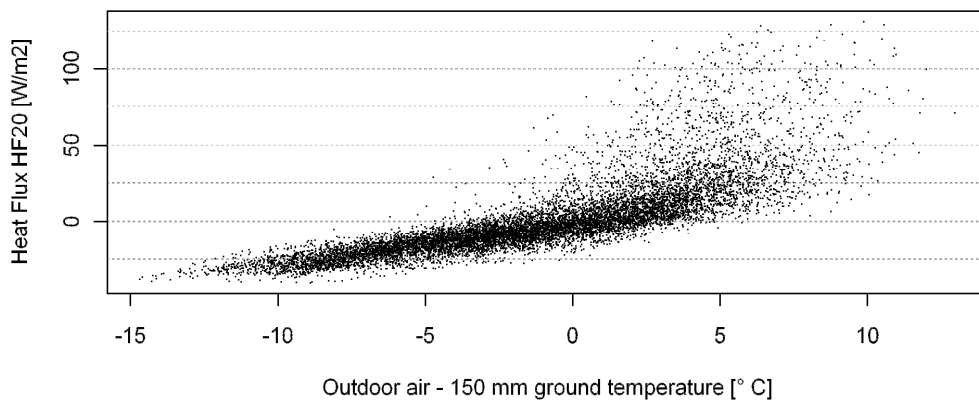


Figure 6.11: Outdoor heat flux versus difference between air and ground temperature

6.2.2 Room and subfloor climate

The three dry bulb room temperatures and the room globe temperature are shown in Figure 6.12. All four are measured via IC sensors. The temperature at 600 mm is the lowest, followed by the temperature at 1200 mm and 1800 mm. This trend is expected as hot air, being less dense, tends to rise. The globe temperature sensor is mounted at 1200 mm and the globe temperature is similar to the dry bulb temperature at 1200 mm.

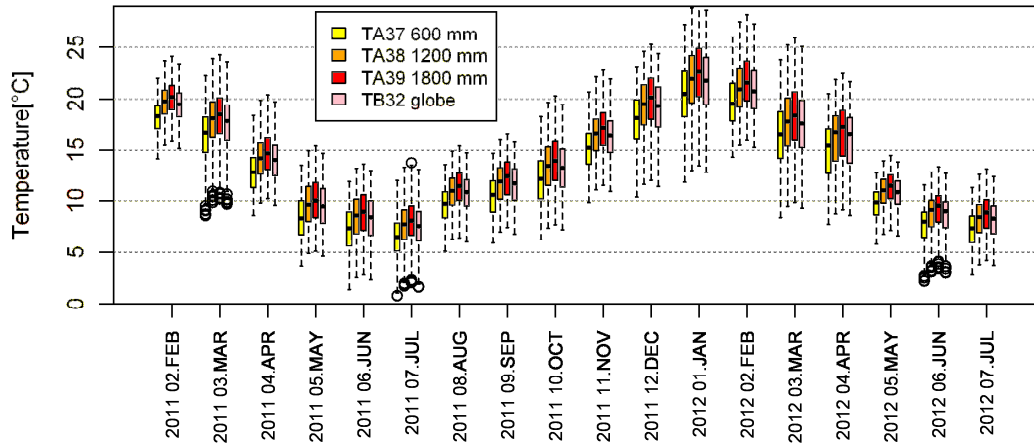


Figure 6.12: Room dry bulb and globe temperatures, by month

The dry bulb air temperature at the centre of the subfloor as measured by RTD is compared to the outdoor air temperature in Figure 6.13. The subfloor centre dry bulb temperature recorded a 0.0 °C error during calibration. The subfloor air temperature follows the same seasonal trend as the outdoor temperature, with a minimum during the winter month of July and a maximum during the summer month of January. The subfloor temperature has a much smaller range than the outside temperature. The monthly average between the outdoor and subfloor temperature is similar. Of all the outdoor climate parameters, the subfloor temperature is most correlated with outdoor temperature. There is a good linear correlation present between the two series, with 64% of the variation in subfloor temperature attributed to the outdoor temperature.

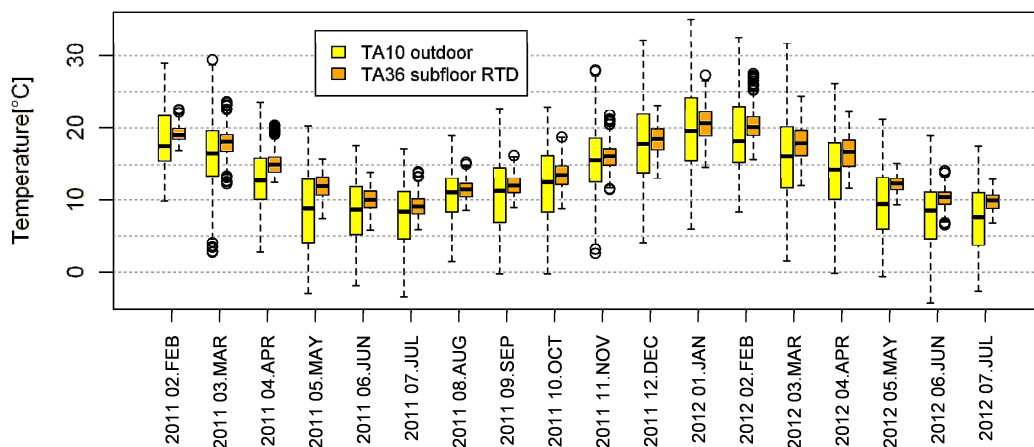


Figure 6.13: Subfloor and outdoor air temperatures, by month

When considering one year from March 2011 through February 2012 the average subfloor air temperature was 14.6 °C, 1.4 °C above the outdoor average. The subfloor temperature reached above 25 °C on nine days: six days in January and three days in February. It reached a high of 27.5

°C at the end of February. The subfloor temperature reached its lowest value of the year of 5.9 °C in mid-June.

The subfloor air temperature is at its minimum at 7am and maximum at 3pm as shown in Figure 6.14.

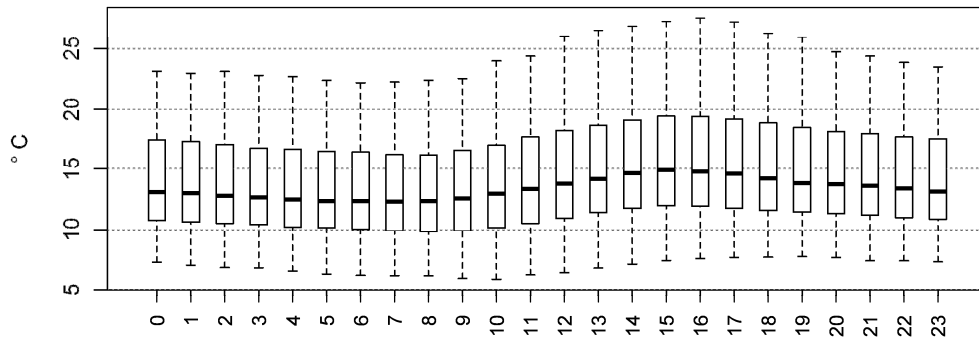


Figure 6.14: Subfloor temperature, by hour

A comparison of three subfloor centre temperatures is provided in Figure 6.15. One sensor is an IC measuring dry bulb temperature (TA35), another is an RTD also measuring dry bulb temperature (TA36) and the third is an RTD measuring globe temperature (TB31). Both the RTDs have a very similar average temperature while the IC is consistently approximately 1°C lower. Because of higher accuracy during calibration, the RTD (TA36) value is used as the subfloor centre dry bulb air temperature in this research unless otherwise specified. Sensor TB31 recorded a 0.0 °C error during calibration.

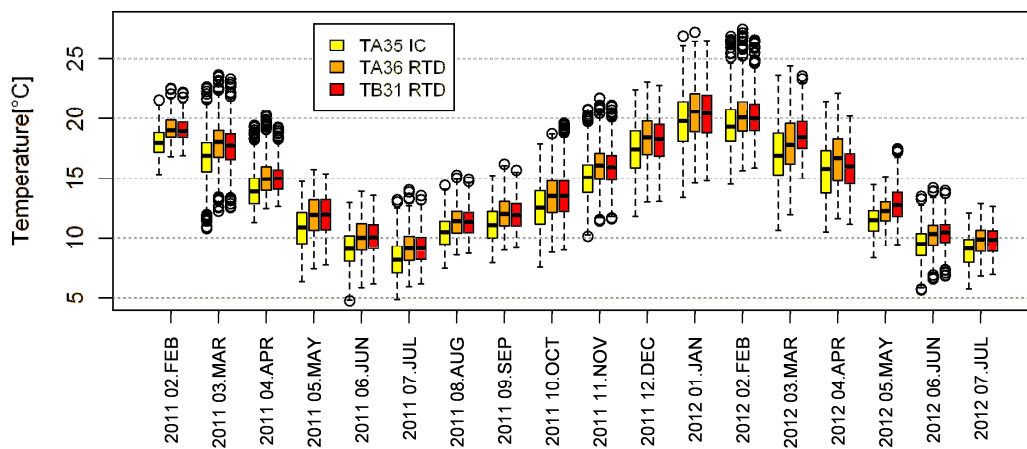


Figure 6.15: Subfloor centre temperatures, by month

The subfloor centre temperature (TA35) is compared to the temperature at the four subfloor corners in Figure 6.16. All five were measured using IC sensors. The NE and SE temperatures are measured at locations above sections of ground that were covered under the ground sheet through

February 2012. The range of the subfloor temperatures is similar to that of the room temperatures, though with a greater number of outlying data points. The centre temperature is generally the highest, followed closely by the NW temperature, then SW, SE then NE. This profile is less pronounced in the summer months. All five sensors show similar variation.

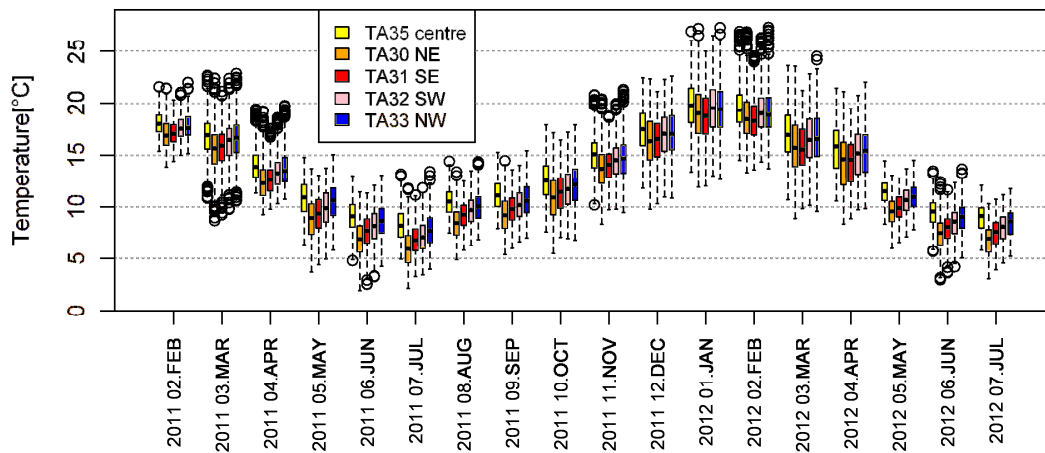


Figure 6.16: Subfloor centre and corner air temperatures, by month

The dry bulb air temperatures at the subfloor centre, NW corner just behind the west vent on the north wall are shown in Figure 6.17. These are all measured via IC sensors. The median values are all similar though the NW vent temperature shows higher variation, as can be expected due to its location directly in the path of the incoming ventilation.

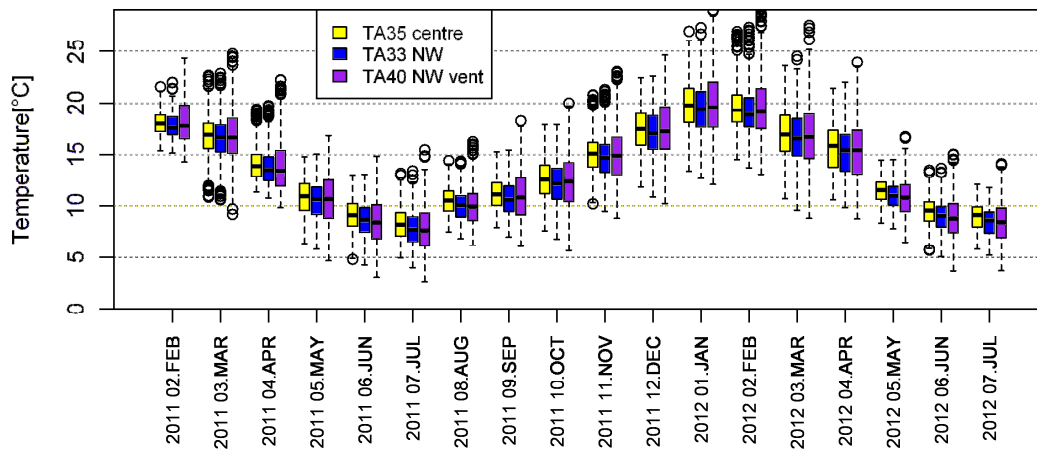


Figure 6.17: Subfloor centre and NW air temperatures, by month

The subfloor dry bulb and globe temperatures at the centre and east side, all measured via RTD sensors, are compared in Figure 6.18. There is no large difference between any of the values, though during the warmer months the east side temperatures are slightly higher than the centre temperatures.

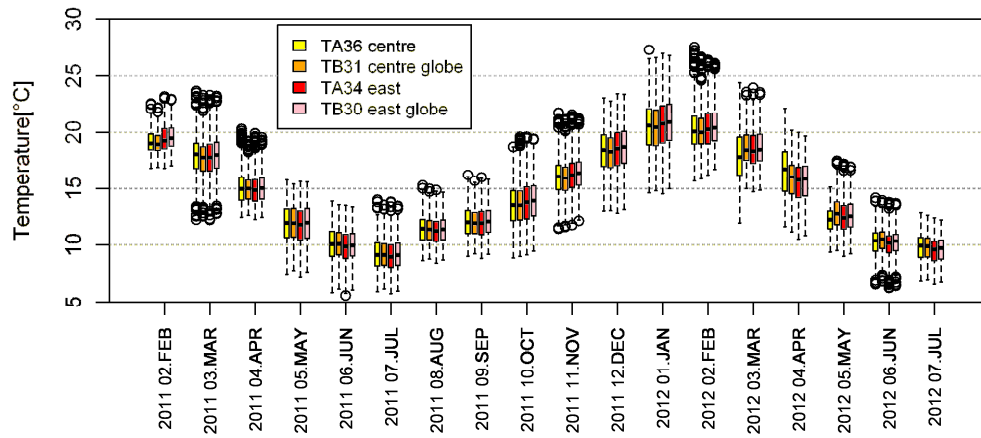


Figure 6.18: Subfloor centre and east side air temperatures, by month

The subfloor centre globe and dry bulb air temperatures are analysed in more detail as these two values contribute to the calculation of the subfloor environmental temperature. The difference between the globe temperature (TB31) and dry bulb air temperature (TA36) is provided by month and by hour in Figure 6.19. The first and third quartiles of data, representing 50% of the data, are nearly always between 0.1 and -0.3 °C. The difference is higher in the winter months than in the summer months. However, the difference is also greater in the early morning when temperatures are low and lower in the afternoon when temperatures are high.

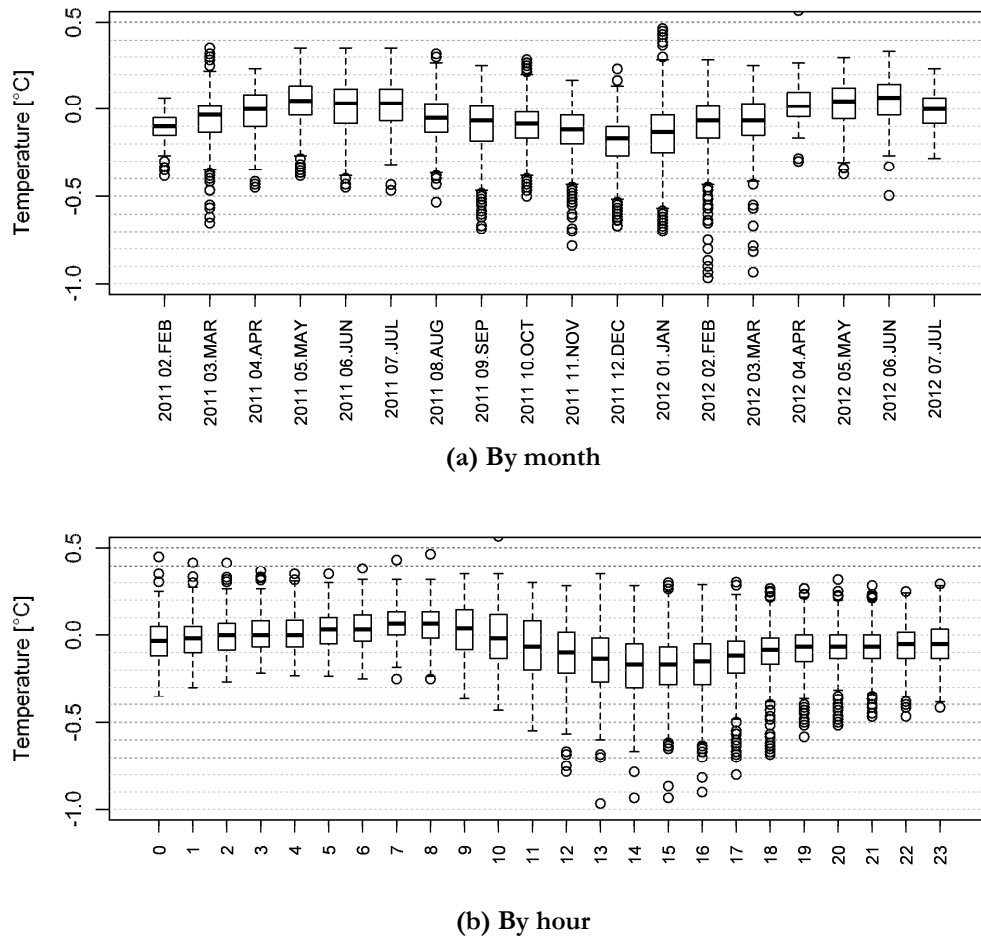


Figure 6.19: Temperature difference, subfloor globe - dry bulb air temperature

The relative humidity at the centre of the subfloor is compared to the outdoor relative humidity in Figure 6.20. The uncertainty in the three subfloor relative humidity sensors was within 3%. The subfloor relative humidity follows the same seasonal trend as the outdoor humidity. It is lowest in the warm months when the temperature is highest, and highest in the cool months when the temperature is lowest. The monthly average subfloor relative humidity is greater than the monthly average outdoor humidity from the beginning of spring through mid-summer. The subfloor relative humidity has a much smaller range than the outside humidity. The cooler months have a smaller range than the warmer months. Of all the outdoor climate parameters, the subfloor relative humidity is most correlated with outdoor relative humidity. There is a good linear correlation present, with 59% of the variation in subfloor relative humidity attributed to the outdoor relative humidity.

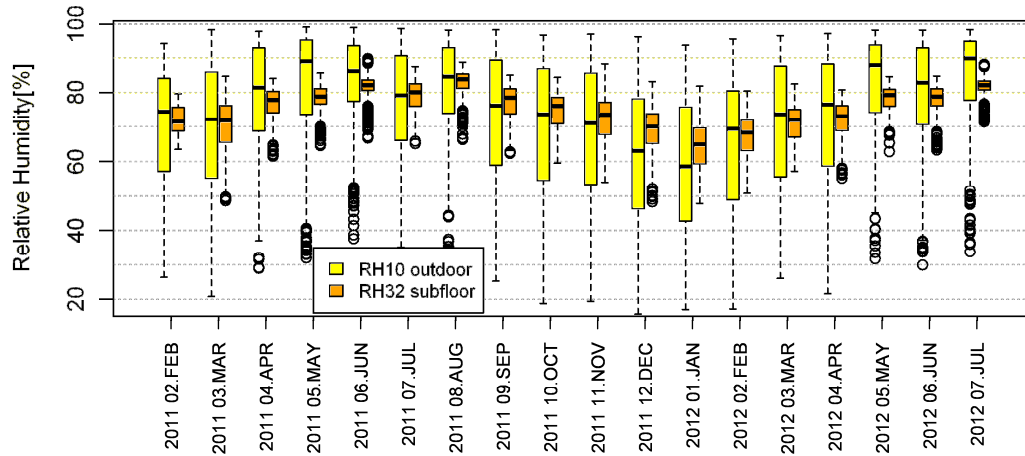


Figure 6.20: Subfloor and outdoor relative humidity, by month

Subfloor humidity by hour is shown in Figure 6.21. It is highest in the early hours of the morning and lowest in the late afternoon, corresponding with the reverse of the subfloor temperature hourly profile.

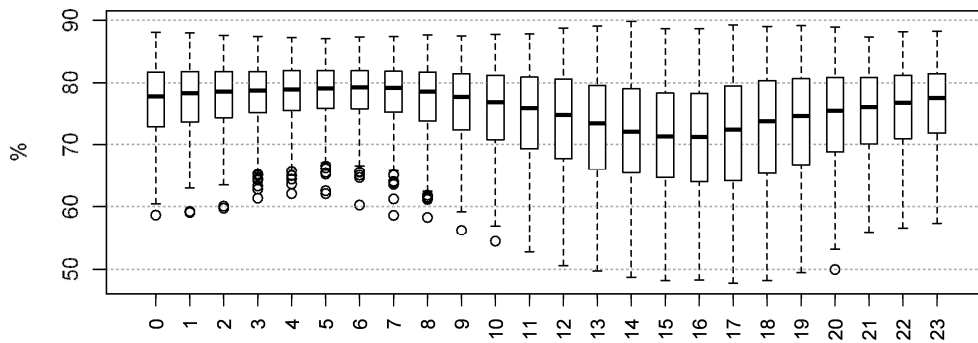


Figure 6.21: Subfloor relative humidity, by hour

The relative humidity at the subfloor centre and near the southeast and northwest corners is presented in Figure 6.22. The relative humidity is fairly similar between the centre and southeast, with the southeast being slightly higher. The northwest humidity is different from the other two, especially in autumn/early winter. It was substantially less in April, May and June of both 2011 and 2012.

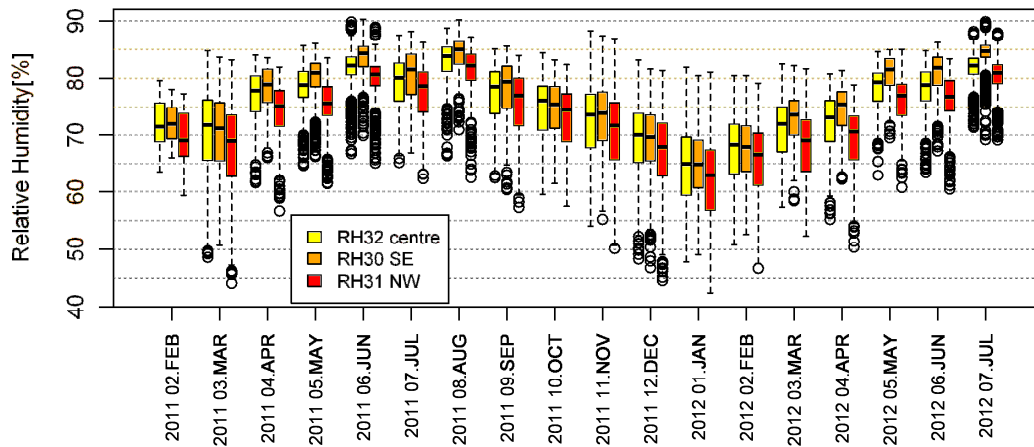


Figure 6.22: Relative humidity throughout subfloor, by month

The relative humidity in the SE corner of the subfloor is considered in more detail and exceedances above 80% and 85% are summarized in Table 6.1. The SE corner location was selected because it displayed higher humidity than the other locations. During the entire test period the humidity reached a high of 90.3% on the 19th of June 2011. The humidity exceeded 90% for a total of five hours; four occurred on that day in June 2011 and the final hour occurred on the 8th of August 2011. In the year from March 2011 through February 2012 the relative humidity exceeded 80% on 198 days, more than half of the year. The humidity exceeded 80% every day during the months of June 2011, August 2011, September 2011 and July 2012.

Table 6.1: Subfloor SE corner relative humidity, time spent above 80% and 85%

Year	Month	Season	# of samples	Subfloor humidity above 80%		Subfloor humidity above 85%	
				Total hours	Number of days with occurrence	# of hours	Number of days with occurrence
2011	March	Autumn	587	61	5	0	0
2011	April	Autumn	564	234	18	0	0
2011	May	Autumn	744	458	28	7	1
2011	June	Winter	720	634	30	263	21
2011	July	Winter	744	440	23	114	11
2011	August	Winter	744	660	31	366	25
2011	September	Spring	720	334	30	5	2
2011	October	Spring	693	73	15	0	0
2011	November	Spring	720	108	13	20	3
2011	December	Summer	744	7	2	0	0
2012	January	Summer	744	3	2	0	0
2012	February	Summer	677	3	1	0	0
2012	March	Autumn	420	16	4	0	0
2012	April	Autumn	275	10	3	0	0
2012	May	Autumn	437	282	17	0	0
2012	June	Winter	652	432	22	55	7
2012	July	Winter	744	688	31	304	25
2012	August	Winter	10	10	0	0	0

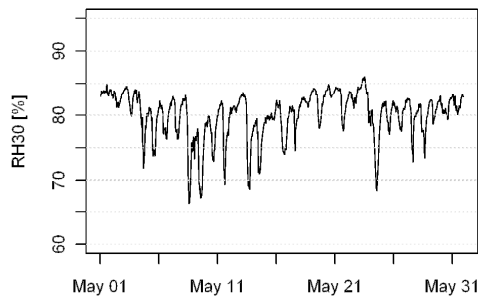
Graphs of the subfloor relative humidity in the SE corner during these cooler months are provided in Figure 6.23. For ease of comparison all graphs have the same scale of 60–90 %. During the

months of June 2011, August 2011 and July 2012, the relative humidity in the SE corner dropped below 80% for only 85 hours, 84 hours and 56 hours, respectively.

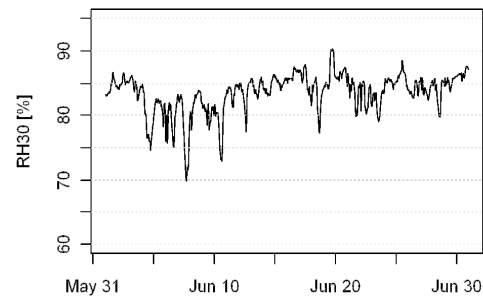
One high humidity stretch occurred between late June and mid-July of 2012. From 9pm on the 29th of June until 7am on the 15th of July, a time period of 15 ½ days, the relative humidity was above 80% for all but five hours. These five hours occurred on the 3rd and 4th of July. Another high humidity stretch occurred between late June and early July of 2011. From 6pm on the 10th of June until 2am on the 5th of July, a time period of 24 ½ days, the relative humidity was above 80 % for all but 17 hours. These 17 hours were scattered with three hours occurring on the 12th, four occurring on the 18th, two occurring on the 21st, five on the 23rd, and three occurring on the 28th.

The longest period where the SE corner relative humidity stayed continuously above 80% was 10 ½ days, or 255 hours, from 2pm on the 4th of July 2012 to 6am on the 15th of July. The second longest period was also 10 ½ days, or 252 hours, from the 1am on the 28th of July 2011 until noon on the 7th of August. There is also an eight day period, or 190 hours, from 5pm on 20th July to 2pm on 28th July 2012.

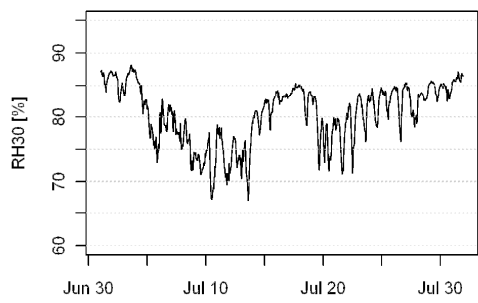
For comparison, graphs of the subfloor air temperature corner during these cooler months are provided in Figure 6.24. For ease of comparison, all graphs have the same scale of 4-18 °C. Generally the periods with high relative humidity correspond with cooler subfloor temperatures.



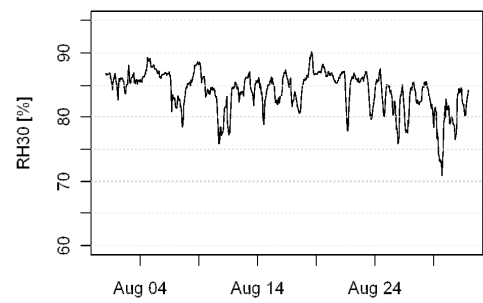
(a) May 2011



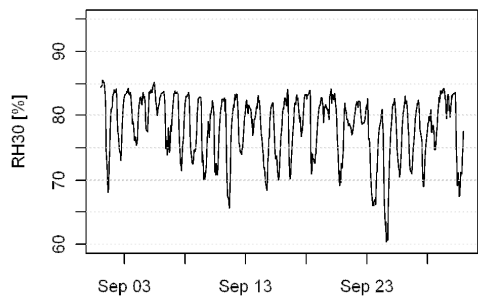
(b) June 2011



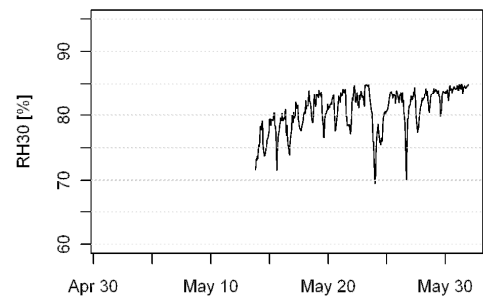
(c) July 2011



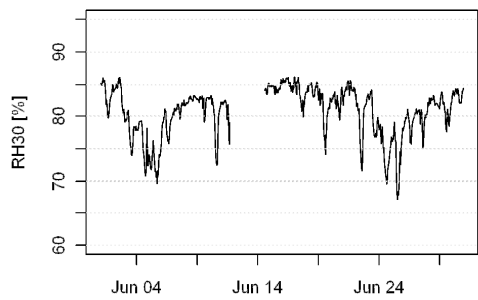
(d) August 2011



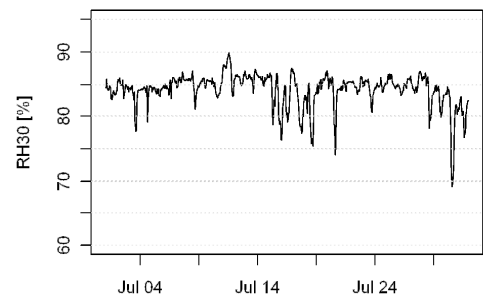
(e) September 2011



(f) May 2012

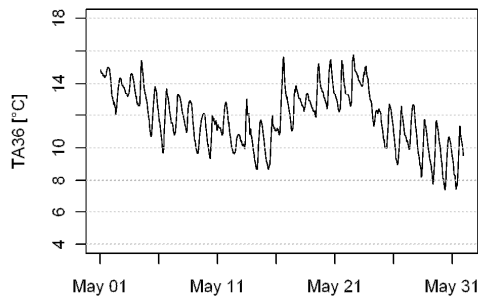


(g) June 2012

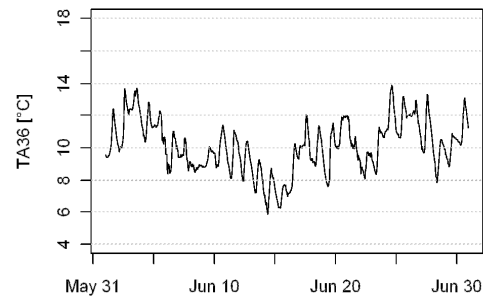


(h) July 2012

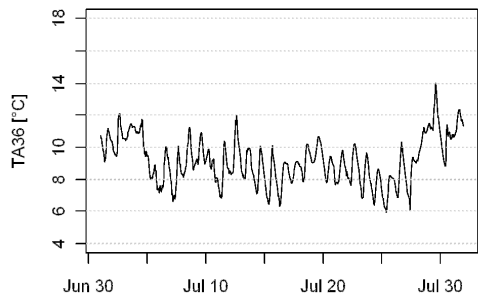
Figure 6.23: Subfloor SE corner relative humidity during cool months



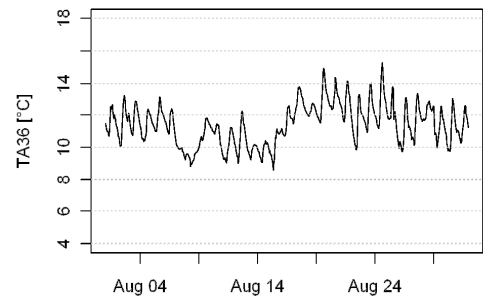
(a) May 2011



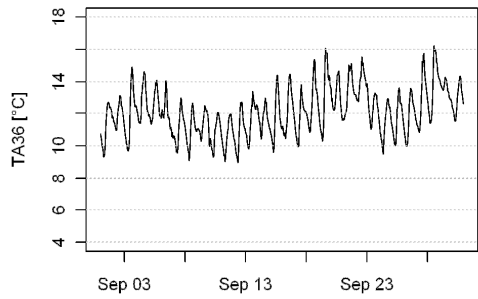
(b) June 2011



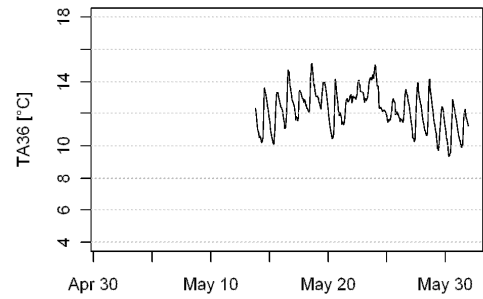
(c) July 2011



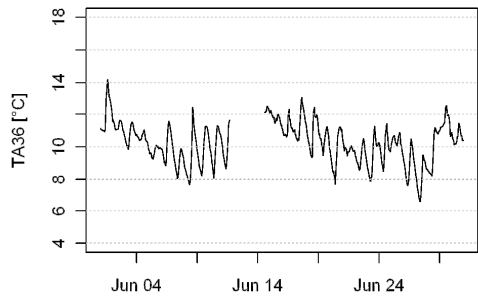
(d) August 2011



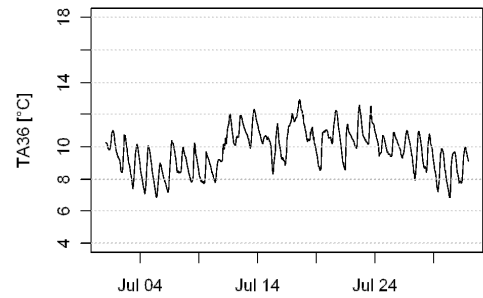
(e) September 2011



(f) May 2012



(g) June 2012



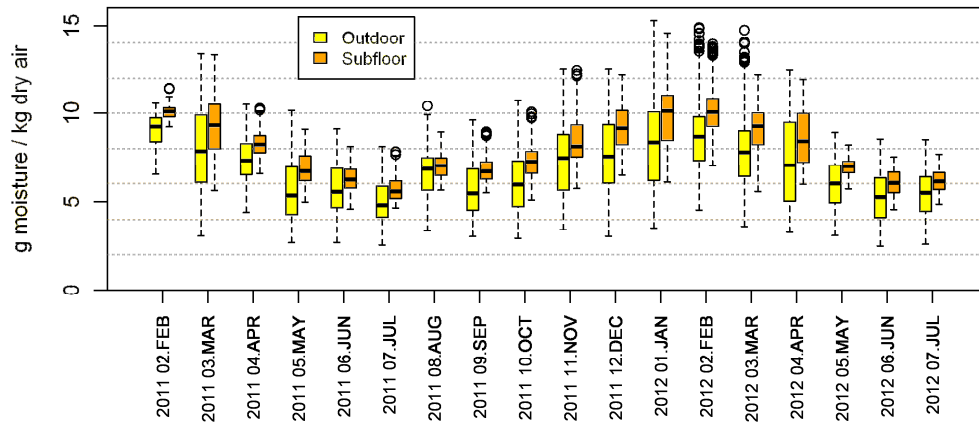
(h) July 2012

Figure 6.24: Subfloor temperature during cool months

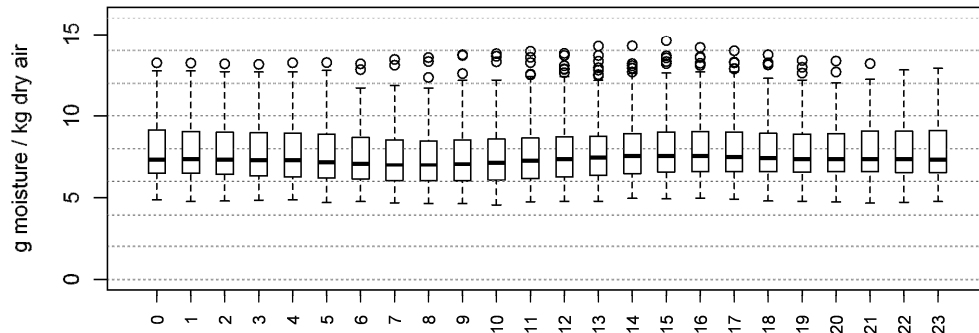
A subfloor temperature of 12 °C has been suggested as the temperature threshold to be applied in conjunction with the 80% relative humidity limit (Williamson and Delsante 2006b). Around the 18th of May 2011 there is approximately a one week period where the subfloor temperature is above 12 °C. The relative humidity is mostly above 80% though it does drop below that occasionally. After approximately the 25th of May the subfloor temperature drops to mostly below 12 °C where it remains during the high humidity periods of June, July and early to mid-August. Starting approximately the 16th of August there is a period of five days where the relative humidity is above 80% and the temperature is mostly above 12 °C. The temperature drops three times and the longest continuous time the subfloor spends above both limits concurrently is two days. After that five day period the temperature routinely drops below 12 °C. Throughout September 2011 on a daily basis the relative humidity drops below 80% and the temperature drops below 12 °C.

In May 2012 the temperature is predominantly above 12 °C though the relative humidity drops below 80% every day. In June and July the relative humidity is quite frequently above 80% though the subfloor temperature is quite cool and very infrequently exceeds 12 °C.

The specific humidity of the subfloor air based on the subfloor centre air temperature as measured by RTD sensor and relative humidity at the centre of the subfloor is compared to the outdoor specific humidity in Figure 6.25(a). The uncertainty in subfloor specific humidity is calculated to be 0.4 g/kg, based on the uncertainty of temperature of 0.1 °C and the uncertainty in relative humidity of 3%. The subfloor specific humidity, like the outdoor specific humidity, is higher in warmer months and lower in cooler months. However, the subfloor specific humidity is generally higher and has less variation. Figure 6.25(b) shows the hourly profile of specific humidity. Compared to the range of values there is little variation by the time of day, indicating that the subfloor specific humidity changes slowly with time. There is a strong linear correlation present, with 74% of the variation in subfloor specific humidity attributed to the outdoor specific humidity.



(a) Compared to outdoor specific humidity, by month



(b) By hour

Figure 6.25: Subfloor specific humidity, TP1-3

The variation of specific humidity throughout the subfloor is shown in Figure 6.26. Each of the three specific humidities is calculated using the IC temperature and relative humidity at its location. The specific humidity at the subfloor centre is higher than the specific humidity at either the southeast or northwest corners. This trend is constant throughout all seasons. There is hardly any distinction between the specific humidity at the southeast and northwest corners.

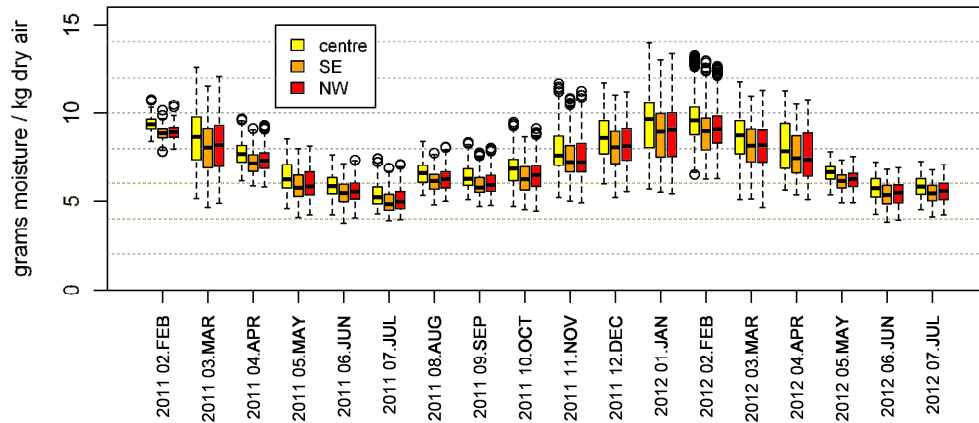


Figure 6.26: Specific humidity throughout subfloor, by month

The ground heat flux at the centre of the subfloor and east side locations is shown in Figure 6.27(a). The east side sensor was under the ground sheet until its removal in February 2012. In the colder months heat tends to flow upward, as the air temperature is relatively cool compared to subground temperatures. In the warmer months the reverse occurs. As can be expected due to shielding from the sun, these internal heat fluxes have a much smaller range than the outside heat flux shown in Figure 6.8, which ranges from approximately -50 to more than 100 W/m². The heat flux at these two subfloor locations is similar in mid-autumn and winter but the centre heat flux is noticeably higher than the east side heat flux in the late spring and summer. There is less variation in the east side heat flux than there is in the centre heat flux.

The daily heat flux profile between the two subfloor locations is similar, as shown in Figure 6.27(b). The heat flux is at a minimum, meaning flowing most upward, at 8 to 9am and at a maximum at 5 to 6pm. As opposed to the outdoors, which is exposed to solar radiation, there is no great difference in the subfloor heat flux with time of day.

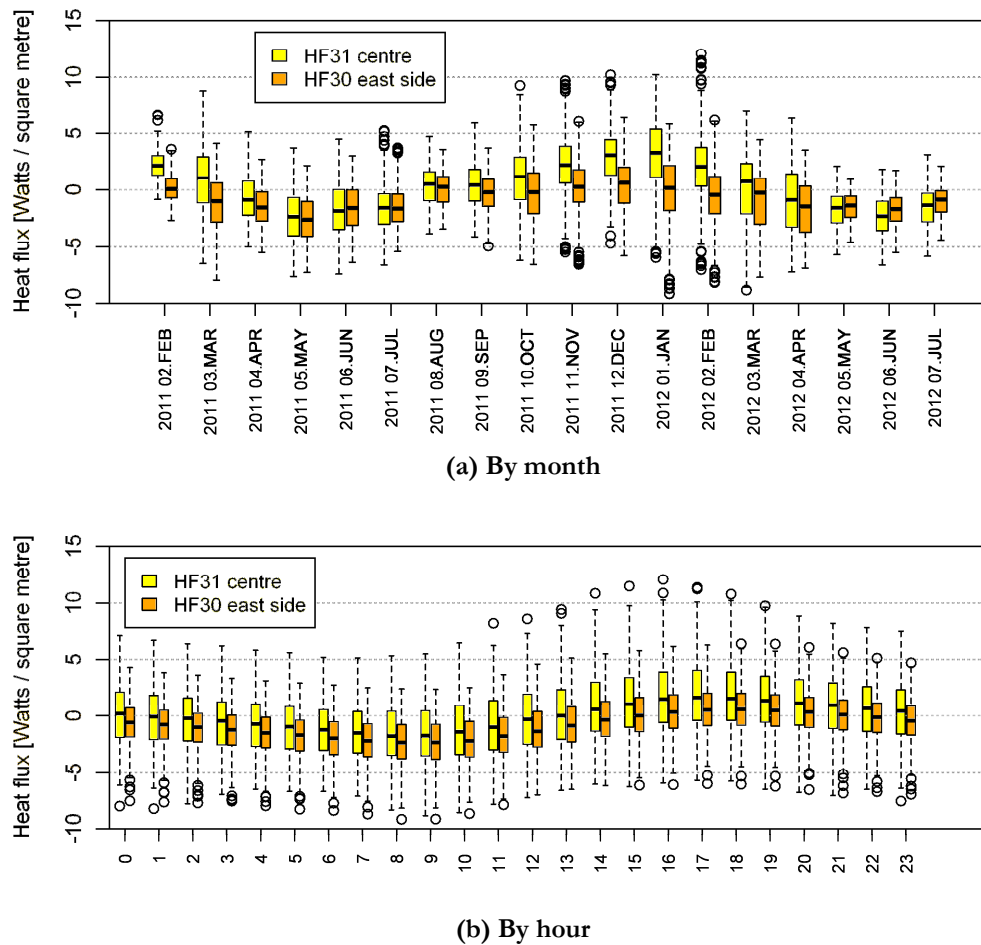


Figure 6.27: Subfloor centre and east side heat flux

The ground temperatures at the centre of the subfloor are shown in Figure 6.28. The calibration error in ground temperatures ranged from -0.2°C to $+0.3^{\circ}\text{C}$. The variation at 600 mm deep is less than the variation at 150 mm deep. Similar to the outside ground temperatures, the lowest temperature occurs in July and the highest temperature occurs in February. The annual average subfloor air temperature of 14.6°C is indicated on the graph. This is nearly one degree above the annual average ground temperatures at 150mm deep (13.8°C) and 600mm deep (13.9°C). Outside the test cell the annual ground temperature averages were each over 1°C higher than the annual air temperature average. Research has shown that the subfloor air temperature and ground surface temperature are generally quite close in value (Hartless 1996; Kurnitski 2000; Olweny et al. 1998).

The relationship between the two subfloor ground temperatures is similar to that outside the test cell. The average monthly 150mm deep temperature drops below the average monthly 600mm deep temperature in mid-autumn and it rises above at the end of winter. The range of subfloor

ground temperatures (Figure 6.28) is less than the range of outdoor ground temperatures, as shown in Figure 6.29(a) and (b).

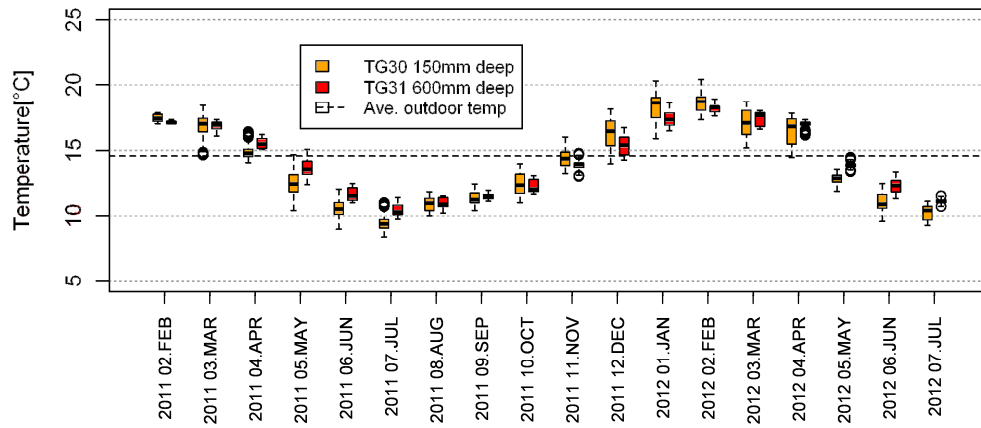


Figure 6.28: Subfloor centre ground temperatures, by month

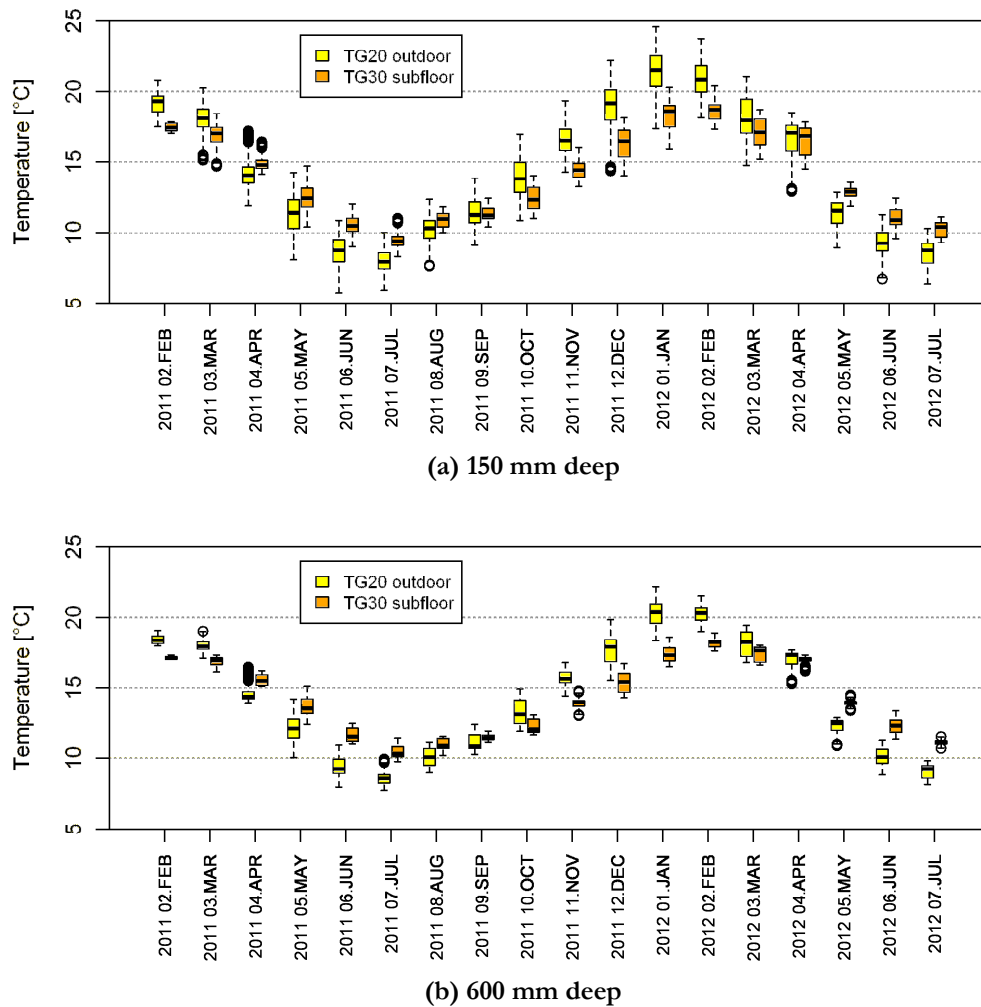


Figure 6.29: Comparison of subfloor and outdoor ground temperatures

Subfloor centre heat flux is related to the difference between subfloor air and subfloor centre 150 mm ground temperature as shown in Figure 6.30. The correlation has an R^2 of 0.68. Similar to what was done with the outdoor parameters, applying Fourier's law of heat conduction, and substituting air temperature for ground surface temperature, yields an observed soil thermal conductivity of 0.18 ± 0.03 W/mK inside the subfloor. This is lower than the conductivity measured outside the subfloor though still within the typical range (Hillel 2004). The uncertainty stems from an assumed uncertainty in heat flux of 10%, and the uncertainty in the temperature difference of 0.1 °C.

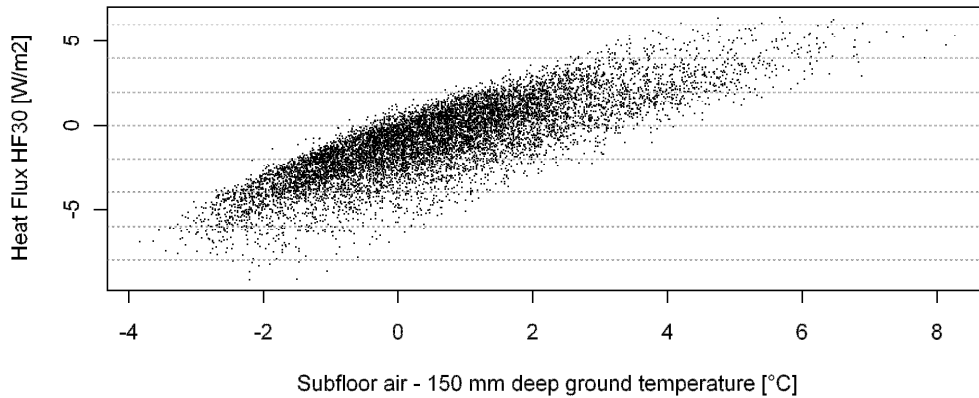


Figure 6.30: Subfloor heat flux versus air and ground temperature difference

Soil samples were taken on a summer day in February 2012, immediately after the subfloor ground cover was removed. Upon entering into the subfloor no odour was present, but when the ground sheet was removed a damp odour was immediately noticed. The odour emanated only from the freshly uncovered ground surface. It is not known for how long the odour remained. There were no other signs of subfloor deterioration observed. Observations of the soil samples noted during the test preparations were that SM1 was moist, SM2 was dry, SM3 was moist and contained less plant material than either SM1 or SM2, SM4 had a moisture between SM2 and SM1/SM3, and that SM5 looked very dry, even drier than SM2, and contained the most plant material. The observations are supported by the photo of the pre-test samples of Figure 5.19 where it is clear that SM1 and SM3 are the darkest, followed by SM4, with SM2 and SM5 the lightest.

The calculated soil moisture results are shown in Table 6.2. The results align with the observations, with SM5 being the driest and SM1 and SM3 being the wettest. The results are as expected based on the location of sampling, as SM1 and SM3 had been covered by the ground sheet, and both SM2 and SM5 being the most exposed to incoming ventilation at the northwest corner. SM4 was just in from the edge of the building and it was neither in the direct path of the vents, nor had it been covered by the ground sheet. The moisture content of SM4 was in the middle of the others.

Table 6.2: Soil moisture content

ID	Location relative to ground sheet	Soil moisture content [%]
SM1	underneath	36
SM2	not covered	6
SM3	underneath but near edge	36
SM4	not covered	20
SM5	not covered	4

Soil samples were taken only once, and that was during the summer. A separate study considering a similar style brick veneer residential building (Olweny et al. 1998) showed the soil moisture content

underneath the building remained relatively constant throughout the year, only changing by 1%. The uncovered soil moisture contents are less than the critical topsoil moisture content of 35%, and thus the evaporation rate of water from the soil is expected to be less than the evaporation rate of a free surface of water (Abbott 1983). The vapour pressure at the ground surface is therefore not simply a function of the surface temperature. In addition, a significant amount of the evaporation would be expected to occur from as far as 500 mm below the surface (Trethowen 1988).

The wood moisture content at all six locations throughout the test period is provided in Figure 6.31. Two of the locations, WM30 and WM31, were in the hardwood joists of the subfloor. These two locations consistently yielded lower moisture contents than did the other four locations. The other four locations were in the softer floor board. One of those, WM33, was inside the room while the other three, WM32, WM34 and WM35, were in the subfloor. The room wood moisture content, WM33, was consistently higher than the subfloor joist moisture content and lower than the other subfloor floor board moisture contents. Of the three subfloor floor board moisture contents, the northwest location, WM34, was consistently the lowest. The southeast location, WM35, generally had the highest moisture content, except for twice during March 2011 when the centre floor board, WM32, moisture content was higher, and for February 2012 when those two locations had equal moisture contents. In winter of 2011 the southeast moisture content reached 2% above that at the centre location.

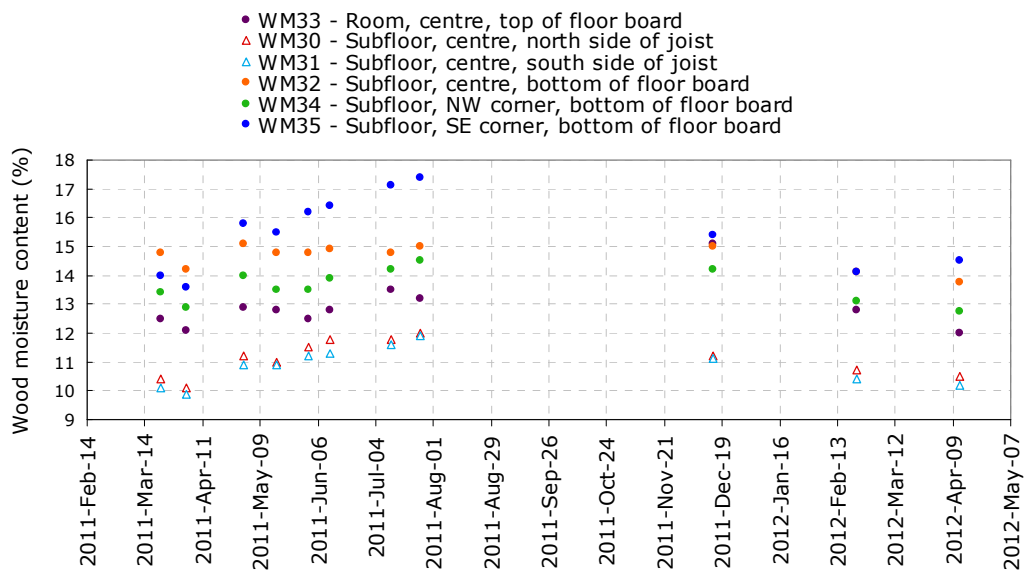


Figure 6.31: Wood moisture content

6.2.3 Air, moisture and energy flows in the subfloor

Ventilation through the subfloor is calculated as described in Section 5.5.5. The relationship between subfloor humidity and ventilation is provided in Figure 6.32. There is a negative slope as expected and as seen in the literature but the correlation is very weak. Similar ventilation studies in the literature show a stronger correlation (Kurnitski 2000).

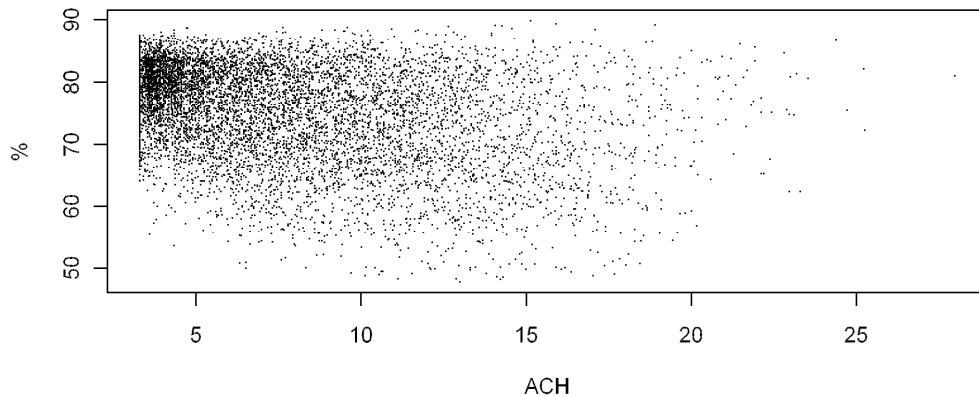


Figure 6.32: Subfloor centre relative humidity vs ventilation

The net moisture flow through the vents is calculated as described in Section 5.5.5 as a function of the subfloor and outdoor air properties and the ventilation. The net moisture exiting the vents is shown in Figure 6.33. The uncertainty in moisture flow is approximately 15%. This is based on the uncertainty in indoor and outdoor specific humidity, the assumed uncertainty in ventilation rate of 10%, and the uncertainty in air density resulting from the errors in the temperature and humidity measurements. The moisture flow is sometimes negative, indicating that 24% of the time the net effect of the vents is to introduce and deposit moisture into the subfloor. The moisture flow is higher in the warmer months than in the cooler months. This contradicts theories that vents can be problematic in summer (Kurnitski and Matilainen 2000).

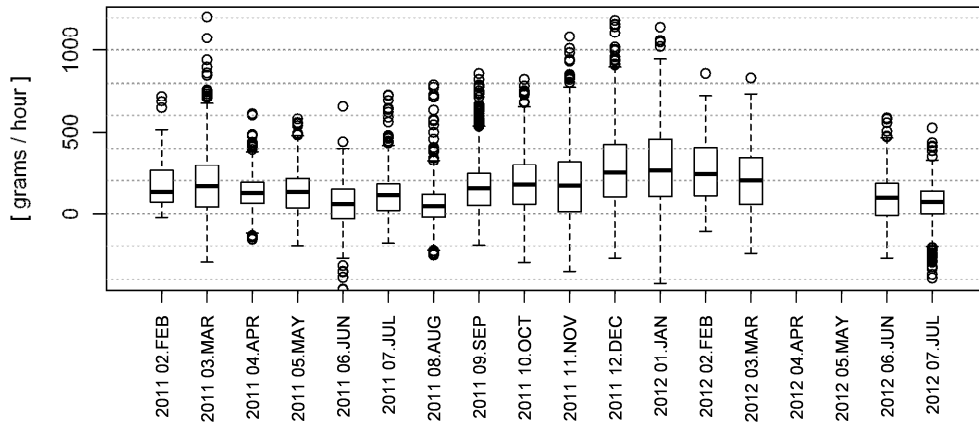


Figure 6.33: Net moisture exiting subfloor vents

The vents tend to increase subfloor moisture when the relative humidity is high and decrease moisture when the relative humidity is low, as shown in Figure 6.34. When the outside humidity drops below about 70% the vents primarily decrease subfloor moisture.

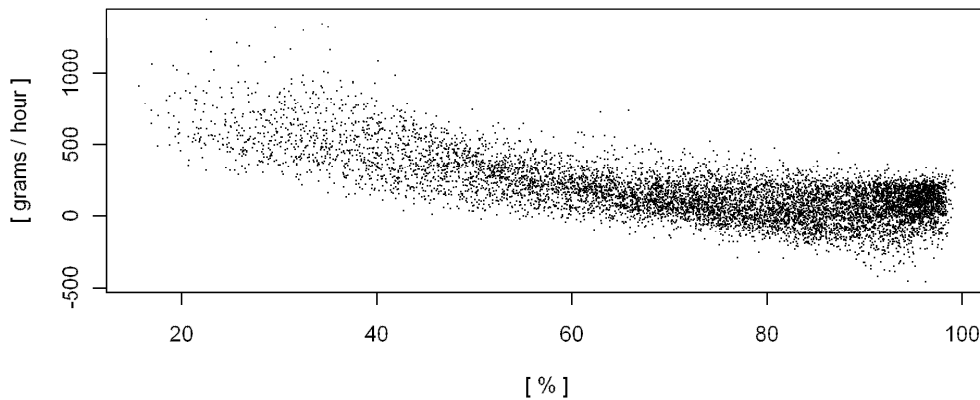


Figure 6.34: Net moisture exiting vents versus outside relative humidity

Evaporation was calculated as a function of the net moisture flow through the vents and the subfloor cavity moisture storage rate as shown in Equation 5.4. The moisture storage rate is calculated to be negligible in all cases. This was not unexpected as the specific humidity was observed to vary very slowly with time, as shown in Figure 6.25(b). Hence the evaporation term is equal to the net moisture exiting the subfloor via the vents. As the wood moisture content was also observed to vary slowly with time, as shown in Figure 6.31, any moisture exchange between the subfloor air and the wood elements in the subfloor is negligible. Thus, the source of evaporation in the subfloor can be considered to be solely from the ground.

There are two methods for moisture to enter the subfloor air as shown in the control volume of Figure 5.20. Moisture can enter from the ground via evaporation or from the vents via direct

transport. These two sources of moisture are compared in Figure 6.35. In nearly all cases, 99.6% of the time, more moisture enters the subfloor from the vents than from the ground. On average the vents introduce 8 times the moisture than the ground does. This relationship varies with the ventilation. With a low ventilation rate of 5 ACH, the vents bring in approximately four times the moisture than does the ground. At a mid-range ventilation rate of 12 ACH this ratio grows to 10, and the ratio increases as ventilation rate increases.

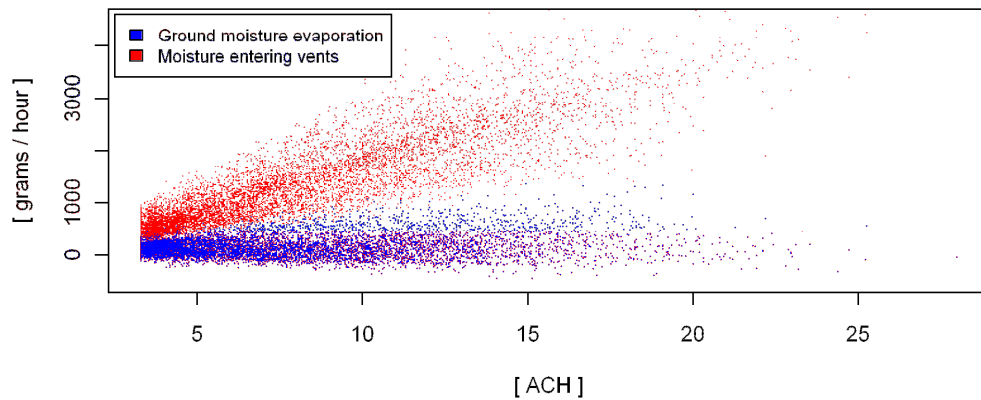


Figure 6.35: Subfloor cavity moisture sources versus ventilation

This high vent-to-evaporation ratio is comparable to that found in the British study described in Section 2.5.2 (Hartless and Llewellyn 1999) where it was found that the vents' contribution of moisture was an order of magnitude greater than the contribution from the ground evaporation.

The relationship between ground moisture evaporation and ventilation is shown in greater detail in Figure 6.36. The evaporation rate, averaging 5 g/m²/hour over the test period, is at the lower end of the range observed in the published studies from New Zealand and Finland (Abbott 1983; Bassett 1988; Kurnitski 2000; Trethowen 1994, 1998) as described in Section 2.5.2.

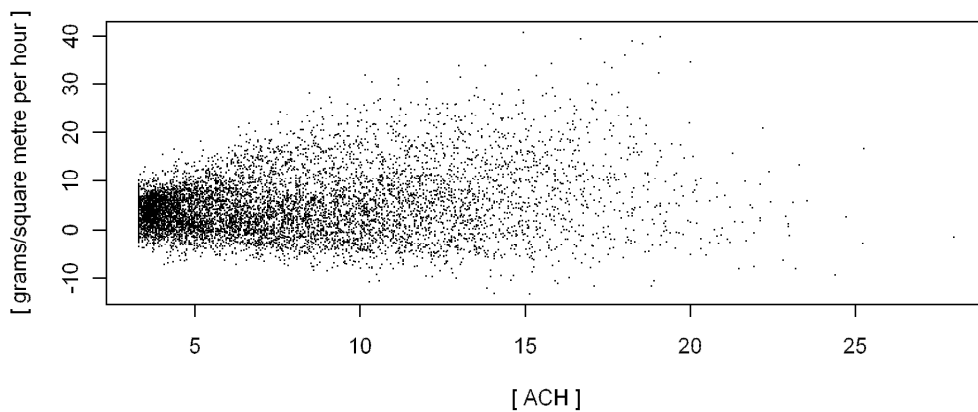


Figure 6.36: Ground moisture evaporation as a function of ventilation

The data in Figure 6.36 show no correlation with an R^2 of 0.05 and a slope of near 0. The uncertainty of 15% in evaporation rate is not enough to account for this lack of correlation. This differs from the literature, which shows evaporation to have a weak correlation with ventilation but a clearly positive slope (Kurnitski 2000). However, as ventilation is only one contributor to the evaporation potential as described in Section 5.5.5 and there may be substantial confounding between ventilation and the other contributors to evaporation potential, the lack of a strongly positive correlation between evaporation and ventilation does not indicate an unexplainable phenomenon. Nevertheless, the relationship between evaporation and ventilation was investigated further and is documented in Appendix A.5.1.

The evaporation potential is the product of ground surface vapour pressure deficit and wind speed. The ground surface vapour pressure is a function of the ground surface temperature and amount of moisture at the surface. However, the thermocouples measuring ground surface temperatures are not reliable. In addition, the soil moisture content has been observed to be lower than the critical value at which it can be treated as free water, and this alters the relationship between ground surface vapour pressure and temperature. Thus, the evaporation potential cannot be determined with great accuracy. An estimated evaporation potential is calculated using ground temperature at 150 mm deep and assuming the vapour pressure is equal to that of fully saturated conditions.

The observed evaporation versus evaporation potential is provided in Figure 6.37. The scale and units of the evaporation potential are arbitrary and thus the value of slope has no meaning. However, the slope is clearly positive as expected and the correlation R^2 of 0.30 is better than observed in Figure 6.36. Thus, the calculated value of evaporation is within expectation.

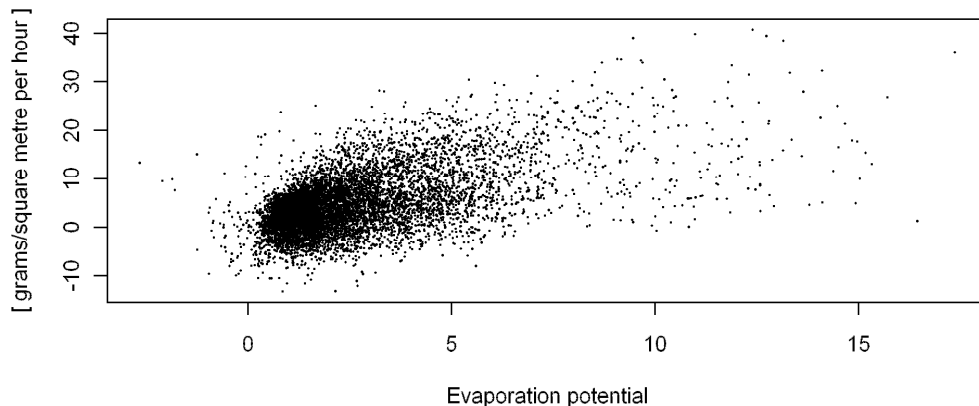


Figure 6.37: Ground moisture evaporation vs. evaporation potential

The net enthalpy flow through the vents is calculated as described in Section 5.5.5 as a function of the subfloor and outdoor air properties and the ventilation. The net enthalpy exiting the subfloor via the vents is shown in Figure 6.38. The energy flow is often negative, indicating that 35% of the

time the net effect of the vents is to increase the energy content of the subfloor cavity air. The net amount of energy exiting the vents is higher in the warmer months than in the cooler months.

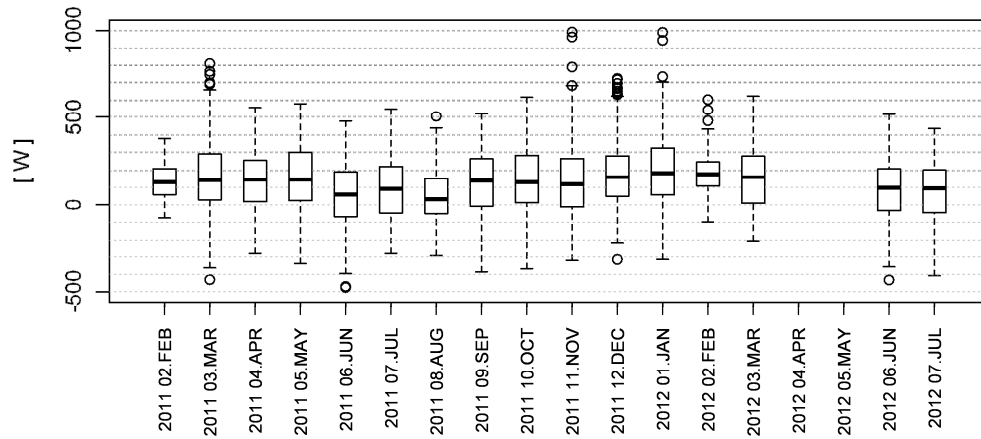


Figure 6.38: Net energy exiting subfloor vents

There is no strong correlation between the net energy through the vents and subfloor ventilation. The strongest correlation between the energy flow and any environmental parameter is with the outdoor specific humidity, as shown in Figure 6.39.

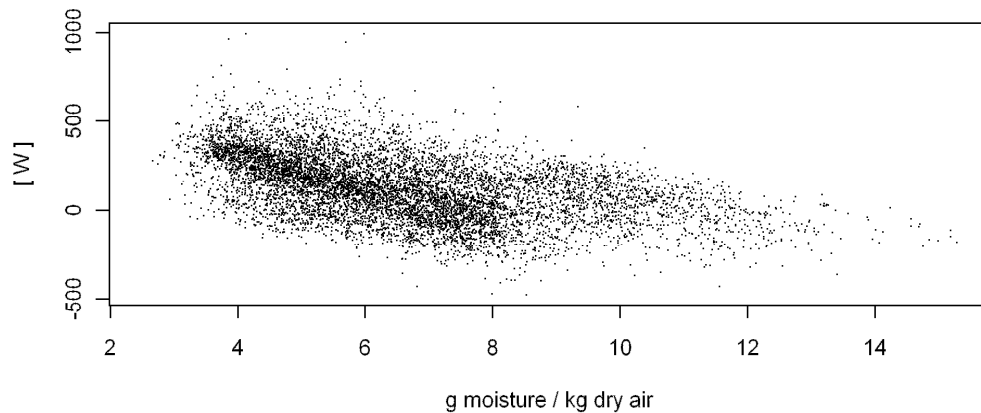


Figure 6.39: Net energy exiting subfloor vents versus outdoor specific humidity

6.2.4 Different time periods and historical data

As an initial part of this research, test cell data from 2007 (Dewsbury 2011) was investigated to reveal patterns of the subfloor climate environment and moisture and energy flows (Sequeira et al. 2010b). The comparison of the subfloor and outdoor air temperatures from that study is provided in Figure 6.40.

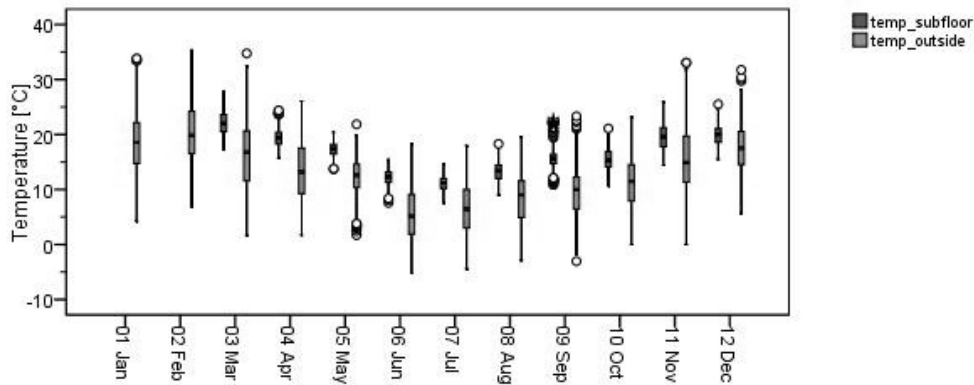
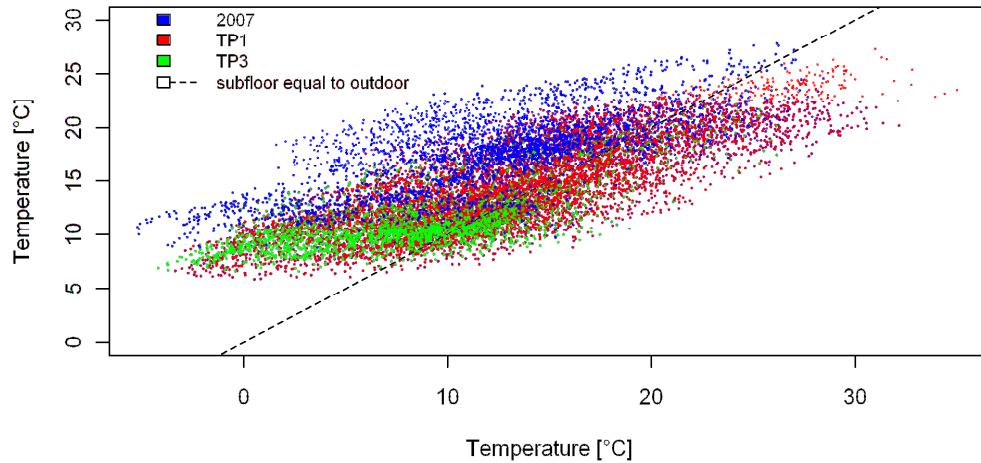


Figure 6.40: 2007 Subfloor and outdoor air temperatures (Sequeira et al. 2010b)

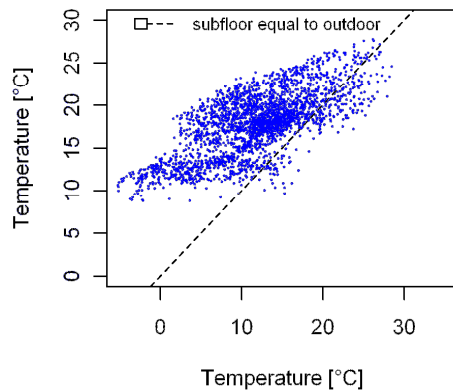
In 2007, the subfloor median temperature by month is nearly always greater than the third quartile of outdoor temperature. However, Figure 6.13 from 2011-2012 displays a subfloor temperature much closer in value to the outdoor temperature. This change in subfloor conditions between 2007 and 2011-2012 is investigated further.

Subfloor parameters of air temperature, relative humidity and specific humidity from 2007 are compared to those parameters from 2011-2012 TP1 and TP3. Each parameter is graphed against the corresponding outdoor parameter, as they were found to have the highest correlations. The 2007 data series spans January through December, though temperature is missing in January and February and relative humidity is missing in December. The TP1 data series spans one year from February 2011 through February 2012. The TP3 data series is smaller than the others as it spans only March to August of 2012. In 2007, as in TP3, there was no ground sheet present and the room ceiling hatch was in place. During TP1, however, the ground sheet was in place and the ceiling hatch was off.

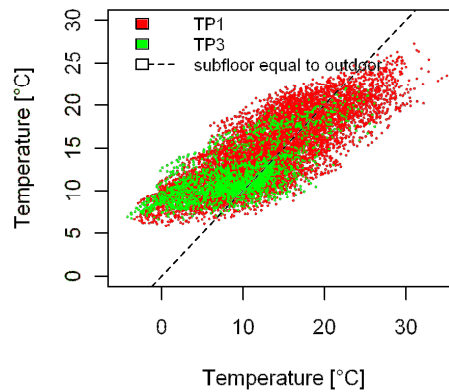
Figure 6.41(a) compares the subfloor temperatures from 2007 to 2011-2012. All three data sets span a similar range of outdoor temperature. There is an obvious difference in the subfloor temperature between 2007 and 2011-2012. The subfloor temperature in 2007 is a few degrees higher. In 2007 the subfloor temperature rarely drops below 10 °C but in 2011-2012 it appears to do that approximately one fifth of the time. This difference in subfloor temperature is easier to see in Figure 6.41(b) and (c). In Figure 6.41(b) the data is mostly above the line of equal subfloor and outdoor temperature, while in Figure 6.41(c) a substantial number of data points are below.



(a) 2007, 2011-2012 TP1 and TP3



(b) 2007 only



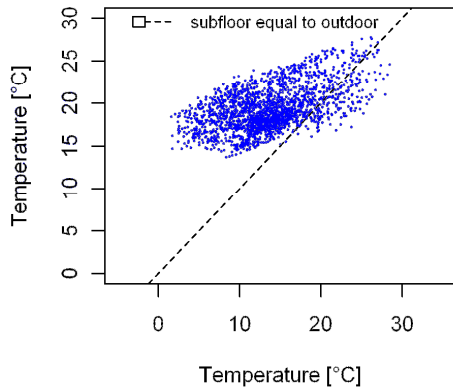
(c) 2011-2012 TP1 and TP3 only

Figure 6.41: Subfloor temperature vs. outdoor temperature, by time period

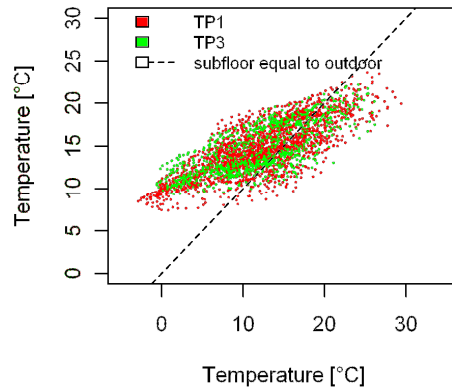
The TP1 and TP3 data of Figure 6.41(c) are mostly interspersed though it appears that TP1 subfloor temperature is a few degrees higher than TP3 subfloor temperature when the outdoor temperature is between 10 and 20 °C. It is possible that there is a seasonal trend in the data causing this difference.

As the TP3 data only spans autumn and winter, only data from these seasons are compared in Figure 6.42. The autumn data of Figure 6.42(a) and (b) shows that the 2007 subfloor temperature is still higher than the 2011-2012 temperature, and also that the TP1 and TP3 subfloor temperatures are clearly interspersed. The winter data of Figure 6.42(c) and (d) show the same two trends. Thus, the visible difference in subfloor temperature between TP1 and TP3 observed in Figure 6.41(c) is attributed to seasonal differences and not an actual physical phenomenon. Comparison between

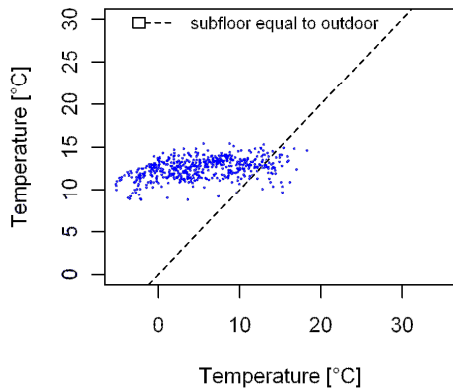
seasons shows that in winter the subfloor temperature is relatively constant and less sensitive to the outdoor temperature than it is in autumn.



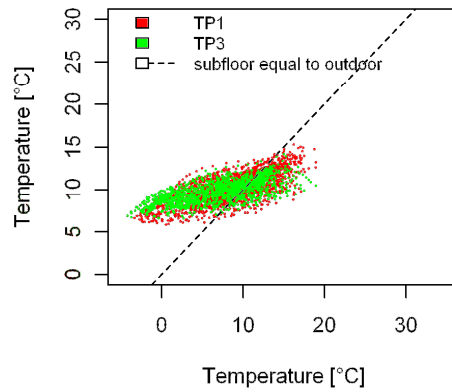
(a) 2007 autumn



(b) 2011-2012 autumn



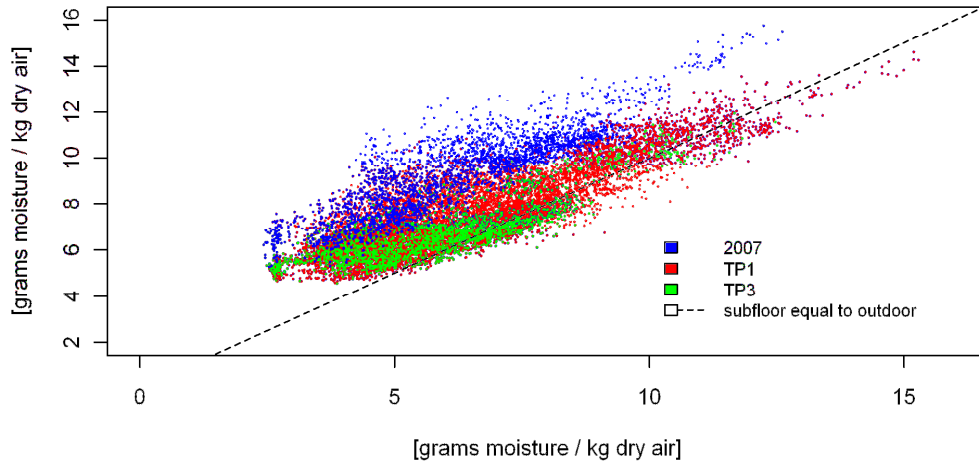
(c) 2007 winter



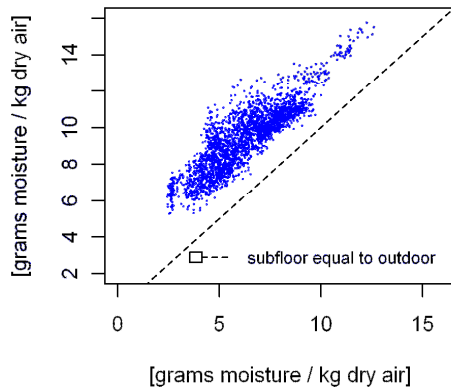
(d) 2011-2012 winter

Figure 6.42: Subfloor temperature, by time period and season

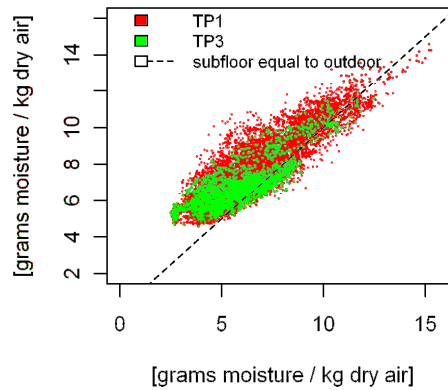
Specific humidity of the 2007 and 2011-2012 data is compared in Figure 6.43(a). The TP1 data spans a larger range of outdoor humidity than does either the 2007 or TP3 data. There is a noticeable difference in the subfloor humidity between 2007 and 2011-2012. This difference is displayed in Figure 6.43(b) and (c). All the 2007 data of Figure 6.43(b) is well above the line, indicating that the specific humidity in the subfloor is always greater than in the outdoors. However, Figure 6.43(c) shows that approximately one quarter of the time, the 2011-2012 subfloor specific humidity is below the outdoor specific humidity.



(a) 2007, 2011-2012 TP1 and TP3



(b) 2007 only

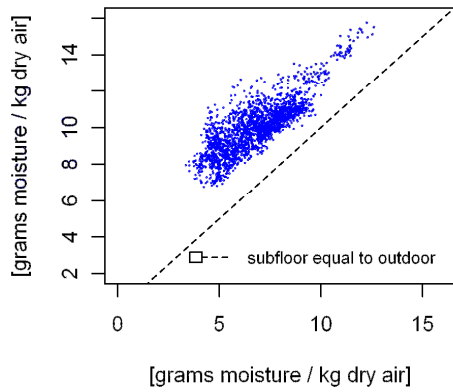


(c) 2011-2012 TP1 and TP3 only

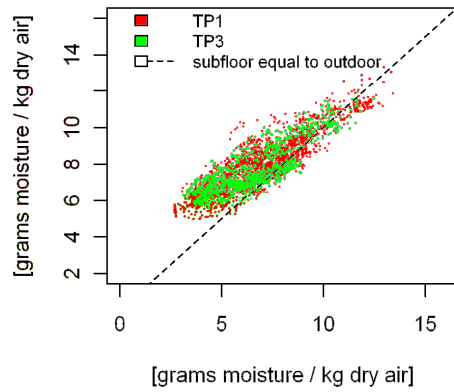
Figure 6.43: Subfloor specific humidity vs. outdoor specific humidity, by time period

The TP1 and TP3 data of Figure 6.43(c) are mostly interspersed though it appears that TP1 specific humidity is greater than the TP3 specific humidity. As was done for the subfloor temperature, the subfloor specific humidity is investigated by season in Figure 6.44.

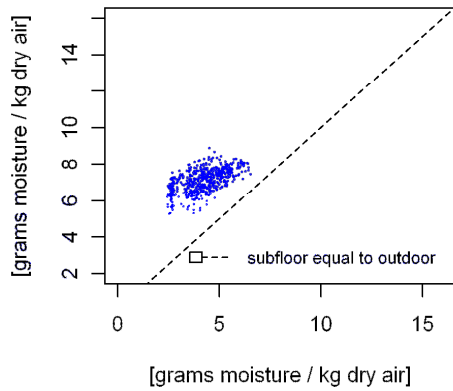
The autumn data in Figure 6.44 (a) and (b) show that the 2007 subfloor specific humidity is higher than the 2011-2012 specific humidity, and that the TP1 and TP3 specific humidities are clearly interspersed. The winter data of Figure 6.44 (c) and (d) show the same two trends. Thus, the visible difference in specific humidity between TP1 and TP3 observed in Figure 6.43(c) is attributed to seasonal differences and not an actual physical phenomenon. Comparison between seasons shows that in winter the subfloor specific humidity is less sensitive to the outdoor specific humidity than it is in autumn.



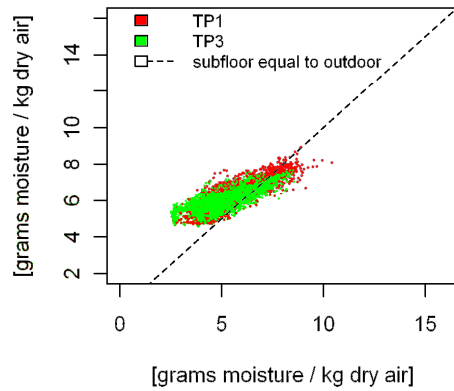
(a) 2007 autumn



(b) 2011-2012 TP1 and TP3 autumn



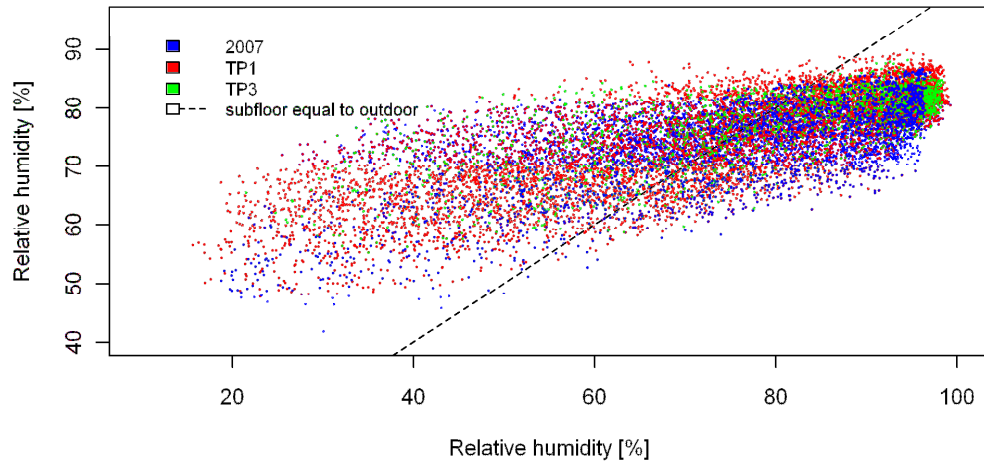
(a) 2007 winter



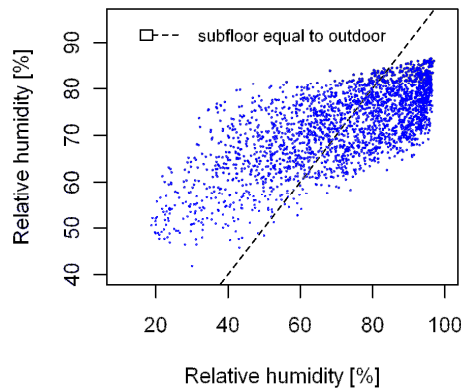
(b) 2011-2012 TP1 and TP3 winter

Figure 6.44: Subfloor specific humidity, by time period and season

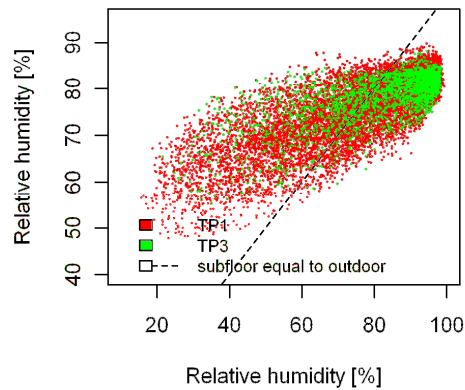
Figure 6.45(a), (b) and (c) show the subfloor relative humidity for the three series of data. There is little difference between the three series. The 2007 subfloor data do not reach as high a value as the 2011-2012 data, though that is expected to be caused by nuances in the data acquisition and reduction processes and not an actual physical phenomenon.



(a) 2007, 2011-2012 TP1 and TP3



(b) 2007 only



(c) 2011-2012 TP1 and TP3 only

Figure 6.45: Subfloor relative humidity vs. outdoor relative humidity, by time period

The pattern of moisture flows throughout the subfloor in 2011-2012 differs from that of 2007. This is displayed in the ground moisture evaporation as shown in Figure 6.46. In the 2007 data set, missing wind speed values limit the calculation of evaporation to only March through June, or autumn and winter. The 2007 evaporation has a number of data points clustered between 10 and 20 g/m²/hr, whereas the 2011-2012 data is mostly under 10 g/m²/hr. The 2007 evaporation data set has a strong, positive correlation with ventilation with an R² of 0.78, whereas the 2011-2012 data set as shown in Figure 6.36 correlates poorly with ventilation. The 2007 relationship between evaporation rate and ventilation rate is similar to other studies in the literature (Kurnitski 2000).

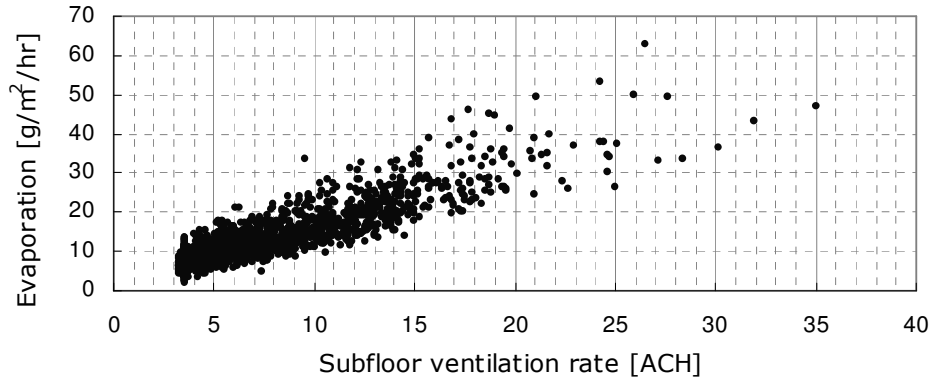
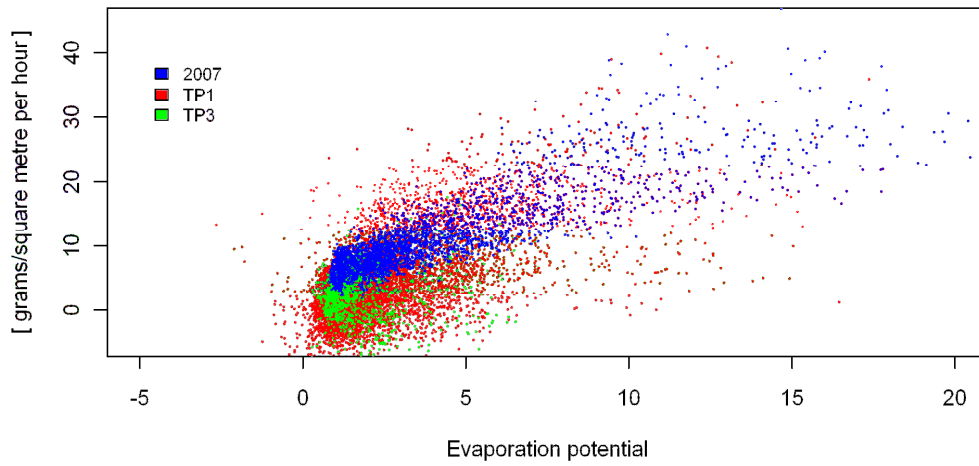
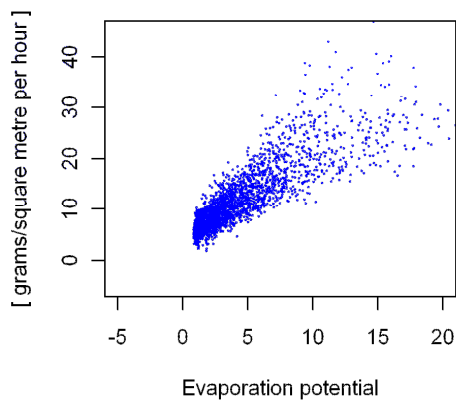


Figure 6.46: 2007 Ground moisture evaporation vs. subfloor ventilation (Sequeira et al. 2010b)

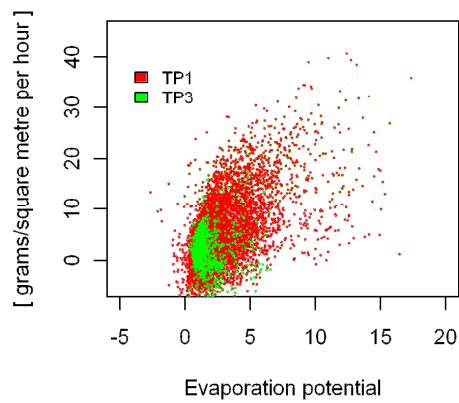
The 2007 evaporation data also show a correlation with evaporation potential, as shown in Figure 6.47. The 2007 data have a strong, positive correlation with evaporation potential with an R^2 of 0.75, which is stronger than the 2011-2012 data R^2 of 0.30 as shown in Figure 6.37.



(a) 2007, 2011-2012 TP1 and TP3



(b) 2007 only



(c) 2011-2012 TP1 and TP3 only

Figure 6.47: Evaporation vs. evaporation potential, by time period

Figure 6.47 shows the TP1 and TP3 evaporation data to display different trends. However, when only the winter data is selected the two series of data collapse, as shown in Figure 6.48. Only winter data are shown as there are no evaporation data for TP3 in autumn, as the observed wind speed data were not available.

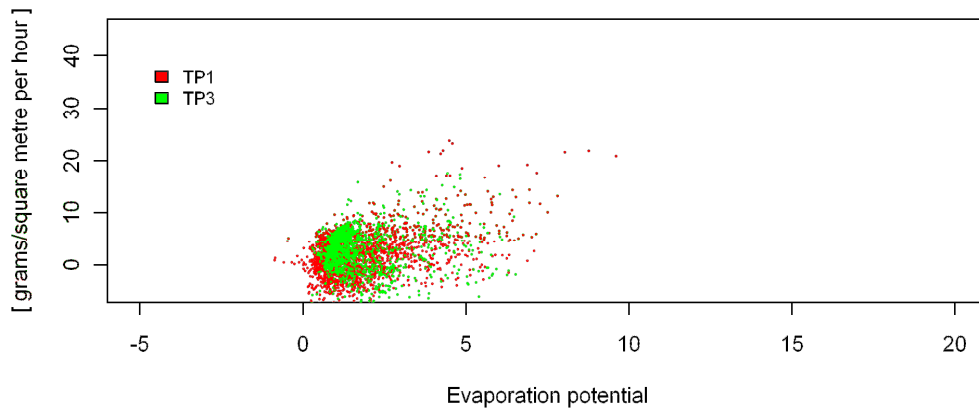


Figure 6.48: Subfloor evaporation vs. evaporation potential, TP1 and TP3 winter data

In 2011-2012, 24% of the time the net effect of vents was to actually increase the moisture of the subfloor. However, in 2007 this was never the case (Sequeira et al. 2010b). This is supported by Figure 6.43(b), which shows the subfloor specific humidity was always greater than the outdoor specific humidity during 2007.

The source of subfloor moisture also differs between 2007 and 2011-2012. In 2011-2012 the vents introduce on average 8 times as much moisture to the subfloor than the ground does via evaporation. In 2007, however, the vents introduce only 2.5 times as much (Sequeira et al. 2010b).

There is also a difference in the energy flow through the subfloor vents between 2007 and 2011-2012. In 2011-2012 the vents' net effect is to introduce energy into the subfloor 35% of the time. However, in 2007 this was the case for less than 1% of the time. In the two of the 2500 instances in 2007 when the vents did introduce energy, it was in both instances less than 15 W (Sequeira et al. 2010b).

6.3 Presentation of AccuRate data

AccuRate subfloor temperature is analysed and compared to the observed dry bulb and environmental temperatures. Only limited results are presented for the room zone as that is mostly out of the scope of this research. The AccuRate data are generated and reduced as described in Section 5.6.

AccuRate Run 1 (AR1) data are presented and related to previous test cell research. AccuRate Run 2 (AR2) data are then presented and compared to Run 1 data. Run 2 data include corrections of errors and are thus more representative of the capabilities of the AccuRate program. Subfloor data for TP1, TP2 and TP3 are presented, but only TP3 data are presented for the room zone, due to the inability of AccuRate to model the open ceiling hatch present during TP1 and TP2.

6.3.1 AccuRate Run 1 results

Graphs of AccuRate room temperature, observed dry bulb temperature (ODB) and observed environmental temperature (OE) for two weeks are shown in Figure 6.49. Graphs of test cell room temperatures during all weeks of TP3 containing AccuRate AR1 data are provided in Appendix A.5.2. The three data series generally follow the same daily pattern, though the AccuRate room temperature mostly remains above the observed room temperatures. There is no noticeable time shift between the three data series, with all maximum and minimum daily temperatures occurring at nearly identical times.

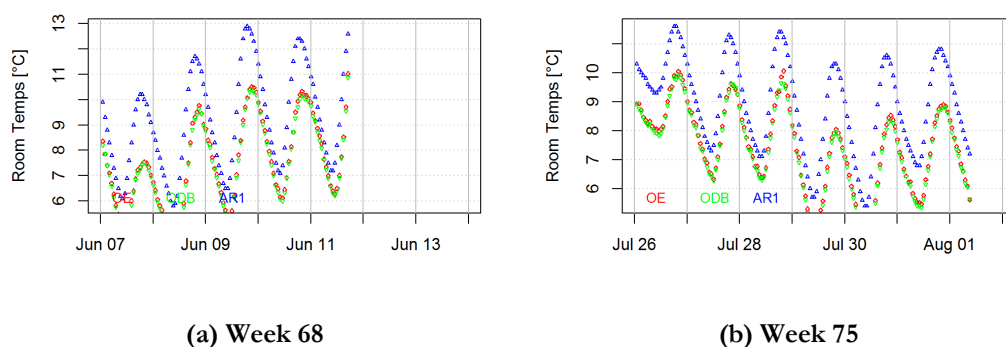


Figure 6.49: Observed and AR1 room temperatures for selected weeks

Graphs of AccuRate subfloor temperature, observed dry bulb temperature and observed environmental temperature for four representative weeks are shown in Figure 6.50. Similar graphs of subfloor temperature throughout the entire test period are in Appendix A.5.3, for all weeks that contain AccuRate data. The AccuRate and observed data generally follow the same daily pattern. There is no noticeable time shift between the three data series, with all peaks and troughs occurring at nearly identical times.

The greatest difference between the AccuRate and observed data appear to occur at the daily maximum and minimum temperatures when the AccuRate data overshoot and undershoot the observed data. Thus the AccuRate data has the largest daily temperature range of the three series. The dry bulb temperature has slightly higher daily maximums and slightly lower daily minimums than the environmental temperature.

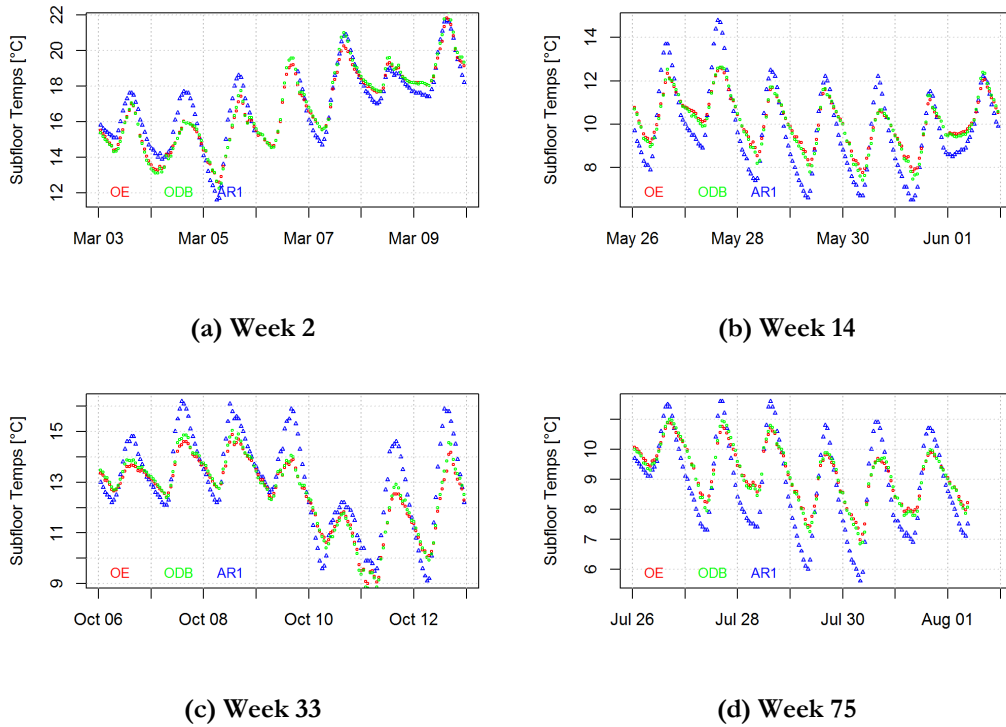


Figure 6.50: Observed and AR1 subfloor temperatures for selected weeks

The subfloor temperature from AccuRate Run 1 is compared to observed subfloor temperatures at different time periods in Figure 6.51(a) through (d). A line of perfect fit, indicating an equal AccuRate and observed temperature, is displayed in red on each graph. As AccuRate TP3 data only occur in winter, the temperature range evident in Figure 6.51(a) and (c) is much smaller than in (b) and (d).

The relationship between AccuRate subfloor temperature and dry bulb temperature in Figure 6.51(a) and (b) is similar to the relationship with environmental temperature in Figure 6.51(c) and (d). The AccuRate data span both higher and lower than the observed data and generally remains within two degrees of the observed data. This concurs with the trends observed in Figure 6.50.

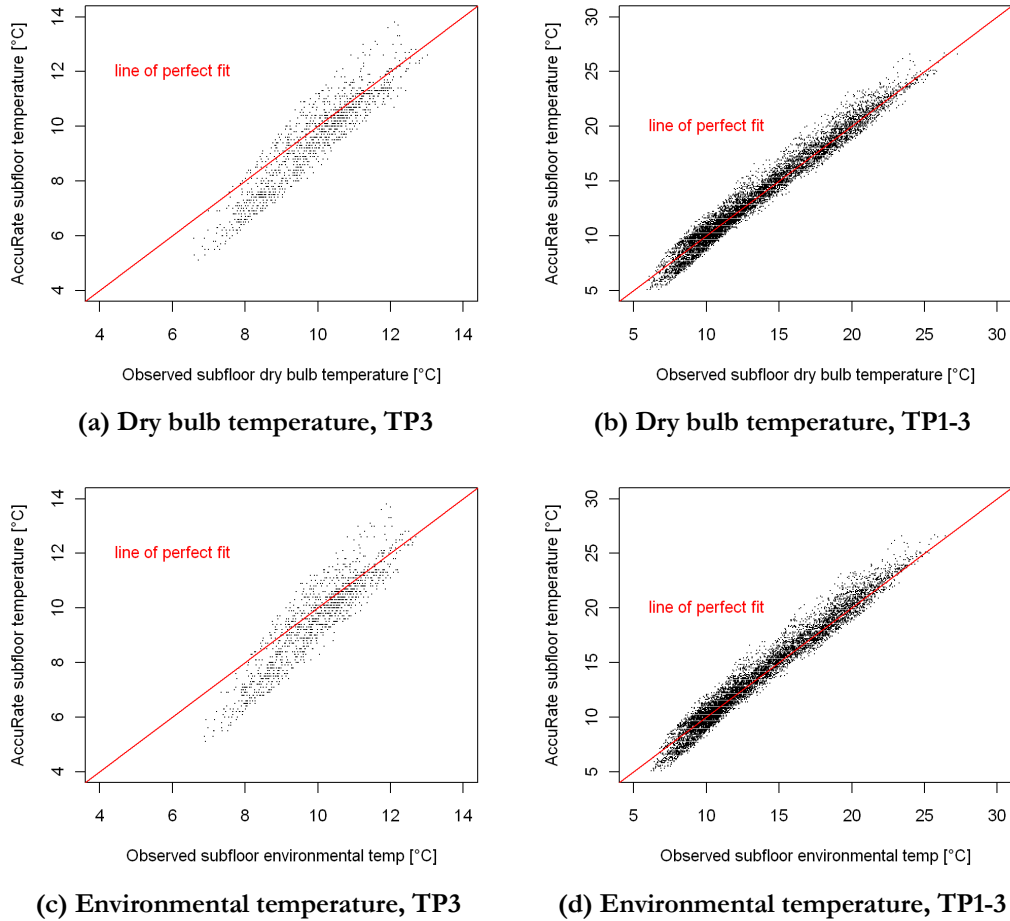


Figure 6.51: AR1 temperature vs. observed subfloor temperatures

The correlation of AccuRate subfloor temperature with observed subfloor temperatures is summarized in Table 6.3. There is no notable difference in the correlation between dry bulb and environmental temperature. The lower correlation values during TP3 is not unexpected as the number of observations is lower.

Table 6.3: Correlation of AR1 subfloor temperature to observed temperatures

Time Period	Observed Temperature	R^2
TP1-3	Dry bulb	0.97
TP3 only	Dry bulb	0.86
TP1-3	Environmental	0.97
TP3 only	Environmental	0.85

The data from Figure 6.51 (a) and (b) is compared to similar 2007 data from previous research shown in Figure 6.52. The 2007 data show a shift in the relation between AccuRate and observed temperature when the observed temperature is below 15 °C. That shift is not apparent in the 2011-

2012 data. The correlation of the 2007 data has an R^2 of 0.92 (Dewsbury 2011), similar to the 2011-2012 data.

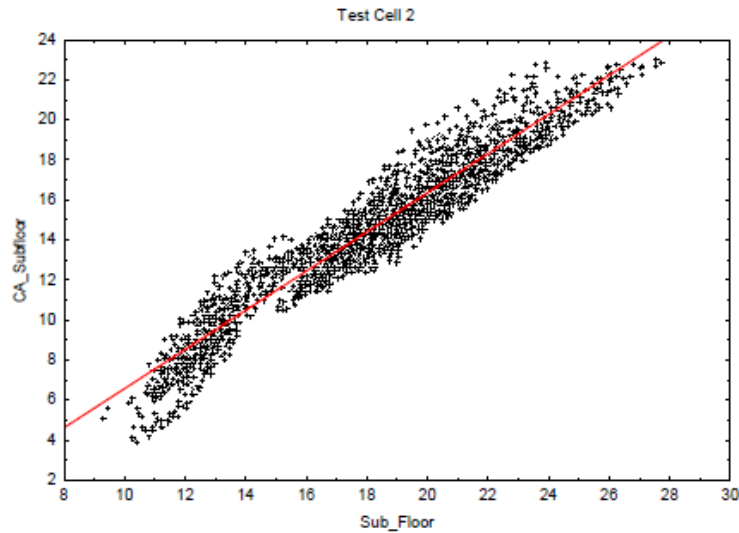


Figure 6.52: 2007 Simulated subfloor temperature versus observed subfloor dry bulb temperature (Dewsbury 2011)

Figure 6.50 and Figure 6.51 consider all hours of data. One way to summarize the AccuRate and observed data is to consider only the maximum and minimum daily temperatures. Considering only the extrema minimizes the effect of any transient lags in the data. Figure 6.53 shows the daily maximum and minimum AccuRate and observed subfloor temperatures for July 2012 in TP3. The graphs for all months of data are provided in Appendix A.5.4.

Figure 6.53 shows that the AccuRate data mostly have a larger range than the observed data. The maximum daily temperatures are higher and the minimum daily temperatures are lower. This agrees with the trends observed in Figure 6.50.

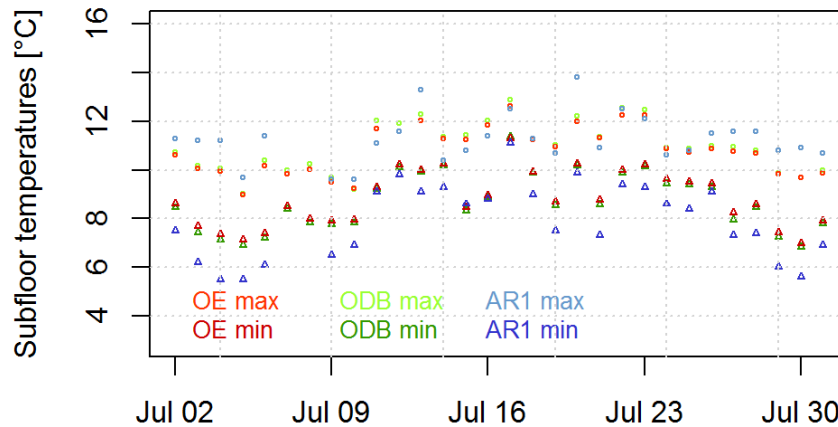


Figure 6.53: Observed and AR1 daily min. and max. subfloor temperatures, July 2012

The differences in these daily minimum and maximum temperatures, observed minus AccuRate, are the daily minimum and maximum residuals. The daily minimum residual is the difference between the temperatures when each is at its daily minimum, and the daily maximum residual is the difference when each is at its daily maximum. Use of daily residuals avoids any complication due to time shifts between the AccuRate and observed data, because they only consider the maximum and minimum temperature values and are not a function of the times at which those values occur. For direct comparison to prior studies the dry bulb temperatures is used instead of the environmental temperature. The room and subfloor daily residuals are tabulated by month and the average values are presented in Table 6.4.

Table 6.4: Daily minimum and maximum residuals (ODB – AR1), averaged by month

Month	# of Data points		Daily Minimum Residual [°C] (Observed - AccuRate)		Daily Maximum Residual [°C] (Observed - AccuRate)	
	Subfloor	Room	Subfloor	Room	Subfloor	Room
2011 February	0					
2011 March	13		0.4		-0.3	
2011 April	3		-0.5		0.0	
2011 May	17		0.7		-0.4	
2011 June	29		0.3		-0.2	
2011 July	31		0.0		-0.8	
2011 August	29		0.0		-0.4	
2011 September	30		0.4		-0.5	
2011 October	25		0.4		-0.7	
2011 November	30		0.2		-0.2	
2011 December	31		0.4		-0.8	
2012 January	30		0.4		-0.4	
2012 February	4		0.6		-1.0	
2012 March	5	0	0.5		-0.1	
2012 April	0	0				
2012 May	0	0				
2012 June	19	19	0.8	-1.4	-0.2	-1.8
2012 July	29	29	0.8	-1.3	-0.2	-1.6

The subfloor minimum residuals are mostly positive and the maximum residuals are mostly negative, supporting the trends observed in Figure 6.50 and Figure 6.53 that AccuRate data both

undershoot and overshoot the observed data. The highest minimum daily subfloor residuals occur in May 2011 and June and July 2012. The lowest maximum daily subfloor residuals occur in July, October and December 2011, and February 2012. The room temperature average daily residuals are all negative with roughly the same values, concurring with the trend observed in Figure 6.49 that the AccuRate room temperature is shifted above the test cell room temperature with a similar daily temperature range.

The average daily residuals from previous test cell research in 2007 are provided in Table 6.5. All subfloor and rooms residuals are lower in 2011-2012 than in 2007.

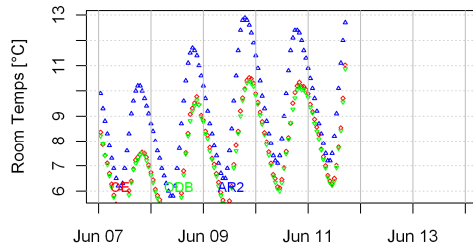
Table 6.5: Average daily minimum and maximum residuals (ODB – AccuRate) from 2007 (Dewsbury 2011)

	Daily Minimum Temperature (Measured – Simulated)			Daily Maximum Temperature (Measured – Simulated)		
	Subfloor	Room	Roof	Subfloor	Room	Roof
January		4.65			4.18	
February		4.48			3.40	
March	4.75	5.58	9.24	4.83	5.40	3.45
April	4.31	4.90	8.85	3.13	4.00	3.25
May	3.93	4.50	8.87	3.83	4.55	6.31
June	5.67	4.08	8.76	3.66	3.08	5.07#
# This does not include the maximum value for June 22 Note: The measured data for the months of January and February is unavailable for the subfloor and roof space.						

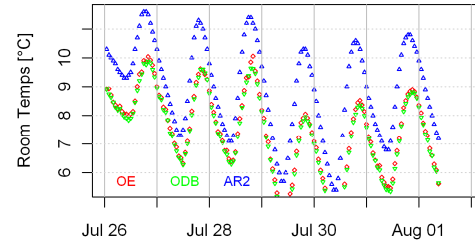
The 2011-2012 subfloor and room average daily residuals are several degrees lower than those from 2007, which are a positive value for each month. The largest subfloor minimum residual for both the 2011-2012 and 2007 data occurred in June. There is little difference in the daily temperature range between the current data and 2007 data, as indicated by the difference between the daily maximum and daily minimum residuals for each zone. This indicates that there may not be a fundamental change in the profile of any of the data series between 2007 and 2011-2012, but instead a simple shifting up or down.

6.3.2 AccuRate Run 2 results

Graphs of AccuRate room temperature, observed dry bulb temperature and observed environmental temperature for two weeks are shown in Figure 6.54. Graphs of test cell room temperatures during all weeks of TP3 containing AccuRate AR2 data are provided in Appendix A.5.5. The three data series generally follow the same daily pattern, though as the case with the AR1 data, the AR2 room temperature mostly remains above the observed room temperatures. There is no noticeable time shift between the three data series, with all maximum and minimum daily temperatures occurring at nearly identical times.



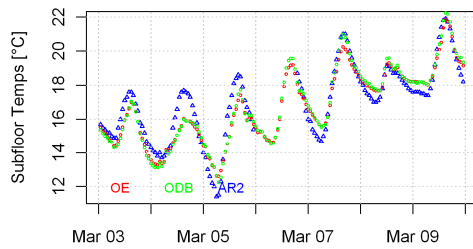
(a) Week 68



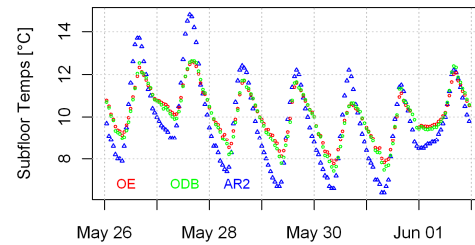
(b) Week 75

Figure 6.54: Observed and AR2 room temperatures for selected weeks

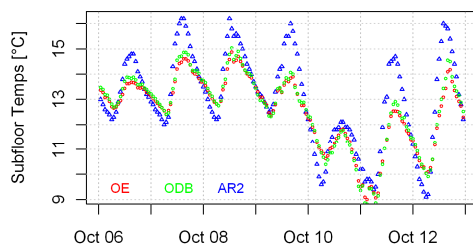
Graphs of AccuRate subfloor temperature, observed dry bulb temperature and observed environmental temperature for four representative weeks are shown in Figure 6.55. Similar graphs of subfloor temperature throughout the entire test period are in Appendix A.5.6, but only for the weeks that contain AccuRate data. The AccuRate and observed data generally follow the same daily pattern. There is no noticeable time shift between the three data series, with all peaks and troughs occurring at nearly identical times. At this scale there is no readily observable difference between the AR2 and AR1 data.



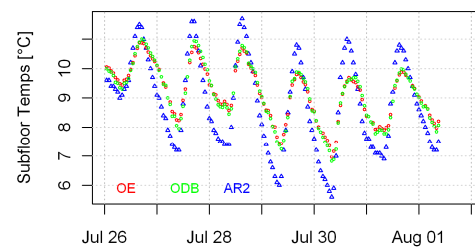
(a) Week 2



(b) Week 14



(c) Week 33



(d) Week 75

Figure 6.55: Observed and AR2 subfloor temperatures for selected weeks

As was the case with the AR1 data, the greatest difference between the AR2 and observed data appear to occur at the daily maximum and minimum temperatures when the AccuRate data overshoot and undershoot the observed data. Thus the AccuRate data has the largest daily temperature range of the three series. The dry bulb temperature has slightly higher daily maximums and slightly lower daily minimums than the environmental temperature.

The subfloor temperature from AccuRate Run 2 is compared to observed subfloor temperatures at different time periods in Figure 6.56(a) through (d). A line of perfect fit, indicating an equal AccuRate and observed temperature, is displayed in red on each graph. As AccuRate TP3 data only occur in winter, the temperature range evident in Figure 6.56(a) and (c) is much smaller than in (b) and (d).

The relationship between AR2 subfloor temperature and dry bulb temperature in Figure 6.56(a) and (b) is similar to the relationship with environmental temperature in Figure 6.56(c) and (d). The AccuRate data span both higher and lower than the observed data and generally remain within two degrees of the observed data. This concurs with the trends observed in Figure 6.55.

On these graphs there is no discernible difference between the AR1 and AR2 data. Similar to the AR1 data, the AR2 data show no shift in the AccuRate and observed data relationship below 15 °C as did the 2007 data (Dewsbury 2007).

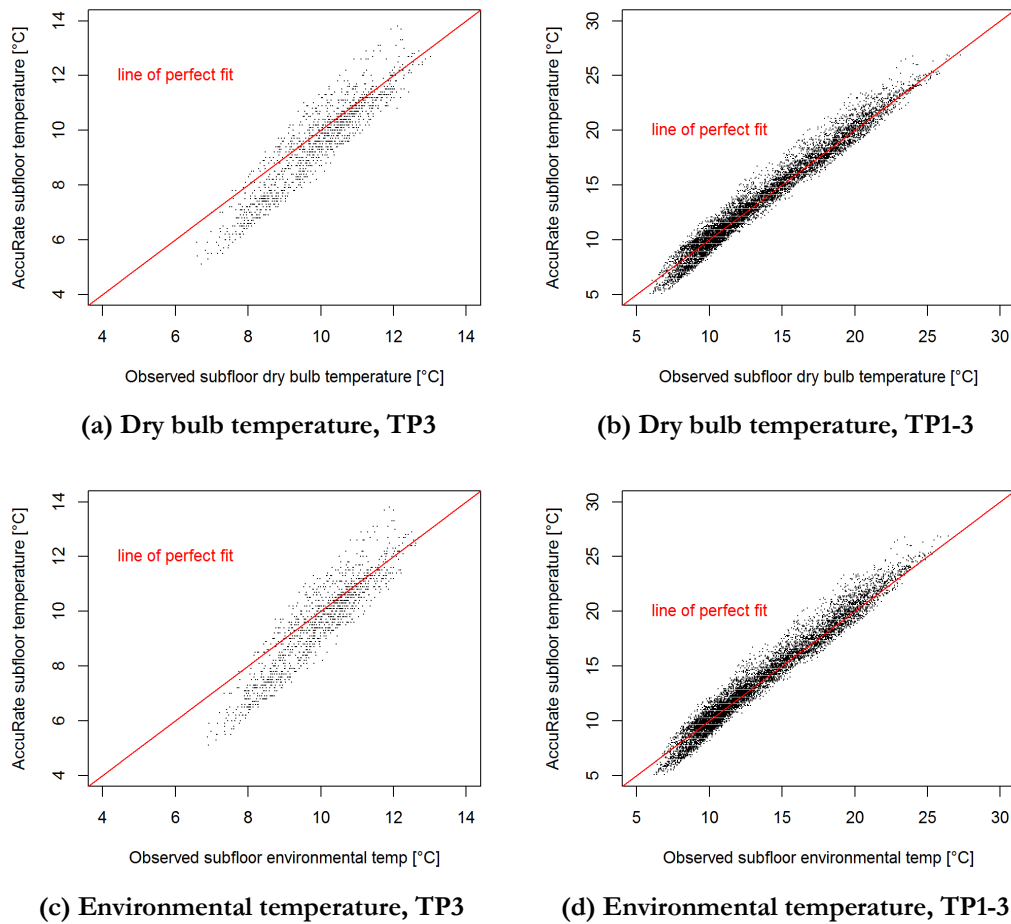


Figure 6.56: AR2 temperature vs. observed subfloor temperatures

The correlation of AR2 subfloor temperature with observed subfloor temperature is summarized in Table 6.6. The correlation values are identical to those of AR1.

Table 6.6: Correlation of AR2 subfloor temperature to observed temperatures

Time Period	Observed Temperature	R^2
TP1-3	Dry bulb	0.97
TP3 only	Dry bulb	0.86
TP1-3	Environmental	0.97
TP3 only	Environmental	0.85

Figure 6.57 shows the daily maximum and minimum AR2 and observed subfloor temperatures for July 2012 in TP3. The graphs for all months of data are provided in Appendix A.5.7. These graphs show that the AccuRate temperature generally has a higher daily range than the observed temperatures. Comparing the AR2 daily temperatures to those of AR1 in Figure 6.53 shows no noticeable difference.

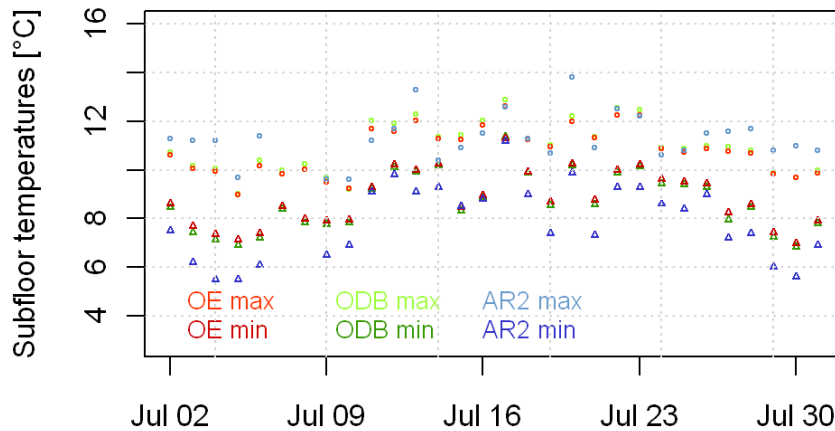


Figure 6.57: Observed and AR2 daily min. and max. subfloor temperatures, July 2012

The minimum daily residual is the AccuRate daily minimum temperature subtracted from the observed daily minimum temperature. The maximum daily residual is calculated similarly. Both the minimum and maximum daily residuals can be calculated via four different methods. The AccuRate temperature can be from either Run 1 or Run 2, and the observed temperature can be either from dry bulb or environmental temperature. A comparison of the daily subfloor residuals averaged by month and calculated via all four methods is provided in Figure 6.58. Data from months containing five or fewer observations have been removed.

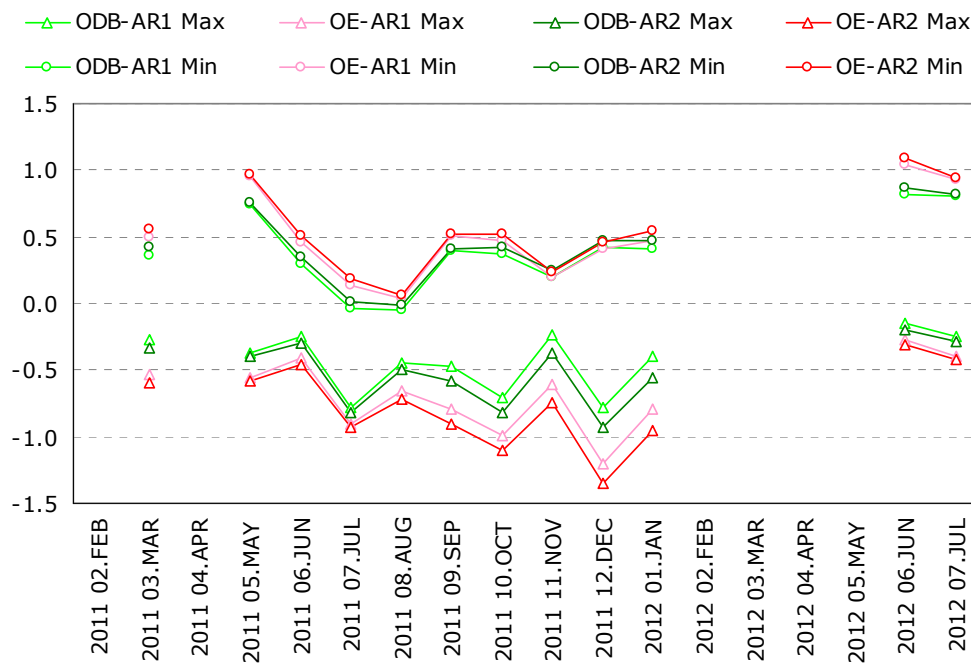


Figure 6.58: Monthly average of AR1 and AR2 daily residuals

The minimum daily residuals are mostly positive, supporting the observed patterns that the AccuRate minimum temperature is mostly less than that of the observed data. All four series have a very similar monthly pattern. The residuals are greater when calculated using environmental temperature instead of dry bulb temperature, and this trend holds for both the AR1 and AR2 data. This is not unexpected as the dry bulb temperature also overshoot and undershot the environmental temperature. The AR1 and AR2 values are very similar. The difference in minimum daily residuals when going from dry bulb to environmental temperature is greater than the difference when going from AR1 to AR2.

The maximum daily residuals are all negative, supporting the observed patterns that the AccuRate maximum daily temperature is mostly greater than that of the observed data. All four series have a very similar monthly pattern, and the relationship between the four series of the maximum daily residuals is similar to that of minimum daily residuals. The maximum daily residuals are greatest, in this case meaning furthest from zero, when calculated using environmental temperature instead of dry bulb temperature, and this trend holds for both the AR1 and AR2 data. The AR1 and AR2 values are very similar. The difference in maximum daily residuals when going from dry bulb to environmental temperature is greater than the difference when going from AR1 to AR2.

Residuals calculated based on dry bulb temperature were provided for purposes of direct comparison to previous research. However, environmental temperature better represents AccuRate's output (Chen 2013a). Additionally, AR2 represents the test cell and climate better than AR1 does. Thus, the room and subfloor residuals are best calculated using AR2 AccuRate temperature and environmental observed temperature.

Throughout the entire test period the subfloor daily minimum residuals range from 1.9 °C to -1.0 °C. The subfloor daily maximum residuals range from 0.9 °C to -3.4 °C. The daily residuals are averaged by month and presented in Table 6.7.

Table 6.7: Daily minimum and maximum residuals (OE – AR2), averaged by month

Month	# of Data points		Daily Minimum Residual [°C] (Observed - AccuRate)		Daily Maximum Residual [°C] (Observed - AccuRate)	
	Subfloor	Room	Subfloor	Room	Subfloor	Room
2011 February	0					
2011 March	13		0.6		-0.6	
2011 April	3		-0.3		-0.2	
2011 May	17		1.0		-0.6	
2011 June	29		0.5		-0.5	
2011 July	31		0.2		-0.9	
2011 August	29		0.1		-0.7	
2011 September	30		0.5		-0.9	
2011 October	25		0.5		-1.1	
2011 November	30		0.2		-0.7	
2011 December	31		0.5		-1.3	
2012 January	30		0.5		-1.0	
2012 February	4		0.8		-1.5	
2012 March	5		0.7		-0.5	
2012 April	0					
2012 May	0					
2012 June	19	19	1.1	-1.3	-0.3	-1.6
2012 July	29	29	0.9	-1.2	-0.4	-1.5

The highest average minimum daily subfloor residuals occur in May 2011 and June and July 2012.

The lowest average maximum daily subfloor residuals occur in December 2011 and February 2012.

6.4 Correlation of residuals

The correlation between the room and subfloor residuals using AR2 AccuRate data and observed environmental temperature during TP3 is shown in Figure 6.59. The room residuals are generally approximately two degrees lower than the subfloor residuals. During TP3 the room residuals range from 0.2 °C to -3.2 °C and the subfloor residuals range from 2.0 °C to -1.9 °C. The correlation has an R^2 of 0.42. The room and subfloor residuals correlation in 2007 data had an R^2 value of 0.75 (Dewsbury 2011).

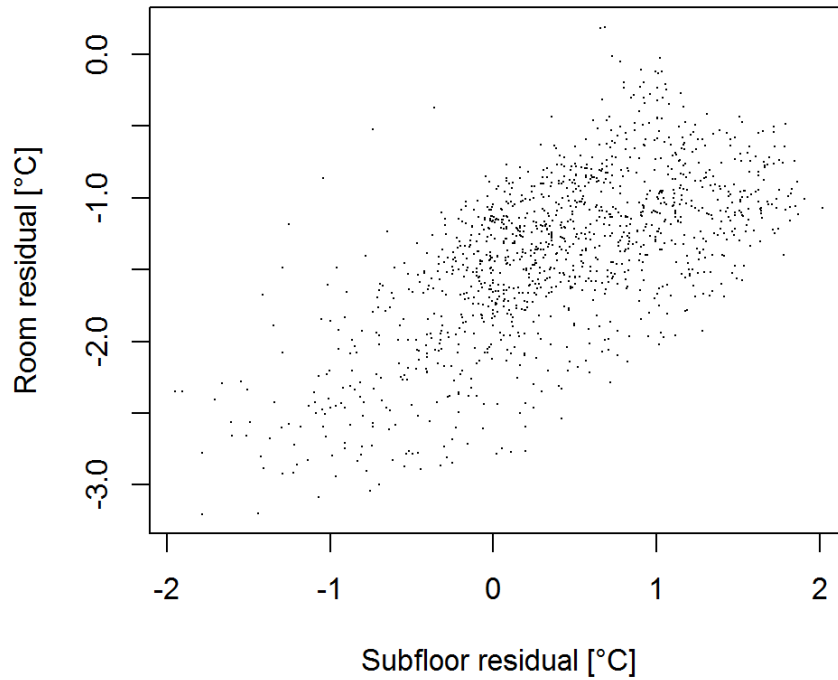


Figure 6.59: Correlation of room residuals with subfloor residuals (OE-AR2), TP3

The TP3 subfloor residuals at all hours are graphed against various observed parameters in Figure 6.60 and Figure 6.61. Similar graphs showing data from all time periods are in Appendix A.6.1. When considering the data from all time periods, the subfloor residuals range from 2.0 to -4.0 °C. The subfloor ground temperature is not the surface temperature but rather the temperature 150 mm below the surface at the subfloor centre. The wind direction is grouped into bins as it was for input into the AccuRate climate file. The subfloor temperature difference is the difference between the subfloor dry bulb air temperature and the ground temperature measured at 150 mm below the surface.

Figure 6.60 and Figure 6.61 show a correlation between the subfloor residuals and outdoor temperature, outdoor relative humidity, subfloor dry bulb temperature and the difference between subfloor dry bulb and subfloor ground temperatures.

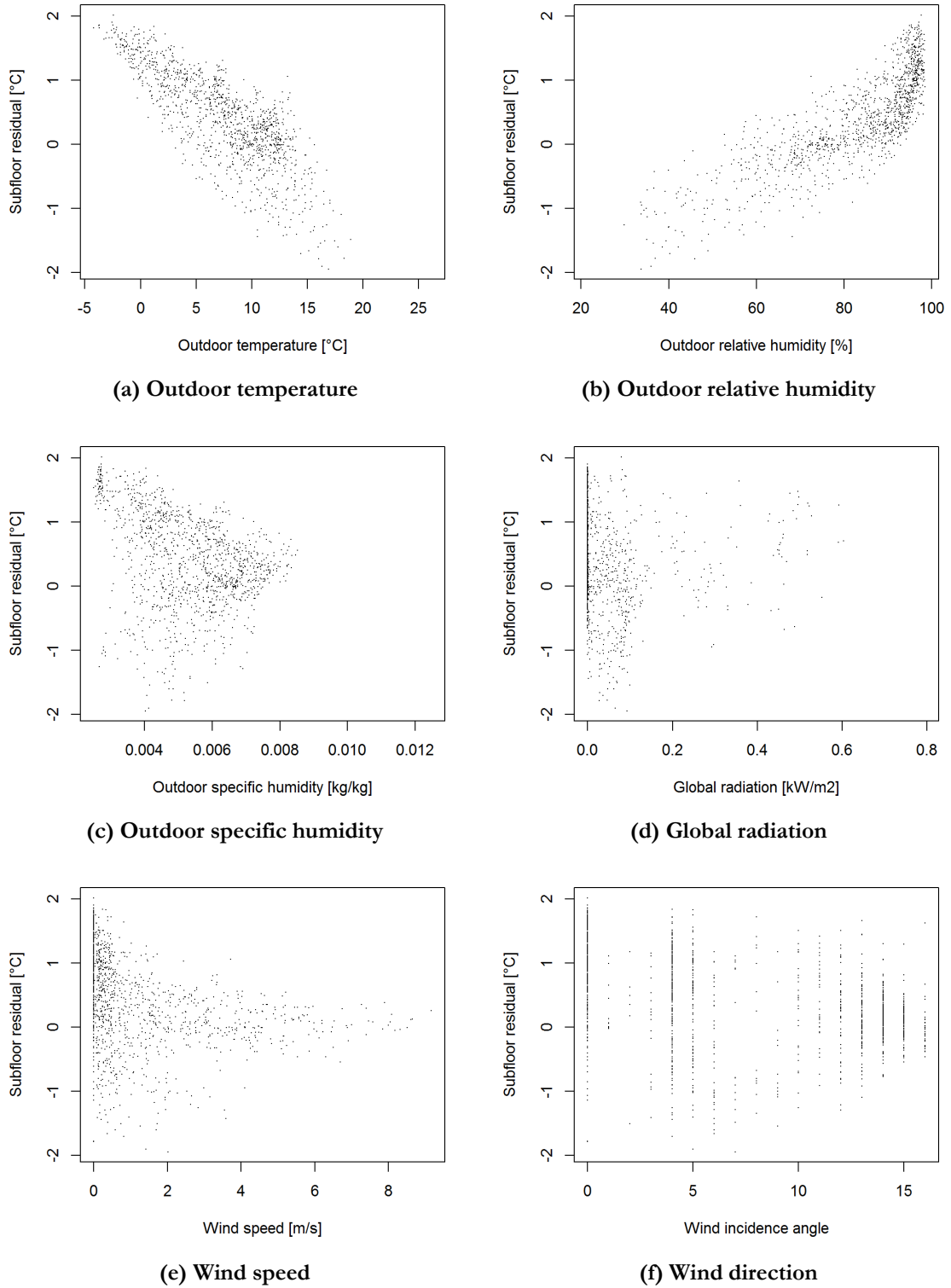


Figure 6.60: Correlation of subfloor residuals (OE-AR2) with various parameters, TP3, batch 1

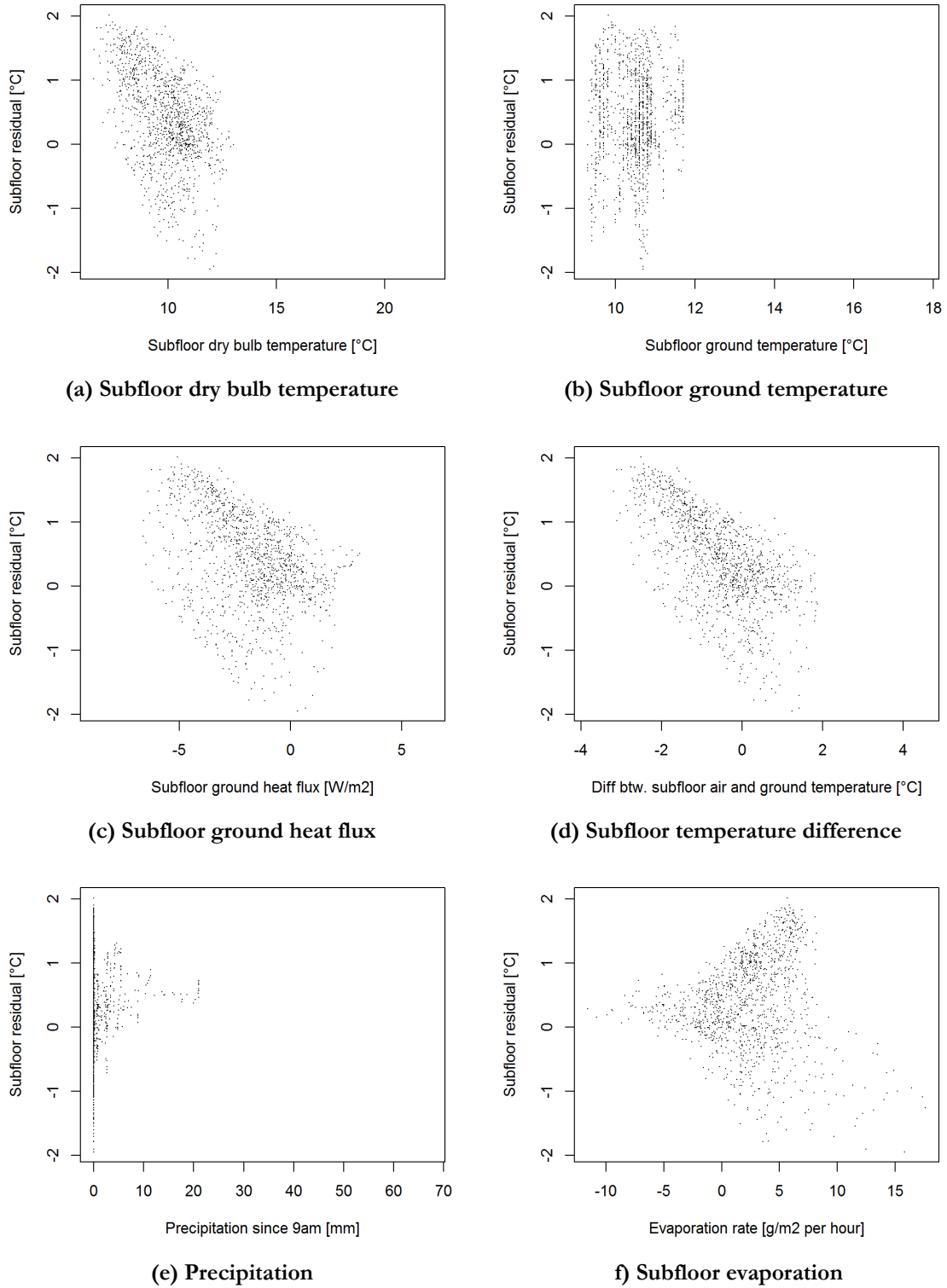


Figure 6.61: Correlation of subfloor residuals (OE-AR2) with various parameters, TP3, batch 2

A linear model was run between the subfloor residuals and 11 of the observed parameters. The wind angle was not included due to its circular nature, though from Figure 6.60(f) there is no visible correlation with the subfloor residuals and wind angle. The linear model mostly supports the observations from Figure 6.60 and Figure 6.61, showing that 79% of the variation in TP3 subfloor residuals is attributable to a combination of the outdoor temperature and outdoor relative humidity, with humidity being just slightly more influential. Wind speed and global radiation together combine to account for an additional 4% in the variation, but no other parameters have a major effect on the subfloor residuals.

When considering data from all time periods, there is similarity in the parameters driving the subfloor residuals. Relative humidity alone accounts for 66% of the variation in the subfloor residuals. Once variation due to relative humidity is considered the only other influential parameter is evaporation, which accounts for an additional 5% of the variation. The outdoor temperature has little additional influence on the subfloor residuals.

Figure 6.59 through Figure 6.61 consider all hours of data. However, it is shown throughout Sections 6.2.1 and 6.2.2 that many of the outdoor and subfloor climate parameters have distinct hourly profiles. Thus, by their nature the climate parameters are all confounded. If data at all hours is considered it is therefore difficult to determine if relationships between the residuals and the climate parameters are due to true physical interactions or instead due to the confounding of the climate parameters with time.

The hourly profiles of the room and subfloor residuals during TP3 are shown in Figure 6.62. The room residuals are highest at approximately 7 to 8am and lowest at about 5pm. The subfloor residuals have a similar daily profile though with a steeper hourly profile. The subfloor residuals encounter their highest and lowest values at similar times, approximately 7am and 3 to 4pm.

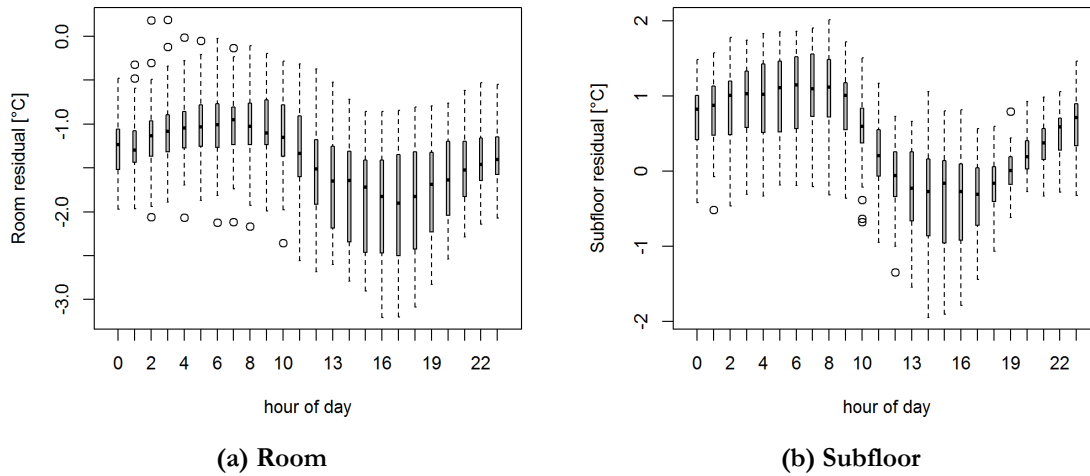


Figure 6.62: Residuals by hour, TP3

The hourly profiles of the room and subfloor environmental temperatures during TP3 are shown in Figure 6.63. The room temperature is lowest in the late morning and highest in the evening. The subfloor temperature follows a similar pattern though steeper and shifted forward in time. The subfloor temperature is lowest at approximately 9am and highest at 4pm.

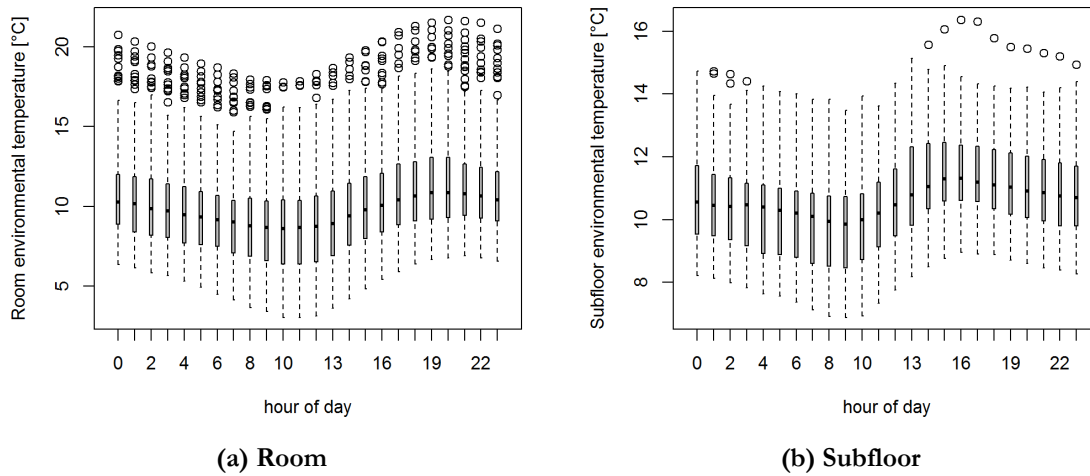


Figure 6.63: Environmental temperatures by hour, TP3

A comparison of the hours where the minimum and maximum values occur in Figure 6.62(b) and Figure 6.63(b) generally supports the observation that the subfloor residuals are at their highest and lowest values when the subfloor temperature is approximately at its highest and lowest values. This is also supported by Figure 6.61(a) where the correlation between subfloor residuals and subfloor dry bulb air temperature display a correlation with negative slope. However, the time shift of two

hours from 7am, when the highest residual occurs, to 9am, when the subfloor temperature is at its lowest, indicates a time shift between the AccuRate and observed temperature does exist.

An example day displaying the relationship between subfloor residual and temperature is shown in Figure 6.64. On this day the minimum AccuRate and observed temperatures occur at 8am. This is also the time when the residual is highest. The maximum AccuRate and observed subfloor temperatures occur at 4pm, near the time when the difference between the observed and AccuRate temperatures is highest. The AccuRate temperature data are mostly lower than the observed temperatures, except for the daytime hours between noon and 6pm.

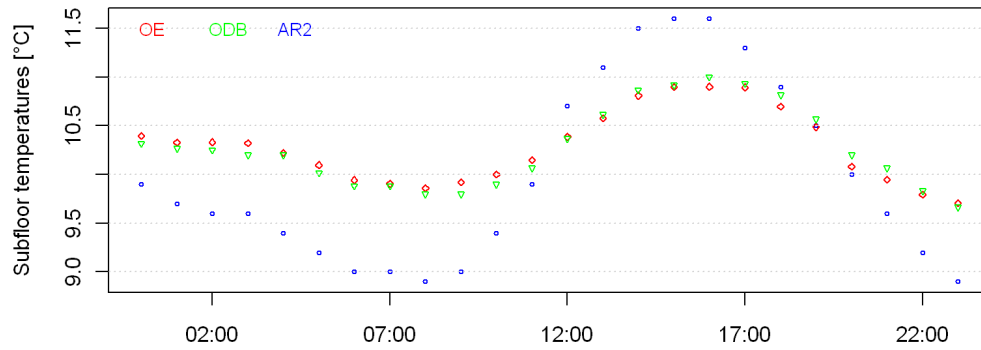


Figure 6.64: Subfloor temperatures by hour on July 01 2012

The hourly profiles of the room residuals, subfloor residuals and subfloor temperatures are similar, suggesting that these values are indeed confounded. To eliminate the confounding factor of time the data is investigated at only selected hours. The hours of 9am and 4pm are selected as those align with the times of the minimum and maximum subfloor environmental temperature.

The correlation of the room and subfloor residuals at 9am and 4pm is shown in Figure 6.65. Both graphs have a positive slope but at 9am the correlation is weak with an R^2 of 0.18. At 4pm the correlation is stronger with an R^2 of 0.55.

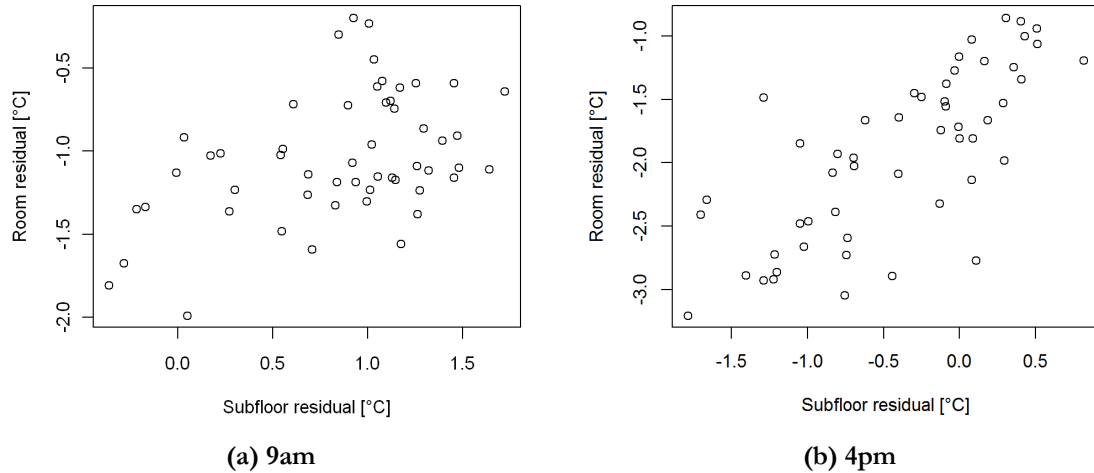


Figure 6.65: Correlation of room residuals to subfloor residuals by hour, TP3

The room and subfloor daily minimum and maximum residuals are also compared in Figure 6.66. This compares the residuals between the room and subfloor when each zone is at its minimum temperature, and then again at its maximum. These extrema are possibly occurring hours apart, as each zone's temperatures have a different hourly profile as shown in Figure 6.63, but in general for each zone the data contributing to the minimum daily residuals occur in the morning and the data contributing to the minimum daily residuals occur in the afternoon or evening.

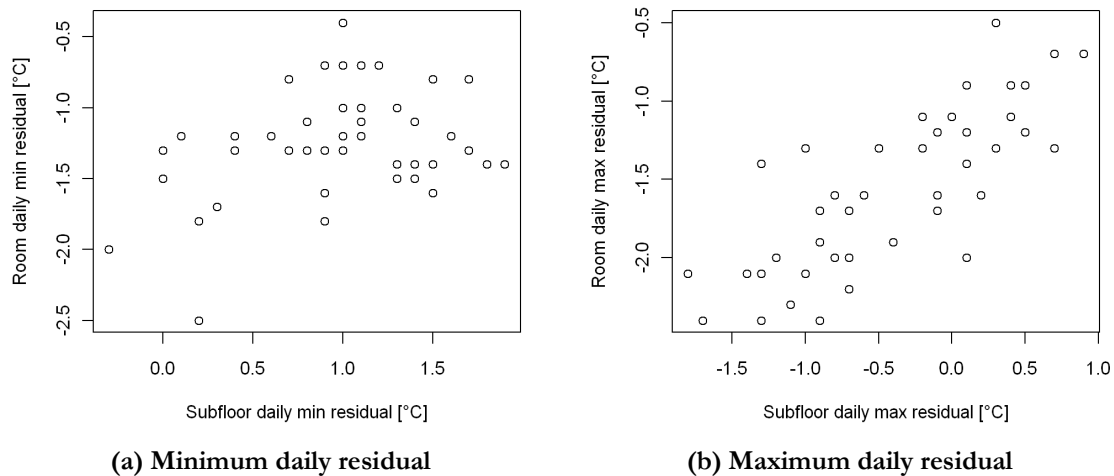


Figure 6.66: Correlation of daily room residuals to subfloor residuals, TP3

The daily minimum residuals have no correlation with an R^2 of 0.06, similar to the 9am correlation. The daily maximum residuals show a positive slope with a correlation R^2 of 0.62, similar to the 4pm correlation. Figure 6.65(a) and Figure 6.66(a) look similar, and Figure 6.65(b) and Figure 6.66(b) look similar. Both figures demonstrate that the room and subfloor residuals correlate poorly in the morning but better in the afternoon/evening.

The relationship between AccuRate and observed subfloor data at 9am during TP3 is shown in Figure 6.67. As expected at that time, the AccuRate temperature is mostly lower than the observed temperature.

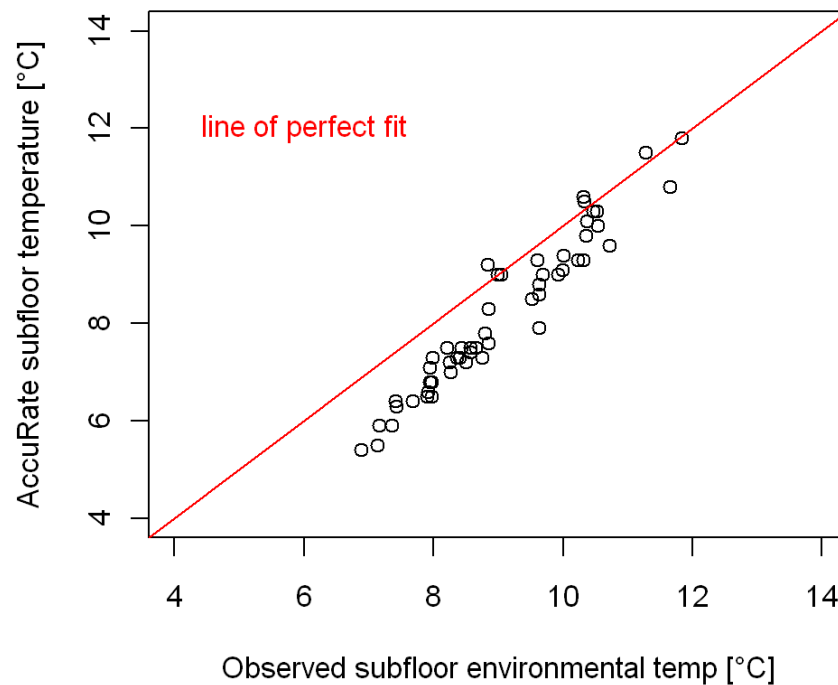
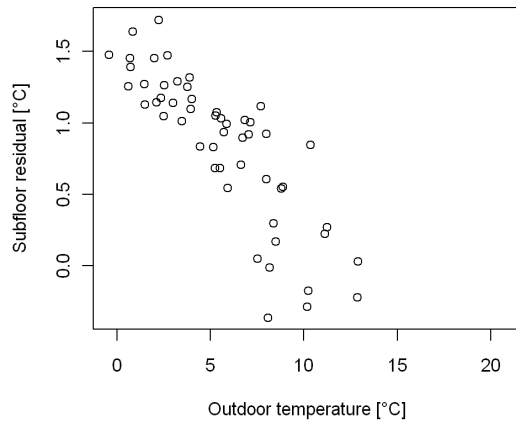


Figure 6.67: AccuRate vs. observed temperature, 9am, TP3

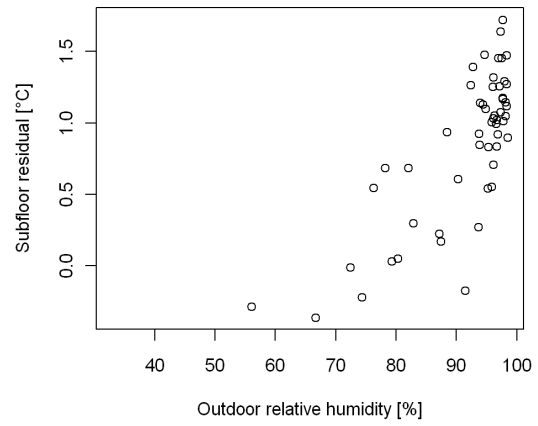
The subfloor residuals at 9am are graphed against the set of 12 observed climate parameters and shown in Figure 6.68 and Figure 6.69.

Figure 6.68 and Figure 6.69 show that at 9am there still exists a correlation between the subfloor residuals and both outdoor temperature and outdoor relative humidity. There is also a visible correlation to outdoor specific humidity, the air and ground temperatures in the subfloor, the subfloor ground heat flux, and to a lesser extent a correlation with wind speed, wind direction and evaporation.

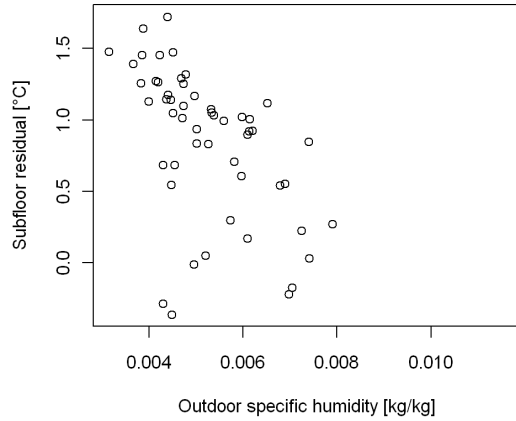
A linear regression shows that outdoor temperature accounts for 69% of the variation in the subfloor residuals. Relative humidity is of secondary importance and when included in the regression the R^2 is brought up to 0.86. The other parameters which indicated a correlation to the residuals do not explain any more of the variation when added to the linear model.



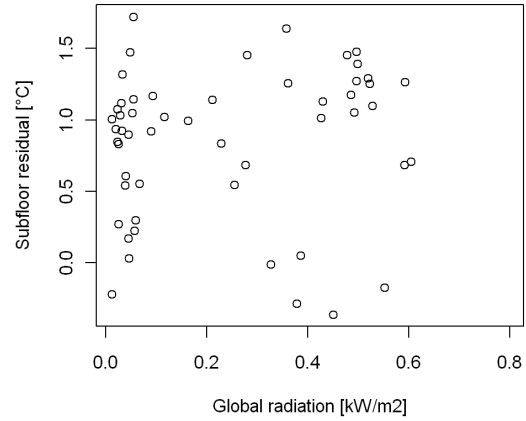
(a) Outdoor temperature



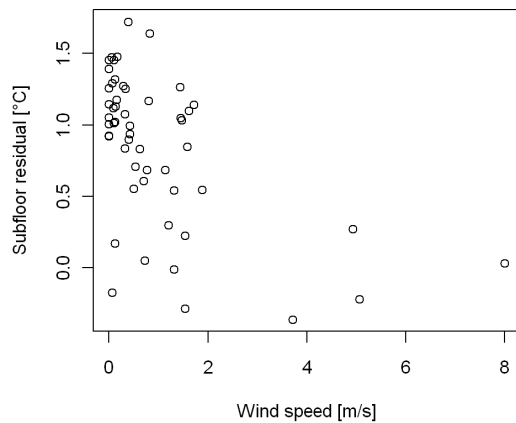
(b) Outdoor relative humidity



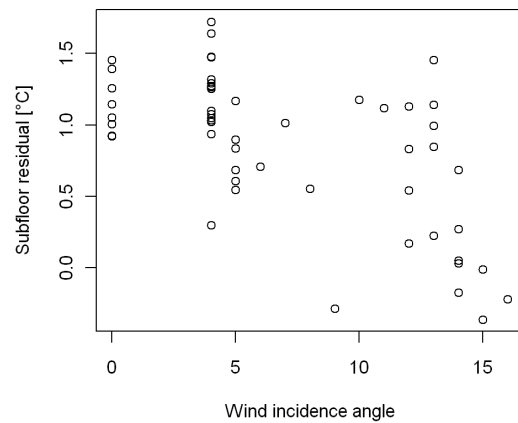
(c) Outdoor specific humidity



(d) Global radiation

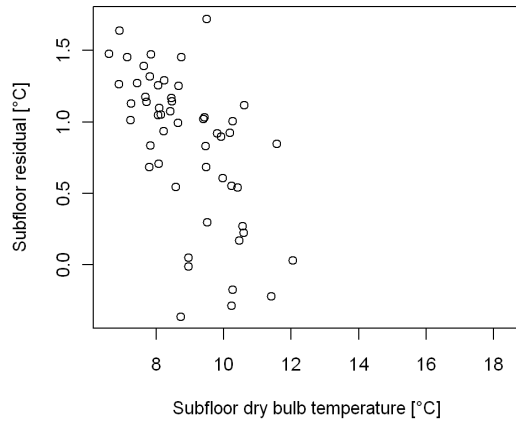


(e) Wind speed

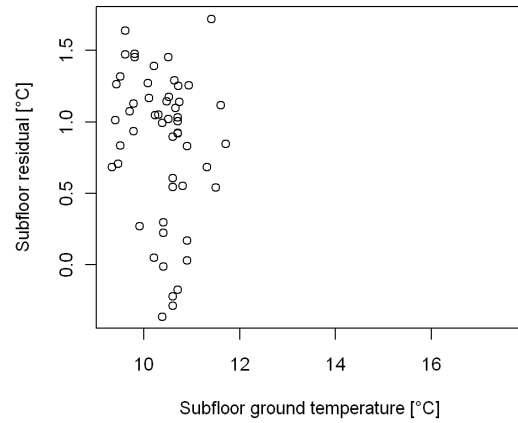


(f) Wind direction

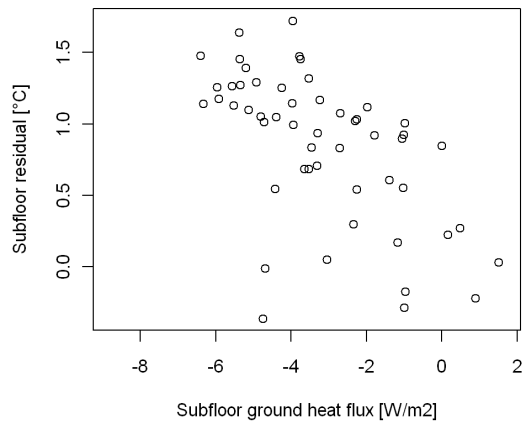
Figure 6.68: Correlation of subfloor residuals (OE-AR2) w/various parameters, 9am,TP3,batch 1



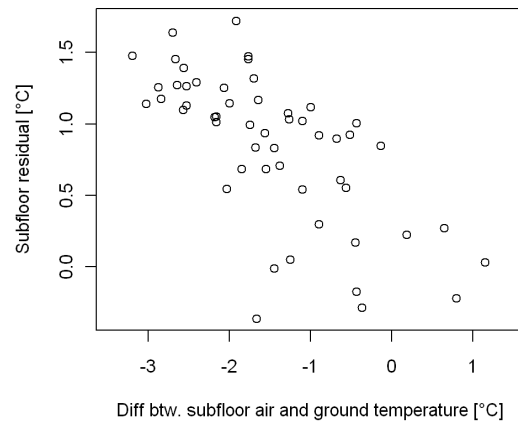
(a) Subfloor dry bulb temperature



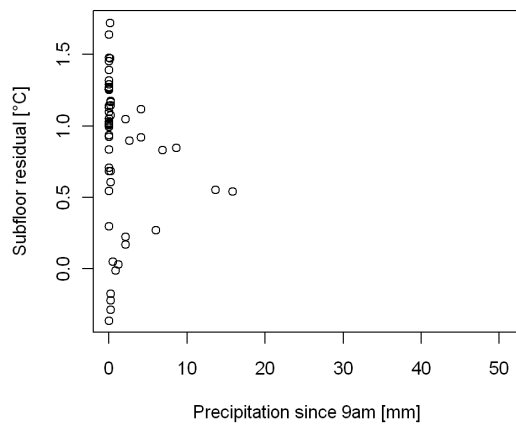
(b) Subfloor ground temperature



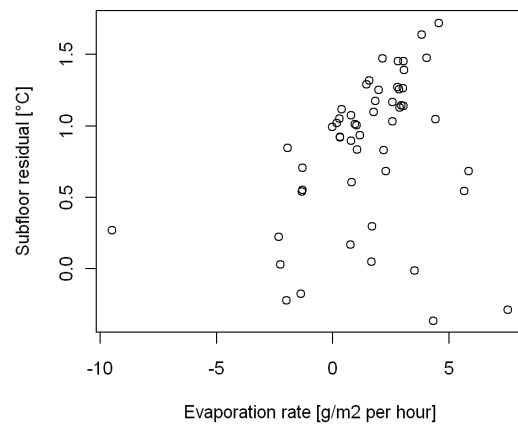
(c) Subfloor ground heat flux



(d) Subfloor temperature difference



(e) Precipitation



f) Subfloor evaporation

Figure 6.69: Correlation of subfloor residuals (OE-AR2) w/various parameters, 9am,TP3,batch 2

Graphs of the AccuRate subfloor temperature and the correlation of subfloor residuals with observed parameters at 9am for all time periods are provided in Appendix A.6.2. The AccuRate temperature is not distinctly less than the observed temperature as it was during TP3. This is not surprising as Table 6.7 shows the daily minimum residuals for TP1 were much lower than they were during TP3. The subfloor residuals show a correlation with outdoor temperature, relative humidity, radiation, wind speed and wind direction, and to a lesser extent a correlation with the heat flux and temperatures in the subfloor. A linear model of the subfloor residuals shows that of all the climate parameters outdoor relative humidity has the highest correlation and accounts for 71% of the variation in the subfloor residuals. No other parameter makes a substantial contribution to the model beyond that.

The relationship between AccuRate and observed subfloor data at 4pm during TP3 is shown in Figure 6.70. As expected at that time, the AccuRate temperature is mostly higher than the observed temperature.

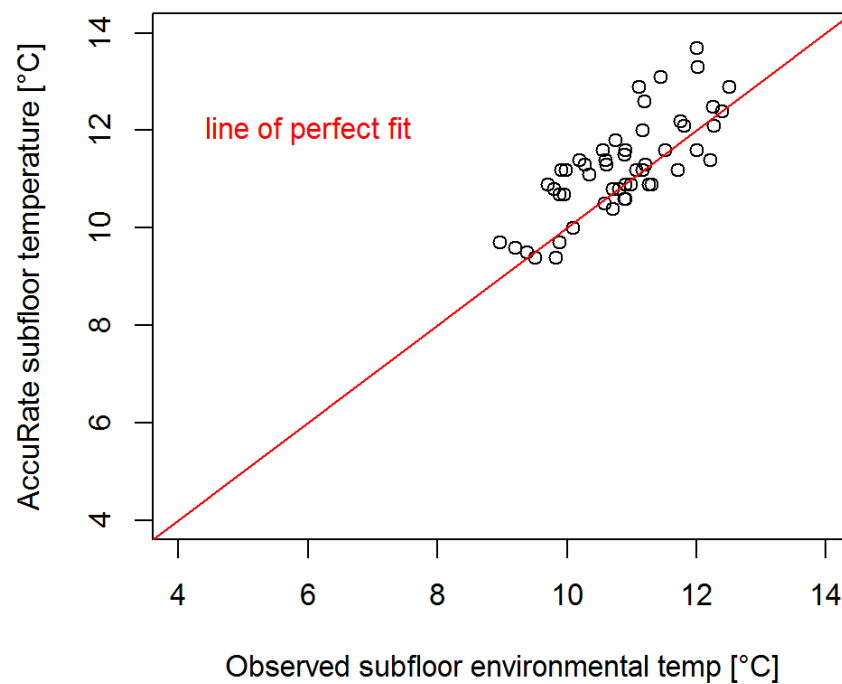


Figure 6.70: AccuRate vs. observed temperature, 4pm, TP3

The subfloor residuals at 4pm are graphed against the same 12 observed parameters and shown in Figure 6.71 and Figure 6.72.

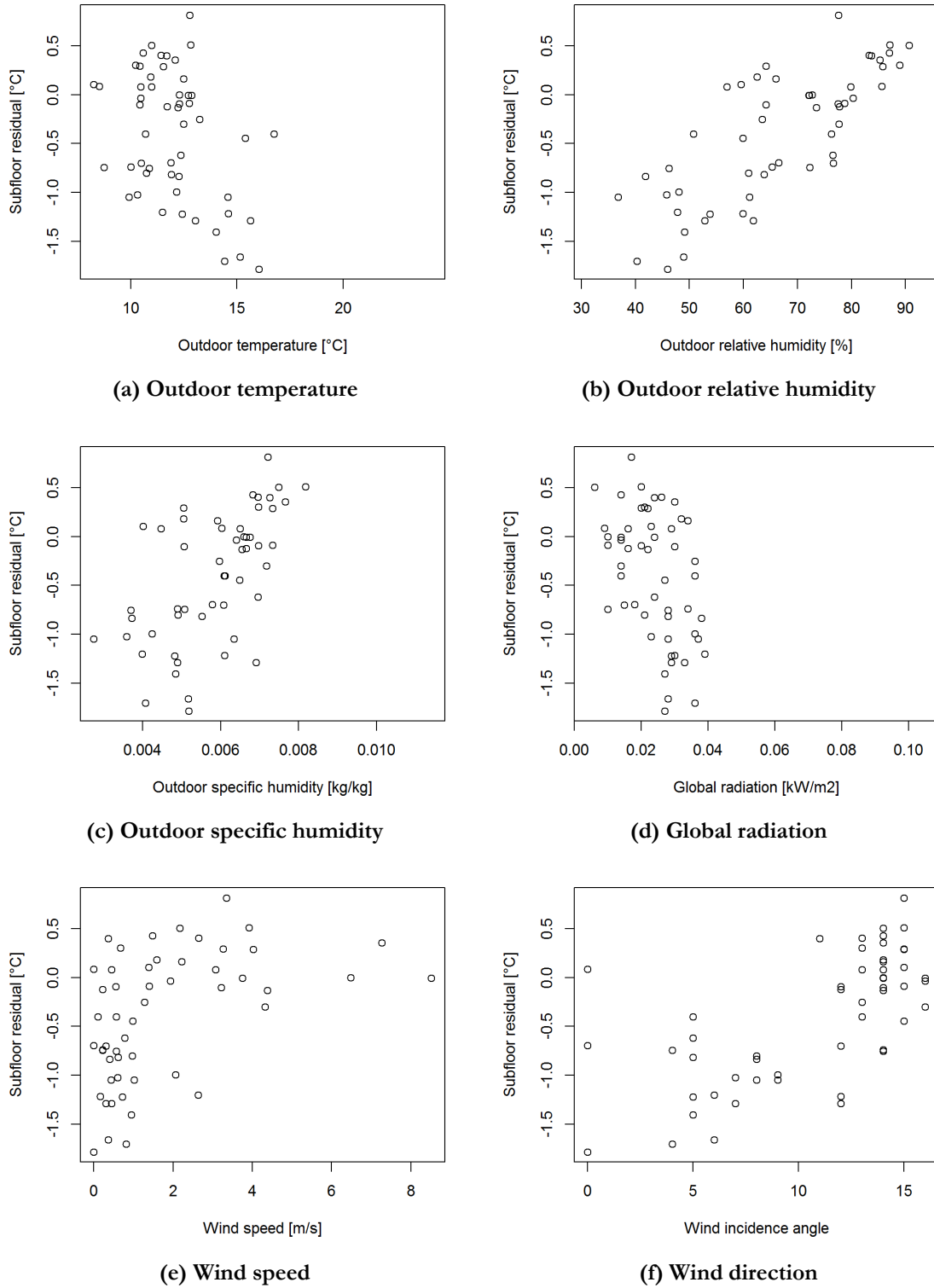
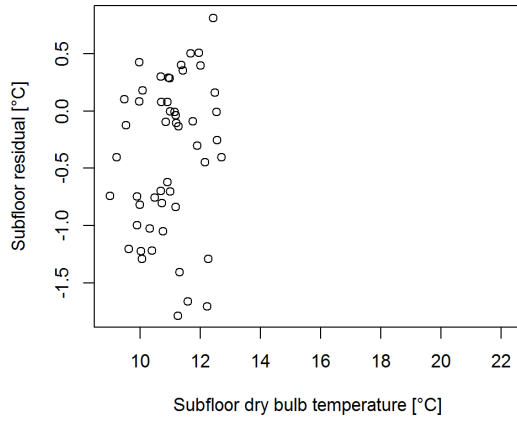
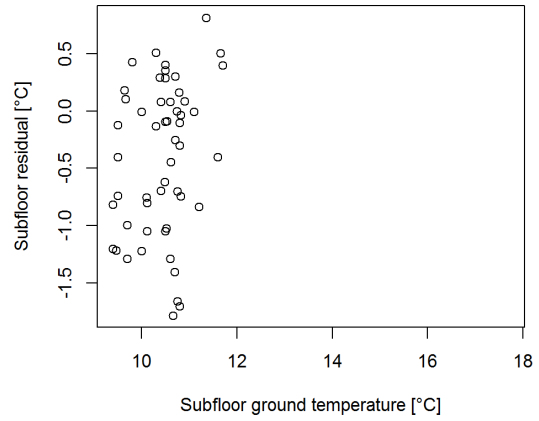


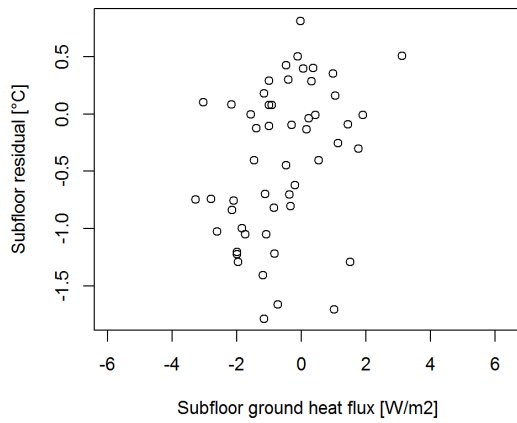
Figure 6.71: Correlation of subfloor residuals (OE-AR2) w/various parameters, 4pm,TP3,batch 1



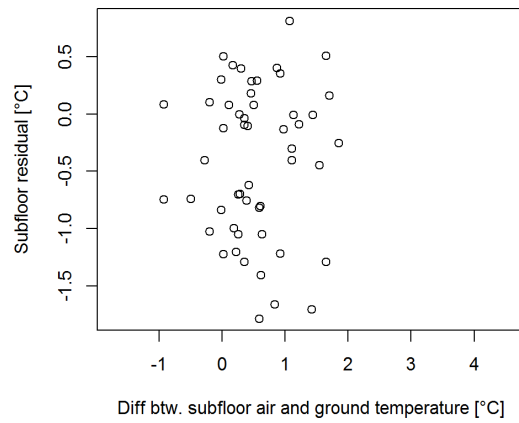
(a) Subfloor dry bulb temperature



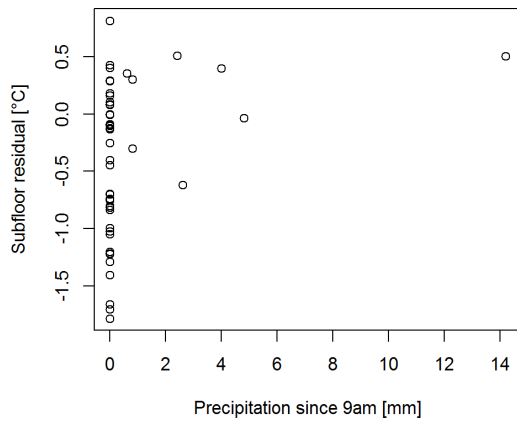
(b) Subfloor ground temperature



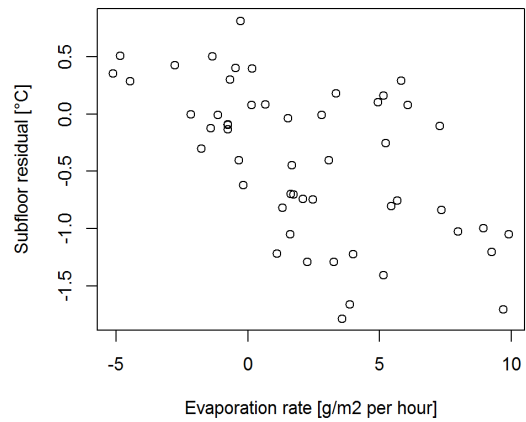
(c) Subfloor ground heat flux



(d) Subfloor temperature difference



(e) Precipitation



(f) Subfloor evaporation

Figure 6.72: Correlation of subfloor residuals (OE-AR2) w/various parameters, 4pm,TP3,batch 2

Figure 6.71 and Figure 6.72 show that the correlation between subfloor residuals and outdoor temperature is not as strong as previously observed. There is, however, a visible correlation to humidity, evaporation and wind direction, and radiation to a lesser extent. A linear regression shows that outdoor relative humidity alone accounts for 60% of the variation in the subfloor residuals, and adding wind speed to the model accounts for an additional 5%. Adding neither evaporation nor radiation increases the strength of the correlation. The correlation of subfloor residuals to outdoor temperature is weak with an R^2 of 0.16.

Graphs of the AccuRate subfloor temperature and the correlation of subfloor residuals with observed parameters at 4pm for all time periods are provided in Appendix A.6.3. The AccuRate subfloor temperature is mostly greater than the observed subfloor temperature, as expected.

The graphs of 4pm data for the entire test period show correlations between subfloor residuals and outdoor temperature, humidity, radiation and evaporation. A linear model shows that outdoor relative humidity is the biggest driver of the residuals, accounting for 48% of the variation.

Including either evaporation or wind speed into the model does improve it, with the effect of wind speed being stronger and raising the R^2 to 0.64. The effect of including outdoor temperature in the model is negligible.

6.5 Measurement system analysis

The uncertainty in subfloor dry bulb temperature is ± 0.05 °C, subfloor environmental temperature is ± 0.1 °C, and subfloor relative humidity is $\pm 3\%$. These uncertainties are based upon the sensor calibration information provided in Appendix A2.1 and in the case of subfloor environmental temperature, the propagation of uncertainties in subfloor dry bulb and globe (± 0.05 °C) temperatures.

A measurement system analysis was performed using the sequential perturbation method (Taylor 1982) to calculate the uncertainty in the AccuRate subfloor temperature due only to the uncertainty in the input weather parameters. Supporting analysis is provided in Appendix A.7.

First the uncertainty was estimated for each of the five weather parameters that are input into the AccuRate climate file. Four of these parameters are directly measured: air temperature, global irradiation, wind speed and wind direction. The uncertainties for those four inputs are based upon sensor calibration or manufacturers' specifications. The fifth parameter, specific humidity, was calculated as a function of air temperature, relative humidity and pressure, and thus the uncertainty of specific humidity is a function of the nominal values and uncertainty of its three inputs.

The relationship between AccuRate subfloor temperature and the five weather inputs was determined via linear model using TP1-TP3 data, thus encompassing all seasons. Each of the five inputs was varied from its nominal value by its uncertainty and the corresponding effect on calculated subfloor temperature was assessed. The total uncertainty in subfloor temperature was calculated via square root of the sum of the square of each input's effect. This process was done four times with four different sets of nominal conditions, each representing a different season, and the results were averaged.

The uncertainty in AccuRate's subfloor temperature is thus found to be ± 0.4 °C. This yields an uncertainty of ± 0.4 °C in both the OE and the ODB residuals.

6.6 Conclusion

The outdoor and subfloor parameters generally followed expected trends, although the subfloor was noticeably cooler and drier in 2011-2012 than it was in 2007. Variations in temperature and humidity were found throughout the subfloor. The vents frequently introduced both moisture and energy into the subfloor cavity. The subfloor relative humidity was found to frequently exceed and remain above 80%, the criterion for the subfloor ventilation design.

AccuRate's predicted subfloor temperature varied from 2.0 °C below, to 4.0 °C above the observed subfloor environmental temperature. When considering only the minimum daily temperatures, the difference was 1.9 °C below, to 1.0 °C above. When considering only the maximum daily temperatures, the difference was 0.9 °C below, to 3.4 °C above. In comparison, the uncertainty in the difference between AccuRate and observed subfloor temperature was 0.4 °C. The climate parameter found to most consistently correlate with the subfloor residuals was the outdoor relative humidity.

7 • DISCUSSION: SUBFLOOR VENTILATION AND CLIMATE

7.1 Introduction

Chapter 4 presents the results of Investigation 1, the subfloor ventilation investigation, and Chapter 6 presents the results of Investigation 2, the subfloor climate investigation. This chapter interprets those results and considers the implications of the two investigations. First the observed and AccuRate results are examined in Sections 7.2 and 7.3. Then the sources of error and shortcomings of both investigations are discussed in Section 7.4.

The four research questions proposed in Chapter 3 are addressed in Chapter 8, along with the significance of the findings and recommendations for future action.

7.2 Trends in observed subfloor data

7.2.1 Subfloor ventilation

The observed subfloor ventilation rate as calculated from the 2007 tracer gas test is higher than theoretically predicted, though it does support the model in that it is linear with wind speed. Since AccuRate was run only with the observed ventilation data overwriting the default ventilation data, the effect of this higher ventilation data on the AccuRate output temperatures is not known. Assessment of the AccuRate output with the default subfloor ventilation is the first recommendation provided in Section 8.2.

The tracer gas ventilation test was assumed to have an uncertainty of $\pm 10\%$ ACH. A measurement system analysis was performed to gauge the effects of ventilation uncertainty on the AccuRate output. The process was similar to that described in Section 6.5 and Appendix A.7. As ventilation is calculated in AccuRate as a linear function of outdoor windspeed, the outdoor windspeed was altered to gauge the effect of ventilation on AccuRate output. Accurate was run nominally, and then with a severe offset to windspeed of 5 m/s. This represents 10 times the

manufacturer's uncertainty in the instrument and is thus would be a large error. A windspeed uncertainty of 5 m/s resulted in an AccuRate subfloor temperature uncertainty of 0.8 °C, and uncertainty of subfloor residuals of 0.8 °C. This information is provided to bound the AccuRate expected uncertainty, should future ventilation testing be investigated.

The ventilation rate shows no dependence on wind direction, though there are very few data points upon which this claim is based. It is possible that two different wind direction phenomena are counter-acting each other. The CFD analysis summarized in Table 4.2 on page 52 indicates that wind speed at the subfloor vent is higher when the wind is from the northwest, with a diagonal incidence angle, than when it is from either the north or west, with a perpendicular incidence angle. However, the literature suggests (ASHRAE 2005) as described in Section 2.4.2 that wind with a diagonal incidence angle is less effective at entering vents, and thus for equivalent wind speeds perpendicular vents would result in a higher subfloor ventilation rate than would angled vents.

These two phenomena could combine as follows: a northwest wind would produce a high wind speed at the vent height, but a small proportion of that would be realized as subfloor ventilation. A northerly wind would produce a lower wind speed at the vent height, but a higher proportion of that would be realized as subfloor ventilation. Thus, the lack of dependency of subfloor ventilation on wind direction may actually be concealing two separate phenomena. If these two phenomena are to be investigated further, more experimental data are required.

Equation 2.6 on page 21 provides the ventilation equation used in AccuRate. This shows the stack component, A_1 , as a constant. When creating the stack component in the AccuRate subfloor ventilation model it was assumed that changes in the stack component were negligible in comparison to the ventilation component, and hence a constant value for the stack component was used. However that stack component actually represents a function of subfloor and outdoor temperatures (Delsante 2007) and a preliminary assessment of a small range of data indicates that the stack component can fluctuate greatly (Sequeira et al. 2010a).

The subfloor ventilation test did not measure temperature concurrently with ventilation so the influence of the stack effect (the buoyancy caused by the difference between subfloor and outdoor temperature) could not be investigated. The observed stack effect was larger than it was predicted to be. More work can be performed with existing data to investigate this. The stack component can be calculated with data recorded in Investigation 2, as subfloor and outdoor temperature have been recorded over a broad range of weather conditions. This can then be compared to the wind component of ventilation, and then the assumption of the stack term being negligible can be tested. This work is suggested as part of Recommendation 3 in Section 8.2.

This research used a theoretical relationship to relate the meteorological wind speed and building height wind speed to the wind speed at the subfloor vent height. However, the CFD results showed that the relationship between these three wind speeds was quite dependent on the layout of the test site and obstructions in the wind path. Additional study into the subfloor ventilation model should seek to examine these trends observed in the CFD results and investigate the relationship between wind speeds at different heights. Further investigation should start with a review of the CFD results and a comparison to wind and pressure studies (Swami and Chandra 1988). The CFD analysis may benefit by including the presence of cars in the nearby car park. Existing data can support this work, as the wind speed observed at three locations in the face of the west vent on the north side of the subfloor was recorded via hot-wire anemometers and went through the error-checking routine. This work is suggested as part of Recommendation 3 in Section 8.2.

7.2.2 Temporal variations

Between one year and five years after construction of the test cell, the subfloor cavity air cooled significantly as shown in Figure 6.41 and Figure 6.42 on pages 142 and 143. One explanation for this is that the presence of the test cell blocked the radiation energy that the subfloor ground would otherwise have absorbed. This is supported by Figure 6.8 and Figure 6.27 on pages 115 and 131, which show that the peak monthly heat flux into the ground reaches over 50 W/m^2 outside of the test cell in an area which often has unobstructed access to solar radiation, but within the test cell the heat flux reaches only a fifth of that.

During those four years the subfloor cavity air also became drier, as shown in Figure 6.43 and Figure 6.44 on pages 144 and 145. In 2007 the subfloor specific humidity was always greater than the outdoor specific humidity and thus the net effect of the subfloor ventilation was always to carry moisture out of the subfloor. However, in 2011-2012 the net effect of the ventilation was to deposit moisture into the subfloor 24% of the time.

The cooler and drier subfloor conditions reduced the enthalpy of the subfloor air over time. The enthalpy reduction also changed the pattern of the energy transfer through the vents. Data from 2007 (Sequeira et al. 2010b) indicates that in nearly all instances the net effect of the ventilation was to reduce the enthalpy of the subfloor cavity air. However, in 2011-2012 the net effect of the ventilation 35% of the time was to increase the enthalpy of the subfloor air.

As the net moisture transfer rate through the vents is equivalent to the ground moisture evaporation rate as discussed in Section 6.2.3, the evaporation rate thus also dropped significantly from one to five years after construction of the test cell as shown in Figure 6.47 on page 148. This changed the influence of the vents as the predominant source of subfloor moisture. In 2007 150%

more moisture entered the subfloor cavity from the vents than from ground (Sequeira et al. 2010b). However, in 2011-2012 the vents introduced 700% more moisture than did ground evaporation.

Soil moisture content was not recorded in 2007 and thus no direct comparison can be made to confirm that the subfloor ground dried over time. However, it is possible that the ground did dry as the soil from uncovered locations in the subfloor in 2012 was qualitatively observed to be quite dry, drier than the outside soil at the time that the soil samples were collected. In addition, the evaporation rate from damp soil is known to be similar to the evaporation rate of free water (Abbott 1983) and observed evaporation rates have been shown to correlate well with prediction. In contrast, evaporation from drier soil is a more complex process with the amount of water vaporizing half a metre below the surface being significant in comparison to that vaporizing at the surface (Trethowen 1988). As the 2007 evaporation rate correlates better with evaporation potential than the 2011-2012 does, as shown in Figure 6.47 on page 148, it seems likely that in 2007 the ground was wetter than it was in 2011-2012.

It is not surprising that the subfloor would dry over time because the presence of the test cell itself blocks the precipitation that would otherwise have reached the subfloor ground surface. This reasoning is supported by the observed soil thermal conductivity. Outside the test cell the conductivity was found to be 250% higher than it was inside the test cell. One reason for this could be that the ground was much drier inside the test cell than it was outside, as water presence is known to increase soil thermal conductivity (Hillel 2004).

The cooling and drying of the subfloor air over time had no considerable impact on the relative humidity. This is demonstrated in Figure 6.45 on page 146.

7.2.3 Spatial variations

Parameters of interest in the subfloor vary between the subfloor centre, the edge and the corners.

Figure 6.18 on page 121 shows that during the warmer months the east side subfloor temperatures are slightly higher than the centre temperatures. These east side temperatures are measured between the two vents on the east side. Figure 6.16 on page 120 shows that the centre temperature is generally higher than the temperature at any of the corners. Those corner temperatures are measured just inside from each corner vent.

It is possible that subfloor air movement has a first-order effect on the temperature distribution in the subfloor, with higher air speeds yielding lower temperatures. This is supported by the CFD results of Figure 4.3(d), Figure 4.4(d) and Figure 4.5(d), on pages 48, 49 and 51, which show that the air speed in the subfloor is generally higher behind the vents than it is at the centre, and at the centre it is higher than it is along the subfloor perimeter between the vents.

There is also the possibility of a second order effect of ventilation on temperature resulting from the relationship between air movement and thermal resistance. Research from an instrumented test building in the UK investigated the interaction between subfloor air movement and floor thermal resistance. It was found that differing air speeds throughout the subfloor corresponded to fluctuations in the effective thermal resistance of the floor assembly above (Harris and Dudek 1993). As air speed increased, thermal resistance was reduced by 40%. Thus, at different locations in the subfloor the heat transfer rate through the floor assembly may vary, depending on local air speed. This may be affecting the profile of the observed temperature data.

The variation of the specific humidity throughout the subfloor is similar to that of the temperature. As shown in Figure 6.26 on page 130 the specific humidity is higher at the subfloor centre than it is at either the northwest or southeast corners, two locations which would be subjected to higher air speeds.

The soil moisture variation is also similar as shown in Table 6.2 on page 134. The soil moisture contents at the two locations most exposed to the incoming ventilation at the northwest corner, SM2 and SM5, are lower than the soil moisture content along the perimeter of the subfloor between two vents, SM4, where the CFD predicted a lower wind speed.

The variation of relative humidity reflects the variation in both temperature and specific humidity. The subfloor humidity at the northwest corner, generally the windward corner, is substantially lower than that of the centre and southeast corner humidity, especially during the cooler months. As the prevailing wind is from the northwest, air speed at the location of the northwest corner humidity sensor, directly behind the vents, is predicted by CFD as shown in Figure 4.5(d) on page 51 to have higher air speeds than elsewhere throughout the subfloor. The relative humidity at the southeast corner, the leeward corner, is greater than the centre humidity though the difference is slight.

The wood moisture variation as shown in Figure 6.31 on page 135 is similar to that of the relative humidity. The floor board at the northwest corner was consistently drier than the floor board at the centre, and the floor board at the centre was drier than the floor board at the southeast corner.

Both the relative humidity and wood moisture are higher in the southeast corner, the leeward corner, than they are in the centre. This is different to the temperature and specific humidity, which are higher in the centre than in the southeast corner. It is not surprising that the wood moisture trends with relative humidity instead of specific humidity as wood moisture is driven primarily by relative humidity (Williamson and Delsante 2006b).

These variations in temperature and moisture throughout the subfloor appear correlated with air speed. The southeast corner showed the highest relative humidity. However, it is likely that the

relative humidity at a location with less air movement, such as between the vents on the south or east side of the building, would have been higher. Thus, it is possible that the highest relative humidity in the subfloor has not been recorded. There were no relative humidity sensors placed between the vents.

It was been shown that the vent placement on the leeward side of a building does not have any effect on the pattern of air movement in a subfloor (Harris and Dudek 1994). It is possible then that the vent placement may not affect the rate of subfloor ventilation, either. Further study should therefore consider the addition of vents on the windward side of a building. This may increase the local air speeds and reduce the relative humidity at the location where it is expected to be highest.

The heat flux at the subfloor centre and east side of the test cell is compared in Figure 6.27 on page 131. The heat flux has a smaller range at the east side than it does at the subfloor centre. The heat flux is consistently lower at the east side than at the centre at all times. This indicates that when heat is flowing upward, there is less heat flux at the east side than the centre, but when heat is flowing downward there is more heat flux at the east side than the centre. The difference is more pronounced in the late spring and summer when the heat is predominantly flowing downward.

This pattern agrees with laboratory testing from the UK based on a test cell with similar vent placement. That research found that when the test cell chamber was heated the heat flux into the ground was higher along the perimeter of the subfloor wall than it was at the subfloor centre. That research also found that heat flux into the ground was higher still at the subfloor corners (Harris and Dudek 1997). These results are not surprising, as the horizontal temperature gradient in the soil would be greater at the subfloor perimeter than it is in the centre, and thus there would be more potential for heat transfer at the perimeter.

Various perimeter and edge effects are observed in the data. Further study may find that these effects are not worth examining, as real buildings are generally larger than the test cell and therefore the area effects would outweigh the boundary effects. However, in larger buildings the variation between centre and edge parameters may be more dramatic.

7.2.4 Seasonal variations

The relationship between subfloor and outdoor parameters changes between autumn and winter. Figure 6.42 on page 143 compares the subfloor temperature to outdoor temperature. Figure 6.42(a) and (c) compares the 2007 autumn data to winter data, and Figure 6.42(b) and (d) compares the 2011-2012 autumn data to winter data. Both data sets indicate that in winter the subfloor temperature is relatively constant and less sensitive to the outdoor temperature than it is in autumn. Figure 6.44 on page 145 shows similar graphs for specific humidity, and both data sets indicate that in winter the subfloor specific humidity is less sensitive to the outdoor specific humidity than it is

in autumn. Further investigation into this seasonal trend is suggested as Recommendation 2 in Section 8.2.

7.2.5 Effect of ground cover and ceiling hatch

The plastic ground sheet covering the length of the east side of the subfloor was removed at the end of February 2012, thus ending TP1 and commencing TP2. The ceiling hatch between the room and roof space was not put in place until March 2012, thus ending TP2 and commencing TP3. It is not expected that the presence of the ceiling hatch would have a noticeable effect on the subfloor cavity conditions, nor is it expected that the ground sheet removal would have a noticeable effect on the room conditions.

The profile of the three room dry bulb air temperatures and the room globe temperature is shown in Figure 6.12 on page 118. The profile between the four sensors is consistent before and after the ceiling hatch was installed. Thus, it does not appear that the absence of the ceiling hatch affected the room temperatures.

The subfloor temperature profiles of Figure 6.13 through Figure 6.19 on pages 118 through 122 are considered before and after February 2012. The only time the ground cover seems to have made a difference in the profile between temperatures is in Figure 6.18 on page 121, which compares the subfloor centre temperatures to the temperatures along the east side of the subfloor. All four measurements were recorded via RTD sensors. The profile of these four temperatures appears different in March, April and May 2012 than it did in March, April and May 2011. By June 2012 the profile returns to the baseline state. However when the subfloor centre dry bulb temperature using that same RTD sensor is compared to outdoor temperature with and without the ground cover in place as shown in Figure 6.41 and Figure 6.42 on pages 142 and 143, the ground cover removal shows no apparent effect on the relationship between subfloor and outdoor air temperature.

There is no apparent effect of ground cover removal in the variation of specific humidity throughout the subfloor as shown in Figure 6.27 on page 131. Also, Figure 6.43 and Figure 6.44 on pages 144 and 145 show no effect of ground cover removal on the relationship between subfloor and outdoor specific humidity. There is also no evident effect of ground cover removal in the variation of relative humidity throughout the subfloor as shown in Figure 6.22 on page 124. Similarly, Figure 6.45 on page 146 shows no effect of ground cover removal on the relationship between subfloor and outdoor relative humidity. Figure 6.48 on page 149 shows that there is no evident effect of ground cover removal on the subfloor evaporation rate.

Figure 6.27(a) on page 131 compares the heat flux at the centre of the subfloor to that at the east side. In June and July 2011, both the centre and east side heat flux values are similar, but in June and July 2012 the east side heat flux shows a higher value than the centre sensor does, indicating

less heat flowing upward. This change in the profile between locations may not directly result from ground sheet removal, though, as the ground cover was removed at the end of February 2012, and the March, April and May 2012 profiles are similar to the March, April and May 2011 profiles.

The observed changes in the subfloor temperature before and after ground cover removal are minor, and there are no evident effects of ground cover removal on the humidity or moisture in the subfloor. It is not surprising that there is no change in the moisture characteristic of the subfloor, as the amount of moisture entering from the ground is minor compared to the amount of moisture entering via the vents. Thus, reducing the exposed ground surface area by 20% would not greatly affect the amount of introduced moisture. In addition, because the ground is relatively dry, a significant amount of the evaporation is from moisture which vaporizes below the surface. Thus, the vapour has some distance to travel to reach the surface and the effect of the blockage directly at the surface is reduced.

It is well documented that ground cover reduces relative humidity in subfloors (Kurnitski 2000, 2001; Rose and TenWolde 1994). However, in those instances the ground sheet covers the entire subfloor and thus those are not comparable situations.

7.2.6 Subfloor moisture and deterioration criteria

The original criterion for the ventilation design was to ensure the subfloor relative humidity remained below 80% (Williamson and Delsante 2006b). The subfloor humidity is shown to exceed 80% persistently in the cooler months of the year, at one instance for as long as 10 consecutive days, and thus the observed relative humidity fails to comply. However, this alone does not indicate that the subfloor climate is actually conducive to corrosion, mould growth or durability issues, the avoidance of which was the intent of the design criterion.

There are a variety of publications linking the deterioration in subfloors, the subfloor climate and presence of odour from buildings throughout varying geographical areas (Flynn, Quarles, and Dost 1994; Fugler and Moffatt 1994; Stiles and Custer 1994; Tsongas 1994). There are also several publications that summarize the history, regulation or technical aspects of the matter (DeWitt and Bunn 1994; Rose 1994; Samuelson 1994; Williamson and Delsante 2006b). These publications link subfloor deterioration to not only high relative humidity but also high temperature, high wood moisture content, the presence of free water or condensation, and the time spent under such conditions.

The aim of the 80% humidity criterion used in Australia's ventilation design was to keep the moisture content of the wood under 18% (Williamson and Delsante 2006b). Figure 6.31 on page 135 shows that the wood moisture at the southeast corner approached 18% in August 2011.

However, wood moisture content was not recorded again for nearly five months, so it is not known whether it would have surpassed 18% or not.

A subfloor temperature of 12 °C was suggested as the temperature threshold to be applied in conjunction with the 80% relative humidity limit (Williamson and Delsante 2006b). It is not known for how long the subfloor climate must remain above 80% relative humidity and 12 °C for deterioration to occur. The interaction between relative humidity, temperature and time can be observed in Figure 6.23 and Figure 6.24 on pages 126 and 127. The periods with high relative humidity correspond with cooler subfloor temperatures. There are two time periods, each of approximately one week, when the relative humidity is mostly above 80% and the subfloor temperature is mostly above 12 °C. The longest continuous time the subfloor spends above both limits concurrently is two days.

The presence of free water was never observed on the subfloor ground surface, except on the east side immediately after the ground cover was removed.

The net effect of the vents was to increase the moisture in the subfloor 24% of the time. As the rate of moisture absorption into the subfloor cavity air was found to be very slow, this moisture would therefore have been realized as condensation on any of the subfloor surfaces, including the ground, walls, underside of the floor or the piers. Moisture condensed when the outside relative humidity was high, as shown in Figure 6.34 on page 137. It would require further investigation to see if the periods of condensation coincide with the periods of high relative humidity or temperature.

It should be noted that it is a relatively simple task to determine if vents are increasing or decreasing the moisture of a subfloor, as was done in this research. Thus, the calculation is one that can be applied to historical data. Temperature and relative humidity both inside and outside the test cell are the only needed measurements. Atmospheric pressure is also needed, but that can be estimated or purchased from a nearby BOM location with minimal loss in accuracy. From temperature, relative humidity and pressure the absolute humidity, the mass of moisture per unit volume, both inside and outside the subfloor can be calculated.

If the absolute humidity is greater outside the test cell than inside the subfloor, then the vents are increasing the moisture of the subfloor. For the small range of climate conditions considered in the present research, the fluctuation in air density is small and comparing specific humidities, the mass of moisture per unit mass of dry air, yields similar results as when comparing absolute humidities. The rate of subfloor ventilation is only needed if the rate of moisture addition or removal needs to be quantified.

7.3 Trends in AccuRate data

The AccuRate program was run to best mimic the actual test conditions encountered. The observed climate data was fused into the program to overwrite the RMY data, thereby avoiding differences between the observed and AccuRate temperatures due to differences between actual and predicted climate. The default values for the subfloor, room and roof zones were also overwritten by the observed ventilation rates. This was done for the purpose of comparing the results to that of previous research on the test cell. Consequently, the results of this research do not quantify the effect of subfloor ventilation on the accuracy of the AccuRate output.

The AccuRate results presented in this research are not representative of what the typical user would obtain. This is not only because of the overwritten outdoor climate and ventilation data, but also because the program was altered to represent free-running conditions. The program was adjusted to eliminate the addition of energy for space heating or cooling, thereby allowing the test cell's predicted temperatures to fluctuate at will, without being controlled. Thus, in this research the only outputs of AccuRate considered are the zone temperatures. This is in contrast to typical use, where the building's temperatures would be controlled to a pre-defined range by the addition of heating or cooling energy as described in Sections 2.2.1 and 5.6.1, and the main output of AccuRate would be the sum of that space conditioning energy.

Throughout this research AccuRate's output temperature is compared to the corresponding observed test cell temperature. The baseline residuals are the AccuRate temperature subtracted from the observed temperature. This calculation is performance on all hours of data and for both the room and subfloor zones. The daily minimum residuals are the minimum daily AccuRate temperatures subtracted from the minimum daily observed temperatures. These two temperatures may occur at different times of the day. However, the minimum, and similarly the maximum, daily residuals are considered a more useful metric than the baseline residuals for two reasons.

Firstly, the daily extrema residuals better represent the output of the AccuRate program from the typical users' standpoint. The typical user is most interested in the energy rating output from AccuRate, as that is regulated by the Australian government. The energy rating is assessed in the AccuRate program based on each zone's potential for exceeding the pre-defined temperature thresholds. Thus, the extreme daily temperatures are those most likely to influence the energy assessment.

Secondly, the data sets of minimum and maximum daily residuals eliminate the residual values that result strictly from the transient capability of the AccuRate program or time shifts between the AccuRate and observed data. These residuals are more likely to be larger at times of day when the temperatures are rapidly changing. This concept is best illustrated in Figure 7.1.

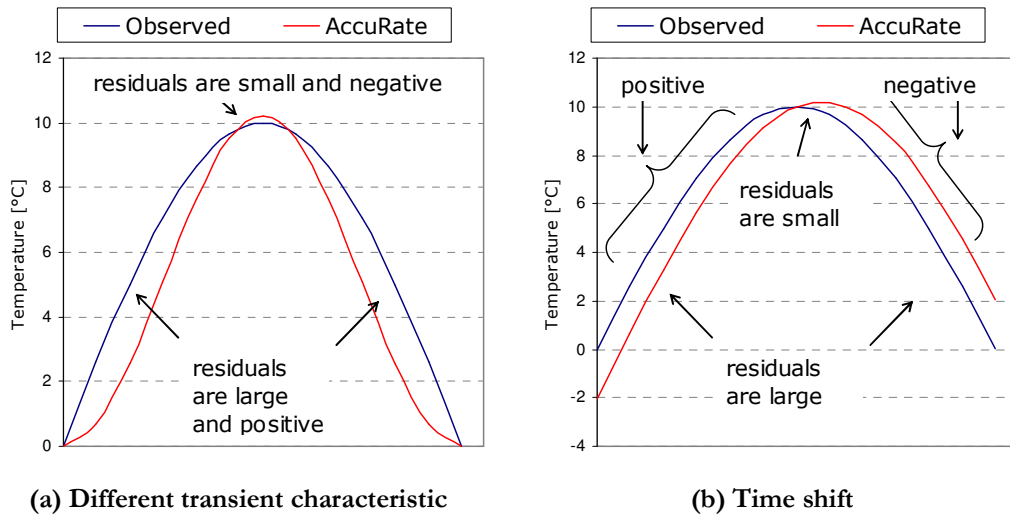


Figure 7.1: Example characteristics of residuals, using contrived data

Figure 7.1(a) and (b) each compare a series of example AccuRate and observed temperatures. Both comparisons would yield a daily maximum residual value of $-0.2\text{ }^{\circ}\text{C}$ but they would yield a different set of baseline residuals. The AccuRate temperature in Figure 7.1(a) has a faster rate of increase and decrease than the observed data does. This would result in mostly positive residuals as high as $2.5\text{ }^{\circ}\text{C}$, and then a few negative residuals as low as $-0.2\text{ }^{\circ}\text{C}$. The AccuRate temperature in Figure 7.1(b) has the same rate of temperature increase and decrease as the observed temperature does but is delayed in time. This would result in residuals ranging from $+2.0$ to $-2.0\text{ }^{\circ}\text{C}$.

In both cases demonstrated in Figure 7.1, consideration of all the baseline residuals may cloud the issue if what is considered most important is that $0.2\text{ }^{\circ}\text{C}$ overshoot at the peak temperature. However, it is still useful sometimes to consider the baseline set of residuals. Since they are linked to corresponding hours, the baseline residuals can be correlated with other observed parameters. If those hours are isolated to those near the expected maximum and minimum temperatures, the effect of transient differences or time shifts are minimized.

Consideration of just the daily extrema residuals, as summarized in Table 6.7 on page 161, indicates that for the subfloor zone AccuRate generally has a larger daily temperature range than does the observed data, exceeding the observed data at both the minimum and maximum temperatures. This indicates that in typical use, AccuRate would likely err on the side of over-predicting the amount of energy required for both space heating and cooling.

The subfloor residuals were lower in 2011-2012 than they were in 2007. In 2007 the subfloor model consistently predicted lower temperatures than were observed, at both the high and low temperature times of the day as shown in Table 6.5 on page 155. But five years later the subfloor

has cooled as discussed in Section 7.2.2, coinciding with lower residuals as shown in Figure 6.58 on page 159. The room residuals are also lower in 2011-2012 than they were in 2007, which is an improvement.

This subfloor investigation was initially triggered by a thermal performance study into the room zone. This demonstrated a correlation between the room and subfloor residuals with an R^2 of approximately 0.75 (Dewsbury 2011), based on data observed in 2007. Five years later the subfloor and room residuals have a poorer correlation with an R^2 of 0.42. One explanation for the poorer correlation is simply that the data set is smaller. Another reason is that between the two studies the test cell floor was carpeted, which would increase the floor system thermal resistance and hence contribute to de-coupling the two zones. As the correlation between room and subfloor residuals is now weaker, further investigation into the AccuRate subfloor model may not be needed if the goal is to improve thermal performance accuracy, which takes only room accuracy into account.

The correlation between room and subfloor residuals is present at 4pm, as shown in 6.64(b) on page 167. This is at the time when subfloor temperatures are high and the AccuRate temperature tends to overshoot the observed temperature. This correlation is supported by the correlation between daily maximum room and subfloor residuals as shown in Figure 6.66(b) on page 168, because those maximum temperatures occur near 4pm.

However, the correlation between room and subfloor residuals no longer exists in the morning. At 9am there is no correlation between room and subfloor residuals, as shown in 6.64(a) on page 167. This is at the time when subfloor temperatures are low and the AccuRate temperature tends to undershoot the observed temperature. There is also no correlation between the daily minimum room and subfloor residuals, as shown in Figure 6.66(a) on page 168. Those minimum temperatures also occur near 9am.

This shift in the residuals' correlation by time of day is comparable to the seasonal phenomena discussed in Section 7.2.4, where the observed parameters of temperature and specific humidity show less sensitivity to their corresponding outdoor parameters in winter than they do in autumn. Compared to 4pm, at 9am the subfloor is generally cool and has a high relative humidity. Similarly, compared to autumn, in winter the subfloor is generally cool and has a high relative humidity. Thus, the relationship between the room and subfloor residuals no longer exists under the same circumstances under which the subfloor conditions become less sensitive to the outdoor conditions. This indicates the presence of a lurking variable, one with an unequal effect on the room and subfloor zones. Further investigation into this area should focus on the ground model, as was recommended in previous thermal performance research (Dewsbury 2011; Geard 2011).

The reduced sensitivity of subfloor to outdoor parameters in winter is present in both the 2007 and current data as shown in Section 6.2.4 and discussed in Section 7.2.4. An additional low temperature trend is observed in the 2007 data. The relationship between the simulated and observed dry bulb subfloor temperatures, shown in Figure 6.52 on page 153, displays a shift in sensitivity when the subfloor temperature is 15 °C. However, this relationship differs in the 2011-2012 data. As shown in Figure 6.51(b) on page 152 there is no shift in the relationship at low temperature. The relationship is linear with a seemingly constant slope throughout the range of temperatures.

It is possible that the temperature and moisture stabilization over time has a different effect in cool versus warm conditions, and that this has contributed to the more constant relationship between the AccuRate and observed subfloor temperatures in 2011-2012, as observed in Figure 6.51(b) on page 152.

Regardless of the change in relationship between the subfloor and room residuals, the subfloor residuals themselves demonstrate a correlation with relative humidity more than any other weather parameter. There is also a consistent correlation with temperature, although it is not as strong. The only group of subfloor residuals shown to be more strongly correlated with the outdoor temperature than with relative humidity is the subset of TP3 residuals at 9am. As TP3 AccuRate data only exists in winter months, this subset of residuals therefore represents the coolest times.

Though the graphs throughout Section 6.4 show correlations between the residuals and the subfloor parameters, these correlations are found to be statistically weaker than the correlations between the residuals and outdoor parameters. This is not surprising as the subfloor conditions themselves are driven by the outdoor conditions. The graphs show correlations between the residuals and other outdoor parameters as well. This is also not surprising as several of the outdoor parameters are confounded. For example high wind speed and high temperature, and thus low relative humidity, tend to occur several hours after peak radiation, as indicated in Section 6.2.1 via comparison of the hourly profile graphs of each parameter. Consideration of the residuals at only certain hours, or at the daily maxima and minima, reduces the effect that the confounding of parameters has on the study of the residuals.

The subfloor residuals have a negative correlation with the outdoor temperature and a positive correlation with outdoor relative humidity. This correlation with outdoor temperature was also observed in previous thermal performance research on the test cell (Dewsbury 2011). The correlations indicate that improvements to the AccuRate program should be in the direction of increasing the predicted temperature when the outside temperature is low and the relative humidity is high, and decreasing the predicted temperature when the outside temperature is high and the relative humidity is low. As the subfloor residuals are correlated more strongly with humidity, this

suggests that improvements to the AccuRate program should focus on the contribution of the relative humidity to the enthalpy of the subfloor air. Currently the enthalpy is too low at times of high humidity, and too high at times of low humidity.

The details of the manner in which the AccuRate model accounts for humidity are not known. However, a typical energy balance of subfloor cavity air is shown in Figure 2.2 on page 17 and summarized in Equation 2.3 on page 18. The left-hand side of the equation represents the energy storage rate of the subfloor air. It represents only the enthalpy contribution due to the rate of change in temperature of the air, whereas the enthalpy contribution due to rate of change in humidity is neglected. Even though the observed data indicate that the specific humidity of the subfloor cavity changed quite slowly with time, the contribution of moisture storage to the enthalpy of the subfloor cavity air should be investigated further.

The only other terms in Equation 2.3 with a first-order effect from humidity are the last two terms. These terms represent the net energy transfer into the subfloor air due to ventilation. It is not known whether AccuRate accounts for the contribution of moisture in these terms. This should be investigated. The net energy transfer based on observed data is calculated as described in Section 5.5.5 and that calculation does consider the enthalpy contribution of both the temperature and the moisture in the air. It is this energy transfer that is shown in Figure 6.38 on page 140 and is found to have the net effect of increasing the energy of the subfloor cavity 35% of the time.

One physical occurrence that may affect the enthalpy of the subfloor air or energy transfer through the vents is evaporation. If the subfloor air temperature is equal to the ground moisture temperature then evaporation would not affect the energy balance of the subfloor air, as the heat loss represented by air temperature reduction would be nearly identical to the enthalpy increase due to moisture gain (Cengel and Boles 2006). However, the process becomes more complex when the air and ground moisture temperatures are different, due to additional heat transfer taking place. In this case the evaporation would no longer be a constant-enthalpy process (Stoecker and Jones 1982).

The graphs of subfloor residuals as a function of evaporation at 9am and 4pm are shown in Figure 6.69(f) and Figure 6.72(f) on pages 171 and 174. Both graphs indicate that the residuals are near zero when evaporation is low, but the slope at 9am is positive whereas the slope at 4pm is negative. The value of incorporating evaporation into AccuRate should be investigated further.

As summarized in Section 4.2.3, CFD predicts that the wind speed at the test cell roof varies as a function of wind direction. Although no effect of wind direction is apparent in the observed ventilation data as discussed in Section 7.2.1, the subfloor residuals do have different correlations with wind direction at 9am than they do at 4pm, as shown in Figure 6.68(f) and Figure 6.71(f) on

pages 170 and 173. Wind direction, due to its circular nature, was not included in the linear model described in Section 6.4. Thus the effect of wind direction on thermal performance, not just subfloor ventilation, should be reviewed further. Wind speed was rarely found to have a substantial correlation with the subfloor residuals.

7.4 Sources of error and limitations

The measurement system analysis described in Section 6.5 shows that the uncertainty in the observed subfloor environmental temperature is 0.1 °C, and due to the uncertainty in the weather inputs, the uncertainty in AccuRate subfloor temperature is 0.4 °C. These combine (Taylor 1982) to yield an uncertainty in the subfloor residuals of 0.4 °C.

The range in residuals at the minimum and maximum daily temperature is 2.9 °C and 4.3 °C, respectively. These ranges are large compared to the uncertainty in the residuals. Additionally, the effect of uncertainty is minimized in this research as discussion focuses on general trends and most parameters are discussed on their relative, not absolute value. Some exceptions to this are the tabulation of time spent at high humidity, and the presentation of soil moisture and wood moisture contents. The assessment of time spent at high humidity is compared against vague criteria and therefore the accuracy in humidity is not crucial. Soil moisture and wood moisture contents are both used to support trends observed in other parameters, and no calculations are based on either parameter.

It is not known why the observed subfloor centre dry bulb air temperature is approximately one degree lower when measured by the IC sensor, TA35, than by the RTD sensor, TA36. Sensor TA35 was calibrated in June 2011 and sensor TA36 was calibrated in September 2012. This research uses TA36 as the subfloor centre temperature unless where otherwise specified, as the RTD sensors have shown through experience to shift less with time. Compared to using the sensor TA35, using sensor TA36 errs on the side of indicating less temperature drop between 2007 to 2011-2012. It also results in higher quantifications of subfloor specific humidity, thus higher values of evaporation and moisture exiting the vents.

The tracer gas ventilation test was performed in March 2007, before the carpet was installed and several years before the test period began. The airtightness of the building could have changed in those years. Tracer gas data obtained from the carpeted test cell in September 2007 do exist, but the results are suspected to be corrupt. It is assumed in this research that any subfloor air leakage is negligible compared to the rate of air flow through the vents and thus the rate of air flow entering the vents equals that exiting. Data do exist from the tracer gas ventilation test to confirm this assumption if needed.

Moisture exchange in the subfloor is assumed to occur only through the vents and between the air and ground. Moisture transfer through the brick is neglected. The effect of perimeter moisture transfer plays a larger role in the test cell than it would be in a larger building, due to the relative importance of perimeter effects in a smaller building.

In addition to measurement uncertainty it is possible that the wind speed input into AccuRate has uncertainty as high as 30% due to directional influence. Wind speed was observed at the building height and then projected to the meteorological height via a constant value as described in Section 5.5.3. However, the CFD results summarized in Table 4.1 indicate that the relationship between the wind speeds at building height and meteorological height is not constant, and that it varies with wind direction by as much as 30%. The effect of this directional error is dampened by the fact that most high wind speeds are from only one direction, the northwest.

Apart from the weather inputs, there are other sources of uncertainty in the AccuRate temperature results. Classifying the terrain as open or suburban, etc., involves user assumption. With such room for variation it is therefore assumed that the program is not expected to have a very high accuracy, and the uncertainty added by the nuances of this non-standard application of AccuRate do not contribute much more to the nominal uncertainty.

There are also characteristics of the test cell not adequately represented in AccuRate. Some items were inside the test cell while data was being gathered, such as small working desks, chairs and a portable refrigerator. Though mostly lightweight, these items would have an influence on the thermal mass of the room.

The AccuRate model was not adjusted to incorporate the plastic ground sheet or the missing ceiling hatch. Though there were no substantial differences noted in the observed or AccuRate data as a result of either the ground cover or the ceiling hatch, AccuRate room data was only considered during TP3, when the ground sheet was removed and the ceiling hatch was on. A comparison of the AccuRate subfloor residuals shows similar trends between TP1 and TP3 data subsets.

Some assumptions in the AccuRate program may be valid for larger buildings but may affect the accuracy of modelling a building as small as the test cell. AccuRate is known to neglect convective heat transfer between the subfloor air and the subfloor walls. Further, AccuRate considers that the ground exchanges radiation energy only to the bottom of the subfloor, and neglects radiation between the ground surface and subfloor walls (Delsante 2005). These factors may be valid omissions when considering buildings with larger floor areas, but they are of greater significance when considering a building as small as the test cell.

8 • CONCLUSIONS AND RECOMMENDATIONS

8.1 Findings

The aim of this research was to investigate experimentally the subfloor cavity conditions of a residential building in a cool temperate climate. The research method devised to fulfil this aim led to the formation of four Research Questions. Those four Research Questions are addressed here:

1. How accurate is the subfloor ventilation model in AccuRate? The observed subfloor ventilation rate was 60% higher than predicted by AccuRate, though as expected it had a linear dependence on wind speed. The effect of this offset on the accuracy of the AccuRate results was not quantified.
2. Are the subfloor ventilation requirements effective at maintaining a relative dry subfloor? The vents are not effective at maintaining a relatively dry subfloor as the subfloor climate consistently exceeded the desired limit of 80% relative humidity. However, the extent of these exceedances are not expected to contribute to subfloor deterioration as they were short in duration and generally occurred when the subfloor dry bulb air temperature was below 12 °C. It is also noted that no signs of deterioration were observed in the subfloor.
3. How accurate is AccuRate's predicted subfloor temperature? The AccuRate subfloor temperature generally followed the same daily pattern as the observed subfloor temperature, with no noticeable time shift. At the warmest part of the day, AccuRate's predicted subfloor temperature tended to overshoot the observed temperature. The amount of this difference ranged from AccuRate being 3.4 °C above to 0.9 °C below the observed subfloor temperature. At the coolest part of the day, AccuRate's predicted subfloor temperature tended to drop below the observed subfloor temperature. The amount of the difference ranged from AccuRate being 1.9 °C below to 1.0 °C above the observed subfloor temperature. The uncertainty in these temperature differences is 0.4 °C.

4. How can the AccuRate subfloor model be improved? The AccuRate subfloor model can be improved by incorporating physical processes that decrease the enthalpy of the subfloor cavity air when the outside relative humidity is low, and increase the enthalpy when the outside relative is high. As ground moisture evaporation would affect the subfloor air enthalpy, its effects should be investigated. It is noted that the actual contents of the AccuRate calculation engine are not currently known and that there may be other considerations in addition to evaporation.

Additionally, this research found the following shifts when comparing the subfloor climate conditions and corresponding AccuRate prediction from five years after construction of the test cell to one year after construction:

5. The subfloor was noticeably cooler and contained less moisture, and the amount of ground moisture evaporation was lower. The relative humidity remained constant.
6. AccuRate more accurately predicted the subfloor temperature five years after construction than it did one year after construction. This improvement was not due to intentional modifications to the test cell or the AccuRate program itself but instead due to the reduction of energy and moisture in the subfloor cavity as the ground reacted over time to the presence of the test cell above. The room model's accuracy also increased over this time, though that comparison is based on limited data.
7. Five years after construction, the net effect of the subfloor vents was to frequently increase both the moisture and energy in the subfloor cavity. One year after construction, the net effect of the vents was to always decrease moisture and nearly always decrease energy. Thus, the effectiveness of the vents has decreased over time.

The initial driver of this research was the desire to increase the accuracy of AccuRate's prediction of a building's thermal performance. The subfloor model in AccuRate was specifically targeted as it was thought that its improvement would improve the accuracy of the room model. It is worthwhile to note that all results presented in this thesis were generated using observed data to overwrite the default subfloor ventilation model in AccuRate. Thus, these results are not what the typical AccuRate user would obtain.

The recent research that drove this current study was based on buildings that had been newly constructed. Those studies considered both test cells and houses with varying building constructions including a concrete slab on ground. As the current research shows shifts in the subfloor climate due to time elapsed since construction, the relevance of those previous studies must be reconsidered.

At this stage a reassessment is needed by CSIRO and industry representatives to determine if improvements to the AccuRate model are still worth pursuing.

Further investigation into the subfloor may not be warranted for the sake of improving thermal performance accuracy alone, as the correlation between room and subfloor accuracy was found to be inconsistent. Additionally, the presence of subfloor insulation, as is now mandated by the Building Code of Australia, would further de-couple the room and subfloor zones.

Further investigation into the subfloor may be worthwhile in relation to the deterioration of timber due to high relative humidity. The subfloor did exceed the design criteria of 80% relative humidity and the conditions are on the boundary of what is considered favorable for mould growth or decay. In addition, the subfloor relative humidity was assessed at a location that was likely not the most damp. However, as time since construction increased, the relative humidity remained constant while the subfloor temperature decreased, hence reducing the likelihood of deterioration. These moisture characteristics are likely very site-specific.

8.2 Recommendations for further research

It is crucial when undertaking any research into building thermal or moisture performance to account for stabilization of the subfloor cavity and ground. The subfloor and ground conditions of any test building should be periodically monitored until a steady state has been reached. Any results from data observed before the subfloor and ground have stabilized are subject to change.

Data obtained from this research may be available to others subject to research institution agreement. Data include the measurements recorded on-site and recorded in the data loggers as summarized in Table 5.3, as well as the hand measured wood moisture and soil moisture data.

Recommendations for additional thermal performance and subfloor climate research are as follows.

1. AccuRate should be re-run with the default ventilation models. The results would represent those closer to what the typical user would obtain. The results could then be compared to the observed data. This task can be performed with existing data.
2. By comparing the results from Recommendation 1 to the results provided in this thesis, the effect of subfloor ventilation on the building's thermal performance could be quantified. A decision should then be made on the acceptability of AccuRate's subfloor ventilation model, the entire subfloor model, and the performance of the program as a whole.
3. If the outcome of Recommendation 2 is that the effect of the subfloor ventilation model on thermal performance is significant, then AccuRate's subfloor ventilation model may need improvement. If so, additional ventilation testing would be required. The test period should cover

a broad range of climate zones and weather conditions and not only should wind speed and direction be recorded, but also subfloor and outdoor temperature for quantification of stack effect. Wind speed and/or pressure at meteorological height, building roof height and vent height should be simultaneously recorded to investigate trends evident in the CFD results and support the theoretical relationship between wind speed at different heights. Existing data can be assessed to quantify the air infiltration from the subfloor to the room zone and to assess the expected contribution of temperature on ventilation.

4. The outcome of Recommendation 2 may be that the thermal performance of AccuRate needs improvement beyond that of the ventilation model. If so, the correlations between room and subfloor residuals should be further reviewed. This should be done concurrently with further analysis of observed data, especially the differences between cool and warm weather characteristics. The effect of wind direction on AccuRate's output should also be assessed. These tasks can be performed using existing data. This task should identify specific conditions under which the accuracy of AccuRate's room and subfloor models are correlated.
5. The outcome of Recommendations 2 and 4 may be that the AccuRate subfloor model is worth investigating further. If so, particular attention should be paid to the conditions under which the room and subfloor models are correlated, as identified in Recommendation 4. The enthalpy contribution of moisture to the subfloor energy balance should be assessed. The quantification of energy transfer due to evaporation and the effects of wind direction should also be explored. These tasks can be performed using existing data, but would likely require that full access to the AccuRate calculation engine be provided.
6. Previous research recommended that the AccuRate ground model be investigated. That task was not completed as part of the current research, though data was generated that would be of assistance. This task should be performed if Recommendation 5 does not yield suitable accuracy, or if the thermal performance investigation broadens to include slab floor construction.
7. The subfloor cavity conditions should be further reviewed for their likelihood to contribute to timber deterioration. Additional data should be gathered including relative humidity, soil moisture content and wood moisture content. These should be measured at a location with low air speed, such as between the vents of the south perimeter wall. Measurements should be recorded for one year. Analysis of these data will indicate if the likelihood of subfloor climate to be conducive to deterioration continues to decrease as time since construction increases.
8. The role of the subfloor vents should be further investigated. It should be determined if the periods of condensation coincide with the periods of high relative humidity or temperature. If they do not, then the increase of moisture due to the vents' contribution may not be significant. This

task can be performed with existing data. The role of the vents should also be assessed as time since construction increases.

9. The effect of adding more vents on the windward side of a building should be investigated as a method for reducing subfloor relative humidity.

REFERENCES

- ASHRAE Handbook of Fundamentals*. 2005. Atlanta: American Society of Heating, Refrigerating and Air-Conditioning Engineers, Inc.
- Abbott, J. E. 1983. Paper 31, subfloor evaporation rates. In *Institute of Professional Engineers New Zealand Annual Conference*. 507-522. University of Waikato, Hamilton, New Zealand.
- American Society for Testing and Materials, 2006. ASTM E741-00. *Standard Test Method for Determining Air Change in a Single Zone by Means of a Tracer Gas Dilution*.
- Australian Bureau of Agricultural and Resource Economics and Sciences. 2011. *Energy in Australia*.
- Australian Bureau of Statistics. 2008. *Environmental Issues: Energy Use and Conservation*. Report No. 4602.0.55.001.
- Awbi, H. B. 2003. *Ventilation of buildings*. New York: Spon Press, Taylor & Francis Group.
- Bassett, M. R. 1988. Natural airflows between roof, subfloor, and living spaces. In *AIVC 9th Conference, Effective Ventilation*:5-26. Gent, Belgium.
- Batlles, F.J., M.A. Rubio, J. Tovar, F.J. Olmo, and L. Alados-Arboledas. 2000. Empirical modeling of hourly direct irradiance by means of hourly global irradiance. *Energy* 25: 675–688.
- Boland, J., 2013. Personal communication: March 7, 2013.
- Building Code of Australia*. 2011. Canberra, Australia: Australian Building Control Board.
- Cengel, Y. A. and M. A. Boles. 2006. *Thermodynamics: An Engineering Approach, Fifth Edition*. Sydney: McGraw Hill Higher Education.
- Chen, D. 2010. Personal communication: August 26, 2010.
- Chen, D. 2013a. Personal communication: July 22, 2013.
- Chen, D. 2013b. Personal communication: September 6, 2013.
- Delsante, A. 2004. *A Validation of the 'AccuRate' Simulation Engine using BESTEST*. CSIRO, Report No.CMIT(C)-2004-152.
- Delsante, A. 2005. Is the new generation of building energy rating software up to the task? A review of accurate. In *ABCB, Building Australia's Future 2005*. Surfer's Paradise, Australia: ABCB.
- Delsante, A. 2007. *A Comparison of NATHERS, FirstRate and AccuRate Predictions of the Differences between Slab-on-ground Floors and Suspended Timber Floors*. Forest and Wood Products Research and Development Corporation, Report No. PN04.1008.

- Delsante, A. 1997. The development of an hourly thermal simulation program for use in the Australian nationwide house energy rating scheme. In *Clima 2000 Conference*. Brussels, Belgium.
- Delsante, A. 2006. A comparison of 'AccuRate' predictions with measured data from a mud brick house. In *Investigating the roles and challenges of building performance simulation in achieving a sustainable built environment: Proceedings of the IBPSA Australasia 2006 conference*, ed. Veronica Soebarto and Patrick Marhsallsay: 96-103. Adelaide, Australia: University of Adelaide.
- Department of Climate Change and Energy Efficiency. 2012. NATHERS - nationwide house energy rating scheme. Website www.nathers.gov.au/index.html accessed March 7, 2012.
- Department of Climate Change and Energy Efficiency. 2014. NATHERS - nationwide house energy rating scheme. Website www.nathers.gov.au/index.html accessed January 25, 2014.
- Department of Energy, Water, Heritage and the Arts. 2008. *Energy use in the Australian residential sector 1986-2020*. Commonwealth of Australia.
- Deru, M. and P. Burns. 2003. Infiltration and natural ventilation model for whole-building energy simulation of residential buildings. In *ASHRAE 2003*:1-23. Kansas City, Missouri, USA.
- DeWitt, C.A. and J.M. Bunn. 1994. Airflow through crawl space foundation vents. *ASHRAE Transactions* 100, No. 1: 1439-1452.
- Dewsbury, M. 2011. *The empirical validation of house energy rating (HER) software for lightweight housing in cool temperate climate*. PhD Thesis, University of Tasmania.
- Dewsbury, M., R. Fay, G. Nolan, and R. Vale. 2007. The design of three thermal performance test cells in launceston. In *41st Annual Conference of the Architectural Science Association ANZAScA*, ed. Coulson, J., Schwede, D. and R. Tucker: 92-100. Deakin University, Geelong, Australia.
- Dewsbury, M. and G. Nolan. 2006. Improving the thermal performance of light weight timber construction: A review of approaches and impediments relevant to six test buildings. In *Challenges for Architectural Science in Changing Climates: Proceedings of the 40th Annual Conference of the Architectural Science Association ANZAScA*, ed. Shannon, S., V. Soebarto and T. J. Williamson: 17-25. Adelaide, Australia.
- Dewsbury, M., G. Nolan, and Roger Fay. 2008. Thermal performance of light-weight timber test buildings. In *10th World conference of Timber Engineering*. 216-223. Miyazaki, Japan.
- Dewsbury, M., L. Wallis, R. Fay, and G. Nolan. 2009. The influence of residential framing practices on thermal performance. In *Performative ecologies in the built environment | Sustainable research across disciplines : Proceedings of the 43rd Annual Conference of the Architectural Science Association*, ed. Loo, S., G. Nolan, S. Sequeira and F. Soriano. Launceston, Tasmania: University of Tasmania.
- Edwards, R., R. Hartless, and A. Gaze. 1990. Measurement of sub-floor ventilation rates -- comparison with brevent predictions. In *11th AIVC Conference, Ventilation system Performance*. 1-16. Belgirate, Italy.

- Flynn, K. A., S. L. Quarles, and W. A. Dost. 1994. Comparison of ambient conditions and wood moisture contents in crawl spaces in a California condominium complex. *ASHRAE Transactions* 100, no. 1: 1302-1313.
- Fugler, D. W. and S. D. Moffatt. 1994. Investigation of crawl space performance in British Columbia. *ASHRAE Transactions* 100, no. 1: 1411-1419.
- Geard, D. 2011. *An empirical validation of the house energy rating software accurate for residential buildings in cool temperate climates of Australia*. PhD Thesis, University of Tasmania.
- Geard, D., G. Nolan, and R. Fay. 2008. The comparative thermal performance of three purpose designed houses in Australia. In *Innovation, Inspiration and Instruction: New Knowledge in the Architectural Sciences | Proceedings of the 42nd Annual Conference of the Australian and New Zealand Architectural Science Association*, ed. Ning Gu, Leman Figen Gul, Michael J Ostwald and Anthony Williams:213-220. Newcastle, Australia: University of Newcastle.
- GoogleEarth. Accessed April 3, 2013.
- Harris, D. J. and S. J. M. Dudek. 1993. The variation of heat loss through suspended floors with ventilation rate. In *AIVC 14th Conference*: 337-345. Copenhagen, Denmark.
- Harris, D. J. and S. J. M. Dudek. 1994. Heat losses from suspended timber floors with insulation. In *AIVC 15th Conference*: 387-395. Buxton, Great Britain.
- Harris, D. J. and S. J. M. Dudek. 1997. Heat losses from suspended timber floors - laboratory experiments measuring heat losses through flooring utilizing a variety of insulation and ventilation rates to determine appropriate strategies for retrofitting insulation. *Building Research and Information* 25, no. 4: 226-233.
- Hartless, R. P. 1996. Subfloor and house ventilation rates: Comparing measured and predicted values. In *AIVC 17th Conference*: 1:331-342. Gothenburg, Sweden.
- Hartless, R. P. and J. W. Llewellyn. 1999. Measuring and modelling moisture and temperature beneath a suspended timber floor. In *AIVC 20th Conference*: 1-6. Edinburgh, Scotland.
- Hartless, R. and M. K. White. 1994. Measuring subfloor ventilation rates. In *AIVC 15th Conference*, 2:687-696. Buxton, UK.
- Helec. Website <http://www.helec.com.au> referenced 18 Nov 2013.
- Hillel, D. 2004. *Environmental soil physics*. Burlington, MA USA: Academic Press.
- Kurnitski, J. 2000. Crawl space air change, heat and moisture behaviour. *Energy and Buildings* 32: 19-39.
- Kurnitski, J. 2001. Ground moisture evaporation in crawl spaces. *Building and Environment* 36, No. 1: 359-373.
- Kurnitski, J. and M. Matilainen. 2000. Moisture conditions of outdoor air ventilated crawl spaces in apartment buildings in a cold climate. *Energy and Buildings* 33, no. 1: 15-29.

- Lauret, P., J. Boland, and B. Ridley. 2010. Derivation of a solar diffuse fraction model in a bayesian framework. *Case Studies in Business, Industry and Government Statistics : CSBIGS* 3, no. 2: 108-122.
- Luther, M. B. 2008. *University of Tasmania - Test Cells and Houses*. Geelong: Deakin University, Mobile Architecture & Built Environment Laboratory.
- McInnes, K. 2005. *Encyclopedia of Soil Science, Second Edition*, s.v. "Temperature Measurement". Boca Raton: Taylor and Francis Group / CRC Press.
- McWilliams, J. 2002. *Review of Airflow Measurement Techniques*. Berkeley, California, USA: Energy Performance of Buildings Group, Environmental Energy Technologies Division, Lawrence Berkeley National Laboratory, Report No. LBNL-49747.
- Olweny, M., T.J. Williamson, A. Delsante, C. Chan, and G. Threlfall. 1998. An investigation of the thermal performance of suspended timber floors. In *32nd Annual Conference of the Australia and New Zealand Architectural Science Association*: 219-226. Victoria University of Wellington, Wellington, New Zealand.
- Rose, W. B. 1994. A review of the regulatory and technical literature related to crawl space moisture control. *ASHRAE Transactions* 100, No. 1: 1289-1301.
- Rose, W. B. and A. TenWolde. 1994. Moisture control in crawl spaces. *Wood Design Focus* 5, no. 4: 11-14.
- Roulet, C. A. and L. Vandaale. 1991. *Airflow Patterns Within Buildings, Measurement Techniques*. Coventry, U.K.: Air Infiltration and Ventilation Centre, Technical Note AIVC 34.
- Samuelson, I. 1994. Moisture control in crawl spaces. *ASHRAE Transactions* 100, No. 1: 1420-1426.
- Sequeira, S., D. Chen, R. Fay, J. Sargison, and F. Soriano. 2010b. A heat and mass transfer analysis of the subfloor cavity of a residential building. In *On the edge: Cross-disciplinary & intra-disciplinary connections in architectural science | Proceedings of the 44th Annual Conference of the Australian and New Zealand Architectural Science Association*, ed. Murphy, C., S. J. Wake, D. Turner, G. McConchie and D. Rhodes. Auckland, New Zealand: Unitec Institute of Technology.
- Sequeira, S., R. Fay, J. Sargison, and F. Soriano. 2010a. A preliminary analysis of subfloor ventilation data: Bridging the gap between theory and experiment. *Architectural Science Review* 53, No. 3: 315-322.
- Sherman, M. H. 1990. Tracer-gas techniques for measuring ventilation in a single zone. *Building and Environment* 25, No. 4: 365-374.
- Shuttleworth, W. J. 2007. Putting the "Vap" Into evaporation. *Hydrology & Earth System Sciences* 11, No. 1: 210-244.
- Standards Australia. 2000. AS 1289.0-2000 *Methods of testing soils for engineering purposes - general requirements and list of methods*.
- Stiles, L. and M. Custer. 1994. Reduction of moisture in wood joists in crawl spaces - a study of seventeen houses in southern New Jersey. *ASHRAE Transactions* 100, No. 1: 1314-1324.

- Stoecker, W. F. and J. W. Jones. 1982. *Refrigeration and Air Conditioning*. Edited by J. P. Holman. Sydney: McGraw-Hill Book Company.
- Strangeways, I. 2003. *Measuring the Natural Environment*. Cambridge, UK: Cambridge University Press.
- Sugo, H.O., A.W. Page, and B. Moghtaderi. 2004. A comparative study of the thermal performance of cavity and brick veneer construction. In *13th International Brick and Block Masonry Conference*, 3:767-776. Eindhoven, Holland.
- Sugo, H.O., A.W. Page, and B. Moghtaderi. 2005. The study of heat flows in masonry walls in a thermal test building incorporating a window. In *10th Canadian Masonry Symposium*. Banff, Alberta.
- Swami, M. V. and S. Chandra. 1988. Correlations for pressure distribution of buildings and calculation of natural ventilation airflow. *ASHRAE Transactions* 94(1): 243-266.
- Taylor, J. R. 1982. *An introduction to error analysis*. Edited by Eugene D. Commins. Sausalito, CA USA: University Science Books.
- Thomas, H. 2010a. Software glitch undermines green houses. *The Australian*, July 27, 2010.
- Thomas, H. 2010b. Home building guided by stars. *The Australian*, July 31, 2010.
- Trethowen, H. A. 1988. *A Survey of Subfloor Ground Evaporation Rates*. Report No. 13. Porirua, New Zealand: Building Research Association of New Zealand.
- Trethowen, H. A. 1994. Three surveys of subfloor moisture in New Zealand. *ASHRAE Transactions* 100, No. 1: 1427-1438.
- Tsongas, G. A. 1994. Crawl space moisture conditions in new and existing northwest homes. *ASHRAE Transactions* 100, No. 1: 1325-1332.
- Williamson, T. J. 1984. *An Evaluation of Thermal Performance Computer Programs*. Australian Housing Research Council, Department of Housing and Construction, AHRC Project 89. Melbourne, Australia.
- Williamson, T. J. and A. Delsante. 2006a. Investigation of a model for the ventilation of suspended floors. In *Challenges for Architectural Science in Changing Climates: Proceedings of the 40th Annual Conference of the Architectural Science Association ANZAScA*, ed. Shannon, S., V. Soebarto and T. J. Williamson: 143-150. Adelaide, Australia.
- Williamson, T. J. and A. Delsante. 2006b. An investigation of the ventilation requirements to prevent deterioration of timber and mould growth beneath suspended floors. In *Challenges for Architectural Science in Changing Climates: Proceedings of the 40th Annual Conference of the Architectural Science Association ANZAScA*, ed. Shannon, S., V. Soebarto and T. J. Williamson: 159-166. Adelaide, Australia.
- Wu, J. and D. L. Nofziger. 1999. Incorporating Temperature Effects on Pesticide Degradation into a Management Model. *Journal of Environmental Quality* 28 No. 1: p. 92-100.

APPENDIX

APPENDIX TABLE OF CONTENTS

A.1 Test cell drawings.....	209
A.2 Observed data calibration, acquisition, data reduction and calculations.....	213
A.2.1 Calibration and sensor resolution.....	213
A.2.2 Data acquisition, reduction and calculations	214
A.3 AccuRate input files	243
A.4 AccuRate data reduction	279
A.5 Observed and AccuRate Results	283
A.5.1 Observed ground moisture evaporation	283
A.5.2 Observed and AR1 room temperatures, TP3.....	288
A.5.3 Observed and AR1 subfloor temperatures, TP1-3.....	290
A.5.4 Observed and AR1 subfloor daily max. and min. temperatures, TP1-3	298
A.5.5 Observed and AR2 room temperatures, TP3.....	305
A.5.6 Observed and AR2 subfloor temperatures, TP1-3.....	307
A.5.7 Observed and AR2 subfloor daily max. and min. temperatures, TP1-3	315
A.6 Analysis of Residuals.....	322
A.6.1 Subfloor residuals (OE-AR2), TP1-TP3	323
A.6.2 AccuRate temperature and subfloor residuals (OE-AR2), 9am, TP1-TP3	325
A.6.3 AccuRate temperature and subfloor residuals (OE-AR2), 4pm, TP1-TP3	328
A.7 Measurement system analysis	331

LIST OF APPENDIX FIGURES

Figure A.1: Footing plan, floor plan, roof plan (Dewsbury 2011).....	210
Figure A.2: Test cell elevations (Dewsbury 2011)	211
Figure A.3: Test cell section drawing (Dewsbury 2011)	212
Figure A.4: Data acquisition schematic	215
Figure A.5: DT0 data acquisition script, page 1	216
Figure A.6: DT0 data acquisition script, page 2.....	217
Figure A.7: DT2 data acquisition script	218
Figure A.8: instr_range.R, page 1	219
Figure A.9: instr_range.R, page 2	220
Figure A.10: instr_limits.txt.....	221
Figure A.11: instr_step.R, page 1.....	222
Figure A.12: instr_step.R, page 2.....	223
Figure A.13: instr_maxmin.R, page 1	224
Figure A.14: instr_maxmin.R, page 2	225
Figure A.15: instr_graph.R, page 1.....	226
Figure A.16: instr_graph.R, page 2.....	227
Figure A.17: instr_graph.R, page 3.....	228
Figure A.18: instr_graph.R, page 4.....	229
Figure A.19: instr_graph.R, page 5.....	230
Figure A.20: instr_ave.R, page 1	231
Figure A.21: instr_ave.R, page 2.....	232
Figure A.22: ana_calcs.R, page 1	233
Figure A.23: ana_calcs.R, page 2	234
Figure A.24: ana_calcs.R, page 3	235
Figure A.25: ana_calcs.R, page 4	236
Figure A.26: ana_calcs.R, page 5	237
Figure A.27: ana_calcs.R, page 6	238
Figure A.28: ana_calcs.R, page 7	239
Figure A.29: ana_maxmin.R, page 1	240
Figure A.30: ana_maxmin.R, page 2	241
Figure A.31: AR1 Building report, page 1.....	244
Figure A.32: AR1 Building report, page 2.....	245
Figure A.33: AR1 Building report, page 3.....	246
Figure A.34: AR1 Building report, page 4.....	247

Figure A.35: AR1 Building report, page 5.....	248
Figure A.36: AR1 Building report, page 6.....	249
Figure A.37: AR1 Building report, page 7.....	250
Figure A.38: AR1 Building report, page 8.....	251
Figure A.39: AR1 Scratch file, page 1.....	252
Figure A.40: AR1 Scratch file, page 2.....	253
Figure A.41: AR1 Scratch file, page 3.....	254
Figure A.42: AR1 Scratch file, page 4.....	255
Figure A.43: AR1 Scratch file, page 5.....	256
Figure A.44: AR1 Scratch file, page 6.....	257
Figure A.45: AR1 Scratch file, page 7.....	258
Figure A.46: AR2 Building report, page 1.....	259
Figure A.47: AR2 Building report, page 2.....	260
Figure A.48: AR2 Building report, page 3.....	261
Figure A.49: AR2 Building report, page 4.....	262
Figure A.50: AR2 Building report, page 5.....	263
Figure A.51: AR2 Building report, page 6.....	264
Figure A.52: AR2 Building report, page 7.....	265
Figure A.53: AR2 Building report, page 8.....	266
Figure A.54: AR2 Scratch file, page 1.....	267
Figure A.55: AR2 Scratch file, page 2.....	268
Figure A.56: AR2 Scratch file, page 3.....	269
Figure A.57: AR2 Scratch file, page 4.....	270
Figure A.58: AR2 Scratch file, page 5.....	271
Figure A.59: AR2 Scratch file, page 6.....	272
Figure A.60: AR2 Scratch file, page 7.....	273
Figure A.61: ana_climate.R, page 1.....	274
Figure A.62: ana_climate.R, page 2.....	275
Figure A.63: ana_climate.R, page 3.....	277
Figure A.64: ana_climate.R, page 4.....	277
Figure A.65: AR1 and AR2 Climate file, first page	278
Figure A.66: acc_check.R	280
Figure A.67: acc_maxmin.R, page 1.....	281
Figure A.68: acc_maxmin.R, page 2.....	282
Figure A.69: 2011-2012 Ground moisture evaporation vs. ventilation, by month	284
Figure A.70: 2011-2012 Ground moisture evaporation vs. ventilation, by outdoor temperature	285
Figure A.71: 2007 Ground moisture evaporation vs. ventilation, by month	286
Figure A.72: 2007 Ground moisture evaporation vs. ventilation, by outdoor temperature	286

Figure A.73: 2007 Ground moisture evaporation vs. ventilation, by subfloor temperature	287
Figure A.74: Observed and AR1 room temperatures, TP1-3, page 1	288
Figure A.75: Observed and AR1 room temperatures, TP1-3, page 2	289
Figure A.76: Observed and AR1 subfloor temperatures, TP1-3, page 1	290
Figure A.77: Observed and AR1 subfloor temperatures, TP1-3, page 2	291
Figure A.78: Observed and AR1 subfloor temperatures, TP1-3, page 3	292
Figure A.79: Observed and AR1 subfloor temperatures, TP1-3, page 4	293
Figure A.80: Observed and AR1 subfloor temperatures, TP1-3, page 5	294
Figure A.81: Observed and AR1 subfloor temperatures, TP1-3, page 6	295
Figure A.82: Observed and AR1 subfloor temperatures, TP1-3, page 7	296
Figure A.83: Observed and AR1 subfloor temperatures, TP1-3, page 8	297
Figure A.84: AR1 and observed daily max. and min. subfloor temperatures, page 1	298
Figure A.85: AR1 and observed daily max. and min. subfloor temperatures, page 2	299
Figure A.86: AR1 and observed daily max. and min. subfloor temperatures, page 3	300
Figure A.87: AR1 and observed daily max. and min. subfloor temperatures, page 4	301
Figure A.88: AR1 and observed daily max. and min. subfloor temperatures, page 5	302
Figure A.89: AR1 and observed daily max. and min. subfloor temperatures, page 5	303
Figure A.90: AR1 and observed daily max. and min. subfloor temperatures, page 6	304
Figure A.91: Observed and AR2 room temperatures, TP1-3, page 1	305
Figure A.92: Observed and AR2 room temperatures, TP1-3, page 2	306
Figure A.93: Observed and AR2 subfloor temperatures, TP1-3, page 1	307
Figure A.94: Observed and AR2 subfloor temperatures, TP1-3, page 2	308
Figure A.95: Observed and AR2 subfloor temperatures, TP1-3, page 3	309
Figure A.96: Observed and AR2 subfloor temperatures, TP1-3, page 4	310
Figure A.97: Observed and AR2 subfloor temperatures, TP1-3, page 5	311
Figure A.98: Observed and AR2 subfloor temperatures, TP1-3, page 6	312
Figure A.99: Observed and AR2 subfloor temperatures, TP1-3, page 7	313
Figure A.100: Observed and AR2 subfloor temperatures, TP1-3, page 8	314
Figure A.101: AR2 and observed daily max. and min. subfloor temperatures, page 1	315
Figure A.102: AR2 and observed daily max. and min. subfloor temperatures, page 2	316
Figure A.103: AR2 and observed daily max. and min. subfloor temperatures, page 3	317
Figure A.104: AR2 and observed daily max. and min. subfloor temperatures, page 4	318
Figure A.105: AR2 and observed daily max. and min. subfloor temperatures, page 5	319
Figure A.106: AR2 and observed daily max. and min. subfloor temperatures, page 5	320
Figure A.107: AR2 and observed daily max. and min. subfloor temperatures, page 6	321
Figure A.108: Subfloor residuals (OE-AR2), TP1-TP3, batch 1	323
Figure A.109: Subfloor residuals (OE-AR2), TP1-TP3, batch 2	324
Figure A.110: AccuRate vs. observed temperature, 9am, TP1-3	325

Figure A.111: Subfloor residuals (OE-AR2), 9am, TP1-TP3, batch 1	326
Figure A.112: Subfloor residuals (OE-AR2), 9am, TP1-TP3, batch 2.....	327
Figure A.113: AccuRate vs. observed temperature, 4pm, TP1-3.....	328
Figure A.114: Subfloor residuals (OE-AR2), 4pm, TP1-TP3, batch 1	329
Figure A.115: Subfloor residuals (OE-AR2), 4pm, TP1-TP3, batch 2	330
Figure A.116: Uncertainty in specific humidity.....	332
Figure A.117: Uncertainty in predicted subfloor temperature.....	333

A.1 Test cell drawings

The footing plan, floor plan and roofing plan for the tell cell are provided in Figure A.1. The elevations are provided in Figure A.2. Note that the northern elevation omits the subfloor access door at the east end of the wall and the resulting spacing change for the subfloor vents. The section drawing is provided in Figure A.3.

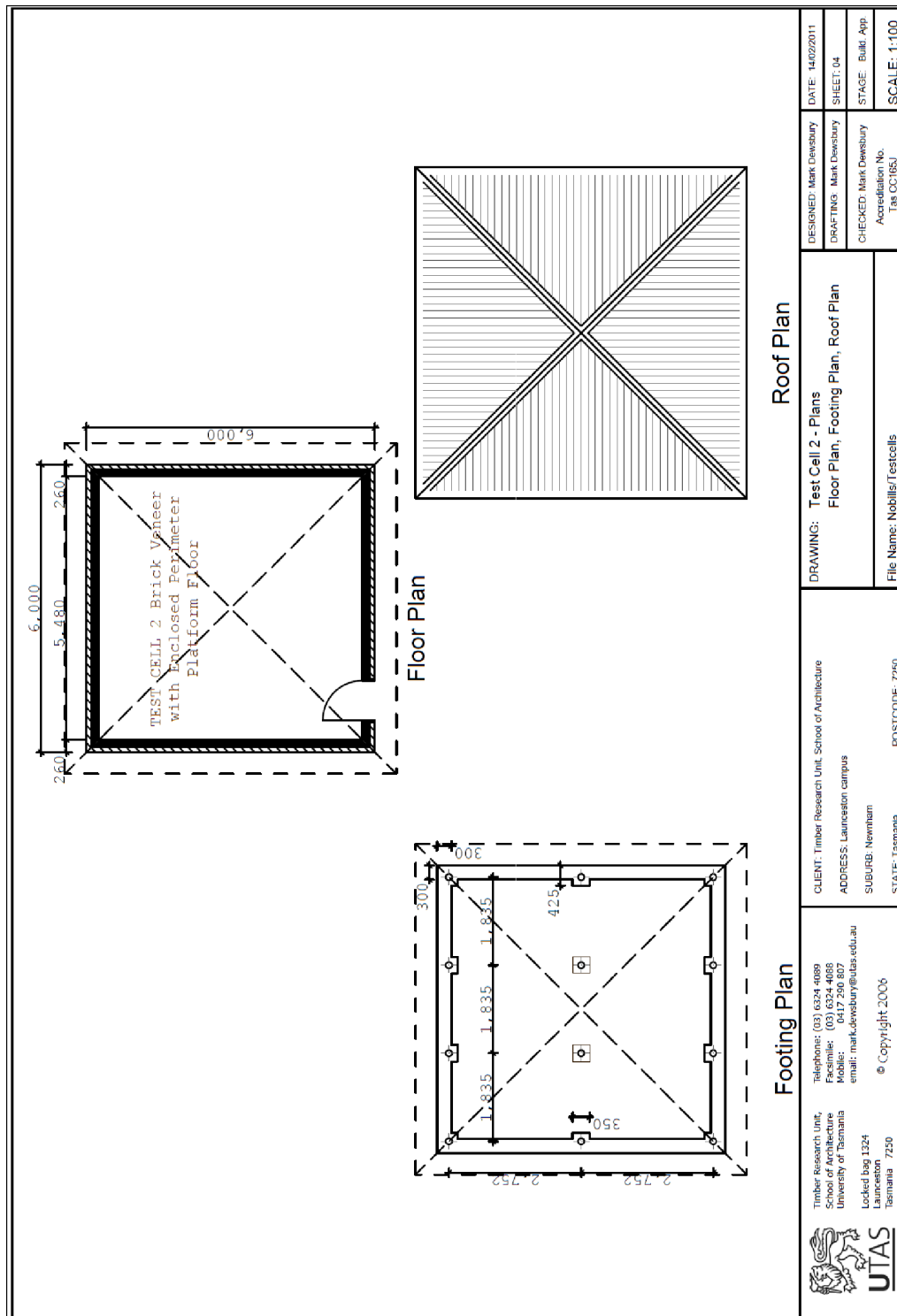


Figure A.1: Footing plan, floor plan, roof plan (Dewsbury 2011)

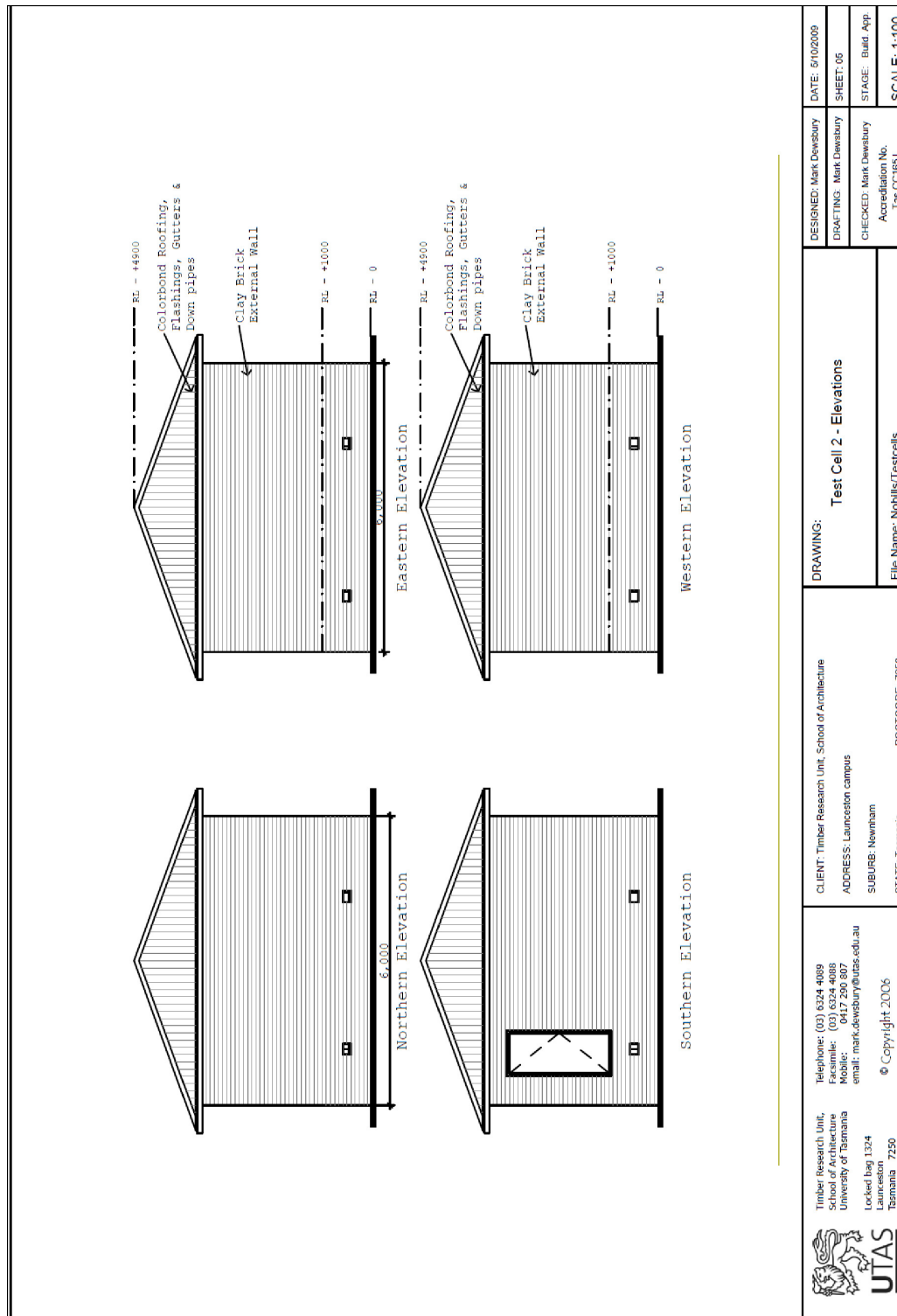
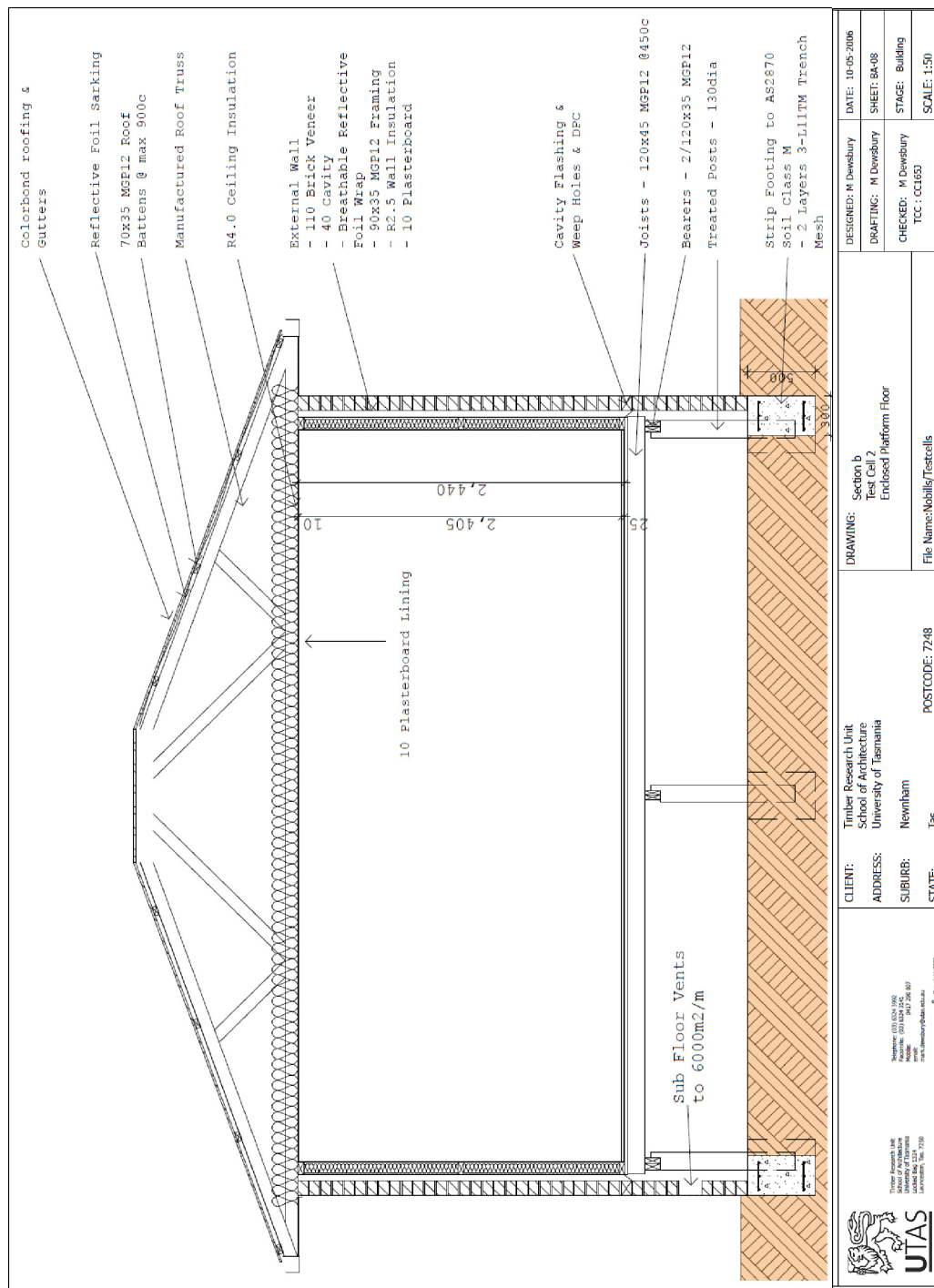


Figure A.2: Test cell elevations (Dewsbury 2011)



A.2 Observed data calibration, acquisition, data reduction and calculations

A.2.1 Calibration and sensor resolution

Calibration and/or manufacturers' stated accuracy is presented for all parameters used in the measurement system analysis. Calibration of equipment began in June 2010 with installation of sensors beginning later that year and finishing in February 2011. Calibration of certain sensors was performed before June 2010 as part of another research program.

Wind angle (AD10) was calibrated on-site in April 2011 by comparing the observed wind direction to that using Google Earth. Wind direction was found to be accurate within 4 °. Manufacturer claims for the wind speed (AS10) sensor is a speed threshold of 0.5 m/s and accuracy of 0.5 m/s. Wind speed was calibrated by Industrial Technik in May 2010.

Both the weather station temperature (TA10) and humidity (RH10) sensors were calibrated by Industrial Technik during October 2010. The temperature calibration was between -0.6 and 0.4 °C and relative humidity was -0.8% and -0.1%.

Global irradiation was measured via a SolData 80SPC pyranometer. Manufacturer stated accuracy is within 3% of actual value with variation within 2% for two years.

Integrated circuit (AD592CN) sensors used throughout the subfloor and room zones were calibrated on-site, via the data acquisition system in June 2010. The sensors were calibrated against two Industrial Technik PT100 sensors: TK06, which was calibrated 8th July 2009; and TK52, which was calibrated 8th July 2009. Calibration was performed at 0 °C, 17 °C and 24 °C. The resulting calibration adders and scalars were applied to the raw data in the data acquisition scripts.

RTD (PT100) sensors measuring subfloor air and ground temperature were calibrated on-site, via the data acquisitions system in September 2012 by Industrial Technik. All eight sensors were calibrated at approximately 0 °C, 24 °C and 60 °C. At 0 °C the eight PT100s had offsets ranging from 0 °C to +0.3 °C. The one sensor recording an offset of +0.3 °C was TA34, the subfloor air temp near east wall. The two sensors that had offsets of +0.2 °C were TG30, the 150 mm ground temp at subfloor centre, and TG21, the 600 mm ground temp at the east wall. At 24 °C all eight PT100s had offsets between -0.1 °C and +0.1 °C. At 60 °C the offsets were between -0.3 °C to +0.1 °C. TG31, the sensor buried 600 mm in the ground at the subfloor centre had the -0.3 °C offset. All other seven sensor were between -0.1 °C and +0.1 °C at 24 °C. Both TA36, the subfloor centre dry bulb temperature, and TB31, the subfloor centre globe temperature, recorded a 0.0 °C offset at all three temperature settings.

The thermocouples were also calibrated on-site, via the data acquisitions system in September 2012 by Industrial Technik. The thermocouples were consistently reading 2.5 °C to 3.0 °C too high. The thermocouples were all between 1.9 °C and 3.0 °C except for TS32, the surface temperature of brick inside the west wall, TS38, the surface temperature of the floor in the room, and TS39, the surface temperature of a pier at the subfloor centre.

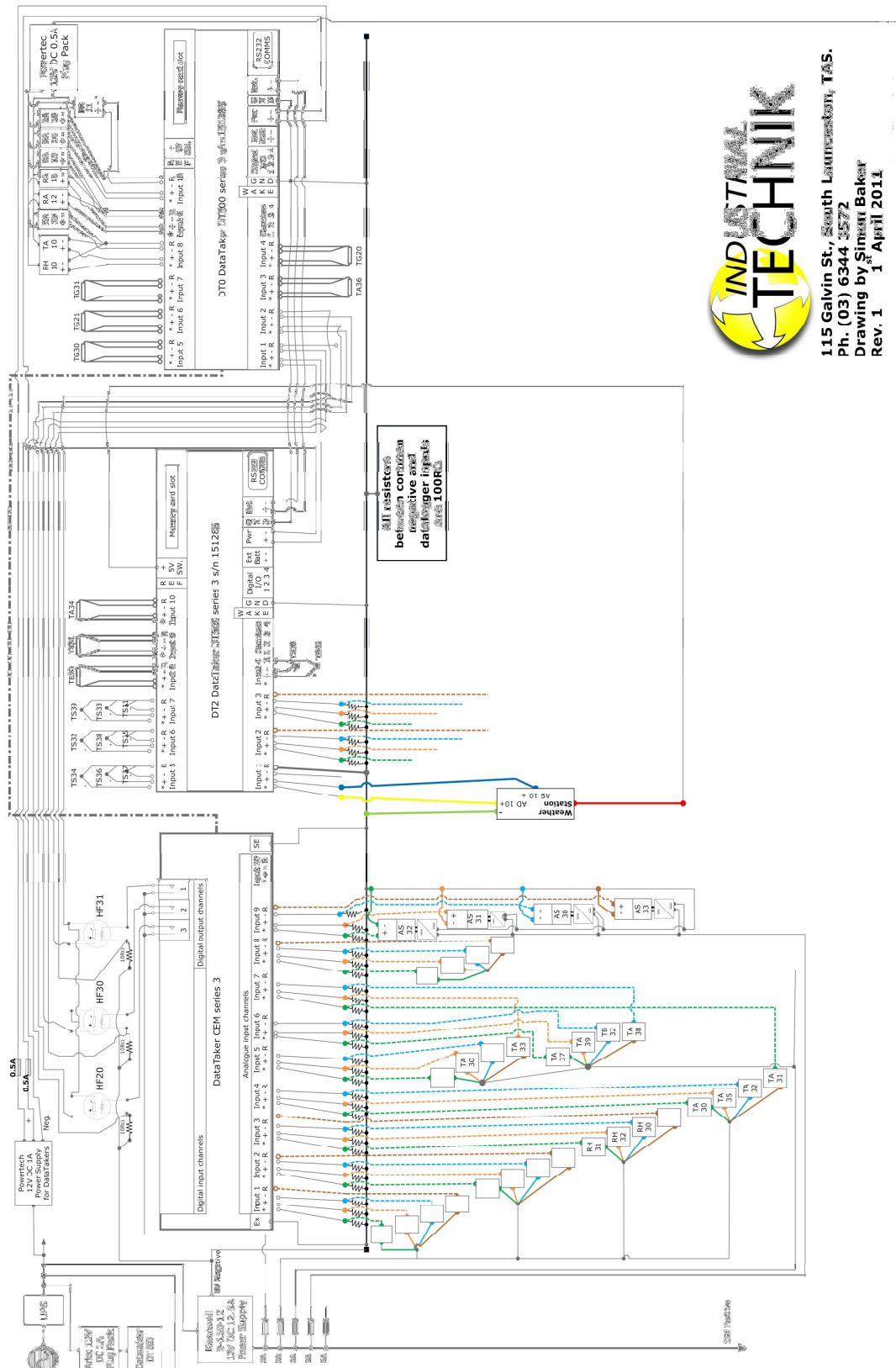
The three humidity sensors used throughout the subfloor were calibrated by Industrial Technik in October 2010. They met the manufacturer's stated accuracy, which is 3%.

A.2.2 Data acquisition, reduction and calculations

The data acquisition schematic is shown in Figure A.4. The scripts for the data acquisition from the data loggers are presented here. The DT0 script is two pages long and is provided in Figure A.5 and Figure A.6. The DT2 script is provided in Figure A.7.

Also provided are several scripts for the error checking. The first file is the range checking script, `instr_range.R`, provided in Figure A.8 and Figure A.9. That script calls the file `instr_limits.txt`, provided in Figure A.10. Next is the step checking script, `instr_step.R`, in Figure A.11 and Figure A.12; the script for calculating daily maximum and minimum values, `instr_maxmin.R`, in Figure A.13 and Figure A.14; the script for creating graphs for error-checking instrumentation, `instr_graph.R`, in Figure A.15 through Figure A.19, and finally the script for taking hourly averages of the 10-minute interval data, `instr_ave.R`, in Figure A.20 and Figure A.21. The error checking scripts were run several times and occasionally the limits were changed. The actual values run during different passes are documented. This limits file is shown as an example. The `instr_limits.txt` file is normally in CSV format but it is shown here tabulated for ease of reading. The `instr_maxmin.R` script though not computationally efficient was effective.

The script for incorporating the purchased weather data from BOM and the calculated diffuse and direct radiation values, as well as performing calculations on the weather data and many other calculations in general, is `ana_calcs.R` in Figure A.22 through Figure A.28. Once all the calculations are performed, the daily maximum and minimum values for some calculated parameters are calculated to supplement the set of daily max and min values of directly measured values. This is performed in the `ana_maxmin.R` script in Figure A.29 and Figure A.30. The calculation of daily extrema is performed far more efficiently in `ana_maxmin.R` than in `instr_maxmin.R`.



115 Galvin St., South Launceston, TAS.
Ph. (03) 6344 3572
Drawing by Simon Baker
Rev. 1 1 April 2011

```

H
CLEAR
\W3
CDATA
\W3
RESET
\W4
S1=-100,100,61.5,138.5"DegC"
S2=0,5,400,2000"m/s"
S4=0,100,400,2000"%"
S5=0,100,0,1000"%RH"
S6=-40,60,0,1000"DegC"
S7=0,1,0,181"kW/m2"
S8=0,1,0,155"kW/m2"
S12=0,1,0,182"kW/m2"
S13=0,1,0,184"kW/m2"
S14=0,1,0,181"kW/m2"
S16=-45.79,63.87,-40,60"CalDegC"
S17=-40.38,60.17,-40,60"CalDegC"
S18=-44.71,63.02,-40,60"CalDegC"
S19=-39.91,58.63,-40,60"CalDegC"
S20=-40.04,59.51,-40,60"CalDegC"
S3=-44.00,62.90,-40,60"CalDegC"
S9=-42.93,60.89,-40,60"CalDegC"
S10=-44.18,62.56,-40,60"CalDegC"
S11=-44.25,63.20,-40,60"CalDegC"
S15=-40.95,59.59,-40,60"CalDegC"
BEGIN
RA10M
D 'DAY
T 'TIME
2-V("HF20")
1-V("HF20HEATER")
4R(S1,4W,"TG20")
6R(S1,4W,"TG21")
10*V(S7,"RA14",X,N)
9-V(S8,"RA15",X,N)
10+V(S8,"RA16",X,N)
8*V(S5,"RH10",X,N)
8+V(S6,"TA10",X,N)
8-V(S12,"RA10",X,N)
10-V(S13,"RA11",X,N)
9*V(S14,"RA12",X,N)
9+V(S14,"RA13",X,N)
1:9#V(S2,"AS33",N)
2+V("HF30")
1+V("HF30HEATER")

```

Figure A.5: DT0 data acquisition script, page 1

```

2*v("HF31")
1*v("HF31HEATER")
1:3-v(S4,"RH30",X,N)
1:3*v(S4,"RH31",X,N)
1:3+v(S4,"RH32",X,N)
1:4*AD590(S16,"TA30",X,N)
1:7*AD590(S17,"TA31",X,N)
1:4-AD590(S18,"TA32",X,N)
1:7+AD590(S19,"TA33",X,N)
1:4+AD590(S20,"TA35",X,N)
3R(S1,4W,"TA36")
5R(S1,4W,"TG30")
7R(S1,4W,"TG31")
1:9-v(S2,"AS30",X,N)
1:9+v(S2,"AS31",X,N)
1:9*v(S2,"AS32",X,N)
1:6-AD590(S3,"TB32",X,N)
1:6*AD590(S9,"TA37",X,N)
1:7-AD590(S10,"TA38",X,N)
1:6+AD590(S11,"TA39",X,N)
1:5+AD590(S15,"TA40",X,N)
RZ1S
ALARM2(2ST<3)AND
ALARM3(3ST<1)"TURN HEATERS ON[2*v("flux 1 sensor heater on")
2+v("flux 2 sensor heater on") 2-v("flux 3 sensor heater on")
1:1DSO=1 1:2DSO=1 1:3DSO=1]"
ALARM4(2ST<3)AND
ALARM5(3ST>5)AND
ALARM6(3ST<7)"TURN HEATERS ON[2*v("flux 1 sensor heater on")
2+v("flux 2 sensor heater on") 2-v("flux 3 sensor heater on")
1:1DSO=1 1:2DSO=1 1:3DSO=1]"
ALARM7(2ST<3)AND
ALARM8(3ST>11)AND
ALARM9(3ST<13)"TURN HEATERS ON[2*v("flux 1 sensor heater on")
2+v("flux 2 sensor heater on") 2-v("flux 3 sensor heater on")
1:1DSO=1 1:2DSO=1 1:3DSO=1]"
ALARM10(2ST<3)AND
ALARM11(3ST>17)AND
ALARM12(3ST<19)"TURN HEATERS ON[2*v("flux 1 sensor heater on")
2+v("flux 2 sensor heater on") 2-v("flux 3 sensor heater on")
1:1DSO=1 1:2DSO=1 1:3DSO=1]"
ALARM13(2ST>3)"TURN HEATERS OFF[1:1DSO=0 1:2DSO=0 1:3DSO=0]"
END
LOGON
G

```

Figure A.6: DT0 data acquisition script, page 2

```

H
CLEAR
\W3
CDATA
\W3
RESET
\W4

S1=-100,100,61.5,138.5"Deg C"
S10=0,360,0,1000"Degrees"
S3=0,27.78,0,1000"m/s"

BEGIN
RA10M
D 'DAY
T 'TIME
1*V(S10,"AD10")
1+V(S11,"AS10")
10R(S1,4W,"TA34")
8R(S1,4W,"TB30")
9R(S1,4W,"TB31")
4-TK("TS30",X,N)
7-TK("TS31",X,N)
6*TK("TS32",X,N)
7+TK("TS33",X,N)
5*TK("TS34",X,N)
6-TK("TS35",X,N)
5+TK("TS36",X,N)
5-TK("TS37",X,N)
6+TK("TS38",X,N)
7*TK("TS39",X,N)
4+TK("TS40",X,N)

END

LOGON

G

```

Figure A.7: DT2 data acquisition script

```
#####
## instr_range.R
##
## December 1 2011, Sabrina Sequeira
## Checks data for range violations
## Input: data02.csv (master spreadsheet of data)
## Input: instr_limits.txt (listing of parameter min and max)
## Output: each param has range violations file in the range_output folder)
## Output: summary file in range_output folder
##
## tested: if input data is missing values, output file show NA for that time step
## tested: if parameter is not in limits file, no output file is created
## tested: if parameter is in limits file but has no minmax, this script crashes
##
## To change between 10-minute & hourly:
##   search/replace: data02 is 10-minute & data05 is hourly
##   search/replace. DTstandard is for 10-minute & DateTime is hourly
##   start parameter loop at 7 for 10-minute and 3 for hourly
#####

# set working directory
setwd("F:/sabs uni files/project/test cell data/scripts")

# load in the data into a data frame named all.df, and shorten to some.df
# for easy testing just change range that gets into some.df
#all.df <- read.csv("data05.csv",sep=" ",header=T)
#some.df <- all.df[,]
some.df <- read.csv("data05.csv",sep=" ",header=T)
# load in the range limits file
d <- read.table("instr_limits.txt",header=T)

# create output file
str1 <- c("Summary of Range Violations Check. Run at",date(),"\n")
cat(str1,file="range_check_output/summary_range.txt")
cat("Parameter\tMin\tMax\t# Inputs\t# NA\t# Violations\n",
    file="range_check_output/summary_range.txt",append=TRUE)

# loop through the parameters in main data frame
for (i in 3:length(names(some.df)))
```

Figure A.8: instr_range.R, page 1

```

{
param <- names(some.df)[i]; # identify param by column name
min <- d[d$parameter == param,"ranmin"]; # identify min val using param, min cols
max <- d[d$parameter == param,"ranmax"]; # identify max val using param, max cols
# if the parameter is not in limits file then skip to next parameter
if ('TRUE' %in% (d$parameter == param))
{
str2 <- c("starting",param,"..... "); message(str2); # print status to screen
# create an output vector (not a data frame) for desired param and fill with NA
# that comma before "param" makes it a vector, not a data frame
var_ran <- numeric(length(some.df[,param]))
var_ran[1:length(some.df[,param])] <- NA
# loop through each value of parameter
for (j in 1:length(some.df[,param]))
{
# if input data is NA then skip to next value of parameter
if (is.na(some.df[,param][j])) next else
{
var_ran[j] <- 1 ; # if there is input data, assign the value of 1
# now assign the value of 0 only if the data is within range
if (some.df[,param][j] > min) if (some.df[,param][j] < max) var_ran[j] <- 0
}
}
# compile the three useful vectors into a data frame
range_output <- data.frame(some.df$DateTime,some.df[,param],var_ran)
# rename the variables in the data frame
colnames(range_output) <- c("DateTime","orig","error")
# export the data frame to a csv file in the range_check folder
write.table(range_output,file=paste("range_check_output/range",param,".csv"),
sep=",",row.names=FALSE)
# create the output summary file.
str3 <- c(param,"\t\t",min,"\t",max,"\t",length(var_ran),"\t\t",
sum(is.na(var_ran)), "\t",sum(var_ran,na.rm=TRUE),"\n")
cat(str3,file="range_check_output/summary_range.txt",append=TRUE)
str4 <- c("done\n"); message(str4); # print status to screen
}
else next
}
}
file.show("range_check_output/summary_range.txt")

```

Figure A.9: instr_range.R, page 2

parameter	ranmin	ranmax	step	stephr	digs	units
AD10	-0.001	360	40	240		0 °
AS10	-0.001	20	10	60		1 m/s
AS30	-0.001	5	0.5	3		1 m/s
AS31	-0.001	5	0.5	3		1 m/s
AS32	-0.001	5	0.5	3		1 m/s
AS33	-0.001	5	0.1	0.6		1 m/s
HF20	-50	125	2.5	15		1 W/m2
HF30	-10	10	0.3	1.8		1 W/m2
HF31	-10	10	0.3	1.8		1 W/m2
RA10	-1.3	1.3	0.2	1.2		3 kW/m2
RA11	-1.3	1.3	0.2	1.2		3 kW/m2
RA12	-1.3	1.3	0.2	1.2		3 kW/m2
RA13	-1.3	1.3	0.2	1.2		3 kW/m2
RA14	-1.3	1.3	0.2	1.2		3 kW/m2
RA15	-1.3	1.3	0.05	0.3		3 kW/m2
RA16	-1.3	1.3	0.05	0.3		3 kW/m2
RH10	20	100	3	18		1 %
RH30	35	100	1	6		1 %
RH31	35	100	1	6		1 %
RH32	35	100	1	6		1 %
TA10	0	35	0.3	1.8		1 °C
TA30	5	25	1.2	7.2		1 °C
TA31	5	25	1.2	7.2		1 °C
TA32	5	25	1.2	7.2		1 °C
TA33	5	25	1.2	7.2		1 °C
TA34	5	25	0.5	3		1 °C
TA35	5	25	0.5	3		1 °C
TA36	5	25	0.5	3		1 °C
TA37	5	25	0.3	1.8		1 °C
TA38	5	25	0.3	1.8		1 °C
TA39	5	25	0.3	1.8		1 °C
TA40	5	25	1.5	9		1 °C
TB30	5	25	0.3	1.8		1 °C
TB31	5	25	0.3	1.8		1 °C
TB32	5	25	0.3	1.8		1 °C
TG20	5	25	0.5	3		1 °C
TG21	5	25	0.5	3		1 °C
TG30	7	23	0.2	1.2		1 °C
TG31	7	23	0.2	1.2		1 °C
TS30	0	38	1	6		1 °C
TS31	0	38	1	6		1 °C
TS32	0	38	1	6		1 °C
TS33	0	38	1	6		1 °C
TS34	5	27	1	6		1 °C
TS35	5	25	1	6		1 °C
TS36	5	28	1	6		1 °C
TS37	5	25	1	6		1 °C
TS38	5	25	1	6		1 °C
TS39	5	26.5	1	6		1 °C
TS40	0	41	1	6		1 °C

Figure A.10: instr_limits.txt

```
#####
## instr_step.R
##
## December 1 2011, Sabrina Sequeira. Updated October 24, 2012.
## Checks data for step violations
## Input: data04.csv or data04e.csv
## Input: instr_limits.txt (listing of parameter min and max)
## Output: each parameter has a step violations file in the step_output folder)
## Output: summary file in step_output folder
##
## NOTE: swap input file between data04.csv and data04e.csv
##
## this works! but still do the routine checking
## tested: if input data file is missing some values, output file show NA
## for that and next time step
## tested: if parameter is not in limits file, no output file is created
## tested: if param is in limits file but has no step defined, this script crashes
##
## To change between 10-minute & hourly:
## search/replace: data04 is 10-minute & data05 is hourly
## search/replace. DTstandard is for 10-minute & DateTime is hourly
## search/replace. in "max" definition step is for 10-minute and stephr is hourly
## start parameter loop at 7 for 10-minute and 3 for hourly
#####

# set working directory
setwd("F:/sabs uni files/project/test cell data/scripts")

# load in the data into a data frame named all.df, and shorten to some.df
# for easy testing just change what data gets read into some.df
some.df <- read.csv("data05.csv", sep=",", header=T)
#some.df <- all.df[50:60,]
#some.df <- read.csv("data04e.csv", sep=",", header=T)
# load in the range limits file
d <- read.table("instr_limits.txt", header=T)

# create output file
str1 <- c("Summary of Step Violations Check. Run at", date(), "\n")
cat(str1, file="step_check_output/summary_step.txt")
cat("Parameter\tMaxStep\t# Inputs\t# NA\t# Violations\n",
    file="step_check_output/summary_step.txt", append=TRUE)

# loop through the parameters in main data frame
for (i in 3:length(names(some.df)))
```

Figure A.11: instr_step.R, page 1

```

{
param <- names(some.df)[i]; # identify param by column name
max <- d[d$parameter == param,"stephr"]
# identify max step value using param and max column
# if the parameter is not in limits file then skip to next parameter
if ('TRUE' %in% (d$parameter == param))
{
str2 <- c("starting",param,"..... "); message(str2); # print status to screen
# create output vector (not a data frame) for the desired param and fill w/ NA
# that comma before "param" makes it a vector, not a data frame
var_step <- numeric(length(some.df[,param]))
var_step[1:length(some.df[,param])] <- NA
# create a diff vector (not a data frame) for desired param and fill with NA
var_diff <- numeric(length(some.df[,param]))
var_diff[1:length(some.df[,param])] <- NA
# loop through each value of parameter
for (j in 2:length(some.df[,param]))
{
# if current value or previous value is NA then skip to next value of param
if ((is.na(some.df[,param][j]))|(is.na(some.df[,param][j-1]))) next else
{
var_step[j] <- 1 ; # if there is input data, assign the value of 1
# calculate the diff between current and previous value. goes into var_diff
var_diff[j] <- some.df[,param][j] - some.df[,param][j-1]
# now assign the value of 0 only if the diff is within step limit
if (abs(var_diff[j]) < max) var_step[j] <- 0
}
}
# compile the four useful vectors into a data frame
step_output <- data.frame(some.df$DateTime,some.df[,param],var_diff,var_step)
# rename the variables in the data frame
colnames(step_output) <- c("DTact","orig","step","error")
# export the data frame to a csv file in the step_check folder
write.table(step_output,file=paste("step_check_output/step",param,".csv",sep=""),
,sep=";",row.names=FALSE)
# create the output summary file.
str3 <- c(param,"\t\t",max,"\t",length(var_step),"\t\t",sum(is.na(var_step)),
\t",sum(var_step,na.rm=TRUE),"\n")
cat(str3,file="step_check_output/summary_step.txt",append=TRUE)
str4 <- c("done\n"); message(str4); # print status to screen
}
else next
}
file.show("step_check_output/summary_step.txt")

```

Figure A.12: instr_step.R, page 2

```
#####
## instr_maxmin.R
##
## November 1 2012, Sabrina Sequeira
## November 9 2012: edited to include two input files
## January 23 2013: edited for hourly data
##
## Calculates max and min measured values
## Input: data03.csv or data05.csv
## Input: data03e.csv or nothing
## Input: instr_names.txt (listing of sensor descriptions and units)
## Output: maxmin_output/maxmin.csv
## Supercedes: instr_maxmin_old.R
##
## This script loops through all parameters in data04 and data04e.
## For each parameters, the daily max and min are calculated.
## inner loop (i) is parameter. outer loop (j) is date.
##
## Assumptions:
## data in 10-minute increments (or hourly)
## data is chronological
## no time step is missing
## missing sensor data (NA) is OK though
## data03 and data03e input must be consecutive (10 minutes apart)
##
## To change between 10-minute & hourly:
##   search/replace: data03 is 10-minute & data05 is hourly
##   search/replace. DTstandard is for 10-minute & DateTime is hourly
##   start parameter loop at 7 for 10-minute and 3 for hourly
##   change counter from 143 (10-minute) to 23 (hourly)
##   search the word CHANGE and comment out line as needed
##
## Improvements: Can make much faster using factors like in
##               ana_calcs.R and ana_stats.R
#####

# set working directory
setwd("F:/sabs uni files/project/test cell data/scripts")

# load in the data into a data frame named some.df
first.df <- read.csv("data05.csv",sep=",",header=T)

# add a 2nd data file
second.df <- read.csv("data05e.csv",sep=",",header=T)
# append 2nd data file if in time sequence
end <- as.POSIXct(tail(first.df$DateTime,n=1))
start <- as.POSIXct(head(second.df$DateTime,n=1))
if ((as.character(start-end))==10) some.df <- rbind(first.df,second.df)

# CHANGE comment out the following line if using 10minute data
some.df <- first.df

param_count <- length(names(some.df)); #count the number of columns

# create output data frame and print starting status message
datefirst <- as.Date(strftime(head(some.df$DateTime, n=1),format="%Y/%m/%d"))
datelast <- as.Date(strftime(tail(some.df$DateTime, n=1),format="%Y/%m/%d"))
seqdays <- seq(datefirst,datelast,by="1 day"); numdays<- length(seqdays)
maxmin.df <- data.frame(seqdays)
```

Figure A.13: instr_maxmin.R, page 1

```

# print status message to screen
str01 <- c("Will analyze from",as.character(datefirst)," to ",as.character(datelast))
message(str01)

stepfirst <- 1
day_tally <- 1
count_steps <- NA; count_NA <- NA
# steplast <- 216 ; # uncomment for testing.
# j <- 72 ;# uncomment for testing
# param <- "RH10"; # uncomment for testing
param_max <- NA; param_min <- NA

# loop through all dates
for (j in 2:length(some.df[,1]))
{
  id_day <- as.Date(strftime(some.df$DateTime[j],format="%Y/%m/%d"))
  id_yest <- as.Date(strftime(some.df$DateTime[j-1],format="%Y/%m/%d"))
  # only go forward if the date has changed
  if (id_day!=id_yest)
  {
    str02 <- c("Starting ",as.character(id_day)); message(str02)
    steplast <- j-1
    # count how many time steps since last swapped days
    count_steps <- steplast - stepfirst; count_steps
    # only go forward if 23 steps in day.
    if (count_steps==23)
    {
      # loop through all parameters
      for (i in 3:param_count)
      {
        # identify param name by column name from main data frame
        param <- names(some.df)[i]
        # count how many times parameter was NA since last day
        count_NA <- tail(cumsum(is.na(some.df[stepfirst:steplast,param])),n=1)
        # only go forward if all data for that parameter was good
        if (count_NA==0)
        {
          param_max <- tail(cummax(some.df[stepfirst:steplast,param]),n=1)
          param_min <- tail(cummin(some.df[stepfirst:steplast,param]),n=1)
        }
        # write max and min to output data frame
        maxname <- paste(param,"max",sep=""); minname <- paste(param,"min",sep="")
        maxmin.df[day_tally,maxname] <- param_max
        maxmin.df[day_tally,minname] <- param_min
        # comment next line when testing
        param_max <- NA; param_min <- NA
        # uncomment next line when testing
        # str16 <- c(id_day,"\t",param_max,"\t",param_min); message(str16)
      }
    }
  }
  # reset counters at the start of a new day
  day_tally <- day_tally + 1; stepfirst <- j
  # comment next line when testing
  count_steps <- NA; count_NA <- NA
}
# end loop through dates
}
# write entire new data frame to output file
write.table(maxmin.df,file=paste("maxmin_output/maxmin.csv"),sep=",",row.names=FALSE)

```

Figure A.14: instr_maxmin.R, page 2

```
#####
##
## instr_graph.R
##
## October 31 2012, Sabrina Sequeira
## November 9 2012: editted to include two input files
## November 23 2012: added weekly TC graphs at bottom
## January 08 2013: set system time to GMT-10 to ignore DST
## January 23 2013: made changes for hourly data
##
## Graphical checks of data
## Inputs: data03.csv
##         data03e.csv
##         maxmin.csv (output of instr_maxmin.R)
##         instr_names.txt (listing of sensor descriptions and units)
##         instr_lims.txt (listing of scales for sensors)
## Output: graphs to graph_output folder
##
## Desc: i is outer loop (sensors)
##       j is inner loop (for monthly graphs)
##       k is inner loop (for weekly graphs)
##
## Note: comments in 4 plot areas to go btw pre-defined and auto scales
##       weekly graph only done if data is there
##       (otherwise auto-scale crashes. for pre-defined scales it works tho.)
##       montly graph 12 has Jan2011 not Jan2012 in graph title. Don't know why.
##       Adding time zone (thus avoiding DST) has fixed wonky scales
##
## must have chron library installed (use Packages menu in gui)
##
## To change between 10-minute & hourly:
##   search/replace: data03 is 10-minute & data05 is hourly
##   search/replace. DTstandard is for 10-minute & DateTime is hourly
##   search the word CHANGE and comment out line as needed
##   start parameter loop at 7 for 10-minute and 3 for hourly
##
#####

# set working directory
setwd("F:/sabs uni files/project/test cell data/scripts")

# Must install package chron and then load into library. Only once.
library(chron)
# Change time zone to GMT-10 to ignore daylight savings.
# All calcs done in current time zone.
Sys.setenv(tz='Etc/GMT-10')

# load in the data into a data frame named some.df
first.df <- read.csv("data05.csv",sep=",",header=T)

# add a 2nd data file
second.df <- read.csv("data05e.csv",sep=",",header=T)
# append 2nd data file if in time sequence
end <- as.POSIXct(tail(first.df$DateTime,n=1))
start <- as.POSIXct(head(second.df$DateTime,n=1))
if ((as.character(start-end))==10) some.df <- rbind(first.df,second.df)

# CHANGE comment out the following line if using 10minute data
some.df <- first.df

param_count <- length(names(some.df)); #count the number of columns
```

Figure A.15: instr_graph.R, page 1

```

# load in the max and min data
maxmin.df <- read.csv("maxmin_output/maxmin.csv",sep=",",header=T)
# convert seqdays to date parameter
maxmin.df$dates <- as.Date(maxmin.df$seqdays)

# load in the sensor file names. needed only for the graph titles
names.df <- read.table("instr_names.txt",sep=",",header=T)

# load in the sensor scales. needed only for the graph scales
scales.df <- read.table("instr_scales.txt",sep=",",header=T)

# Change the DateTime to character format then date & time format
some.df$DTconvert <- strptime(as.character(some.df$DateTime), "%Y/%m/%d %H:%M")
some.df$dnt <- as.POSIXct(some.df$DTconvert)

# find first day of first month of data (scales, monthly/weekly graphs)
mon1 <- as.character(months(as.POSIXct(head(some.df$DateTime,n=1)), abbreviate=TRUE))
yr1 <- as.character(years(as.POSIXct(head(some.df$DateTime,n=1))))
yrmon1 <- paste(yr1,mon1,"1",sep=""); yrmonfirst <- strptime(yrmon1, "%Y%b%d")
datefirst <- as.POSIXct(as.character(as.Date(head(some.df$DateTime,n=1))))

# yrmonlast is first day of first month with no data (scales, monthly/weekly graphs)
mon2 <- as.character(months(as.POSIXct(tail(some.df$DateTime,n=1)), abbreviate=TRUE))
yr2 <- as.character(years(as.POSIXct(tail(some.df$DateTime,n=1))))
yrmon2 <- paste(yr2,mon2,"1",sep=""); yrmon3 <- strptime(yrmon2, "%Y%b%d")
yrmonlast <- tail(seq(yrmon3, by = "months", len = 2),n=1)
datelast <- as.POSIXct(as.character(as.Date(tail(some.df$DateTime,n=1))+1))

#####

# to test one parameter only: i <- 50
# loop through all parameters
for (i in 3:param_count)
{

param <- names(some.df)[i];# identify param by column name from main data frame
desc <- names.df[names.df$sensor == param,"description"]; # identify sensor description
uni <- names.df[names.df$sensor == param,"unit"]; # identify sensor units
str3 <- paste(param," [",uni,"]",sep=""); # create y-axis string
maxname <- paste(param,"max",sep=""); minname <- paste(param,"min",sep="")
miny <- scales.df[scales.df$sensor == param,"ymingraph"]; # find predefined min y scale
maxy <- scales.df[scales.df$sensor == param,"ymaxgraph"]; # find predefined max y scale

str02 <- c("Starting ",param); message(str02)

# alldata graph
str1 <- paste("graph_check_output/all/",param,"_all.png",sep=""); # output filename
str2 <- paste(param,": ",desc,sep=""); # create string for plot graph title
png(str1,width=8,height=4,units="in",res=500)
# windows(str1,width=8,height=4)
# toggle between two following lines for auto-scaling
plot(some.df$dnt,some.df[,param],type="p",xlab="",ylab="",pch=".",ylim=c(miny,maxy))
# plot(some.df$dnt,some.df[,param],type="p",xlab="",ylab="",pch=".")
# figure out how to remove the 2012 from x-axis
axis.POSIXct(1,Day,at=seq(as.POSIXct(yrmonfirst), as.POSIXct(tail(some.df$DateTime,
n=1)),by="months"),format="%b")
abline(v=seq(as.POSIXct(yrmonfirst),as.POSIXct(tail(some.df$DateTime,n=1)),
by="months"), lty = FALSE, col="gray")
title(main=str2,xlab="Date",ylab=str3)
grid(col = "lightgray", lty = "dotted",lwd = par("lwd"))

```

Figure A.16: instr_graph.R, page 2

```

dev.off()

# monthly graph. note that this scrolls through months
yrmonstart <- yrmonfirst
for (j in 2:length(seq(yrmonfirst, yrmonlast, by = "months")))
{
  graphnum <- formatC(j-1,width=2,format = "d",flag = "0"); # seq graph for file name
  yrmonend <- seq(yrmonfirst, yrmonlast, by = "months")[j]; # end of data get graphed
  # create output filename
  str1 <- paste("graph_check_output/monthly/",param,"_monthly",graphnum,".png",sep="")
  # create string for plot graph title
  str2 <- paste(param,": ",desc,". ",months(yrmonstart)," ",years(yrmonstart),sep="")
  if (sum(!is.na(some.df[ ((some.df$dnt>yrmonstart)&(some.df$dnt<yrmonend)),param])))
  {
    png(str1,width=8,height=4,units="in",res=500)
    # windows(str1,width=8,height=4)
    # toggle between two following lines for auto-scaling
    plot(some.df$dnt[ (some.df$dnt>yrmonstart)&(some.df$dnt<yrmonend)],
         some.df[ ((some.df$dnt>yrmonstart)&(some.df$dnt<yrmonend)),param],
         type="l",xlab="",ylab="",pch=".",ylim=c(miny,maxy))
    # plot(some.df$dnt[ (some.df$dnt>yrmonstart)&(some.df$dnt<yrmonend)],
    #      some.df[ ((some.df$dnt>yrmonstart)&(some.df$dnt<yrmonend)),param],
    #      type="l",xlab="",ylab="",pch=".")
    # next 2 lines are being ignored. figure out one day.
    axis.Date(1,at=seq(as.Date(yrmonstart)+1, as.Date(yrmonend),by="weeks"),format="%d")
    xtickplaces <- seq(as.Date(yrmonstart)+1, as.Date(yrmonend),by="weeks")
    axis(side=1, at=xtickplaces)
    title(main=str2,xlab="Date",ylab=str3)
    grid(col = "lightgray", lty = "dotted",lwd = par("lwd"))
    dev.off()
  }
  yrmonstart <- yrmonend
}

# weekly graph. note that this scrolls through weeks
datestart <- datefirst
for (k in 2:length(seq(datefirst, datelast, by = "weeks")))
{
  graphnumw <- formatC(k-1,width=3,format = "d",flag = "0"); # seq of graph file name
  dateend <- seq(datefirst, datelast, by = "weeks")[k]; # end of data to get graphed
  # create output filename
  str1 <- paste("graph_check_output/weekly/",param,"_weekly",graphnumw,".png",sep="")
  # create string for plot graph title
  str2 <- paste(param,": ",desc,". ",months(datestart)," ",years(datestart),sep="")
  # only make the plot if there is data in there
  if (sum(!is.na(some.df[ ((some.df$dnt>datestart)&(some.df$dnt<dateend)),param])))
  {
    png(str1,width=8,height=4,units="in",res=500)
    # windows(str1,width=8,height=4)
    # toggle between two following lines for auto-scaling
    plot(some.df$dnt[ (some.df$dnt>datestart)&(some.df$dnt<dateend)],
         some.df[ ((some.df$dnt>datestart)&(some.df$dnt<dateend)),param],
         type="l",xlab="",ylab="",pch=".",ylim=c(miny,maxy))
    # plot(some.df$dnt[ (some.df$dnt>datestart)&(some.df$dnt<dateend)],
    #      some.df[ ((some.df$dnt>datestart)&(some.df$dnt<dateend)),param],type="l",
    #      xlab="",ylab="",pch=".")
    axis.POSIXct(1,at=seq(datestart,dateend,by="days"),format="%b %d")
    abline(v=seq(datestart,dateend,by="days"), lty = FALSE, col="gray")
    title(main=str2,xlab="Date",ylab=str3)
    grid(col = "lightgray", lty = "dotted",lwd = par("lwd"))
    dev.off()
  }
}

```

Figure A.17: instr_graph.R, page 3


```

    }
    datestart <- dateend
  }

# maxmin graph
# maxmin graph must be last cos it redefines the miny and maxy values
# maxmin graph always must set ylim otherwise axis is based on 1st data series only
# create output filename
str1 <- paste("graph_check_output/maxmin/",param,"_maxmin.png",sep="")
# create string for plot graph title
str2 <- paste(param,": ",desc,". Daily max and min.",sep="")
png(str1,width=8,height=4,units="in",res=500)
# windows(str1,width=8,height=4)
# comment out next line to go back to pre-defined scales
miny <- min(maxmin.df[,minname],na.rm=TRUE)
maxy <- max(maxmin.df[,maxname],na.rm=TRUE)
plot(maxmin.df$dates,maxmin.df[,minname],type="p",xlab="",ylab="",pch=5,col="blue",
     ylim=c(miny,maxy))
points(maxmin.df$dates,maxmin.df[,maxname],type="p",xlab="",ylab="",pch=1,col="red")
# figure out how to remove the 2012 from x-axis
axis.Date(1,Day,at=seq(as.Date(yrmonfirst), as.Date(tail(maxmin.df$dates,n=1)),
    by="months"),format="%b")
title(main=str2,xlab="Month",ylab=str3)
grid(col="lightgray", lty="dotted",lwd=par("lwd"))
dev.off()

# close the parameter loop
}

#####

# TC weekly graphs. note that this scrolls through weeks
# must load in the data from the top section first
datestart <- datefirst
for (k in 2:length(seq(datefirst, datelast, by="weeks")))
{
  graphnumw <- formatC(k-1,width=3,format="d",flag="0"); # seq of graph file name
  dateend <- seq(datefirst, datelast, by="weeks")[k]; # end of data to get graphed
  # create output filename
  str1 <- paste("graph_check_output/weekly/","TC1_",graphnumw,".png",sep="")
  # create graph title
  str2 <- paste("TC Batch 1. ",months(datestart)," ",years(datestart),sep="")
  # create output filename
  str3 <- paste("graph_check_output/weekly/","TC2_",graphnumw,".png",sep="")
  # create graph title
  str4 <- paste("TC Batch 2. ",months(datestart)," ",years(datestart),sep="")
  str5 <- paste("Temperature [°C]")
  # only make plot 1 if there is data in there
  if (sum(!is.na(some.df$TS30[(some.df$dnt>datestart)&(some.df$dnt<dateend)])))
  {
    png(str1,width=10,height=6,units="in",res=500)
    # windows(str1,width=10,height=6)
    layout(rbind(1,2), heights=c(7,1))
    par(mar=c(1,5,2,1))
    miny<-min(some.df$TS33[(some.df$dnt>datestart)&(some.df$dnt<dateend)]),na.rm=TRUE)-2
    maxy <- max(some.df$TS33[(some.df$dnt>datestart)&(some.df$dnt<dateend)]),na.rm=TRUE)
    plot(some.df$dnt[(some.df$dnt>datestart)&(some.df$dnt<dateend)],
        some.df$TS30[(some.df$dnt>datestart)&(some.df$dnt<dateend)]),
        type="l",xlab="",ylab="",ylim=c(miny,maxy),col="hotpink")
    lines(some.df$dnt[(some.df$dnt>datestart)&(some.df$dnt<dateend)],

```

Figure A.18: instr_graph.R, page 4

```

    some.df$TS31[ ((some.df$dnt>datestart)&(some.df$dnt<dateend)) ],
    ,xlab="", ylab="", col="skyblue")
lines(some.df$dnt[ (some.df$dnt>datestart)&(some.df$dnt<dateend) ],
    some.df$TS32[ ((some.df$dnt>datestart)&(some.df$dnt<dateend)) ],
    ,xlab="", ylab="", col="orange")
lines(some.df$dnt[ (some.df$dnt>datestart)&(some.df$dnt<dateend) ],
    some.df$TS33[ ((some.df$dnt>datestart)&(some.df$dnt<dateend)) ],
    ,xlab="", ylab="", col="blue")
lines(some.df$dnt[ (some.df$dnt>datestart)&(some.df$dnt<dateend) ],
    some.df$TS39[ ((some.df$dnt>datestart)&(some.df$dnt<dateend)) ],
    ,xlab="", ylab="", col="red")
lines(some.df$dnt[ (some.df$dnt>datestart)&(some.df$dnt<dateend) ],
    some.df$TS40[ ((some.df$dnt>datestart)&(some.df$dnt<dateend)) ],
    ,xlab="", ylab="", col="green")
leg.txt <- c("TS30-E-brick ", "TS31-S-brick", "TS32-W-brick", "TS33-N-brick",
    TS39-pier, "TS40-E-embed-brick")
leg.col <- c("hotpink", "skyblue", "orange", "blue", "red", "green")
legend("bottomleft", legend=leg.txt, ncol=3, bty="n", text.col=leg.col)
axis.POSIXct(1, at=seq(datestart, dateend, by="days"), format="%b %d")
abline(v=seq(datestart, dateend, by="days"), lty = FALSE, col="gray")
title(main=str2, xlab="Date", ylab=str5)
grid(col = "lightgray", lty = "dotted", lwd = par("lwd"))
dev.off()
}
# only make plot 2 if there is data in there
if (sum(!is.na(some.df$TS34[ ((some.df$dnt>datestart)&(some.df$dnt<dateend)) ])))
{
png(str3, width=10, height=6, units="in", res=500)
# windows(str3, width=10, height=6)
layout(rbind(1,2), heights=c(7,1))
par(mar=c(1,5,2,1))
plot(some.df$dnt[ (some.df$dnt>datestart)&(some.df$dnt<dateend) ],
    some.df$TS34[ ((some.df$dnt>datestart)&(some.df$dnt<dateend)) ],
    type="l", xlab="", ylab="", ylim=c(miny, maxy), col="green")
lines(some.df$dnt[ (some.df$dnt>datestart)&(some.df$dnt<dateend) ],
    some.df$TS35[ ((some.df$dnt>datestart)&(some.df$dnt<dateend)) ],
    ,xlab="", ylab="", col="red")
lines(some.df$dnt[ (some.df$dnt>datestart)&(some.df$dnt<dateend) ],
    some.df$TS36[ ((some.df$dnt>datestart)&(some.df$dnt<dateend)) ],
    ,xlab="", ylab="", col="skyblue")
lines(some.df$dnt[ (some.df$dnt>datestart)&(some.df$dnt<dateend) ],
    some.df$TS37[ ((some.df$dnt>datestart)&(some.df$dnt<dateend)) ],
    ,xlab="", ylab="", col="orange")
lines(some.df$dnt[ (some.df$dnt>datestart)&(some.df$dnt<dateend) ],
    some.df$TS38[ ((some.df$dnt>datestart)&(some.df$dnt<dateend)) ],
    ,xlab="", ylab="", col="hotpink")
leg.txt <- c("TS34-E-underfloor", "TS35-E-ground", "TS36-C-underfloor",
    "TS37-C-ground", "TS38-C-topfloor")
leg.col <- c("green", "red", "skyblue", "orange", "hotpink")
legend("bottomleft", legend=leg.txt, ncol=3, bty="n", text.col=leg.col)
axis.POSIXct(1, at=seq(datestart, dateend, by="days"), format="%b %d")
abline(v=seq(datestart, dateend, by="days"), lty = FALSE, col="gray")
title(main=str4, xlab="Date", ylab=str5)
grid(col = "lightgray", lty = "dotted", lwd = par("lwd"))
dev.off()
}
datestart <- dateend
}

#####

```

Figure A.19: instr_graph.R, page 5

```
#####
##
## instr_ave.R
##
## January 16 2012, Sabrina Sequeira
##
## Calculates average hourly values
##
## Input: data04.csv
## Input: data04e.csv
## Output: hourly.csv
##
## This script loops through all parameters in data04 and data04e
## and creates the hourly average values. Takes about 4 hours
##
## Note: Must still clean up hourly.csv output for AD10 and AS10.
##
## Assumptions:
## 40,50,0,10,20,30 minutes make the hourly average (Mark thesis p156)
## input data is chronological in 10-min increments
## no time step is missing
## missing sensor data (NA) is OK though
## data04 and data04e input must be consecutive (10 minutes apart)
## Note column is retained
## special average NOT DONE for outdoor wind speed and direction
## DTstandard in input files must have format: yyyy/mm/dd hh:mm
## Neglects daylight savings. So no two outputs for April 03 2011 2:00 or
## April 01 2012. Also doesn't skip Also Oct 2nd, 2011 2am.
##
#####

# set working directory
setwd("F:/sabs uni files/project/test cell data/scripts")

# Must install package chron and then load into library. Only once.
library(chron)
# Change tz to GMT-10 to ignore daylight savings. Calcs done in current time zone.
Sys.setenv(tz='Etc/GMT-10')

# load in the data into a data frame named some.df
first.df <- read.csv("data04.csv",sep=" ",header=T)
# add a 2nd data file
second.df <- read.csv("data04e.csv",sep=" ",header=T)
# append 2nd data file if in time sequence
end <- as.POSIXct(tail(first.df$DTstandard,n=1))
start <- as.POSIXct(head(second.df$DTstandard,n=1))
if ((as.character(start-end))==10) some.df <- rbind(first.df,second.df)

param_count <- length(names(some.df)); #count the number of columns
```

Figure A.20: instr_ave.R, page 1

```

# create output data frame with hours and empty note column
datefirst <- as.POSIXct(strftime(head(some.df$DTstandard, n=1),format="%Y/%m/%d"))
datelast <- as.POSIXct(strftime(tail(some.df$DTstandard, n=1),format="%Y/%m/%d"))
DateTime <- seq(datefirst,datelast,by="1 hour"); numhours<- length(DateTime)
hourly.df <- data.frame(DateTime); hourly.df$Note <- NA

# Change the DTstandard to character format then date & time format
some.df$DTconvert <- strptime(as.character(some.df$DTstandard), "%Y/%m/%d %H:%M")
some.df$dnt <- as.POSIXct(some.df$DTconvert)

# loop through all hours
# j<- 16
for (j in 1:numhours)
{

# find the row number when hours match
current <- match(hourly.df$DateTime[j],some.df$dnt,
  nomatch=NA_integer_,incomparables=NULL)
# only proceed if hour is in original data
if (!is.na(current))
{
# define row id for input data as :40,:50,:00,:10,:20,:30
seq.average <- seq.int(current-2,current+3,1)
# create a vector of all the notes
notevector<-some.df$Note[seq.average]
# combine and sort all the notes within the hour
notesort <- sort(as.numeric(unlist(strsplit(as.character(notevector),split="-"))))
# keep only the unique ones and format to 3-digit character
noteunique <- formatC(unique(notesort,incomparables=FALSE),width=3,flag = "0")
# put back into original format
hourly.df$Note[j]<-paste(noteunique,collapse="-")
# start parameter loop
# i <- 15
for (i in 7:param_count)
{
param <- names(some.df)[i]
# remove from hourly calc: HF heaters,DTconvert,dnt,AS10,AD10
# define how many decimal spaces to keep! here default is 3
hourly.df[j,param]<-round(mean(some.df[seq.average,param],na.rm=TRUE),digits=3)
# end parameter loop here
}
# close if statement
}

# close hours loop
}

# write entire new data frame to output file
write.table(hourly.df,file=paste("hourly.csv"),sep=",",row.names=FALSE)

```

Figure A.21: instr_ave.R, page 2

```
#####
##
## ana_calcs.R
##
## December 20 2012, Sabrina Sequeira
## January 8 2013, updated
##
## Analyzes the measured data, merges in weather data
## Performs many calculations
##
## Input: data05.csv (best hourly data)
## bom.csv (supplemental data purchased from BOM)
## radiation.csv (diffuse irradiance, direct irradiance, solar altitude)
## Output: data06.csv (hourly dataset with calculated params)
##
## Assumptions:
## must have chron library installed (use Packages menu in gui)
## Checked first half thoroughly Feb 19 2013
##
## Needed:
##
## check value of TC calibrations
## Search on "Need"
## Search on "ANZASCA" as needed to process 2007 data
## Search on "Option" to see what calc options are available
##
#####
# set working directory
setwd("F:/sabs uni files/project/test cell data/scripts")

# load in the test cell data into a data frame named input.df
input.df <- read.csv("data05.csv", sep=",", header=T)
# load the BOM data into a data frame
bom.df <- read.csv("bom.csv", sep=",", header=T)
# load the other weather data into a data frame
radiation.df <- read.csv("radiation.csv", sep=",", header=T)
output.df <- cbind(input.df, bom.df, radiation.df)

# the following 2 lines are for ANZASCA (year 2007) data only
```

Figure A.22: ana_calcs.R, page 1

```

# input.df <- read.csv("data_anzinp.csv", sep=",", header=T)
# output.df <- input.df

# Must install package chron and then load into library. Only once.
library(chron)

# Change time zone to GMT-10 to ignore daylight savings. All calcs done in current time zone.
Sys.setenv(tz='Etc/GMT-10')

output.df$DTconvert <- strptime(as.character(input.df$DateTime), "%Y/%m/%d %H:%M")
output.df$dnt <- as.POSIXct(output.df$DTconvert)

# Load in thermo tables and make interpolation functions
table_pg.df <- read.table("table_pg.txt", sep=",", header=T); # Cengel & Boles 5th, Appendix A-4, tsat
table_psat <- approxfun(table_pg.df$Tsats, table_pg.df$Psats)
table_tsat <- approxfun(table_pg.df$Psats, table_pg.df$Tsats)
table_h.df <- read.table("table_h.txt", sep=",", header=T); # Cengel & Boles 5th, Appendix A-4
table_hg <- approxfun(table_h.df$Tsats, table_h.df$hg)
table_hf <- approxfun(table_h.df$Tsats, table_h.df$hf)

# Define constants
# Temp calibration from 09/20/2012 report. 23.9°C values.
TS30cal <- -2.4; TS31cal <- -2.7; TS32cal <- -8.2; # all from 2012-09 calibration [C]
TS33cal <- -2.4; TS36cal <- -2.8; TS37cal <- -2.6; # all from 2012-09 calibration [C]
ventscales <- 2.3; ventadd <- 3.3; # from ANZASCA 2009 paper [ACH/mps] and [ACH]
Rair <- 0.287; Rv <- 0.4615; Ratio <- Rair/Rv; # gas consts and ratio for air, water [kPa m3/kgK]
ptot <- 101.325; # total sea-level pressure, assumed constant
# subfloor cavity volume [m3], ground area [m2], under-floor area [m2], uncovered ground area [m2]
volssf <- 20.04; areasf <- 33.4084; areauf <- 30.03; areasfuncov <- 0.8*areasf
areawl <- 11.93; # total area of subfloor walls [m2]
tempadd <- 273.15; # adder to go from C to K
hconv_g <- 1.5; # convective heat transfer coefficient from ground to air [W/m2K]. Need to validate this!
sbconst <- 0.0000000567; # stefan-boltzmann constant [W/m2K4]
emis <- 0.9; #emissivity of surfaces
vf_gf <- 0.9; vf_gw <- 0.1; # view factor from ground to floor and walls

# Calibrate thermocouples
output.df$TS30cor <- input.df$TS30 + TS30cal
output.df$TS31cor <- input.df$TS31 + TS31cal
output.df$TS32cor <- input.df$TS32 + TS32cal
output.df$TS33cor <- input.df$TS33 + TS33cal

```

Figure A.23: ana_calcs.R, page 2

```

output.df$TS36cor <- input.df$TS36 + TS36cal
output.df$TS37cor <- input.df$TS37 + TS37cal

# Choose between options
# Option. Use either TA35 (IC) or TA36 (PT100) as subfloor air temp. Default TA35.
output.df$tempsf <- input.df$TA36; # air temp for subfloor [C]
# Option. Use either TS37, TS37cor, TG30 as subfloor ground surface temp. Default TS37.
output.df$tempsg <- output.df$TG30; # ground surface temp for subfloor [C]
# Option. Sea-level pressure from either constant ptot or BOM Pmsl. Default is BOM Pmsl.
output.df$psl <- output.df$Pmsl
# output.df$psl <- ptot

# Weather calcs
output.df$windmet <- 1.36*input.df$AS10 ; # windspeed at 10m [m/s]. (Note used 1.2036 in ANZAScA 2009)
output.df$cloud <- 4; # define Cloud cover as 4 on scale of 0 to 8
# Pressure at 15m (decreases 1.19 kPa per 100m, Cenglel & Boles 5th, Appendix A-16)
output.df$ptc <- output.df$psl - 1.19*15/100

# General calcs
output.df$ventach <- ventscal*input.df$AS10 + ventadd ; # subfloor ventilation [air changes/hour]
output.df$ventvsf <- 1.2*input.df$TB31 - 0.2*output.df$tempsf ; # Environmental temp of subfloor, Muncey method [C]
output.df$tairm <- (input.df$TA37+input.df$TA38+input.df$TA39)/3 ; # dry bulb air temp of room [C]
output.df$tenvrm <- 1.2*input.df$TB32 - 0.2*output.df$tairm ; # Environmental temp of room, Muncey method [C]

# Subfloor air calcs
output.df$psatsf <- table_psat(output.df$tempsf) ; # saturation vapor pressure [kPa]
output.df$pvsvf <- (input.df$RH32)*(output.df$psatsf)/100 ; # vapor pressure [kPa]
# Option next two lines. Choose between approx or table for water enthalpy hgsvf
# output.df$hgsvf <- 2500.9+ 1.82*output.df$tempsf ; # enthalpy of water vapor [kJ/kg]
output.df$gsvf <- table_hg(output.df$tempsf) ; # enthalpy of water vapor [kJ/kg]
output.df$psat_g <- table_psat(output.df$tempsg) ; # saturation vapor pressure at ground temp [kPa]
output.df$pv_df <- output.df$psat_g - output.df$pvsvf ; # diff in vapor pres. btw ground & subfloor [kPa]
output.df$dqpsf <- table_tsat(output.df$pvsvf) ; # subfloor air dew point [C]
output.df$tdp_df <- output.df$tempsg-output.df$tdpsf ; # diff in temp btw ground & dew point [C]
output.df$hg_g <- table_hg(output.df$tempsg) ; # enthalpy of water vapor at ground temp [kJ/kg]
output.df$hf_g <- table_hf(output.df$tempsg) ; # enthalpy of liquid water at ground temp [kJ/kg]
output.df$tdf <- output.df$tempsf - output.df$tempsg ; # diff in temp btw subfloor air and ground [C]
output.df$wsf <- Ratio*output.df$pvsvf/(output.df$ptc-output.df$pvsvf) ; # spec humidity [kg water / kg dry air]
output.df$hasf <- 1.005*output.df$tempsf ; # spec enthalpy of subfloor dry air [kJ/kg dry air]
output.df$hsvf <- output.df$wsf*output.df$hgsvf ; # spec enthalpy of subfloor water vapor [kJ/kg dry air]

```

Figure A.24: ana_calcs.R, page 3

```

output.df$hsf <- output.df$hasf + output.df$hvsvf ; # spec enthalpy of subfloor air [kJ/kg dry air]
output.df$masf <- (output.df$ptc-output.df$psvf)*volrf/(Rair*(output.df$tempsf+tempadd)) ; # mass of dry air in subfloor[kg]
output.df$dendasf <- output.df$masf/volsf ; # density of dry air in subfloor [kg dry air /m3]
output.df$mvsvf <- (output.df$psvf)*volrf/(Rv*(output.df$tempsf+tempadd)) ; # mass of vapor in subfloor [kg]
output.df$Hsaf <- output.df$hasf*output.df$masf ; # total enthalpy of dry air [kJ]
output.df$Hsvf <- output.df$hvsvf*output.df$masf ; # total enthalpy of vapor [kJ]
output.df$Hsf <- output.df$Hsaf + output.df$Hsvf ; # total enthalpy of subfloor air [kJ]
output.df$Qgovent <- output.df$mvsvf*output.df$ventach ; # mass flowrate of water exiting vent [kg/hour]
output.df$Qovent <- output.df$Hsf*output.df$ventach ; # rate of enthalpy exiting vent [kJ/hour]
output.df$masfdiff[1] <- 0 ; # initial derivative of subfloor dry air mass is 0 [kg/hr]
output.df$masfdiff[2:length(output.df$masfdiff)] <- diff(output.df$masf) ; # subfloor vapor mass deriv [kg/hr]
output.df$mvsvfdiff[1] <- 0 ; # initial derivative of subfloor vapor mass is 0 [kg/hr]
output.df$mvsvfdiff[2:length(output.df$mvsvfdiff)] <- diff(output.df$mvsvf) ; # subfloor vapor mass deriv [kg/hr]
output.df$Hsfdiff[1] <- 0 ; # initial derivative of subfloor total enthalpy is 0 [kJ]
output.df$Hsfdiff[2:length(output.df$Hsfdiff)] <- (diff(output.df$Hsf))/3.6 ; # subfloor total enthalpy deriv [W]

# Outdoor air calcs
output.df$psatos <- table_psat(input.df$TA10) ; # saturation vapor pressure [kPa]
output.df$psvos <- (input.df$RH10)*(output.df$psatos)/100 ; # vapor pressure [kPa]
output.df$hg <- table_hg(input.df$TA10) ; # enthalpy of water vapor [kJ/kg]
output.df$swos <- Ratio*output.df$psvos/(output.df$ptc-output.df$psvos) ; # spec humidity [kg water / kg dry air]
output.df$shaos <- 1.005*input.df$TA10 ; # spec enthalpy of outdoor dry air [kJ/kg dry air]
output.df$shvos <- output.df$swos*output.df$hg ; # spec enthalpy of outdoor water vapor [kJ/kg dry air]
output.df$shos <- output.df$shaos + output.df$shvos ; # spec enthalpy of outdoor air [kJ/kg dry air]
output.df$maos <- (output.df$ptc-output.df$psvos)*volrf/(Rair*(output.df$TA10+tempadd)) ; # mass of dry air [kg/subfloor size]
output.df$dendaos <- output.df$maos/volsf ; # density of dry air [kg dry air /m3]
output.df$mvsvos <- (output.df$psvos)*volrf/(Rv*(output.df$TA10+tempadd)) ; # mass of vapor in outside air [kg]
output.df$shaos <- output.df$haos*output.df$maos ; # total enthalpy of dry air [kJ/ subfloor size]
output.df$shvos <- output.df$shvos*output.df$maos ; # total enthalpy of vapor [kJ/ subfloor size]
output.df$shos <- output.df$shos + output.df$shvos ; # total enthalpy of air [kJ/subfloor size]
output.df$Qgivent <- output.df$mvsvos*output.df$ventach ; # mass flowrate of water entering vent [kg/hour]
output.df$Qivent <- output.df$shos*output.df$ventach ; # rate of enthalpy entering vent [kJ/hour]

# Net calcs: moisture and energy flows
output.df$ventcalch <- (output.df$masfdiff/volsf)/(output.df$dendaos-output.df$dendasf)
output.df$gnetvent <- output.df$govent-output.df$givent ; # net water flowrate exiting vents [kg/hour]
output.df$gevap <- output.df$gnetvent+output.df$mvsvfdiff ; # evap rate [kg/hour]
# Option. may want to change areasf to uncovered areasfuncov if ground cover there
output.df$gevap2 <- output.df$gevap*1000/areasf ; # evap rate [g/m2/hour]
output.df$ration <- output.df$givent/output.df$gevap ; # ratio of water entering vent/evaporation

```

Figure A.25: ana_calcs.R, page 4


```

output.df$Qnetvent <- output.df$Qovent-output.df$Qivent ; # net enthalpy exiting the vents [kJ/hour]
output.df$Qnetvent2 <- output.df$Qnetvent*1000/3600 ; # net enthalpy exiting the vents [W]
output.df$Qeva_hf <- output.df$gevap*output.df$hf_g*1000/3600 ; # energy of evap assuming hf, low bound [W]
output.df$Qeva_hg <- output.df$gevap*output.df$hg_g*1000/3600 ; # energy of evap assuming hg, upper bound [W]

## CHECKED THOROUGHLY UP TO HERE

# Energy balance over ground surface - this may not get used
output.df$Qcond_g <- input.df$HF31*areaf ; # energy conducted from subground to surface [W]
output.df$Qconv_g <- -hconv_g*areaf*output.df$t_df ; # energy convected from ground surface to air [W]
# energy radiated from ground surface to underfloor surface [W]
output.df$Qrad_gf <- vf_gf*areaf*emis*sbconst*((output.df$TS37cor+tempadd)^4)-((output.df$TS36cor+tempadd)^4))
# energy radiated from ground surface to under floor [W]
output.df$Qrad_gf <- vf_gf*areaf*emis*sbconst*((output.df$TS37cor+tempadd)^4)-((output.df$TS36cor+tempadd)^4))
# Need to check this calc - do by hand
# energy radiated from ground surface to walls [W]; # view factor per p 729 Fundamentals h&mt incopera
output.df$Qrad_gw <- vf_gw*areaf*emis*sbconst*0.25*((4*((output.df$TS37cor+tempadd)^4))-((output.df$TS30cor+tempadd)^4))-
((output.df$TS31cor+tempadd)^4))-((output.df$TS32cor+tempadd)^4))-((output.df$TS33cor+tempadd)^4))
output.df$Qeva_1 <- output.df$Qcond_g - output.df$Qconv_g - output.df$Qrad_gf - output.df$Qrad_gw

# Define factors for stats analysis or AccuRate
# hours used DateTime. Others use dnt. Don't know why.
# hour of day
output.df$hour <- hours(output.df$DateTime); output.df$hour <- factor(output.df$hour)
# month of year
output.df$month <- months(output.df$dnt)
output.df$month[output.df$month=="January"] <- "01.JAN"
output.df$month[output.df$month=="February"] <- "02.FEB"
output.df$month[output.df$month=="March"] <- "03.MAR"
output.df$month[output.df$month=="April"] <- "04.APR"
output.df$month[output.df$month=="May"] <- "05.MAY"
output.df$month[output.df$month=="June"] <- "06.JUN"
output.df$month[output.df$month=="July"] <- "07.JUL"
output.df$month[output.df$month=="August"] <- "08.AUG"
output.df$month[output.df$month=="September"] <- "09.SEP"
output.df$month[output.df$month=="October"] <- "10.OCT"
output.df$month[output.df$month=="November"] <- "11.NOV"
output.df$month[output.df$month=="December"] <- "12.DEC"
output.df$month <- factor(output.df$month)
# season, using month

```

Figure A.26: ana_calcs.R, page 5

```

summer <- c("12.DEC", "01.JAN", "02.FEB"); autumn <- c("03.MAR", "04.APR", "05.MAY")
winter <- c("06.JUN", "07.JUL", "08.AUG"); spring <- c("09.SEP", "10.OCT", "11.NOV")
output.df$season[output.df$month %in% summer] <- "04.SUM"
output.df$season[output.df$month %in% autumn] <- "01.AUT"
output.df$season[output.df$month %in% winter] <- "02.WIN"
output.df$season[output.df$month %in% spring] <- "03.SPR"
output.df$season <- factor(output.df$season)
# month of which year
output.df$month2 <- paste(years(output.df$DateTime), output.df$month)
output.df$month2 <- factor(output.df$month2)
# season of which year
# put jan and feb into summer season starting previous year
output.df$season2 <- paste(years(output.df$DateTime), output.df$season)
output.df$season2[years(output.df$DateTime)=="2011" & output.df$month=="02.FEB"] <- "2010 04.SUM"
output.df$season2[years(output.df$DateTime)=="2012" & output.df$month=="01.JAN"] <- "2011 04.SUM"
output.df$season2[years(output.df$DateTime)=="2012" & output.df$month=="02.FEB"] <- "2011 04.SUM"
output.df$season2 <- factor(output.df$season2)
# daylight, by using global radiation.
output.df$daynight <- "DAY"; output.df$daynight[output.df$RA14==0] <- "NIGHT"
output.df$daynight[is.na(output.df$RA14)] <- "NA"
output.df$daynight <- factor(output.df$daynight)
# ground cover
# Need to fix this. why doesn't it work as function of note? Fix: just define basic factor as function of time
output.df$ground <- "COVERED"
output.df$ground[as.character(output.df$DateTime)>"2012/02/22 15:00"] <- "UNCOVERED"
# Make factor based on wsf:wsf relation of above or below the line wsf = wos + 0.0018
output.df$wsfabove <- (output.df$wsf > output.df$ws + 0.0018)
output.df$wsfabove <- factor(output.df$wsfabove)
# Define wind angle 16th-tants
output.df$windbin <- "NA"
output.df$windbin[(input.df$AD10 > 0.00) & (input.df$AD10 < 11.25)] <- 16
output.df$windbin[(input.df$AD10 > 11.25) & (input.df$AD10 < 33.75)] <- 1
output.df$windbin[(input.df$AD10 > 33.75) & (input.df$AD10 < 56.25)] <- 2
output.df$windbin[(input.df$AD10 > 56.25) & (input.df$AD10 < 78.75)] <- 3
output.df$windbin[(input.df$AD10 > 78.75) & (input.df$AD10 < 101.25)] <- 4
output.df$windbin[(input.df$AD10 > 101.25) & (input.df$AD10 < 123.75)] <- 5
output.df$windbin[(input.df$AD10 > 123.75) & (input.df$AD10 < 146.25)] <- 6
output.df$windbin[(input.df$AD10 > 146.25) & (input.df$AD10 < 168.75)] <- 7
output.df$windbin[(input.df$AD10 > 168.75) & (input.df$AD10 < 191.25)] <- 8

```

Figure A.27: ana_calcs.R, page 6

```

output.df$windbin[((input.df$AD10 > 191.25) & (input.df$AD10 < 213.75))] <- 9
output.df$windbin[((input.df$AD10 > 213.75) & (input.df$AD10 < 236.25))] <- 10
output.df$windbin[((input.df$AD10 > 236.25) & (input.df$AD10 < 258.75))] <- 11
output.df$windbin[((input.df$AD10 > 258.75) & (input.df$AD10 < 281.25))] <- 12
output.df$windbin[((input.df$AD10 > 281.25) & (input.df$AD10 < 303.75))] <- 13
output.df$windbin[((input.df$AD10 > 303.75) & (input.df$AD10 < 326.25))] <- 14
output.df$windbin[((input.df$AD10 > 326.25) & (input.df$AD10 < 348.75))] <- 15
output.df$windbin[((input.df$AD10 > 348.75) & (input.df$AD10 < 360.00))] <- 16
output.df$windbin[(input.df$AD10 > 0.00) & (input.df$AS10 < 0.001))] <- 0
# time periods
output.df$tp <- "TP2"
output.df$tp[as.character(output.df$DateTime) < "2012/02/22 16:00"] <- "TP1"
output.df$tp[as.character(output.df$DateTime) > "2012/03/22 11:00"] <- "TP3"
output.df$tp <- factor(output.df$tp)

# write entire output data frame to output file
write.table(output.df, file=paste("data06.csv"), sep=",", row.names=FALSE)
# the following is for ANZASCA data only
# write.table(output.df, file=paste("data_anzout.csv"), sep=",", row.names=FALSE)

```

Figure A.28: ana_calcs.R, page 7

```
#####
##
## ana_stats.R
##
## January 27 2013, Sabrina Sequeira
## Edited July 28, 2013 to calc more maxmins as needed.
##
## Create factors on maxmin data
## Add max mins for some calculated params
##
## must have chron library installed (use Packages menu in gui)
##
## Inputs: maxmin.csv (output of instr_maxmin.R)
## Output: maxmin_factors.csv
##
## Notes:
##
## The factors should exactly match those from ana_calcs.R
##
#####

# set working directory
setwd("F:/sabs uni files/project/test cell data/scripts")

# Must install package chron and then load into library. Only once.
library(chron)
# Change time zone to GMT-10 to ignore DST. All calcs done in current time zone.
Sys.setenv(tz='Etc/GMT-10')

# load output from maxmin data into a data frame named maxmin.df
maxmin.df <- read.csv("maxmin_output/maxmin.csv", sep=",", header=T)
# convert seqdays to date parameter
maxmin.df$date <- as.Date(maxmin.df$seqdays)

# load in data after calculations
input.df <- read.csv("data06.csv", sep=",", header=T)
input.df$date <- as.Date(input.df$dateTime)

# do more maxmins on selected calculated parameters
for (i in 1:nrow(maxmin.df))
{
  j <- maxmin.df$date[i]
  # print(j)
  maxmin.df$tempsfmax[i] <- max(input.df$tempsf[input.df$date==j])
  maxmin.df$tempsfmin[i] <- min(input.df$tempsf[input.df$date==j])
  maxmin.df$tenvsfmax[i] <- max(input.df$tenvsf[input.df$date==j])
  maxmin.df$tenvsfmin[i] <- min(input.df$tenvsf[input.df$date==j])
  maxmin.df$stairrmmax[i] <- max(input.df$stairrm[input.df$date==j])
  maxmin.df$stairrmmin[i] <- min(input.df$stairrm[input.df$date==j])
  maxmin.df$stenvrmmax[i] <- max(input.df$stenvrm[input.df$date==j])
  maxmin.df$stenvrmmin[i] <- min(input.df$stenvrm[input.df$date==j])
}

# Define factors for maxmin stats analysis
# month of year
maxmin.df$month <- months(maxmin.df$date)
maxmin.df$month[maxmin.df$month=="January"] <- "01.JAN"
maxmin.df$month[maxmin.df$month=="February"] <- "02.FEB"
maxmin.df$month[maxmin.df$month=="March"] <- "03.MAR"
maxmin.df$month[maxmin.df$month=="April"] <- "04.APR"
maxmin.df$month[maxmin.df$month=="May"] <- "05.MAY"
maxmin.df$month[maxmin.df$month=="June"] <- "06.JUN"
maxmin.df$month[maxmin.df$month=="July"] <- "07.JUL"
maxmin.df$month[maxmin.df$month=="August"] <- "08.AUG"
maxmin.df$month[maxmin.df$month=="September"] <- "09.SEP"
maxmin.df$month[maxmin.df$month=="October"] <- "10.OCT"
maxmin.df$month[maxmin.df$month=="November"] <- "11.NOV"
maxmin.df$month[maxmin.df$month=="December"] <- "12.DEC"
maxmin.df$month <- factor(maxmin.df$month)
```

Figure A.29: ana_maxmin.R, page 1

```

# season, using month
summer <- c("12.DEC", "01.JAN", "02.FEB"); autumn <- c("03.MAR", "04.APR", "05.MAY")
winter <- c("06.JUN", "07.JUL", "08.AUG"); spring <- c("09.SEP", "10.OCT", "11.NOV")
maxmin.df$season[maxmin.df$month %in% summer] <- "04.SUM"
maxmin.df$season[maxmin.df$month %in% autumn] <- "01.AUT"
maxmin.df$season[maxmin.df$month %in% winter] <- "02.WIN"
maxmin.df$season[maxmin.df$month %in% spring] <- "03.SPR"
maxmin.df$season <- factor(maxmin.df$season)

# month of which year
maxmin.df$month2 <- paste(years(maxmin.df$date), maxmin.df$month)
maxmin.df$month2 <- factor(maxmin.df$month2)

# season of which year
# put jan and feb into summer season starting previous year
maxmin.df$season2 <- paste(years(maxmin.df$date), maxmin.df$season)
maxmin.df$season2[years(maxmin.df$date)=="2011" & maxmin.df$month=="02.FEB"] <- "2010 04.SUM"
maxmin.df$season2[years(maxmin.df$date)=="2012" & maxmin.df$month=="01.JAN"] <- "2011 04.SUM"
maxmin.df$season2[years(maxmin.df$date)=="2012" & maxmin.df$month=="02.FEB"] <- "2011 04.SUM"
maxmin.df$season2 <- factor(maxmin.df$season2)

# ground cover
# Need to fix this. why doesn't it work? Fix: just define basic factor as function of time
maxmin.df$ground <- "COVERED"
maxmin.df$ground[as.character(maxmin.df$date) > "2012-02-22"] <- "UNCOVERED"
maxmin.df$ground <- factor(maxmin.df$ground)

# time periods
maxmin.df$tp <- "TP2"
maxmin.df$tp[as.character(maxmin.df$date) < "2012/02/22 16:00"] <- "TP1"
maxmin.df$tp[as.character(maxmin.df$date) > "2012/03/22 11:00"] <- "TP3"
maxmin.df$tp <- factor(maxmin.df$tp)

# write entire new data frame to output file
write.table(maxmin.df, file=paste("maxmin_output/maxmin_factors.csv"), sep=",", row.names=FALSE)



```

Figure A.30: ana_maxmin.R, page 2

A.3 AccuRate input files

Information can be input into the AccuRate program in two formats: the project file and the scratch file. The project file data can be output into the building data report. It is not typical for the standard user to modify the scratch file. For AR1 the building data report is provided in Figure A.31 through Figure A.38, and the scratch file is provided in Figure A.39 through Figure A.45. For AR2 the building data report is provided in Figure A.46 through Figure A.53, and the scratch file is provided in Figure A.54 through Figure A.60.

The `ana_climate.R` script creates the on-site climate data by merging observed data into the lengthened default climate file. This script is provided in Figure A.61 through Figure A.64. The beginning of the climate file used for both AR1 and AR2 is provided in Figure A.65. Only the first page is provided because the file is hundreds of pages long.

	<h2 style="margin: 0;">AccuRate V1.1.4.1</h2> <h3 style="margin: 10px 0 0 0;">Nationwide House Energy Rating Scheme</h3>	
Project Name: Test Cell 2		
File Name: F:\sabs uni		
files\AccuRate\AccuRate1.1.4.1\Projects\tc2_2013_05_14.PRO		
Postcode: 7250		Climate Zone: 23
Client Name:		
Site Address:		
Design Option: V1.0		
Date: 2/07/2013		Time: 12:34
		Page: 1



Construction details: External Walls		
Description: Sub floor wall		
External colour: Medium	Internal colour: Medium	Area: 13.9 m ²
External absorptance (%): 50	Internal absorptance (%): 50	
Layer	Material	Thickness (mm)
1	Brickwork: generic extruded clay brick (typical density)	110

Description: brick veneer framing factor East west north		
External colour: Medium	Internal colour: Paint: light cream	Area: 39.9 m ²
External absorptance (%): 50	Internal absorptance (%): 30	
Layer	Material	Thickness (mm)
1	Brickwork: generic extruded clay brick (typical density)	110
2	Air gap vertical 31-65 mm (40 nominal) unventilated reflective (0.4/0.9; E = 0.38)	40
3	Rockwool batt (k = 0.033)	61
4	Plasterboard	10

Description: Brick veneer Wall Bridged South		
External colour: Medium	Internal colour: Paint: light cream	Area: 13.2 m ²
External absorptance (%): 50	Internal absorptance (%): 30	
Layer	Material	Thickness (mm)
1	Brickwork: generic extruded clay brick (typical density)	110
2	Air gap vertical 31-65 mm (40 nominal) unventilated reflective (0.4/0.9; E = 0.38)	40
3	Rockwool batt (k = 0.033)	59
4	Plasterboard	10

Description: north wall without plasterboard (base wall #4)		
External colour: Medium	Internal colour: Paint: light cream	Area: 0.2 m ²
External absorptance (%): 50	Internal absorptance (%): 30	
Layer	Material	Thickness (mm)
1	Brickwork: generic extruded clay brick (typical density)	110
2	Air gap vertical 31-65 mm (40 nominal) unventilated reflective (0.4/0.9; E = 0.38)	40
3	Rockwool batt (k = 0.033)	61

Figure A.31: AR1 Building report, page 1

	<h2 style="margin: 0;">AccuRate V1.1.4.1</h2> <h3 style="margin: 10px 0 0 0;">Nationwide House Energy Rating Scheme</h3>	
Project Name: Test Cell 2		
File Name: F:\sabs uni		
files\AccuRate\AccuRate1.1.4.1\Projects\tc2_2013_05_14.PRO		
Postcode: 7250		Climate Zone: 23
Client Name:		
Site Address:		
Design Option: V1.0		
Date: 2/07/2013		Time: 12:34
		Page: 2

Description: south wall without plasterboard (base wall #5)		
External colour: Medium	Internal colour: Paint: light cream	Area: 0.2 m ²
External absorptance (%) : 50	Internal absorptance (%) : 30	
Layer	Material	Thickness (mm)
1	Brickwork: generic extruded clay brick (typical density)	110
2	Air gap vertical 31-65 mm (40 nominal) unventilated reflective (0.4/0.9; E = 0.38)	40
3	Rockwool batt (k = 0.033)	59

Construction details: External Doors		
Description: Timber (solid)		
External colour: Medium	Internal colour: Medium	Area: 1.7 m ²
External absorptance (%) : 50	Internal absorptance (%) : 50	
Layer	Material	Thickness (mm)
1	Timber (Mountain ash)	40

Description: Sub Floor Door		
External colour: Medium	Internal colour: Medium	Area: 0.4 m ²
External absorptance (%) : 50	Internal absorptance (%) : 50	
Layer	Material	Thickness (mm)
1	Plywood (softwood)	12

Construction details: Floor/Ceilings		
Description: Plasterboard 10 mm bridged		
Top colour: Medium	Bottom colour: Light	Area: 30.0 m ²
Top absorptance (%) : 50	Bottom absorptance (%) : 30	
Layer	Material	Thickness (mm)
1	Glass fibre batt (k = 0.044 density = 12 kg/m ³)	158
2	Plasterboard	10

Description: Bare ground		
Top colour: Medium	Bottom colour: Dark	Area: 33.4 m ²
Top absorptance (%) : 50	Bottom absorptance (%) : 85	
Layer	Material	Thickness (mm)
1	Ground	0

Figure A.32: AR1 Building report, page 2





	<p>AccuRate V1.1.4.1</p> <p>Nationwide House Energy Rating Scheme</p>	
Project Name: Test Cell 2		
File Name: F:\sabs uni		
files\AccuRate\AccuRate1.1.4.1\Projects\tc2_2013_05_14.PRO		
Postcode: 7250		Climate Zone: 23
Client Name:		
Site Address:		
Design Option: V1.0		
Date: 2/07/2013		Time: 12:34
		Page: 3
Description: Particle Board Floor Bridged plus carpet & underlay		
Top colour: Medium		Bottom colour: Not Specified
		Area: 30.0 m ²
Top absorptance (%) : 50		Bottom absorptance (%) : Not Specified
Layer	Material	Thickness (mm)
1	Carpet 10 + rubber underlay 8	18
2	Particleboard	21
Construction details: Roofs		
Description: Metal deck		
External colour: Medium		Internal colour: Light
		Area: 50.9 m ²
External absorptance (%) : 50		Internal absorptance (%) : 30
Layer	Material	Thickness (mm)
1	Steel	1
2	Air gap 22.5° 31-65 mm (40 nominal) ventilated reflective (0.4/0.9; E = 0.38)	40

Figure A.33: AR1 Building report, page 3

	<h2 style="margin: 0;">AccuRate V1.1.4.1</h2> <h3 style="margin: 10px 0 0 0;">Nationwide House Energy Rating Scheme</h3>	
Project Name: Test Cell 2		
File Name: F:\sabs uni		
files\AccuRate\AccuRate1.1.4.1\Projects\tc2_2013_05_14.PRO		
Postcode: 7250		Climate Zone: 23
Client Name:		
Site Address:		
Design Option: V1.0		
Date: 2/07/2013		Time: 12:34
Page: 4		



Habitable zones						
Name	Type	Volume (m³)	Floor height (m)	Ceiling height above floor (m)	Heated	Cooled
Test cell	Living/Kitchen	73.3	0.6	2.4	Y	Y

Habitable zones (continued)									
Name	Chimneys		Wall/Ceiling vents	Exhaust fans		Vented downlights	Unflued gas heaters	Ceiling fans	Type
	U/S	S		U/S	S				
Test cell	0	0	0	0	0	0	0	0	-

Roofspace zones						
Name	Volume (m³)	Reflective	Sarking	Roof surface	Openness	
Roof Space	19.7	Y	Sarked	Continuous	Standard	

Sub-floor zones							
Name	Volume (m³)	Floor height (m)	Ceiling height above floor (m)	Reflective	Openness	Wall cavity	Vent area (mm²/m wall)
Sub Floor	20.0	0.0	0.6	N	Enclosed	N	6000.0

Figure A.34: AR1 Building report, page 4

	<h1 style="margin: 0;">AccuRate V1.1.4.1</h1> <h2 style="margin: 10px 0 0 0;">Nationwide House Energy Rating Scheme</h2>	
Project Name: Test Cell 2		
File Name: F:\sabs uni		
files\AccuRate\AccuRate1.1.4.1\Projects\tc2_2013_05_14.PRO		
Postcode: 7250		Climate Zone: 23
Client Name:		
Site Address:		
Design Option: V1.0		
Date: 2/07/2013		Time: 12:34
		Page: 5

Test cell: External walls main data									
Wall	Construction	Azi (deg.)	L (m)	H (m)	Area (gross) (m²)	Area (net) (m²)	Fixed shade	Opening (m²)	Opening Type
1	brick veneer framing factor East west no	0	5.40	2.44	13.18	13.18	Eave all	0.00	Controlled
2	brick veneer framing factor East west no	90	5.48	2.44	13.37	13.37	Eave all	0.00	Controlled
3	Brick veneer Wall Bridged South	180	5.40	2.44	13.18	11.45	Eave all	0.00	Controlled
4	brick veneer framing factor East west no	270	5.48	2.44	13.37	13.37	Eave all	0.00	Controlled
5	north wall without plasterboard (base wa	0	0.08	2.44	0.20	0.20	Eave all	0.00	Controlled
6	south wall without plasterboard (base wa	180	0.08	2.44	0.20	0.20	Eave all	0.00	Controlled



Test cell: External walls screen data						
Wall	Screen	Height (m)	Width (m)	Horizontal Offset (m)	Vertical Offset (m)	Monthly blocking factors
1	1	7.0	44.0	56.6	-1.6	100,100,100,100,100,100,100,100,100,100,100,100
1	2	4.2	5.8	1.0	-1.0	100,100,100,100,100,100,100,100,100,100,100,100
2	1	3.6	37.0	3.5	-0.6	100,100,100,100,100,100,100,100,100,100,100,100
2	2	3.6	12.0	15.0	-0.6	100,100,100,100,100,100,100,100,100,100,100,100
2	3	7.0	26.0	-22.5	-0.6	100,100,100,100,100,100,100,100,100,100,100,100
3	1	6.0	9.0	13.5	-0.6	95,95,95,95,95,95,95,95,95,95,95,95
3	2	11.0	21.0	-6.0	1.4	95,95,70,50,30,20,15,15,20,50,70,95
3	3	3.6	7.0	-1.0	-0.3	100,100,100,100,100,100,100,100,100,100,100,100
5	1	7.0	44.0	56.6	-1.6	100,100,100,100,100,100,100,100,100,100,100,100
5	2	4.2	5.8	1.0	-1.0	100,100,100,100,100,100,100,100,100,100,100,100
6	1	6.0	9.0	13.5	-6.0	95,95,95,95,95,95,95,95,95,95,95,95
6	2	11.0	21.0	-6.0	1.4	95,95,70,50,30,20,15,15,20,50,70,95
6	3	3.6	7.0	-1.0	-0.3	100,100,100,100,100,100,100,100,100,100,100,100

Test cell: Doors in walls											
Wall	Door Name	Construction	Azi (deg.)	H (m)	W (m)	Area (m²)	HO (m)	Openable (%)	Weather stripped	Gap size	
3	Door 1	Timber(solid)	180	2.10	0.82	1.72	0.00	0	Y	M	

Test cell: Floors							
Floor	Construction	Area (gross) (m²)	Area (net) (m²)	Under the floor	Edge Ins.	Opening (m²)	Opening Type
1	Particle Board Floor Bridged plus carpet & um	30.0	30.0	Sub Floor		0.00	Controlled

Test cell: Ceilings						
Ceiling	Construction	Area (gross) (m²)	Area (net) (m²)	Above the ceiling	Opening (m²)	Opening Type
1	Plasterboard 10 mm bridged	30.0	30.0	Roof Space	0.00	Controlled



Figure A.35: AR1 Building report, page 5

	<h2 style="margin: 0;">AccuRate V1.1.4.1</h2> <h3 style="margin: 10px 0 0 0;">Nationwide House Energy Rating Scheme</h3>	
Project Name: Test Cell 2		
File Name: F:\sabs uni		
files\AccuRate\AccuRate1.1.4.1\Projects\tc2_2013_05_14.PRO		
Postcode: 7250		Climate Zone: 23
Client Name:		
Site Address:		
Design Option: V1.0		
Date: 2/07/2013		Time: 12:34
Page: 6		

Roof Space: Floors							
Floor	Construction	Area (gross) (m²)	Area (net) (m²)	Under the floor	Edge Ins.	Opening (m²)	Opening Type
1	Plasterboard 10 mm bridged	30.0	30.0	Test cell		0.00	Controlled

Roof Space: Roofs						
Roof	Construction	Area (gross) (m²)	Area (net) (m²)	Azi (deg.)	Pitch (deg.)	Exposure
1	Metal deck	12.73	12.73	0	23	Normal
2	Metal deck	12.73	12.73	90	23	Normal
3	Metal deck	12.73	12.73	180	23	Normal
4	Metal deck	12.73	12.73	270	23	Normal

Figure A.36: AR1 Building report, page 6

		AccuRate V1.1.4.1							
Nationwide House Energy Rating Scheme									
Project Name: Test Cell 2									
File Name: F:\sabs uni									
files\AccuRate\AccuRate1.1.4.1\Projects\tc2_2013_05_14.PRO									
Postcode: 7250					Climate Zone: 23				
Client Name:									
Site Address:									
Design Option: V1.0									
Date: 2/07/2013				Time: 12:34			Page: 7		

Sub Floor: External walls main data									
Wall	Construction	Azi (deg.)	L (m)	H (m)	Area (gross) (m²)	Area (net) (m²)	Fixed shade	Opening (m²)	Opening Type
1	Sub floor wall	0	5.78	0.60	3.47	3.47	Sub floor	0.00	Controlled
2	Sub floor wall	90	5.78	0.60	3.47	3.47	Sub floor	0.00	Controlled
3	Sub floor wall	180	5.78	0.60	3.47	3.04	Sub floor	0.00	Controlled
4	Sub floor wall	270	5.78	0.60	3.47	3.47	Sub floor	0.00	Controlled



Sub Floor: External walls screen data									
Wall	Screen	Height (m)	Width (m)	Horizontal Offset (m)	Vertical Offset (m)	Monthly blocking factors			
1	1	7.0	44.0	55.6	-1.0	100,100,100,100,100,100,100,100,100,100,100			
1	2	4.2	5.8	1.0	-0.4	100,100,100,100,100,100,100,100,100,100,100			
2	1	3.6	37.0	3.5	0.0	100,100,100,100,100,100,100,100,100,100,100			
2	2	3.6	12.0	15.0	0.0	100,100,100,100,100,100,100,100,100,100,100			
2	3	7.0	26.0	-22.5	0.0	100,100,100,100,100,100,100,100,100,100,100			
3	1	6.0	9.0	13.5	0.0	95,95,95,95,95,95,95,95,95,95,95			
3	2	11.0	21.0	-6.0	2.0	95,95,70,50,30,20,15,15,20,50,70,95			
3	3	3.6	7.0	-1.0	0.3	100,100,100,100,100,100,100,100,100,100,100			

Sub Floor: Doors in walls											
Wall	Door Name	Construction	Azi (deg.)	H (m)	W (m)	Area (m²)	HO (m)	Openable (%)	Weather stripped	Gap size	
3	subfloor	Sub Floor Door	180	0.60	0.72	0.43	0.00	90	N	L	

Sub Floor: Floors									
Floor	Construction	Area (gross) (m²)	Area (net) (m²)	Under the floor		Edge Ins.	Opening (m²)	Opening Type	
1	Bare ground	33.4	33.4	Ground			0.00	Controlled	

Sub Floor: Ceilings									
Ceiling	Construction	Area (gross) (m²)	Area (net) (m²)	Above the ceiling		Opening (m²)	Opening Type		
1	Particle Board Floor Bridged plus carpet & un	30.0	30.0	Test cell		0.00	Controlled		

Figure A.37: AR1 Building report, page 7

	<h2 style="margin: 0;">AccuRate V1.1.4.1</h2> <h3 style="margin: 10px 0 0 0;">Nationwide House Energy Rating Scheme</h3>	
Project Name: Test Cell 2		
File Name: F:\sabs uni		
files\AccuRate\AccuRate1.1.4.1\Projects\tc2_2013_05_14.PRO		
Postcode: 7250		Climate Zone: 23
Client Name:		
Site Address:		
Design Option: V1.0		
Date: 2/07/2013		Time: 12:34
Page: 8		

Shading Schemes					
Name	Eaves		Other fixed shading		
	Projection (m)	Offset (m)	Projection (m)	Offset (m)	Monthly blocking factors (%)
Eave all	0.58	0.00	0.00	0.00	100,100,100,100,100,100,100,100,100,100
Sub floor	0.58	2.40	0.00	0.00	100,100,100,100,100,100,100,100,100,100

Ventilation			
Footprint: vertical dimension (m)	Footprint: horizontal dimension (m)	Azimuth of highlighted facade (degrees)	Insect screens
5.5	5.5	0	N

Figure A.38: AR1 Building report, page 8


```

C Horizontal shading schemes. 999 maximum
C Scheme no., eave proj., eave offset, pergola proj., pergola offset, pergola shading factors
C
  EaveP EaveO PergP PergO
1 20 1 0.58 0.00 0.00 0.00 1.00 1.00 1.00 1.00 1.00 1.00 1.00 1.00 1.00
1 20 2 0.58 0.00 0.00 0.00 1.00 1.00 1.00 1.00 1.00 1.00 1.00 1.00 1.00
1 20 3 0.58 0.00 0.00 0.00 1.00 1.00 1.00 1.00 1.00 1.00 1.00 1.00 1.00
1 20 4 0.58 0.34 0.00 0.00 1.00 1.00 1.00 1.00 1.00 1.00 1.00 1.00 1.00
1 20 5 0.58 0.00 0.00 0.00 1.00 1.00 1.00 1.00 1.00 1.00 1.00 1.00 1.00
1 20 6 0.58 0.00 0.00 0.00 1.00 1.00 1.00 1.00 1.00 1.00 1.00 1.00 1.00
1 20 7 0.58 0.00 0.00 0.00 1.00 1.00 1.00 1.00 1.00 1.00 1.00 1.00 1.00
1 20 8 0.58 2.40 0.00 0.00 1.00 1.00 1.00 1.00 1.00 1.00 1.00 1.00 1.00
1 20 9 0.58 2.40 0.00 0.00 1.00 1.00 1.00 1.00 1.00 1.00 1.00 1.00 1.00
1 20 10 0.58 2.40 0.00 0.00 1.00 1.00 1.00 1.00 1.00 1.00 1.00 1.00 1.00
1 20 11 0.58 2.40 0.00 0.00 1.00 1.00 1.00 1.00 1.00 1.00 1.00 1.00 1.00
1 20 12 0.58 2.40 0.00 0.00 1.00 1.00 1.00 1.00 1.00 1.00 1.00 1.00 1.00
C
C Vertical shading schemes. 999 maximum
C Left proj., left offset, right proj., right offset
C
  LeftP LeftRightRightO
1 22 1 7.0 44.0 35.5 56.6 -1.6 1.00 1.00 1.00 1.00 1.00 1.00 1.00 1.00 1.00
1 22 2 4.2 5.8 7.5 1.0 -1.0 1.00 1.00 1.00 1.00 1.00 1.00 1.00 1.00 1.00
1 22 3 3.6 37.0 66.0 3.5 -0.6 1.00 1.00 1.00 1.00 1.00 1.00 1.00 1.00 1.00
1 22 4 3.6 12.0 50.0 15.0 -0.6 1.00 1.00 1.00 1.00 1.00 1.00 1.00 1.00 1.00
1 22 5 7.0 26.0 25.0 -22.5 -0.6 1.00 1.00 1.00 1.00 1.00 1.00 1.00 1.00 1.00
1 22 6 6.0 9.0 17.0 13.5 -0.6 0.95 0.95 0.95 0.95 0.95 0.95 0.95 0.95 0.95
1 22 7 6.0 9.0 17.0 13.5 -0.6 0.95 0.95 0.95 0.95 0.95 0.95 0.95 0.95 0.95
1 22 8 11.0 21.0 19.0 -6.0 1.4 0.95 0.95 0.70 0.50 0.30 0.20 0.15 0.15 0.20 0.50 0.70 0.95
1 22 9 11.0 21.0 19.0 -6.0 1.4 0.95 0.95 0.70 0.50 0.30 0.20 0.15 0.15 0.20 0.50 0.70 0.95
1 22 10 3.6 7.0 7.5 -1.0 -0.3 1.00 1.00 1.00 1.00 1.00 1.00 1.00 1.00 1.00
1 22 11 3.6 7.0 7.5 -1.0 -0.3 1.00 1.00 1.00 1.00 1.00 1.00 1.00 1.00 1.00
1 22 12 7.0 44.0 35.5 56.6 -1.6 1.00 1.00 1.00 1.00 1.00 1.00 1.00 1.00 1.00
1 22 13 4.2 5.8 7.5 1.0 -1.0 1.00 1.00 1.00 1.00 1.00 1.00 1.00 1.00 1.00
1 22 14 6.0 9.0 17.0 13.5 -0.6 0.95 0.95 0.95 0.95 0.95 0.95 0.95 0.95 0.95
1 22 15 11.0 21.0 19.0 -6.0 1.4 0.95 0.95 0.70 0.50 0.30 0.20 0.15 0.15 0.20 0.50 0.70 0.95
1 22 16 3.6 7.0 7.5 -1.0 -0.3 1.00 1.00 1.00 1.00 1.00 1.00 1.00 1.00 1.00
1 22 17 7.0 44.0 35.5 55.6 -1.0 1.00 1.00 1.00 1.00 1.00 1.00 1.00 1.00 1.00
1 22 18 4.2 5.8 7.5 1.0 -0.4 1.00 1.00 1.00 1.00 1.00 1.00 1.00 1.00 1.00
1 22 19 3.6 37.0 66.0 3.5 0.0 1.00 1.00 1.00 1.00 1.00 1.00 1.00 1.00 1.00
1 22 20 3.6 12.0 50.0 15.0 0.0 1.00 1.00 1.00 1.00 1.00 1.00 1.00 1.00 1.00
1 22 21 7.0 26.0 25.0 -22.5 0.0 1.00 1.00 1.00 1.00 1.00 1.00 1.00 1.00 1.00
1 22 22 6.0 9.0 17.0 13.5 0.0 0.95 0.95 0.95 0.95 0.95 0.95 0.95 0.95 0.95
1 22 23 6.0 9.0 17.0 13.5 0.0 0.95 0.95 0.95 0.95 0.95 0.95 0.95 0.95 0.95
1 22 24 11.0 21.0 19.0 -6.0 2.0 0.95 0.95 0.70 0.50 0.30 0.20 0.15 0.15 0.20 0.50 0.70 0.95
1 22 25 11.0 21.0 19.0 -6.0 2.0 0.95 0.95 0.70 0.50 0.30 0.20 0.15 0.15 0.20 0.50 0.70 0.95
1 22 26 3.6 7.0 7.5 -1.0 0.3 1.00 1.00 1.00 1.00 1.00 1.00 1.00 1.00 1.00
1 22 27 3.6 7.0 7.5 -1.0 0.3 1.00 1.00 1.00 1.00 1.00 1.00 1.00 1.00 1.00
C
C Screen schemes. 20 maximum
C Scheme no., screen height, width, distance, offset horiz, offset vert, shading factors
C
  Height Width Dist OffH OffV
1 22 1 7.0 44.0 35.5 56.6 -1.6 1.00 1.00 1.00 1.00 1.00 1.00 1.00 1.00 1.00
1 22 2 4.2 5.8 7.5 1.0 -1.0 1.00 1.00 1.00 1.00 1.00 1.00 1.00 1.00 1.00
1 22 3 3.6 37.0 66.0 3.5 -0.6 1.00 1.00 1.00 1.00 1.00 1.00 1.00 1.00 1.00
1 22 4 3.6 12.0 50.0 15.0 -0.6 1.00 1.00 1.00 1.00 1.00 1.00 1.00 1.00 1.00
1 22 5 7.0 26.0 25.0 -22.5 -0.6 1.00 1.00 1.00 1.00 1.00 1.00 1.00 1.00 1.00
1 22 6 6.0 9.0 17.0 13.5 -0.6 0.95 0.95 0.95 0.95 0.95 0.95 0.95 0.95 0.95
1 22 7 6.0 9.0 17.0 13.5 -0.6 0.95 0.95 0.95 0.95 0.95 0.95 0.95 0.95 0.95
1 22 8 11.0 21.0 19.0 -6.0 1.4 0.95 0.95 0.70 0.50 0.30 0.20 0.15 0.15 0.20 0.50 0.70 0.95
1 22 9 11.0 21.0 19.0 -6.0 1.4 0.95 0.95 0.70 0.50 0.30 0.20 0.15 0.15 0.20 0.50 0.70 0.95
1 22 10 3.6 7.0 7.5 -1.0 -0.3 1.00 1.00 1.00 1.00 1.00 1.00 1.00 1.00 1.00
1 22 11 3.6 7.0 7.5 -1.0 -0.3 1.00 1.00 1.00 1.00 1.00 1.00 1.00 1.00 1.00
1 22 12 7.0 44.0 35.5 56.6 -1.6 1.00 1.00 1.00 1.00 1.00 1.00 1.00 1.00 1.00
1 22 13 4.2 5.8 7.5 1.0 -1.0 1.00 1.00 1.00 1.00 1.00 1.00 1.00 1.00 1.00
1 22 14 6.0 9.0 17.0 13.5 -0.6 0.95 0.95 0.95 0.95 0.95 0.95 0.95 0.95 0.95
1 22 15 11.0 21.0 19.0 -6.0 1.4 0.95 0.95 0.70 0.50 0.30 0.20 0.15 0.15 0.20 0.50 0.70 0.95
1 22 16 3.6 7.0 7.5 -1.0 -0.3 1.00 1.00 1.00 1.00 1.00 1.00 1.00 1.00 1.00
1 22 17 7.0 44.0 35.5 55.6 -1.0 1.00 1.00 1.00 1.00 1.00 1.00 1.00 1.00 1.00
1 22 18 4.2 5.8 7.5 1.0 -0.4 1.00 1.00 1.00 1.00 1.00 1.00 1.00 1.00 1.00
1 22 19 3.6 37.0 66.0 3.5 0.0 1.00 1.00 1.00 1.00 1.00 1.00 1.00 1.00 1.00
1 22 20 3.6 12.0 50.0 15.0 0.0 1.00 1.00 1.00 1.00 1.00 1.00 1.00 1.00 1.00
1 22 21 7.0 26.0 25.0 -22.5 0.0 1.00 1.00 1.00 1.00 1.00 1.00 1.00 1.00 1.00
1 22 22 6.0 9.0 17.0 13.5 0.0 0.95 0.95 0.95 0.95 0.95 0.95 0.95 0.95 0.95
1 22 23 6.0 9.0 17.0 13.5 0.0 0.95 0.95 0.95 0.95 0.95 0.95 0.95 0.95 0.95
1 22 24 11.0 21.0 19.0 -6.0 2.0 0.95 0.95 0.70 0.50 0.30 0.20 0.15 0.15 0.20 0.50 0.70 0.95
1 22 25 11.0 21.0 19.0 -6.0 2.0 0.95 0.95 0.70 0.50 0.30 0.20 0.15 0.15 0.20 0.50 0.70 0.95
1 22 26 3.6 7.0 7.5 -1.0 0.3 1.00 1.00 1.00 1.00 1.00 1.00 1.00 1.00 1.00
1 22 27 3.6 7.0 7.5 -1.0 0.3 1.00 1.00 1.00 1.00 1.00 1.00 1.00 1.00 1.00
C

```

Figure A.40: AR1 Scratch file, page 2


```

C Zone 2
C
C Name, volume, infiltration data, wind speed reduction factor, type, SHG dist. fractions
C      Name Vol A B WsRed Type EstSG CeilZ RoofZ REmis
3 2      Roof Space 19.7 0.40 0.26 0.67RoofSA 1 5 4 0.05
C Skylights
C      Area Azim Slope ShadI ShadEZonlit ShLenShAreaShRef1 ShRes Diff VArea VType
C Roofs
C      Area Azim Slope AbsE AbsI Emiss SHGFra
C Floors, Ceilings, Partitions
C      Area AbsI AdjZ SHGF
3 2 51 30.03 0.50 5
3 2111 52.00 0.50 4
C
C
C Zone 3
C
C Name, volume, infiltration data, wind speed reduction factor, type, SHG dist. fractions
C      Name Vol A B WsRed Type EstSG FlorZ GrndZ REmis
3 3      Sub Floor 20.0 3.29 1.91 0.67SubFlA 1 6 7 0.82
C Windows
C      Height Width AzimHSSch1HSSch2VShSchScSch1ScSch2ScSch3 Curtn Blind
C Doors
C      Height Width NArea Azim AbsE AbsI EmissHShSchVShSchScSch1ScSch2ScSch3SHGFra
3 3 29 0.60 0.72 0.43 180 0.50 0.50 1.00 11 0 23 25 27
C OpaqueLouvres
C      Height Width NArea Azim AbsE AbsI EmissHShSchVShSchScSch1ScSch2ScSch3SHGFraLouvre
C Walls
C      Height Width NArea Azim AbsE AbsI EmissHShSchVShSchScSch1ScSch2ScSch3SHGFra
3 3 21 0.60 5.78 3.47 0 0.50 0.50 1.00 8 0 17 18 0
3 3 21 0.60 5.78 3.47 90 0.50 0.50 1.00 9 0 19 20 21
3 3 21 0.60 5.78 3.04 180 0.50 0.50 1.00 10 0 22 24 26
3 3 21 0.60 5.78 3.47 270 0.50 0.50 1.00 12 0 0 0 0
C Floors, Ceilings, Partitions
C      Area AbsI AdjZ SHGF
3 3 82 30.03 0.50 6
3 3113 30.03 0.50 7
C
C
C Zone 4
C
C Name, volume, infiltration data, wind speed reduction factor, type, SHG dist. fractions
C      Name Vol A B WsRed Type EstSG
3 4      Underside of Ro 0.0 0.00 0.00 0.67Normal 1 1
C Skylights
C      Area Azim Slope ShadI ShadEZonlit ShLenShAreaShRef1 ShRes Diff VArea VType
C Roofs
C      Area Azim Slope AbsE AbsI Emiss SHGFra
C Floors, Ceilings, Partitions
C      Area AbsI AdjZ SHGF
3 4111 52.00 0.50 2
3 4112 30.03 0.50 5
3 4116 12.73 0.50 9
3 4116 12.73 0.50 11
3 4116 12.73 0.50 13
3 4116 12.73 0.50 15
C
C
C Zone 5
C
C Name, volume, infiltration data, wind speed reduction factor, type, SHG dist. fractions
C      Name Vol A B WsRed Type EstSG
3 5      Top of Ceilings 0.0 0.00 0.00 0.67Normal 1 1
C Floors, Ceilings, Partitions
C      Area AbsI AdjZ SHGF
3 5 53 30.03 0.50 1
3 5 81 30.03 0.50 2
3 5112 30.03 0.50 4
C
C

```

Figure A.43: AR1 Scratch file, page 5

```

C Zone 6
C
C Name, volume, infiltration data, wind speed reduction factor, type, SHG dist. fractions
C      Name Vol A B WsRed Type EstSG
3 6 Underside of fl 0.0 0.00 0.00 0.67Normal 1
C Floors, Ceilings, Partitions
C      Area AbsI AdjZ SHGF
3 6 52 30.03 0.50 3
3 6 84 30.03 0.50 1
3 6 114 30.03 0.50 7
C
C
C Zone 7
C
C Name, volume, infiltration data, wind speed reduction factor, type, SHG dist. fractions
C      Name Vol A B WsRed Type EstSG
3 7 Top of ground 0.0 0.00 0.00 0.67Normal 1
C Floors, Ceilings, Partitions
C      Area AbsI AdjZ SHGF
3 7 41 30.03 0.50
3 7 113 30.03 0.50 3
3 7 114 30.03 0.50 6
C
C
C Zone 8
C
C Name, volume, infiltration data, wind speed reduction factor, type, SHG dist. fractions
C      Name Vol A B WsRed Type EstSG BotZ
3 8 Air Gap Top 1 0.0 0.00 0.00 0.67AirGpT 1 9
C Skylights
C      Area Azim Slope ShadI ShadEZonlit ShLenShAreaShRefl ShRes Diff VArea VType
C Roofs
C      Area Azim Slope AbsE AbsI Emiss SHGFra
3 8 31 12.73 0 23 0.50 0.90
C Floors, Ceilings, Partitions
C      Area AbsI AdjZ SHGF
3 8 115 12.73 0.50 9
C
C
C Zone 9
C
C Name, volume, infiltration data, wind speed reduction factor, type, SHG dist. fractions
C      Name Vol A B WsRed Type EstSG BotZ
3 9 Air Gap Bot 1 0.0 0.00 0.00 0.67Normal 1
C Floors, Ceilings, Partitions
C      Area AbsI AdjZ SHGF
3 9 116 12.73 0.50 4
3 9 115 12.73 0.50 8
C
C
C Zone 10
C
C Name, volume, infiltration data, wind speed reduction factor, type, SHG dist. fractions
C      Name Vol A B WsRed Type EstSG BotZ
3 10 Air Gap Top 2 0.0 0.00 0.00 0.67AirGpT 1 11
C Skylights
C      Area Azim Slope ShadI ShadEZonlit ShLenShAreaShRefl ShRes Diff VArea VType
C Roofs
C      Area Azim Slope AbsE AbsI Emiss SHGFra
3 10 31 12.73 90 23 0.50 0.90
C Floors, Ceilings, Partitions
C      Area AbsI AdjZ SHGF
3 10 115 12.73 0.50 11
C
C

```

Figure A.44: AR1 Scratch file, page 6



```

C Zone 11
C
C Name, volume, infiltration data, wind speed reduction factor, type, SHG dist. fractions
C      Name Vol      A      B WsRed Type EstSG
3 11      Air Gap Bot 2  0.0  0.00  0.00  0.67Normal 1
C Floors, Ceilings, Partitions
C      Area AbsI AdjZ SHGF
3 11116 12.73 0.50 4
3 11115 12.73 0.50 10
C
C
C Zone 12
C
C Name, volume, infiltration data, wind speed reduction factor, type, SHG dist. fractions
C      Name Vol      A      B WsRed Type EstSG BotZ
3 12      Air Gap Top 3  0.0  0.00  0.00  0.67AirGpT 1 13
C Skylights
C      Area Azim Slope ShadI ShadEZonlit ShLenShAreaShRefl ShRes Diff VArea VType
C Roofs
C      Area Azim Slope AbsE AbsI Emiss SHGFra
3 12 31 12.73 180 23 0.50 0.50 0.90
C Floors, Ceilings, Partitions
C      Area AbsI AdjZ SHGF
3 12115 12.73 0.50 13
C
C
C Zone 13
C
C Name, volume, infiltration data, wind speed reduction factor, type, SHG dist. fractions
C      Name Vol      A      B WsRed Type EstSG
3 13      Air Gap Bot 3  0.0  0.00  0.00  0.67Normal 1
C Floors, Ceilings, Partitions
C      Area AbsI AdjZ SHGF
3 13116 12.73 0.50 4
3 13115 12.73 0.50 12
C
C
C Zone 14
C
C Name, volume, infiltration data, wind speed reduction factor, type, SHG dist. fractions
C      Name Vol      A      B WsRed Type EstSG BotZ
3 14      Air Gap Top 4  0.0  0.00  0.00  0.67AirGpT 1 15
C Skylights
C      Area Azim Slope ShadI ShadEZonlit ShLenShAreaShRefl ShRes Diff VArea VType
C Roofs
C      Area Azim Slope AbsE AbsI Emiss SHGFra
3 14 31 12.73 270 23 0.50 0.50 0.90
C Floors, Ceilings, Partitions
C      Area AbsI AdjZ SHGF
3 14115 12.73 0.50 15
C
C
C Zone 15
C
C Name, volume, infiltration data, wind speed reduction factor, type, SHG dist. fractions
C      Name Vol      A      B WsRed Type EstSG
3 15      Air Gap Bot 4  0.0  0.00  0.00  0.67Normal 1
C Floors, Ceilings, Partitions
C      Area AbsI AdjZ SHGF
3 15116 12.73 0.50 4
3 15115 12.73 0.50 14
C

```

9

Figure A.45: AR1 Scratch file, page 7

	<h2 style="margin: 0;">AccuRate V1.1.4.1</h2> <h3 style="margin: 10px 0 0 0;">Nationwide House Energy Rating Scheme</h3>	
Project Name: Test Cell 2		
File Name: F:\sabs uni		
files\AccuRate\AccuRate1.1.4.1\Projects\tc2_2013_05_14.PRO		
Postcode: 7250		Climate Zone: 23
Client Name:		
Site Address:		
Design Option: V2.0		
Date: 2/07/2013		Time: 12:34
		Page: 1



Construction details: External Walls		
Description: Sub floor wall		
External colour: Medium		Internal colour: Medium
Area: 13.9 m ²		
External absorptance (%): 50		Internal absorptance (%): 50
Layer	Material	Thickness (mm)
1	Brickwork: generic extruded clay brick (typical density)	110

Description: brick veneer framing factor East west north		
External colour: Medium		Internal colour: Paint: light cream
Area: 39.9 m ²		
External absorptance (%): 50		Internal absorptance (%): 30
Layer	Material	Thickness (mm)
1	Brickwork: generic extruded clay brick (typical density)	110
2	Air gap vertical 31-65 mm (40 nominal) unventilated reflective (0.4/0.9; E = 0.38)	40
3	Rockwool batt (k = 0.033)	61
4	Plasterboard	10

Description: Brick veneer Wall Bridged South		
External colour: Medium		Internal colour: Paint: light cream
Area: 13.2 m ²		
External absorptance (%): 50		Internal absorptance (%): 30
Layer	Material	Thickness (mm)
1	Brickwork: generic extruded clay brick (typical density)	110
2	Air gap vertical 31-65 mm (40 nominal) unventilated reflective (0.4/0.9; E = 0.38)	40
3	Rockwool batt (k = 0.033)	59
4	Plasterboard	10

Description: north wall without plasterboard (base wall #4)		
External colour: Medium		Internal colour: Paint: light cream
Area: 0.2 m ²		
External absorptance (%): 50		Internal absorptance (%): 30
Layer	Material	Thickness (mm)
1	Brickwork: generic extruded clay brick (typical density)	110
2	Air gap vertical 31-65 mm (40 nominal) unventilated reflective (0.4/0.9; E = 0.38)	40
3	Rockwool batt (k = 0.033)	61

Figure A.46: AR2 Building report, page 1

	<h2 style="margin: 0;">AccuRate V1.1.4.1</h2> <h3 style="margin: 10px 0 0 0;">Nationwide House Energy Rating Scheme</h3>	
Project Name: Test Cell 2		
File Name: F:\sabs uni files\AccuRate\AccuRate1.1.4.1\Projects\tc2_2013_05_14.PRO		
Postcode: 7250		Climate Zone: 23
Client Name:		
Site Address:		
Design Option: V2.0		
Date: 2/07/2013	Time: 12:34	Page: 2

Description: south wall without plasterboard (base wall #5)		
External colour: Medium	Internal colour: Paint: light cream	Area: 0.2 m ²
External absorptance (%) : 50	Internal absorptance (%) : 30	
Layer	Material	Thickness (mm)
1	Brickwork: generic extruded clay brick (typical density)	110
2	Air gap vertical 31-65 mm (40 nominal) unventilated reflective (0.4/0.9; E = 0.38)	40
3	Rockwool batt (k = 0.033)	59



Construction details: External Doors		
Description: Timber (solid)		
External colour: Medium	Internal colour: Medium	Area: 1.7 m ²
External absorptance (%) : 50	Internal absorptance (%) : 50	
Layer	Material	Thickness (mm)
1	Timber (Mountain ash)	40

Description: Sub Floor Door		
External colour: Medium	Internal colour: Medium	Area: 0.4 m ²
External absorptance (%) : 50	Internal absorptance (%) : 50	
Layer	Material	Thickness (mm)
1	Plywood (softwood)	12

Construction details: Floor/Ceilings		
Description: Plasterboard 10 mm bridged		
Top colour: Medium	Bottom colour: Light	Area: 30.0 m ²
Top absorptance (%) : 50	Bottom absorptance (%) : 30	
Layer	Material	Thickness (mm)
1	Glass fibre batt (k = 0.044 density = 12 kg/m ³)	158
2	Plasterboard	10

Description: Bare ground		
Top colour: Medium	Bottom colour: Dark	Area: 33.4 m ²
Top absorptance (%) : 50	Bottom absorptance (%) : 85	
Layer	Material	Thickness (mm)
1	Ground	0



Figure A.47: AR2 Building report, page 2

	<p>AccuRate V1.1.4.1</p> <p>Nationwide House Energy Rating Scheme</p>	
Project Name: Test Cell 2		
File Name: F:\sabs uni		
files\AccuRate\AccuRate1.1.4.1\Projects\tc2_2013_05_14.PRO		
Postcode: 7250		Climate Zone: 23
Client Name:		
Site Address:		
Design Option: V2.0		
Date: 2/07/2013	Time: 12:34	Page: 3

Description: Particle Board Floor Bridged plus carpet & underlay		
Top colour: Medium	Bottom colour: Not Specified	Area: 30.0 m ²
Top absorptance (%): 50	Bottom absorptance (%): Not Specified	
Layer	Material	Thickness (mm)
1	Carpet 10 + rubber underlay 8	18
2	Particleboard	21

Construction details: Roofs		
Description: Metal deck		
External colour: Medium	Internal colour: Light	Area: 50.9 m ²
External absorptance (%): 50	Internal absorptance (%): 30	
Layer	Material	Thickness (mm)
1	Steel	1
2	Air gap 22.5° 31-65 mm (40 nominal) ventilated reflective (0.4/0.9; E = 0.38)	40

Figure A.48: AR2 Building report, page 3

	<h2 style="margin: 0;">AccuRate V1.1.4.1</h2> <h3 style="margin: 10px 0 0 0;">Nationwide House Energy Rating Scheme</h3>	
Project Name: Test Cell 2		
File Name: F:\sabs uni		
files\AccuRate\AccuRate1.1.4.1\Projects\tc2_2013_05_14.PRO		
Postcode: 7250		Climate Zone: 23
Client Name:		
Site Address:		
Design Option: V2.0		
Date: 2/07/2013		Time: 12:34
Page: 4		



Habitable zones						
Name	Type	Volume (m³)	Floor height (m)	Ceiling height above floor (m)	Heated	Cooled
Test cell	Living/Kitchen	73.3	0.6	2.4	Y	Y

Habitable zones (continued)									
Name	Chimneys		Wall/Ceiling vents	Exhaust fans		Vented downlights	Unflued gas heaters	Ceiling fans	Type
	U/S	S		U/S	S				
Test cell	0	0	0	0	0	0	0	0	-

Roofspace zones						
Name	Volume (m³)	Reflective	Sarking	Roof surface	Openness	
Roof Space	19.7	Y	Sarked	Continuous	Standard	

Sub-floor zones							
Name	Volume (m³)	Floor height (m)	Ceiling height above floor (m)	Reflective	Openness	Wall cavity	Vent area (mm²/m wall)
Sub Floor	20.0	0.0	0.6	N	Enclosed	N	6000.0

Figure A.49: AR2 Building report, page 4

	<h1 style="margin: 0;">AccuRate V1.1.4.1</h1> <h2 style="margin: 10px 0 0 0;">Nationwide House Energy Rating Scheme</h2>	
Project Name: Test Cell 2		
File Name: F:\sabs uni		
files\AccuRate\AccuRate1.1.4.1\Projects\tc2_2013_05_14.PRO		
Postcode: 7250		Climate Zone: 23
Client Name:		
Site Address:		
Design Option: V2.0		
Date: 2/07/2013		Time: 12:34
		Page: 5

Test cell: External walls main data									
Wall	Construction	Azi (deg.)	L (m)	H (m)	Area (gross) (m²)	Area (net) (m²)	Fixed shade	Opening (m²)	Opening Type
1	brick veneer framing factor East west no	0	5.40	2.44	13.18	13.18	Eave all	0.00	Controlled
2	brick veneer framing factor East west no	90	5.48	2.44	13.37	13.37	Eave all	0.00	Controlled
3	Brick veneer Wall Bridged South	180	5.40	2.44	13.18	11.45	Eave all	0.00	Controlled
4	brick veneer framing factor East west no	270	5.48	2.44	13.37	13.37	Eave all	0.00	Controlled
5	north wall without plasterboard (base wa	0	0.08	2.44	0.20	0.20	Eave all	0.00	Controlled
6	south wall without plasterboard (base wa	180	0.08	2.44	0.20	0.20	Eave all	0.00	Controlled



Test cell: External walls screen data						
Wall	Screen	Height (m)	Width (m)	Horizontal Offset (m)	Vertical Offset (m)	Monthly blocking factors
1	1	7.0	44.0	56.6	-1.6	100,100,100,100,100,100,100,100,100,100,100,100
1	2	4.2	5.8	1.0	-1.0	100,100,100,100,100,100,100,100,100,100,100,100
2	1	3.6	37.0	3.5	-0.6	100,100,100,100,100,100,100,100,100,100,100,100
2	2	3.6	12.0	15.0	-0.6	100,100,100,100,100,100,100,100,100,100,100,100
2	3	7.0	26.0	-22.5	-0.6	100,100,100,100,100,100,100,100,100,100,100,100
3	1	6.0	9.0	13.5	-0.6	95,95,95,95,95,95,95,95,95,95,95,95
3	2	11.0	21.0	-6.0	1.4	95,95,70,50,30,20,15,15,20,50,70,95
3	3	3.6	7.0	-1.0	-0.3	100,100,100,100,100,100,100,100,100,100,100,100
5	1	7.0	44.0	56.6	-1.6	100,100,100,100,100,100,100,100,100,100,100,100
5	2	4.2	5.8	1.0	-1.0	100,100,100,100,100,100,100,100,100,100,100,100
6	1	6.0	9.0	13.5	-6.0	95,95,95,95,95,95,95,95,95,95,95,95
6	2	11.0	21.0	-6.0	1.4	95,95,70,50,30,20,15,15,20,50,70,95
6	3	3.6	7.0	-1.0	-0.3	100,100,100,100,100,100,100,100,100,100,100,100

Test cell: Doors in walls										
Wall	Door Name	Construction	Azi (deg.)	H (m)	W (m)	Area (m²)	RO (m)	Openable (%)	Weather stripped	Gap size
3	Door 1	Timber(solid)	180	2.10	0.82	1.72	0.00	0	Y	M

Test cell: Floors							
Floor	Construction	Area (gross) (m²)	Area (net) (m²)	Under the floor	Edge Ins.	Opening (m²)	Opening Type
1	Particle Board Floor Bridged plus carpet & um	30.0	30.0	Sub Floor		0.00	Controlled

Test cell: Ceilings						
Ceiling	Construction	Area (gross) (m²)	Area (net) (m²)	Above the ceiling	Opening (m²)	Opening Type
1	Plasterboard 10 mm bridged	30.0	30.0	Roof Space	0.00	Controlled



Figure A.50: AR2 Building report, page 5

	<h2 style="margin: 0;">AccuRate V1.1.4.1</h2> <h3 style="margin: 10px 0 0 0;">Nationwide House Energy Rating Scheme</h3>	
Project Name: Test Cell 2		
File Name: F:\sabs uni		
files\AccuRate\AccuRate1.1.4.1\Projects\tc2_2013_05_14.PRO		
Postcode: 7250		Climate Zone: 23
Client Name:		
Site Address:		
Design Option: V2.0		
Date: 2/07/2013		Time: 12:34
Page: 6		

Roof Space: Floors							
Floor	Construction	Area (gross) (m²)	Area (net) (m²)	Under the floor	Edge Ins.	Opening (m²)	Opening Type
1	Plasterboard 10 mm bridged	30.0	30.0	Test cell		0.00	Controlled

Roof Space: Roofs						
Roof	Construction	Area (gross) (m²)	Area (net) (m²)	Azi (deg.)	Pitch (deg.)	Exposure
1	Metal deck	12.73	12.73	0	23	Normal
2	Metal deck	12.73	12.73	90	23	Normal
3	Metal deck	12.73	12.73	180	23	Normal
4	Metal deck	12.73	12.73	270	23	Normal

Figure A.51: AR2 Building report, page 6

	<h1 style="margin: 0;">AccuRate V1.1.4.1</h1> <h2 style="margin: 10px 0 0 0;">Nationwide House Energy Rating Scheme</h2>	
Project Name: Test Cell 2		
File Name: F:\sabs uni		
files\AccuRate\AccuRate1.1.4.1\Projects\tc2_2013_05_14.PRO		
Postcode: 7250		Climate Zone: 23
Client Name:		
Site Address:		
Design Option: V2.0		
Date: 2/07/2013		Time: 12:34
		Page: 7

Sub Floor: External walls main data									
Wall	Construction	Azi (deg.)	L (m)	H (m)	Area (gross) (m²)	Area (net) (m²)	Fixed shade	Opening (m²)	Opening Type
1	Sub floor wall	0	5.78	0.60	3.47	3.04	Sub floor	0.00	Controlled
2	Sub floor wall	90	5.78	0.60	3.47	3.47	Sub floor	0.00	Controlled
3	Sub floor wall	180	5.78	0.60	3.47	3.47	Sub floor	0.00	Controlled
4	Sub floor wall	270	5.78	0.60	3.47	3.47	Sub floor	0.00	Controlled



Sub Floor: External walls screen data						
Wall	Screen	Height (m)	Width (m)	Horizontal Offset (m)	Vertical Offset (m)	Monthly blocking factors
1	1	7.0	44.0	55.6	-1.0	100,100,100,100,100,100,100,100,100,100,100
1	2	4.2	5.8	1.0	-0.4	100,100,100,100,100,100,100,100,100,100,100
2	1	3.6	37.0	3.5	0.0	100,100,100,100,100,100,100,100,100,100,100
2	2	3.6	12.0	15.0	0.0	100,100,100,100,100,100,100,100,100,100,100
2	3	7.0	26.0	-22.5	0.0	100,100,100,100,100,100,100,100,100,100,100
3	1	6.0	9.0	13.5	0.0	95,95,95,95,95,95,95,95,95,95,95
3	2	11.0	21.0	-6.0	2.0	95,95,70,50,30,20,15,15,20,50,70,95
3	3	3.6	7.0	-1.0	0.3	100,100,100,100,100,100,100,100,100,100,100

Sub Floor: Doors in walls										
Wall	Door Name	Construction	Azi (deg.)	H (m)	W (m)	Area (m²)	HO (m)	Openable (%)	Weather stripped	Gap size
1	subfloor	Sub Floor Door	0	0.60	0.72	0.43	0.00	90	N	L

Sub Floor: Floors							
Floor	Construction	Area (gross) (m²)	Area (net) (m²)	Under the floor	Edge Ins.	Opening (m²)	Opening Type
1	Bare ground	33.4	33.4	Ground		0.00	Controlled

Sub Floor: Ceilings						
Ceiling	Construction	Area (gross) (m²)	Area (net) (m²)	Above the ceiling	Opening (m²)	Opening Type
1	Particle Board Floor Bridged plus carpet & um	30.0	30.0	Test cell	0.00	Controlled

Figure A.52: AR2 Building report, page 7

	<p style="text-align: center;">AccuRate V1.1.4.1</p> <p style="text-align: center;">Nationwide House Energy Rating Scheme</p>	
Project Name: Test Cell 2		
File Name: F:\sabs uni		
files\AccuRate\AccuRate1.1.4.1\Projects\tc2_2013_05_14.PRO		
Postcode: 7250	Climate Zone: 23	
Client Name:		
Site Address:		
Design Option: V2.0		
Date: 2/07/2013	Time: 12:34	Page: 8

Shading Schemes					
Name	Eaves		Other fixed shading		
	Projection (m)	Offset (m)	Projection (m)	Offset (m)	Monthly blocking factors (%)
Eave all	0.58	0.00	0.00	0.00	100,100,100,100,100,100,100,100,100,100,100
Sub floor	0.58	2.40	0.00	0.00	100,100,100,100,100,100,100,100,100,100,100

Ventilation			
Footprint: vertical dimension (m)	Footprint: horizontal dimension (m)	Azimuth of highlighted facade (degree)	Insect screens
5.9	5.9	0	N

Figure A.53: AR2 Building report, page 8


```

C Horizontal shading schemes. 999 maximum
C Scheme no., eave proj., eave offset, pergola proj, pergola offset, pergola shading factors
C
  EaveP EaveO PergP PergO
1 20 1 0.58 0.00 0.00 0.00 1.00 1.00 1.00 1.00 1.00 1.00 1.00 1.00 1.00 1.00
1 20 2 0.58 0.00 0.00 0.00 1.00 1.00 1.00 1.00 1.00 1.00 1.00 1.00 1.00 1.00
1 20 3 0.58 0.00 0.00 0.00 1.00 1.00 1.00 1.00 1.00 1.00 1.00 1.00 1.00 1.00
1 20 4 0.58 0.34 0.00 0.00 1.00 1.00 1.00 1.00 1.00 1.00 1.00 1.00 1.00 1.00
1 20 5 0.58 0.00 0.00 0.00 1.00 1.00 1.00 1.00 1.00 1.00 1.00 1.00 1.00 1.00
1 20 6 0.58 0.00 0.00 0.00 1.00 1.00 1.00 1.00 1.00 1.00 1.00 1.00 1.00 1.00
1 20 7 0.58 0.00 0.00 0.00 1.00 1.00 1.00 1.00 1.00 1.00 1.00 1.00 1.00 1.00
1 20 8 0.58 2.40 0.00 0.00 1.00 1.00 1.00 1.00 1.00 1.00 1.00 1.00 1.00 1.00
1 20 9 0.58 2.40 0.00 0.00 1.00 1.00 1.00 1.00 1.00 1.00 1.00 1.00 1.00 1.00
1 20 10 0.58 2.40 0.00 0.00 1.00 1.00 1.00 1.00 1.00 1.00 1.00 1.00 1.00 1.00
1 20 11 0.58 2.40 0.00 0.00 1.00 1.00 1.00 1.00 1.00 1.00 1.00 1.00 1.00 1.00
1 20 12 0.58 2.40 0.00 0.00 1.00 1.00 1.00 1.00 1.00 1.00 1.00 1.00 1.00 1.00
C
C Vertical shading schemes. 999 maximum
C Left proj., left offset, right proj., right offset
C
  LeftP LeftRightRightO
C Screen schemes. 20 maximum
C Scheme no., screen height, width, distance, offset horiz, offset vert, shading factors
C
  Height Width Dist OffH OffV
1 22 1 7.0 44.0 35.5 56.6 -1.6 1.00 1.00 1.00 1.00 1.00 1.00 1.00 1.00 1.00
1 22 2 4.2 5.8 7.5 1.0 -1.0 1.00 1.00 1.00 1.00 1.00 1.00 1.00 1.00 1.00
1 22 3 3.6 37.0 66.0 3.5 -0.6 1.00 1.00 1.00 1.00 1.00 1.00 1.00 1.00 1.00
1 22 4 3.6 12.0 50.0 15.0 -0.6 1.00 1.00 1.00 1.00 1.00 1.00 1.00 1.00 1.00
1 22 5 7.0 26.0 25.0 -22.5 -0.6 1.00 1.00 1.00 1.00 1.00 1.00 1.00 1.00 1.00
1 22 6 6.0 9.0 17.0 13.5 -0.6 0.95 0.95 0.95 0.95 0.95 0.95 0.95 0.95 0.95
1 22 7 6.0 9.0 17.0 13.5 -0.6 0.95 0.95 0.95 0.95 0.95 0.95 0.95 0.95 0.95
1 22 8 11.0 21.0 19.0 -6.0 1.4 0.95 0.95 0.70 0.50 0.30 0.20 0.15 0.15 0.20 0.50 0.70 0.95
1 22 9 11.0 21.0 19.0 -6.0 1.4 0.95 0.95 0.70 0.50 0.30 0.20 0.15 0.15 0.20 0.50 0.70 0.95
1 22 10 3.6 7.0 7.5 -1.0 -0.3 1.00 1.00 1.00 1.00 1.00 1.00 1.00 1.00 1.00
1 22 11 3.6 7.0 7.5 -1.0 -0.3 1.00 1.00 1.00 1.00 1.00 1.00 1.00 1.00 1.00
1 22 12 7.0 44.0 35.5 56.6 -1.6 1.00 1.00 1.00 1.00 1.00 1.00 1.00 1.00 1.00
1 22 13 4.2 5.8 7.5 1.0 -1.0 1.00 1.00 1.00 1.00 1.00 1.00 1.00 1.00 1.00
1 22 14 6.0 9.0 17.0 13.5 -6.0 0.95 0.95 0.95 0.95 0.95 0.95 0.95 0.95 0.95
1 22 15 11.0 21.0 19.0 -6.0 1.4 0.95 0.95 0.70 0.50 0.30 0.20 0.15 0.15 0.20 0.50 0.70 0.95
1 22 16 3.6 7.0 7.5 -1.0 -0.3 1.00 1.00 1.00 1.00 1.00 1.00 1.00 1.00 1.00
1 22 17 7.0 44.0 35.5 55.6 -1.0 1.00 1.00 1.00 1.00 1.00 1.00 1.00 1.00 1.00
1 22 18 7.0 44.0 35.5 55.6 -1.0 1.00 1.00 1.00 1.00 1.00 1.00 1.00 1.00 1.00
1 22 19 4.2 5.8 7.5 1.0 -0.4 1.00 1.00 1.00 1.00 1.00 1.00 1.00 1.00 1.00
1 22 20 4.2 5.8 7.5 1.0 -0.4 1.00 1.00 1.00 1.00 1.00 1.00 1.00 1.00 1.00
1 22 21 3.6 37.0 66.0 3.5 0.0 1.00 1.00 1.00 1.00 1.00 1.00 1.00 1.00 1.00
1 22 22 3.6 12.0 50.0 15.0 0.0 1.00 1.00 1.00 1.00 1.00 1.00 1.00 1.00 1.00
1 22 23 7.0 26.0 25.0 -22.5 0.0 1.00 1.00 1.00 1.00 1.00 1.00 1.00 1.00 1.00
1 22 24 6.0 9.0 17.0 13.5 0.0 0.95 0.95 0.95 0.95 0.95 0.95 0.95 0.95 0.95
1 22 25 11.0 21.0 19.0 -6.0 2.0 0.95 0.95 0.70 0.50 0.30 0.20 0.15 0.15 0.20 0.50 0.70 0.95
1 22 26 3.6 7.0 7.5 -1.0 0.3 1.00 1.00 1.00 1.00 1.00 1.00 1.00 1.00 1.00
C

```

Figure A.55: AR2 Scratch file, page 2


```

C
C
CCCCCCCCCCCCCCCCCCCCCCCCCCCCCCCCCCCCCCCCCCCCCCCCCCCCCCCCCCCC
C
C Data type 3: Zone data
C
C
C
C Zone 1
C
C Name, volume, infiltration data, wind speed reduction factor, type, SHG dist. fractions
C      Name Vol A B WsRed Type EstSG
C 3 1 Test cell 73.3 0.00 0.03 0.67Normal 1
C Windows
C      Height Width AzimHSSch1HSSch2VShSchScSch1ScSch2ScSch3 Curtn Blind
C Doors
C      Height Width NArea Azim AbsE AbsI EmissHShSchVShSchScSch1ScSch2ScSch3SHGFra
C 3 1 28 2.10 0.82 1.72 180 0.50 0.50 1.00 4 0 7 9 11
C OpaqueLouvres
C      Height Width NArea Azim AbsE AbsI EmissHShSchVShSchScSch1ScSch2ScSch3SHGFraLouvre
C Walls
C      Height Width NArea Azim AbsE AbsI EmissHShSchVShSchScSch1ScSch2ScSch3SHGFra
C 3 1 22 2.44 5.40 13.18 0 0.50 0.30 1.00 1 0 1 2 0
C 3 1 22 2.44 5.48 13.37 90 0.50 0.30 1.00 2 0 3 4 5
C 3 1 23 2.44 5.40 11.45 180 0.50 0.30 1.00 3 0 6 8 10
C 3 1 22 2.44 5.48 13.37 270 0.50 0.30 1.00 5 0 0 0 0
C 3 1 24 2.44 0.08 0.20 0 0.50 0.30 1.00 6 0 12 13 0
C 3 1 25 2.44 0.08 0.20 180 0.50 0.30 1.00 7 0 14 15 16
C Floors, Ceilings, Partitions
C      Area AbsI AdjZ SHGF
C 3 1 54 30.03 0.50 6
C 3 1 83 30.03 0.30 5
C
C Sensible internal heat gain (watts), [hours 1-12]
C 3 1401 30 30 30 30 30 30 30 30 30 30 30 30
C Sensible internal heat gain (watts), [hours 13-24]
C 3 1402 30 30 30 30 30 30 30 30 30 30 30 30
C Latent internal heat gain (watts), [hours 1-12]
C 3 1403 0 0 0 0 0 0 0 0 0 0 0 0
C Latent internal heat gain (watts), [hours 13-24]
C 3 1404 0 0 0 0 0 0 0 0 0 0 0 0
C
C Heating thermostat settings [hours 1-12]
C 3 1501 0.0 0.0 0.0 0.0 0.0 0.0 0.0 0.0 0.0 0.0 0.0
C Heating thermostat settings [hours 13-24]
C 3 1502 0.0 0.0 0.0 0.0 0.0 0.0 0.0 0.0 0.0 0.0 0.0
C Cooling thermostat settings [hours 1-12]
C 3 1503 0.0 0.0 0.0 0.0 0.0 0.0 0.0 0.0 0.0 0.0 0.0
C Cooling thermostat settings [hours 13-24]
C 3 1504 0.0 0.0 0.0 0.0 0.0 0.0 0.0 0.0 0.0 0.0 0.0
C
C Indoor covering closing & opening times, drawing temp, drawing solar for windows
C 3 1601 18 7 25.0 200.0
C Indoor covering closing & opening times, drawing temp, drawing solar for roof windows
C 3 1602 18 7 25.0 200.0
C Outdoor covering drawing temp, drawing solar for windows
C 3 1603 22.5 75.0
C Outdoor covering drawing temp, drawing solar for skylights and roof windows
C 3 1604 22.5 75.0
C Ventilation on & off times, on & off temps, A factor, B factor
C 3 1605 0 24 22.5 22.0 0.0 0.0
C
C

```

Figure A.57: AR2 Scratch file, page 4

```

C Zone 2
C
C Name, volume, infiltration data, wind speed reduction factor, type, SHG dist. fractions
C      Name Vol A B WsRed Type EstSG CeilZ RoofZ REmis
3 2      Roof Space 19.7 0.40 0.34 0.67RoofSA 1 5 4 0.05
C Skylights
C      Area Azim Slope ShadI ShadEZonlit ShLenShAreaShRef1 ShRes Diff VArea VType
C Roofs
C      Area Azim Slope AbsE AbsI Emiss SHGFra
C Floors, Ceilings, Partitions
C      Area AbsI AdjZ SHGF
3 2 51 30.03 0.50 5
3 2111 52.00 0.50 4
C
C
C Zone 3
C
C Name, volume, infiltration data, wind speed reduction factor, type, SHG dist. fractions
C      Name Vol A B WsRed Type EstSG FlorZ GrndZ REmis
3 3      Sub Floor 20.0 3.29 2.53 0.67SubFlA 1 6 7 0.82
C Windows
C      Height Width AzimHSSch1HSSch2VShSchScSch1ScSch2ScSch3 Curtn Blind
C Doors
C      Height Width NArea Azim AbsE AbsI EmissHShSchVShSchScSch1ScSch2ScSch3SHGFra
3 3 29 0.60 0.72 0.43 0 0.50 0.50 1.00 9 0 18 20 0
C OpaqueLouvres
C      Height Width NArea Azim AbsE AbsI EmissHShSchVShSchScSch1ScSch2ScSch3SHGFraLouvre
C Walls
C      Height Width NArea Azim AbsE AbsI EmissHShSchVShSchScSch1ScSch2ScSch3SHGFra
3 3 21 0.60 5.78 3.04 0 0.50 0.50 1.00 8 0 17 19 0
3 3 21 0.60 5.78 3.47 90 0.50 0.50 1.00 10 0 21 22 23
3 3 21 0.60 5.78 3.47 180 0.50 0.50 1.00 11 0 24 25 26
3 3 21 0.60 5.78 3.47 270 0.50 0.50 1.00 12 0 0 0 0
C Floors, Ceilings, Partitions
C      Area AbsI AdjZ SHGF
3 3 82 30.03 0.50 6
3 3113 30.03 0.50 7
C
C
C Zone 4
C
C Name, volume, infiltration data, wind speed reduction factor, type, SHG dist. fractions
C      Name Vol A B WsRed Type EstSG
3 4      Underside of Ro 0.0 0.00 0.00 0.67Normal 1 1
C Skylights
C      Area Azim Slope ShadI ShadEZonlit ShLenShAreaShRef1 ShRes Diff VArea VType
C Roofs
C      Area Azim Slope AbsE AbsI Emiss SHGFra
C Floors, Ceilings, Partitions
C      Area AbsI AdjZ SHGF
3 4111 52.00 0.50 2
3 4112 30.03 0.50 5
3 4116 12.73 0.50 9
3 4116 12.73 0.50 11
3 4116 12.73 0.50 13
3 4116 12.73 0.50 15
C
C
C Zone 5
C
C Name, volume, infiltration data, wind speed reduction factor, type, SHG dist. fractions
C      Name Vol A B WsRed Type EstSG
3 5      Top of Ceilings 0.0 0.00 0.00 0.67Normal 1 1
C Floors, Ceilings, Partitions
C      Area AbsI AdjZ SHGF
3 5 53 30.03 0.50 1
3 5 81 30.03 0.50 2
3 5112 30.03 0.50 4
C
C

```

Figure A.58: AR2 Scratch file, page 5

```

C Zone 6
C
C Name, volume, infiltration data, wind speed reduction factor, type, SHG dist. fractions
C      Name Vol A B WsRed Type EstSG
3 6 Underside of fl 0.0 0.00 0.00 0.67Normal 1 1
C Floors, Ceilings, Partitions
C      Area AbsI AdjZ SHGF
3 6 52 30.03 0.50 3
3 6 84 30.03 0.50 1
3 6 114 30.03 0.50 7
C
C
C Zone 7
C
C Name, volume, infiltration data, wind speed reduction factor, type, SHG dist. fractions
C      Name Vol A B WsRed Type EstSG
3 7 Top of ground 0.0 0.00 0.00 0.67Normal 1 1
C Floors, Ceilings, Partitions
C      Area AbsI AdjZ SHGF
3 7 41 30.03 0.50
3 7 113 30.03 0.50 3
3 7 114 30.03 0.50 6
C
C
C Zone 8
C
C Name, volume, infiltration data, wind speed reduction factor, type, SHG dist. fractions
C      Name Vol A B WsRed Type EstSG BotZ
3 8 Air Gap Top 1 0.0 0.00 0.00 0.67AirGpT 1 9 1
C Skylights
C      Area Azim Slope ShadI ShadEZonlit ShLenShAreaShRefl ShRes Diff VArea VType
C Roofs
C      Area Azim Slope AbsE AbsI Emiss SHGFra
3 8 31 12.73 0 23 0.50 0.50 0.90
C Floors, Ceilings, Partitions
C      Area AbsI AdjZ SHGF
3 8 115 12.73 0.50 9
C
C
C Zone 9
C
C Name, volume, infiltration data, wind speed reduction factor, type, SHG dist. fractions
C      Name Vol A B WsRed Type EstSG
3 9 Air Gap Bot 1 0.0 0.00 0.00 0.67Normal 1 1
C Floors, Ceilings, Partitions
C      Area AbsI AdjZ SHGF
3 9 116 12.73 0.50 4
3 9 115 12.73 0.50 8
C
C
C Zone 10
C
C Name, volume, infiltration data, wind speed reduction factor, type, SHG dist. fractions
C      Name Vol A B WsRed Type EstSG BotZ
3 10 Air Gap Top 2 0.0 0.00 0.00 0.67AirGpT 1 11 1
C Skylights
C      Area Azim Slope ShadI ShadEZonlit ShLenShAreaShRefl ShRes Diff VArea VType
C Roofs
C      Area Azim Slope AbsE AbsI Emiss SHGFra
3 10 31 12.73 90 23 0.50 0.50 0.90
C Floors, Ceilings, Partitions
C      Area AbsI AdjZ SHGF
3 10 115 12.73 0.50 11
C
C

```

Figure A.59: AR2 Scratch file, page 6

```

C Zone 11
C
C Name, volume, infiltration data, wind speed reduction factor, type, SHG dist. fractions
C      Name Vol A B WsRed Type EstSG
3 11 Air Gap Bot 2 0.0 0.00 0.00 0.67Normal 1 1
C Floors, Ceilings, Partitions
C      Area AbsI AdjZ SHGF
3 11116 12.73 0.50 4
3 11115 12.73 0.50 10
C
C
C Zone 12
C
C Name, volume, infiltration data, wind speed reduction factor, type, SHG dist. fractions
C      Name Vol A B WsRed Type EstSG BotZ
3 12 Air Gap Top 3 0.0 0.00 0.00 0.67AirGpT 1 13 1
C Skylights
C      Area Azim Slope ShadI ShadEZonlit ShLenShAreaShRefl ShRes Diff VArea VType
C Roofs
C      Area Azim Slope AbsE AbsI Emiss SHGFra
3 12 31 12.73 180 23 0.50 0.50 0.90
C Floors, Ceilings, Partitions
C      Area AbsI AdjZ SHGF
3 12115 12.73 0.50 13
C
C
C Zone 13
C
C Name, volume, infiltration data, wind speed reduction factor, type, SHG dist. fractions
C      Name Vol A B WsRed Type EstSG
3 13 Air Gap Bot 3 0.0 0.00 0.00 0.67Normal 1 1
C Floors, Ceilings, Partitions
C      Area AbsI AdjZ SHGF
3 13116 12.73 0.50 4
3 13115 12.73 0.50 12
C
C
C Zone 14
C
C Name, volume, infiltration data, wind speed reduction factor, type, SHG dist. fractions
C      Name Vol A B WsRed Type EstSG BotZ
3 14 Air Gap Top 4 0.0 0.00 0.00 0.67AirGpT 1 15 1
C Skylights
C      Area Azim Slope ShadI ShadEZonlit ShLenShAreaShRefl ShRes Diff VArea VType
C Roofs
C      Area Azim Slope AbsE AbsI Emiss SHGFra
3 14 31 12.73 270 23 0.50 0.50 0.90
C Floors, Ceilings, Partitions
C      Area AbsI AdjZ SHGF
3 14115 12.73 0.50 15
C
C
C Zone 15
C
C Name, volume, infiltration data, wind speed reduction factor, type, SHG dist. fractions
C      Name Vol A B WsRed Type EstSG
3 15 Air Gap Bot 4 0.0 0.00 0.00 0.67Normal 1 1
C Floors, Ceilings, Partitions
C      Area AbsI AdjZ SHGF
3 15116 12.73 0.50 4
3 15115 12.73 0.50 14
C

```

9

Figure A.60: AR2 Scratch file, page 7

```
#####
##
## ana_climate.R
##
## February 25 2013, Sabrina Sequeira
##
## Creates the climate file for AccuRate
##
## Input: data06.csv
##         climate23_long.txt
##
## Output: climateNA.csv
##          climate_site1
##          climate_site2.txt
##          climate_tp1.txt, climate_tp2.txt, climate_tp3.txt
##
## How it works:
## The best data with calculations is loaded into tc.df.
## Then parameters are added into climate.df in certain order
## and formatted as needed to match the AccuRate climate file.
## Then climate_site1.txt is created, which may contain NAs.
## Stats on this file are shown. The file climateNA.csv is
## created. This shows each date and then TRUE if there are
## any NAs in the observed data. Then climate_site2.txt is
## created. This file replaces any row with observed NA data
## with the original AccuRate climate data for that same row.
##
#####

# set working directory
setwd("F:/sabs uni files/project/test cell data/scripts")

# load in the test cell data into a data frame
tc.df <- read.csv("data06.csv", sep=",", header=T)

# Must install package chron and then load into library. Only once.
library(chron)
# Change time zone to GMT-10 to ignore DST. All calcs in current time zone.
Sys.setenv(tz='Etc/GMT-10')

tc.df$DTconvert <- strptime(as.character(tc.df$DateTime), "%Y/%m/%d %H:%M")
tc.df$dnt <- as.POSIXct(tc.df$DTconvert)

# Define climate data frame.
climate.df <- data.frame(vector(mode="character", length = nrow(tc.df)))
# Define other things
flag1 <- "111111"
flag2 <- "111"
yrstart <- "20      " ;# putting six extra spaces at the end of the file
```

Figure A.61: ana_climate.R, page 1

```

# Calculate and format things for climate file
climate.df$loc <- "LT" ;# LT is location for Launceston
climate.df$yrend <- as.character(tc.df$dnt,format="%y") ;# year, last two digits
climate.df$mon <- as.character(tc.df$dnt,format="%m");# month, two digits, prec. zeros
climate.df$day <- as.character(tc.df$dnt,format="%d");# day, two digits, prec. zeros
climate.df$hour <- formatC(tc.df$hour,width=2);# day, two spaces, no preceding zeros
tc.df$temp1 <- round(tc.df$TA10*10) ;# temp [1/10 degs]
climate.df$temp <- formatC(tc.df$temp1,format="d",width=4) ;# temp [1/10 degs] 4 spaces
tc.df$specum1 <- round(tc.df$wos*10000) ;# spec hum [1/10 g/kg]
climate.df$specum <- formatC(tc.df$specum1,format="d",width=3) ;# temp [1/10 g/kg] as int
tc.df$pres <- round(tc.df$ptc*10) ;# pressure [mbar]
climate.df$pres <- formatC(tc.df$pres,format="d",width=4) ;# pressure [mbar] as integer
tc.df$spd1 <- round(tc.df$windmet*10) ;# windspeed [1/10 m/s]
climate.df$spd <- formatC(tc.df$spd1,format="d",width=3) ;# windspeed [1/10 m/s] as integer

```

Figure A.62: ana_climate.R, page 2

```

climate.df$dir <- formatC(tc.df$windbin,width=2);# wind dir 16tant, two spaces, no prec zeros
climate.df$cloud <- formatC(tc.df$cloud,width=1);# cloud cover, one space
climate.df$flag1 <- flag1
tc.df$global <- tc.df$A14*1000 ;# global solar radiation [W/m2]
climate.df$global <- formatC(tc.df$global,format="d",width=4);# global solar radiation [W/m2]
tc.df$diffrad <- tc.df$Diffuse*1000 ;# diffuse solar radiation [W/m2]
climate.df$diffuse <- formatC(tc.df$diffrad,format="d",width=3);# diffuse solar rad [W/m2]
tc.df$dirrad <- tc.df$Direct*1000 ;# direct solar radiation [W/m2]
climate.df$direct <- formatC(tc.df$dirrad,format="d",width=4);# diffuse solar radiation [W/m2]
climate.df$salt <- formatC(tc.df$Solaralt,width=2);# solar altitude [degs], two spaces
climate.df$azi <- formatC(tc.df$Solarazi,width=3);# solar azimuth[degs], three spaces
climate.df$flag2 <- flag2
climate.df$ystart <- yrstart

# write out climate data to climate_sitel.txt
write.table(climate.df,file=paste("climate_sitel.txt"),quote=FALSE,sep=" ",
            col.names=FALSE,row.names=FALSE)

# Note any rows where the climate.df inputs are NA. Output to climateNA.csv
output.df <- data.frame(tc.df$DateTime)
colnames(output.df) <- c("DateTime")
output.df$climateNA <- FALSE
for (j in 1:length(climate.df[,1]))
{
  output.df$climateNA[j]<-(!("NA"%in%climate.df[j,])|(" NA"%in%climate.df[j,]))
}
write.table(output.df,file=paste("climateNA.csv"),quote=FALSE,sep=" ",row.names=FALSE)

# Print out stats on climate file
paste("Of ",length(output.df$climateNA)," rows of data,")
paste(sum(output.df$climateNA)," are missing weather parameters and need replacement")

```


Figure A.63: ana_climate.R, page 3

```
# load in the climateNA.csv if starting from here
# output.df <- read.csv("climateNA.csv",sep=" ",header=T)

# For each row where climateNA is T, replace observed data with AccuRate climate
# First read in climate_site1.txt and climate23_long.txt
long.df <- read.fwf("climate23_long.txt",widths=c(10,50),header=F,as.is=T)
obs.df <- read.fwf("climate_site1.txt",widths=c(10,50),header=F,as.is=T)
# Only replace after the data & time because AccuRate climate has no Feb29th
# So keep the test cell date & time.
for (j in 1:length(climate.df[,1]))
{
  if (output.df$climateNA[j]) obs.df$V2[j] <- as.character(long.df$V2[j])
}

# Output the climate data without NAs to climate_site2.txt
write.table(obs.df,file=paste("climate_site2.txt"),quote=FALSE,sep=" ",
           col.names=FALSE,row.names=FALSE)

# Output the climate data into different runs for AccuRate
write.table(obs.df[1:8728,],file=paste("climate_tp1.txt"),quote=FALSE,sep=" ",
           col.names=FALSE,row.names=FALSE)
write.table(obs.df[8729:9420,],file=paste("climate_tp2.txt"),quote=FALSE,sep=" ",
           col.names=FALSE,row.names=FALSE)
write.table(obs.df[9421:13609,],file=paste("climate_tp3.txt"),quote=FALSE,sep=" ",
           col.names=FALSE,row.names=FALSE)
# tp1 is rows 1 to 8728 (Contains notes 014 and 015)
# tp2 is rows 8729 to 9420 (Contains note 015 but not 014)
# tp3 is rows 9421 to 13609 (contains neither 014 nor 015)
```

Figure A.64: ana_climate.R, page 4

```

LT110224 0 118 561003 17165111111 0 0 0 0 011119
LT110224 1 114 571003 0 051111111 0 0 0 0 011119
LT110224 2 109 591003 0 071000000 0 0 0 0 011119
LT110224 3 104 601003 0 051111111 0 0 0 0 011119
LT110224 4 99 611003 0 051111111 0 0 0 0 011119
LT110224 5 97 591003 0 061000000 0 0 0 0 011119
LT110224 6 98 631004 0 051111111 17 14 7 4 9911119
LT110224 7 104 631004 0 041111111 149 89 22015 8911119
LT110224 8 120 691005 0 050000000 347108 60826 7911119
LT110224 9 133 611005 0 041111111 540109 77437 6711119
LT11022410 154 591005 41153111111 682132 79446 5211119
LT11022411 176 511004 62157100000 762173 74754 3211119
LT11022412 196 551004 58153111111 795207 70158 611119
LT11022413 245 791012 14124111111 887 010705633911120
LT11022414 217 841011 40124111111 396338 765031611120
LT11022415 214 941011 33134111111 358313 694129911120
LT11022416 200 951010 31144111111 209193 313128611120
LT11022417 194 941011 31134111111 170153 512027511120
LT11022418 189 911011 24144111111 69 64 33 926511120
LT11022419 178 871012 6 441111111 7 0 401 125911120
LT11022420 176 721013 19 541111111 0 0 0 0 011120
LT11022421 170 721013 29 541111111 0 0 0 0 011120
LT11022422 153 731013 7 441111111 0 0 0 0 011120
LT11022423 128 711013 2 441111111 0 0 0 0 011120
LT110225 0 120 721013 0 441111111 0 0 0 0 011120
LT110225 1 140 451005 0 051111111 0 0 0 0 011119
LT110225 2 136 471005 0 051000000 0 0 0 0 011119
LT110225 3 114 751013 8 441111111 0 0 0 0 011120
LT110225 4 120 481005 0 041111111 0 0 0 0 011119
LT110225 5 99 691013 1 441111111 0 0 0 0 011120
LT110225 6 98 701014 1 441111111 42 20 323 4 9811120
LT110225 7 126 821014 11441111111 163 94 26515 8911120
LT110225 8 175 891015 16 441111111 459 84 85526 7911120
LT110225 9 222 841014 15 641111111 613115 82837 6711120
LT11022510 255 711014 9 341111111 754141 85346 5211120
LT11022511 256 701014 23134111111 893165 90054 3211120
LT11022512 225 801013 29144111111 526378 17757 611120
LT11022513 215 831013 40134111111 356308 585633911120
LT11022514 222 881012 54134111111 716267 5865031711120
LT11022515 231 861011 60134111111 628180 6824130011120
LT11022516 224 891011 44134111111 491140 6823128611120
LT11022517 216 891011 55134111111 274128 4282027511120
LT11022518 201 901011 58134111111 81 64 124 826511120
LT11022519 184 911011 33144111111 8 0 458 125911120
LT11022520 172 921012 19144111111 0 0 0 0 011120
LT11022521 161 931012 24134111111 0 0 0 0 011120
LT11022522 156 941012 19134111111 0 0 0 0 011120
LT11022523 153 941012 91341111111 0 0 0 0 011120
LT110226 0 142 901012 3 441111111 0 0 0 0 011120
LT110226 1 134 891011 4 341111111 0 0 0 0 011120
LT110226 2 141 931010 2 441111111 0 0 0 0 011120
LT110226 3 140 931009 3 441111111 0 0 0 0 011120
LT110226 4 134 901009 3 441111111 0 0 0 0 011120
LT110226 5 130 891009 4 541111111 0 0 0 0 011120
LT110226 6 126 871009 7 441111111 26 24 25 4 9811120
LT110226 7 140 941009 6 441111111 90 84 2314 8911120
LT110226 8 1681021008 41141111111 197176 4726 7811120
LT110226 9 1901031008 29124111111 472295 30136 6611120
LT11022610 208 991007 32124111111 618325 40846 5111120
LT11022611 220 921007 41124111111 667358 38753 3111120
LT11022612 225 921006 41124111111 849318 63357 611120
LT11022613 229 941005 48124111111 486397 1085633911120
LT11022614 218 931005 43134111111 285267 235031711120
LT11022615 200 971005 51134111111 170164 94130011120
LT11022616 187 951004 45134111111 100 97 53028711120

```

Figure A.65: AR1 and AR2 Climate file, first page

A.4 AccuRate data reduction

These files reduce the AccuRate data set and make the data comparable to the observed data set. The script `acc_check.R` provided in Figure A.66 expunges the AccuRate output data from any date and time when the observed weather data was missing. The data is also cleared for the following 12 hours as well. The script `acc_maxmin.R` provided in Figure A.67 and Figure A.68 calculates the daily extrema for the test cell and subfloor zone temperatures.

```
#####
##
## acc_check.R
##
## May 14 2013, Sabrina Sequeira
##
## Takes the AccuRate output, removes NA rows and adds Date&Time
## Also removes 12 hours after the last NA
##
## Inputs: data06.csv (output from the ana_calcs.R program)
##          tc2_2013_05_14_V2.0.tem (output from Accurate program)
##          climateNA.csv (rows with NA in AccuRate climate input)
##
## Output: acc_V2.0.csv (AccuRate data with NAs removed)
##
## To-do:
##          search on "Need"
##          change V1.0 to V2.0 to V3.0 as needed
##
#####

# set working directory
setwd("F:/sabs uni files/project/test cell data/scripts")

# Install packages. Then load into library. Only once per computer.
library(chron)

# Change time zone to GMT-10 to ignore DST. All calcs done in current time zone.
Sys.setenv(tz='Etc/GMT-10')

# load in the test cell data
tc.df <- read.csv("data06.csv",sep=",",header=T)
# load in the AccuRate data
acc.df <- read.table("tc2_2013_05_14_V2.0.tem",sep="",header=F,skip=4)
# load in climate NA data
climateNA.df <- read.csv("climateNA.csv",sep=",",header=T)

# assign column names to AccuRate data
colnames(acc.df) <- c("Month","Day","Hour","Outdoor","TestCell","RoofSpace","Subfloor")

# Add an ending row if needed to acc.df to get to 13609 lines
newrow = c(NA)
acc.df = rbind(acc.df,newrow)

# nrow(tc.df); # should have 13609 lines now

## Remove NAs based on climateNA.csv, for current hour and 12 hours ahead
for (j in 1:length(acc.df[,1]))
{
  jend<-min(j+12,nrow(acc.df)) ;# hours after last NA to clear data
  if (climateNA.df$climateNA[j]) acc.df[j:jend,4:7] <- NA
}

# Add dnt column to acc.df for easy graphing
acc.df$DateTime <- tc.df$DateTime

# Output NA-removed AccuRate data, may need to change name as required
write.table(acc.df,file=paste("acc_V2.0.csv"),sep=",",row.names=FALSE)
```

Figure A.66: acc_check.R

```
#####
##
## acc_maxmin.R
##
## June 18 2013, Sabrina Sequeira
##
## Does daily maxmin on AccuRate data
##
## Inputs: acc_V1.0.csv (output from acc_check.R program)
##
## Output: maxmin_acc.csv to maxmin folder
##
##
## To-do:
##     search on "Need"
##     Check which version of AccuRate data is being used
##
#####

# set working directory
setwd("F:/sabs uni files/project/test cell data/scripts")

# Install packages. Then load into library. Only once per computer.
library(chron)

# Change time zone to GMT-10 to ignore DST. Calcs done in current time zone.
Sys.setenv(tz='Etc/GMT-10')

# load in the AccuRate data
# Need to swap between V1.0 and V2.0 and V3.0
acc.df <- read.csv("acc_V3.0.csv", sep=",", header=T)
# load in list of dates and add to AccuRate data
dates.df <- read.table("dates.txt", sep=",", header=T)
acc.df$Date <- as.Date(dates.df$Dates)

# oops. instead of importing another way would have been this:
# as.Date(strftime(acc.df$DateTime, format="%Y/%m/%d"))

# Start output data frame and columns
maxmin.df <- data.frame(as.Date(levels(dates.df$Dates)))
names(maxmin.df)[1] <- "Date"
outmax <- numeric(nrow(maxmin.df)); outmax[1:nrow(maxmin.df)] <- NA
outmin <- numeric(nrow(maxmin.df)); outmin[1:nrow(maxmin.df)] <- NA
tcmax <- numeric(nrow(maxmin.df)); tcmax[1:nrow(maxmin.df)] <- NA
tcmin <- numeric(nrow(maxmin.df)); tcmin[1:nrow(maxmin.df)] <- NA
roofmax <- numeric(nrow(maxmin.df)); roofmax[1:nrow(maxmin.df)] <- NA
roofmin <- numeric(nrow(maxmin.df)); roofmin[1:nrow(maxmin.df)] <- NA
submax <- numeric(nrow(maxmin.df)); submax[1:nrow(maxmin.df)] <- NA
submin <- numeric(nrow(maxmin.df)); submin[1:nrow(maxmin.df)] <- NA

# Scroll through all dates
for (i in 1:nrow(maxmin.df))
{
  j <- maxmin.df$Date[i]
  outmax[i] <- max(acc.df[,4][acc.df$Date==j])
  outmin[i] <- min(acc.df[,4][acc.df$Date==j])
  tcmax[i] <- max(acc.df[,5][acc.df$Date==j])
  tcmin[i] <- min(acc.df[,5][acc.df$Date==j])
  roofmax[i] <- max(acc.df[,6][acc.df$Date==j])
  roofmin[i] <- min(acc.df[,6][acc.df$Date==j])
  submax[i] <- max(acc.df[,7][acc.df$Date==j])
  submin[i] <- min(acc.df[,7][acc.df$Date==j])
}

```

Figure A.67: acc_maxmin.R, page 1

```

# Add output vectors and names to maxmin dataframe
maxmin.df[,2] <- outmax; maxmin.df[,3] <- outmin
maxmin.df[,4] <- tcmax; maxmin.df[,5] <- tcmin
maxmin.df[,6] <- roofmax; maxmin.df[,7] <- roofmin
maxmin.df[,8] <- submax; maxmin.df[,9] <- submin
names(maxmin.df)[2:9] <-
  c("outmax","outmin","tcmax","tcmin","roofmax","roofmin","submax","submin")

# Define factors for maxmin stats analysis
# month of year
maxmin.df$month <- months(maxmin.df$Date)
maxmin.df$month[maxmin.df$month=="January"] <- "01.JAN"
maxmin.df$month[maxmin.df$month=="February"] <- "02.FEB"
maxmin.df$month[maxmin.df$month=="March"] <- "03.MAR"
maxmin.df$month[maxmin.df$month=="April"] <- "04.APR"
maxmin.df$month[maxmin.df$month=="May"] <- "05.MAY"
maxmin.df$month[maxmin.df$month=="June"] <- "06.JUN"
maxmin.df$month[maxmin.df$month=="July"] <- "07.JUL"
maxmin.df$month[maxmin.df$month=="August"] <- "08.AUG"
maxmin.df$month[maxmin.df$month=="September"] <- "09.SEP"
maxmin.df$month[maxmin.df$month=="October"] <- "10.OCT"
maxmin.df$month[maxmin.df$month=="November"] <- "11.NOV"
maxmin.df$month[maxmin.df$month=="December"] <- "12.DEC"
maxmin.df$month <- factor(maxmin.df$month)
# season, using month
summer <- c("12.DEC","01.JAN","02.FEB"); autumn<- c("03.MAR","04.APR","05.MAY")
winter <- c("06.JUN","07.JUL","08.AUG"); spring<- c("09.SEP","10.OCT","11.NOV")
maxmin.df$season[maxmin.df$month %in% summer] <- "04.SUM"
maxmin.df$season[maxmin.df$month %in% autumn] <- "01.AUT"
maxmin.df$season[maxmin.df$month %in% winter] <- "02.WIN"
maxmin.df$season[maxmin.df$month %in% spring] <- "03.SPR"
maxmin.df$season <- factor(maxmin.df$season)
# month of which year
maxmin.df$month2 <- paste(years(maxmin.df$Date),maxmin.df$month)
maxmin.df$month2 <- factor(maxmin.df$month2)
# season of which year
# put jan and feb into summer season starting previous year
maxmin.df$season2 <- paste(years(maxmin.df$Date),maxmin.df$season)
maxmin.df$season2[years(maxmin.df$Date=="2011" & maxmin.df$month=="02.FEB")]
  <- "2010 04.SUM"
maxmin.df$season2[years(maxmin.df$Date=="2012" & maxmin.df$month=="01.JAN")]
  <- "2011 04.SUM"
maxmin.df$season2[years(maxmin.df$Date=="2012" & maxmin.df$month=="02.FEB")]
  <- "2011 04.SUM"
maxmin.df$season2 <- factor(maxmin.df$season2)
# ground cover
# Need to fix this. Fix: just define basic factor as function of time
maxmin.df$ground <- "COVERED"
maxmin.df$ground[as.character(maxmin.df$Date)>"2012-02-22"] <- "UNCOVERED"
maxmin.df$ground <- factor(maxmin.df$ground)
# time periods
maxmin.df$tp <- "TP2"
maxmin.df$tp[as.character(maxmin.df$Date)<"2012-02-22 16:00"] <- "TP1"
maxmin.df$tp[as.character(maxmin.df$Date)>"2012-03-22 11:00"] <- "TP3"
maxmin.df$tp <- factor(maxmin.df$tp)

# write entire new data frame to output file
write.table(maxmin.df, file=paste("maxmin_output/maxmin_acc_V3.0.csv"),
  sep="," , row.names=FALSE)

```

Figure A.68: acc_maxmin.R, page 2

A.5 Observed and AccuRate Results

Appendix A.5 is divided into several sections.

The investigation between ground moisture evaporation and climate data is presented in A.5.1.

Observed and AR1 room temperature graphs from TP3 are provided in A.5.2, and observed and AR1 subfloor temperature graphs from TP1-3 are provided in A.5.3. Observed and AR1 daily maximum and minimum subfloor temperature graphs are provided in A.5.4.

Observed and AR2 room temperature graphs from TP3 are provided in A.5.5, and observed and AR2 subfloor temperature graphs from TP1-3 are provided in A.5.6. Observed and AR2 daily maximum and minimum subfloor temperature graphs are provided in A.5.7.

A.5.1 Observed ground moisture evaporation

Data from TP1-TP3 is shown in Figure A.69 and Figure A.70. Both these figures contain a matrix of small graphs. Each small graph plots the term 'gevap2', the ground moisture evaporation in units of g/m²/hour, against the term 'ventach', the subfloor ventilation in units of ACH. The smaller graphs are organized by different confounding parameters. Figure A.69 is organized by month and Figure A.70 is organized by outdoor air temperature. The first graph in the series is the bottom left graph. As the confounding parameter increases the next graph in the series is the one to the right. This continues until the row is complete and then the next graph in the series is the left graph in the next higher up row. For example, the left-most graph in the top row of Figure A.70 represents evaporation vs ventilation for the data point where the outdoor temperature is approximately 12 °C to 16 °C. Figure A.69 starts with February 2011 in the bottom left-hand corner and increases monthly, such that April, May and September 2012 contain no data.

It is observed in Figure A.69 that the evaporation relationship with ventilation has no clear pattern in the warmer months but has a distinct negative slope in the cooler months. This trend is confirmed in Figure A.70 which shows the confounding with outdoor temperature. The first few graphs in the series have a negative slope but the shape of the data changes as temperature increases. It appears from these graphs that ventilation is not a significant driver of evaporation. It also appears that the subfloor thermal and moisture performance is different at lower temperatures than it is at high temperatures, as seen in previous test cell research (Dewsbury 2011).

This trend is not evident in the test cell data from 2007. The relationship between evaporation and ventilation is always strong and positive, even when segregated by month as in Figure A.71, outdoor temperature as in Figure A.72, or subfloor temperature as in Figure A.73.

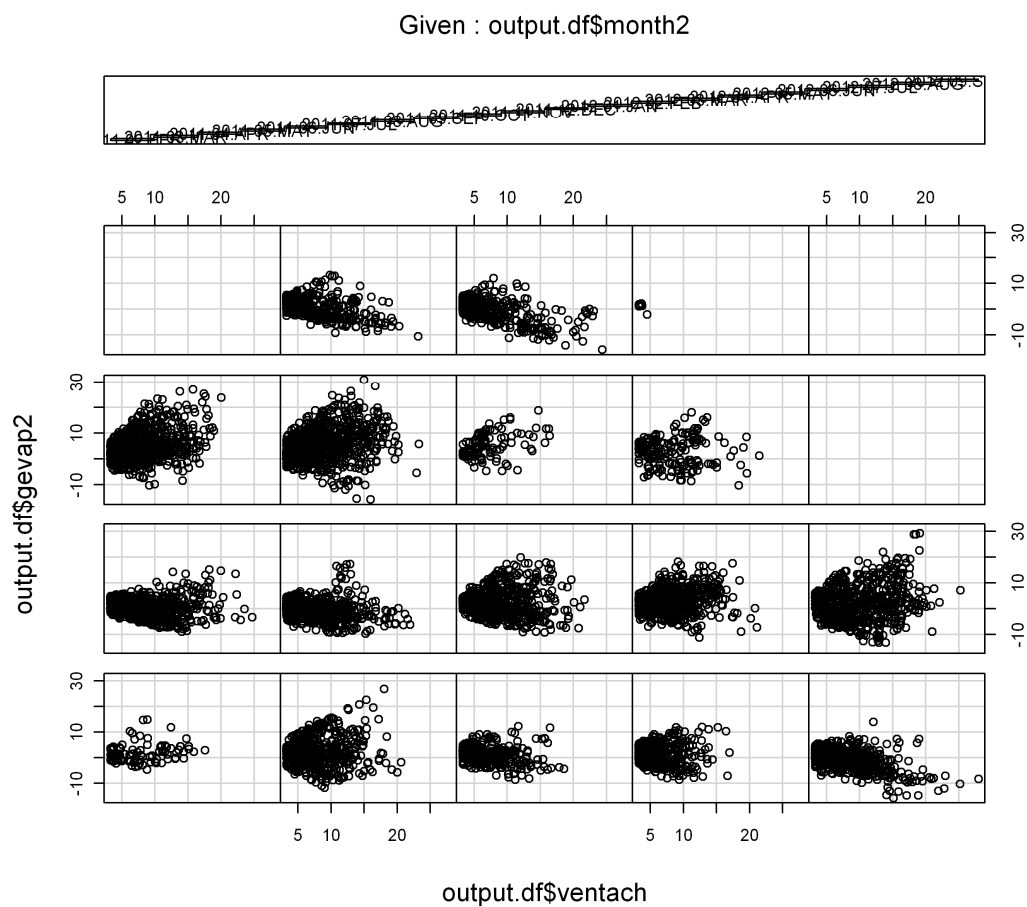


Figure A.69: 2011-2012 Ground moisture evaporation vs. ventilation, by month

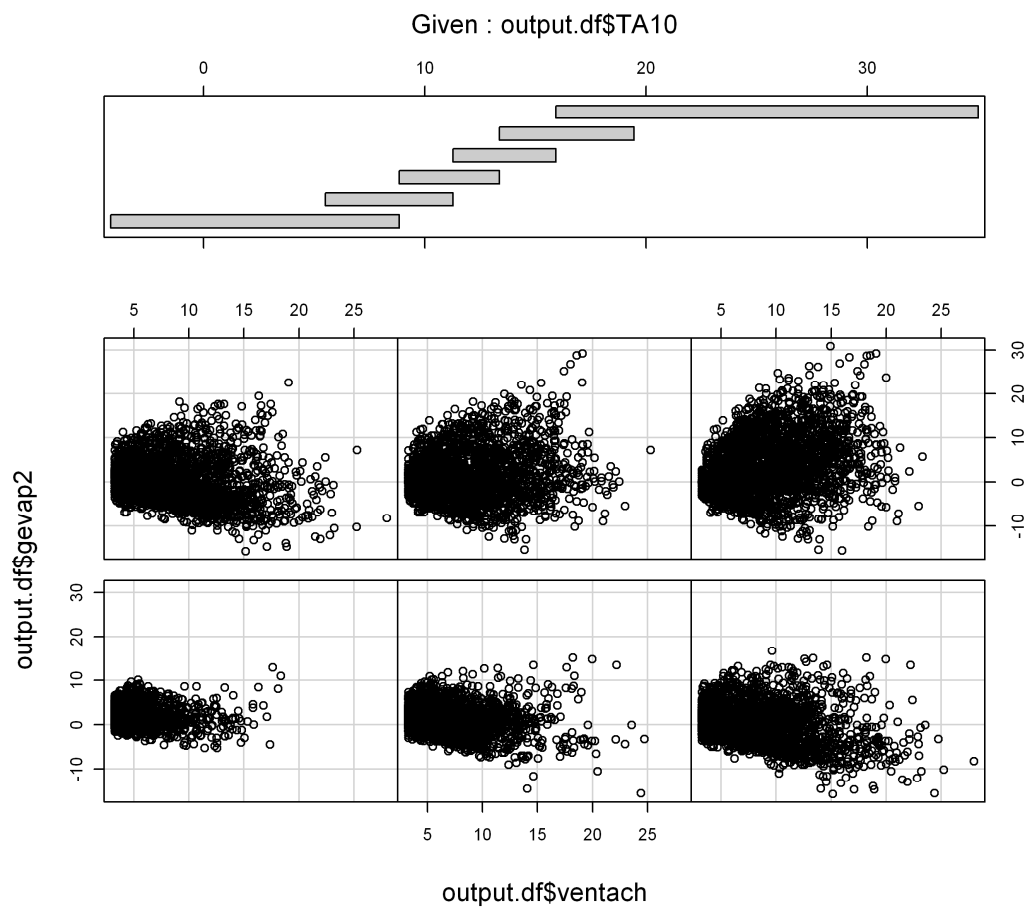


Figure A.70: 2011-2012 Ground moisture evaporation vs. ventilation, by outdoor temperature

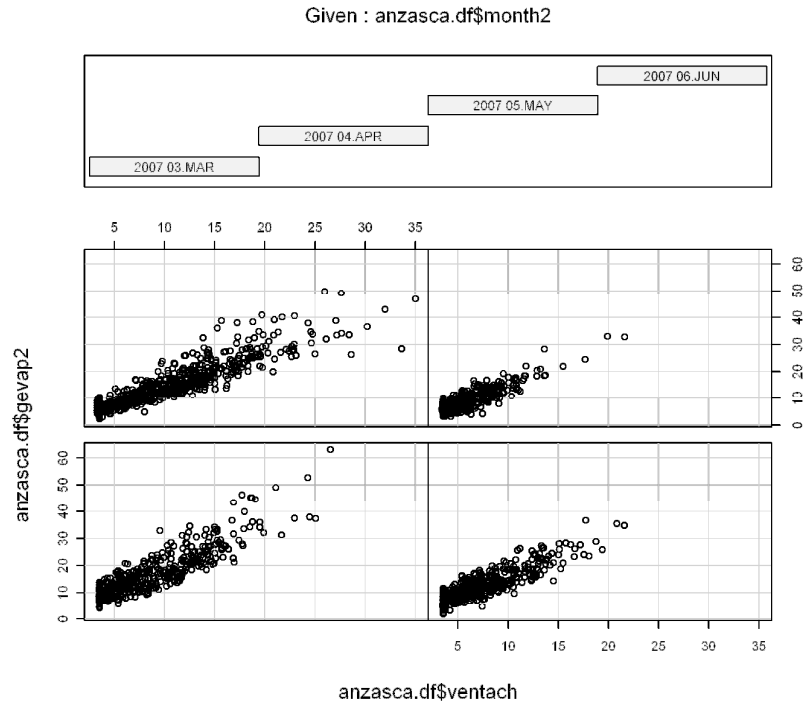


Figure A.71: 2007 Ground moisture evaporation vs. ventilation, by month

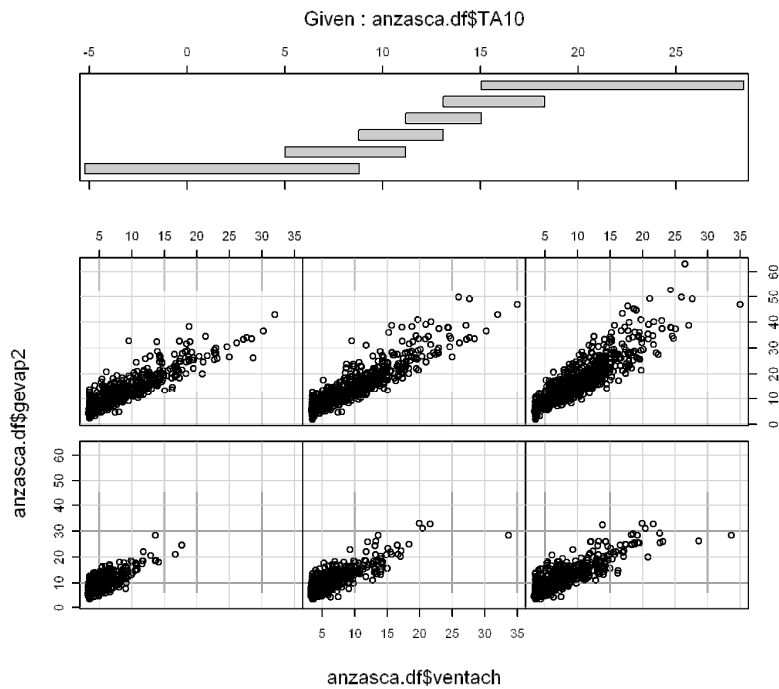


Figure A.72: 2007 Ground moisture evaporation vs. ventilation, by outdoor temperature

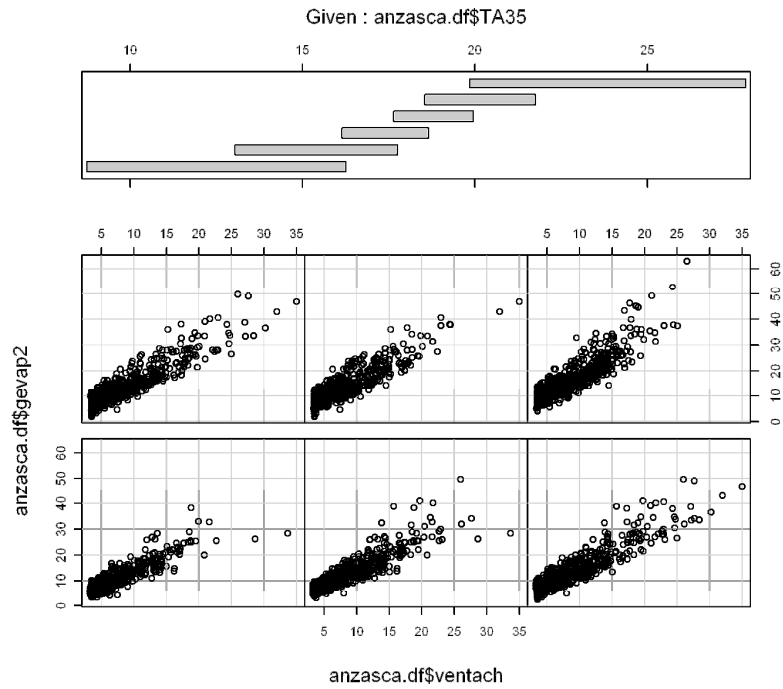
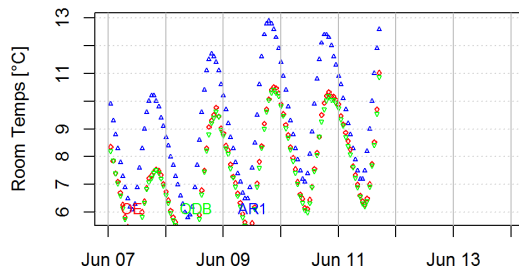


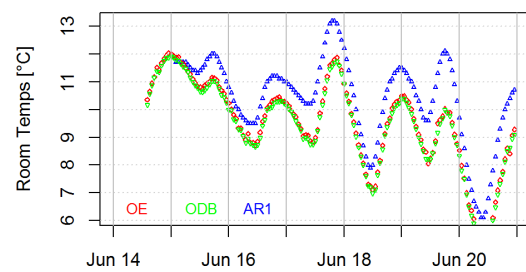
Figure A.73: 2007 Ground moisture evaporation vs. ventilation, by subfloor temperature

A.5.2 Observed and AR1 room temperatures, TP3

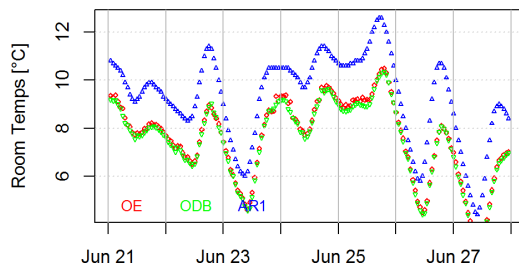
Figure A.74 and Figure A.75 display the AR1, observed dry bulb and observed environmental room temperatures for every week in the entire test period that contain AccuRate data.



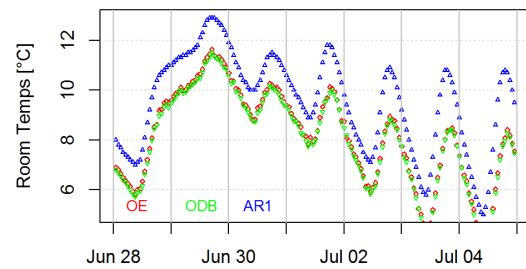
(a) Week 68



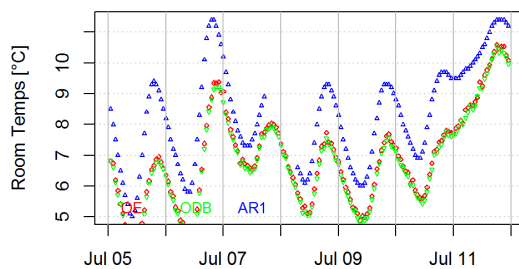
(b) Week 69



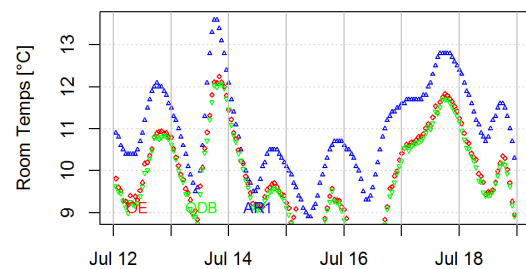
(c) Week 70



(d) Week 71

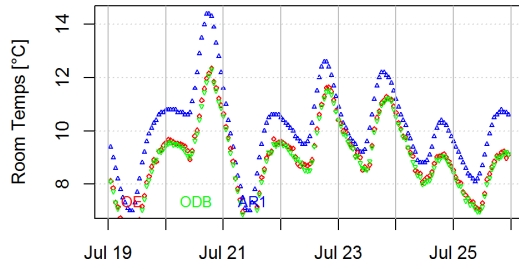


(e) Week 72

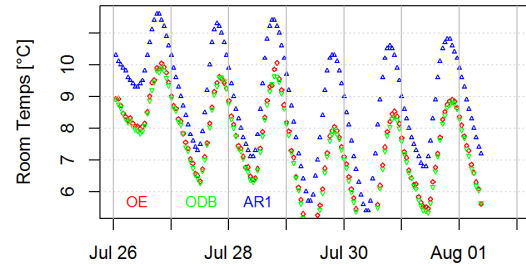


(f) Week 73

Figure A.74: Observed and AR1 room temperatures, TP1-3, page 1



(c) Week 74



(f) Week 75

Figure A.75: Observed and AR1 room temperatures, TP1-3, page 2

A.5.3 Observed and AR1 subfloor temperatures, TP1-3

Figure A.76 through Figure A.83 display the AR1, observed dry bulb and observed environmental subfloor temperatures for every week in the entire test period that contain AccuRate data.

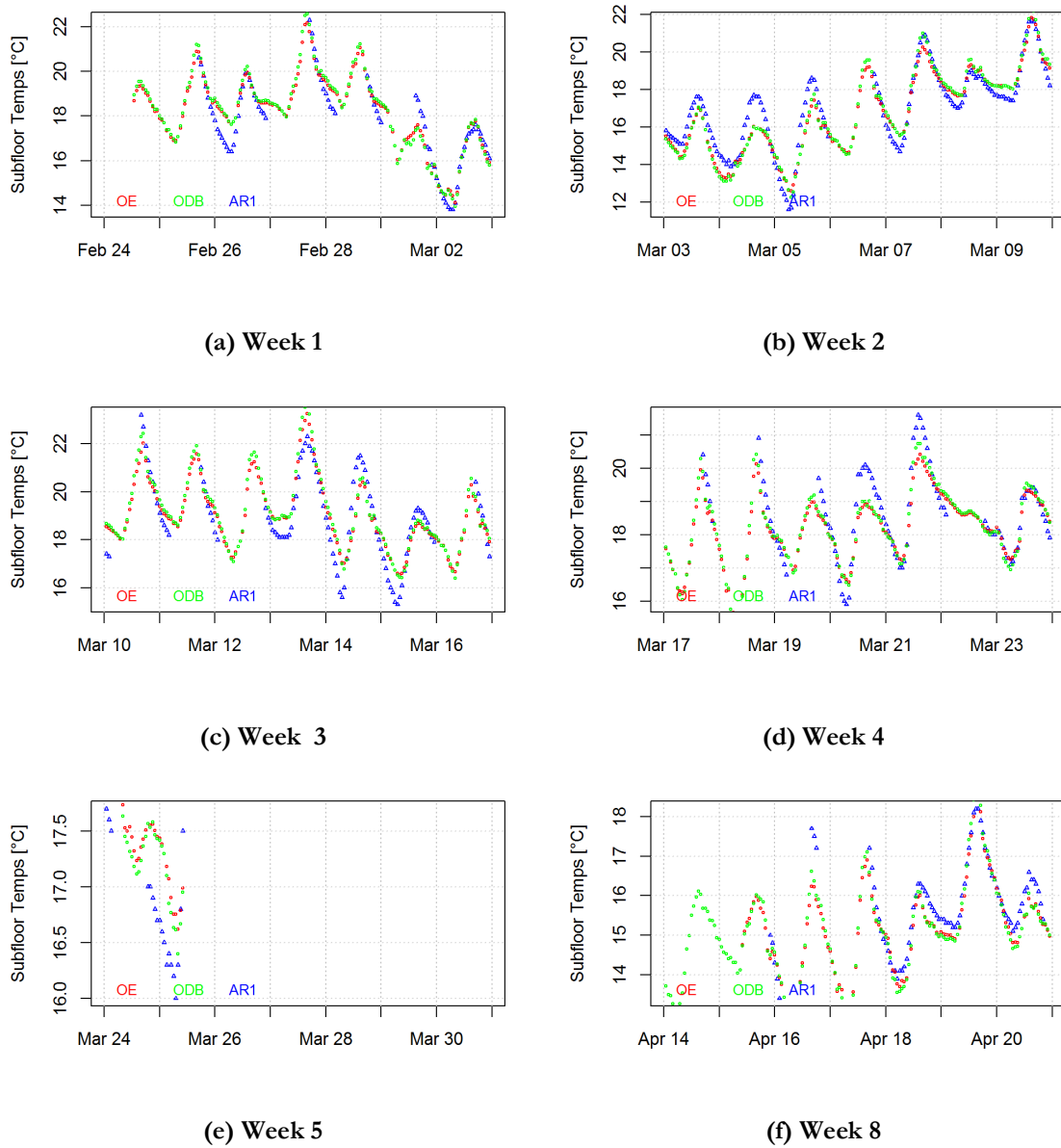
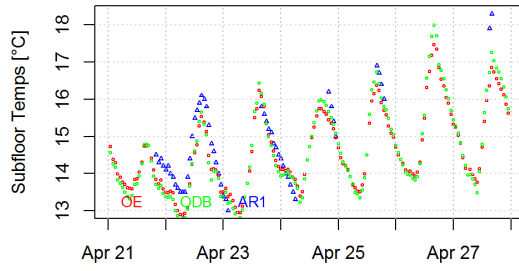
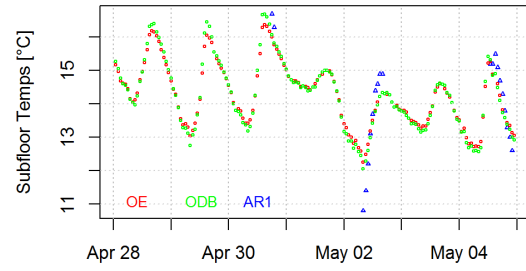


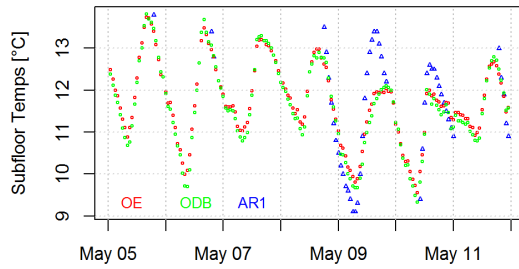
Figure A.76: Observed and AR1 subfloor temperatures, TP1-3, page 1



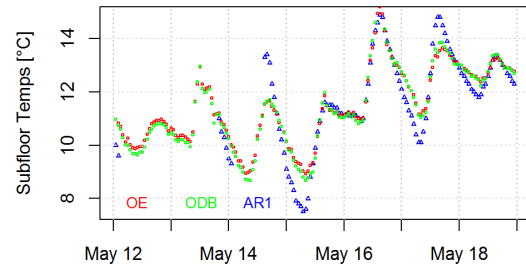
(a) Week 9



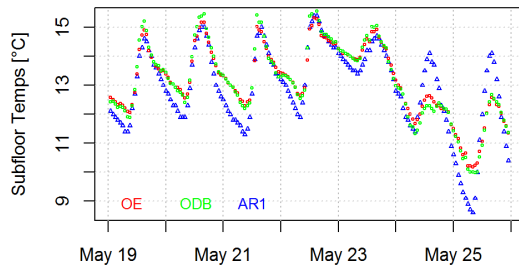
(b) Week 10



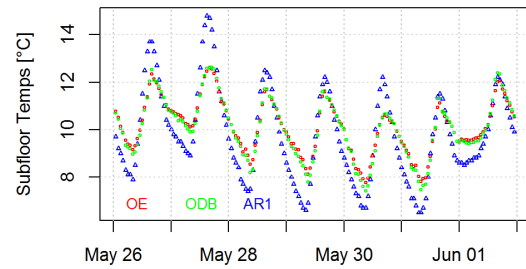
(c) Week 11



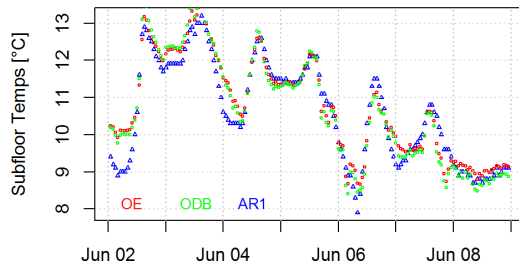
(d) Week 12



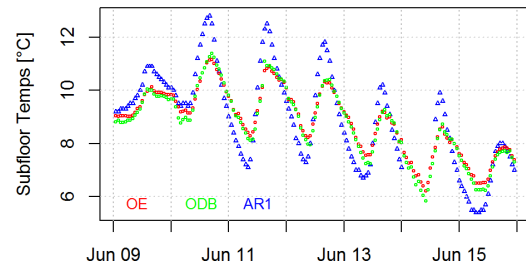
(e) Week 13



(f) Week 14

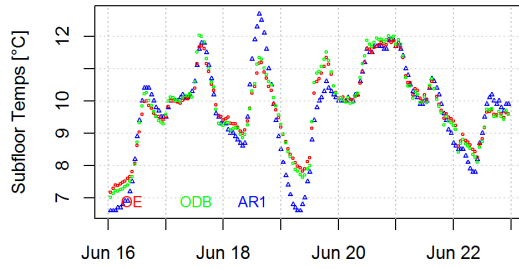


(e) Week 15

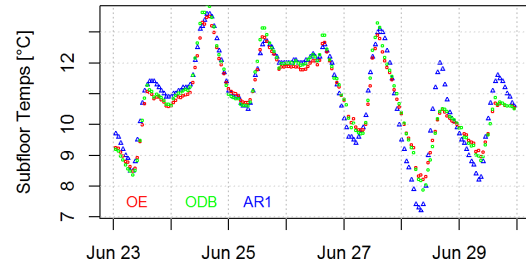


(f) Week 16

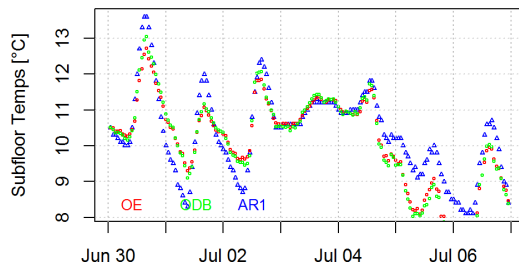
Figure A.77: Observed and AR1 subfloor temperatures, TP1-3, page 2



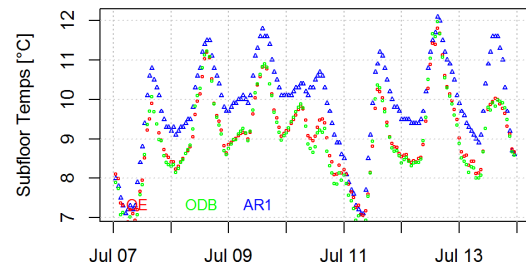
(a) Week 17



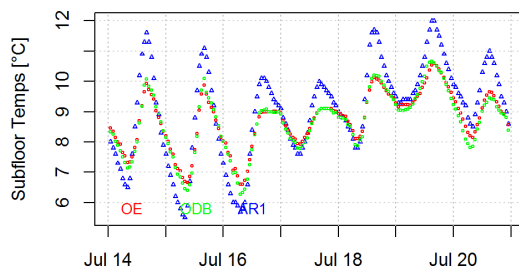
(b) Week 18



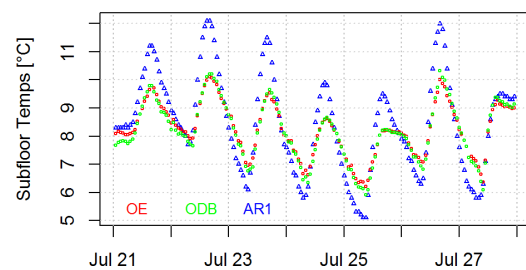
(c) Week 19



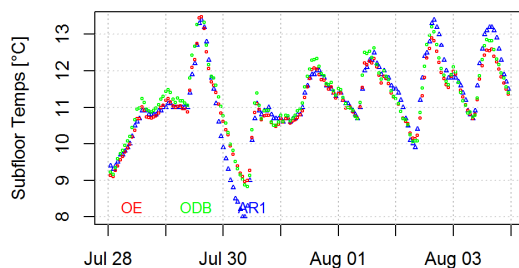
(d) Week 20



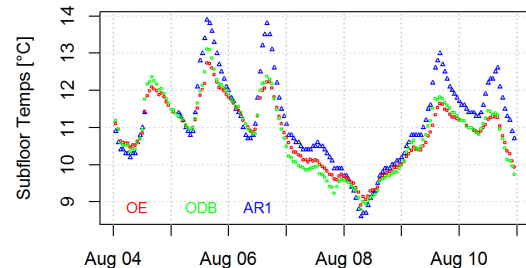
(e) Week 21



(f) Week 22

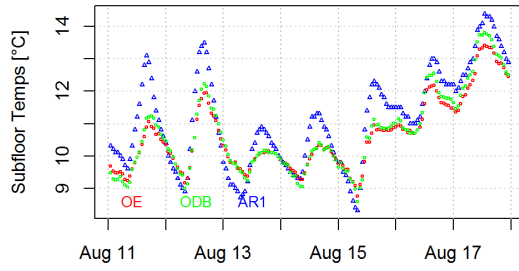


(e) Week 23

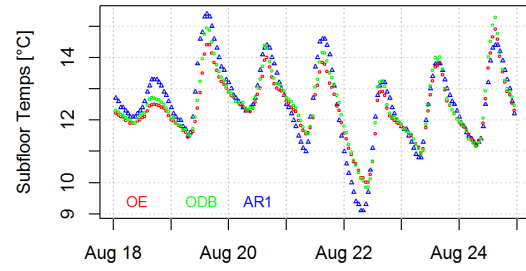


(f) Week 24

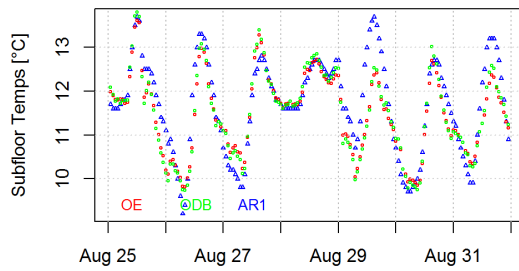
Figure A.78: Observed and AR1 subfloor temperatures, TP1-3, page 3



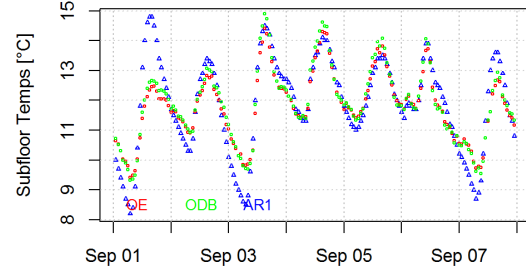
(a) Week 25



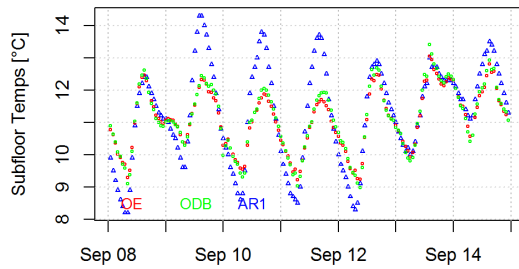
(b) Week 26



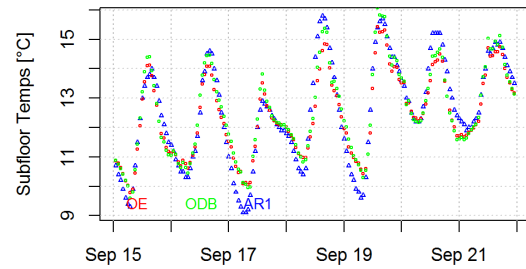
(c) Week 27



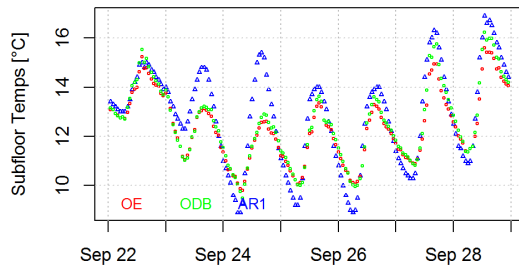
(d) Week 28



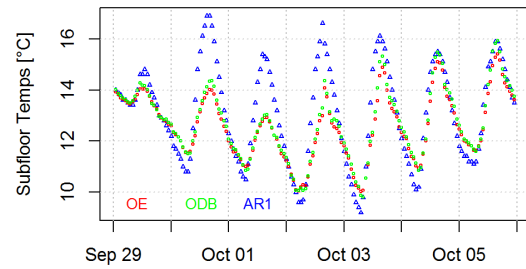
(e) Week 29



(f) Week 30

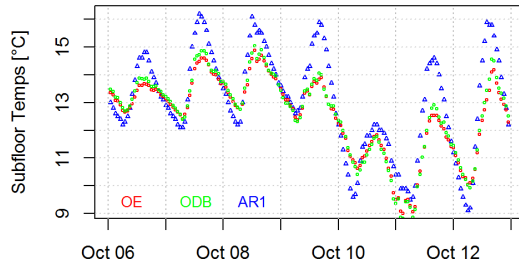


(g) Week 31

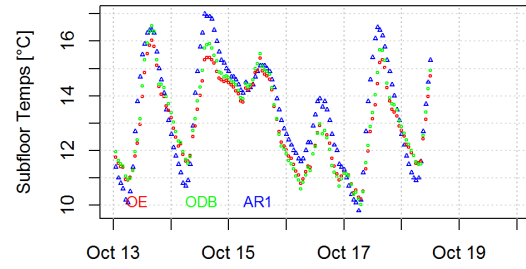


(h) Week 32

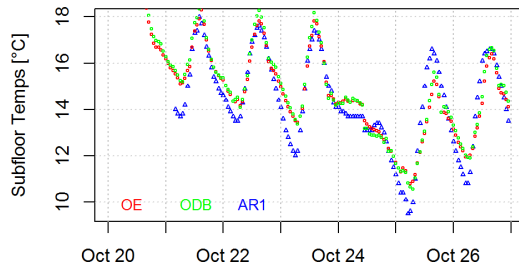
Figure A.79: Observed and AR1 subfloor temperatures, TP1-3, page 4



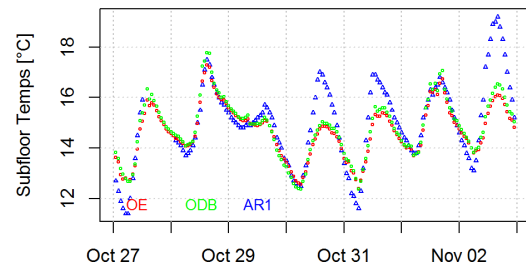
(a) Week 33



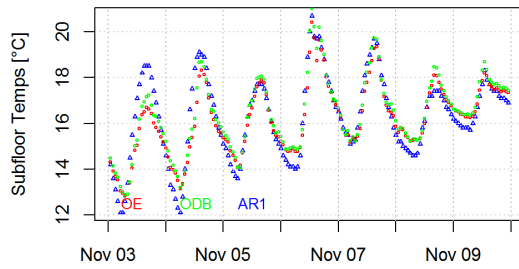
(b) Week 34



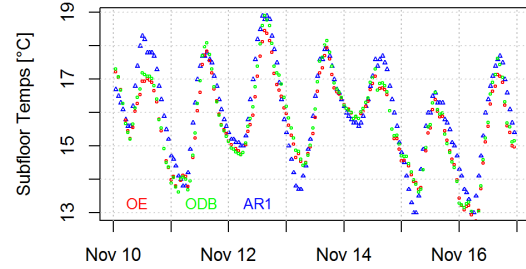
(c) Week 35



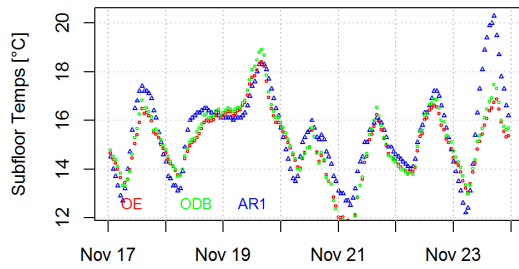
(d) Week 36



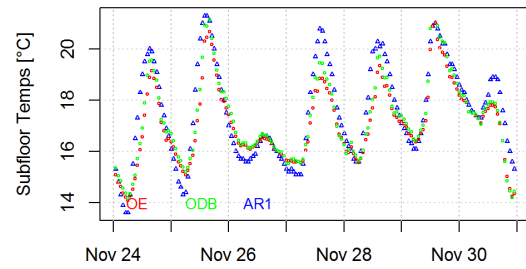
(e) Week 37



(f) Week 38

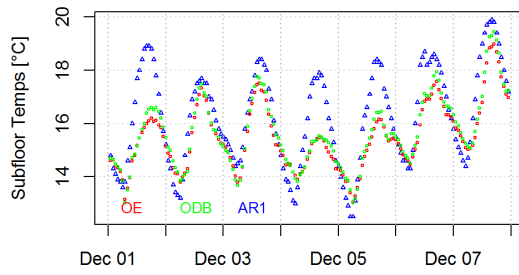


(e) Week 39

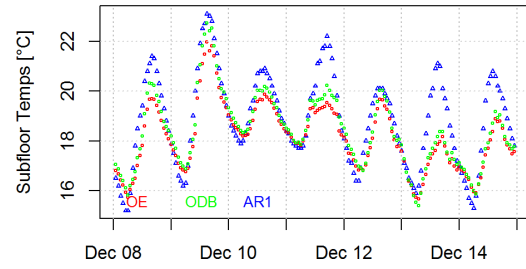


(f) Week 40

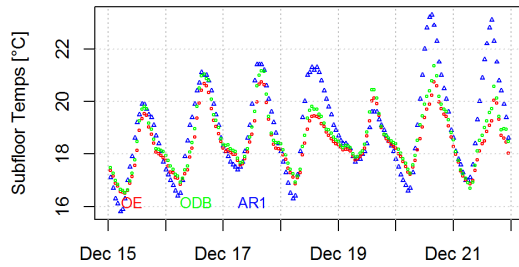
Figure A.80: Observed and AR1 subfloor temperatures, TP1-3, page 5



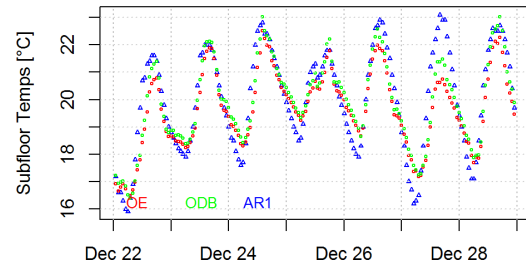
(a) Week 41



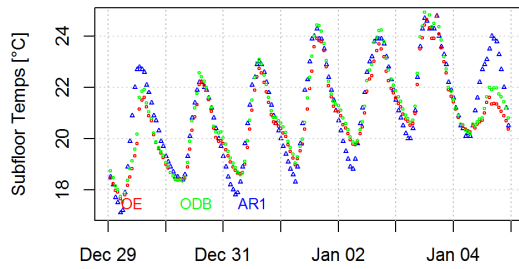
(b) Week 42



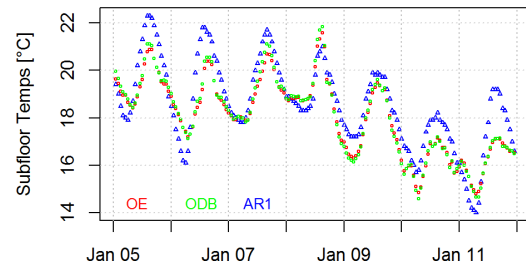
(c) Week 43



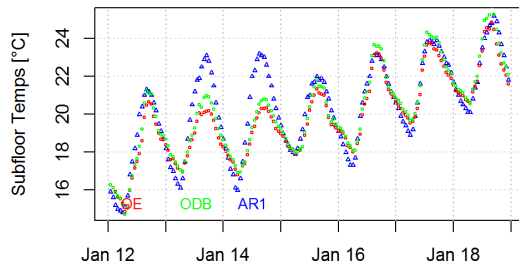
(d) Week 44



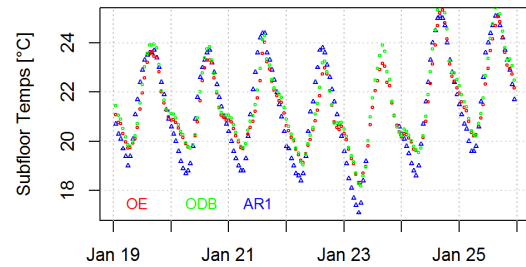
(e) Week 45



(f) Week 46

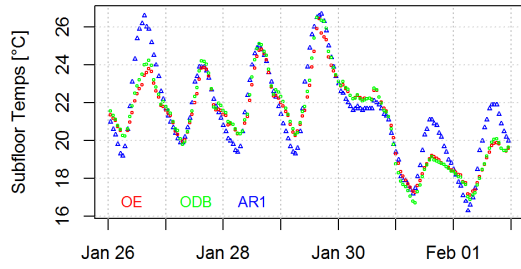


(e) Week 47

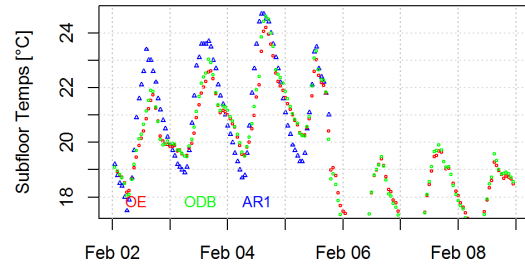


(f) Week 48

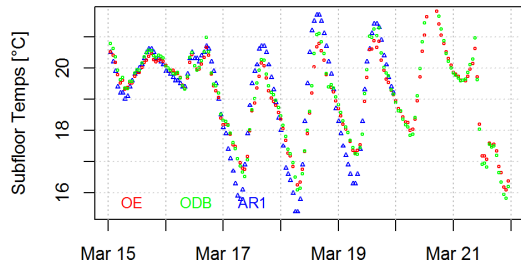
Figure A.81: Observed and AR1 subfloor temperatures, TP1-3, page 6



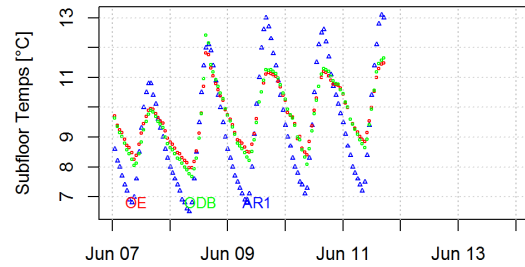
(a) Week 49



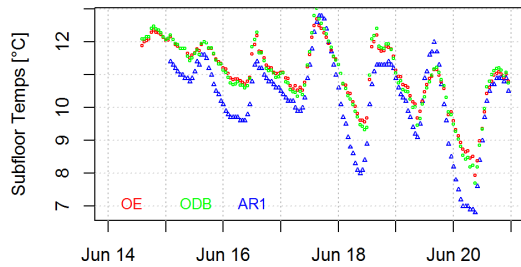
(b) Week 50



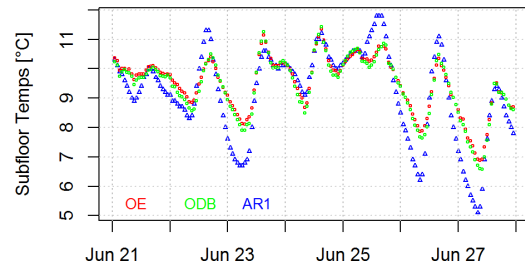
(c) Week 56



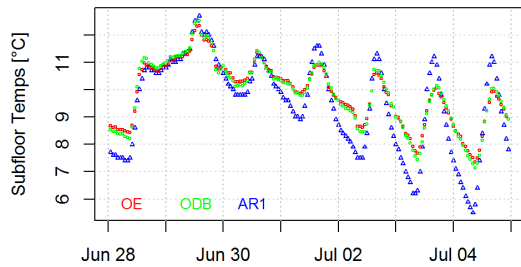
(d) Week 68



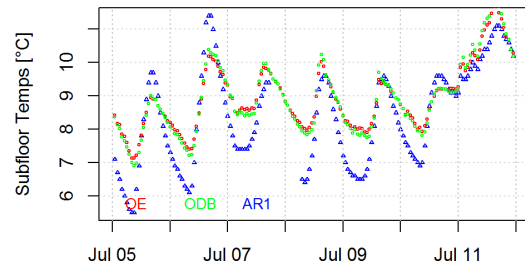
(e) Week 69



(f) Week 70

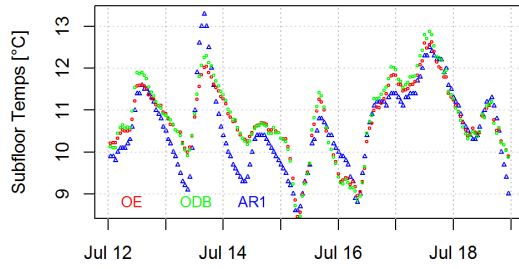


(e) Week 71

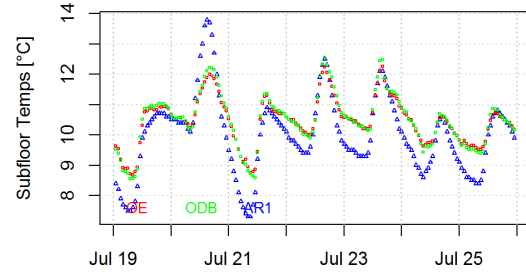


(f) Week 72

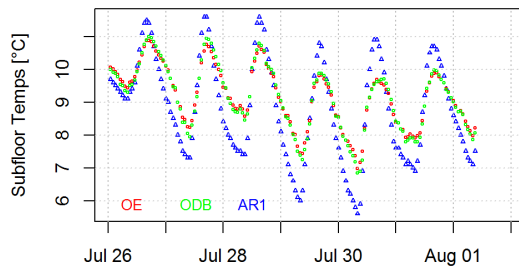
Figure A.82: Observed and AR1 subfloor temperatures, TP1-3, page 7



(a) Week 73



(b) Week 74

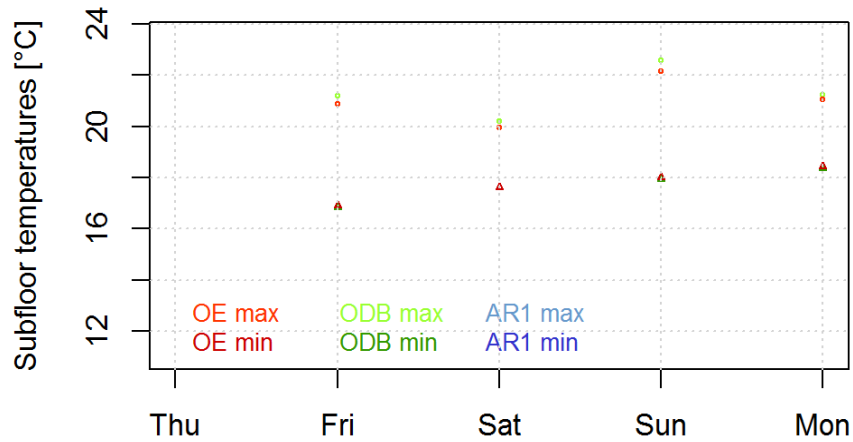


(c) Week 75

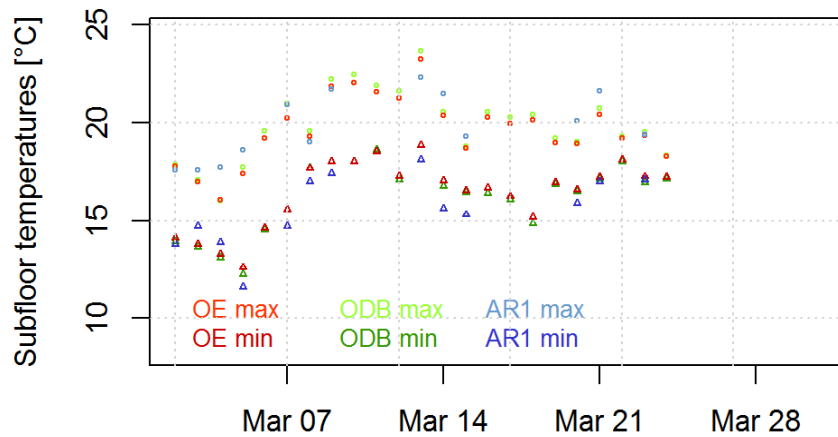
Figure A.83: Observed and AR1 subfloor temperatures, TP1-3, page 8

A.5.4 Observed and AR1 subfloor daily max. and min. temperatures, TP1-3

Figure A.84 through Figure A.90 display the AR1, observed dry bulb and observed environmental subfloor daily maximum and minimum temperatures for every month in the entire test period.

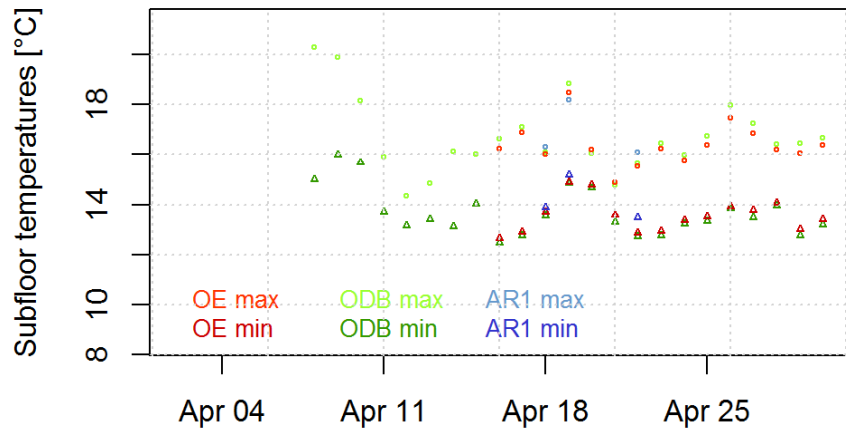


(a) February 2011

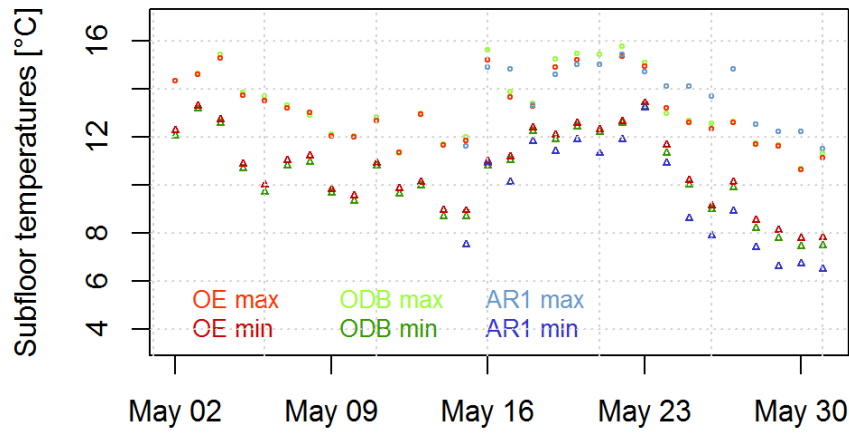


(b) March 2011

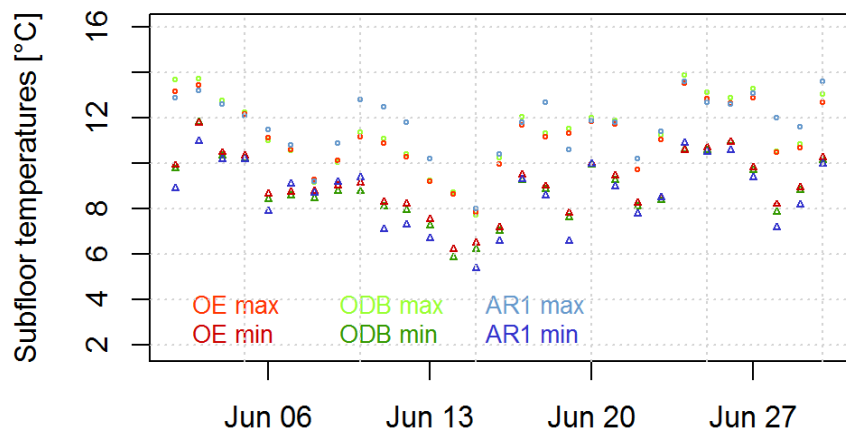
Figure A.84: AR1 and observed daily max. and min. subfloor temperatures, page 1



(a) April 2011

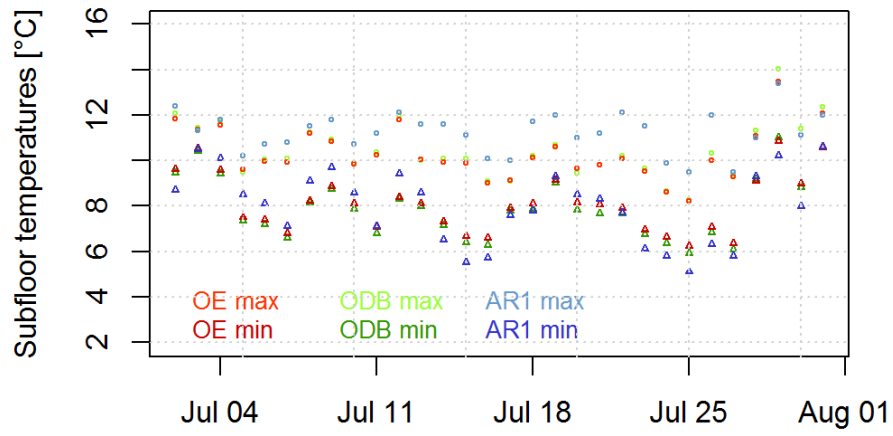


(b) May 2011

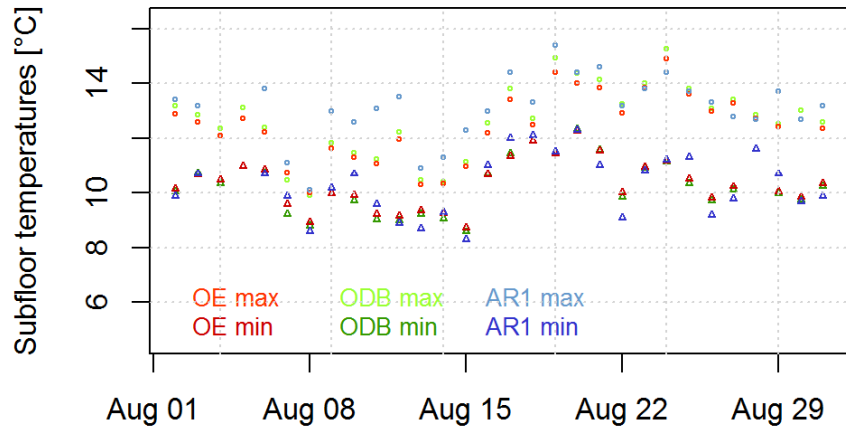


(c) June 2011

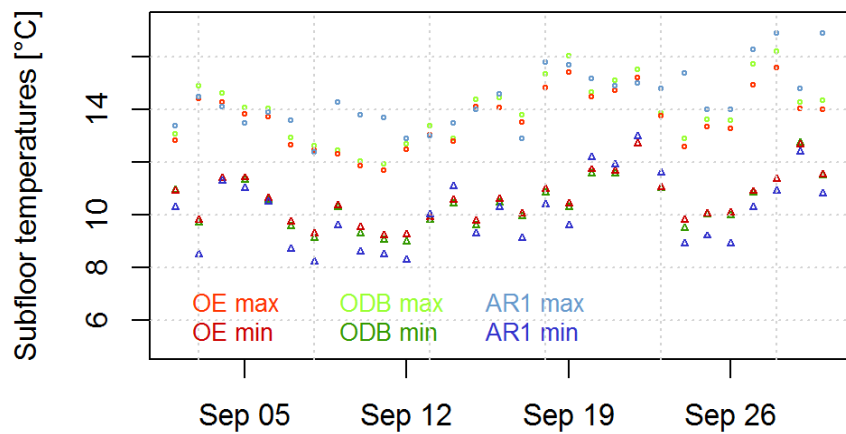
Figure A.85: AR1 and observed daily max. and min. subfloor temperatures, page 2



(a) July 2011



(b) August 2011



(c) September 2011

Figure A.86: AR1 and observed daily max. and min. subfloor temperatures, page 3

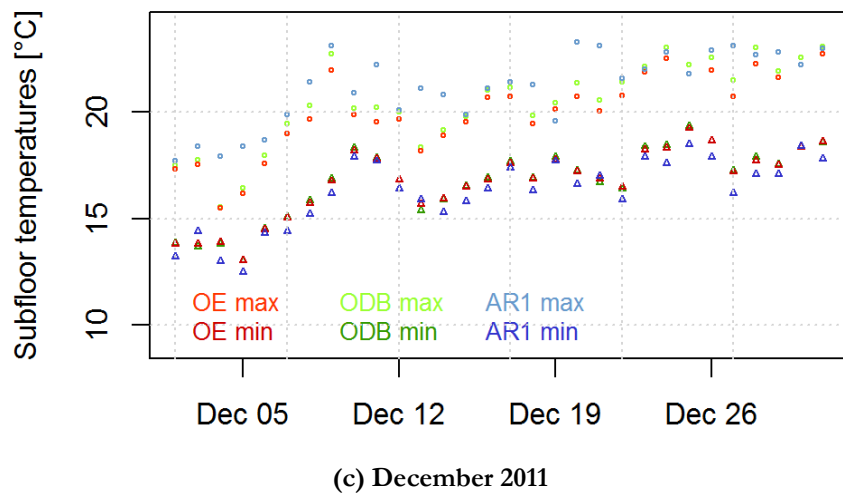
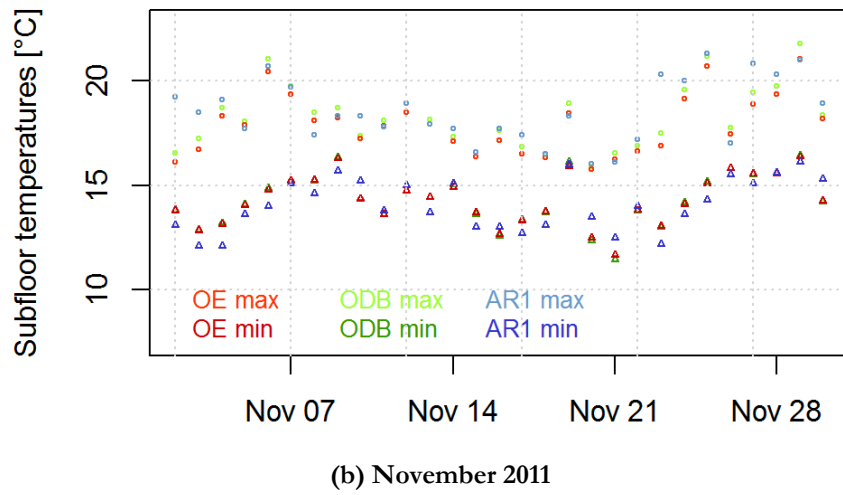
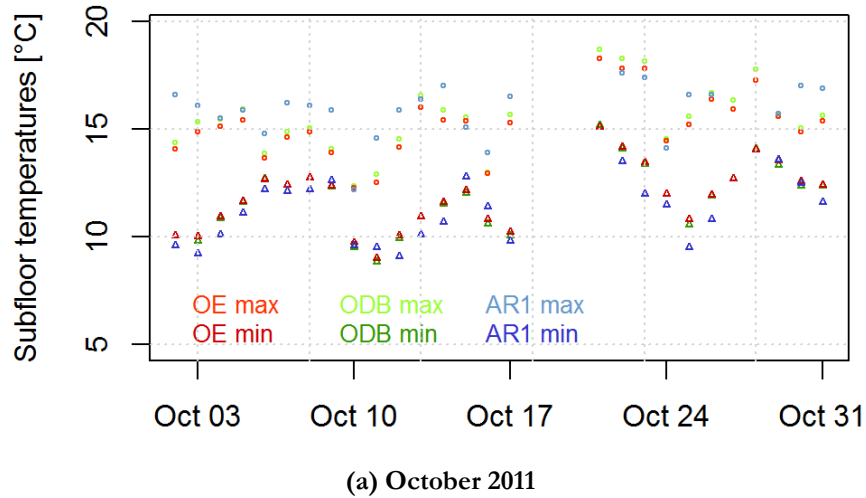


Figure A.87: AR1 and observed daily max. and min. subfloor temperatures, page 4

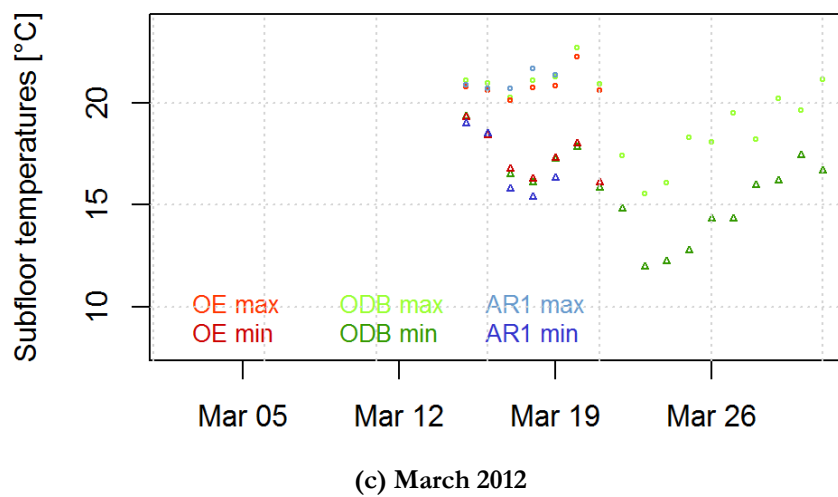
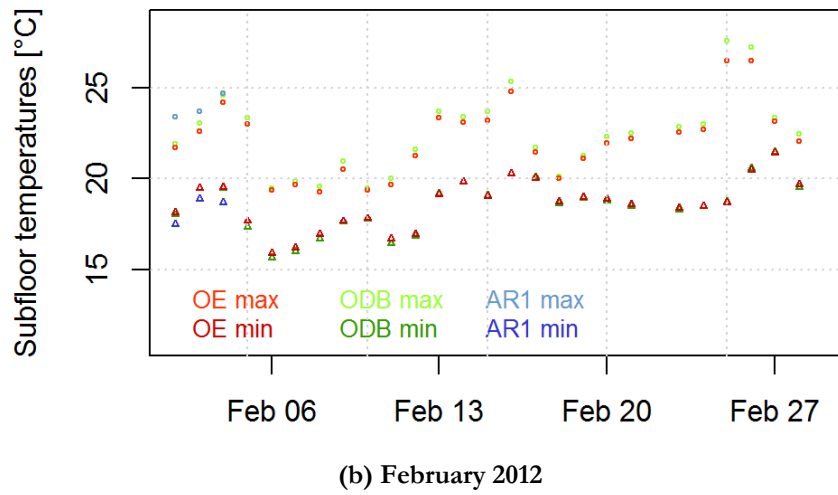
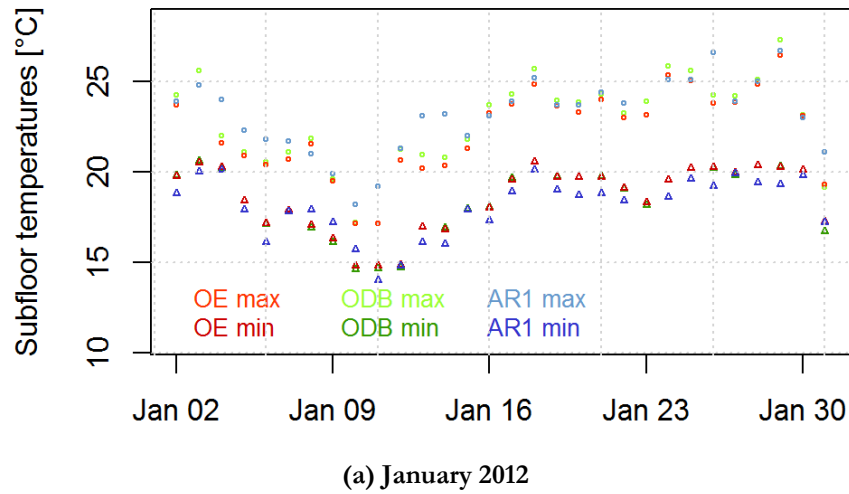
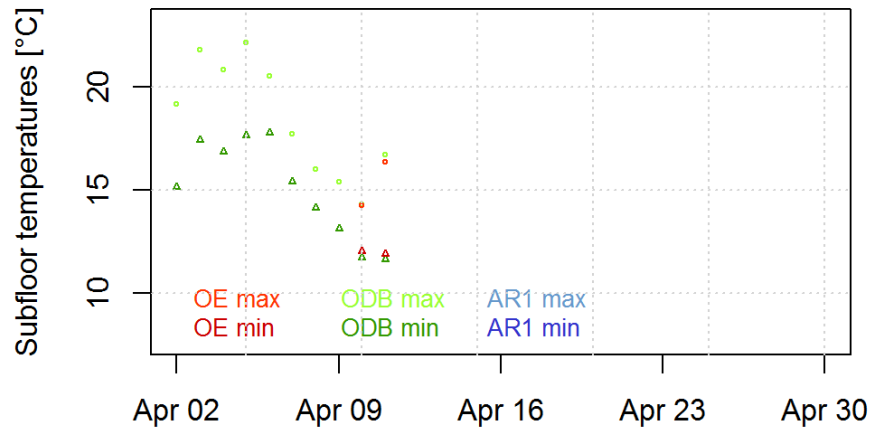
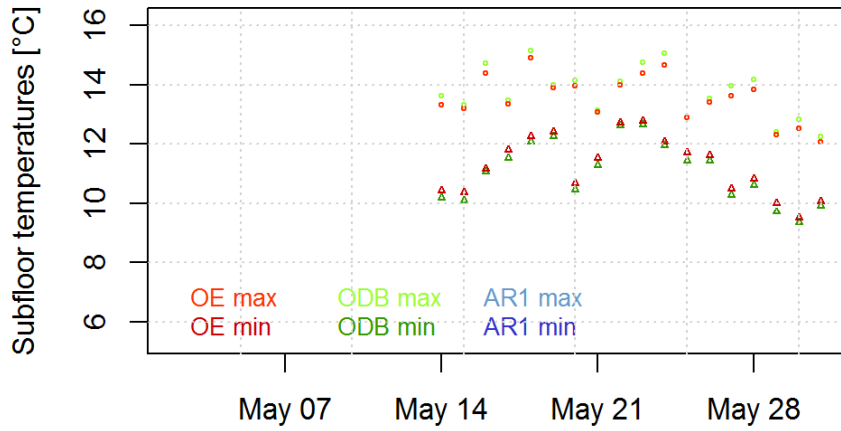


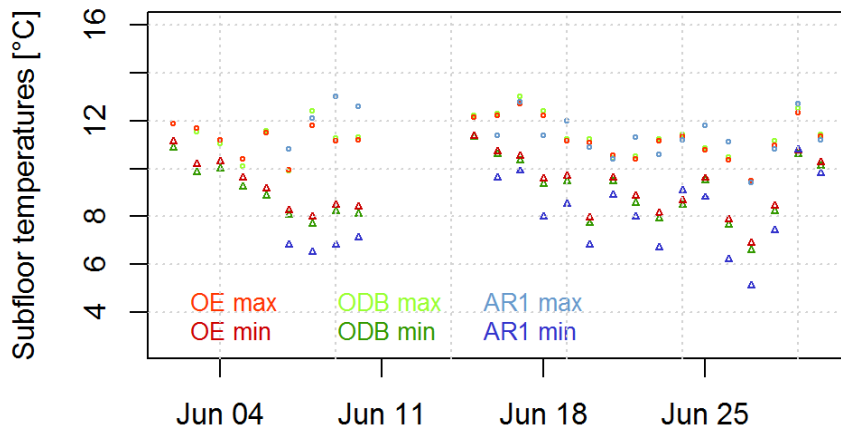
Figure A.88: AR1 and observed daily max. and min. subfloor temperatures, page 5



(a) April 2012



(b) May 2012



(c) June 2012

Figure A.89: AR1 and observed daily max. and min. subfloor temperatures, page 5

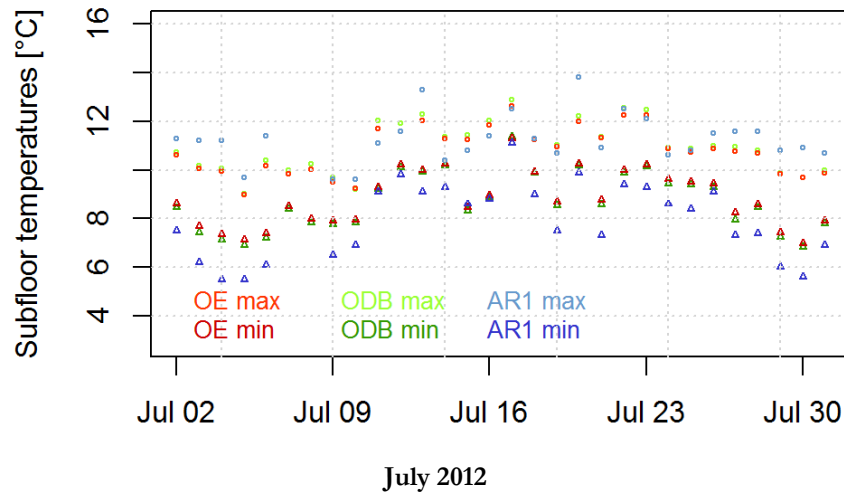


Figure A.90: AR1 and observed daily max. and min. subfloor temperatures, page 6

A.5.5 Observed and AR2 room temperatures, TP3

Figure A.91 and Figure A.92 display the AR2, observed dry bulb and observed environmental room temperatures for every week in the entire test period that contain AccuRate data.

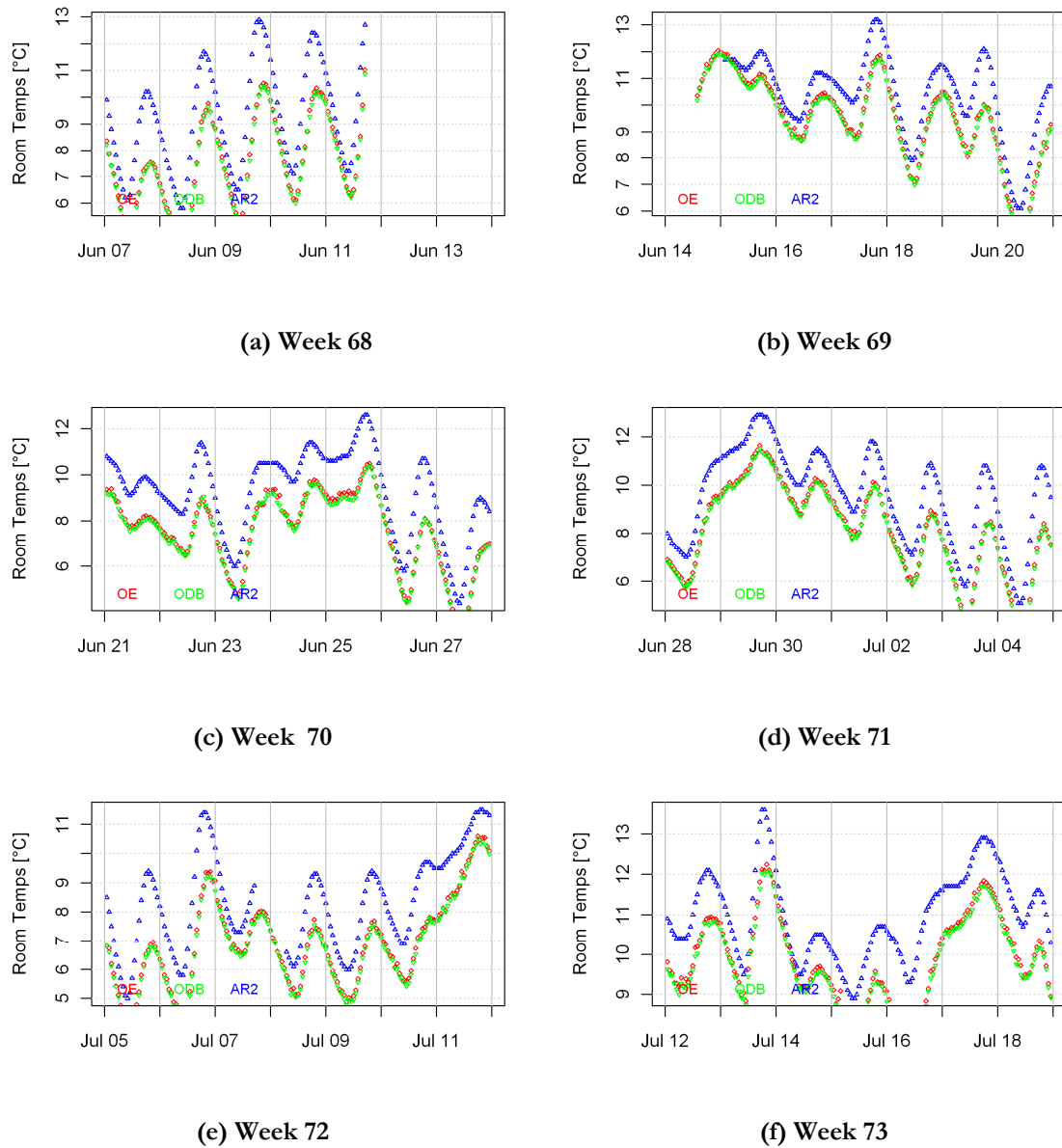
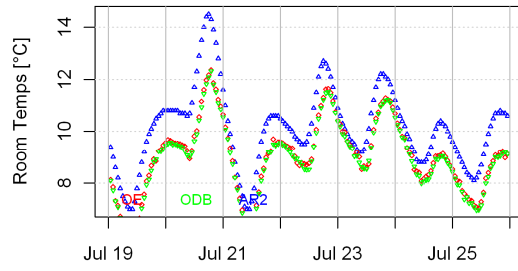
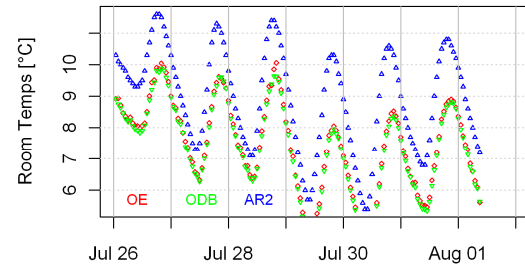


Figure A.91: Observed and AR2 room temperatures, TP1-3, page 1



(c) Week 74



(f) Week 75

Figure A.92: Observed and AR2 room temperatures, TP1-3, page 2

A.5.6 Observed and AR2 subfloor temperatures, TP1-3

Figure A.93 through Figure A.100 display the AR2, observed dry bulb and observed environmental subfloor temperatures for every week in the entire test period that contain AccuRate data.

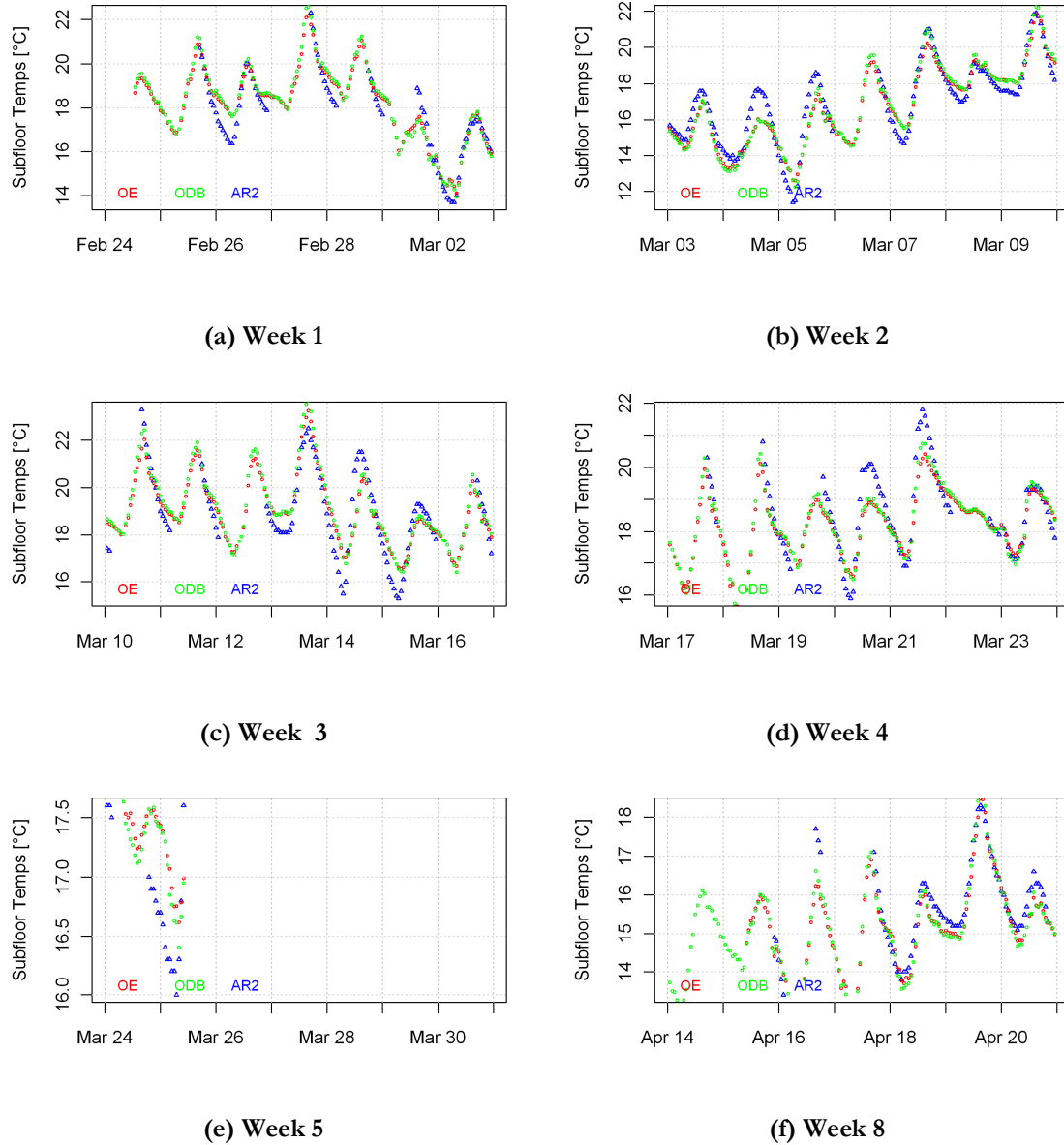
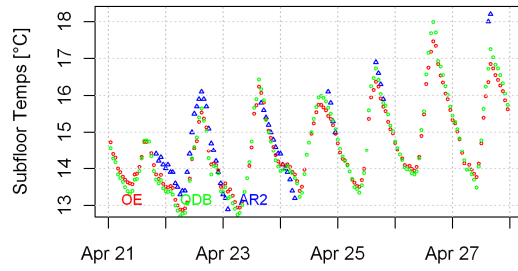
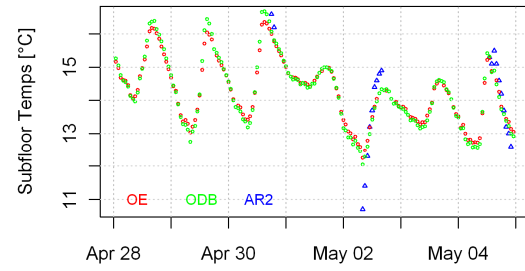


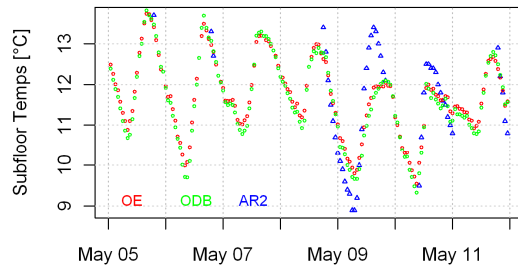
Figure A.93: Observed and AR2 subfloor temperatures, TP1-3, page 1



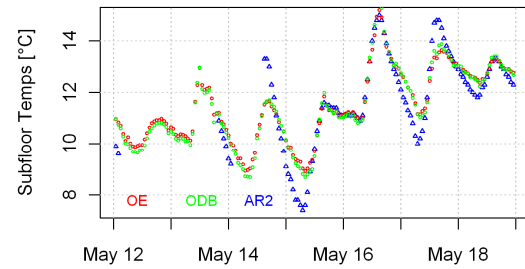
(a) Week 9



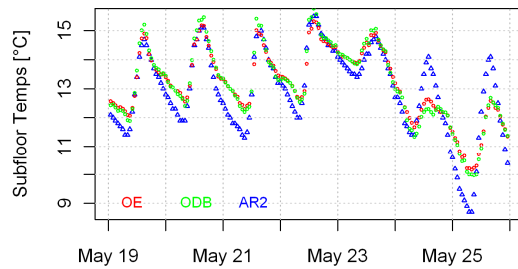
(b) Week 10



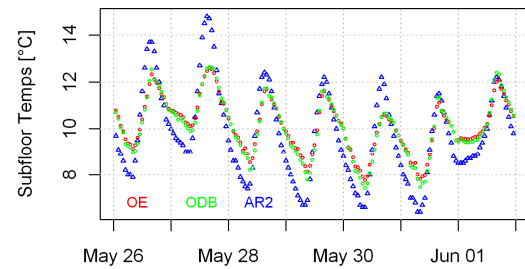
(c) Week 11



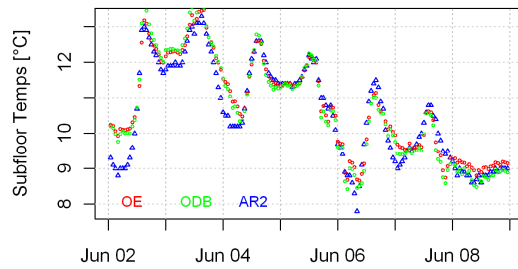
(d) Week 12



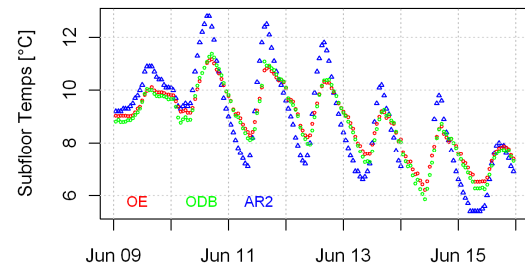
(e) Week 13



(f) Week 14

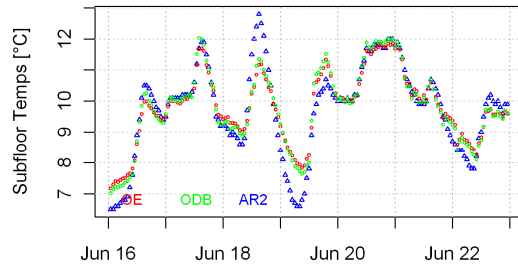


(e) Week 15

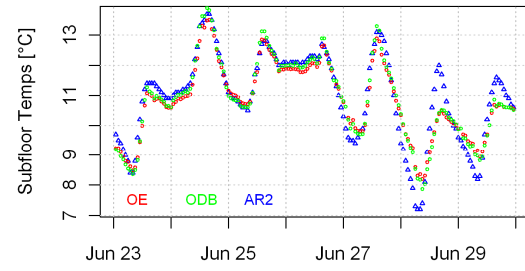


(f) Week 16

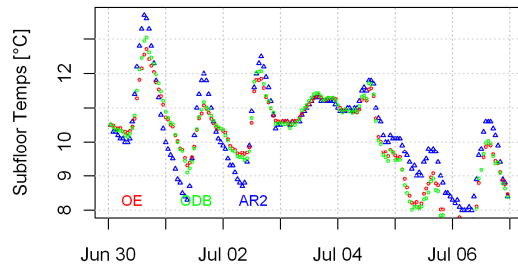
Figure A.94: Observed and AR2 subfloor temperatures, TP1-3, page 2



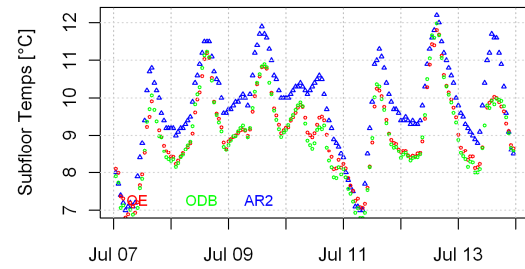
(a) Week 17



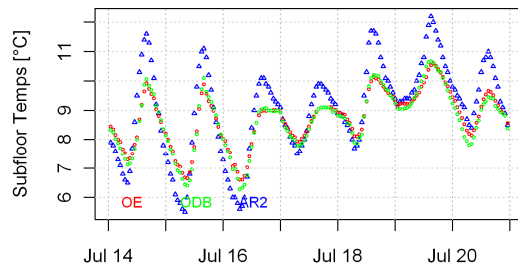
(b) Week 18



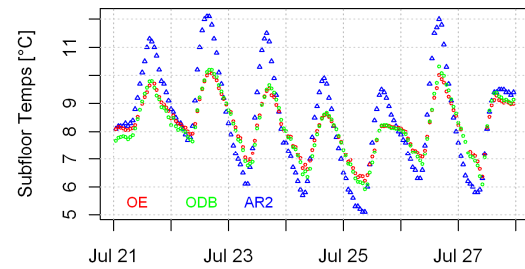
(c) Week 19



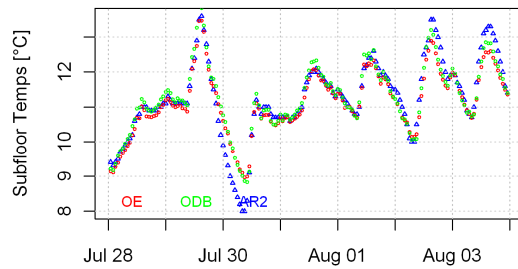
(d) Week 20



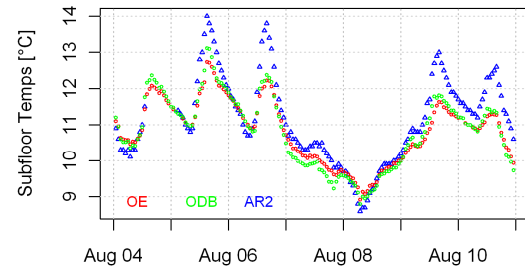
(e) Week 21



(f) Week 22

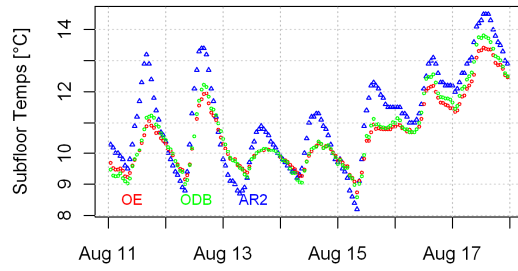


(e) Week 23

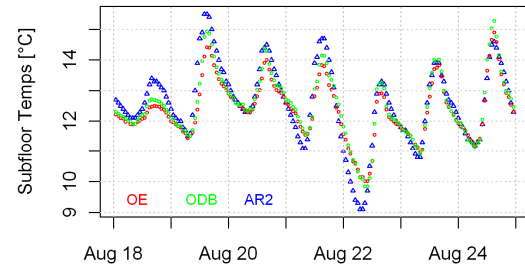


(f) Week 24

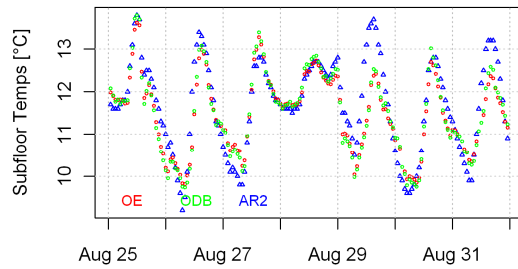
Figure A.95: Observed and AR2 subfloor temperatures, TP1-3, page 3



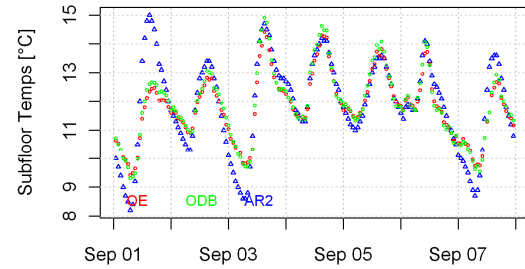
(a) Week 25



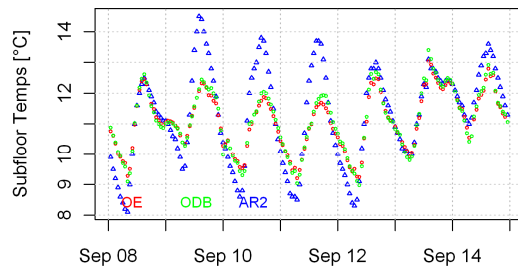
(b) Week 26



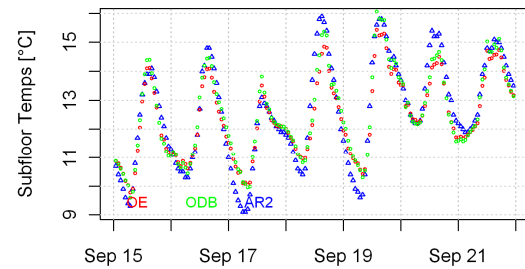
(c) Week 27



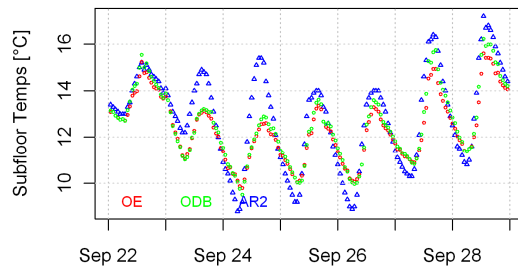
(d) Week 28



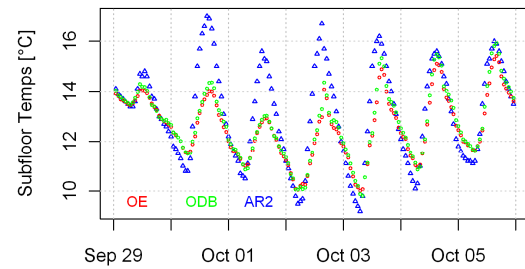
(e) Week 29



(f) Week 30

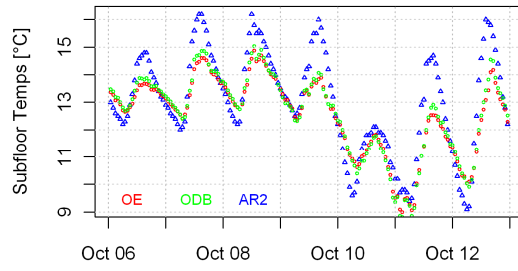


(e) Week 31

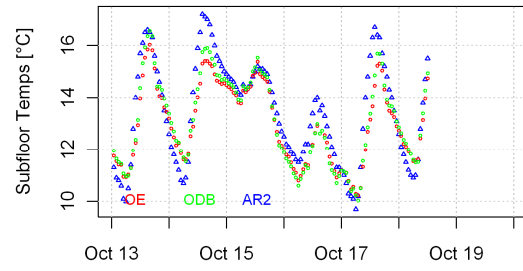


(f) Week 32

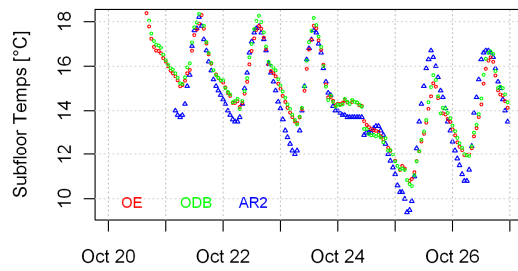
Figure A.96: Observed and AR2 subfloor temperatures, TP1-3, page 4



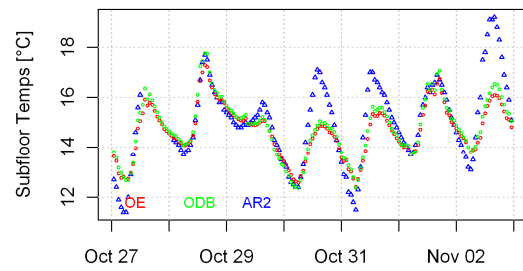
(a) Week 33



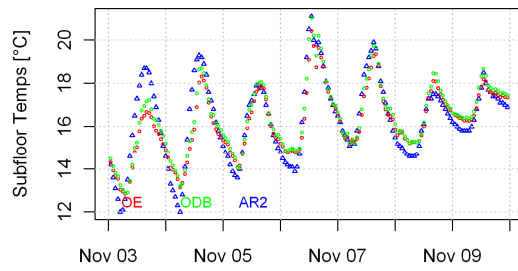
(b) Week 34



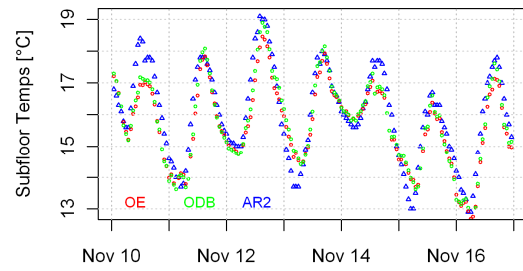
(c) Week 35



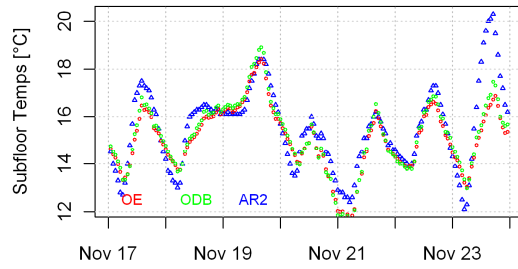
(d) Week 36



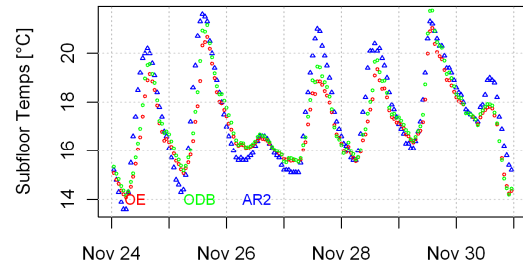
(e) Week 37



(f) Week 38

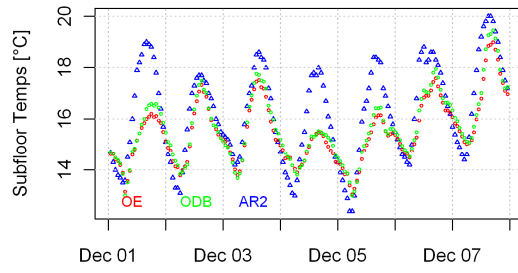


(e) Week 39

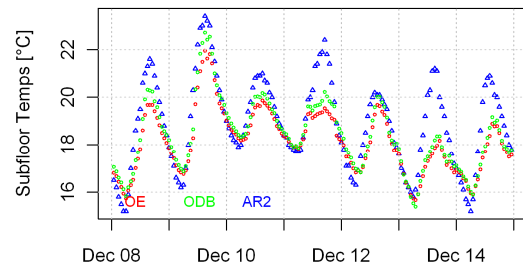


(f) Week 40

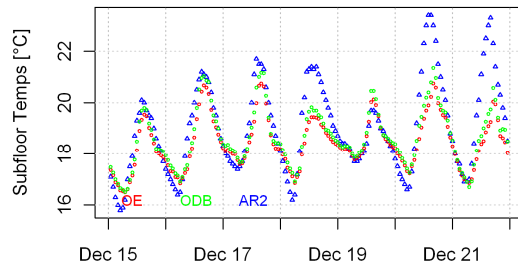
Figure A.97: Observed and AR2 subfloor temperatures, TP1-3, page 5



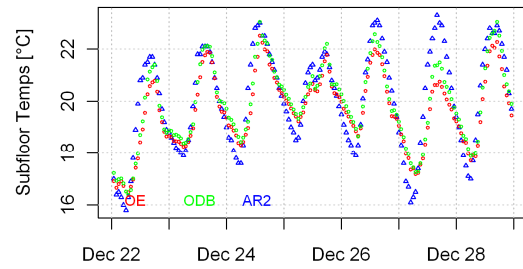
(a) Week 41



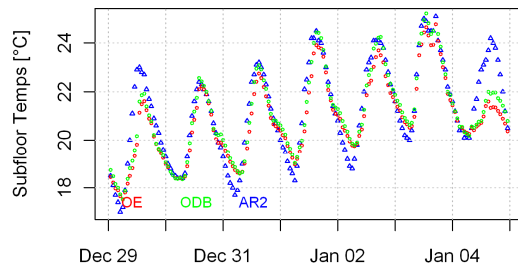
(b) Week 42



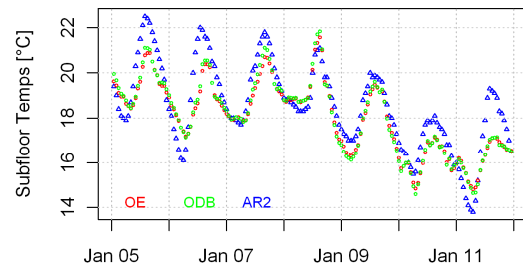
(c) Week 43



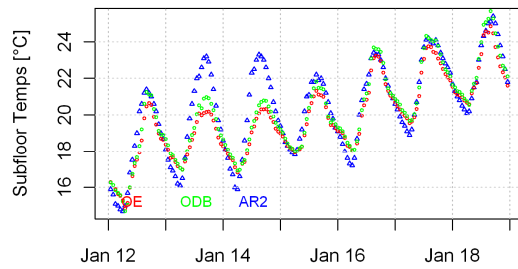
(d) Week 44



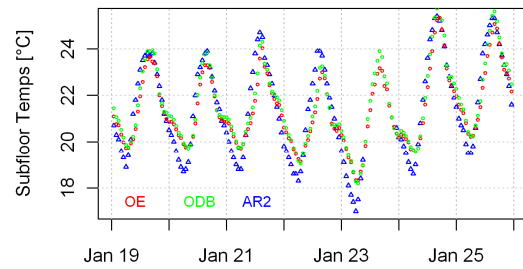
(e) Week 45



(f) Week 46

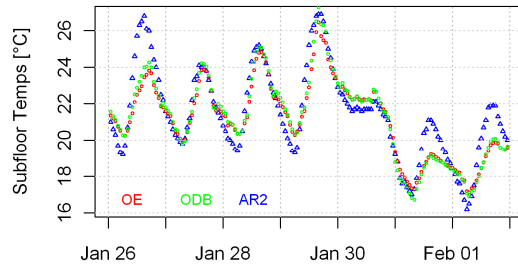


(e) Week 47

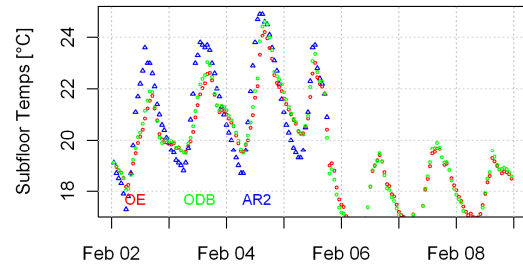


(f) Week 48

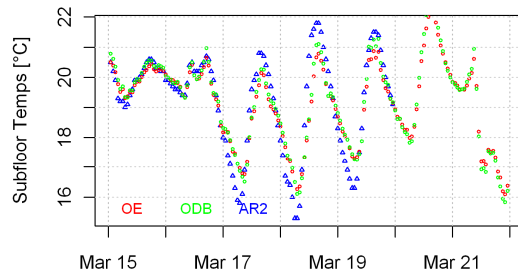
Figure A.98: Observed and AR2 subfloor temperatures, TP1-3, page 6



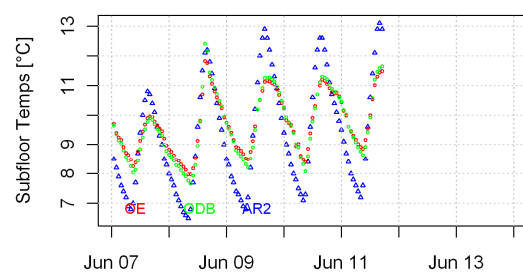
(a) Week 49



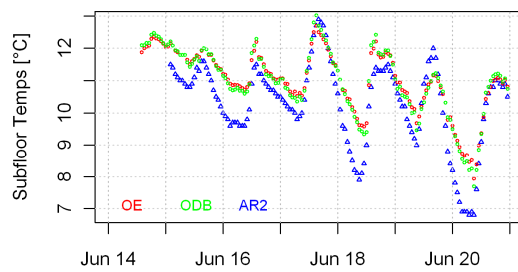
(b) Week 50



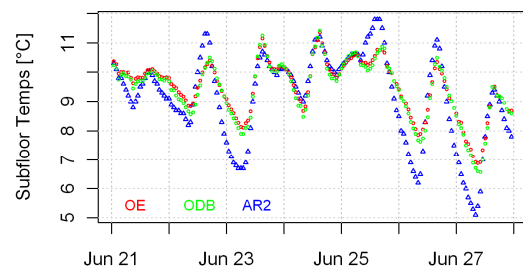
(c) Week 56



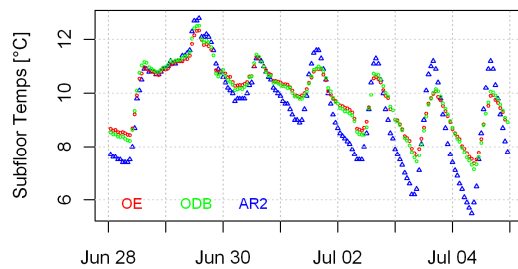
(d) Week 68



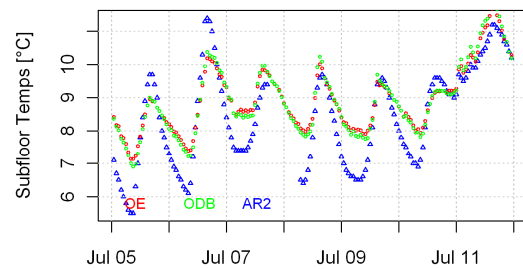
(e) Week 69



(f) Week 70

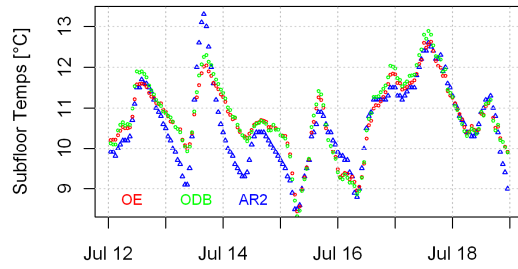


(e) Week 71

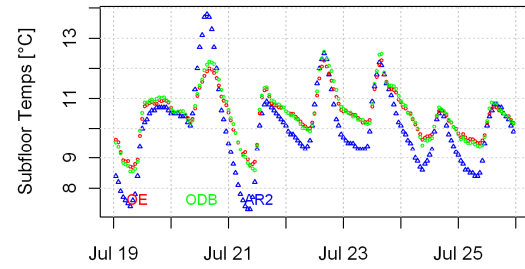


(f) Week 72

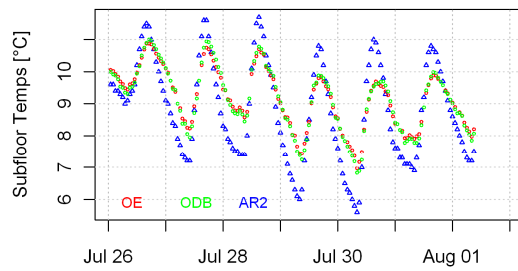
Figure A.99: Observed and AR2 subfloor temperatures, TP1-3, page 7



(a) Week 73



(b) Week 74



(c) Week 75

Figure A.100: Observed and AR2 subfloor temperatures, TP1-3, page 8

A.5.7 Observed and AR2 subfloor daily max. and min. temperatures, TP1-3

Figure A.101 through Figure A.107 display the AR2, observed dry bulb and observed environmental subfloor daily maximum and minimum temperatures for every month in the entire test period.

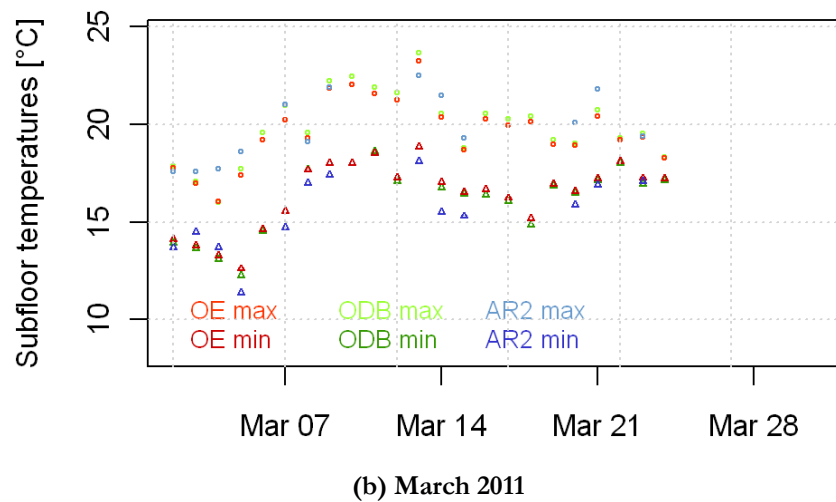
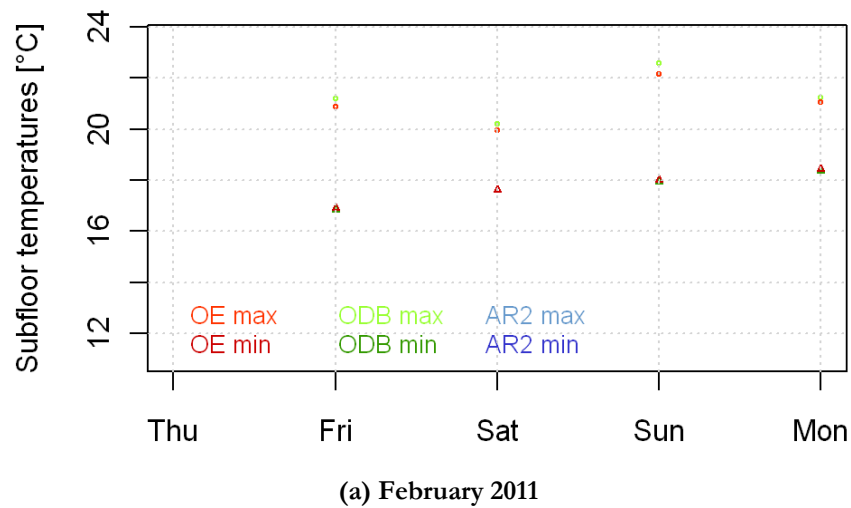
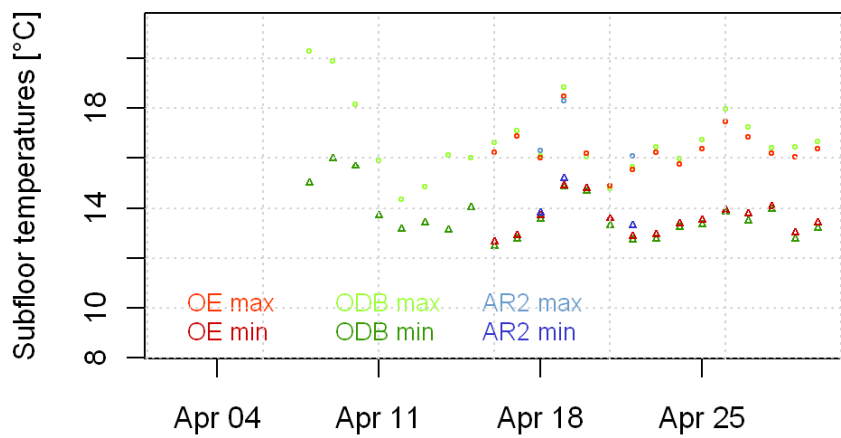
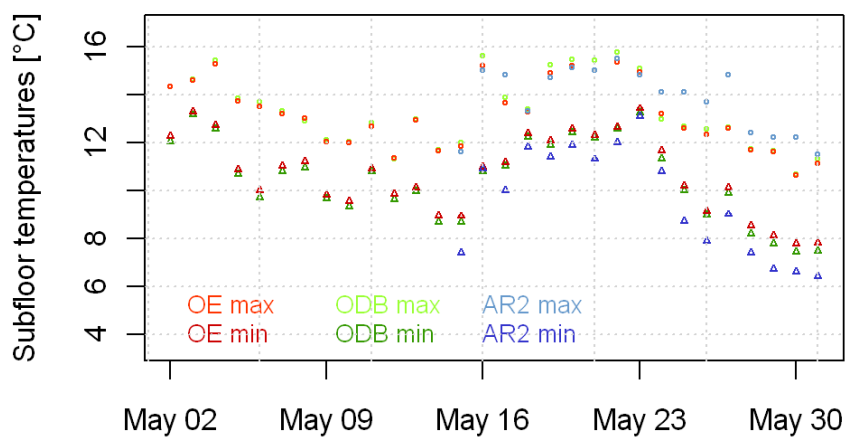


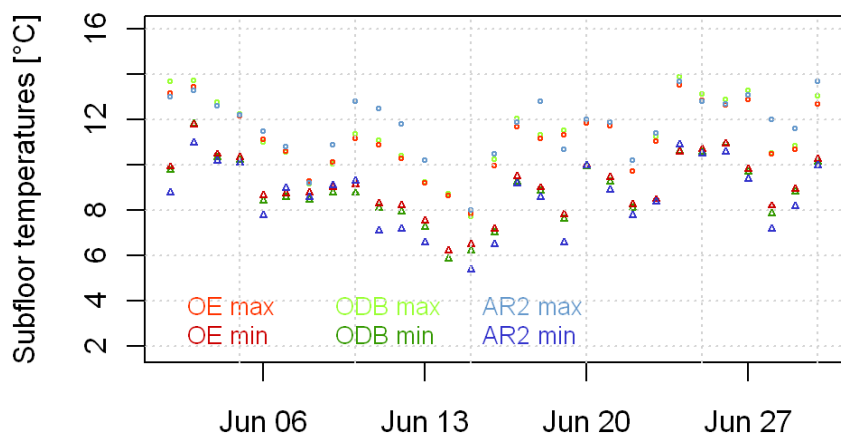
Figure A.101: AR2 and observed daily max. and min. subfloor temperatures, page 1



(a) April 2011

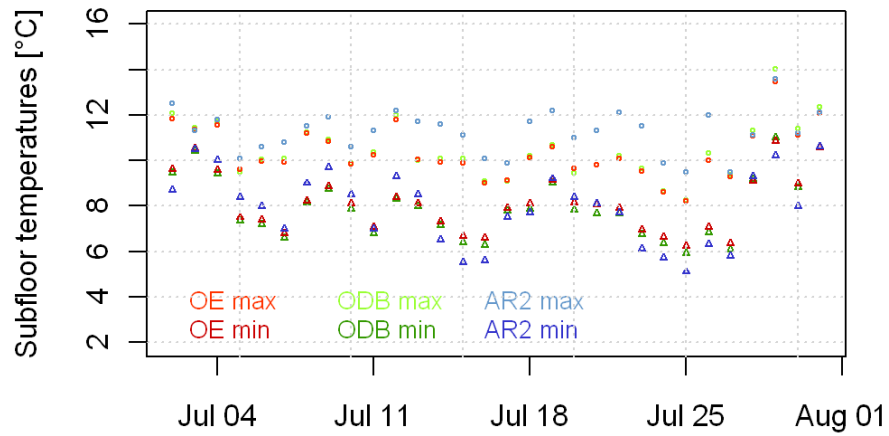


(b) May 2011

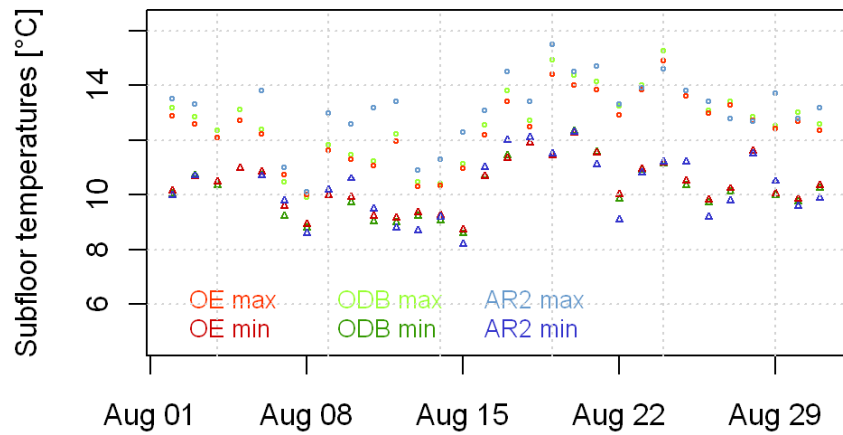


(c) June 2011

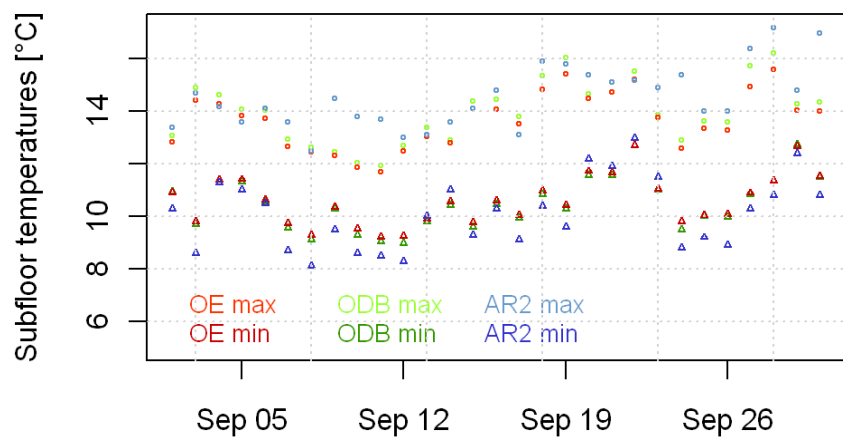
Figure A.102: AR2 and observed daily max. and min. subfloor temperatures, page 2



(a) July 2011

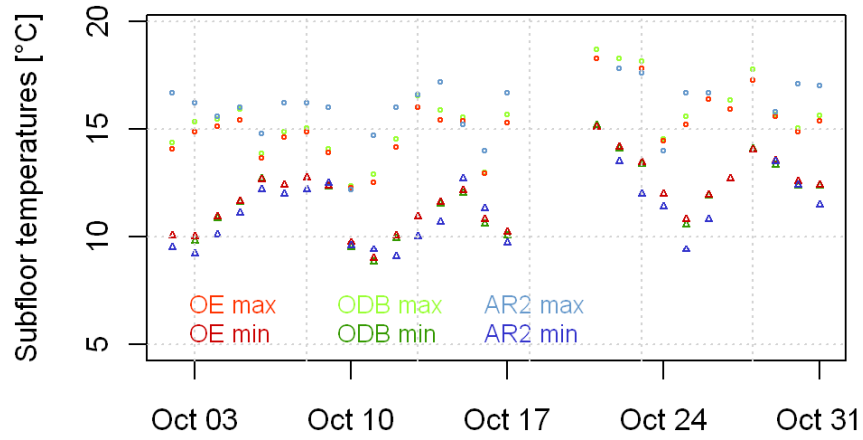


(b) August 2011

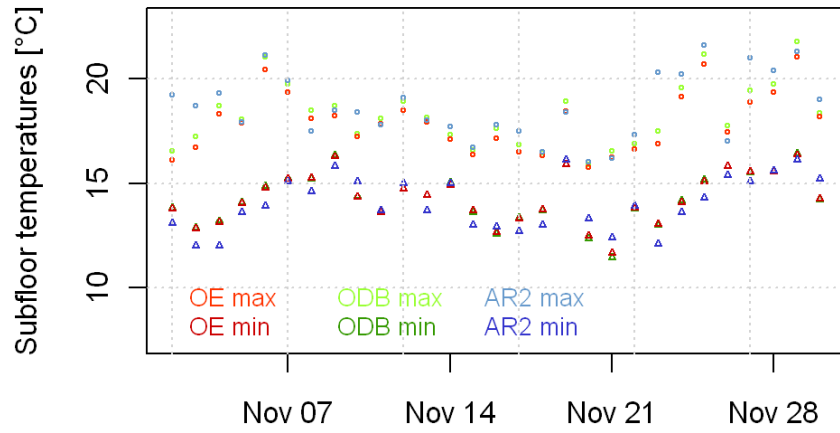


(c) September 2011

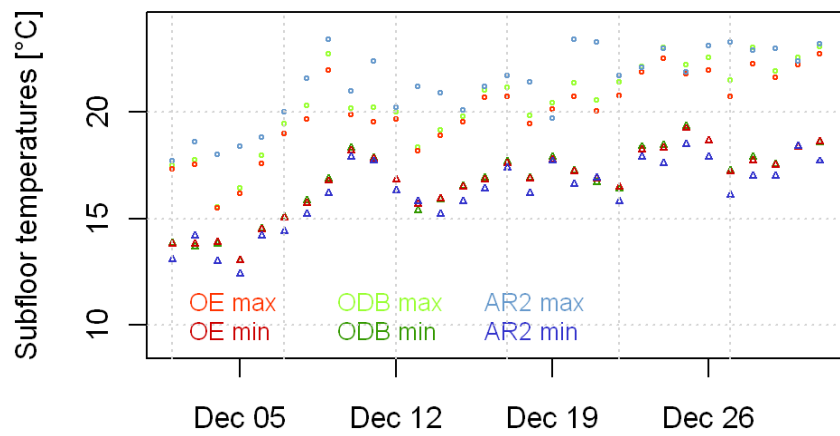
Figure A.103: AR2 and observed daily max. and min. subfloor temperatures, page 3



(a) October 2011

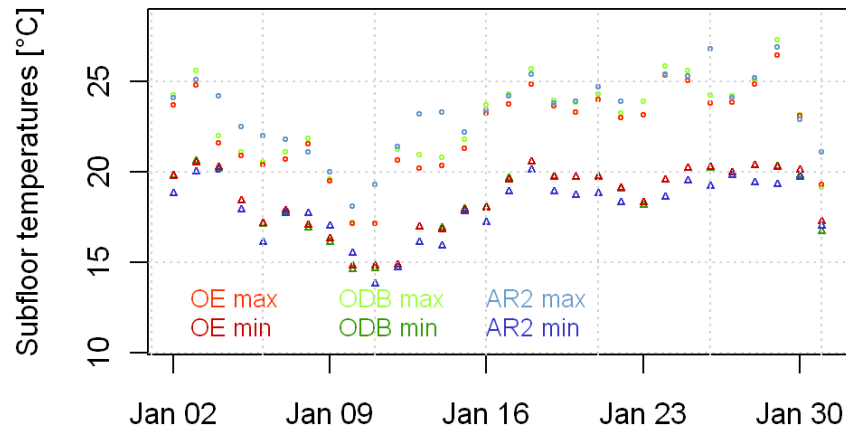


(b) November 2011

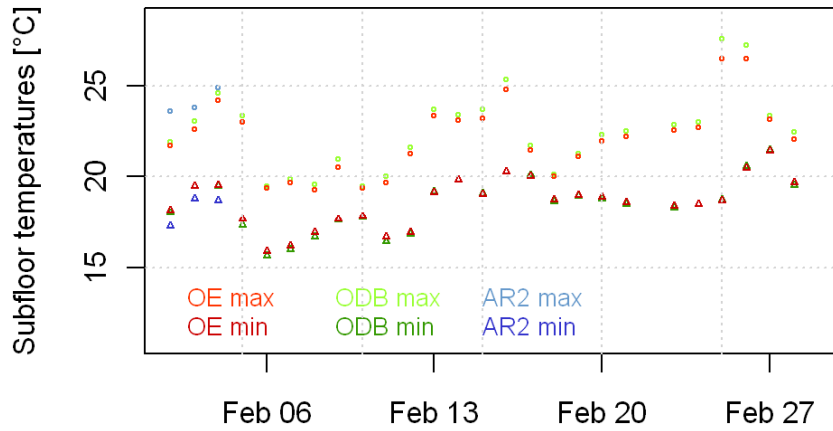


(c) December 2011

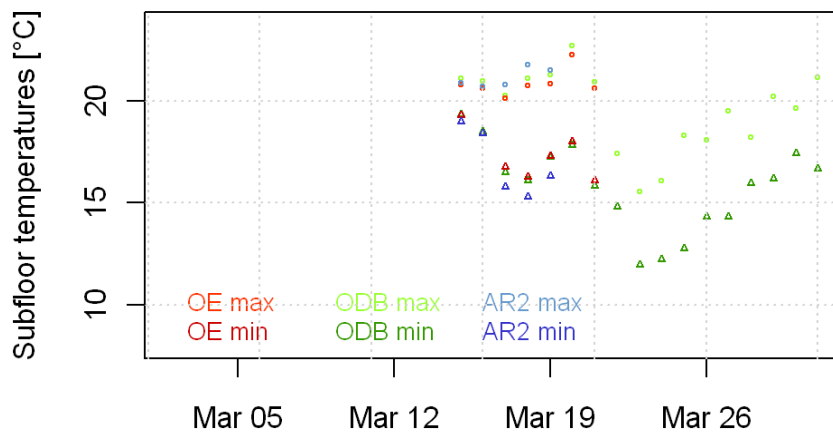
Figure A.104: AR2 and observed daily max. and min. subfloor temperatures, page 4



(a) January 2012

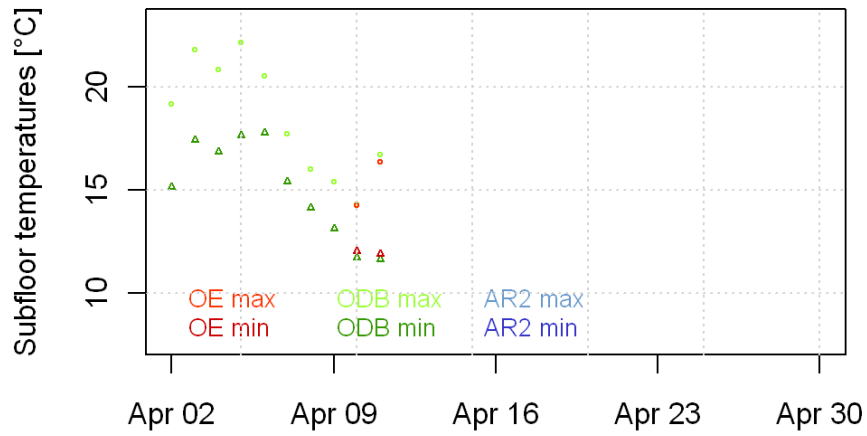


(b) February 2012

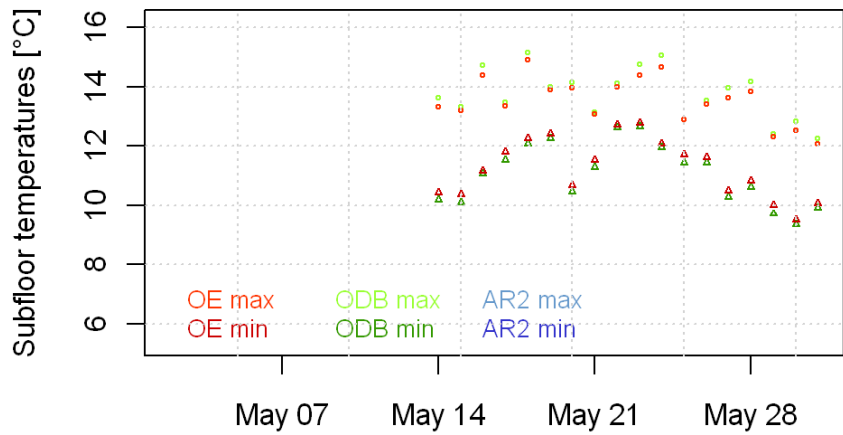


(c) March 2012

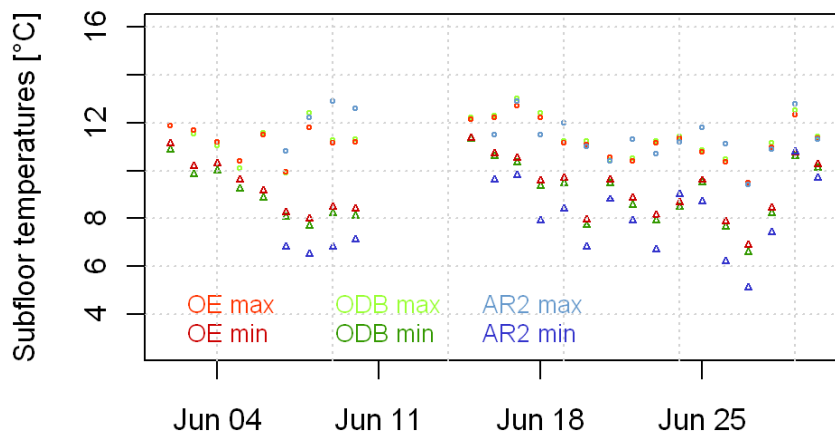
Figure A.105: AR2 and observed daily max. and min. subfloor temperatures, page 5



(a) April 2012



(b) May 2012



(c) June 2012

Figure A.106: AR2 and observed daily max. and min. subfloor temperatures, page 5

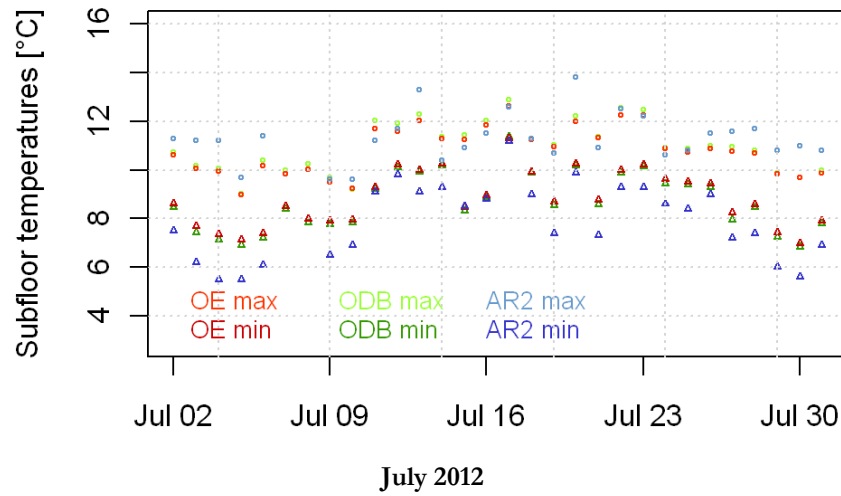


Figure A.107: AR2 and observed daily max. and min. subfloor temperatures, page 6

A.6 Analysis of Residuals

Appendix A.6 is divided into several sections.

A.6.1 contains Figure A.108 and Figure A.109, the correlation of subfloor residuals (OE-AR2) with various parameters from all time periods.

A.6.2 contains Figure A.110, Figure A.111 and Figure A.112 displaying the AccuRate subfloor temperature and subfloor residuals at 4pm from all time periods.

A.6.3 contains Figure A.113, Figure A.114 and Figure A.115, displaying the AccuRate subfloor temperature and subfloor residuals at 4pm from all time periods.

A.6.1 Subfloor residuals (OE-AR2), TP1-TP3

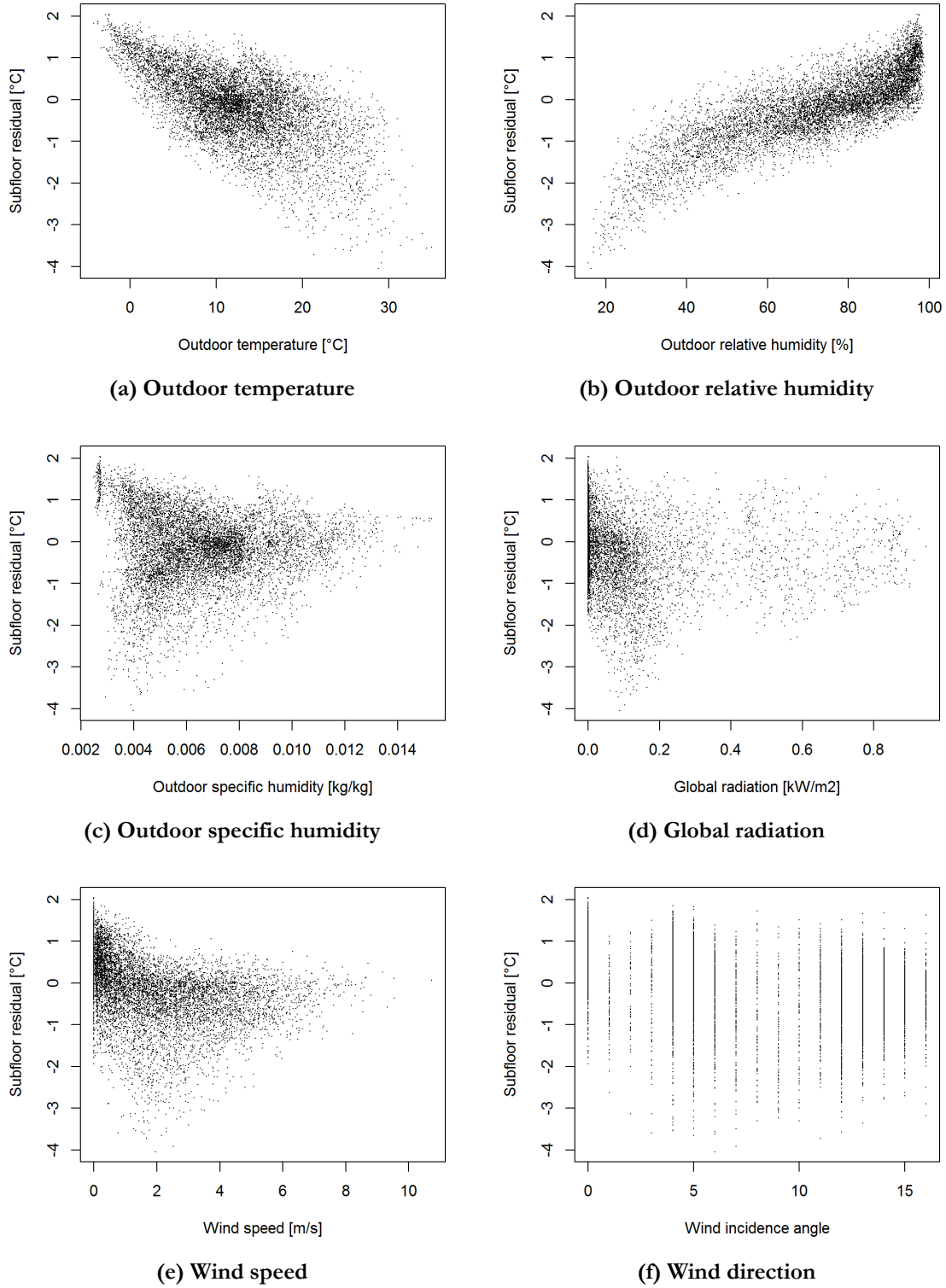
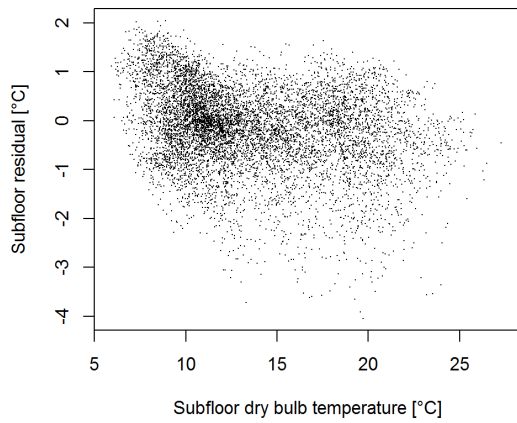
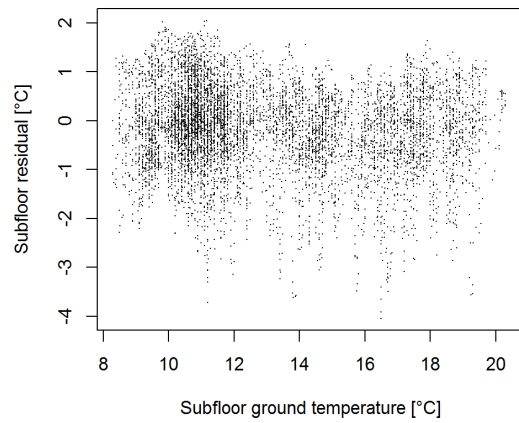


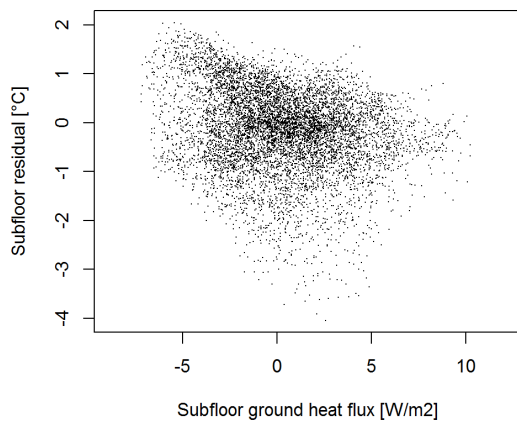
Figure A.108: Subfloor residuals (OE-AR2), TP1-TP3, batch 1



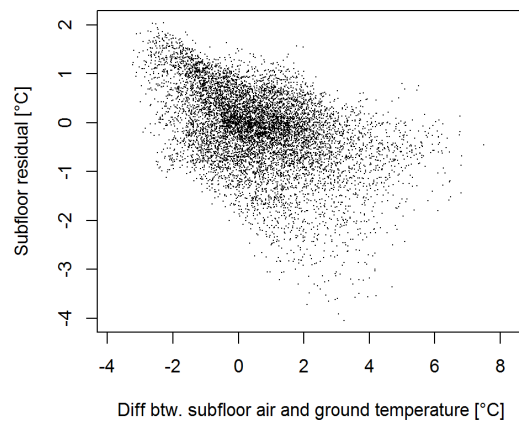
(a) Subfloor dry bulb temperature



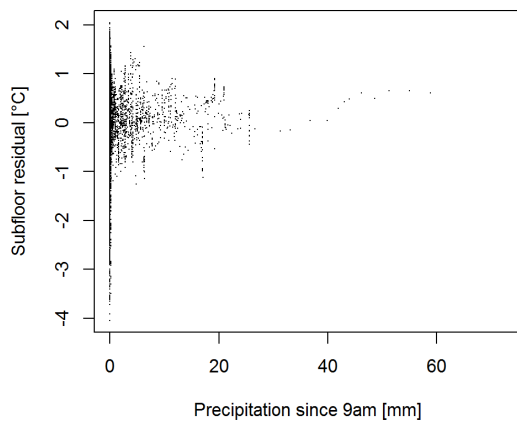
(b) Subfloor ground temperature



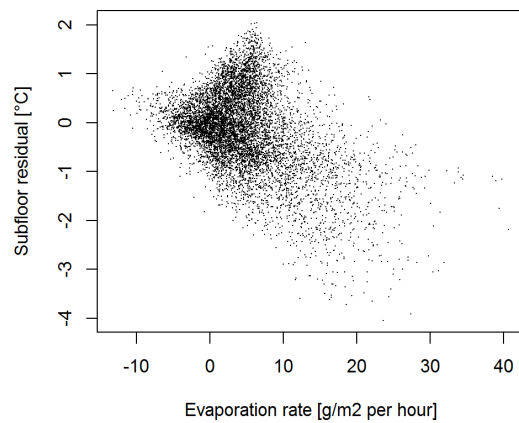
(c) Subfloor ground heat flux



(d) Subfloor temperature difference



(e) Precipitation



(f) Subfloor evaporation

Figure A.109: Subfloor residuals (OE-AR2), TP1-TP3, batch 2

A.6.2 AccuRate temperature and subfloor residuals (OE-AR2), 9am, TP1-TP3

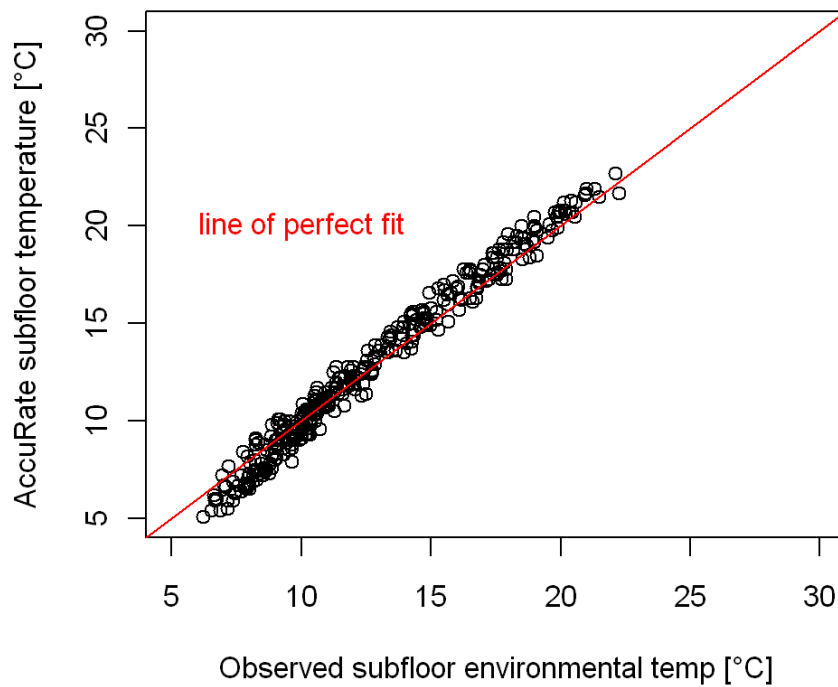
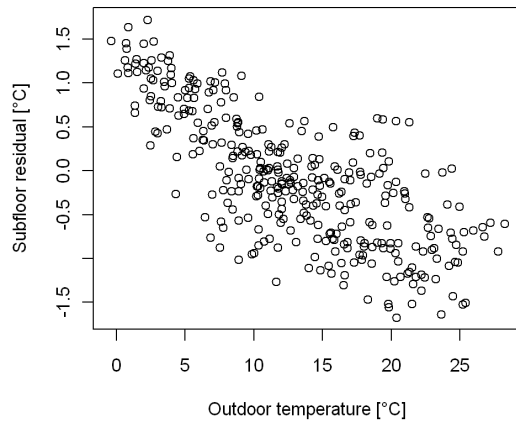
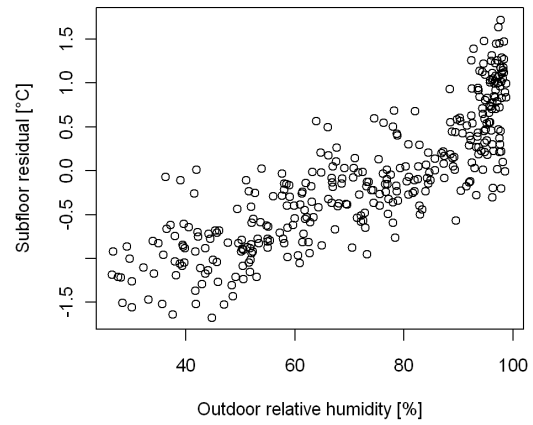


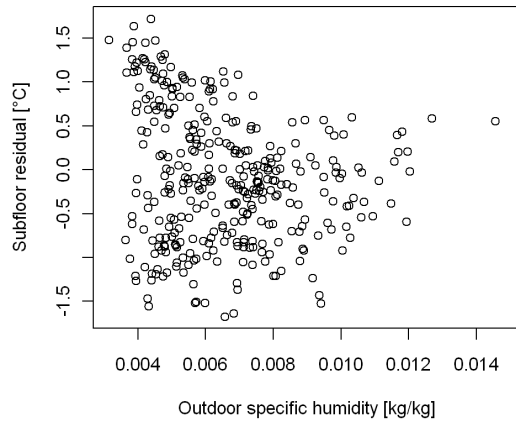
Figure A.110: AccuRate vs. observed temperature, 9am, TP1-3



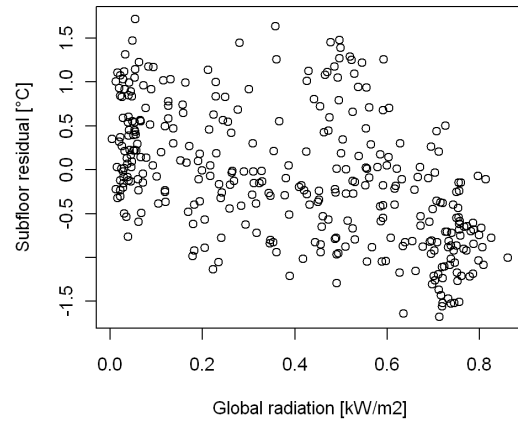
(a) Outdoor temperature



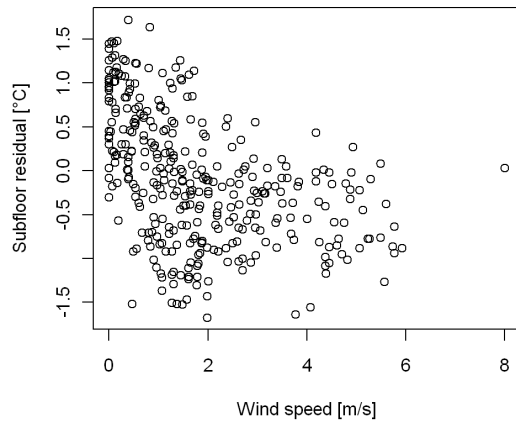
(b) Outdoor relative humidity



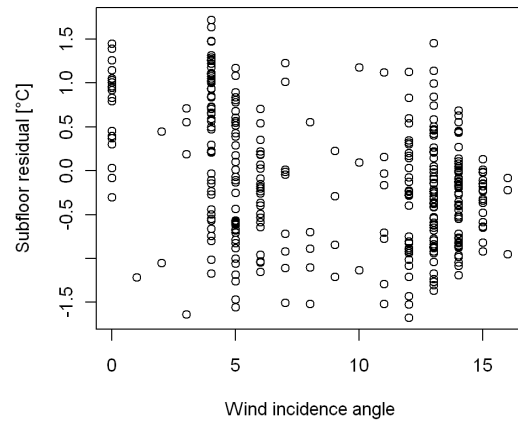
(c) Outdoor specific humidity



(d) Global radiation

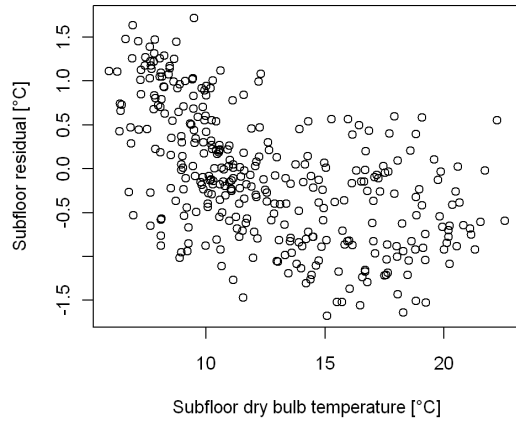


(e) Wind speed

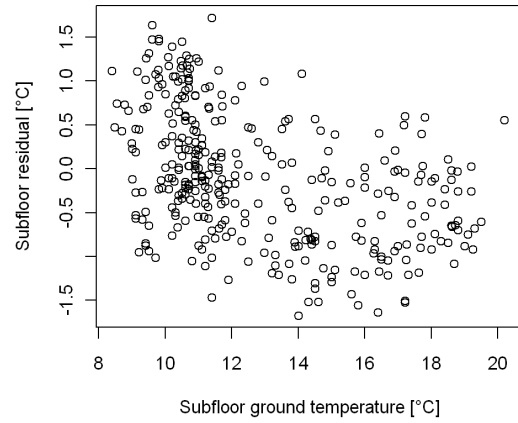


(f) Wind direction

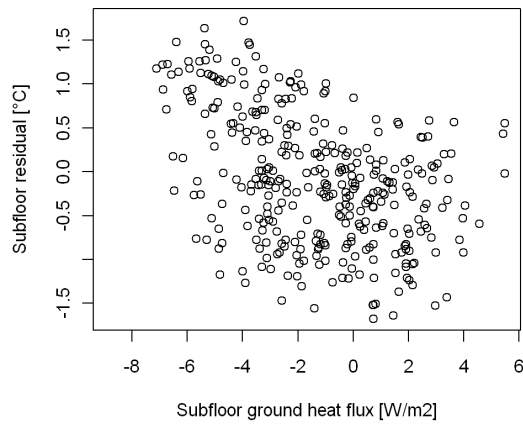
Figure A.111: Subfloor residuals (OE-AR2), 9am, TP1-TP3, batch 1



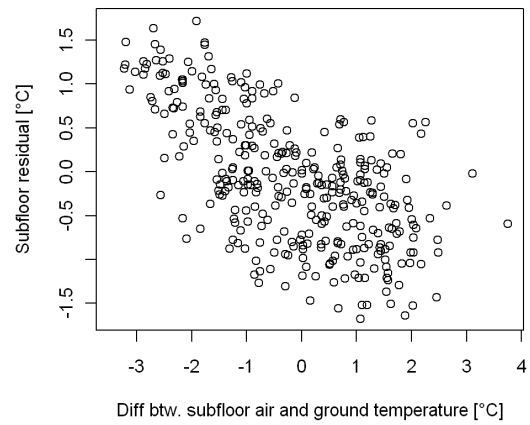
(a) Subfloor dry bulb temperature



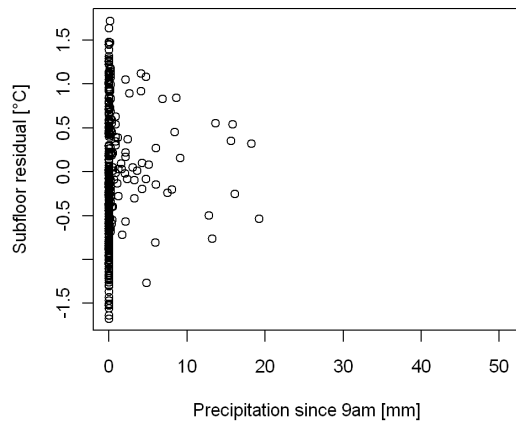
(b) Subfloor ground temperature



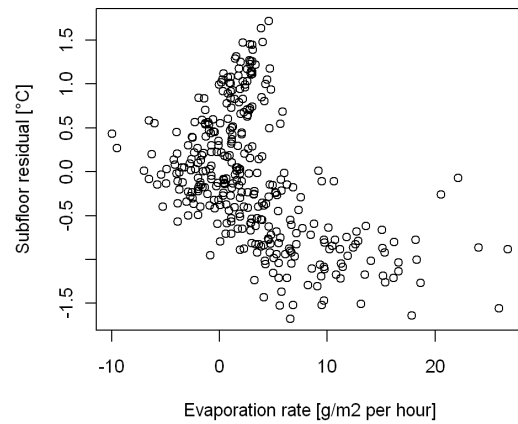
(c) Subfloor ground heat flux



(d) Subfloor temperature difference



(e) Precipitation



(f) Subfloor evaporation

Figure A.112: Subfloor residuals (OE-AR2), 9am, TP1-TP3, batch 2

A.6.3 AccuRate temperature and subfloor residuals (OE-AR2), 4pm, TP1-TP3

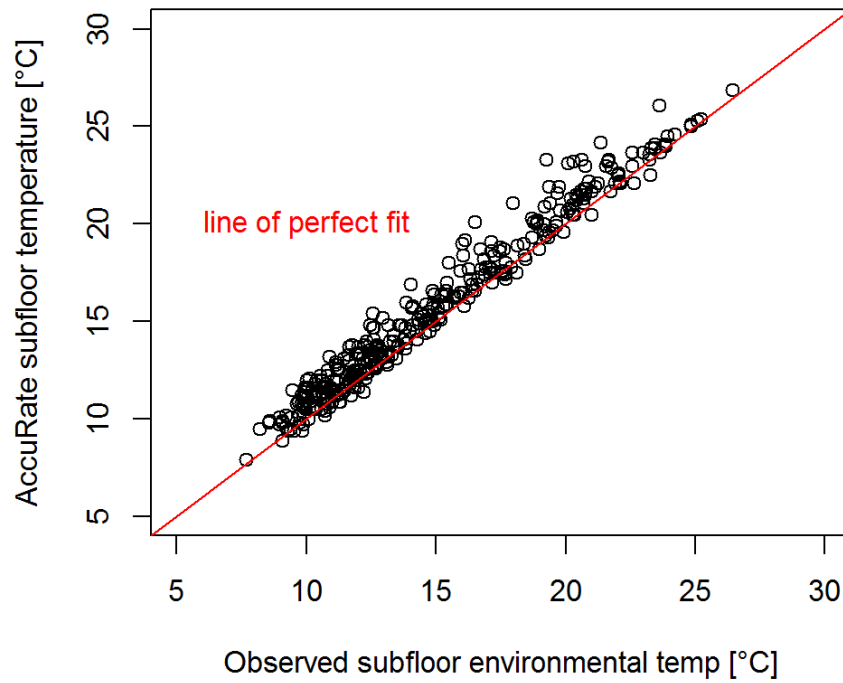
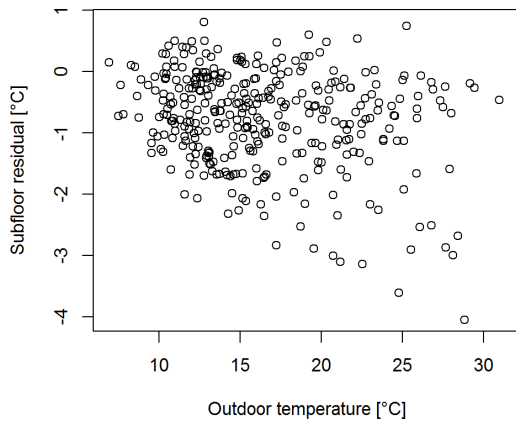
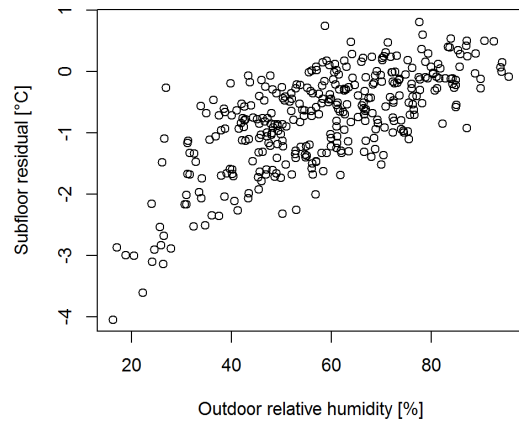


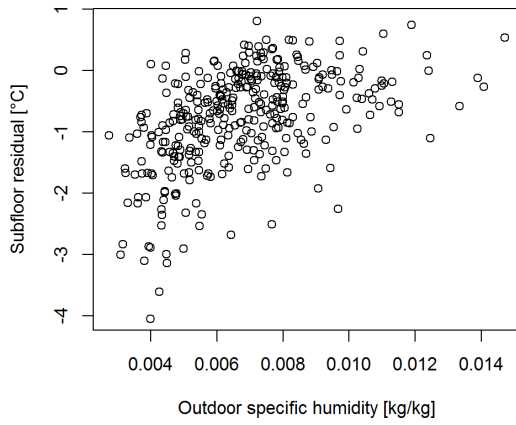
Figure A.113: AccuRate vs. observed temperature, 4pm, TP1-3



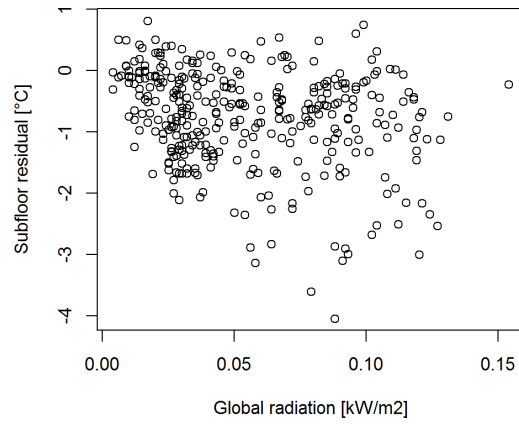
(a) Outdoor temperature



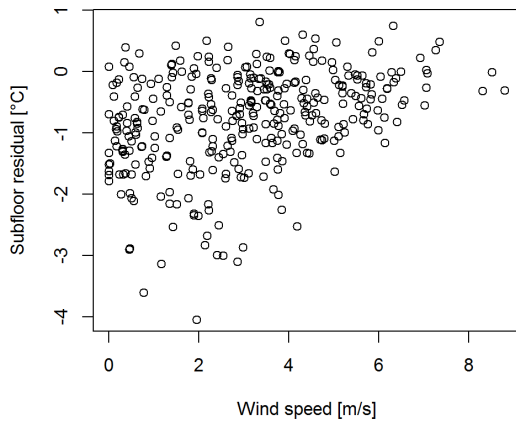
(b) Outdoor relative humidity



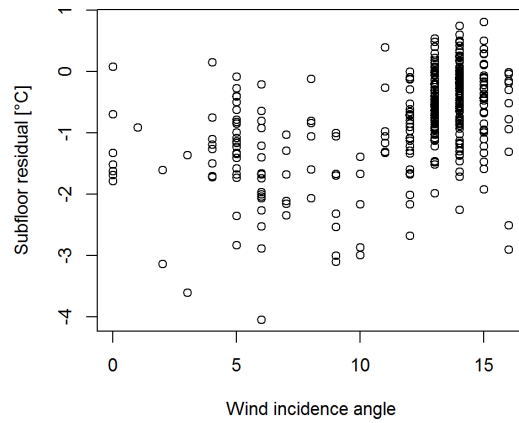
(c) Outdoor specific humidity



(d) Global radiation

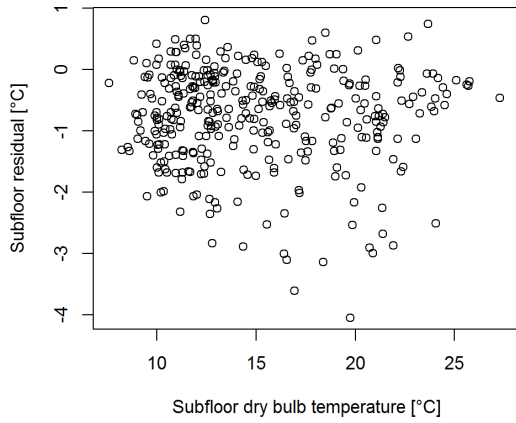


(e) Wind speed

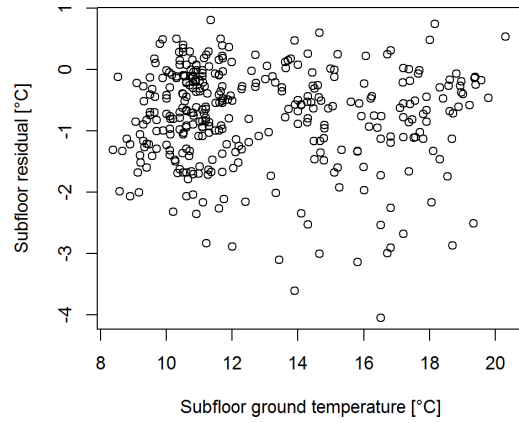


(f) Wind direction

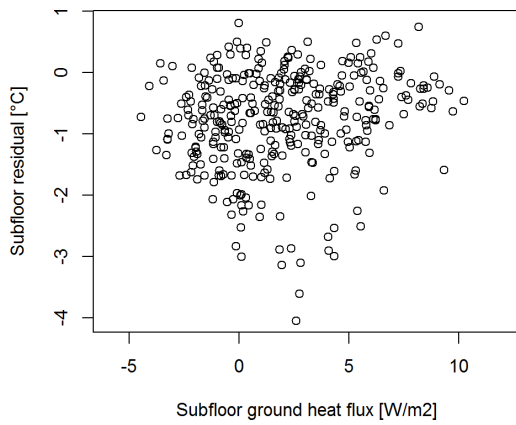
Figure A.114: Subfloor residuals (OE-AR2), 4pm, TP1-TP3, batch 1



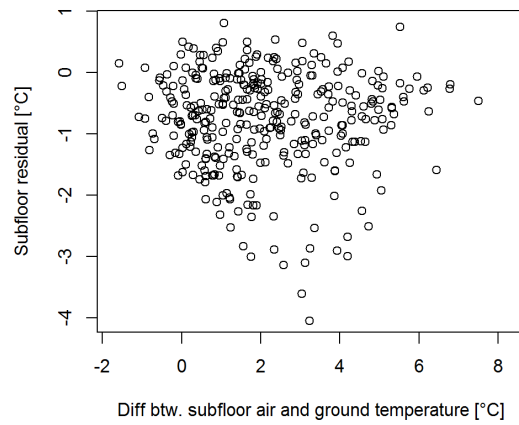
(a) Subfloor dry bulb temperature



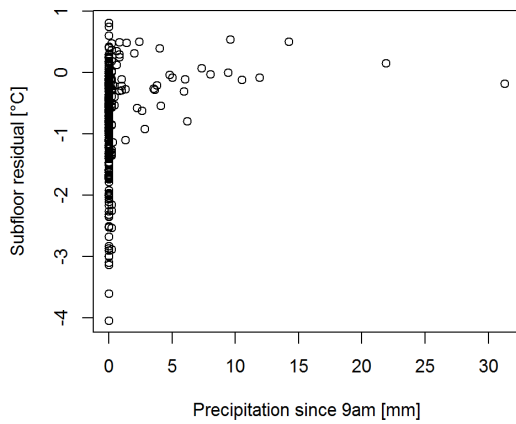
(b) Subfloor ground temperature



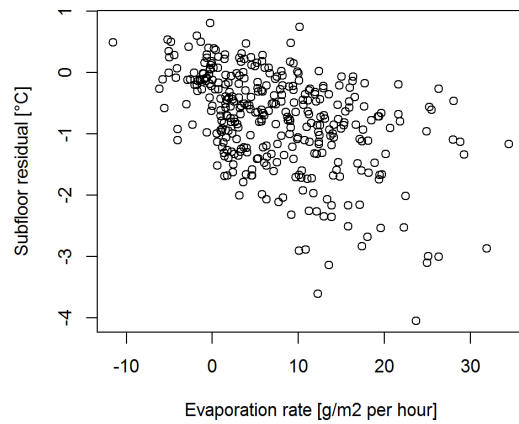
(c) Subfloor ground heat flux



(d) Subfloor temperature difference



(e) Precipitation



(f) Subfloor evaporation

Figure A.115: Subfloor residuals (OE-AR2), 4pm, TP1-TP3, batch 2

A.7 Measurement system analysis

Sensors TA36, the observed subfloor dry bulb temperature, and TB31, the observed subfloor globe temperature, were calibrated in September 2012. The offset was 0.0 °C for both sensors. Assuming an uncertainty of 0.05 °C for each sensor due to resolution, these uncertainties propagate to yield an uncertainty of 0.1 °C for the observed subfloor environmental temperature.

The uncertainty in the AccuRate subfloor temperature due only to the uncertainty in the input weather parameters was calculated. First the uncertainty in specific humidity was found. Specific humidity is not measured directly. It is calculated as a function of outdoor air pressure, temperature and relative humidity. Pressure was provided by the Bureau of Meteorology and its uncertainty is unknown. Its contribution is likely negligible compared to the contribution of temperature and relative humidity. Thus, the uncertainty in specific humidity is calculated as a function of the nominal values and uncertainty in outdoor temperature and relative humidity.

The uncertainty in relative humidity is 0.8% and the uncertainty in temperature is 0.6 °C, both obtained during the October 2010 calibration. Four sets of nominal values for each parameter are used, each representing a different season. In each of the four cases the effect of temperature on the specific humidity's uncertainty is larger than the effect of relative humidity. Averaging across the four seasons yields an uncertainty in specific humidity of 0.00021 kg moisture/kg dry air. The Excel worksheet containing these calculations is provided in Figure A.116.

Temperature and specific humidity are two of the five weather parameters input into the AccuRate model. The other three parameters are wind speed, wind direction and radiation. Uncertainty in wind speed was estimated at 1.0 m/s which is twice the manufacturer's stated accuracy. Uncertainty in wind direction was taken from the April 2011 calibration which yielded 4°. Global, direct and diffuse radiation are input into AccuRate, but only uncertainty in global radiation was modeled. The uncertainty in global radiation was assumed to be 49 W/m², which was twice the manufacture's stated accuracy.

A linear model of AccuRate subfloor temperature as a function of the weather inputs was created. Each of the five values was perturbed by its uncertainty and its effect on the change in calculated subfloor temperature was quantified. This process was performed four times, each time with nominal values representing a different season, but because the model was linear the results of the four trials was identical. The resulting uncertainty in AccuRate subfloor temperature was 0.4 °C. The Excel worksheet containing these calculations is provided in Figure A.117.

The uncertainties in AccuRate subfloor temperature and the observed subfloor temperature combine to yield an uncertainty in the residuals of 0.4 °C

Uncertainty in wos from uncertainty in RH10 and TA10

Parameter	Unit	Uncertainty	Source
RH10	%	0.8	Calibration October 2010
TA10	°C	0.6	Calibration October 2010
Psatos	kPa	NA	Function of temperature TA10
Ptot	kPa	NA	From BOM, adjusted for altitude

Spring 2011	Nominal	+ RH10	- RH10	+ TA10	- TA10	Uncertainty
RH10	37.5	38.3	36.7	37.5	37.5	
TA10	16.5	16.5	16.5	17.1	15.9	
Psatos	1.9	1.9	1.9	2.0	1.8	
Ptot	102.3	102.3	102.3	102.3	102.3	
Calculated wos	0.00434	0.00443	0.00425	0.00452	0.00416	
Difference		0.00009	0.00009	0.00018	0.00018	0.00020

Summer 2011	Nominal	+ RH10	- RH10	+ TA10	- TA10	Uncertainty
RH10	20.5	21.3	19.7	20.5	20.5	
TA10	20.7	20.7	20.7	21.3	20.1	
Psatos	2.5	2.5	2.5	2.6	2.4	
Ptot	102.0	102.0	102.0	102.0	102.0	
Calculated wos	0.00308	0.00320	0.00296	0.00321	0.00296	
Difference		0.00012	0.00012	0.00013	0.00013	0.00017

Autumn 2011	Nominal	+ RH10	- RH10	+ TA10	- TA10	Uncertainty
RH10	26.5	27.3	25.7	26.5	26.5	
TA10	17.6	17.6	17.6	18.2	17.0	
Psatos	2.0	2.0	2.0	2.1	2.0	
Ptot	100.5	100.5	100.5	100.5	100.5	
Calculated wos	0.00336	0.00346	0.00326	0.00348	0.00323	
Difference		0.00010	0.00010	0.00013	0.00013	0.00016

Winter 2011	Nominal	+ RH10	- RH10	+ TA10	- TA10	Uncertainty
RH10	76.0	76.8	75.2	76.0	76.0	
TA10	15.2	15.2	15.2	15.8	14.6	
Psatos	1.7	1.7	1.7	1.8	1.7	
Ptot	102.5	102.5	102.5	102.5	102.5	
Calculated wos	0.00811	0.00820	0.00802	0.00847	0.00781	
Difference		0.00009	0.00009	0.00036	0.00031	0.00032

Average across seasons, uncertainty in wos	0.00021
The uncertainty varies with season and in positive,negative direction.	

Figure A.116: Uncertainty in specific humidity

Now vary each parameter by its uncertainty. Do four times, once for each month of data

Spring 2011	Nominal	+ TA10	- TA10	+ wos	- wos	+ RA14	- RA14	+ AS10	- AS10	+ AD10	- AD10
TA10	16.5	17.1	15.9	16.5	16.5	16.5	16.5	16.5	16.5	16.5	16.5
wos	0.0043	0.0043	0.0043	0.0046	0.0041	0.0043	0.0043	0.0043	0.0043	0.0043	0.0043
RA14	0.186	0.186	0.186	0.186	0.186	0.235	0.137	0.186	0.186	0.186	0.186
AS10	2.0	2.0	2.0	2.0	2.0	2.0	2.0	3.0	1.9	2.0	2.0
AD10	108	108	108	108	108	108	108	108	108	112	104
Calculated Subfloor Temp	16.0	16.3	15.6	16.0	15.9	15.8	16.1	15.7	16.0	15.9	16.0
Difference		0.4	-0.4	0.0	0.0	-0.2	0.2	-0.3	0.0	0.0	0.0
Average effect by parameter		0.4	0.0	0.0	0.2	0.1	0.0	0.0			
Summer 2011	Nominal	+ TA10	- TA10	+ wos	- wos	+ RA14	- RA14	+ AS10	- AS10	+ AD10	- AD10
TA10	20.7	21.3	20.1	20.7	20.7	20.7	20.7	20.7	20.7	20.7	20.7
wos	0.0031	0.0031	0.0031	0.0033	0.0029	0.0031	0.0031	0.0031	0.0031	0.0031	0.0031
RA14	0.58	0.580	0.580	0.580	0.580	0.629	0.531	0.580	0.580	0.580	0.580
AS10	2.5	2.5	2.5	2.5	2.5	2.5	2.5	3.5	2.5	2.5	2.5
AD10	209	209	209	209	209	209	209	209	209	213	205
Calculated Subfloor Temp	16.6	17.0	16.2	16.6	16.6	16.4	16.7	16.3	16.6	16.6	16.6
Difference		0.4	-0.4	0.0	0.0	-0.2	0.2	-0.3	0.0	0.0	0.0
Average effect by parameter		0.4	0.0	0.0	0.2	0.1	0.0	0.0			
Autumn 2011	Nominal	+ TA10	- TA10	+ wos	- wos	+ RA14	- RA14	+ AS10	- AS10	+ AD10	- AD10
TA10	17.6	18.2	17.0	17.6	17.6	17.6	17.6	17.6	17.6	17.6	17.6
wos	0.0034	0.0034	0.0034	0.0036	0.0031	0.0034	0.0034	0.0034	0.0034	0.0034	0.0034
RA14	0.486	0.486	0.486	0.486	0.486	0.535	0.437	0.486	0.486	0.486	0.486
AS10	4.8	4.8	4.8	4.8	4.8	4.8	4.8	5.8	4.7	4.8	4.8
AD10	269	269	269	269	269	269	269	269	269	273	265
Calculated Subfloor Temp	14.2	14.6	13.8	14.3	14.2	14.1	14.4	14.0	14.2	14.2	14.2
Difference		0.4	-0.4	0.0	0.0	-0.2	0.2	-0.3	0.0	0.0	0.0
Average effect by parameter		0.4	0.0	0.0	0.2	0.1	0.0	0.0			
Winter 2011	Nominal	+ TA10	- TA10	+ wos	- wos	+ RA14	- RA14	+ AS10	- AS10	+ AD10	- AD10
TA10	15.2	15.8	14.6	15.2	15.2	15.2	15.2	15.2	15.2	15.2	15.2
wos	0.0081	0.0081	0.0081	0.0083	0.0079	0.0081	0.0081	0.0081	0.0081	0.0081	0.0081
RA14	0.048	0.048	0.048	0.048	0.048	0.097	-0.001	0.048	0.048	0.048	0.048
AS10	0.9	0.9	0.9	0.9	0.9	0.9	0.9	1.9	0.9	0.9	0.9
AD10	290	290	290	290	290	290	290	290	290	294	286
Calculated Subfloor Temp	16.0	16.4	15.7	16.1	16.0	15.9	16.2	15.8	16.0	16.0	16.1
Difference		0.4	-0.4	0.0	0.0	-0.2	0.2	-0.3	0.0	0.0	0.0
Average effect by parameter		0.4	0.0	0.0	0.2	0.1	0.0	0.0			
Uncertainty in AccuRate subfloor temperature: 0.4 °C By RSS of the above 5 values											
The uncertainty is constant by season and in positive, negative direction because the model is linear.											

Figure A.117: Uncertainty in predicted subfloor temperature